PHAGOCYTES IN IMMUNITY: LINKING MATERIAL INTERNALIZATION TO IMMUNE RESPONSES AND THERAPEUTIC STRATEGIES

EDITED BY: Johnathan Canton, Gregory D. Fairn and Valentin Jaumouillé
PUBLISHED IN: Frontiers in Immunology

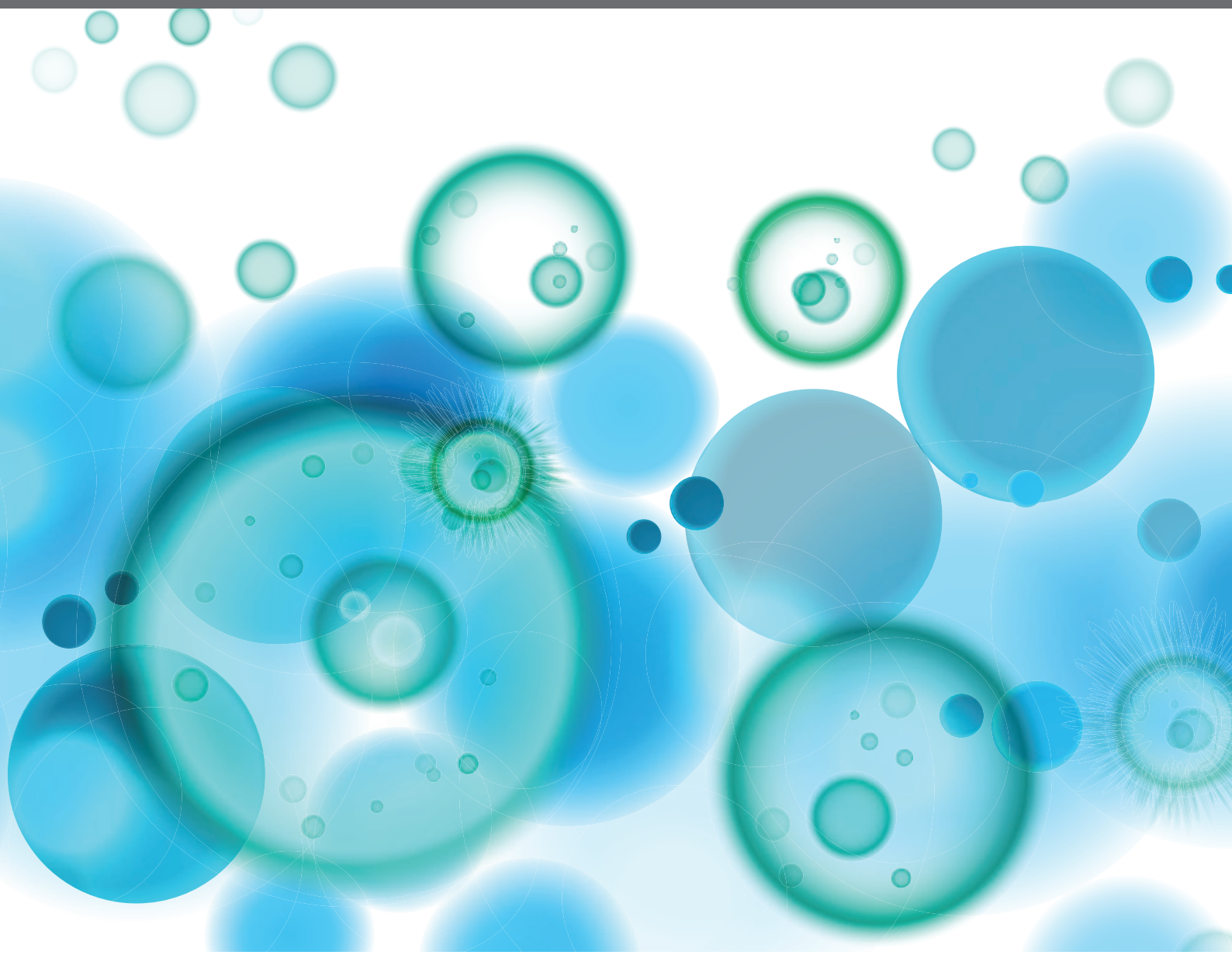

frontiers Research Topics

Frontiers eBook Copyright Statement

The copyright in the text of individual articles in this eBook is the property of their respective authors or their respective institutions or funders. The copyright in graphics and images within each article may be subject to copyright of other parties. In both cases this is subject to a license granted to Frontiers.

The compilation of articles constituting this eBook is the property of Frontiers.

Each article within this eBook, and the eBook itself, are published under the most recent version of the Creative Commons CC-BY licence. The version current at the date of publication of this eBook is CC-BY 4.0. If the CC-BY licence is updated, the licence granted by Frontiers is automatically updated to the new version.

When exercising any right under the CC-BY licence, Frontiers must be attributed as the original publisher of the article or eBook, as applicable.

Authors have the responsibility of ensuring that any graphics or other materials which are the property of others may be included in the CC-BY licence, but this should be checked before relying on the CC-BY licence to reproduce those materials. Any copyright notices relating to those materials must be complied with.

Copyright and source acknowledgement notices may not be removed and must be displayed in any copy, derivative work or partial copy which includes the elements in question.

All copyright, and all rights therein, are protected by national and international copyright laws. The above represents a summary only. For further information please read Frontiers' Conditions for Website Use and Copyright Statement, and the applicable CC-BY licence.

ISSN 1664-8714
ISBN 978-2-88971-631-9
DOI 10.3389/978-2-88971-631-9

About Frontiers

Frontiers is more than just an open-access publisher of scholarly articles: it is a pioneering approach to the world of academia, radically improving the way scholarly research is managed. The grand vision of Frontiers is a world where all people have an equal opportunity to seek, share and generate knowledge. Frontiers provides immediate and permanent online open access to all its publications, but this alone is not enough to realize our grand goals.

Frontiers Journal Series

The Frontiers Journal Series is a multi-tier and interdisciplinary set of open-access, online journals, promising a paradigm shift from the current review, selection and dissemination processes in academic publishing. All Frontiers journals are driven by researchers for researchers; therefore, they constitute a service to the scholarly community. At the same time, the Frontiers Journal Series operates on a revolutionary invention, the tiered publishing system, initially addressing specific communities of scholars, and gradually climbing up to broader public understanding, thus serving the interests of the lay society, too.

Dedication to Quality

Each Frontiers article is a landmark of the highest quality, thanks to genuinely collaborative interactions between authors and review editors, who include some of the world's best academicians. Research must be certified by peers before entering a stream of knowledge that may eventually reach the public - and shape society; therefore, Frontiers only applies the most rigorous and unbiased reviews.
Frontiers revolutionizes research publishing by freely delivering the most outstanding research, evaluated with no bias from both the academic and social point of view. By applying the most advanced information technologies, Frontiers is catapulting scholarly publishing into a new generation.

What are Frontiers Research Topics?

Frontiers Research Topics are very popular trademarks of the Frontiers Journals Series: they are collections of at least ten articles, all centered on a particular subject. With their unique mix of varied contributions from Original Research to Review Articles, Frontiers Research Topics unify the most influential researchers, the latest key findings and historical advances in a hot research area! Find out more on how to host your own Frontiers Research Topic or contribute to one as an author by contacting the Frontiers Editorial Office: frontiersin.org/about/contact

PHAGOCYTES IN IMMUNITY: LINKING MATERIAL INTERNALIZATION TO IMMUNE RESPONSES AND THERAPEUTIC STRATEGIES

Topic Editors:
Johnathan Canton, University of Calgary, Canada
Gregory D. Fairn, Dalhousie University, Canada
Valentin Jaumouillé, Simon Fraser University, Canada

Citation: Canton, J., Fairn, G. D., Jaumouillé, V., eds. (2021). Phagocytes in Immunity: Linking Material Internalization to Immune Responses and Therapeutic Strategies. Lausanne: Frontiers Media SA. doi: 10.3389/978-2-88971-631-9

Table of Contents

05 ***Editorial: Phagocytes in Immunity: Linking Material Internalization to Immune Responses and Therapeutic Strategies***
Johnathan Canton, Gregory D. Fairn and Valentin Jaumouillé

07 ***Phagocytosis by the Retinal Pigment Epithelium: Recognition, Resolution, Recycling***
Whijin Kwon and Spencer A. Freeman

22 ***Warburg Effect is a Cancer Immune Evasion Mechanism Against Macrophage Immunosurveillance***
Jing Chen, Xu Cao, Bolei Li, Zhangchen Zhao, Siqi Chen, Seigmund W. T. Lai, Sabina A. Muend, Gianna K. Nossa, Lei Wang, Weihua Guo, Jian Ye, Peter P. Lee and Mingye Feng

38 ***Bacterial and Fungal Toll-Like Receptor Activation Elicits Type I IFN Responses in Mast Cells***
Lisa Kornstädt, Sandra Pierre, Andreas Weigert, Stefanie Ebersberger, Tim J. Schäufele, Anja Kolbinger, Tobias Schmid, Jennifer Cohnen, Dominique Thomas, Nerea Ferreirós, Bernhard Brüne, Ingo Ebersberger and Klaus Scholich

53 ***Modulation of Immune Responses by Particle Size and Shape***
Maksim V. Baranov, Manoj Kumar, Stefano Sacanna, Shashi Thutupalli and Geert van den Bogaart

76 ***Engineered IgG1-Fc Molecules Define Valency Control of Cell Surface Fcγ Receptor Inhibition and Activation in Endosomes***
Elizabeth M. Bailey, Amit Choudhury, Harika Vuppula, Daniel F. Ortiz, John Schaeck, Anthony M. Manning, Carlos J. Bosques and Adam D. Hoppe

91 ***Use of Flow Cytometry to Evaluate Phagocytosis of* Staphylococcus aureus *by Human Neutrophils***
Elena Boero, Iris Brinkman, Thessely Juliet, Eline van Yperen, Jos A. G. van Strijp, Suzan H. M. Rooijakkers and Kok P. M. van Kessel

106 ***Better Together: Current Insights Into Phagosome-Lysosome Fusion***
Jenny A. Nguyen and Robin M. Yates

125 ***Harnessing and Enhancing Macrophage Phagocytosis for Cancer Therapy***
Siqi Chen, Seigmund W. T. Lai, Christine E. Brown and Mingye Feng

141 ***The Activation and Regulation of β2 Integrins in Phagocytes and Phagocytosis***
Hao Sun, Kangkang Zhi, Liang Hu and Zhichao Fan

152 ***Examining the Underappreciated Role of S-Acylated Proteins as Critical Regulators of Phagocytosis and Phagosome Maturation in Macrophages***
Charneal L. Dixon, Katrina Mekhail and Gregory D. Fairn

163 ***Modular Organization of Engulfment Receptors and Proximal Signaling Networks: Avenues to Reprogram Phagocytosis***
Emily A. Britt, Vanessa Gitau, Amara Saha and Adam P. Williamson

169 ***Intravacuolar Pathogens Hijack Host Extracellular Vesicle Biogenesis to Secrete Virulence Factors***
Anna Gioseffi, Mariola J. Edelmann and Peter E. Kima

183 ***Cellular Responses to the Efferocytosis of Apoptotic Cells***
Charles Yin and Bryan Heit

195 ***Microbial Phagocytic Receptors and Their Potential Involvement in Cytokine Induction in Macrophages***
Yan Lin Fu and Rene E. Harrison

211 ***Rab10-Positive Tubular Structures Represent a Novel Endocytic Pathway That Diverges From Canonical Macropinocytosis in RAW264 Macrophages***
Katsuhisa Kawai, Arata Nishigaki, Seiji Moriya, Youhei Egami and Nobukazu Araki

225 ***Pro-Resolving Ligands Orchestrate Phagocytosis***
Christa Decker, Sudeshna Sadhu and Gabrielle Fredman

frontiers in Immunology

EDITORIAL
published: 24 September 2021
doi: 10.3389/fimmu.2021.772256

Editorial: Phagocytes in Immunity: Linking Material Internalization to Immune Responses and Therapeutic Strategies

Johnathan Canton[1]*, *Gregory D. Fairn*[2]* and *Valentin Jaumouillé*[3]*

[1] Comparative Biology and Experimental Medicine, University of Calgary, Calgary, AB, Canada, [2] Department of Biology, Dalhousie University, Halifax, NS, Canada, [3] Molecular Biology and Biochemistry, Simon Fraser University, Burnaby, BC, Canada

Keywords: macrophage, dendritic cell, neutrophil, phagocytosis, efferocytosis, macropinocytosis, immunotherapy, host-pathogen interactions

Editorial on the Research Topic

Phagocytes in Immunity: Linking Material Internalization to Immune Responses and Therapeutic Strategies

OPEN ACCESS

Edited and reviewed by:
Francesca Granucci,
University of Milano-Bicocca, Italy

***Correspondence:**
Johnathan Canton
Johnathan.Canton@ucalgary.ca
Gregory D. Fairn
gfairn@dal.ca
Valentin Jaumouillé
v_jaumouille@sfu.ca

Specialty section:
This article was submitted to Molecular Innate Immunity, a section of the journal Frontiers in Immunology

Received: *07 September 2021*
Accepted: *08 September 2021*
Published: *24 September 2021*

Citation:
Canton J, Fairn GD and Jaumouillé V (2021) Editorial: Phagocytes in Immunity: Linking Material Internalization to Immune Responses and Therapeutic Strategies. Front. Immunol. 12:772256. doi: 10.3389/fimmu.2021.772256

In this collection, a series of primary research articles and reviews cover the impressive functional diversity of phagocytes in the maintenance of organismal homeostasis and immunity. Phagocytes, including neutrophils, macrophages and dendritic cells, are endowed with the unique capacity to internalize large quantities of exogenous material. This can occur through the receptor-dependent uptake of particulate material by phagocytosis or through the uptake of fluid-phase material by macropinocytosis. In both cases, the internalized material is processed and information is extracted allowing phagocytes to discern homeostatic debris from any potential threats. A failure in phagocyte function results in a departure from homeostasis. The study of phagocytes serves as a venue for interrogating fundamental questions in the biology of molecules, cells and organisms. Here we highlight the contributions to this Research Topic:

Both phagocytosis and macropinocytosis are initiated by receptors. One commonly studied phagocytic receptor is the Fcγ receptor (FcγR), which binds to antibodies attached to phagocytic targets. A prerequisite for FcγR signaling involves their clustering in the plane of the plasma membrane. Clustering is achieved when large, multivalent targets, such as immune complexes, come into contact with the phagocyte. In this collection, Bailey et al. demonstrate that, below a critical threshold, FcγR clustering can in fact be inhibitory, adding another layer to our understanding of the regulation of phagocytic receptor function. In many instances, including in the case of FcγR-mediated phagocytosis, transmembrane proteins called integrins are intimately involved, and indeed required, for efficient phagocytosis. Sun et al. describe the activation of and mechanisms by which integrins contribute to phagocytosis and phagocyte function.

Phagocytes encounter a diverse array of targets. Indeed, targets may be completely immobile, or, as is the case for many pathogens, may be swimming away at high speed! Targets may be less than a micron across, or may be filamentous, extending many microns away from the phagocyte. Yet, phagocytes have evolved mechanisms for dealing with the vast diversity of targets they could encounter. Baranov et al. discuss in detail how particle size and shape affect phagocytosis.

One commonly encountered phagocytic target is homeostatic debris. Endowed with an array of receptors, phagocytes can bind to and internalize dead and damaged cells. Internalization is followed by digestion of the homeostatic debris into exportable components, such as amino acids, nucleotides and lipids which are transferred out of the phagosome by transmembrane transporters for recycling or export from the cell. This process is best exemplified by the clearance of dead and dying cells through a process known as efferocytosis. Yin and Heit provide a comprehensive review of efferocytosis and discuss its salient features including phagocyte metabolism during efferocytosis, antigen extraction from internalized cells and the coupling of efferocytosis to the resolution of inflammation. The clearance of spent cells is not restricted to professional phagocytes. Tissue-resident non-myeloid cells can harbor phagocyte receptors and play key roles in the maintenance of tissue homeostasis. Kwon and Freeman describe how retinal pigment epithelial (RPE) cells contribute to the optimal functioning of tissues in the eye. Finally, the scavenging activity of phagocytes is tunable. They remain responsive to external cues and can therefore regulate both phagocytic and macropinocytic activity in a context-dependent manner. Decker et al. describe how specialized pro-resolving mediators contribute to the resolution of inflammation by modulating the phagocytic and efferocytic activity of phagocytes.

Phagocytes can also contribute to immunity through the direct clearance of pathogens by phagocytosis. Interestingly, Kornstädt et al. show that during inflammation, mast cells serve as critical regulators of the phagocytic activity of neighboring phagocytes. Despite phagocyte specialization for rapid and contained killing, many pathogens have evolved means of either evading or indeed parasitizing phagocytes. Gioseffi et al. review how pathogens parasitize phagocyte membrane trafficking pathways to optimize their own survival.

Phagocytosis and macropinocytosis generate nascent vacuoles, which must mature into degradative organelles akin to endosomal maturation. The harsh environment within these compartments allows for the killing of microbial threats, the extraction of antigen for presentation to cells of the adaptive immune system, and the delivery of pathogen-associated molecular patterns (PAMPs) to intracellular pattern recognition receptors (PRRs). Critical for this maturation is the fusion of phagosomes/macropinosomes with lysosomes, which deliver hydrolases and promote lumen acidification. Nguyen and Yates discuss the current understanding of the molecular mechanisms of the fusion of phagosomes with lysosomes. Protein S-acylation is a post-translational modification that alters the function of many cellular proteins including those involved in phagocytosis and phagosome maturation. Dixon et al., discuss what is known and highlight many questions that remain to understand this modification during these processes. Additionally, Kawai et al. describe endocytic structures marked by Rab10 that occur in response to macropinocytic stimuli but are instead tubular in nature.

Altering and exploiting the adaptive immune response to combat tumors has been a popular area for many years. Chen et al. and Britt et al. discuss how manipulating the innate immune response and in particular harnessing macrophages and phagocytosis can be beneficial as a targeted cancer therapy. The direct clearance of malignant tumor cells by macrophages and presentation of cell-associated antigen by dendritic cells to T cells have both emerged as areas of intense study in cancer research. As we continue to learn about phagocytes, new avenues for understanding the basic biology of organisms and leveraging that information for future therapies will undoubtedly continue to emerge.

AUTHOR CONTRIBUTIONS

All authors listed have made a substantial, direct, and intellectual contribution to the work and approved it for publication.

ACKNOWLEDGMENTS

VJ acknowledges the support of the Natural Sciences and Engineering Research Council of Canada (NSERC RGPIN-2021-03727).

Conflict of Interest: The authors declare that the research was conducted in the absence of any commercial or financial relationships that could be construed as a potential conflict of interest.

Publisher's Note: All claims expressed in this article are solely those of the authors and do not necessarily represent those of their affiliated organizations, or those of the publisher, the editors and the reviewers. Any product that may be evaluated in this article, or claim that may be made by its manufacturer, is not guaranteed or endorsed by the publisher.

Copyright © 2021 Canton, Fairn and Jaumouillé. This is an open-access article distributed under the terms of the Creative Commons Attribution License (CC BY). The use, distribution or reproduction in other forums is permitted, provided the original author(s) and the copyright owner(s) are credited and that the original publication in this journal is cited, in accordance with accepted academic practice. No use, distribution or reproduction is permitted which does not comply with these terms.

frontiers in Immunology

REVIEW
published: 13 November 2020
doi: 10.3389/fimmu.2020.604205

Phagocytosis by the Retinal Pigment Epithelium: Recognition, Resolution, Recycling

Whijin Kwon[1] *and Spencer A. Freeman*[1,2]*

[1] Program in Cell Biology, Peter Gilgan Centre for Research and Learning, Hospital for Sick Children, Toronto, ON, Canada, [2] Department of Biochemistry, University of Toronto, Toronto, ON, Canada

Tissue-resident phagocytes are responsible for the routine binding, engulfment, and resolution of their meals. Such populations of cells express appropriate surface receptors that are tailored to recognize the phagocytic targets of their niche and initiate the actin polymerization that drives internalization. Tissue-resident phagocytes also harbor enzymes and transporters along the endocytic pathway that orchestrate the resolution of ingested macromolecules from the phagolysosome. Solutes fluxed from the endocytic pathway and into the cytosol can then be reutilized by the phagocyte or exported for their use by neighboring cells. Such a fundamental metabolic coupling between resident phagocytes and the tissue in which they reside is well-emphasized in the case of retinal pigment epithelial (RPE) cells; specialized phagocytes that are responsible for the turnover of photoreceptor outer segments (POS). Photoreceptors are prone to photo-oxidative damage and their long-term health depends enormously on the disposal of aged portions of the outer segment. The phagocytosis of the POS by the RPE is the sole means of this turnover and clearance. RPE are themselves mitotically quiescent and therefore must resolve the ingested material to prevent their toxic accumulation in the lysosome that otherwise leads to retinal disorders. Here we describe the sequence of events underlying the healthy turnover of photoreceptors by the RPE with an emphasis on the signaling that ensures the phagocytosis of the distal POS and on the transport of solutes from the phagosome that supersedes its resolution. While other systems may utilize different receptors and transporters, the biophysical and metabolic manifestations of such events are expected to apply to all tissue-resident phagocytes that perform regular phagocytic programs.

Keywords: cholesterol, integrins, actin cytoskeleton, MerTK, glucose transport, V-ATPase, resolvins, phosphatidylserine (PtdSer)

OPEN ACCESS

Edited by:
Gregory D. Fairn,
St. Michael's Hospital, Canada

Reviewed by:
Tobias Dallenga,
Research Center Borstel (LG), Germany
Raymond B. Birge,
The State University of New Jersey, United States

***Correspondence:**
Spencer A. Freeman
spencer.freeman@sickkids.ca

Specialty section:
This article was submitted to Molecular Innate Immunity, a section of the journal Frontiers in Immunology

Received: *08 September 2020*
Accepted: *20 October 2020*
Published: *13 November 2020*

Citation:
Kwon W and Freeman SA (2020) Phagocytosis by the Retinal Pigment Epithelium: Recognition, Resolution, Recycling. Front. Immunol. 11:604205. doi: 10.3389/fimmu.2020.604205

INTRODUCTION

Phagocytosis, the ingestion of large (>0.5 um) particles, is an evolutionarily conserved, actin-driven process with roles in nutrient acquisition, immunity, and tissue homeostasis (1–3). The ongoing, routine phagocytic programs that maintain tissue homeostasis in the absence of infection or injury are largely performed by tissue-resident phagocytes. These cells are non-migratory and are therefore

strategically positioned for phagocytic encounters. In some cases, resident phagocytes are uniformly distributed to optimally survey the whole tissue by probing the space between them (4, 5). In other cases, they are localized to particular regions that favor their collection and engulfment of phagocytic loads [e.g. splenic red pulp macrophages that turnover red blood cells (6) or bone marrow-resident macrophages that remove nuclei extruded during erythropoiesis (7, 8)]. In all cases, the efficient removal of dead cells, parts of cells, and debris by these phagocytes is essential to prevent secondary necrosis, inflammation, and autoimmunity (9, 10).

Within the category of tissue resident phagocytes are "specialized phagocytes"; epithelial derived stromal cells including the retinal pigment epithelium (RPE) of the eye and Sertoli cells of the testes (10, 11). As epithelia, these cells contribute to the formation of blood-tissue barriers while facilitating the directional transport of oxygen, glucose, cholesterol, etc. to the tissue from circulation. As specialized phagocytes, these cells also actively turnover theirs neighbors. Perhaps the best studied example of specialized phagocytes is indeed the RPE that intimately associates with photoreceptors and mediates their turnover (12). A single RPE cell is in contact with ~30 photoreceptor cells (rods and cones) and is responsible for the phagocytosis and removal of the distal portions of the photoreceptor outer segments (POS) that are phagocytosed in a diurnal fashion (13, 14) (**Figure 1**). The removed mass is not trivial; 7–10% is eliminated daily meaning the entire POS population is turned over every 2 weeks (15). Remarkably, a burst of phagocytosis is timed with the entry of light to the retina and, within hours, the phagosomes formed in each healthy RPE cell are resolved (14, 16).

Expectedly, the removal of the aged regions of the POS and of metabolic wastes by the RPE is essential for the homeostasis of the retina (17, 18). Just as critically, the ingested material by the RPE needs to be resolved otherwise it accumulates and forms lipofuscin (comprised of oxidized proteins and lipids), eventually leading to retinal disorders (19). Lipofuscin also accumulates in the eye with healthy aging (20, 21), so an understanding of when and how this causes disease is fundamental. RPE cells are themselves post-mitotic and therefore resolution of the vacuoles formed during phagocytosis is integral to RPE longevity. The resolution process can be envisaged as a sequence of steps that includes the maturation of the nascent phagosome, the digestion of luminal macromolecules, the efflux of solutes from the phagolysosomes, and the resorption of the phagosomal membrane. Interestingly, the building blocks from the ingested photoreceptor outer segments (POS) are thought to be shuttled back to the photoreceptor cells (22), supporting their continuous regeneration and completing a "heterocellular metabolic circuit." Importantly, in the RPE-photoreceptor relationship, it is appreciated that dysfunction in one cell type leads to degeneration in the other. Such metabolic coupling and the sequence of events that complete these circuits, while recognized in the case of the RPE and photoreceptors, are poorly understood for other tissue-resident phagocytes (23).

Here we describe the phagocytosis, breakdown, and resolution of ingested POS by RPE cells. We first illustrate phagocytosis by the RPE including the binding, ensheathment, and ingestion of the POS driven by the RPE actin cytoskeleton. We subsequently describe the maturation steps of the phagosome that confer on the vacuole its degradative capacity. The eventual efflux of solutes from the phagolysosome is discussed in some detail and we describe how these fluxes are expected to lead to the remodeling of the phagosomal membrane including its vesiculation and tubulation. Finally, we propose that the delivery of building blocks back to the tissue microenvironment supports the health of neighboring cells and we speculate on how such events may occur.

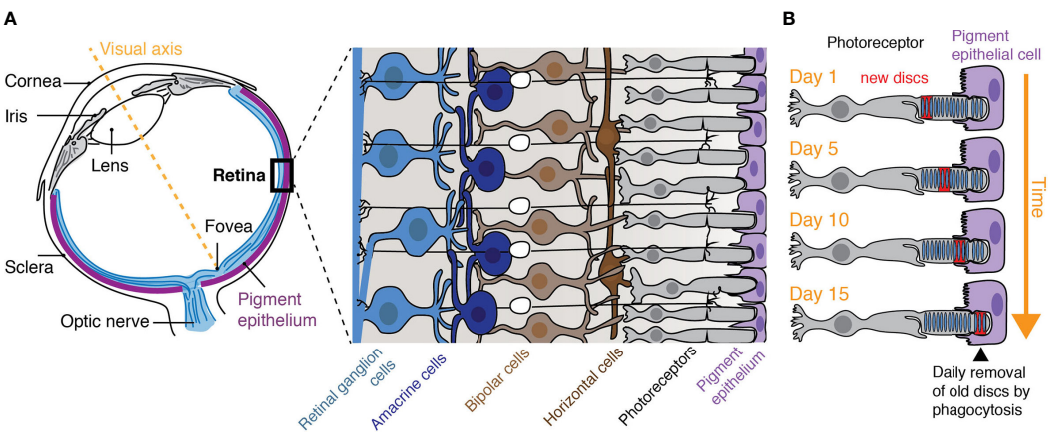

FIGURE 1 | The retinal pigment epithelium. **(A)** The retina lines the back of the eye and is comprised of five cell types: rod and cone photoreceptors, bipolar, horizontal, amacrine, and retinal ganglion cells. **(B)** The retinal pigment epithelium that underlies the retina is responsible for the turnover of photoreceptor outer segments (POS) by their phagocytosis and is critical for photoreceptor function. Photoreceptors are choc-a-bloc with membrane discs that harbor opsins which are susceptible to phototoxic damage. The most distal segments of the POS that contain the oldest discs are therefore removed from the live photoreceptors while new discs are made at the beginning of the outer segment. Note: as new discs are formed at the base of the POS, old discs are removed by phagocytosis, a process that takes approximately 2 weeks.

Photoreceptors and the Retinal Pigment Epithelium: Close Encounters

Light that enters the vertebrate eye is focused onto the neural retina, a thin tissue (~200 μm) comprised of five main classes of cells including photoreceptors, bipolar cells, amacrine cells, horizontal cells, and ganglion cells (**Figure 1**). These cells work concertedly to process and transmit visual information to the midbrain, thalamus, and visual cortex *via* the optic nerve (24). Despite their posterior positioning (e.g. at the back layer of the retina and the region farthest from incoming light), it is with the photoreceptor cells where light is captured and the visual pathway is initiated. The light is entirely absorbed in outer segments of the photoreceptor. The POS consists of membranous discs packed with integral membrane proteins called opsins. Opsins are made to be light-sensitive by their covalent association with the chromophore retinal (e.g. rhodopsin in the case of rods) (25) and are perhaps the best studied of the G-protein coupled receptors. Upon light exposure, rhodopsin undergoes immediate bleaching which triggers the visual transduction pathway. Over time, and with repetitive bleaching and regeneration of rhodopsin, phototoxic damage can occur in the neighboring proteins and lipids of the discs (26). To circumvent the accumulation of damaged components, photoreceptors undergo continuous turnover facilitated by the synthesis and assembly of new discs at the base of the outer segment and the simultaneous shedding of the oldest discs from the growing tips of the POS (**Figure 1**). This mechanism results in photoreceptors that are long-lived and discs of the POS that are short-lived (~2 weeks).

At the tip of the POS facing the RPE, is the marked accumulation of phosphatidylserine (PtdSer) exposed on the outer leaflet of the cell which becomes much more pronounced with light onset (16) (**Figure 2**). In virtually all other healthy cell types, the asymmetric distribution of PtdSer to the inner leaflet is tightly maintained by the ongoing activity of phospholipid translocases or "flippases" including ATP11A and ATP11C (27–30). Only under apoptotic conditions are these flippases cleaved and inactivated by caspases. The same caspases also cleave and activate scramblases, which can alternatively be activated by Ca^{2+}, that begin to randomly flip membrane phospholipids like PtdSer between the two leaflets (31–34). Given the tight control over the asymmetric distribution of PtdSer in most cells, the polarized and relatively sustained exposure of the phospholipid in the non-apoptotic photoreceptor is a unique phenomenon. It must require 1) the very local disruption of flippases/activation of scramblases and 2) a barrier to the free diffusion of exofacial PtdSer from the distal POS tip.

The latter may be achieved by secreted molecules that bridge and tether the PtdSer to RPE receptors. Plenty of bridging molecules may participate in trapping the exposed PtdSer including Gas6, Protein S, Tubby, and Tubby-like protein 1 which connect PtdSer to the RPE-expressed MerTK receptor (35–38) and MFG-E8 which does the same for αvβ5 integrins (39). Given that exposed PtdSer remains polarized to the distal tips of POS in *Mfge8*-/- and *Itgb5*-/- (β5 integrin) mice (16), there may be functional redundancy to this effect or the MerTK ligands may be the essential factors. Here, at least Gas6 and Protein S are provided to the interphotoreceptor matrix by their synthesis and release from the RPEs themselves (35, 37, 40). At least some of these bridging molecules were recently shown to be transcribed by the RPE in a circadian fashion (41). Fittingly, experiments challenging RPEs with POS *in vitro* are often performed by augmenting the culture with exogenous Gas6 and/or Protein S (42) suggesting their requirement and some mechanism(s) of regulation to their expression by light.

How the local inactivation or exclusion of flippases and activation of scramblases at the distal tip of the POS occurs and is regulated in a diurnal fashion, on the other hand, remains entirely unclear. Notably, scramblases of the anoctamin/TMEM16 family show a polarized localization in other cell types (43) and their activation causes membrane expansion and shedding (44). A role for local Ca^{2+} flux and caspase activation has also been suggested (27).

Photoreceptors and the Retinal Pigment Epithelium: Phagocytosis

The association between the POS of the photoreceptor and the RPEs is constant: The apical microvilli of the RPE probe and become elaborated to "ensheath" the outer segments as they accumulate PtdSer, long before their phagocytosis (**Figure 2**) (45–47). Such membrane projections from the RPE can reach nearly half-way up the POS (up to ~15 μm), yet little is known about the cytoskeleton and the associated membrane remodeling that supports these structures. It is unlikely to be mediated by the features shared between the RPE microvilli and those found in other epithelial cells like ezrin/radixin/moesin (ERM) proteins (45, 48) and ERM-binding proteins including NHERF1 (49), which tend to oppose broad ruffling events (50, 51). Other features of the RPE apical membrane including the Na^+/K^+-ATPase pump, while also unique, are unlikely to directly drive ensheathment.

Instead, it is known that the ensheathment of POS requires the engagement of apically targeted MerTK, a member of the Tyro/Axl/Mer family of receptor tyrosine kinases (52, 53). Once MerTK is engaged by Gas6 or Protein S, ligand binding induces its multimerization and trans-autophosphorylation by the kinase domain. This leads to the recruitment of a number of adaptors and effectors that facilitate pseudopod extension (**Figure 2**). For example, the phosphorylated tyrosines in the cytosolic aspect of the receptor serve as docking sites for Vav, a potent GEF for Rac GTPases (54). The ensheathment structures indeed resemble those of spontaneous ruffles that are observed in macrophages (55) or that can be stimulated by pathogens (56) in a manner dependent on the activation of Rac GTPases. MerTK also stimulates Rac activation by recruiting the p130Cas/CrkII/Dock180 GEF complex (57). Rac-GTP can then bind and activate the WASP-family verprolin-homologous protein (WAVE) regulatory complex (WRC), (58, 59) which functions as a nucleation promoting factor for Arp2/3-branching of the F-actin cytoskeleton. Though less appreciated in recent literature, F-actin branching has long been known to also be mediated by

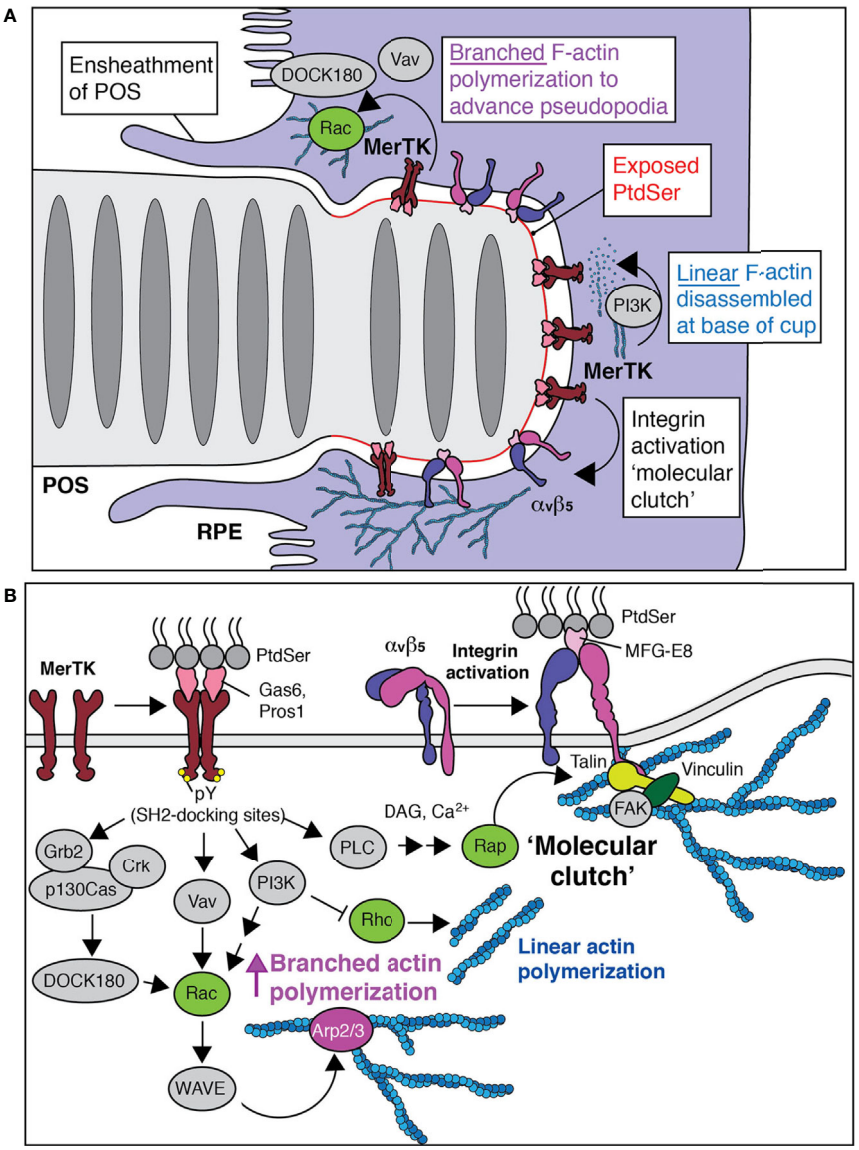

FIGURE 2 | Phagocytosis by the retinal pigment epithelium. **(A)** Like all types of phagocytosis, the engulfment of POS by the RPE is driven by actin polymerization. PtdSer is first exposed and tethered by bridging molecules that bind the distal portion of the POS and MerTK receptors. To relieve membrane tension, linear networks are removed by the activation of PI3K. Branched networks are stimulated by nucleation promoting factors that bring actin monomers to the Arp2/3 complex. Both activities are mediated by MerTK (see also panel **B**). **(B)** MerTK initiates a series of signaling pathways that stimulate branched actin polymerization, networks that attach to the membrane *via* integrins. The major RPE integrin is αvβ5, which also binds to PtdSer but *via* MFG-E8. As actin advances the pseudopodia tips of the RPE and facilitates severing of the POS, clearance of actin from the base of the cup allows for the delivery of new membrane, a PI3K-dependent process.

flexible dimers of filamins including filA (60). No matter how they are formed, heavily branched networks of F-actin are indeed associated with broad membrane ruffling events akin to those of ensheathing RPEs (61). That Rac activation is associated with ensheathment is supported by data demonstrating Rac is indeed essential for the phagocytosis of POS (62).

MerTK also recruits and activates PI3K which in turn phosphorylates PtdIns(4,5)P_2 to generate PtdIns(3,4,5)P_3 a phosphoinositide that can subsequently be converted to PtdIns (3,4)P_2 (63). PtdIns(3,4,5)P_3 and potentially PtdIns(3,4)P_2 support Rac activation by recruiting Rac GEFs and also dismantle linear actin networks by recruiting Rho specific GAPs (64) (**Figure 2**). The latter is critical for removing the submembrane highly bundled actin cables of the cortex that allows for the focal delivery of membrane from the endocytic pathway. Collectively, these actions relieve membrane tension that opposes membrane ruffling (65–68) and helps to explain why PI3 kinases are critical for the phagocytosis of large particles

but not small ones (69, 70). While the phagosomes formed by the RPE are only 1-2 μm in diameter, a single RPE needs to engulf ~30 targets at once—a number that can in fact be much higher in the center of the retina—while maintaining junctions with its neighbors. Given the amount of new membrane delivered and/or the unfurling of the microvillar membrane that would require substantive F-actin disassembly for ensheathment, it makes sense that PI3K activation is indeed a prerequisite for synchronized POS phagocytosis and that its inhibition leads to increased F-actin at aborted phagocytic cups (71). That Rho inactivation is central to the process is supported by experiments demonstrating decreased phagocytosis when Rho kinase is made to be constitutively active (72).

While branched networks of F-actin propel and advance broad regions of the plasma membrane, they must be stabilized and connected to adhered transmembrane proteins to prevent the retrograde flow and collapse of the entire effort (**Figure 2**). Such points of stability are described as "molecular clutches" that limit the slipping of the branched F-actin networks (73) and yield efficiency to phagocytosis in many contexts (74, 75). A molecular clutch in the RPE membrane could be facilitated by the binding of the RPE cadherins to the neural cell adhesion molecule (N-CAM) expressed in the POS (76). Interestingly, aged whole animal KO *Ncam*$^{-/-}$ mice have thinned photoreceptor cell layers and premature vision-loss (77). A specific role for N-CAM in the RPE has not been identified but is well-expressed in these cells. Another obvious molecular clutch for the ruffling RPEs is the major RPE integrin, αvβ5 which is targeted apically. A role for the integrin here would explain why ensheathment is not stimulated by peppering the RPEs with MFG-E8 alone (45) but that the efficient, diurnal removal of the portions of the POS indeed requires the integrin and its ligand (16, 78).

Crosstalk Between MerTK and αvβ5

The MerTK and αvβ5 pathways are not mutually exclusive (**Figure 2**) (57). Like other integrins, αvβ5 is thought to exist primarily in a "bent" or closed conformation with low affinity for ligand (79). Its inside-out activation is triggered by receptor tyrosine kinases like MerTK. Once MerTK is engaged, a number of SH2-containing proteins are then recruited to the phosphorylated tyrosine residues including the adaptors Vav, Crk, and Grb2 as well as the phospholipase C gamma (PLCγ) (80–82) (**Figure 2**). Importantly, these multi-molecular assemblies favor the recruitment and activation of Rap GTPases which in turn recruit the proteins necessary to disrupt the inactive conformation of the integrin including the Rap1-GTP-interacting adapter molecule (RIAM) and Talin (83) leading to its inside-out activation. Talin, once bound to the β5 subunit of the integrin heterodimer, provides binding sites for F-actin and F-actin-binding proteins like vinculin.

Such an effect is critical in the case of MerTK which itself does not bind F-actin directly or even, to our knowledge, indirectly. Since integrins provide the mechanical linkage between actin polymerization to the ruffling/ensheathing membrane to yield traction, it makes sense that their activation by primary phagocytic receptors is observed in many types of phagocytosis (84). In this regard, it is noteworthy that MerTK-mediated phagocytosis involves focal adhesion kinase (FAK) (85), regulation of FAK activity (62), and the cleavage of PtdIns(4,5)P_2 to generate Ins3P/diacylglycerol (DAG), which are normally associated with integrin and Rap activation respectively (86). Still, and as previously described, other ancillary transmembrane clutches are possible. Just as integrins can augment MerTK initiated phagocytosis, other receptors also participate including Tyro3 of the Tyro/Axl/Mer family of receptor tyrosine kinases (87) and the scavenger receptor CD36 (88). The relative contribution of Tyro3 and CD36 is still unclear and MerTK remains the canonical phagocytic receptor of the RPE; only the ablation of MerTK in the RPE leads to severe photoreceptor degeneration.

Sealing of the Nascent RPE Phagosome

The final steps of phagocytosis—sealing of the nascent phagosome by fusion of the pseudopodia tips—is the least understood step in all instances of engulfment and is especially poorly understood in the case of the RPE. This is remarkable since the RPE must apply a sufficient amount of local force on the POS to deform and generate scission through two lipid bilayers of an intact, live cell. The nascent phagosomes formed by RPE cells are indeed regular in their size (1–2 μm in diameter) as observed by electron (18) and light microscopy (89), as would be expected given the regular turnover of the POS, so the steps leading to scission must also be regulated. The site of eventual scission may be demarcated on the POS by the polarized distribution of PtdSer, which expands just before the scission event (16). However, the final, inward constricting force to complete phagocytosis remains enigmatic. In other systems, this has been attributed to the dynamin machinery employed in generic forms of endocytosis (90) and this could also be the case for the RPE. Alternatively, or in addition to dynamin, myosins may provide a "purse-string" constricting force as has been observed during the phagocytosis of targets by macrophages (91). Impressively, such a constricting force is sufficient to deform the skeleton of red cells (91) and to remove parts of live cells during 'trogocytosis" (92). Indeed, MerTK activation in the RPE leads to the marked recruitment of Myosin II-A and Myosin II-B to the phagocytic cup, and the pharmacological or genetic ablation of Myosin II partially prevents POS engulfment *in vitro* (93). However, like the majority of the systems used to investigate RPE phagocytosis, here the targets were delivered in a pre-severed state. Clearly, further studies are necessary to visualize these events and to determine the mechanism(s) involved.

Phagosome Maturation

Following its scission from the plasma membrane, the nascent RPE phagosome undergoes graded fusion with endosomes and then lysosomes in a complex process termed "maturation" (**Figure 3**). Maturation can be envisaged as a series of steps marked by changes in the signaling phosphoinositides found within the limiting membrane of the phagosome and changes in its association with Rab GTPases in particular (12, 94). Importantly, maturation results in the acquisition of the

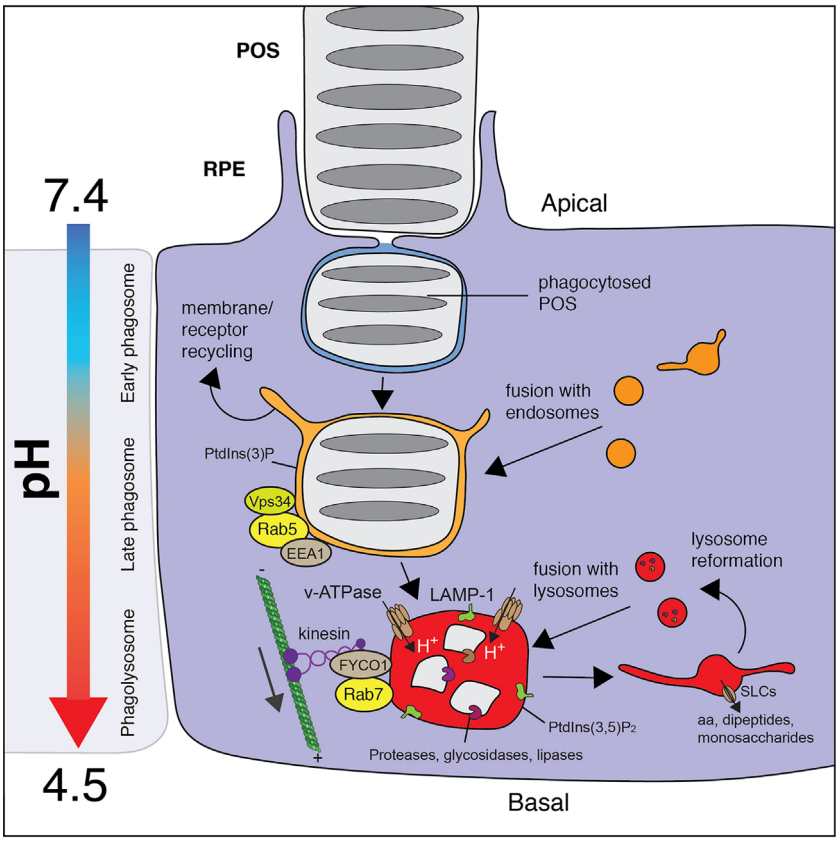

FIGURE 3 | Maturation of the RPE phagosome. Internalized POS particles are sealed in a nascent phagosome that undergoes step-wise maturation which involves the graded fusion of endosomes and then lysosomes. The maturation of the phagosome is delineated by its association with Rab GTPase and its phosphoinositide constituents, which act to coordinate fusion. Maturation also involves microtubule-based movement toward the cell center, a switch in Rabs [Rab5 → Rab7] and phosphoinositide [PI(3)P → PI(3,5)P_2] composition, a drop in pH [6.5 → 4.0], and the activation of phagosomal proteases. In the RPE, the movement of the phagosome is dependent on kinesins which traverse the cytosol towards the plus ends of the microtubules on the basal side of the cell. Once solutes are transported from the phagolysosome, the compartment undergoes fragmentation to reform and replenish the pool of lysosomes.

V-ATPase and the delivery of enzymes from lysosomes that grant the vacuole its degradative properties. Maturation also coincides with—and is highly dependent on—the motor-driven movement of the phagosomes toward the basolateral side of the epithelial cell where they collect in a juxtanuclear location (95, 96). While the movement of the POS-containing phagosome through the cytosol differs markedly from the phagosomes formed in myeloid cells, the maturation process otherwise shares many of its salient molecular features. In this section, we therefore describe maturation in general terms and highlight what is known in the RPE system.

The Rab family of GTPases that orchestrate membrane fusion events and organellar trafficking are indispensable for maturation (94). Following its sealing, Rabex-5, a guanine nucleotide exchange factor (GEF), is targeted to the early phagosome to recruit and activate Rab5, Rab21, and Rab22 (97). While these Rab5 subfamily members all play important roles in phagosome maturation (98), Rab5 remains the best characterized member (99). Once active, Rab5 binds to its effectors including Rabaptin-5 which in turn re-stimulates Rabex-5, triggering a positive-feedback loop (100). Additionally, Rab5 exerts its function through the recruitment and activation of the phosphatidylinositol 3-kinase (PI3K) Vps34, which results in the rapid production of phosphatidylinositol 3-phosphate (PI3P). PI3P is necessary for the recruitment of early endosomal antigen 1 (EEA1), a protein that is essential for phagosome maturation by promoting its fusion with endosomes (99).

Rab5 and EEA1 are indeed reported to localize to the early RPE phagosome along with PI3P (101). Moreover, the conditional knockout of Vps34 leads to disordered phagosome trafficking, impaired lysosome fusion, and retinal degeneration in mice, supporting a similar role for PI3P in the RPE system (102). As the RPE phagosome matures, marked by its incorporation of LAMP proteins, the localization of Rab5 and EEA1 are expectedly depressed (101). Though mechanisms remain to be elucidated, the LAMP family of lysosome-resident glycoproteins is indeed required for the fusion of lysosomes with the phagosome (103). It is therefore noteworthy, that the loss of

just one of these family members, LAMP2, in the murine RPE causes delayed POS degradation and the build-up of POS debris (104). In fact, the loss-of-function mutations in *LAMP2* that cause Danon disease in humans is also associated with retinal and macular degeneration (105).

In all cases, progression to the late phagosome is marked not just by the acquisition of LAMP proteins and its luminal acidification (described later), but also by the transition from being Rab5- to Rab7-positive, known as a Rab5-Rab7 "switch" (106). The sharp transition between Rab5 and Rab7 is explained by Rab7 GEFs that inhibit Rab5 activation. Specifically, Mon1, a subunit of the Rab7 GEF Mon1-Ccz1 that recruits and activates Rab7, also ousts Rabex-5 and arrests the Rab5 feedback loop (107). The Rab5-Rab7 transition promotes the subunit substitution necessary for the transformation of CORVET, a protein complex associated with early endosomal fusion, to HOPS, associated with later stage endosomal fusion (108).

In addition to facilitating fusion with late endosomes and lysosomes, Rab7 activation also coordinates the inward movement of the phagosome. In myeloid cells, the Rab7 effectors Rab7-interacting lysosomal protein (RILP) (109) and OSBP-related protein 1 (ORP1L) (110) form complexes that cluster dynein motors on the phagosome to cooperatively facilitate retrograde movement (111). The apical to basal movement of phagosomes in the RPE, while indeed dependent on Rab7 and microtubules (112, 113), differs markedly. First, the phagosomes formed by the RPE are initially engaged by Myosin VIIa, an unconventional myosin that moves along F-actin. Myosin VIIa is of particular interest since mutations in the MYO7A gene cause Usher syndrome 1B which involves progressive retinal degeneration (114). Fittingly, Myosin VIIa is largely expressed in the apical region of the RPE where it may facilitate the initial transport of the phagosome through a dense apical F-actin network until it can latch on to microtubule motors (96, 115). Second, the RPE phagosomes are then bound by kinesin motors and their associated kinesin-1 light chain 1 (KLC1), rather than dynein. The RPE phagosomes on the apical side of the cell lose their association with Myosin-VIIa as they begin to associate with KLC1, an event that coincides with their movement toward the basolateral side (95, 116). Mice lacking KLC1 show delayed phagosome progression to the basal region of the cell, the accumulation of debris and drusen, and ultimately the loss of photoreceptors (96, 116). In contrast to myeloid cells, a strong association with dynein motor complexes is in fact associated with delayed phagosome maturation and impaired phagosome motility in RPE (95). The obvious difference in phagosomal transport through the cytosol between cell types is attributed to the polarity of the microtubule tracks that are inversely oriented in the RPE (12): The plus ends of the microtubules are found at the basolateral side of the RPE. Rab7-GTP on the RPE phagosome must therefore mediate connections between the organelle and kinesins. Interestingly, active Rab7 binds FYCO1 and kinesin light chain/KIF5 (117). A role for this complex in orchestrating phagosome motility in the RPE is unknown, though FYCO1 is known to at least control the positioning of lysosomes in RPE cells (118).

The precise regulation of Rabs by their posttranslational modification is also essential for phagosome maturation, especially in the RPE. For example, the ablation of the Rab escort protein (*Rep1*), a geranylgeranyltransferase that acts on Rab7 and others, causes a delay in phagosome maturation and POS clearance, the accumulation of debris in the RPE, and a pathology resembling age-related macular degeneration (119, 120). Clearly, the efficient mobilization and maturation of the RPE phagosome is critical for retinal health and homeostasis and has some unique features that warrant further study.

Acidification of the Phagosome

As phagosomes form in the RPE every morning, their lumens acidify. The drop in pH is largely driven by the vacuolar ATPase (V-ATPase) that hydrolyzes ATP to pump protons into the lumen. Many of the digestive hydrolases, delivered to the phagosome by its fusion with endolysosomes, are then activated by the decrease in pH. That the acidification of the phagosome is indeed critical for the proper digestion of POS is exemplified by experiments demonstrating that inhibiting the V-ATPase in the RPE causes their accumulation of swollen phagolysosomes that do not degrade opsin proteins (121–123). This ultimately leads to the build-up of undigested debris between the Bruch's membrane of the choroid and the RPE, a phenotype akin to age-related macular degeneration (AMD) in humans (12).

Despite the imperative role for acidification of the phagosome *via* the V-ATPase, it is a process that remains remarkably enigmatic in the RPE system. This is partly explained from an operational standpoint. Reliable measurements of phagosomal pH entail the selection of a suitable probe and the ability to target it to the phagosome. In the case of retinal flat mounts, phagocytic targets (i.e. POS) cannot be readily and specifically labeled. Most pH determinations of the RPE phagosome, and even of their lysosomes, have therefore been estimated by qualitative or semiquantitative means using predominantly membrane-permeant weak bases that accumulate in acidic organelles (89, 124). These include fluorescent dyes like LysoTracker (89), that accumulates in the phagosome without altering its fluorescence or LysoSensor that undergoes a pH-dependent spectral shift (124). While such sensors are acceptable indicators of acidity, they come with limitations (125). For example, when used at sufficiently high concentrations, membrane-permeant basic probes can themselves alter the pH of the (phago)lysosome. Nevertheless, LysoSensor has been used to determine that lysosomes in RPE cells in culture are pH 4.5 on average (124).

More recently, a genetically encoded chimera of an intralumenal, pH-sensitive GFP tethered to a cytosolic mCherry *via* a lysosomal transmembrane domain has been utilized to measure the pH of RPE lysosomes (126). Such a system also has caveats. First, the pKa of GFP is ~6.0 which is not optimal for determinations of the more acidic pH values expected within lysosomes and phagolysosomes. Second, the proteases within the lysosome are expected to degrade the internal GFP thereby conflating measurements of the proteolytic activity and the pH of the compartments.

Generally, the pH of the POS-containing phagosome or the rate at which it acidifies has not been formally assessed but has been inferred by the degradation of its contents (123) or by LysoTracker (89). Other, non-ratiometric dyes like rhodamine-based pHrodo®, that exhibit strong fluorescence in acidic environments have also been used to grossly estimate the pH of RPE phagosomes (127, 128).

The rates and extent of acidification should not be tacitly assumed to occur in all phagocytes similarly. One consideration is that in isolation, the V-ATPase driven proton influx required for acidification is self-limiting as it creates a membrane potential detrimental to the efficient acidification of the phagolysosome. Such an undesirable electrogenic consequence is circumvented by accompanied counterion fluxes that dissipate the building voltage. This can be achieved by cation efflux (e.g. the expulsion of Na^+ or K^+) or concurrent anion influx (e.g. of Cl^-) (129) and these pathways may differ widely between cell types. Little is known about counterion flux mechanisms in any phagocyte, however, it is noteworthy that the whole animal loss of ClC7 or ClC3, chloride exchangers that can provide such counterion fluxes, results in retinal degeneration. While a direct role for ClCs in the RPE is not yet known, this phenotype could suggest that Cl- flux into the RPE phagosome may be critical for its acidification and breakdown of POS (130, 131).

Taken together, given that the rapid acidification supersedes enzymatic breakdown of the POS in the phagosome and is critical in maintaining retinal health, additional experiments should be done in this area. Clearly, a complete picture for the mechanisms that regulate the V-ATPase, pH, and maturation of the RPE phagosome has yet to emerge.

Distilling and Breaking Down Macromolecules

The delivery of the V-ATPase and acidification of the phagosome is concomitant with the enzymatic breakdown of its contents (**Figure 3**). Though published results vary, as much as 70% of the POS dry mass is heavily glycosylated opsin, and the remaining 30% is polyunsaturated lipids, and therefore the proper digestion in the phagosome requires the delivery and activation of proteases, glycosidases, and lipases (132). The removal of water from the phagosome is also thought to be an important early step that facilitates membrane recycling, decreases the volume required for the pump to acidify, and increases the contact between enzymes and their substrates (133). This early step is initiated by monovalent ion efflux followed by outward movement of osmotically-obliged water (5) that presumably exits through aquaporins or other pores and channels that make mammalian membranes water-permeant.

The proteases involved in breaking down opsins which account for >95% of the protein content of the shed POS (134) into peptides and amino acids are primarily cathepsins. Cathepsin D, a ubiquitously expressed aspartyl protease, has garnered particular attention as it is both highly-expressed in the RPE and its genetic inactivation in mice leads to incompletely digested rhodopsins in the phagosome, the general accumulation of undigested phagocytic debris, and photoreceptor death (135, 136). There are numerous cathepsins that function as cysteine proteases in the RPE, on the other hand, so while these have also been suggested to play a role in proteolytic degradation of the OS target, there is likely functional redundancy between them (12). Making matters more complex, in addition to their autoactivation, aspartyl proteases like cathepsin D can be cleaved and activated by these cysteine proteases in the RPE lysosome (137).

The major phospholipids of the POS are phosphatidylcholine and phosphatidylethanolamine which account for ~80% of the total lipid, followed by phosphatidylserine (13%), and minor contributors like phosphatidylinositol and sphingomyelin (138). As the photoreceptor discs age, their cholesterol content tends to decrease, going from 30% of the molar lipid when first generated by their invagination from the plasma membrane to 10% when shed as part of the distal POS (139). Ingested photoreceptor lipids, including phospholipids and glycolipids, are broken down in the RPE phagolysosome by pH-dependent lipid hydrolases, namely phospholipase A_1 and A_2 (140). Cholesterol, on the other hand, is liberated from the POS and possibly de-esterified *via* the lysosomal acid lipase type A (141) and once soluble, transported into the limiting membrane of the phagosome. This requires a system of cholesterol-binding proteins that support movement of the hydrophobic molecule through tunnel-like structures. It can be achieved by the concerted action of Niemann–Pick type C (NPC) 1 and 2 (142) as well as by LIMP-2 (143). Niemann-Pick proteins are indeed necessary for normal retinal function (144). Upon its incorporation into the phagolysosomal membrane, cholesterol transport to extra-lysosomal destinations occurs through vesicular and non-vesicular routes (i.e. membrane contact sites). By these means, cholesterol can be delivered to lysosomes and/or trafficked to the plasma membrane, the Golgi apparatus and the endoplasmic reticulum. Remarkably, as discussed later, the efflux of POS-derived cholesterol back to the photoreceptor by the RPE appears to be a means for its reutilization.

As opsins are replete with glycans, a series of glycosidases are also deployed by the RPE to the phagosome including alpha-mannosidase, beta-glucouronidase and alpha fucosidase (145). Human diseases involving a deficiency of these enzymes commonly have retinal phenotypes, including degeneration, photoreceptor death, vision loss, and undigested phagocytic debris, suggesting that these enzymes play an important role in POS catabolism (146, 147).

Finally, the POS is in fact embedded within an interphotoreceptor matrix (IPM) that has a unique molecular composition that differs from other extracellular matrices. The major insoluble components of the IPM are in fact glycosaminoglycans (i.e. hyaluronic acid and proteoglycans with heparan, chondroitin, and keratan sulfate chains) (148). While the soluble fraction of the IPM contains only small amounts of these, the RPE is expected to take up portions of the IPM along with the POS during phagocytosis and may even facilitate the turnover of the IPM over time. It follows that deficiencies in the enzymes responsible for the breakdown of the glycosaminoglycans (mucopolysaccharidoses) have some sort of retinal phenotype (149).

Solute Efflux and Resolution of the RPE Phagolysosome

Organic and inorganic solutes liberated or accumulated in the phagosome need to be effluxed from the vacuole in order for the compartment to "resolve" (**Figure 3**). Resolution is a normal part of the phagocytic process but remains the least understood aspect. In the case of the RPE, the return of the phagosomal membrane to replenish the pool of lysosomes is essential. Indeed, there are no observed circadian changes in the expression of prototypical lysosomal proteins in the RPE and so the pool of lysosomes used by the phagosomes must be returned to the cell (89).

In the final stages of resolution, the efflux of solutes is in fact proposed as the mechanism that drives the reformation of lysosomes (**Figure 4**). Here, tubulation and vesiculation requires extreme deformations to the limiting phagosomal membrane and is opposed by any tension on the vacuole (133). Tension comes in the form of osmotic pressure, generated because the solute concentrations of the phagosome can be higher than those of the cytosol. As solutes flux out of the phagosome, such pressure is relieved and the membrane becomes more pliable to these deformations by clathrin for example (150).

The exit pathways for solutes come in the form of solute carrier proteins (SLCs), and enormous family of transporters. While SLCs that flux amino acids and dipeptides out of the phagolysosome are the best appreciate in this regard (151–154), others that flux monosaccharides, metals, Na^+ (155), Ca^{2+} (156), etc. will all be critical to the resolution process. The control of the efflux pathways is only recently becoming appreciated. The mammalian target of rapamycin (mTOR) and its associated complexes form major regulatory hubs that can both inhibit and stimulate amino acid efflux by SLCs (151, 152, 157) and even inhibit Na^+ channels (155). We anticipate that the "phagosome-lysosome reformation" (PLR) will require exquisite control over its timing. For example, the organic solutes that contribute less osmotically to the compartment overall may be effluxed before more prevalent monovalent ions to ensure that the complete digestion and efflux of proteins and amino acids precedes the reformation of lysosomes. Of course, these ideas remain to be tested.

Recycling Between the RPE and Photoreceptors

The photoreceptor outer segment (POS) grows as it is consumed by the RPE, marking a coupling between a highly anabolic cell type and a catabolic one (**Figure 4**). Throughout this review, we have emphasized the astonishing amount of material that the RPE must turnover per day. As 90% of the membrane shed in the POS derives from the photosensitive membranes of the internal discs, the total surface membrane of a phagosome is ~30 μm^2 and the RPE consumes ~900 μm^2 of surface membrane on average daily. It is not surprising that membrane-associated elements can be recycled by the RPE back to the photoreceptor (18). In some cases, the recycling pathways between the RPE and photoreceptors are well-established, especially for the retinoid cycle (158). As described previously, the phototransduction by opsins occur when the bound 11-*cis*-retinal undergoes isomerization to all-*trans*-retinal which in turns alters the conformation of the opsin. The return to the photosensitive receptor conformation requires the rejuvenation of the 11-*cis*-retinal from all-*trans*-retinal. Aside from the reduction of the all-

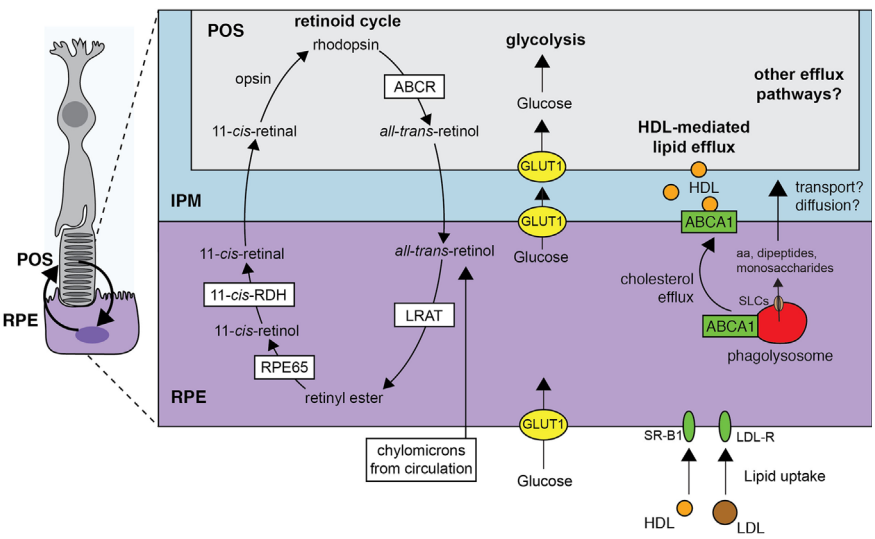

FIGURE 4 | Digestion and solute efflux in the mature RPE phagolysosome. The retinoid cycle necessitates the active participation of the RPE. Upon photoisomerization of 11-cis-retinal to *all-trans*-retinal, the chromophore activates opsins and phototransduction. The removal of *all-trans*-retinal can then occurs by active means or passive diffusion but importantly, is delivered to the RPE for its esterification (catalyzed by lecithin:retinol acyltransferase/LRAT). Isomerization to 11-*cis*-retinol and oxidation to 11-*cis*-retinal also occurs in the RPE before diffusion back to the POS. The coupling between the POS and the RPE does not stop there. Glucose is transported to the interphotoreceptor matrix from circulation by the RPE and could conceivably also come from the phagolysosome. Similarly, high density lipoprotein mediates lipid efflux from the RPE to be used by the photoreceptors. Lipids, including cholesterol, are either transported from circulation or recycled from the POS-containing phagosome. Finally, other building blocks like amino acids may be supplied to the IPM by means not yet determined.

trans-retinal to retinol, all reactions that support the retinoid cycle in fact take place in the RPE (159). The all-*trans*-retinol enters the RPE from circulation but a significant portion seems to be shuttled through the IPM (159) or by phagocytosis of the POS. The return of the 11-*cis*-retinal to the photoreceptor is in turn mediated by binding proteins, passive diffusion through the IPM, or direct transport.

The retinoid cycle represents just one of the recycling pathways between the cells. For example, the phospholipids of the photosensitive membrane discs of the POS are enriched in docosahexanoic acid (DHA), an omega-3 fatty acid. Remarkably, the retina can retain DHA even during long periods of dietary deprivation of omega-3 fatty acids (160). Careful experiments using radiolabeled DHA tracked the fatty acid through the POS and into the RPE and found that phagosomes are indeed packed with DHA to the same extent as the distal POS. Moreover, these types of experiments found that labelling in the RPE cytosol remains low and diffuse throughout extended (days long) periods of tracing, demonstrating that the DHA is quickly recycled back to the photoreceptors (22, 161).

While beyond the scope of this review, it should be mentioned that normal functions of RPE include maintaining an anti-inflammatory microenvironment and this is owed to the ongoing lipid metabolism of the phagosome. In particular, not all of the DHA is necessarily recycled back to the POS as is. The DHA supplied to the RPE can also be enzymatically converted to derive resolvins including neuroprotection D1 (NPD1) (162). NPD1 is a potent anti-inflammatory mediator that inhibits pro-apoptotic proteins and induces anti-apoptotic proteins, yielding cell-protective effects (162). On the other hand, the RPE can also contribute to pro-inflammatory pathways in certain contexts. Under sustained oxidative stress, for example, the RPE makes inflammatory cytokines including IL-6 and IL-1β and this can lead to AMD (163).

In addition to supplying the photoreceptor with retinal and DHA, the RPE sources the photoreceptors with glucose. To do so, the RPE expresses remarkably high levels of GLUT1 at their apical and basolateral surface (164). Glucose in the cytosol would normally be quickly converted for its use in glycolysis, but this is effectively suppressed in the RPE by the lactate that is produced and exported by the photoreceptor and because kinases that act on sugars are inhibited or expressed at sufficient low levels (164, 165). Conversely, such kinases (e.g. pyruvate kinase) are highly enriched in the photoreceptor making the cell highly glycolytic (164). When the RPE is made to consume more glucose, the neighboring photoreceptors become starved and ultimately degenerate. Using the same Glut1-based transport and others, we anticipate monosaccharides could be recycled from the RPE phagosome back to the IPM as well.

Finally, like other phagocytes, the RPE specialize in lipid/cholesterol efflux as emphasized by their robust expression and use of the cholesterol efflux regulatory protein ATP-binding cassette transporter A1 (ABCA1) (166). Here, ABCA1 shuttles cholesterol from the cytoplasm onto HDL. In the RPE, ABCA1 is targeted to both basolateral and apical membranes and can mediate efflux towards the subretinal space (i.e. the IPM) or, to a lesser extent, the choroidal space. Such efflux is more evident when the cells are given liver X receptor agonists or POS targets. Notably, the RPE is well-endowed with other cholesterol efflux proteins like SRB1 and ABCG1 (166). The RPE also metabolizes fatty acids found in the POS like palmitate to produce beta-hydroxybutyrate (167). Interestingly, photoreceptors were also recently found to use palmitate as an energy source through oxidative phosphorylation (168). The shuttling of palmitate or beta-hydroxybutyrate from the RPE to the photoreceptor as potential substates could therefore generally serve to maintain photoreceptor function (169).

It remains to be tested if other building blocks like sugars and amino acids are indeed recycled back to the photoreceptor once fluxed out of the RPE phagosome. Forms of direct transport, where photoreceptors and the RPE could be coupled by GAP junction proteins that support direct connections of the cytosol, are conceivable.

CONCLUSION

The routine phagocytosis performed by the RPE of their photoreceptor neighbors serves as a reasonable guide for future investigations of heterocellular metabolic circuits as formed by tissue-resident phagocytes and the cells they prune and turnover. Unlike in the retina, other tissues can quite readily expand and contract with abrupt dietary changes or with developmental programs like involution. In these cases, the growth of resident populations of phagocytes are kept in check by the stroma: Well-defined paracrine growth factor circuits between stromal cells and macrophages can stabilize the ratios of these populations and this requires intimate contacts between the cells (170). Supporting mitogenesis in such circuits with nutrient supplies may be an overlooked feature of the coupling. A recent emphasis on cell-cell competition in tissues (171) may benefit from understanding the circuits, cell-cell sharing and recycling, and the metabolic ecosystems that ensure tissue homeostasis. Such studies would immediately lend themselves to an appreciation for how tumor-associated macrophages support the growth of lesions. Additionally, more emphasis on phagosome resolution and the handling of solutes in the endocytic pathway of phagocytes is will certainly lead to strategies that break or support such processes and cycles. The RPE-photoreceptor coupling is a well-defined Yin and Yang relationship but represents one of many more circuits to be uncovered.

AUTHOR CONTRIBUTIONS

WK and SF constructed figures and wrote/reviewed the manuscript. All authors contributed to the article and approved the submitted version.

FUNDING

This work was supported by a CIHR Project Grant PJT #169180 (SAF).

REFERENCES

1. Freeman SA, Grinstein S. Phagocytosis: receptors, signal integration, and the cytoskeleton. *Immunol Rev* (2014) 262:193–215. doi: 10.1111/imr.12212
2. Underhill DM, Goodridge HS. Information processing during phagocytosis. *Nat Rev Immunol* (2012) 12:492–502. doi: 10.1038/nri3244
3. Aderem A, Underhill DM. Mechanisms of phagocytosis in macrophages. *Annu Rev Immunol* (1999) 17:593–623. doi: 10.1146/annurev.immunol.17.1.593
4. Uderhardt S, Martins AJ, Tsang JS, Lammermann T, Germain RN. Resident Macrophages Cloak Tissue Microlesions to Prevent Neutrophil-Driven Inflammatory Damage. *Cell* (2019) 177:541–555 e17. doi: 10.1016/j.cell.2019.02.028
5. Freeman SA, Uderhardt S, Saric A, Collins RF, Buckley CM, Mylvaganam S, et al. Lipid-gated monovalent ion fluxes regulate endocytic traffic and support immune surveillance. *Science* (2020) 367:301–5. doi: 10.1126/science.aaw9544
6. Kohyama M, Ise W, Edelson BT, Wilker PR, Hildner K, Mejia C, et al. Role for Spi-C in the development of red pulp macrophages and splenic iron homeostasis. *Nature* (2009) 457:318–21. doi: 10.1038/nature07472
7. Klei TR, Meinderts SM, van den Berg TK, van Bruggen R. From the Cradle to the Grave: The Role of Macrophages in Erythropoiesis and Erythrophagocytosis. *Front Immunol* (2017) 8:73. doi: 10.3389/fimmu.2017.00073
8. de Back DZ, Kostova EB, van Kraaij M, van den Berg TK, van Bruggen R. Of macrophages and red blood cells; a complex love story. *Front Physiol* (2014) 5:9. doi: 10.3389/fphys.2014.00009
9. Mahajan A, Herrmann M, Munoz LE. Clearance Deficiency and Cell Death Pathways: A Model for the Pathogenesis of SLE. *Front Immunol* (2016) 7:35. doi: 10.3389/fimmu.2016.00035
10. Arandjelovic S, Ravichandran KS. Phagocytosis of apoptotic cells in homeostasis. *Nat Immunol* (2015) 16:907–17. doi: 10.1038/ni.3253
11. Penberthy KK, Lysiak JJ, Ravichandran KS. Rethinking Phagocytes: Clues from the Retina and Testes. *Trends Cell Biol* (2018) 28:317–27. doi: 10.1016/j.tcb.2018.01.004
12. Lakkaraju A, Umapathy A, Tan LX, Daniele L, Philp NJ, Boesze-Battaglia K, et al. The cell biology of the retinal pigment epithelium. *Prog Retin Eye Res* (2020), 100846. doi: 10.1016/j.preteyeres.2020.100846
13. Young RW, Bok D. Participation of the retinal pigment epithelium in the rod outer segment renewal process. *J Cell Biol* (1969) 42:392–403. doi: 10.1083/jcb.42.2.392
14. LaVail MM. Rod outer segment disk shedding in rat retina: relationship to cyclic lighting. *Science* (1976) 194:1071–4. doi: 10.1126/science.982063
15. Kevany BM, Palczewski K. Phagocytosis of retinal rod and cone photoreceptors. *Physiol (Bethesda)* (2010) 25:8–15. doi: 10.1152/physiol.00038.2009
16. Ruggiero L, Connor MP, Chen J, Langen R, Finnemann SC. Diurnal, localized exposure of phosphatidylserine by rod outer segment tips in wild-type but not Itgb5-/- or Mfge8-/- mouse retina. *Proc Natl Acad Sci U.S.A.* (2012) 109:8145–8. doi: 10.1073/pnas.1121101109
17. Bok D, Hall MO. The role of the pigment epithelium in the etiology of inherited retinal dystrophy in the rat. *J Cell Biol* (1971) 49:664–82. doi: 10.1083/jcb.49.3.664
18. Strauss O. The retinal pigment epithelium in visual function. *Physiol Rev* (2005) 85:845–81. doi: 10.1152/physrev.00021.2004
19. Caceres PS, Rodriguez-Boulan E. Retinal pigment epithelium polarity in health and blinding diseases. *Curr Opin Cell Biol* (2020) 62:37–45. doi: 10.1016/j.ceb.2019.08.001
20. Delori FC, Dorey CK, Staurenghi G, Arend O, Goger DG, Weiter JJ. In vivo fluorescence of the ocular fundus exhibits retinal pigment epithelium lipofuscin characteristics. *Invest Ophthalmol Vis Sci* (1995) 36:718–29.
21. Feeney-Burns L, Hilderbrand ES, Eldridge S. Aging human RPE: morphometric analysis of macular, equatorial, and peripheral cells. *Invest Ophthalmol Vis Sci* (1984) 25:195–200.
22. Bazan NG, Gordon WC, Rodriguez de Turco EB. Docosahexaenoic acid uptake and metabolism in photoreceptors: retinal conservation by an efficient retinal pigment epithelial cell-mediated recycling process. *Adv Exp Med Biol* (1992) 318:295–306. doi: 10.1007/978-1-4615-3426-6_26
23. Han CZ, Ravichandran KS. Metabolic connections during apoptotic cell engulfment. *Cell* (2011) 147:1442–5. doi: 10.1016/j.cell.2011.12.006
24. Masland RH. The neuronal organization of the retina. *Neuron* (2012) 76:266–80. doi: 10.1016/j.neuron.2012.10.002
25. Terakita A. The opsins. *Genome Biol* (2005) 6:213. doi: 10.1186/gb-2005-6-3-213
26. Organisciak DT, Vaughan DK. Retinal light damage: mechanisms and protection. *Prog Retin Eye Res* (2010) 29:113–34. doi: 10.1016/j.preteyeres.2009.11.004
27. Lemke G. How macrophages deal with death. *Nat Rev Immunol* (2019) 19:539–49. doi: 10.1038/s41577-019-0167-y
28. Nagata S, Suzuki J, Segawa K, Fujii T. Exposure of phosphatidylserine on the cell surface. *Cell Death Differ* (2016) 23:952–61. doi: 10.1038/cdd.2016.7
29. Segawa K, Kurata S, Nagata S. Human Type IV P-type ATPases That Work as Plasma Membrane Phospholipid Flippases and Their Regulation by Caspase and Calcium. *J Biol Chem* (2016) 291:762–72. doi: 10.1074/jbc.M115.690727
30. Segawa K, Kurata S, Yanagihashi Y, Brummelkamp TR, Matsuda F, Nagata S. Caspase-mediated cleavage of phospholipid flippase for apoptotic phosphatidylserine exposure. *Science* (2014) 344:1164–8. doi: 10.1126/science.1252809
31. Suzuki J, Imanishi E, Nagata S. Xkr8 phospholipid scrambling complex in apoptotic phosphatidylserine exposure. *Proc Natl Acad Sci U.S.A.* (2016) 113:9509–14. doi: 10.1073/pnas.1610403113
32. Suzuki J, Fujii T, Imao T, Ishihara K, Kuba H, Nagata S. Calcium-dependent phospholipid scramblase activity of TMEM16 protein family members. *J Biol Chem* (2013) 288:13305–16. doi: 10.1074/jbc.M113.457937
33. Suzuki J, Denning DP, Imanishi E, Horvitz HR, Nagata S. Xk-related protein 8 and CED-8 promote phosphatidylserine exposure in apoptotic cells. *Science* (2013) 341:403–6. doi: 10.1126/science.1236758
34. Suzuki J, Umeda M, Sims PJ, Nagata S. Calcium-dependent phospholipid scrambling by TMEM16F. *Nature* (2010) 468:834–8. doi: 10.1038/nature09583
35. Burstyn-Cohen T, Lew ED, Traves PG, Burrola PG, Hash JC, Lemke G. Genetic Dissection of TAM Receptor-Ligand Interaction in Retinal Pigment Epithelial Cell Phagocytosis. *Neuron* (2012) 76:1123–32. doi: 10.1016/j.neuron.2012.10.015
36. Prasad D, Rothlin CV, Burrola P, Burstyn-Cohen T, Lu QX, de Frutos PG, et al. TAM receptor function in the retinal pigment epithelium. *Mol Cell Neurosci* (2006) 33:96–108. doi: 10.1016/j.mcn.2006.06.011
37. Hall MO, Obin MS, Heeb M, Burgess BL, Abrams TA. Both protein S and Gas6 stimulate outer segment phagocytosis by cultured rat retinal pigment epithelial cells. *Exp Eye Res* (2005) 81:581–91. doi: 10.1016/j.exer.2005.03.017
38. Caberoy NB, Zhou Y, Li W. Tubby and tubby-like protein 1 are new MerTK ligands for phagocytosis. *EMBO J* (2010) 29:3898–910. doi: 10.1038/emboj.2010.265
39. Hanayama R, Tanaka M, Miwa K, Shinohara A, Iwamatsu A, Nagata S. Identification of a factor that links apoptotic cells to phagocytes. *Nature* (2002) 417:182–7. doi: 10.1038/417182a
40. Karl MO, Kroeger W, Wimmers S, Milenkovic VM, Valtink M, Engelmann K, et al. Endogenous Gas6 and Ca2+ -channel activation modulate phagocytosis by retinal pigment epithelium. *Cell Signal* (2008) 20:1159–68. doi: 10.1016/j.cellsig.2008.02.005
41. Milicevic N, Mazzaro N, de Bruin I, Wils E, Ten Brink J, Asbroek AT, et al. Rev-Erbalpha and Photoreceptor Outer Segments modulate the Circadian Clock in Retinal Pigment Epithelial Cells. *Sci Rep* (2019) 9:11790. doi: 10.1038/s41598-019-48203-3
42. Law AL, Parinot C, Chatagnon J, Gravez B, Sahel JA, Bhattacharya SS, et al. Cleavage of Mer tyrosine kinase (MerTK) from the cell surface contributes to the regulation of retinal phagocytosis. *J Biol Chem* (2015) 290:4941–52. doi: 10.1074/jbc.M114.628297
43. Stohr H, Heisig JB, Benz PM, Schoberl S, Milenkovic VM, Strauss O, et al. TMEM16B, a novel protein with calcium-dependent chloride channel activity, associates with a presynaptic protein complex in photoreceptor terminals. *J Neurosci* (2009) 29:6809–18. doi: 10.1523/JNEUROSCI.5546-08.2009
44. Bricogne C, Fine M, Pereira PM, Sung J, Tijani M, Wang Y, et al. TMEM16F activation by Ca(2+) triggers plasma membrane expansion and directs PD-1 trafficking. *Sci Rep* (2019) 9:619. doi: 10.1038/s41598-019-43808-0
45. Almedawar S, Vafia K, Schreiter S, Neumann K, Khattak S, Kurth T, et al. MERTK-Dependent Ensheathment of Photoreceptor Outer Segments by

Human Pluripotent Stem Cell-Derived Retinal Pigment Epithelium. *Stem Cell Rep* (2020) 14:374–89. doi: 10.1016/j.stemcr.2020.02.004
46. Matsumoto B, Defoe DM, Besharse JC. Membrane turnover in rod photoreceptors: ensheathment and phagocytosis of outer segment distal tips by pseudopodia of the retinal pigment epithelium. *Proc R Soc Lond B Biol Sci* (1987) 230:339–54. doi: 10.1098/rspb.1987.0023
47. Steinberg RH, Wood I, Hogan MJ. Pigment epithelial ensheathment and phagocytosis of extrafoveal cones in human retina. *Philos Trans R Soc Lond B Biol Sci* (1977) 277:459–74. doi: 10.1098/rstb.1977.0028
48. Nandrot EF, Anand M, Sircar M, Finnemann SC. Novel role for alphavbeta5-integrin in retinal adhesion and its diurnal peak. *Am J Physiol Cell Physiol* (2006) 290:C1256–62. doi: 10.1152/ajpcell.00480.2005
49. Nawrot M, West K, Huang J, Possin DE, Bretscher A, Crabb JW, et al. Cellular retinaldehyde-binding protein interacts with ERM-binding phosphoprotein 50 in retinal pigment epithelium. *Invest Ophthalmol Vis Sci* (2004) 45:393–401. doi: 10.1167/iovs.03-0989
50. Nijhara R, van Hennik PB, Gignac ML, Kruhlak MJ, Hordijk PL, Delon J, et al. Rac1 mediates collapse of microvilli on chemokine-activated T lymphocytes. *J Immunol* (2004) 173:4985–93. doi: 10.4049/jimmunol.173.8.4985
51. Takahashi Y, Morales FC, Kreimann EL, Georgescu MM. PTEN tumor suppressor associates with NHERF proteins to attenuate PDGF receptor signaling. *EMBO J* (2006) 25:910–20. doi: 10.1038/sj.emboj.7600979
52. Rothlin CV, Carrera-Silva EA, Bosurgi L, Ghosh S. TAM receptor signaling in immune homeostasis. *Annu Rev Immunol* (2015) 33:355–91. doi: 10.1146/annurev-immunol-032414-112103
53. D'Cruz PM, Yasumura D, Weir J, Matthes MT, Abderrahim H, LaVail MM, et al. Mutation of the receptor tyrosine kinase gene Mertk in the retinal dystrophic RCS rat. *Hum Mol Genet* (2000) 9:645–51. doi: 10.1093/hmg/9.4.645
54. Patel JC, Hall A, Caron E. Vav regulates activation of Rac but not Cdc42 during FcgammaR-mediated phagocytosis. *Mol Biol Cell* (2002) 13:1215–26. doi: 10.1091/mbc.02-01-0002
55. Swanson JA. Shaping cups into phagosomes and macropinosomes. *Nat Rev Mol Cell Biol* (2008) 9:639–49. doi: 10.1038/nrm2447
56. Francis CL, Ryan TA, Jones BD, Smith SJ, Falkow S. Ruffles induced by Salmonella and other stimuli direct macropinocytosis of bacteria. *Nature* (1993) 364:639–42. doi: 10.1038/364639a0
57. Wu Y, Singh S, Georgescu MM, Birge RB. A role for Mer tyrosine kinase in alphavbeta5 integrin-mediated phagocytosis of apoptotic cells. *J Cell Sci* (2005) 118:539–53. doi: 10.1242/jcs.01632
58. Eden S, Rohatgi R, Podtelejnikov AV, Mann M, Kirschner MW. Mechanism of regulation of WAVE1-induced actin nucleation by Rac1 and Nck. *Nature* (2002) 418:790–3. doi: 10.1038/nature00859
59. Chen Z, Borek D, Padrick SB, Gomez TS, Metlagel Z, Ismail AM, et al. Structure and control of the actin regulatory WAVE complex. *Nature* (2010) 468:533–8. doi: 10.1038/nature09623
60. Nakamura F, Osborn TM, Hartemink CA, Hartwig JH, Stossel TP. Structural basis of filamin A functions. *J Cell Biol* (2007) 179:1011–25. doi: 10.1083/jcb.200707073
61. Svitkina TM, Borisy GG. Arp2/3 complex and actin depolymerizing factor/cofilin in dendritic organization and treadmilling of actin filament array in lamellipodia. *J Cell Biol* (1999) 145:1009–26. doi: 10.1083/jcb.145.5.1009
62. Mao Y, Finnemann SC. Essential diurnal Rac1 activation during retinal phagocytosis requires alphavbeta5 integrin but not tyrosine kinases focal adhesion kinase or Mer tyrosine kinase. *Mol Biol Cell* (2012) 23:1104–14. doi: 10.1091/mbc.e11-10-0840
63. Balla T. Phosphoinositides: tiny lipids with giant impact on cell regulation. *Physiol Rev* (2013) 93:1019–137. doi: 10.1152/physrev.00028.2012
64. Canton J, Schlam D, Breuer C, Gutschow M, Glogauer M, Grinstein S. Calcium-sensing receptors signal constitutive macropinocytosis and facilitate the uptake of NOD2 ligands in macrophages. *Nat Commun* (2016) 7:11284. doi: 10.1038/ncomms11284
65. Scott CC, Dobson W, Botelho RJ, Coady-Osberg N, Chavrier P, Knecht DA, et al. Phosphatidylinositol-4,5-bisphosphate hydrolysis directs actin remodeling during phagocytosis. *J Cell Biol* (2005) 169:139–49. doi: 10.1083/jcb.200412162
66. Bajno L, Peng XR, Schreiber AD, Moore HP, Trimble WS, Grinstein S. Focal exocytosis of VAMP3-containing vesicles at sites of phagosome formation. *J Cell Biol* (2000) 149:697–706. doi: 10.1083/jcb.149.3.697
67. Gauthier NC, Rossier OM, Mathur A, Hone JC, Sheetz MP. Plasma membrane area increases with spread area by exocytosis of a GPI-anchored protein compartment. *Mol Biol Cell* (2009) 20:3261–72. doi: 10.1091/mbc.e09-01-0071
68. Gauthier NC, Masters TA, Sheetz MP. Mechanical feedback between membrane tension and dynamics. *Trends Cell Biol* (2012) 22:527–35. doi: 10.1016/j.tcb.2012.07.005
69. Araki N, Johnson MT, Swanson JA. A role for phosphoinositide 3-kinase in the completion of macropinocytosis and phagocytosis by macrophages. *J Cell Biol* (1996) 135:1249–60. doi: 10.1083/jcb.135.5.1249
70. Cox D, Tseng CC, Bjekic G, Greenberg S. A requirement for phosphatidylinositol 3-kinase in pseudopod extension. *J Biol Chem* (1999) 274:1240–7. doi: 10.1074/jbc.274.3.1240
71. Bulloj A, Duan W, Finnemann SC. PI 3-kinase independent role for AKT in F-actin regulation during outer segment phagocytosis by RPE cells. *Exp Eye Res* (2013) 113:9–18. doi: 10.1016/j.exer.2013.05.002
72. Muller C, Charniga C, Temple S, Finnemann SC. Quantified F-Actin Morphology Is Predictive of Phagocytic Capacity of Stem Cell-Derived Retinal Pigment Epithelium. *Stem Cell Rep* (2018) 10:1075–87. doi: 10.1016/j.stemcr.2018.01.017
73. Case LB, Waterman CM. Integration of actin dynamics and cell adhesion by a three-dimensional, mechanosensitive molecular clutch. *Nat Cell Biol* (2015) 17:955–63. doi: 10.1038/ncb3191
74. Jaumouille V, Cartagena-Rivera AX, Waterman CM. Coupling of beta2 integrins to actin by a mechanosensitive molecular clutch drives complement receptor-mediated phagocytosis. *Nat Cell Biol* (2019) 21:1357–69. doi: 10.1038/s41556-019-0414-2
75. Freeman SA, Goyette J, Furuya W, Woods EC, Bertozzi CR, Bergmeier W, et al. Integrins Form an Expanding Diffusional Barrier that Coordinates Phagocytosis. *Cell* (2016) 164:128–40. doi: 10.1016/j.cell.2015.11.048
76. Marmorstein AD, Gan YC, Bonilha VL, Finnemann SC, Csaky KG, Rodriguez-Boulan E. Apical polarity of N-CAM and EMMPRIN in retinal pigment epithelium resulting from suppression of basolateral signal recognition. *J Cell Biol* (1998) 142:697–710. doi: 10.1083/jcb.142.3.697
77. Luke MP, LeVatte TL, O'Reilly AM, Smith BJ, Tremblay F, Brown RE, et al. Effect of NCAM on aged-related deterioration in vision. *Neurobiol Aging* (2016) 41:93–106. doi: 10.1016/j.neurobiolaging.2016.02.003
78. Nandrot EF, Anand M, Almeida D, Atabai K, Sheppard D, Finnemann SC. Essential role for MFG-E8 as ligand for alphavbeta5 integrin in diurnal retinal phagocytosis. *Proc Natl Acad Sci U.S.A.* (2007) 104:12005–10. doi: 10.1073/pnas.0704756104
79. Springer TA, Dustin ML. Integrin inside-out signaling and the immunological synapse. *Curr Opin Cell Biol* (2012) 24:107–15. doi: 10.1016/j.ceb.2011.10.004
80. Shelby SJ, Colwill K, Dhe-Paganon S, Pawson T, Thompson DA. MERTK Interactions with SH2-Domain Proteins in the Retinal Pigment Epithelium. *PloS One* (2013) 8. doi: 10.1371/journal.pone.0053964
81. Mahajan NP, Earp HS. An SH2 domain-dependent, phosphotyrosine-independent interaction between Vav1 and the Mer receptor tyrosine kinase: a mechanism for localizing guanine nucleotide-exchange factor action. *J Biol Chem* (2003) 278:42596–603. doi: 10.1074/jbc.M305817200
82. Linger RM, Keating AK, Earp HS, Graham DK. TAM receptor tyrosine kinases: biologic functions, signaling, and potential therapeutic targeting in human cancer. *Adv Cancer Res* (2008) 100:35–83. doi: 10.1016/S0065-230X(08)00002-X
83. Lee HS, Lim CJ, Puzon-McLaughlin W, Shattil SJ, Ginsberg MH. RIAM activates integrins by linking talin to ras GTPase membrane-targeting sequences. *J Biol Chem* (2009) 284:5119–27. doi: 10.1074/jbc.M807117200
84. Torres-Gomez A, Cabanas C, Lafuente EM. Phagocytic Integrins: Activation and Signaling. *Front Immunol* (2020) 11:738. doi: 10.3389/fimmu.2020.00738
85. Finnemann SC. Focal adhesion kinase signaling promotes phagocytosis of integrin-bound photoreceptors. *EMBO J* (2003) 22:4143–54. doi: 10.1093/emboj/cdg416

86. Heth CA, Marescalchi PA, Ye L. IP3 generation increases rod outer segment phagocytosis by cultured Royal College of Surgeons retinal pigment epithelium. *Invest Ophthalmol Vis Sci* (1995) 36:984–9.
87. Vollrath D, Yasumura D, Benchorin G, Matthes MT, Feng W, Nguyen NM, et al. Tyro3 Modulates Mertk-Associated Retinal Degeneration. *PloS Genet* (2015) 11:e1005723. doi: 10.1371/journal.pgen.1005723
88. Ryeom SW, Silverstein RL. CD36 participates in the phagocytosis of rod outer segments by retinal pigment epithelium. *J Cell Sci* (1996) 109(Pt 2):387–95.
89. Mao Y, Finnemann SC. Live Imaging of LysoTracker-Labelled Phagolysosomes Tracks Diurnal Phagocytosis of Photoreceptor Outer Segment Fragments in Rat RPE Tissue Ex Vivo. *Adv Exp Med Biol* (2016) 854:717–23. doi: 10.1007/978-3-319-17121-0_95
90. Gold ES, Underhill DM, Morrissette NS, Guo J, McNiven MA, Aderem A. Dynamin 2 is required for phagocytosis in macrophages. *J Exp Med* (1999) 190:1849–56. doi: 10.1084/jem.190.12.1849
91. Swanson JA, Johnson MT, Beningo K, Post P, Mooseker M, Araki N. A contractile activity that closes phagosomes in macrophages. *J Cell Sci* (1999) 112(Pt 3):307–16.
92. Matlung HL, Babes L, Zhao XW, van Houdt M, Treffers LW, van Rees DJ, et al. Neutrophils Kill Antibody-Opsonized Cancer Cells by Trogoptosis. *Cell Rep* (2018) 23:3946–3959 e6. doi: 10.1016/j.celrep.2018.05.082
93. Strick DJ, Feng W, Vollrath D. Mertk Drives Myosin II Redistribution during Retinal Pigment Epithelial Phagocytosis. *Invest Ophth Vis Sci* (2009) 50:2427–35. doi: 10.1167/iovs.08-3058
94. Flannagan RS, Jaumouille V, Grinstein S. The cell biology of phagocytosis. *Annu Rev Pathol* (2012) 7:61–98. doi: 10.1146/annurev-pathol-011811-132445
95. Esteve-Rudd J, Hazim RA, Diemer T, Paniagua AE, Volland S, Umapathy A, et al. Defective phagosome motility and degradation in cell nonautonomous RPE pathogenesis of a dominant macular degeneration. *Proc Natl Acad Sci U.S.A.* (2018) 115:5468–73. doi: 10.1073/pnas.1709211115
96. Gibbs D, Kitamoto J, Williams DS. Abnormal phagocytosis by retinal pigmented epithelium that lacks myosin VIIa, the Usher syndrome 1B protein. *Proc Natl Acad Sci U.S.A.* (2003) 100:6481–6. doi: 10.1073/pnas.1130432100
97. Delprato A, Merithew E, Lambright DG. Structure, exchange determinants, and family-wide rab specificity of the tandem helical bundle and Vps9 domains of Rabex-5. *Cell* (2004) 118:607–17. doi: 10.1016/j.cell.2004.08.009
98. Khurana T, Brzostowski JA, Kimmel AR. A Rab21/LIM-only/CH-LIM complex regulates phagocytosis via both activating and inhibitory mechanisms. *EMBO J* (2005) 24:2254–64. doi: 10.1038/sj.emboj.7600716
99. Fratti RA, Backer JM, Gruenberg J, Corvera S, Deretic V. Role of phosphatidylinositol 3-kinase and Rab5 effectors in phagosomal biogenesis and mycobacterial phagosome maturation arrest. *J Cell Biol* (2001) 154:631–44. doi: 10.1083/jcb.200106049
100. Lippe R, Miaczynska M, Rybin V, Runge A, Zerial M. Functional synergy between Rab5 effector Rabaptin-5 and exchange factor Rabex-5 when physically associated in a complex. *Mol Biol Cell* (2001) 12:2219–28. doi: 10.1091/mbc.12.7.2219
101. Yu B, Egbejimi A, Dharmat R, Xu P, Zhao Z, Long B, et al. Phagocytosed photoreceptor outer segments activate mTORC1 in the retinal pigment epithelium. *Sci Signal* (2018) 11. doi: 10.1126/scisignal.aag3315
102. Wensel TG. Phosphoinositides in Retinal Function and Disease. *Cells* (2020) 9. doi: 10.3390/cells9040866
103. Huynh KK, Eskelinen EL, Scott CC, Malevanets A, Saftig P, Grinstein S. LAMP proteins are required for fusion of lysosomes with phagosomes. *EMBO J* (2007) 26:313–24. doi: 10.1038/sj.emboj.7601511
104. Notomi S, Ishihara K, Efstathiou NE, Lee JJ, Hisatomi T, Tachibana T, et al. Genetic LAMP2 deficiency accelerates the age-associated formation of basal laminar deposits in the retina. *Proc Natl Acad Sci U.S.A.* (2019) 116:23724–34. doi: 10.1073/pnas.1906643116
105. Thompson DA, Constable PA, Liasis A, Walters B, Esteban MT. The Physiology of the Retinal Pigment Epithelium in Danon Disease. *Retina* (2016) 36:629–38. doi: 10.1097/IAE.0000000000000736
106. Fairn GD, Grinstein S. How nascent phagosomes mature to become phagolysosomes. *Trends Immunol* (2012) 33:397–405. doi: 10.1016/j.it.2012.03.003
107. Poteryaev D, Datta S, Ackema K, Zerial M, Spang A. Identification of the switch in early-to-late endosome transition. *Cell* (2010) 141:497–508. doi: 10.1016/j.cell.2010.03.011
108. Levin R, Grinstein S, Canton J. The life cycle of phagosomes: formation, maturation, and resolution. *Immunol Rev* (2016) 273:156–79. doi: 10.1111/imr.12439
109. Harrison RE, Bucci C, Vieira OV, Schroer TA, Grinstein S. Phagosomes fuse with late endosomes and/or lysosomes by extension of membrane protrusions along microtubules: role of Rab7 and RILP. *Mol Cell Biol* (2003) 23:6494–506. doi: 10.1128/MCB.23.18.6494-6506.2003
110. Johansson M, Lehto M, Tanhuanpaa K, Cover TL, Olkkonen VM. The oxysterol-binding protein homologue ORP1L interacts with Rab7 and alters functional properties of late endocytic compartments. *Mol Biol Cell* (2005) 16:5480–92. doi: 10.1091/mbc.e05-03-0189
111. Rai A, Pathak D, Thakur S, Singh S, Dubey AK, Mallik R. Dynein Clusters into Lipid Microdomains on Phagosomes to Drive Rapid Transport toward Lysosomes. *Cell* (2016) 164:722–34. doi: 10.1016/j.cell.2015.12.054
112. Herman KG, Steinberg RH. Phagosome degradation in the tapetal retinal pigment epithelium of the opossum. *Invest Ophthalmol Vis Sci* (1982) 23:291–304.
113. Keller G, Leuenberger PM. Effects of colchicine on phagosome-lysosome interaction in retinal pigment epithelium. II. In vitro observations on histio-organotypical retinal pigment epithelial cells of the pig (a preliminary report). *Albrecht Von Graefes Arch Klin Exp Ophthalmol* (1977) 203:253–9. doi: 10.1007/BF00409831
114. Weil D, Blanchard S, Kaplan J, Guilford P, Gibson F, Walsh J, et al. Defective myosin VIIA gene responsible for Usher syndrome type 1B. *Nature* (1995) 374:60–1. doi: 10.1038/374060a0
115. Williams DS, Lopes VS. The many different cellular functions of MYO7A in the retina. *Biochem Soc Trans* (2011) 39:1207–10. doi: 10.1042/BST0391207
116. Jiang M, Esteve-Rudd J, Lopes VS, Diemer T, Lillo C, Rump A, et al. Microtubule motors transport phagosomes in the RPE, and lack of KLC1 leads to AMD-like pathogenesis. *J Cell Biol* (2015) 210:595–611. doi: 10.1083/jcb.201410112
117. Pankiv S, Alemu EA, Brech A, Bruun JA, Lamark T, Overvatn A, et al. FYCO1 is a Rab7 effector that binds to LC3 and PI3P to mediate microtubule plus end-directed vesicle transport. *J Cell Biol* (2010) 188:253–69. doi: 10.1083/jcb.200907015
118. Hong Z, Pedersen NM, Wang L, Torgersen ML, Raiborg C. PtdIns3P controls mTORC1 signaling through lysosomal positioning. *J Cell Biol* (2017) 216:4217–33. doi: 10.1083/jcb.201611073
119. Gordiyenko NV, Fariss RN, Zhi C, MacDonald IM. Silencing of the CHM gene alters phagocytic and secretory pathways in the retinal pigment epithelium. *Invest Ophthalmol Vis Sci* (2010) 51:1143–50. doi: 10.1167/iovs.09-4117
120. Wavre-Shapton ST, Tolmachova T, Lopes da Silva M, Futter CE, Seabra MC. Conditional ablation of the choroideremia gene causes age-related changes in mouse retinal pigment epithelium. *PloS One* (2013) 8:e57769. doi: 10.1371/journal.pone.0057769
121. Deguchi J, Yamamoto A, Yoshimori T, Sugasawa K, Moriyama Y, Futai M, et al. Acidification of phagosomes and degradation of rod outer segments in rat retinal pigment epithelium. *Invest Ophthalmol Vis Sci* (1994) 35:568–79.
122. Nuckels RJ, Ng A, Darland T, Gross JM. The vacuolar-ATPase complex regulates retinoblast proliferation and survival, photoreceptor morphogenesis, and pigmentation in the zebrafish eye. *Invest Ophthalmol Vis Sci* (2009) 50:893–905. doi: 10.1167/iovs.08-2743
123. Wavre-Shapton ST, Meschede IP, Seabra MC, Futter CE. Phagosome maturation during endosome interaction revealed by partial rhodopsin processing in retinal pigment epithelium. *J Cell Sci* (2014) 127:3852–61. doi: 10.1242/jcs.154757
124. Liu J, Lu W, Reigada D, Nguyen J, Laties AM, Mitchell CH. Restoration of lysosomal pH in RPE cells from cultured human and ABCA4(-/-) mice: pharmacologic approaches and functional recovery. *Invest Ophthalmol Vis Sci* (2008) 49:772–80. doi: 10.1167/iovs.07-0675
125. Saric A, Grinstein S, Freeman SA. Measurement of Autolysosomal pH by Dual-Wavelength Ratio Imaging. *Methods Enzymol* (2017) 588:15–29. doi: 10.1016/bs.mie.2016.09.073

126. Webb JCBA, Wittmann T, Barber DL. pHLARE: A Genetically Encoded Ratiometric Lysosome pH Biosensor. *bioRxiv* (2020). doi: 10.1101/2020.06.03.132720
127. Valapala M, Sergeev Y, Wawrousek E, Hose S, Zigler JSJr, Sinha D. Modulation of V-ATPase by betaA3/A1-Crystallin in Retinal Pigment Epithelial Cells. *Adv Exp Med Biol* (2016) 854:779–84. doi: 10.1007/978-3-319-17121-0_104
128. Zigler JS Jr., Zhang C, Grebe R, Sehrawat G, Hackler L Jr., Adhya S, et al. Mutation in the betaA3/A1-crystallin gene impairs phagosome degradation in the retinal pigmented epithelium of the rat. *J Cell Sci* (2011) 124:523–31. doi: 10.1242/jcs.078790
129. Steinberg BE, Huynh KK, Brodovitch A, Jabs S, Stauber T, Jentsch TJ, et al. A cation counterflux supports lysosomal acidification. *J Cell Biol* (2010) 189:1171–86. doi: 10.1083/jcb.200911083
130. Kasper D, Planells-Cases R, Fuhrmann JC, Scheel O, Zeitz O, Ruether K, et al. Loss of the chloride channel ClC-7 leads to lysosomal storage disease and neurodegeneration. *EMBO J* (2005) 24:1079–91. doi: 10.1038/sj.emboj.7600576
131. Stobrawa SM, Breiderhoff T, Takamori S, Engel D, Schweizer M, Zdebik AA, et al. Disruption of ClC-3, a chloride channel expressed on synaptic vesicles, leads to a loss of the hippocampus. *Neuron* (2001) 29:185–96. doi: 10.1016/S0896-6273(01)00189-1
132. Goldberg AF, Moritz OL, Williams DS. Molecular basis for photoreceptor outer segment architecture. *Prog Retin Eye Res* (2016) 55:52–81. doi: 10.1016/j.preteyeres.2016.05.003
133. Freeman SA, Grinstein S. Resolution of macropinosomes, phagosomes and autolysosomes: Osmotically driven shrinkage enables tubulation and vesiculation. *Traffic* (2018) 19:965–74. doi: 10.1111/tra.12614
134. Papermaster DS, Dreyer WJ. Rhodopsin content in the outer segment membranes of bovine and frog retinal rods. *Biochemistry* (1974) 13:2438–44. doi: 10.1021/bi00708a031
135. Zimmerman WF, Godchaux W,3, Belkin M. The relative proportions of lysosomal enzyme activities in bovine retinal pigment epithelium. *Exp Eye Res* (1983) 36:151–8. doi: 10.1016/0014-4835(83)90098-2
136. Rakoczy PE, Zhang D, Robertson T, Barnett NL, Papadimitriou J, Constable IJ, et al. Progressive age-related changes similar to age-related macular degeneration in a transgenic mouse model. *Am J Pathol* (2002) 161:1515–24. doi: 10.1016/S0002-9440(10)64427-6
137. Rakoczy PE, Lai MC, Baines MG, Spilsbury K, Constable IJ. Expression of cathepsin S antisense transcripts by adenovirus in retinal pigment epithelial cells. *Invest Ophthalmol Vis Sci* (1998) 39:2095–104.
138. Martin RE, Elliott MH, Brush RS, Anderson RE. Detailed characterization of the lipid composition of detergent-resistant membranes from photoreceptor rod outer segment membranes. *Invest Ophthalmol Vis Sci* (2005) 46:1147–54. doi: 10.1167/iovs.04-1207
139. Albert A, Alexander D, Boesze-Battaglia K. Cholesterol in the rod outer segment: A complex role in a "simple" system. *Chem Phys Lipids* (2016) 199:94–105. doi: 10.1016/j.chemphyslip.2016.04.008
140. Swartz JG, Mitchell JE. Phospholipase activity of retina and pigment epithelium. *Biochemistry* (1973) 12:5273–8. doi: 10.1021/bi00750a008
141. Thelen AM, Zoncu R. Emerging Roles for the Lysosome in Lipid Metabolism. *Trends Cell Biol* (2017) 27:833–50. doi: 10.1016/j.tcb.2017.07.006
142. Infante RE, Wang ML, Radhakrishnan A, Kwon HJ, Brown MS, Goldstein JL. NPC2 facilitates bidirectional transfer of cholesterol between NPC1 and lipid bilayers, a step in cholesterol egress from lysosomes. *Proc Natl Acad Sci U.S.A.* (2008) 105:15287–92. doi: 10.1073/pnas.0807328105
143. Heybrock S, Kanerva K, Meng Y, Ing C, Liang A, Xiong ZJ, et al. Lysosomal integral membrane protein-2 (LIMP-2/SCARB2) is involved in lysosomal cholesterol export. *Nat Commun* (2019) 10:3521. doi: 10.1038/s41467-019-11425-0
144. Claudepierre T, Paques M, Simonutti M, Buard I, Sahel J, Maue RA, et al. Lack of Niemann-Pick type C1 induces age-related degeneration in the mouse retina. *Mol Cell Neurosci* (2010) 43:164–76. doi: 10.1016/j.mcn.2009.10.007
145. Kennedy CJ, Rakoczy PE, Constable IJ. Lipofuscin of the retinal pigment epithelium: a review. *Eye (Lond)* (1995) 9(Pt 6):763–71. doi: 10.1038/eye.1995.192
146. Usui T, Sawaguchi S, Abe H, Iwata K, Oyanagi K. Late-infantile type galactosialidosis. Histopathology of the retina and optic nerve. *Arch Ophthalmol* (1991) 109:542–6. doi: 10.1001/archopht.1991.01080040110040
147. Matlach J, Zindel T, Amraoui Y, Arash-Kaps L, Hennermann JB, Pitz S. Retinal and optic nerve degeneration in alpha-mannosidosis. *Orphanet J Rare Dis* (2018) 13:88. doi: 10.1186/s13023-018-0829-z
148. Ishikawa M, Sawada Y, Yoshitomi T. Structure and function of the interphotoreceptor matrix surrounding retinal photoreceptor cells. *Exp Eye Res* (2015) 133:3–18. doi: 10.1016/j.exer.2015.02.017
149. Ashworth JL, Biswas S, Wraith E, Lloyd IC. Mucopolysaccharidoses and the eye. *Surv Ophthalmol* (2006) 51:1–17. doi: 10.1016/j.survophthal.2005.11.007
150. Yu L, McPhee CK, Zheng L, Mardones GA, Rong Y, Peng J, et al. Termination of autophagy and reformation of lysosomes regulated by mTOR. *Nature* (2010) 465:942–6. doi: 10.1038/nature09076
151. Wyant GA, Abu-Remaileh M, Wolfson RL, Chen WW, Freinkman E, Danai LV, et al. mTORC1 Activator SLC38A9 Is Required to Efflux Essential Amino Acids from Lysosomes and Use Protein as a Nutrient. *Cell* (2017) 171:642–654 e12. doi: 10.1016/j.cell.2017.09.046
152. Wang S, Tsun ZY, Wolfson RL, Shen K, Wyant GA, Plovanich ME, et al. Metabolism. Lysosomal amino acid transporter SLC38A9 signals arginine sufficiency to mTORC1. *Science* (2015) 347:188–94. doi: 10.1126/science.1257132
153. Amick J, Tharkeshwar AK, Talaia G, Ferguson SM. PQLC2 recruits the C9orf72 complex to lysosomes in response to cationic amino acid starvation. *J Cell Biol* (2020) 219. doi: 10.1083/jcb.201906076
154. Smith DE, Clemencon B, Hediger MA. Proton-coupled oligopeptide transporter family SLC15: physiological, pharmacological and pathological implications. *Mol Aspects Med* (2013) 34:323–36. doi: 10.1016/j.mam.2012.11.003
155. Wang X, Zhang X, Dong XP, Samie M, Li X, Cheng X, et al. TPC proteins are phosphoinositide- activated sodium-selective ion channels in endosomes and lysosomes. *Cell* (2012) 151:372–83. doi: 10.1016/j.cell.2012.08.036
156. Gomez NM, Lu W, Lim JC, Kiselyov K, Campagno KE, Grishchuk Y, et al. Robust lysosomal calcium signaling through channel TRPML1 is impaired by lysosomal lipid accumulation. *FASEB J* (2018) 32:782–94. doi: 10.1096/fj.201700220RR
157. Nicklin P, Bergman P, Zhang B, Triantafellow E, Wang H, Nyfeler B, et al. Bidirectional transport of amino acids regulates mTOR and autophagy. *Cell* (2009) 136:521–34. doi: 10.1016/j.cell.2008.11.044
158. Baehr W, Wu SM, Bird AC, Palczewski K. The retinoid cycle and retina disease. *Vision Res* (2003) 43:2957–8. doi: 10.1016/j.visres.2003.10.001
159. Travis GH, Golczak M, Moise AR, Palczewski K. Diseases caused by defects in the visual cycle: retinoids as potential therapeutic agents. *Annu Rev Pharmacol Toxicol* (2007) 47:469–512. doi: 10.1146/annurev.pharmtox.47.120505.105225
160. Tinoco J, Miljanich P, Medwadowski B. Depletion of docosahexaenoic acid in retinal lipids of rats fed a linolenic acid-deficient, linoleic acid-containing diet. *Biochim Biophys Acta* (1977) 486:575–8. doi: 10.1016/0005-2760(77)90111-4
161. Gordon WC, Rodriguez de Turco EB, Bazan NG. Retinal pigment epithelial cells play a central role in the conservation of docosahexaenoic acid by photoreceptor cells after shedding and phagocytosis. *Curr Eye Res* (1992) 11:73–83. doi: 10.3109/02713689209069169
162. Bazan NG, Calandria JM, Serhan CN. Rescue and repair during photoreceptor cell renewal mediated by docosahexaenoic acid-derived neuroprotectin D1. *J Lipid Res* (2010) 51:2018–31. doi: 10.1194/jlr.R001131
163. Kauppinen A, Paterno JJ, Blasiak J, Salminen A, Kaarniranta K. Inflammation and its role in age-related macular degeneration. *Cell Mol Life Sci* (2016) 73:1765–86. doi: 10.1007/s00018-016-2147-8
164. Kanow MA, Giarmarco MM, Jankowski CS, Tsantilas K, Engel AL, Du J, et al. Biochemical adaptations of the retina and retinal pigment epithelium support a metabolic ecosystem in the vertebrate eye. *Elife* (2017) 6. doi: 10.7554/eLife.28899
165. Weh E, Lutrzykowska Z, Smith A, Hager H, Pawar M, Wubben TJ, et al. Hexokinase 2 is dispensable for photoreceptor development but is required for survival during aging and outer retinal stress. *Cell Death Dis* (2020) 11:422. doi: 10.1038/s41419-020-2638-2

166. Storti F, Raphael G, Griesser V, Klee K, Drawnel F, Willburger C, et al. Regulated efflux of photoreceptor outer segment-derived cholesterol by human RPE cells. *Exp Eye Res* (2017) 165:65–77. doi: 10.1016/j.exer.2017.09.008
167. Adijanto J, Du J, Moffat C, Seifert EL, Hurle JB, Philp NJ. The retinal pigment epithelium utilizes fatty acids for ketogenesis. *J Biol Chem* (2014) 289:20570–82. doi: 10.1074/jbc.M114.565457
168. Joyal JS, Sun Y, Gantner ML, Shao Z, Evans LP, Saba N, et al. Retinal lipid and glucose metabolism dictates angiogenesis through the lipid sensor Ffar1. *Nat Med* (2016) 22:439–45. doi: 10.1038/nm.4059
169. Fu Z, Kern TS, Hellstrom A, Smith L. Fatty acid oxidation and photoreceptor metabolic needs. *J Lipid Res* (2020). doi: 10.1194/jlr.TR120000618
170. Zhou X, Franklin RA, Adler M, Jacox JB, Bailis W, Shyer JA, et al. Circuit Design Features of a Stable Two-Cell System. *Cell* (2018) 172:744–757 e17. doi: 10.1016/j.cell.2018.01.015
171. Ellis SJ, Gomez NC, Levorse J, Mertz AF, Ge Y, Fuchs E. Distinct modes of cell competition shape mammalian tissue morphogenesis. *Nature* (2019) 569:497–502. doi: 10.1038/s41586-019-1199-y

Conflict of Interest: The authors declare that the research was conducted in the absence of any commercial or financial relationships that could be construed as a potential conflict of interest.

Copyright © 2020 Kwon and Freeman. This is an open-access article distributed under the terms of the Creative Commons Attribution License (CC BY). The use, distribution or reproduction in other forums is permitted, provided the original author(s) and the copyright owner(s) are credited and that the original publication in this journal is cited, in accordance with accepted academic practice. No use, distribution or reproduction is permitted which does not comply with these terms.

frontiers in Immunology

ORIGINAL RESEARCH
published: 02 February 2021
doi: 10.3389/fimmu.2020.621757

Warburg Effect Is a Cancer Immune Evasion Mechanism Against Macrophage Immunosurveillance

Jing Chen[1†], Xu Cao[1†], Bolei Li[1†], Zhangchen Zhao[2], Siqi Chen[1], Seigmund W. T. Lai[1], Sabina A. Muend[1], Gianna K. Nossa[1], Lei Wang[1], Weihua Guo[1], Jian Ye[1], Peter P. Lee[1] and Mingye Feng[1]*

[1] Department of Immuno-Oncology, Beckman Research Institute, City of Hope Comprehensive Cancer Center, Duarte, CA, United States, [2] Department of Biostatistics, University of Michigan School of Public Health, Ann Arbor, MI, United States

OPEN ACCESS

Edited by:
Johnathan Canton, Francis Crick Institute, United Kingdom

Reviewed by:
Raymond B. Birge, Rutgers, The State University of New Jersey, United States
Jaime F. Modiano, University of Minnesota Twin Cities, United States

***Correspondence:**
Mingye Feng
mfeng@coh.org

[†]These authors have contributed equally to this work

Specialty section:
This article was submitted to Molecular Innate Immunity, a section of the journal Frontiers in Immunology

Received: 26 October 2020
Accepted: 22 December 2020
Published: 02 February 2021

Citation:
Chen J, Cao X, Li B, Zhao Z, Chen S, Lai SWT, Muend SA, Nossa GK, Wang L, Guo W, Ye J, Lee PP and Feng M (2021) Warburg Effect Is a Cancer Immune Evasion Mechanism Against Macrophage Immunosurveillance. Front. Immunol. 11:621757. doi: 10.3389/fimmu.2020.621757

Evasion of immunosurveillance is critical for cancer initiation and development. The expression of "don't eat me" signals protects cancer cells from being phagocytosed by macrophages, and the blockade of such signals demonstrates therapeutic potential by restoring the susceptibility of cancer cells to macrophage-mediated phagocytosis. However, whether additional self-protective mechanisms play a role against macrophage surveillance remains unexplored. Here, we derived a macrophage-resistant cancer model from cells deficient in the expression of CD47, a major "don't eat me" signal, *via* a macrophage selection assay. Comparative studies performed between the parental and resistant cells identified self-protective traits independent of CD47, which were examined with both pharmacological or genetic approaches in *in vitro* phagocytosis assays and *in vivo* tumor models for their roles in protecting against macrophage surveillance. Here we demonstrated that extracellular acidification resulting from glycolysis in cancer cells protected them against macrophage-mediated phagocytosis. The acidic tumor microenvironment resulted in direct inhibition of macrophage phagocytic ability and recruitment of weakly phagocytic macrophages. Targeting V-ATPase which transports excessive protons in cancer cells to acidify extracellular medium elicited a pro-phagocytic microenvironment with an increased ratio of M1-/M2-like macrophage populations, therefore inhibiting tumor development and metastasis. In addition, blockade of extracellular acidification enhanced cell surface exposure of CD71, targeting which by antibodies promoted cancer cell phagocytosis. Our results reveal that extracellular acidification due to the Warburg effect confers immune evasion ability on cancer cells. This previously unrecognized role highlights the components mediating the Warburg effect as potential targets for new immunotherapy harnessing the tumoricidal capabilities of macrophages.

Keywords: macrophage, immunotherapy, phagocytosis, V-ATPase, microenvironment

INTRODUCTION

In addition to malignant cells, the tumor microenvironment (TME) comprises a large population of resident-tissue cells and recruited immune cells (1–3). Tumor-associated macrophages (TAMs) are usually the most abundant groups of immune cells found within the TME (4–8). TAMs are generally classified into two major groups depending on their activation states: 1) classically activated macrophages (M1), and 2) alternatively activated macrophages (M2), both of which carry out different functions related to tumor development and angiogenesis (9), although these two populations are not always exclusive.

Recent breakthroughs in cancer immunology have identified a novel role of macrophages in recognizing cancer cells and attacking them *via* cellular engulfment. This process was termed "Programmed Cell Removal" (PrCR), during which cancer cells are directly phagocytosed by macrophages, bypassing the induction of cell death (10, 11). Oftentimes, in established tumors and metastases, cancer cells have evaded PrCR by developing self-protective mechanisms, among which the best known were the upregulation of "don't eat me" signals to directly inhibit PrCR, such as CD47, MHCI and CD24 (12–15). Recent exciting progress demonstrated that PrCR may be induced by blocking "don't eat me" pathways to remove this inhibitory effect, or by activating "eat me" pathways to enhance target cell recognition, therefore reinstating macrophage-mediated immunosurveillance and subsequently the elimination of cancer cells (16–19). CD47 has been identified as one of the most important anti-phagocytic "don't eat me" signals, owing to its upregulation on many different types of human cancer cells (10, 11). Antibodies blocking the interaction between CD47 and its receptor on macrophages, signal regulatory protein alpha (SIRPα), have been shown to diminish the inhibitory signaling transduced to macrophages *via* the CD47-SIRPα axis, thus enabling the phagocytosis of cancer cells (16–19). PrCR induction has proven to be a promising new class of cancer immunotherapy in many preclinical cancer models, as well as clinical trials for hematopoietic malignancies and solid tumors (12, 13, 17, 18, 20–29).

However, the blockade of "don't eat me" or induction of "eat me" signals usually were not sufficient to fully eradicate cancer cells. In addition to "don't eat me" signals, it remains largely unexplored whether there are other self-protective mechanisms exploited by cancer cells to escape PrCR. The identification of such mechanisms may reveal novel therapeutic targets for inducing PrCR which can potentially be combined with existing immunotherapies to achieve a superior anti-cancer efficacy.

Distinct from that in normal tissue, the unique microenvironment in tumors directly impacts the metabolism, signaling and function of T cells, as revealed in previous studies in cancer immunology (30). The effects of tumor microenvironment on PrCR, however, remains largely unexplored. Glucose oxidation is one of the main sources of nutrients for cells and provides cells with energy in the form of ATP. Even in the presence of oxygen, cancer cells with high proliferation rates preferentially rely on glycolysis, an incomplete form of glucose oxidation, for energy production, a phenomenon known as the Warburg effect (31–33). While full oxidation of glucose produces carbon dioxide (CO_2), aerobic glycolysis in cancer cells leads to the production of lactic acid in the form of lactate and protons. Cytosolic lactate is transported out of the cells *via* monocarboxylate transporters (MCT), while protons (H^+) are secreted through membrane-bound transporters, leading to extracellular acidification (34, 35). Vacuolar ATPases (V-ATPase) are one of the most important H^+ transporters responsible for maintaining the acidic extracellular pH (36, 37). V-ATPase is a multi-subunit protein complex, consisting of a membrane-anchored V0 domain, a cytosolic V1 domain, and accessory subunits. ATP hydrolysis in the V1 domain drives the rotation of the V0 domain for H^+ translocation, acidifying the extracellular space (38). An acidic extracellular microenvironment has been shown to benefit cancer cells in their proliferation, survival, metastasis, and signal transduction (39–43), but whether it is involved in mediating the interaction between cancer cells and TAMs and regulating the immune evasion capabilities of cancers from PrCR has not been addressed.

Cancer progression has been positively correlated with the development of an immunosuppressive tumor microenvironment (44). Here, we demonstrate that extracellular acidification maintained by V-ATPase confers a self-protective mechanism on cancer cells independent of anti-PrCR mechanisms elicited by "don't eat me" signals. This mode of defense occurs by attenuating the phagocytic ability of macrophages against the cancer cells. Therefore, targeting V-ATPase with pharmacological or gene editing tactics sensitizes cancer cells to macrophage-mediated immunosurveillance by restoring their susceptibility to PrCR, hampering tumor development. This approach synergizes with CD47 blocking, amplifying PrCR and yielding potent anti-cancer activity. In addition to this, we demonstrate that a blockade of the V-ATPase pathway in cancer cells promotes the expression of a cancer therapeutic target, CD71 (45), and thus can be used in combination with anti-CD71 antibodies to induce a "synthetic" PrCR. Our results reveal a previously unrecognized role of extracellular acidification, a common feature of many cancers, in generating an anti-PrCR immunosuppressive microenvironment, and may inspire future efforts for developing novel PrCR-based cancer immunotherapy for a variety of cancers.

MATERIALS AND METHODS

Animals

BALB/c, NOD.Cg-Prkdc^{scid} Il2rg^{tm1Wjl}/SzJ (NSG), and RAG2$^{-/-}$ γc$^{-/-}$ BALB/c mice were bred in the Animal Resources Center at City of Hope Comprehensive Cancer Center. BALB/c mouse strain was purchased from the Jackson Laboratory. RAG2$^{-/-}$ γc$^{-/-}$ mouse strain was a generous gift from Dr. Irving L. Weissman at Stanford University. All the procedures were approved by the Administrative Panel on Laboratory Animal Care at City of Hope Comprehensive Cancer Center (IACUC17051, approved in August 2017).

Cell Culture

MDA-MB-231 and SW620 were cultured in DMEM (Gibco) supplemented with 10% FBS (Gibco) and 1% penicillin/

streptomycin. DLD1, Raji and U937 cells were cultured in RPMI-1640 (Gibco) medium supplemented with 10% FBS (Gibco) and 1% penicillin/streptomycin. All cell lines were purchased from ATCC and maintained at 37°C in a 5% CO_2 atmosphere. Cryopreservation of large quantities of low passage (below 3) cells was performed and cells with passage number below 20 were used in this study. Mycoplasma examination was routinely performed every two months.

Generation of Macrophages

To generate mouse bone marrow derived macrophages (BMDMs), bone marrow cells were harvested from the femur and tibia of 6–12 weeks old BALB/c mice. After the red blood cells were lysed by ACK buffer for 2 min, the bone marrow cells were filtered through a 70-μm strainer, washed twice with DMEM medium supplemented with 10% FBS and cultured in IMDM medium supplemented with 10% FBS and 10ng/ml of MCSF for 6–8 days to differentiate into macrophages.

To generate human peripheral blood mononuclear cells (hPBMC) derived macrophages, human peripheral blood was obtained from the blood center at City of Hope Helford Clinical Research Hospital. $CD14^+$ monocytes were enriched by Magnetic-activated Cell Sorting (MACS) with CD14 MicroBeads (Miltenyi Biotec) and subsequently cultured in IMDM with 10% human serum (Omega) for 6–8 days.

Bioinformatics Analysis

V-ATPase related gene expression data of normal tissue and primary tumors from TCGA breast datasets were obtained from https://portal.gdc.cancer.gov/. In total, 10 ATPase H+ Transporting V0 subunit protein coding genes, 13 ATPase H+ Transporting V1 subunit protein coding genes and 3 ATPase H+ Transporting accessory protein coding genes were included into the analysis.

The correlation between expression of V-ATPase related genes including ATP6V1A, ATP6V0D1, ATP6AP1 and ATP6AP2 and M1/M2 macrophage infiltration from TCGA breast and colon cancer dataset was analyzed *via* TIMER2.0 (46). Gene expression datasets containing cancer patient outcomes were analyzed *via* PRECOG program (47) to assess the correlation between the expression of V-ATPase subunits and survival outcomes of patients with breast cancer, colon cancer, gastric cancer, lung cancer, pancreatic cancer, brain cancer and hematopoietic malignancies.

Enrichment of PrCR Resistant Cells

A $CD47^{KO}$ SW620 stable line was generated with Transcription activator-like effector nucleases (TALENs), as described previously (23). Briefly, SW620 cells were transfected with constructs containing TALEN pairs TGTCGTCATTCCATG CTTTG and TATACTTCAGTAGTGTTTTG which were designed to target exon2 of CD47. Cells were stained with anti-CD47 or isotype antibodies and $CD47^-$ cells were sorted. $CD47^{KO}$ SW620 cells was cocultured with BMDMs at a 1:1 ratio for 24 h. Surviving cells were detached from the cell culture plate by a brief incubation with trypsin during which majority of the BMDMs were still attached to the plate. The cells were then washed once with PBS and put back to cell culture plate with fresh growth medium (DMEM supplemented with 10% FBS) for a recovery of 2–3 days. Cell numbers were determined by counting GFP+ cells under a fluorescent microscope. The cells were then added to freshly prepared BMDMs at a 1:1 ratio to repeat the phagocytosis selection. After 10 rounds of such selection process, the derived $CD47^{KO}$ SW620 sub-line cells (termed P10) were sorted and cultured in fresh growth medium for a recovery of 7 days. $CD47^{KO}$ SW620 cells that were cultured for the same procedure and time period but in the absence of BMDMs were used as the control line (termed P0).

The expression of CD47 on P0 and P10 cells was examined by flow cytometry with anti-CD47 antibody (clone B6H12, BD Biosciences) to ensure no CD47-expressing cells were enriched. Resistance of P10 cells to PrCR was evaluated by a phagocytosis assay.

Extracellular pH, Lactic Acid, and V-ATPase Activity Measurement

To measure extracellular pH, SW620, DLD1 or MDA-MB-231 cells were seeded into the 6-well plates with $5x10^5$ cells per well, including cells treated with vehicles or concanamycin (10nM), or cells transduced with Cas9 and control sgRNAs (non-targeting) or sgRNAs targeting ATP6AP2, as indicated in the figure legend, and pH of culture medium was measured at the indicated time points by pH meter (ThermoFisher).

To measure lactic acid secretion, SW620 P0 or P10 cells were seeded into the 24-well plates with 10^5 cells per well and cultured with DMEM medium supplemented with 10% dialyzed FBS (Gibco). Culture media of P0 and P10 were collected at 24, 48, and 72h for lactate measurement. Cell numbers were also recorded at these time points. The lactate release was measured by L-Lactate Assay Kit (Eton Bioscience).

To measure V-ATPase activity, SW620 P0 or P10 cells were seeded into the 6-well plates with $5x10^5$ cells per well. After overnight incubation, fresh culture medium with 100 nmol/L Lysotracker Red DND-99 (ThermoFisher) were added to the cells and incubated at 37°C in a 5% CO2 atmosphere for 50 min. Cells were washed once with PBS and incubated with fresh medium for another 10 min before the imaging. Images of brightfield and fluorescence were taken by Cytation 3 (BioTek). The mean (Texas Red 586,647) fluorescent intensity was calculated by Cytation 3 and set as the LysoTracker signal. The V-ATPase activity was quantified by the LysoTracker signal per cell.

CRISPR/Cas9-Mediated Gene Editing

Suppression of gene expression was performed using the CRISPR/Cas9 system in SW620, DLD1 and MDA-MB-231 cells. Pairs of primers containing control sgRNAs (non-targeting) or sgRNAs targeting human CD47, ATP6V1A, ATP6V1D, ATP6V0D1, ATP6AP1, or ATP6AP2 genes were designed and cloned into the all-in-one LentiCRISPR V2 vector (48). The LentiCRISPR V2 vector was transfected with the packing plasmids into HEK293T cells. Forty-eight hours after transfection, lentiviruses were collected and filtered through 0.45um filters to remove residual 293T cells and cell debris. SW620, DLD1 or MDA-MB-231 cells were cultured in 6-well cell culture plates with $2x10^5$ cells per well and incubated with lentiviruses for 48 h in the presence of

polybrene (8μg/ml), recovered for 24 h and selected with puromycin (2μg/ml) for at least 6 days to obtain stable lines with indicated genes suppressed.

The following sgRNA sequences were used:

Control 1 (Non-targeting): GAACGUAGAAAUUCCCAUUU (48)
Control 2 (LacZ): UUGGGAAGGGCGAUCGGUGC (49)
Human CD47: CUACUGAAGUAUACGUAAAG (48)
Human ATP6V1A: UGGAGAGAUUAUUCGAUUGG (48)
Human ATP6V1D: CUGUCGAAAUCGAAGAGUUA (48)
Human ATP6V0D1: AGUCAUCGAUGACCGGCUCA (48)
Human ATP6AP1: UGGUGCUUCCUGCCGUCGAC (48)
Human ATP6AP2: AGGAGAGCGGAUCCCAGACG (48)

For the rescue experiment, sgRNA targeting ATP6AP2 was cloned into the all-in-one LentiCRISPR V2-Blast vector. LentiCRISPR v2-Blast was a gift from Dr. Mohan Babu (Addgene plasmid #83480). ATP6AP2 cDNA with synonymous mutations was cloned into pCDH vector (System Biosciences) with a HA tag (TATCCTTACGACGTGCCTGA CTACGCC) to its C-terminus. The targeting sequence by sgRNA and PAM sequence in ATP6AP2 was mutated from AGGAGAGCGGATCCCAGACGTGG to AGGTGAAC GCATTCCTGATGTAG by site-directed mutagenesis and confirmed by Sanger sequencing. The LentiCRISPR V2-blast vector and pCDH vector were transfected with the packing plasmids into HEK293T cells, respectively. Forty-eight hours after transfection, lentiviruses were collected and filtered through 0.45um filters to remove residual 293T cells and cell debris. SW620 cells were cultured in 6-well cell culture plates with $2x10^5$ cells per well and incubated with lentiviruses generated from LentiCRISPR V2 and pCDH for 48 h in the presence of polybrene (8μg/ml), recovered for 24 h and selected with blasticidin (30μg/ml) and puromycin (2μg/ml) for at least 2 days to obtain stable lines with suppression and/or exogenous expression of ATP6AP2.

Flow Cytometry Analysis

Anti-human CD47 (clone B6H12, BD Biosciences), anti-mouse F4/80 (clone BM8, BioLegend), anti-Sirpα (clone P84, BioLegend), anti-mouse/human CD11b (clone M1/70, BioLegend), anti-mouse CD45 (clone 30-F11, BioLegend), anti-mouse MHC II (clone M5/114.15.2, BioLegend), anti-mouse CD206 (clone C068C2, BioLegend), anti-mouse CD80 (clone 16-10A1, BioLegend), anti-mouse CD86 (clone GL-1, BioLegend), anti-mouse PD-L1 (clone 10F.9G2, BioLegend), anti-mouse Gr1(clone RB6-8C5,BioLegend), anti-human CD14 (clone HCD14, BioLegend), and anti-human CD71 (clone CY1G4, BioLegend; clone OKT9, ThermoFisher; clone L01.1 and clone M-A712, BD Biosciences) were used for FACS analyses. Antibodies were Phycoerythrin (PE)-, PE/Cyanine7, APC, APC/Cyanine7, PerCP/Cyanine5.5, PE/Dazzle™ 594, Alexa Flour® 700 or BV605 conjugated, or fluorophore-conjugated secondary antibodies were used. Annexin V (BD Biosciences), Sytox blue (ThermoFisher), 7-Aminoactinomycin D (7-AAD, ThermoFisher), or Zombie Violet™ Fixable Viability Kit (Biolegend) was used to exclude dead cells. Flow cytometry was performed using the BD LSRFortessa cell analyzers (BD).

Phagocytosis Assay

Phagocytosis assays were performed with mouse bone marrow-derived macrophages (BMDMs) or human peripheral blood monocyte-derived macrophages.

For short-term phagocytosis assays, macrophages and target cancer cells were detached from cell culture plates by incubation with TrypLE (Gibco). Cells were washed twice with PBS and cell numbers were determined by cell counting. For each sample, $0.1x10^6$ BMDMs or hPBMC macrophages were cocultured with $0.2x10^6$ cancer cells expressing a GFP-luciferase fusion protein in IMDM medium at 37°C in the cell culture incubator for 2 h in the presence of CD47-blocking antibodies or other agents as indicated in the figure legend. Cells were washed once with FACS buffer (PBS supplemented with 2% FBS). Mouse macrophages were stained with anti-mouse F4/80 antibody (clone BM8, BioLegend) conjugated with PE-Cy7 and hPBMC macrophages were stained with anti-human CD14 antibody (clone HCD14, BioLegend) conjugated with APC. Phagocytosis index was determined by the percentage of macrophages that have phagocytosed cancer cells, thus becoming double positive (PE-$Cy7^+GFP^+$ or APC^+GFP^+) among the entire macrophage population (PE-$Cy7^+$ or APC^+) by flow cytometry analyses using the BD LSRFortessa cell analyzers. Anti-CD47 antibody (clone B6H12, BioXCell) or anti-Sirpα (clone P84, BioLegend) antibody was used in phagocytosis assays for blocking CD47-Sirpα interaction. Phagocytosis index was normalized to the maximal response by each independent donor (human or mouse) against each cell line.

In some phagocytosis assays as indicated, cancer cells were labeled with pHrodo™ Red succinimidyl ester (Thermo). SW620 cells were washed twice with PBS and resuspended with PBS at 0.2 million cells/ml. The pHrodo™ Red was added to a final concentration of 120 ng/ml. Cells were incubated with pHrodo™ Red for 30 min at room temperature in the dark. Cells were washed twice with PBS and cell numbers were determined by cell counting. For each sample, $0.1x10^6$ BMDMs or hPBMC macrophages were cocultured with $0.2x10^6$ cancer cells expressing a GFP-luciferase fusion protein in IMDM medium at 37°C in the cell culture incubator for 2 h in the presence of CD47-blocking antibodies or other agents as indicated in the figure legend. The pHrodo™ Red dye becomes brightly red in phagosomes, indicating the labeled cells were engulfed by macrophages.

For long-term phagocytosis assays, $0.1x10^6$ macrophages and target cancer cells expressing a GFP-luciferase fusion protein were cocultured in 96-well cell culture plate at ratios of 1:1 to 1:3 for 24 h. Samples with cancer cells alone (without macrophages) were used as controls. The plates were washed once with PBS and luciferin (SYDlabs) was added to the wells. Surviving cancer cells were quantified by reading the luminescence signals with Cytation 3. Cancer cell killing was determined by normalizing the luminescence of surviving cancer cells to that of the same type of cancer cells with the same treatment but in the absence of macrophages.

Western Blotting

The ATP6AP2 gene knockdown efficiency was examined by western blotting. Cells were lysed in lysis buffer (PBS supplemented with 0.5% SDS) along with protease inhibitors and protein concentrations were quantified by BCA protein assay. Protein samples were diluted in the loading buffer (62.5 mM Tris-HCl pH 6.8, 10% Glycerol, 2% SDS, 0.01% Bromophenol Blue, 100 mM DTT) and subjected to SDS-polyacrylamide gel electrophoresis. For immunoblotting, anti-HA (Covance), anti-ATP6AP2 (Novus Biologicals) and anti-GAPDH (Cell Signaling, loading control) primary antibodies and HRP-conjugated anti-rabbit IgG or anti-mouse IgG secondary antibodies were used.

In Vivo Tumor Models

$RAG2^{-/-}$ $\gamma c^{-/-}$ mice were engrafted with SW620, DLD1 or MDA-MB-231 cells expressing a GFP-luciferase fusion protein to evaluate the role of V-ATPase-mediated extracellular acidification in tumor development and metastasis. For the SW620 and DLD1 models, $0.05x10^6$ $Ctrl^{KD}$ (sgRNA targeting LacZ gene) or $ATP6AP2^{KD}$ cells were suspended in RPMI medium with 25% Matrigel Matrix (Corning) and subcutaneously injected into the 6-8 weeks old $RAG2^{-/-}$ $\gamma c^{-/-}$ mice. Mice were treated with PBS (control) or CD47-blocking antibody (clone B6H12, BioXCell) once per week starting 7 days after tumor engraftment. CD47-blocking antibody was diluted in PBS and used as a dose of 2.5mg/kg body weight. For the MDA-MB-231 model, 0.2×10^6 $Ctrl^{KD}$ (sgRNA targeting LacZ gene), $CD47^{KD}$, $ATP6AP2^{KD}$, or $Double^{KD}$ cells were suspended in DMEM medium with 25% Matrigel Matrix (Corning) and injected into the mammary fat pad of 6-8 weeks old female NSG mice. Bioluminescent imaging was used to monitor tumor development and metastasis. In detail, tumor-bearing mice were injected intraperitoneally with D-luciferin in PBS with a dose of 139mg luciferin/kg body weight. Imaging was performed using Lago X (Spectral Instruments Imaging) and bioluminescence signals were analyzed with Aura Image software (Spectral Instruments Imaging). All the tumor-bearing mice were sacrificed at the end point.

The tumors developed by $Ctrl^{KD}$ and $ATP6AP2^{KD}$ DLD1 cells were collected, minced into small pieces, and dissociated in DMEM with Liberase TM enzymes (ThermoFisher) and DNase (ThermoFisher) at 37°C until a single-cell suspension was achieved. Red blood cells were lysed with ACK lysis buffer. Cells from the tumor were washed twice with FACS buffer (PBS supplemented with 2% FBS) and filtered through a 70-um cell strainer to remove undigested pieces. FcR blocker (Miltenyi) was used to treat the cells to block non-specific binding of antibodies and the cells were then stained with indicated antibodies and subjected to flow cytometry analysis. A combination of cell surface markers ($CD45^+$ $F4/80^+CD11b^+Gr\text{-}1^-$) and Zombie $Violet^-$ were used to define tumor-associated macrophages (TAMs). The expression of CD206, MHC II, CD80, CD86, PD-L1 on TAMs was examined.

Quantitative PCR

Total RNA of BMDM cultured under pH 7.4 and 6.5 for 48h was extracted with an RNA extraction kit (Qiagen). cDNA was generated by SuperScript™ VILO™ cDNA Synthesis Kit (Invitrogen) and quantitative PCR was performed with SYBR Green (BIOLINE) and acquired by CXF96 real-time system (BIO-RAD).

The following primer sequences were used:

Gapdh F: CCAGTTGGTAACAATGCCATGT
Gapdh R: GAGTTGCTGTTGAAGTCGCA
Cxcl10 F: CCAAGTGCTGCCGTCATTTTC
Cxcl10 R: GGCTCGCAGGGATGATTTCAA
Tnf F: CTGAACTTCGGGGTGATCGG
Tnf R: GGCTTGTCACTCGAATTTTGAGA
Ccl5 F: GCTGCTTTGCCTACCTCTCC
Ccl5 R: TCGAGTGACAAACACGACTGC
Arg1 F: CTCCAAGCCAAAGTCCTTAGAG
Arg1 R: AGGAGCTGTCATTAGGGACATC
Fn1 F: ATGTGGACCCCTCCTGATAGT
Fn1 R: GCCCAGTGATTTCAGCAAAGG

Cytokine/Chemokine Analysis

$Ctrl^{KD}$ and $ATP6AP2^{KD}$ MDA-MB-231 cells were seeded in the 12-well plates at a density of $5x\ 10^5$ cells per well for 48 h. Cell culture medium from these two lines were collected and centrifuged. The supernatants were collected and submitted to Eve Technologies for Human Cytokine Array/Chemokine Array 48-plex discovery arrays which were analyzed using Millipore MILLIPLEX human cytokine/chemokine kit.

Antibody Array

Cell surface proteome on cancer cells with V-ATPase blockade was examined by a flow cytometry-based high-throughput antibody array.

LEGENDScreen kit purchased from BioLegend contained 332 PE-conjugated monoclonal antibodies against human cell surface proteins. The kit also contains 10 mouse, rat and hamster Ig isotype controls. Lyophilized antibodies in 96-well plates were reconstituted with deionized water. SW620 cells treated with vehicles or concanamycin (10nM) overnight were detached from the cell culture dishes by trypsin and cell numbers were determined by cell counting. Cells were washed twice with cell staining buffer included in the kit and seeded to ultra-low attachment 96-well plate with 10^5 cells per well using multi-channel pipettes. Reconstituted antibodies were added to each well of cells and gently mixed with the cell suspensions. The plates were then incubated at 4°C for 30 min, washed twice with cell staining buffer and subjected to flow cytometry analyses using the High Throughput Sampler (HTS) mode of BD LSRFortessa cell analyzers.

Statistical Analysis

Statistical analyses were performed under GraphPad Prism 8.3.0 (GraphPad Software) and Excel (Microsoft). Data are presented as mean ± SD. Student *t* tests for two group comparisons and one-way *ANOVA* test for multi-group comparisons were

used for the study. A p-value of <0.05 was considered statistically significant.

RESULTS

To identify mechanisms exploited by cancer cells against PrCR beyond CD47 upregulation, we first knocked out CD47 expression in SW620, a human colon cancer line, by transducing the cells with TALEN (transcription activator-like effector nucleases) plasmids and sorting for CD47 negative cells. A phagocytosis assay was then performed to examine the susceptibility of cancer cells to PrCR by macrophages. In most cancers, tumor-associated macrophages (TAMs) originated from bone marrow progenitor cells and monocytes, which were recruited to tumors and differentiated into TAMs. Therefore, bone marrow-derived macrophages (BMDMs) have been established as a sound research tool for assessing the phagocytic ability of macrophages against cancer cells. Next, we designed a PrCR selection assay to enrich for cells resistant to PrCR (**Figure 1A**). In this assay, $CD47^{KO}$ SW620 cells were co-cultured with BMDMs for 24 h. Surviving SW620 cells were collected from the tissue culture plates and subjected to another round of co-culture with freshly prepared BMDMs. We reasoned that the repeated selection would lead to the depletion of cells susceptible to PrCR, and thus the enrichment of cells resistant to PrCR. After ten rounds of such selection, we collected the surviving SW620 $CD47^{KO}$ cells (which we termed P10). We demonstrated that consistent with previous studies, the parental $CD47^{KO}$ cells became much more vulnerable to macrophage phagocytosis due to the loss of CD47 protection (**Figures 1B, C**), while the P10 cells surviving from PrCR selection had become significantly more resistant to PrCR, as compared to the parental cells (which we termed P0) (**Figures 1B, C**, and **Figures S1A, B**). We assessed phagocytosis with two independent approaches: 1) to examine the extent by which macrophages have phagocytosed cancer cells after 2 h of macrophage-SW620 coculture, or 2) to examine surviving cancer cells after an overnight macrophage-SW620 coculture (**Figures 1B, C**). The same conclusions were achieved from both methods, indicating PrCR-resistant cells have been enriched in P10. Importantly, the P10 cells remained CD47 deficient (**Figure 1D** and **Figure S1C**), excluding the possibility that our selection had enriched residual CD47-expressing cells.

During glycolysis in cancer cells, lactic acid resulting from the Warburg effect is transported out of the cells to acidify the extracellular microenvironment (50). Interestingly, a significantly lower pH and higher concentration of lactate were detected in the extracellular medium taken from P10 cells compared to the parental cells (**Figures 1E, F**), although the proliferation rate of P0 and P10 was comparable (**Figure S1D**), suggesting that the P10 cells had acidified the extracellular medium more rapidly. In addition, an increase in lysotracker staining was observed in P10 cells (**Figure 1G**), indicating enhanced assembly and activity of V-ATPases. V-ATPase is critical for maintaining an acidic pH within the lysosomal lumen for protein digestion and recycling (37, 38). Beyond this, V-ATPase also pumps protons out of the cells, leading to an acidic microenvironment in cancer tissues (51, 52). To assess the implications on clinical cases, we analyzed a large cohort of gene expression datasets containing cancer patient outcomes with the PRECOG program (47), including that of breast cancer, colon cancer, and hematopoietic malignancies. We found that a higher expression of V-ATPase subunits, including the V0 domain, V1 domain, and accessory domains, was correlated with a worse overall survival outcome (**Figures 1H, I** and **Figures S1E–S1J**). These data indicate that the hyper-activation of V-ATPase is clinically relevant to the progression of a wide range of cancers.

Because the evasion of PrCR has been shown to be an important mechanism contributing to worse prognosis (53), we decided to examine whether V-ATPase plays a role in inhibiting macrophage-mediated PrCR. First, we used pharmacological inhibitors to block V-ATPase activity in SW620 cells. We found that treating the cells with concanamycin A, which blocks the ATP-binding site in the V1 domain to disrupt its ATPase activity, diminished extracellular acidification (**Figure 2A**) and significantly promoted PrCR of P10 cells to a similar level of that of P0 cells (**Figure 2B**), indicating that V-ATPase-mediated self-protection is a major mechanism accounting for their resistance to PrCR. Previous studies have demonstrated that dysfunction in the subunits of the V0 domain, V1 domain, and accessory subunits AP1 or AP2 compromises the ability for V-ATPase to pump protons (54–56). Analyses of gene expression profiling of patient specimens from GDC TCGA Breast Cancer dataset revealed an enhanced expression of V-ATPase subunits in primary tumors as compared to normal tissues (**Figure 2C**). Therefore, we used a CRISPR/Cas-9-mediated gene editing approach to knock down the expression of these subunits individually in SW620 cells and evaluated their effects by examining SW620 susceptibility to macrophages. Enhanced PrCR was observed across the single subunit knockdowns (**Figure 2D**), indicating that a functional V-ATPase complex is critical for maintaining the anti-PrCR ability of cancer cells.

To evaluate whether targeting V-ATPase can be a widely applicable strategy in inducing PrCR, we then assessed the effects of blocking V-ATP activity by pharmacological inhibitors to inhibit its ATPase function in a wider range of human cancer cells including lymphoma, colon cancer and breast cancer (**Figures 3A–D**). Different concentrations of concanamycin and macrophage models including both BMDMs and human peripheral blood monocyte-derived macrophages were used for assessing the role of V-ATPase in regulating PrCR (**Figures 3A–D** and **Figures S2A, B**). Enhanced elimination of cancer cells by macrophages was observed across all the cancer lines examined, when V-ATPase was inhibited. The blockade of the CD47-SIRPα axis further enhanced PrCR induced by V-ATPase disruption (**Figures 3A–D**), suggesting that the V-ATPase-mediated anti-PrCR effect is independent of the inhibitory signaling transduced by CD47. ATPase H+ Transporting Accessory Protein 2, or ATP6AP2, is a critical component that is essential for the proper assembly and function of the V-ATPase complex (57, 58). We then moved to assess the effects of knocking down ATP6AP2 in a

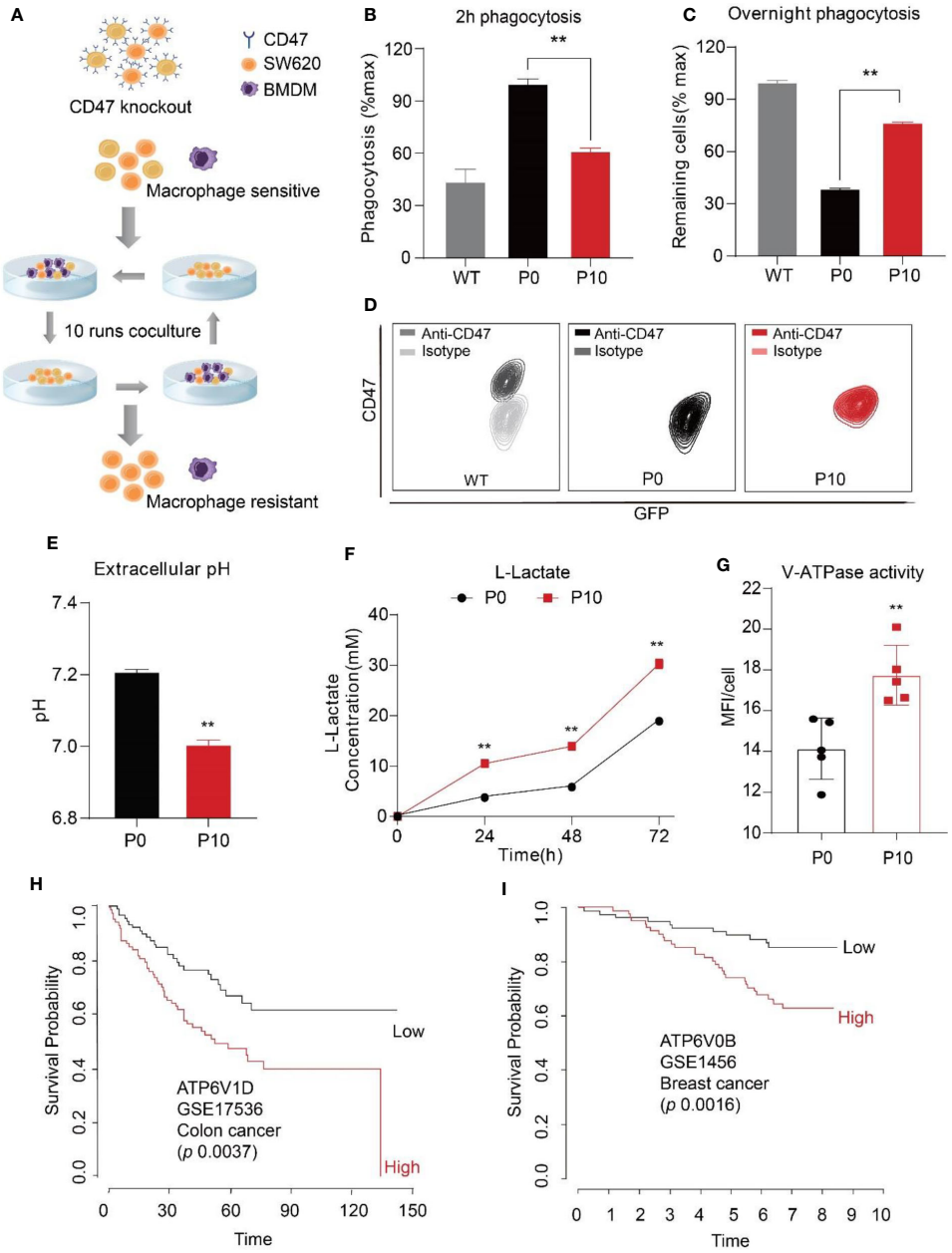

FIGURE 1 | Increased extracellular acidification induced by cancer cells correlated with resistance to macrophage-mediated PrCR and worse prognosis in patients. **(A)** A Schematic showing the strategy to generate cells resistant to macrophage-mediated PrCR. **(B, C)** A 2h phagocytosis assay **(B)** and an overnight phagocytosis assay **(C)** demonstrated the resistance of P10 cells to macrophage-mediated PrCR. P10 group was compared with the P0 group. (Normalization is described in details in "Methods". For overnight assay, the values of WT cells were normalized as 100%) $^{**}P < 0.01$ (*t* test). **(D)** Flow cytometry analysis of CD47 expression on SW620 WT, P0 and P10 cells. **(E)** P10 cells acidified extracellular microenvironment more rapidly than P0 cells. P10 group was compared with the P0 group, 72h culture medium was collected for analysis. $^{**}P < 0.01$ (*t* test). **(F)** A higher concentration of L-lactate was detected in the extracellular medium of P10 cells, as compared to that of P0 cells. P10 group was compared with the P0 group at individual time point. $^{**}P < 0.01$ (*t* test). **(G)** Lysotracker staining indicated an increased activity of V-ATPase in P10 cell, as compared to that in P0 cells. P10 group was compared with the P0 group. $^{**}P < 0.01$ (*t* test). **(H, I)** Upregulation of V-ATPase subunits V1D1 **(H)**, V0B **(I)**] correlates with a worse overall survival rate in patients with colon cancer and breast cancer.

variety of cancer cells, and found a similar enhancement of PrCR (**Figure 3E**). Consistently, exogenous expression of ATP6AP2 led to an inhibition of PrCR and was able to reverse the enhanced PrCR due to ATP6AP2 suppression (**Figure 3F** and **Figure S3A**). Our results suggested that the anti-PrCR effects mediated by V-ATPase on cancer cells was in fact a general mechanism. That is, targeting V-ATPase, either by its subunits or assembly machinery, is sufficient to elicit PrCR.

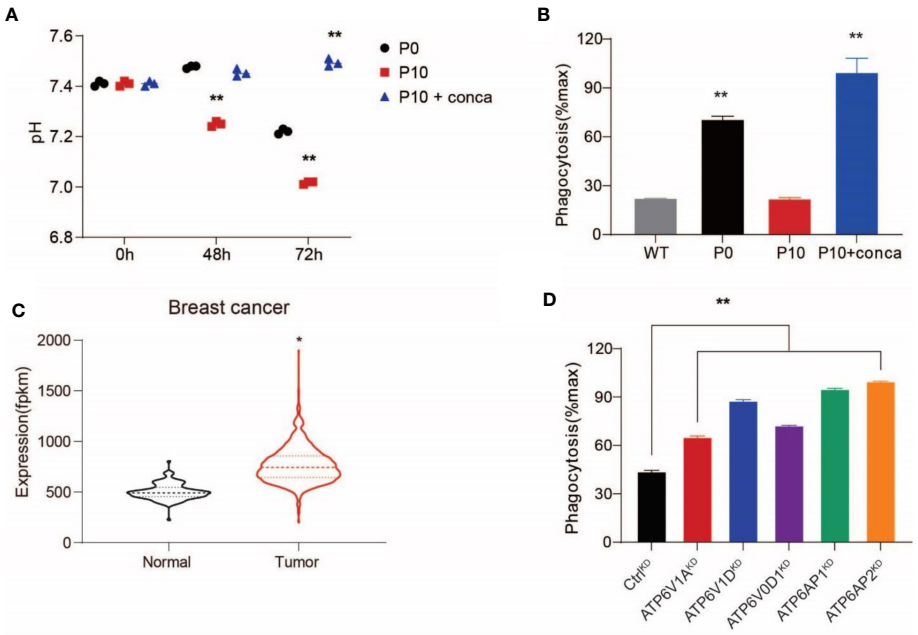

FIGURE 2 | Upregulated V-ATPase activity conferred resistance to macrophage-mediated PrCR. **(A)** Pharmacological inhibition of V-ATPase with concanamycin A (10 nM) diminished extracellular acidification of P10 cells. $^{**}P < 0.01$ (one-way *ANOVA* test). **(B)** A phagocytosis assay with BMDMs showing that concanamycin A treatment restored the vulnerability of P10 cells to macrophage-mediated PrCR. Each group was compared with the WT group. $^{**}P < 0.01$ (one-way *ANOVA* test). **(C)** Significant up-regulation of V-ATPase subunit coding genes in breast cancer (n=1,102) tissues as compared to the adjacent normal tissues, based on TCGA datasets (In total 10 ATPase H^+ Transporting V0 subunit protein coding genes, 13 ATPase H^+ Transporting V1 subunit protein coding genes and 3 ATPase H^+ Transporting accessory protein coding genes were included into the analysis). $^{*}P < 0.05$ (*t* test). **(D)** A phagocytosis assay with BMDMs showing that knocking-down the expression of the individual subunit of V-ATPase with CRISPR increased the susceptibility of SW620 cells to PrCR. Each group was compared with the $Ctrl^{KD}$ group. $^{**}P < 0.01$ (one-way *ANOVA* test).

Next, we examined the anti-cancer effects of blocking V-ATPase in *in vivo* xenotransplantation models. Human colon cancer lines SW620 or DLD1 cells were transduced with lentiviruses expressing a GFP-luciferase fusion protein. Cas9 and non-targeting or ATP6AP2-targeting sgRNAs were transduced into these cells to establish $Ctrl^{KD}$ or $ATP6AP2^{KD}$ stable cell lines, respectively (**Figure S3B**). $RAG2^{-/-}$, $\gamma c^{-/-}$ or NSG mice (deficient in T, B and NK cells but maintain functional phagocytes) were used for tumor engraftment. After engrafted with $Ctrl^{KD}$ or $ATP6AP2^{KD}$ SW620 or DLD1 cells, the mice were treated with a monoclonal antibody blocking CD47-SIRPα interaction, and tumor development was quantified *via* bioluminescence imaging. We showed that ATP6AP2 knockdown or CD47 blockade alone inhibited tumorigenicity of SW620 and DLD1 in mice, and a combination of ATP6AP2 knockdown and CD47 blockade elicited a strong inhibition of tumor growth and development (**Figures 4A, B**). Next, we used a xenotransplantation breast cancer model to examine the effects of blocking V-ATPase on breast tumor development and metastasis. A human breast cancer line MDA-MB-231 stable lines with $Ctrl^{KD}$, $CD47^{KD}$, $ATP6AP2^{KD}$, or a double knockdown were established by CRISPR/Cas9 (**Figure S2B**) and injected into the mammary fat pad of $RAG2^{-/-}$, $\gamma c^{-/-}$ mice (**Figures 4C, D**). Tumor development and lung metastasis were monitored by bioluminescence imaging. Suppression of either CD47 or ATP6AP2 alone in MDA-MB-231 cells demonstrated anti-cancer effects, and a double knockdown revealed a synergistic effect and dramatically inhibited tumor development and lung metastasis (**Figures 4C, D**).

Next, we sought to understand the underlying mechanisms by which V-ATPase in cancer cells confers the ability to escape from PrCR. The extracellular acidification resulting from the Warburg effect leads to an acidic tumor microenvironment with a pH value being as low as 5.8–6.1 (59–62). To investigate the effects of acidic media on PrCR, we performed a phagocytosis assay in media with a pH ranging from 5.8 to 8.8 titrated by lactic acid, and found that cancer cell phagocytosis was dramatically inhibited in the acidic medium compared to the neutral or alkaline medium (**Figure 5A** and **Figure S4A**). The effects of blocking V-ATPase in promoting PrCR were diminished when the extracellular media were maintained acidic by excessive lactic acid (**Figure S4B**). While both M1- and M2-like macrophage respond to blockade of CD47-Sirpα axis to carry out PrCR, stronger phagocytic ability has been associated with M1-polarized macrophages (63). We demonstrated when macrophages were cultured in acidic media, the expression of markers for M1-like states (64, 65) including *Cxcl10, Tnf* and *Ccl5* was downregulated, whereas the expression of key markers for M2-like macrophages (64, 65) including *Arg1* and *Fn1* was dramatically upregulated, in macrophages cultured in acidic media (**Figure 5B**). Next, we assessed the effects of acidic microenvironment in the recruitment and polarization of TAMs

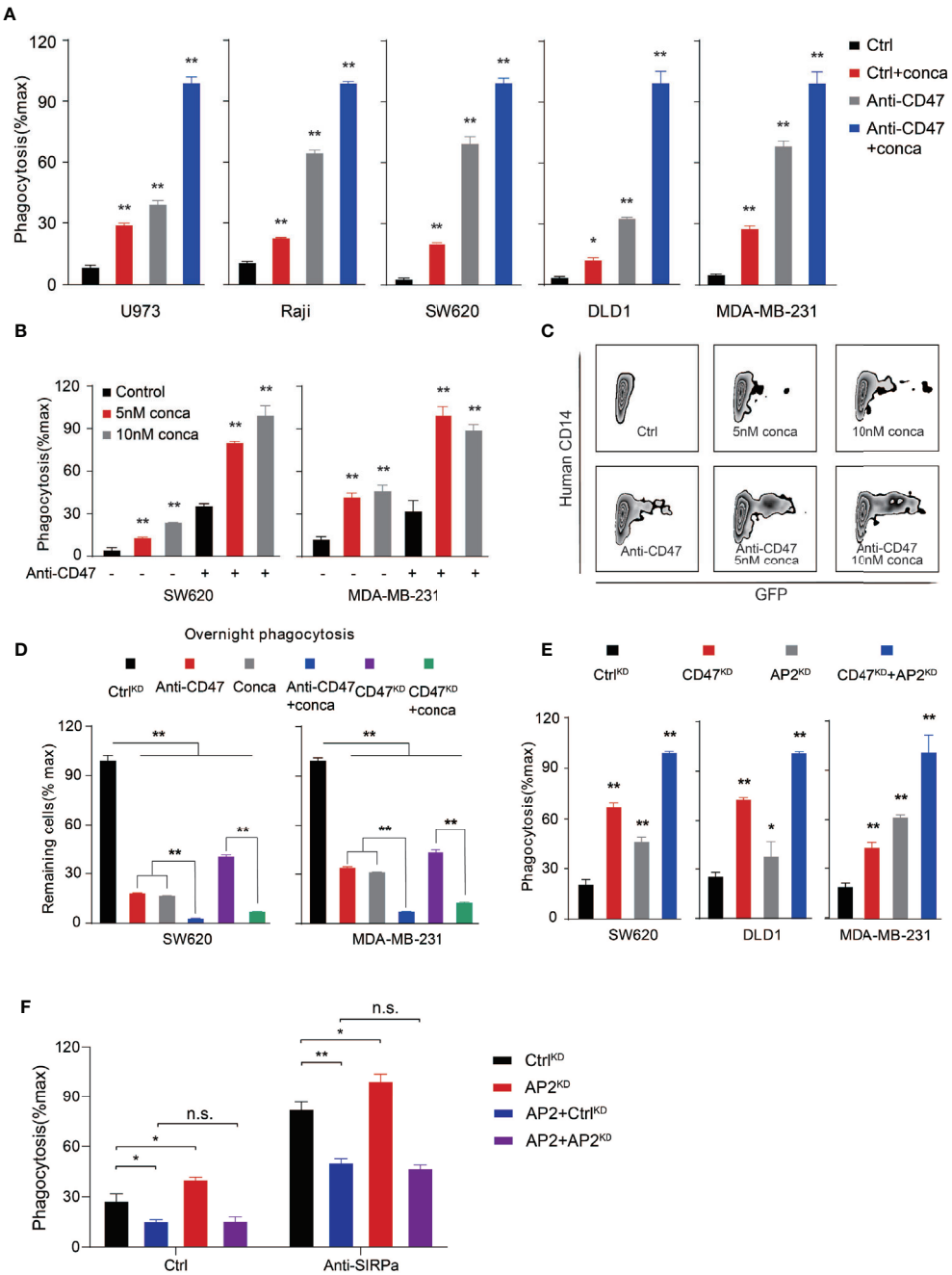

FIGURE 3 | V-ATPase inhibition synergized with CD47 blockades to induce PrCR. **(A)** Phagocytosis assays with BMDMs showing that pharmacological inhibition of V-ATPase with concanamycin A (10 nM) promoted PrCR and increased CD47-blocking antibody-induced phagocytosis. The assays were performed with human lymphoma (U973 and Raji), colon cancer (SW620 and DLD1) and breast cancer (MDA-MB-231) lines. Each group was compared with the Ctrl group. $^{*}P < 0.05$, $^{**}P < 0.01$ (one-way *ANOVA* test). **(B)** A phagocytosis assay with human peripheral blood monocyte-derived macrophages showing that concanamycin A treatment enhanced PrCR of SW620 and MDA-MB-231 cells in the absence or presence of CD47 blocking antibodies. Each group was compared with corresponding non-treated or treated Ctrl group. $^{**}P < 0.01$ (one-way *ANOVA* test). **(C)** Representative flow cytometry plots for **(B)** Macrophages were labeled with anti-CD14. SW620 cells were GFP+. Concanamycin A treatment increased the percentages of human macrophage phagocytosing cancer cells (hCD14+GFP+) with or without anti-CD47 antibody. **(D)** An overnight phagocytosis assay showing macrophage-mediated PrCR induced by either CD47 blocking antibody or genetic deletion of CD47 was largely potentiated by treatment of SW620 and MDA-MB-231 cells with concanamycin A (the values of $Ctrl^{KD}$ were normalized as 100%). $^{**}P < 0.01$ (one-way *ANOVA* test). **(E)** A phagocytosis assay with BMDMs showing that genetic knockdown of ATP6AP2 expression was able to induce PrCR of SW620, DLD1 and MDA-MB-231 cells and synergized with knockdown of CD47 expression. Each group was compared with the $Ctrl^{KD}$ group. $^{*}P < 0.05$, $^{**}P < 0.01$ (one-way *ANOVA* test). **(F)** A phagocytosis assay with BMDMs showing exogenous expression of ATP6AP2 inhibited PrCR of SW620 cells and reversed the enhanced PrCR of $ATP6AP2^{KD}$ cells. $^{*}P < 0.05$, $^{**}P < 0.01$ (*t* test).

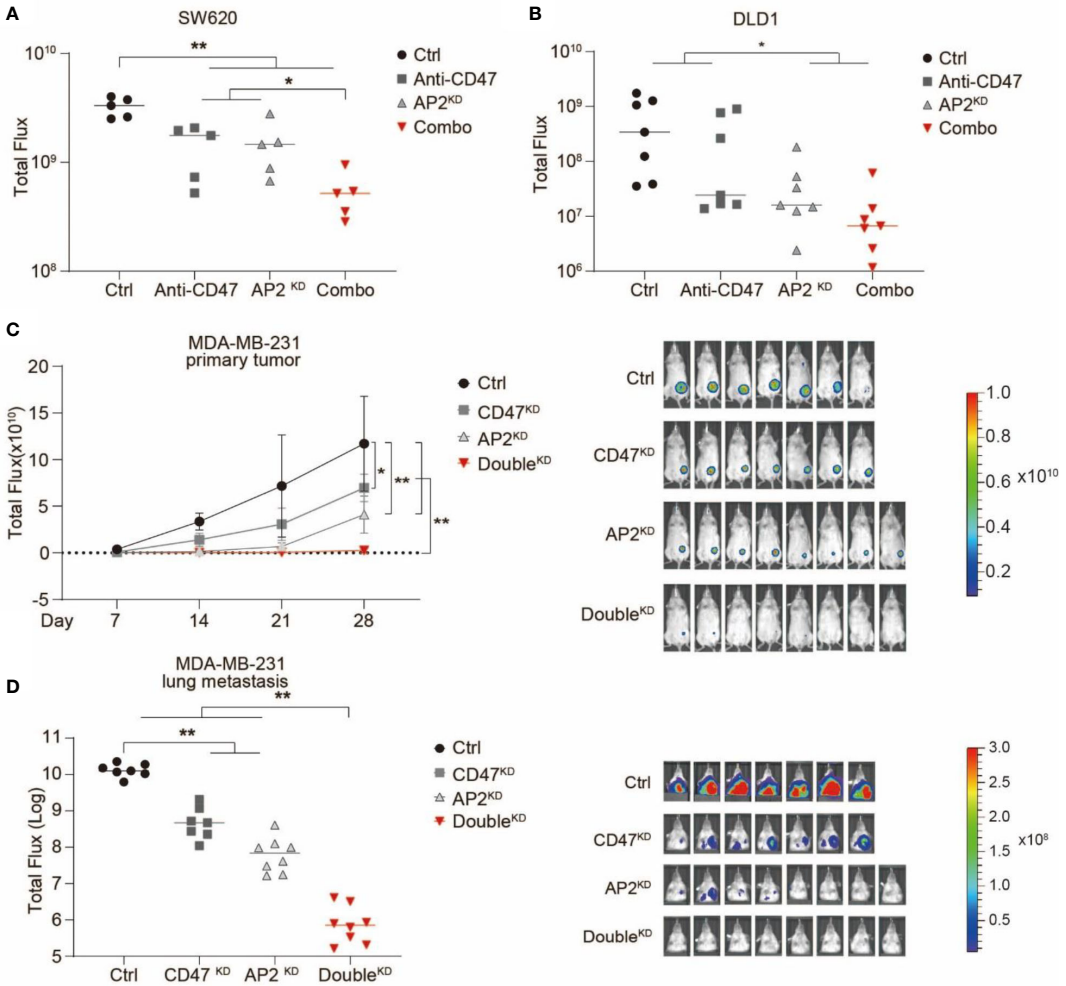

FIGURE 4 | Suppression of ATP6AP2 expression inhibited tumor growth and metastasis in *in vivo* mouse models and synergized with CD47 blockade to yield a dramatic anticancer effect. **(A, B)** Growth of tumors developed by SW620 cells **(A)** and DLD1 **(B)** in RAG2$^{-/-}$ γc$^{-/-}$ mice. Mice engrafted with Ctrl^{KD} cells or ATP6AP2^{KD} cells were treated with PBS or anti-CD47 antibody. Tumor growth was measured by bioluminescence imaging. (n=5 for SW620 model and n=7 for DLD1 model, at 21 days after tumor engraftment). *$P < 0.05$, **$P < 0.01$ (*t* test). **(C, D)** Growth **(C)** and metastasis **(D)** of tumors developed by MDA-MB-231 cells in RAG2$^{-/-}$ γc$^{-/-}$ mice. Mice orthotopically engrafted with Ctrl^{KD}, CD47^{KD}, AP2^{KD}, or double knockdown (Double^{KD}) MDA-MB-231 cells. Tumor growth and metastasis were measured by bioluminescence imaging (n=7, 7, 8, 8). In **(C)** Left, Tumor growth curve, *$P < 0.05$, **$P < 0.01$ (*t* test); Right, animal image from different groups. In **(D)** Left, luminescence signals of lung metastases at day 35, **$P < 0.01$ (*t* test); Right, animal image from different groups.

in the tumors and investigated whether targeting V-ATPase could reverse these effects and generate a pro-phagocytic microenvironment. We demonstrated that disruption of V-ATPase reverted extracellular pH back to a neutral level (**Figure 5C** and **Figures S4C, D**) without directly impacting the viability of cancer cells (**Figures S4E, F**). Therefore, we engrafted mice with Ctrl^{KD} DLD1 cells or ATP6AP2^{KD} DLD1 cells which are deficient in the capability of acidifying extracellular medium, and assessed TAMs from tumors developed by these cells by examining their cell surface marker expression. While the expression of markers related to antigen-presentation, such as CD80 and CD86 (66), as well as ligands for immune checkpoints, such as PD-L1, remained unchanged, there was a significant downregulation of CD206 expression in macrophages taken from tumors resulted from ATP6AP2^{KD} cancer cells (**Figures 5D–I**). Because CD206 is a well-defined marker representing polarization toward M2-like macrophages (67), we then examined the M1- (classically activated macrophages; CD206^{-}, MHC II^{high}) and M2- (alternatively activated macrophages; CD206^{+}, MHC II$^{low/neg}$) like tumor-associated macrophages, and found a significant increase of the ratio of M1:M2 macrophages (**Figures 5J**), suggesting that the disruption of the acidic tumor microenvironment had compromised the recruitment and enrichment of CD206-expressing M2-like TAMs in the tumors. We further investigated the cytokine and chemokine profiling of ATP6AP2 ^{KD} MDA-MB-231 cells by quantifying 48 different human cytokine and chemokine secreted by MDA-MB-231 cells at the protein level. We found

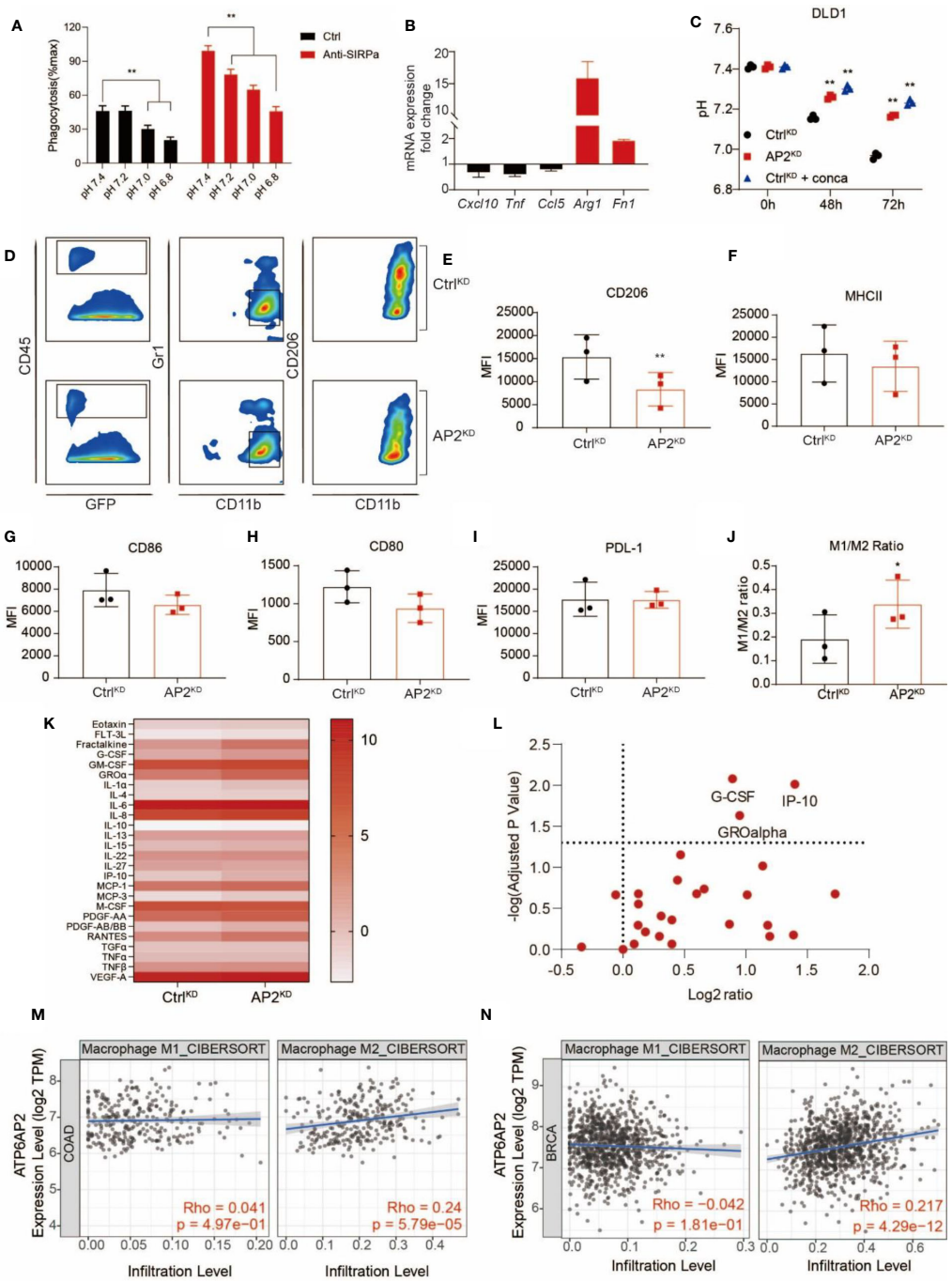

FIGURE 5 | V-ATPase-mediated extracellular acidification facilitated cancer cell evasion of PrCR *via* inhibition of macrophage phagocytic ability and recruitment of M2-like TAMs. **(A)** A phagocytosis assay with BMDMs and SW620 cells in media with a pH ranging from 6.8 to 7.4 showing that acidic medium attenuated macrophage-mediated PrCR toward cancer cells in the absence or presence of CD47 blockades. Each group was compared with corresponding Ctrl group. $^{**}P < 0.01$ (one-way *ANOVA* test). **(B)** mRNA expression of *Cxcl10, Tnf, Ccl5, Arg1* and *Fn1* in BMDMs cultured at acidic pH as compared to that in BMDMs cultured at natural pH. **(C)** V-ATPase inhibition by ATP6AP2 KD or concanamycin A reverted extracellular acidification by DLD1 cells. Each group was compared with the $Ctrl^{KD}$ group. $^{**}P < 0.01$ (one-way *ANOVA* test). **(D)** Representative FACS plots showing the expression of CD206 (bottom) on TAMs from tumors developed by $Ctrl^{KD}$ or $ATPAP2^{KD}$ DLD1 cells in mice. **(E–I)** Mean Fluorescent Intensity (MFI) of CD206, MHC II, CD86, CD80 or PD-L1 expression on TAMs from tumors developed by $Ctrl^{KD}$ or $ATPAP2^{KD}$ DLD1 cells in mice. $^{**}P < 0.01$ (Paired *t* test). **(J)** The ratio of M1:M2 TAMs from tumors developed by $Ctrl^{KD}$ or $ATPAP2^{KD}$ DLD1 cells in mice. $^{*}P < 0.05$ (Paired *t* test). **(K)** Measurement of cytokine and chemokine secretion profiling of $Ctrl^{KD}$ and ATP6AP2 ^{KD} MDA-MB-231 cells. Scale bars indicated Log_2(pg/mL). **(L)** Volcano plot showing the differences of cytokine and chemokine secretion by $Ctrl^{KD}$ and ATP6AP2 ^{KD} MDA-MB-231 cells. **(M, N)** Correlation of ATP6AP2 expression with M1 and M2 macrophage infiltration in TCGA colon cancer (n=458) **(M)** and breast cancer (n=1100) **(N)** datasets.

significantly higher G-CSF, IP-10 and GROα concentration in the ATP6AP2 ^{KD} cell medium (**Figures 5K, L**). Although the roles of G-CSF in macrophage polarization remained to be determined, IP-10 and GROα has been found in many studies to be involved in recruiting proinflammatory leukocytes and reprograming macrophage towards M1 polarization (68, 69). These results suggested that the inhibition of V-ATPase function in cancer cells may be linked to the production in proinflammatory cytokines, although such a link to eliciting the tumor microenvironment toward a proinflammatory state remains to be determined by further analysis. In addition, we found V-ATPase related genes including ATP6V1A, ATP6V0D1, ATP6AP1 and ATP6AP2 expression were positively correlated with M2 macrophage infiltration but not M1 macrophage in TCGA colon cancer and breast cancer dataset (**Figures 5M, N** and **Figures S4G–S4L**), which is consistent with our findings that acidic tumor microenvironment facilitated polarization and recruitment of M2-like macrophages.

Cell surface proteome is the interface mediating intercellular interaction including communications between cancer cells and the immune system, and many of the cell surface receptors have become important therapeutic targets for blocking cancer cell proliferation, survival and immune evasion (70–73). Therefore, we investigated the effects of V-ATPase disruption on cancer cell surface proteomic landscape. SW620 cells were treated with vehicles or concanamycin to inhibit V-ATPase activity and subjected to an antibody array to examine cell surface marker expression. A panel of 332 antibodies were included in the antibody array and cell surface marker expression was assessed by flow cytometry. We discovered that 15 proteins were significantly upregulated on the cell surface, and 3 proteins were significantly downregulated (**Figures 6A–C**). CD71 is one such protein whose expression on SW620 cells was dramatically upregulated upon blockade of V-ATPase (**Figures 6A–C**). CD71, or transferrin receptor 1, was previously identified as a therapeutic target for antibody-mediated cancer therapy (45, 74). The anti-cancer effects of CD71 antibodies can be achieved by direct cytotoxic effect through crosslinking of the receptor, or by antibody-dependent cell-mediated cytotoxicity/phagocytosis (ADCC/ADCP) based on Fc effector functions. We confirmed induction of CD71 surface exposure upon V-ATPase blockade in both SW620 and MDA-MB-231 cells (**Figures 6D, E**) and reasoned that the upregulated exposure of CD71 induced by V-ATPase blockade may further enhance the efficacy of anti-CD71 antibodies in inducing PrCR. Indeed, we found that treatment of SW620 or MDA-MB-231 cells with anti-CD71 antibodies was able to induce PrCR of the cells in a Fc-dependent manner (**Figures 6F, G**). Furthermore, using four different monoclonal antibodies recognizing CD71, we demonstrated that cells with their V-ATPase blocked had become significantly more susceptible to CD71 antibody-induced PrCR (**Figures 6F, G**).

DISCUSSION

The identification of T cell immune checkpoints and the development of therapies targeting these immune inhibitory regulatory mechanisms have revolutionized cancer therapeutics (75, 76). As essential components of immune regulatory programs, negative signaling induced by ligand binding causes a downregulation of the immune response to avoid overactivation of immune activities (77). So far, over ten of such immune checkpoints have been identified, such as PD-1, CTLA4, TIM3, and so on. These immune checkpoints have been found to function at different stages of the T cell's lifecycle, including the priming, proliferation, and effector phases. Blocking immune checkpoints has been found to elicit T and NK cell attack of malignant cells and lead to significant anti-cancer immune responses (78). Tumor-associated macrophages represent the largest population of immune cells present in tumors and metastases (4, 5). The identification of immune checkpoints on TAMs and their ligands on cancer cells revealed the therapeutic potential for re-activating macrophages in the tumor microenvironment for direct phagocytosis and elimination of cancer cells (10, 11). The blockade of immune checkpoints on macrophages subsequently restored their ability to carry out PrCR. Recent progress in numerous preclinical models and clinical trials has revealed the therapeutic potential of inducing PrCR as a new class of promising immunotherapy (21, 22, 53).

Despite the exciting progress, it remains unclear whether and how the tumor microenvironment at different stages of tumor development impacts the PrCR ability of TAMs. The metabolic programs in cancer cells are characterized by aerobic glycolysis even when sufficient oxygen is present, known as the Warburg effect, during which 2 mol of ATP can be generated per mol of glucose (32). This directly contrasts with oxidative phosphorylation, in which 32 mol of ATP can be generated per mol of glucose. Glucose is converted to lactic acid during aerobic glycolysis, which is secreted out of the cell to acidify the microenvironment (40). The Warburg effect allows for rapid ATP synthesis and provides intermediate biosynthetic materials, both of which are critical for meeting the high proliferative demands of cancer cells (33, 43). In addition to this, acidity generated by lactic acid secretion into the extracellular medium leads to remodeling at the tumor-stroma interface to facilitate tumor invasion (79). The accumulation of lactic acid and acidification of tumor sites have been reported to block lymphocyte infiltration into tumors by limiting glucose supply and diminishing T cell and NK cell activity (80, 81).

Here we show that the acidic microenvironment resulting from the Warburg effect significantly attenuates macrophage-mediated PrCR against cancer cells. Interestingly, in addition to directly inhibiting the phagocytic ability of macrophages, an acidic microenvironment may be involved in polarizing TAMs towards a M2-like phenotype, therefore compromising the detection and recognition of cancer cells. We demonstrate that targeting V-ATPase on cancer cells to disrupt their proton pumping machinery dramatically promoted cancer cell recognition and PrCR. Importantly, resistance to PrCR induced by CD47-blockade has been described in several types of cancers, which is not attributable to the deficiency of CD47 expression on these cells nor the contribution of other known "don't eat me" signals, suggesting the existence of additional anti-PrCR mechanisms (82–84). Our results reveal a strategy of activating PrCR

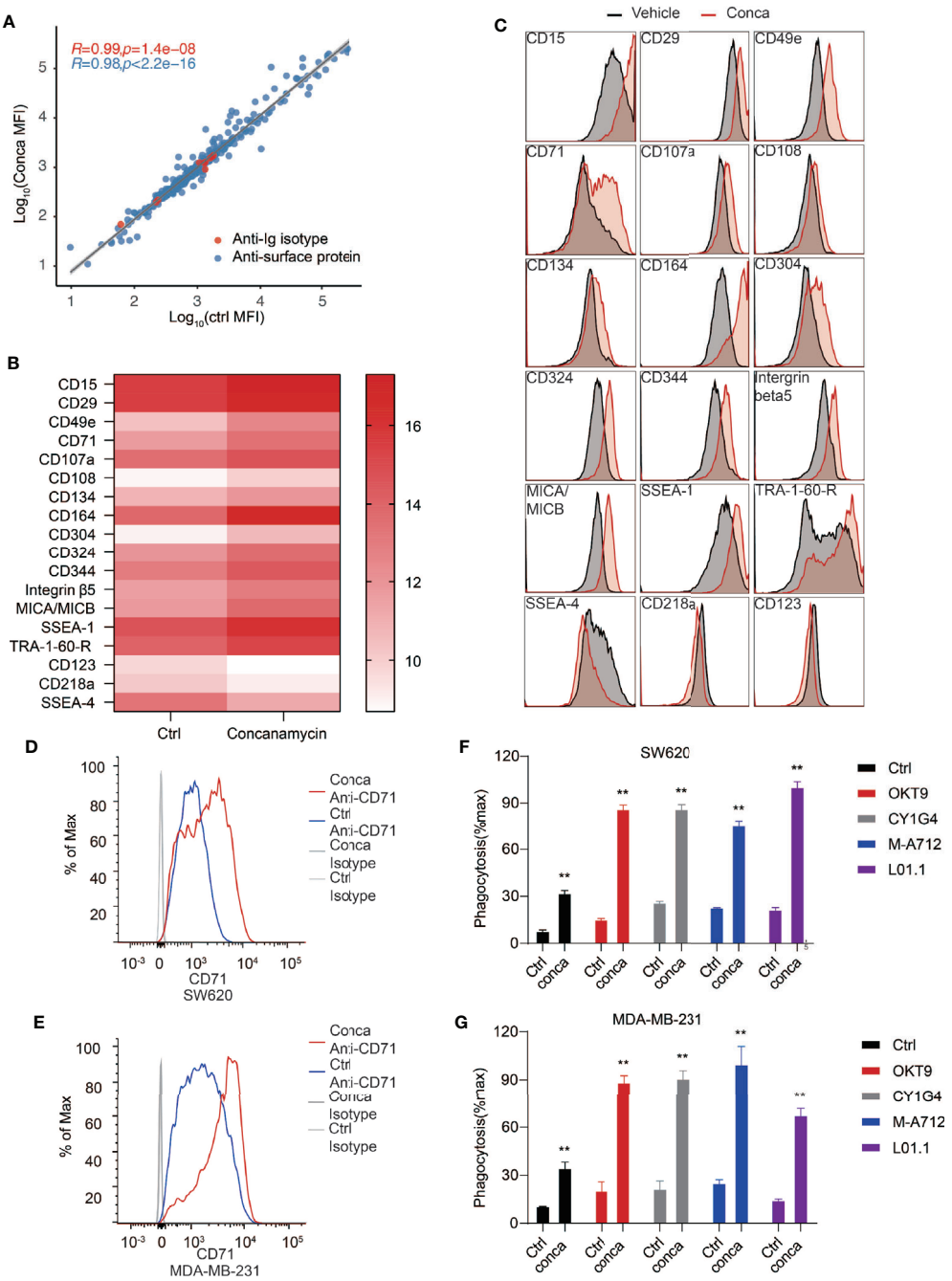

FIGURE 6 | Cell surface proteome analysis revealed CD71 as a potential target for synthetic PrCR upon V-ATPase inhibition. **(A)** Examination of cell surface marker expression on SW620 cells treated with vehicles or concanamycin with an antibody array containing a panel of 332 antibodies. **(B)** Identification of 15 upregulated and 3 downregulated surface proteins upon concanamycin treatment. **(C)** Representative flow cytometry staining of the upregulated and downregulated surface proteins on SW620 upon concanamycin treatment. **(D, E)** Flow cytometry analyses showing the upregulation CD71 expression on the cell surface of concanamycin-treated SW620 **(D)** or MDA-MB-231 **(E)** cells. **(F, G)** Phagocytosis assay with BMDMs showing that concanamycin treatment enabled macrophage-mediated PrCR of SW620 **(F)** or MDA-MB-231 **(G)** cells induced by CD71 antibodies. Each group was compared with corresponding Ctrl group. $^{**}P < 0.01$ (*t* test).

independent of and complementary to current PrCR-based therapies by blocking CD47 on cancer cells. Therefore, this may represent a widely applicable treatment approach for various cancers, including those with limited or no CD47 expression.

Cell surface proteins on cancer cells play important roles in transmitting extracellular signals and mediating their interactions with the immune cells, and thus are critical for cancer cells to maintain a highly proliferative state and escape from

immunosurveillance (70–73). Therefore, cell surface receptors are important therapeutic targets for cancer treatment. In this study, we deduced a "synthetic PrCR" model, in which the blockade of V-ATPase enhances cell surface exposure of therapeutic markers such as CD71 and the ADCP effects from targeting such markers using antibodies was found to be dramatically improved. Future studies will be performed to further characterize subgroups of TAMs and decipher their molecular phenotypes in the acidic tumor microenvironment. This will then be used to develop strategies to convert TAM populations with a hampered PrCR ability to PrCR-competent groups for superior success at cancer detection and subsequent elimination.

DATA AVAILABILITY STATEMENT

The raw data supporting the conclusions of this article will be made available by the authors, without undue reservation.

ETHICS STATEMENT

The animal study was reviewed and approved by Laboratory Animal Care at City of Hope Comprehensive Cancer Center.

AUTHOR CONTRIBUTIONS

JC, XC, BL and MF designed the research, and performed and analyzed the experiments; ZZ, SC, SM, GN and SL performed and analyzed the experiments; LW, WG, JY and PL contributed to the experimental design and scientific input; JC and XC prepared the figures; JC, XC, SL and MF wrote and edited the manuscript; MF supervised the laboratory. All authors contributed to the article and approved the submitted version.

ACKNOWLEDGMENTS

We thank the excellent technical support of Core Facilities at City of Hope, including the Analytical Cytometry, Animal Resource Center and Small Animal Imaging Core Facilities supported by the National Cancer Institute of the National Institutes of Health under award number P30CA033572. This work was supported by the National Cancer Institute of the National Institutes K99/R00 Pathway to Independence Award K99CA201075/R00CA201075 (to MF), the Damon Runyon-Dale F. Frey Award for Breakthrough Scientists DFS-22-16 (to MF), the Margaret E. Early Medical Research Trust Grant (to MF), the V Foundation for Cancer Research V Scholar Award (V2018-012) (MF) and the startup research funding from City of Hope (to MF). Funds from anonymous donors helped accelerate these studies.

SUPPLEMENTARY MATERIAL

The Supplementary Material for this article can be found online at: https://www.frontiersin.org/articles/10.3389/fimmu.2020.621757/full#supplementary-material

REFERENCES

1. Gajewski TF, Schreiber H, Fu YX. Innate and adaptive immune cells in the tumor microenvironment. *Nat Immunol* (2013) 14(10):1014–22. doi: 10.1038/ni.2703
2. Binnewies M, Roberts EW, Kersten K, Chan V, Fearon DF, Merad M, et al. Understanding the tumor immune microenvironment (TIME) for effective therapy. *Nat Med* (2018) 24(5):541–50. doi: 10.1038/s41591-018-0014-x
3. Belli C, Trapani D, Viale G, D'Amico P, Duso BA, Della Vigna P, et al. Targeting the microenvironment in solid tumors. *Cancer Treat Rev* (2018) 65:22–32. doi: 10.1016/j.ctrv.2018.02.004
4. Franklin RA, Liao W, Sarkar A, Kim MV, Bivona MR, Liu K, et al. The cellular and molecular origin of tumor-associated macrophages. *Science* (2014) 344 (6186):921–5. doi: 10.1126/science.1252510
5. Noy R, Pollard JW. Tumor-associated macrophages: from mechanisms to therapy. *Immunity* (2014) 41(1):49–61. doi: 10.1016/j.immuni.2014.06.010
6. O'Sullivan C, Lewis CE. Tumour-associated leucocytes: friends or foes in breast carcinoma. *J Pathol* (1994) 172(3):229–35. doi: 10.1002/path.1711720302
7. Ruffell B, Coussens LM. Macrophages and therapeutic resistance in cancer. *Cancer Cell* (2015) 27(4):462–72. doi: 10.1016/j.ccell.2015.02.015
8. Qian BZ, Li J, Zhang H, Kitamura T, Zhang J, Campion LR, et al. CCL2 recruits inflammatory monocytes to facilitate breast-tumour metastasis. *Nature* (2011) 475(7355):222–5. doi: 10.1038/nature10138
9. Yang M, McKay D, Pollard JW, Lewis CE. Diverse Functions of Macrophages in Different Tumor Microenvironments. *Cancer Res* (2018) 78(19):5492–503. doi: 10.1158/0008-5472.CAN-18-1367
10. Jaiswal S, Chao MP, Majeti R, Weissman IL. Macrophages as mediators of tumor immunosurveillance. *Trends Immunol* (2010) 31(6):212–9. doi: 10.1016/j.it.2010.04.001
11. Chao MP, Majeti R, Weissman IL. Programmed cell removal: a new obstacle in the road to developing cancer. *Nat Rev Cancer* (2012) 12(1):58–67. doi: 10.1038/nrc3171
12. Majeti R, Chao MP, Alizadeh AA, Pang WW, Jaiswal S, Gibbs KD Jr., et al. CD47 is an adverse prognostic factor and therapeutic antibody target on human acute myeloid leukemia stem cells. *Cell* (2009) 138(2):286–99. doi: 10.1016/j.cell.2009.05.045
13. Willingham SB, Volkmer JP, Gentles AJ, Sahoo D, Dalerba P, Mitra SS, et al, et al. The CD47-signal regulatory protein alpha (SIRPa) interaction is a therapeutic target for human solid tumors. *Proc Natl Acad Sci USA* (2012) 109 (17):6662–7. doi: 10.1073/pnas.1121623109
14. Barkal AA, Weiskopf K, Kao KS, Gordon SR, Rosental B, Yiu YY, et al. Engagement of MHC class I by the inhibitory receptor LILRB1 suppresses macrophages and is a target of cancer immunotherapy. *Nat Immunol* (2018) 19(1):76–84. doi: 10.1038/s41590-017-0004-z
15. Barkal AA, Brewer RE, Markovic M, Kowarsky M, Barkal SA, Zaro BW, et al. CD24 signalling through macrophage Siglec-10 is a target for cancer immunotherapy. *Nature* (2019) 572(7769):392–6. doi: 10.1038/s41586-019-1456-0
16. Feng M, Jiang W, Kim BY, Zhang CC, Fu Y-X, Weissman IL. Phagocytosis checkpoints as new targets for cancer immunotherapy. *Nat Rev Cancer* (2019) 19(10):568–86. doi: 10.1038/s41568-019-0183-z
17. Russ A, Hua AB, Montfort WR, Rahman B, Riaz IB, Khalid MU, et al. Blocking "don't eat me" signal of CD47-SIRPalpha in hematological malignancies, an in-depth review. *Blood Rev* (2018) 32(6):480–9. doi: 10.1016/j.blre.2018.04.005
18. Jalil AR, Andrechak JC, Discher DE. Macrophage checkpoint blockade: results from initial clinical trials, binding analyses, and CD47-SIRPalpha structure-function. *Antib Ther* (2020) 3(2):80–94. doi: 10.1093/abt/tbaa006

19. Jaiswal S, Chao MP, Majeti R, Weissman IL. Macrophages as mediators of tumor immunosurveillance. *Trends Immunol* (2010) 31(6):212–9. doi: 10.1016/j.it.2010.04.001
20. Jaiswal S, Jamieson CH, Pang WW, Park CY, Chao MP, Majeti R, et al. CD47 is upregulated on circulating hematopoietic stem cells and leukemia cells to avoid phagocytosis. *Cell* (2009) 138(2):271–85. doi: 10.1016/j.cell.2009.05.046
21. Sikic BI, Lakhani N, Patnaik A, Shah SA, Chandana SR, Rasco D, et al. First-in-Human, First-in-Class Phase I Trial of the Anti-CD47 Antibody Hu5F9-G4 in Patients With Advanced Cancers. *J Clin Oncol* (2019) 37(12):946–53. doi: 10.1200/JCO.18.02018
22. Advani R, Flinn I, Popplewell L, Forero A, Bartlett NL, Ghosh N, et al. CD47 Blockade by Hu5F9-G4 and Rituximab in Non-Hodgkin's Lymphoma. *N Engl J Med* (2018) 379(18):1711–21. doi: 10.1056/NEJMoa1807315
23. Feng M, Chen JY, Weissman-Tsukamoto R, Volkmer JP, Ho PY, McKenna KM, et al. Macrophages eat cancer cells using their own calreticulin as a guide: roles of TLR and Btk. *Proc Natl Acad Sci USA* (2015) 112(7):2145–50. doi: 10.1073/pnas.1424907112
24. Chen J, Zhong MC, Guo H, Davidson D, Mishel S, Lu Y, et al. SLAMF7 is critical for phagocytosis of haematopoietic tumour cells via Mac-1 integrin. *Nature* (2017) 544(7651):493–7. doi: 10.1038/nature22076
25. Chan KS, Espinosa I, Chao M, Wong D, Ailles L, Diehn M, et al. Identification, molecular characterization, clinical prognosis, and therapeutic targeting of human bladder tumor-initiating cells. *Proc Natl Acad Sci USA* (2009) 106(33):14016–21. doi: 10.1073/pnas.0906549106
26. Edris B, Weiskopf K, Volkmer AK, Volkmer JP, Willingham SB, Contreras-Trujillo H, et al. Antibody therapy targeting the CD47 protein is effective in a model of aggressive metastatic leiomyosarcoma. *Proc Natl Acad Sci USA* (2012) 109(17):6656–61. doi: 10.1073/pnas.1121629109
27. Gholamin S, Mitra SS, Feroze AH, Liu J, Kahn SA, Zhang M, et al. Disrupting the CD47-SIRPalpha anti-phagocytic axis by a humanized anti-CD47 antibody is an efficacious treatment for malignant pediatric brain tumors. *Sci Transl Med* (2017) 9(381). doi: 10.1126/scitranslmed.aaf2968
28. Petrova PS, Viller NN, Wong M, Pang X, Lin GH, Dodge K, et al. TTI-621 (SIRPalphaFc): A CD47-Blocking Innate Immune Checkpoint Inhibitor with Broad Antitumor Activity and Minimal Erythrocyte Binding. *Clin Cancer Res* (2017) 23(4):1068–79. doi: 10.1158/1078-0432.CCR-16-1700
29. Xiao Z, Chung H, Banan B, Manning PT, Ott KC, Lin S, et al. Antibody mediated therapy targeting CD47 inhibits tumor progression of hepatocellular carcinoma. *Cancer Lett* (2015) 360(2):302–9. doi: 10.1016/j.canlet.2015.02.036
30. Lim AR, Rathmell WK, Rathmell JC. The tumor microenvironment as a metabolic barrier to effector T cells and immunotherapy. *Elife* (2020) 9. doi: 10.7554/eLife.55185
31. Cairns RA, Harris IS, Mak TW. Regulation of cancer cell metabolism. *Nat Rev Cancer* (2011) 11(2):85–95. doi: 10.1038/nrc2981
32. Hsu PP, Sabatini DM. Cancer cell metabolism: Warburg and beyond. *Cell* (2008) 134(5):703–7. doi: 10.1016/j.cell.2008.08.021
33. Vander Heiden MG, Cantley LC, Thompson CB. Understanding the Warburg Effect: The Metabolic Requirements of Cell Proliferation. *Science* (2009) 324 (5930):1029–33. doi: 10.1126/science.1160809
34. Payen VL, Mina E, Van Hee VF, Porporato PE, Sonveaux P. Monocarboxylate transporters in cancer. *Mol Metab* (2020) 33:48–66. doi: 10.1016/j.molmet.2019.07.006
35. Whitton B, Okamoto H, Packham G, Crabb SJ. Vacuolar ATPase as a potential therapeutic target and mediator of treatment resistance in cancer. *Cancer Med* (2018) 7(8):3800–11. doi: 10.1002/cam4.1594
36. Maxson ME, Grinstein S. The vacuolar-type H+-ATPase at a glance – more than a proton pump. *J Cell Sci* (2014) 127(23):4987–93. doi: 10.1242/jcs.158550
37. Smith GA, Howell GJ, Phillips C, Muench SP, Ponnambalam S, Harrison MA. Extracellular and luminal pH regulation by vacuolar H+-ATPase isoform expression and targeting to the plasma membrane and endosomes. *J Biol Chem* (2016) 291(16):8500–15. doi: 10.1074/jbc.M116.723395
38. Forgac M. Vacuolar ATPases: rotary proton pumps in physiology and pathophysiology. *Nat Rev Mol Cell Biol* (2007) 8(11):917–29. doi: 10.1038/nrm2272
39. Estrella V, Chen T, Lloyd M, Wojtkowiak J, Cornnell HH, Ibrahim-Hashim A, et al. Acidity generated by the tumor microenvironment drives local invasion. *Cancer Res* (2013) 73(5):1524–35. doi: 10.1158/0008-5472.CAN-12-2796
40. Webb BA, Chimenti M, Jacobson MP, Barber DL. Dysregulated pH: a perfect storm for cancer progression. *Nat Rev Cancer* (2011) 11(9):671–7. doi: 10.1038/nrc3110
41. Fais S, Venturi G, Gatenby B. Microenvironmental acidosis in carcinogenesis and metastases: new strategies in prevention and therapy. *Cancer Metastasis Rev* (2014) 33(4):1095–108. doi: 10.1007/s10555-014-9531-3
42. Faes S, Duval AP, Planche A, Uldry E, Santoro T, Pythoud C, et al. Acidic tumor microenvironment abrogates the efficacy of mTORC1 inhibitors. *Mol Cancer* (2016) 15(1):1–11. doi: 10.1186/s12943-016-0562-y
43. Liberti MV, Locasale JW. The Warburg Effect: How Does it Benefit Cancer Cells? *Trends Biochem Sci* (2016) 41(3):211–8. doi: 10.1016/j.tibs.2015.12.001
44. Hegde PS, Karanikas V, Evers S. The where, the when, and the how of immune monitoring for cancer immunotherapies in the era of checkpoint inhibition. *Clin Cancer Res* (2016) 22(8):1865–74. doi: 10.1158/1078-0432.CCR-15-1507
45. Shen Y, Li X, Dong D, Zhang B, Xue Y, Shang P. Transferrin receptor 1 in cancer: a new sight for cancer therapy. *Am J Cancer Res* (2018) 8(6):916–31.
46. Li T, Fu J, Zeng Z, Cohen D, Li J, Chen Q, et al. TIMER2.0 for analysis of tumor-infiltrating immune cells. *Nucleic Acids Res* (2020) 48(W1):W509–14. doi: 10.1093/nar/gkaa407
47. Gentles AJ, Newman AM, Liu CL, Bratman SV, Feng W, Kim D, et al. The prognostic landscape of genes and infiltrating immune cells across human cancers. *Nat Med* (2015) 21(8):938–45. doi: 10.1038/nm.3909
48. Sanjana NE, Shalem O, Zhang F. Improved vectors and genome-wide libraries for CRISPR screening. *Nat Methods* (2014) 11(8):783–4. doi: 10.1038/nmeth.3047
49. Qi LS, Larson MH, Gilbert LA, Doudna JA, Weissman JS, Arkin AP, et al. Repurposing CRISPR as an RNA-guided platform for sequence-specific control of gene expression. *Cell* (2013) 152(5):1173–83. doi: 10.1016/j.cell.2013.02.022
50. Goodwin ML, Gladden LB, Nijsten MW, Jones KB. Lactate and cancer: revisiting the warburg effect in an era of lactate shuttling. *Front Nutr* (2014) 1:27. doi: 10.3389/fnut.2014.00027
51. Lozupone F, Borghi M, Marzoli F, Azzarito T, Matarrese P, Iessi E, et al. TM9SF4 is a novel V-ATPase-interacting protein that modulates tumor pH alterations associated with drug resistance and invasiveness of colon cancer cells. *Oncogene* (2015) 34(40):5163–74. doi: 10.1038/onc.2014.437
52. Damaghi M, Wojtkowiak JW, Gillies RJ. pH sensing and regulation in cancer. *Front Physiol* (2013) 4:370. doi: 10.3389/fphys.2013.00370
53. Majeti R, Chao MP, Alizadeh AA, Pang WW, Jaiswal S, Gibbs KD Jr, et al. CD47 is an adverse prognostic factor and therapeutic antibody target on human acute myeloid leukemia stem cells. *Cell* (2009) 138(2):286–99. doi: 10.1016/j.cell.2009.05.045
54. Drory O, Frolow F, Nelson N. Crystal structure of yeast V-ATPase subunit C reveals its stator function. *EMBO Rep* (2004) 5(12):1148–52. doi: 10.1038/sj.embor.7400294
55. Horng JL, Lin LY, Huang CJ, Katoh F, Kaneko T, Hwang PP. Knockdown of V-ATPase subunit A (atp6v1a) impairs acid secretion and ion balance in zebrafish (Danio rerio). *Am J Physiol Regul Integr Comp Physiol* (2007) 292(5): R2068–76. doi: 10.1152/ajpregu.00578.2006
56. Lee SH, Rho J, Jeong D, Sul JY, Kim T, Kim N, et al. v-ATPase V0 subunit d2-deficient mice exhibit impaired osteoclast fusion and increased bone formation. *Nat Med* (2006) 12(12):1403–9. doi: 10.1038/nm1514
57. Guida MC, Hermle T, Graham LA, Hauser V, Ryan M, Stevens TH, et al. ATP6AP2 functions as a V-ATPase assembly factor in the endoplasmic reticulum. *Mol Biol Cell* (2018) 29(18):2156–64. doi: 10.1091/mbc.E18-04-0234
58. Kinouchi K, Ichihara A, Sano M, Sun-Wada GH, Wada Y, Kurauchi-Mito A, et al. The (pro)renin receptor/ATP6AP2 is essential for vacuolar H+-ATPase assembly in murine cardiomyocytes. *Circ Res* (2010) 107(1):30–4. doi: 10.1161/CIRCRESAHA.110.224667
59. Chen LQ, Pagel MD. Evaluating pH in the Extracellular Tumor Microenvironment Using CEST MRI and Other Imaging Methods. *Adv Radiol* (2015) 2015. doi: 10.1155/2015/206405
60. Tannock IF, Rotin D. Acid pH in tumors and its potential for therapeutic exploitation. *Cancer Res* (1989) 49(16):4373–84.
61. Wike-Hooley JL, Haveman J, Reinhold HS. The relevance of tumour pH to the treatment of malignant disease. *Radiother Oncol* (1984) 2(4):343–66. doi: 10.1016/S0167-8140(84)80077-8

62. Anderson M, Moshnikova A, Engelman DM, Reshetnyak YK, Andreev OA. Probe for the measurement of cell surface pH in vivo and ex vivo. *Proc Natl Acad Sci USA* (2016) 113(29):8177–81. doi: 10.1073/pnas.1608247113
63. Zhang M, Hutter G, Kahn SA, Azad TD, Gholamin S, Xu CY, et al. Anti-CD47 treatment stimulates phagocytosis of glioblastoma by M1 and M2 polarized macrophages and promotes M1 polarized macrophages in vivo. *PloS One* (2016) 11(4):e0153550. doi: 10.1371/journal.pone.0153550
64. Jablonski KA, Amici SA, Webb LM, Ruiz-Rosado Jde D, Popovich PG, Partida-Sanchez S, et al. Novel Markers to Delineate Murine M1 and M2 Macrophages. *PloS One* (2015) 10(12):e0145342. doi: 10.1371/journal.pone.0145342
65. Martinez FO, Gordon S, Locati M, Mantovani A. Transcriptional profiling of the human monocyte-to-macrophage differentiation and polarization: new molecules and patterns of gene expression. *J Immunol* (2006) 177(10):7303–11. doi: 10.4049/jimmunol.177.10.7303
66. Jimenez-Uribe AP, Valencia-Martinez H, Carballo-Uicab G, Vallejo-Castillo L, Medina- Rivero E, Chacon-Salinas R, et al. CD80 Expression Correlates with IL-6 Production in THP-1-Like Macrophages Costimulated with LPS and Dialyzable Leukocyte Extract (Transferon(R)). *J Immunol Res* (2019) 2019:2198508. doi: 10.1155/2019/2198508
67. Jaynes JM, Sable R, Ronzetti M, Bautista W, Knotts Z, Abisoye-Ogunniyan A, et al. Mannose receptor (CD206) activation in tumor-associated macrophages enhances adaptive and innate antitumor immune responses. *Sci Transl Med* (2020) 12(530). doi: 10.1126/scitranslmed.aax6337
68. Mantovani A, Sica A, Sozzani S, Allavena P, Vecchi A, Locati M. The chemokine system in diverse forms of macrophage activation and polarization. *Trends Immunol* (2004) 25(12):677–86. doi: 10.1016/j.it.2004.09.015
69. Upadhyay S, Sharma N, Gupta KB, Dhiman M. Role of immune system in tumor progression and carcinogenesis. *J Cell Biochem* (2018) 119(7):5028–42. doi: 10.1002/jcb.26663
70. Kuhlmann L, Cummins E, Samudio I, Kislinger T. Cell-surface proteomics for the identification of novel therapeutic targets in cancer. *Expert Rev Proteomics* (2018) 15(3):259–75. doi: 10.1080/14789450.2018.1429924
71. Lee JK, Bangayan NJ, Chai T, Smith BA, Pariva TE, Yun S, et al. Systemic surfaceome profiling identifies target antigens for immune-based therapy in subtypes of advanced prostate cancer. *Proc Natl Acad Sci USA* (2018) 115(19):E4473–82. doi: 10.1073/pnas.1802354115
72. Ohaegbulam KC, Assal A, Lazar-Molnar E, Yao Y, Zang X. Human cancer immunotherapy with antibodies to the PD-1 and PD-L1 pathway. *Trends Mol Med* (2015) 21(1):24–33. doi: 10.1016/j.molmed.2014.10.009
73. Das M, Zhu C, Kuchroo VK. Tim-3 and its role in regulating anti-tumor immunity. *Immunol Rev* (2017) 276(1):97–111. doi: 10.1111/imr.12520
74. Tortorella S, Karagiannis TC. Transferrin receptor-mediated endocytosis: a useful target for cancer therapy. *J Membr Biol* (2014) 247(4):291–307. doi: 10.1007/s00232-014-9637-0
75. Sharma P, Allison JP. The future of immune checkpoint therapy. *Science* (2015) 348(6230):56–61. doi: 10.1126/science.aaa8172
76. Topalian SL, Drake CG, Pardoll DM. Immune checkpoint blockade: a common denominator approach to cancer therapy. *Cancer Cell* (2015) 27(4):450–61. doi: 10.1016/j.ccell.2015.03.001
77. Hanahan D, Weinberg RA. Hallmarks of cancer: the next generation. *Cell* (2011) 144(5):646–74. doi: 10.1016/j.cell.2011.02.013
78. Galluzzi L, Chan TA, Kroemer G, Wolchok JD, Lopez-Soto A. The hallmarks of successful anticancer immunotherapy. *Sci Transl Med* (2018) 10(459). doi: 10.1126/scitranslmed.aat7807
79. Ho PC, Liu PS. Metabolic communication in tumors: a new layer of immunoregulation for immune evasion. *J Immunother Cancer* (2016) 4:4. doi: 10.1186/s40425-016-0109-1
80. Brand A, Singer K, Koehl GE, Kolitzus M, Schoenhammer G, Thiel A, et al. LDHA-Associated Lactic Acid Production Blunts Tumor Immunosurveillance by T and NK Cells. *Cell Metab* (2016) 24(5):657–71. doi: 10.1016/j.cmet.2016.08.011
81. Harmon C, Robinson MW, Hand F, Almuaili D, Mentor K, Houlihan DD, et al. Lactate-Mediated Acidification of Tumor Microenvironment Induces Apoptosis of Liver-Resident NK Cells in Colorectal Liver Metastasis. *Cancer Immunol Res* (2019) 7(2):335–46. doi: 10.1158/2326-6066.CIR-18-0481
82. Anderson KL, Snyder KM, Ito D, Lins DC, Mills LJ, Weiskopf K, et al. Evolutionarily conserved resistance to phagocytosis observed in melanoma cells is insensitive to upregulation of pro-phagocytic signals and to CD47 blockade. *Melanoma Res* (2020) 30(2):147–58. doi: 10.1097/CMR.0000000000000629
83. Jain S, Van Scoyk A, Morgan EA, Matthews A, Stevenson K, Newton G, et al. Targeted inhibition of CD47-SIRPalpha requires Fc-FcgammaR interactions to maximize activity in T-cell lymphomas. *Blood* (2019) 134(17):1430–40. doi: 10.1182/blood.2019001744
84. Weiskopf K, Jahchan NS, Schnorr PJ, Cristea S, Ring AM, Maute RL, et al. CD47-blocking immunotherapies stimulate macrophage-mediated destruction of small-cell lung cancer. *J Clin Invest* (2016) 126(7):2610–20. doi: 10.1172/JCI81603

Conflict of Interest: MF declares patent applications pertaining to stimulating TLR/BTK signaling to promote CRT in macrophages assigned to the Stanford University and equity and/or consulting with Forty Seven, Inc.

The remaining authors declare that the research was conducted in the absence of any commercial or financial relationships that could be construed as a potential conflict of interest.

Copyright © 2021 Chen, Cao, Li, Zhao, Chen, Lai, Muend, Nossa, Wang, Guo, Ye, Lee and Feng. This is an open-access article distributed under the terms of the Creative Commons Attribution License (CC BY). The use, distribution or reproduction in other forums is permitted, provided the original author(s) and the copyright owner(s) are credited and that the original publication in this journal is cited, in accordance with accepted academic practice. No use, distribution or reproduction is permitted which does not comply with these terms.

frontiers in Immunology

ORIGINAL RESEARCH
published: 12 February 2021
doi: 10.3389/fimmu.2020.607048

Bacterial and Fungal Toll-Like Receptor Activation Elicits Type I IFN Responses in Mast Cells

*Lisa Kornstädt[1], Sandra Pierre[1], Andreas Weigert[2], Stefanie Ebersberger[3], Tim J. Schäufele[1], Anja Kolbinger[1], Tobias Schmid[2], Jennifer Cohnen[1], Dominique Thomas[1], Nerea Ferreirós[1], Bernhard Brüne[2,4], Ingo Ebersberger[5,6,7] and Klaus Scholich[1,4,8]**

[1] Institute of Clinical Pharmacology, University Hospital Goethe-University Frankfurt, Frankfurt, Germany, [2] Faculty of Medicine, Institute of Biochemistry I, Goethe-University Frankfurt, Frankfurt, Germany, [3] Institute of Molecular Biology gGmbH, Mainz, Germany, [4] Project Group Translational Medicine and Pharmacology, Fraunhofer Institute for Molecular Biology and Applied Ecology IME, Frankfurt am Main, Germany, [5] Department for Applied Bioinformatics, Institute for Cell Biology and Neuroscience, Goethe-University Frankfurt, Frankfurt, Germany, [6] Senckenberg Biodiversity and Climate Research Centre (S-BIKF), Frankfurt am Main, Germany, [7] LOEWE Centre for Translational Biodiversity Genomics (TBG), Frankfurt am Main, Germany, [8] Fraunhofer Cluster of Excellence for Immune-Mediated Diseases (CIMD), Frankfurt am Main, Germany

Next to their role in IgE-mediated allergic diseases and in promoting inflammation, mast cells also have antiinflammatory functions. They release pro- as well as antiinflammatory mediators, depending on the biological setting. Here we aimed to better understand the role of mast cells during the resolution phase of a local inflammation induced with the Toll-like receptor (TLR)-2 agonist zymosan. Multiple sequential immunohistology combined with a statistical neighborhood analysis showed that mast cells are located in a predominantly antiinflammatory microenvironment during resolution of inflammation and that mast cell-deficiency causes decreased efferocytosis in the resolution phase. Accordingly, FACS analysis showed decreased phagocytosis of zymosan and neutrophils by macrophages in mast cell-deficient mice. mRNA sequencing using zymosan-induced bone marrow-derived mast cells (BMMC) revealed a strong type I interferon (IFN) response, which is known to enhance phagocytosis by macrophages. Both, zymosan and lipopolysaccharides (LPS) induced IFN-β synthesis in BMMCs in similar amounts as in bone marrow derived macrophages. IFN-β was expressed by mast cells in paws from naïve mice and during zymosan-induced inflammation. As described for macrophages the release of type I IFNs from mast cells depended on TLR internalization and endosome acidification. In conclusion, mast cells are able to produce several mediators including IFN-β, which are alone or in combination with each other able to regulate the phagocytotic activity of macrophages during resolution of inflammation.

Keywords: mast cells, inflammation, resolution, IFN-β, toll-like receptor, phagocytosis

OPEN ACCESS

Edited by:
Johnathan Canton, Francis Crick Institute, United Kingdom

Reviewed by:
Justine T. Tigno-Aranjuez, University of Central Florida, United States
Claudia Gonzalez-Espinosa, Instituto Politécnico Nacional de México (CINVESTAV), Mexico

***Correspondence:**
Klaus Scholich
scholich@em.uni-frankfurt.de

Specialty section:
This article was submitted to Molecular Innate Immunity, a section of the journal Frontiers in Immunology

Received: *16 September 2020*
Accepted: *29 December 2020*
Published: *12 February 2021*

Citation:
Kornstädt L, Pierre S, Weigert A, Ebersberger S, Schäufele TJ, Kolbinger A, Schmid T, Cohnen J, Thomas D, Ferreirós N, Brüne B, Ebersberger I and Scholich K (2021) Bacterial and Fungal Toll-Like Receptor Activation Elicits Type I IFN Responses in Mast Cells. Front. Immunol. 11:607048. doi: 10.3389/fimmu.2020.607048

INTRODUCTION

Mast cells are part of the first line of defense of the body, protecting against invading pathogens and other environmental harm. They are long-lived, tissue-resident leukocytes, located most abundantly close to surfaces exposed to the environment, like skin and mucosal tissues. Their most characteristic feature is the secretory granules densely packed with pre-formed mediators, which can be released rapidly upon activation by degranulation. Mast cell activation can also induce *de novo* synthesis and release of lipid mediators (e.g. prostaglandin (PG) E2 and thromboxane), cytokines and chemokines (1, 2). The precise response and signaling pathway activated in a mast cell depends on the stimulus activating the cell, which can be recognized and discriminated by an extensive repertoire of receptors. These receptors coordinate the selective release of proinflammatory (e.g. histamine, interleukin (IL)-1β) or antiinflammatory (e.g. IL-4, IL-10, IL-13) mediators (1, 3).

To detect invading pathogens, mast cells express a variety of pattern recognition receptors (PRRs), including Toll-like receptors (TLRs). TLRs are transmembrane proteins located at the cell surface or in intracellular compartments like endosomes or lysosomes. They form homo- or heterodimers and recruit a set of adaptor molecules such as MyD88 and TRIF for signaling (4, 5). While MyD88 is known to be utilized by all TLRs except for TLR3, TRIF is considered to be selectively recruited to TLR3 and TLR4. The MyD88-dependent pathway leads to the activation of the NF-κB pathway and the MAPK pathway, resulting in the induction of pro-inflammatory cytokines like IL-1β. The TRIF-dependent pathway depends on TLRs present on endosomes and mediates the induction of type I IFNs and IFN-inducible genes by activating transcription factors of the IFN regulatory factor (IRF) family (4, 5). Notably, intracellular localization of TLR4 can also be required for the MyD88-dependent pathway (6).

As part of the anti-viral response, e.g. against SARS-CoV-2, mast cells release a specific set of proinflammatory mediators, including IL-1 and IL-6, which are positively associated with COVID-19 severity (7, 8). Also type I IFNs were originally described to be induced as an anti-viral response but are also produced in response to bacterial pathogens (9). The family of type I IFNs consists of at least 13 IFN-α isotypes, one IFN-β isotype and various others. The cytosolic TLR receptors TLR3, TLR7, and TLR9 sense viral nucleic acids and respond by initiating the type I IFN response. TLR4 activates the MyD88-dependent NF-κB pathway while located in the plasma membrane and starts type I IFN signaling through TRIF when internalized into endosomal compartments. Induction of the type I IFN response by TLR2 also takes place from endosomal compartments, but in a MyD88-dependent pathway (10–12).

Here we aimed to investigate the potential roles of antiinflammatory mediators released by mast cells during the resolution phase of a local zymosan-induced inflammation. Zymosan-induced inflammation is a widely used model for local short-lasting inflammation and evokes well-defined inflammatory and behavioral responses. In an untargeted mRNA sequencing approach to identify transcriptional changes in mast cells in response to the TLR2 ligand zymosan, we found strong upregulation of genes involved in the type I IFN response. We further showed that mast cells produce type I IFNs also in response to LPS, which activates TLR4. This was surprising since mast cells were believed to lack the ability to produce type I IFNs as answer to TLR4 activation, due to being unable to internalize surface-bound pathogens (13, 14). Furthermore, as previously shown for macrophages (12, 13) the induction of the type I IFN response is elicited from endosomal compartments also in mast cells.

MATERIALS AND METHODS

Animals

C57BL/6N mice were supplied by Janvier (Le Genest, France). Mcpt5-DTA-Cre mice were originally described and provided by Professor Axel Roers, Technische Universität Dresden, Germany (15). Sex and age matched Mcpt5-DTA-Cre$^-$ litter mates were used as control mice for Mcpt5-DTA-Cre$^+$ mice. The animals were cared for according to the International Association for the Study of Pain guidelines (Grants FK1066, FK1093, and FK1138). For all experiments, the ethics guidelines for investigations in conscious animals were obeyed and the procedures were approved by the local ethics committee (Regierungspräsidium Darmstadt). The animals had free access to food (Sniff standard diet) and water and were maintained in climate- (23°C ± 0.5°C) and light-controlled rooms (light from 6.00 a.m. to 6.00 p.m.).

Behavioral Tests

Inflammation was induced by injection of 10 µl zymosan (12 mg/ml in PBS, #Z4250, Sigma-Aldrich) subcutaneously into the plantar side of one hind paw. Mechanical hypersensitivity was determined by measuring the latency of paw withdrawal using a plantar aesthesiometer (Dynamic Plantar Aesthesiometer, Ugo Basile). A force range of 0 to 5 g with a ramp of 0.5 g/s was applied with a steel rod of 2 mm in diameter, until a strong and immediate withdrawal occurred. The cutoff time was set to 20 s.

Multi Epitope Ligand Cartography (MELC)

MELC technology is an automated immunohistological imaging method and can be used to visualize very high numbers of antibodies on the same sample as described before (16–18). Briefly, tissues were embedded in tissue freezing medium (Tissue-Tek O.C.T. Compound, #4583, Sakura Finetek B.V.), cryosections of 10 µm thickness were applied on silane-coated coverslips, fixed in 4% paraformaldehyde in PBS for 15 min, permeabilized with 0.1% Triton X100 in PBS for 15 min and blocked with 3% BSA in PBS for 1 h. The sample was placed on the stage of a Leica DM IRE2 and a picture was taken. Then, in an automated procedure, the sample was incubated for 15 min with bleachable fluorescence-labeled antibodies and rinsed with PBS. Afterward, the phase contrast and fluorescence signals were imaged by a cooled charge-coupled device camera (Apogee KX4, Apogee Instruments). A bleaching step was performed to delete fluorescence signals, and the post-bleaching image was recorded. Then the next antibody was applied and the process

repeated. For data analysis, fluorescence images produced by each antibody were aligned pixel-wise and were corrected for illumination faults using flat-field correction. The post-bleaching images were subtracted from their following fluorescence image. The antibodies used for MELC analysis were against CD11b (BioRad, #MCA74F), CD11c (Miltenyi Biotec, #130-102-799), CD31 (BD Biosciences, #553373), CD45 (Miltenyi Biotec, #130-091-609), CD54 (Biolegend, #116105), CD80 (Biolegend, #104706), CD86 (Biolegend, #105008), CD117 (Bioss, #bs-10005R-Cy5), CD206 (AbDSerotec, #MCA22335FA), F4 80 (Biolegend, #123107), IL-1β (Thermo Fisher, #11-7114-82), IL-4 (Biolegend, #504109), IL-10 (eBioscience, #11-7101), IL-13 (Invitrogen, #53-7133-82), Ly6C (eBioscience, #17-5932-80), Ly6G (eBioscience, #11-5931-82), MHC II (Miltenyi Biotec, #120-000-810), Siglec F (BD Pharmingen, #562068). Nuclei were stained with propidium iodide (PI) (Sigma-Aldrich, #P4170)

Analysis of MELC Data

In a first step all greyscale antibody channel images were processed using ImageJ 1.52v to diminish noise, background fluorescence and remove artifacts for further analyses if necessary. Subsequently, images for propidium iodide (cell nuclei) and CD45 were used for single-cell segmentation using Cell Profiler (version 3.1.9) (19). The resulting segmentation mask was loaded into histoCAT (version 1.76) (20) together with the corresponding antibody channel images. All images, excluding zymosan images and images used for single-cell mask generation, were z-score normalized and used for Barnes-Hut t-SNE (BH t-SNE) (21) and PhenoGraph analysis (22) as implemented in histoCAT. PhenoGraph defines cell clusters based on single-cell mask and marker colocalization (k was set to 20 or 30). BH t-SNE scatter plot was overlaid with a colored PhenoGraph cluster map. To investigate the relationship between clusters, neighborhood analysis under standard conditions as implemented in histoCAT was used (20).

Multiplex Cytokine Assay

Cytokine and chemokine levels were determined in ipsi- and contralateral paws of Cre^- and Cre^+ Mcpt5-DTA mice 48 h after injection of 10 µl 12 mg/ml zymosan, using the Bio-Plex Pro mouse cytokine group I (Bio-Rad). Tissue samples of paws were dissected and frozen directly at −80°C until protein extraction. The tissue was lysed in 400 µl lysis buffer (1x Protease Inhibitor Cocktail (#11697498001, Roche) in Tissue Extraction Reagent (#FNN0071, Invitrogen). Samples were cut in small pieces and then sonicated twice at 60% power for 10 sec with an Ultrasonic Homogenizer (SONOPULS HD2070 MS73, Bandelin). Afterwards all samples were centrifuged for 10 min at 10,000 g and the supernatant harvested. The concentration of total protein in the samples was assessed by the bicinchoninic acid assay. All samples were diluted to a final protein concentration of 200–900 µg/ml, according to the kit requirements. The concentrations of IL-1α, IL-1β, IL-2, IL-3, IL-4, IL-5, IL-6, IL-9, IL-10, IL-12p40, IL12-p70, IL-13, IL-17, Eotaxin, G-CSF, GM-CSF, IFN-γ, CXCL1 (KC), CCL2 (MCP-1), CCL3 (MIP-1α), CCL4 (MIP-1β), CCL5 (RANTES), TNF-α were measured with a Bioplex 200 (Bio-Rad). The concentration was then normalized to the total protein concentration of the respective sample and is shown as pg/mg protein.

Polychromatic Flow Cytometry

Mcpt5-DTA Cre^- and Cre^+ mice were injected with 10 µl zymosan (12 mg/ml #Z4250, Sigma-Aldrich) and pHrodo Red zymosan Bioparticles (#P35364, Invitrogen) per paw into the plantar side of one hind paw per mouse. Polychromatic flow cytometry was performed essentially as described previously (23). Briefly, single-cell suspensions were generated from solid tissues (<1 mm^3), by digestion with 3 mg/ml Collagenase IA (Sigma) DMEM for 45 min at 37°C, followed by filtration through a 70 µm nylon mesh (BD Life Sciences). Then the cells were incubated for 5 min in DMEM containing 10% FCS to stop the lysis followed by incubation in ACK buffer for 5 min. After centrifugation (1,000 g, 5 min), the cells were washed in PBS and resuspended in 30 µl FACS buffer (1% FCS in PBS), followed by incubation with an antibody cocktail for 1 h at 4°C. Cells were transferred to FACS tubes. Samples were acquired with a FACS Canto II flow cytometer and analyzed using FlowJo software V10 (both BD Biosciences). For gating, fluorescence minus 1 (FMO) controls were used. The antibodies used for FACS analysis were: CD117-PE (Miltenyi, #130-102-795), FcεRIα-FITC (#134305, Biolegend), Ly6C-eFluor450 (eBioscience #48-5932-82) Ly6G/Ly6C-FITC (eBioscience, #11-5931-82), F4/80-PE/Cy7 (Biolegend, #123113), F4/80-PE (Biolegend, #123110), SiglecF-PE-Vio770 (Miltenyi, #130-102-167), CD45-VioGreen (Miltenyi, #130-123-900), CD206-APC (Biolegend, #141708), CD86-BrilliantViolet421 (Biolegend, #105031), CD11b-APC/Cy7 (Biolegend, #101225), MHCII-FITC (Miltenyi, 130-081-601). For analysis of phagocytosed neutrophils, intracellular staining with Ly6G-APC (Biolegend, #127614) was performed. Cells were prepared as described above, incubated with ACK buffer, fixed for 5 min with 1% PFA and washed with PBS. Then the cells were permeabilized with 0.1% Saponin and incubated for 1 h at 4°C with antibodies in FACS buffer containing 0.1% Saponin. After the incubation, the cells were washed with 0.1% Saponin and resuspended in PBS for flow cytometry analysis.

Bone Marrow-Derived Mast Cells (BMMCs)

BMMCs were prepared as described earlier (24). Bone marrow cells were isolated from murine femur and tibia from the hind legs of adult mice. The bones were cut open at one end and centrifuged at 10,000 g for 1 min. The cells of a single animal were resuspended in 40 ml of mast cell medium consisting of RPMI 1640 medium supplemented with 10% fetal bovine serum, 100 U/ml penicillin/streptomycin, 4 mM L-Glutamine, 1 mM sodium pyruvate, 1% MEM nonessential amino acids, 50 µM 2-mercaptoethanol and 10 µg/L IL-3 (#213-13, PeproTech). Forty milliliters of medium was added twice a week. The cells were cultivated for 4 to 6 weeks at 37°C with 5% CO_2 under humidified conditions. After 4–6 weeks, the purity and maturity of the mast cells was assessed by FACS analysis on a

FACS Canto II flow cytometer (BD Life Sciences). For FACS analysis, a portion of the cells was centrifuged at 500 g for 10 min, washed with PBS and then resuspended in FACS buffer (1% FCS in PBS). The cells were then incubated for 1 h with CD117-PE (130-102-795, Miltenyi Biotec) and FcεRIα-FITC (#134305, Biolegend) at 4°C, washed and analyzed on a FACS Canto II flow cytometer (BD Life Sciences) (**Figure S1**).

Bone Marrow-Derived Macrophages (BMDMs)

BMDMs were prepared as described earlier (16). Bone marrow cells were isolated from murine femur and tibia from the hind legs of adult mice. The bones were cut open at one end and centrifuged at 10,000 g for 1 min. The cells were differentiated in macrophage medium consisting of RPMI 1640 GlutaMAX medium supplemented with 10% fetal bovine serum, 100 U/ml penicillin/streptomycin, and 20 ng/ml macrophage colony stimulating factor (M-CSF, #AF-315-02, Peprotech). Non-adherent cells were removed after one day of cultivation by exchange of medium, fresh medium was added after 4 days. Cells were grown for 7 days at 37°C and 5% CO2. Non-adherent cells were removed after one day of cultivation by exchange of medium, fresh medium was added after 4 days.

RNA Sequencing

BMMCs were cultivated for 4–6 weeks as described, then the cell number was adjusted to $8x10^5$ cells/ml and the cells were treated with 10 µg/ml zymosan for 24 h or 48 h or left untreated (0 h). Cells were stained as described above and then sorted using a FACS Aria (BD Biosciences) to obtain a pure population of $CD117^+$/FcεRIα^+ double-positive cells. RNA was isolated from the FACS-sorted cells using the RNeasy micro Kit (Qiagen, #74004). Library preparation was carried out with the QuantSeq 3' mRNA Library Prep Kit FWD (Lexogen). The quality of the libraries was controlled with a Bioanalyzer High Sensitivity DNA Assay (Agilent Technologies), quantification was carried out using a Qubit dsDNA HS assay (Thermo Fisher Scientific). Sequencing was performed on a NextSeq500 using a NextSeq500 High Output (75 cyc) Kit (Illumina).

The raw sequencing reads were preprocessed with the software bcl2fastq. Read mapping against the mouse reference genome (GRCm38.p6, primary assembly) was done with the STAR aligner (version 2.6.0a 2018/04/23) (25). The mapped reads were assigned to annotated features (genes) using the Bioconductor package Rsubread (v1.28.1) (26). Unassignable reads comprise reads overlapping with more than one gene (ambiguous), non-unique mappers and reads that map outside known genes. On average 75% of uniquely mapped reads could be assigned to genes. Differential expression of genes between conditions was assessed with the Bioconductor package DESeq2 (v1.18.1) (27). Gene ontology analysis was performed with the gene set library "GO Biological Processes 2018" by EnrichR (28, 29).

Cytokine Measurements

BMMCs were cultivated for 4–6 weeks as described, then the cell number was adjusted to $8x10^5$ cells/ml in mast cell medium and the cells were pre-incubated and induced as indicated in the respective figure legends with 25 µM Cytochalasin D (#C2618, Sigma-Aldrich), 50 µM Bafilomycin A (#SML1661, Sigma-Aldrich), and 10 µg/ml zymosan (#Z4250, Sigma-Aldrich) or 100 ng/ml LPS (#L3129, Sigma-Aldrich). BMDMs were cultivated for 7 days as described and induced with 10 µg/ml zymosan. Cytokines were measured at the indicated time points after induction using the following ELISA Kits: Mouse IL-10 Quantikine (#M1000B), Mouse IL-1 beta/IL-1F2 Quantikine (#MLB00C), Mouse IFN-beta Quantikine (#MIFNB0, all from R&D Systems), VeriKine-HS (High Sensitivity) Mouse IFN Alpha All Subtype (#42115-1, PBL Assay Science).

LC-MS/MS

LC-MS/MS analysis of PGE_2 in BMMC culture medium was performed as described previously (24). Briefly, 100 µl PBS, 100 µl 150 mM EDTA, and 20 µl internal standard solution (10 ng/ml of [$^2H_4$]-PGE_2 in methanol) were added to 100 µl cell suspension before extraction liquid-liquid extraction using with 600 µl ethyl acetate. Organic layer was separated and the extraction was repeated using again 600 µl ethyl acetate. The organic layers were combined, evaporated at 45°C under a gentle stream of nitrogen and reconstituted with 50 µl of acetonitrile:water:formic acid (20:80:0.0025, v/v). 10 µl of this solution were injected into the LC-MS/MS system. For LC-MS/MS analysis an Agilent 1290 Infinity LC system (Agilent, Waldbronn, Germany) coupled to a hybrid triple quadrupole linear ion trap mass spectrometer QTRAP 6500+ (Sciex, Darmstadt, Germany) equipped with a Turbo-V-source operating in negative ESI mode was used. Chromatographic separation was done using a Synergi Hydro-RP column (2.0 x 150 mm, 4 µm particle size; Phenomenex, Aschaffenburg, Germany), coupled to a precolumn of the same material. 0.0025% formic acid and acetonitrile containing 0.0025% formic acid served as mobile phases. Mass spectrometric parameters were: Ionspray-voltage −4,500 V, source temperature 500°C, curtain-gas 40 psi, nebulizer-gas 40 psi, Turboheater-gas 60 psi. Both quadrupoles were running at unit resolution. For analysis, Analyst Software 1.6 and Multiquant Software 3.0 (both Sciex, Darmstadt, Germany) were used, employing the internal standard method (isotope-dilution mass spectrometry).

Statistical Analysis

Statistical significance was determined by unpaired t-test, one-way ANOVA using a Tukey's post-test or Dunnett's post-test, or two-way ANOVA using a Sidak's post-test through the GraphPad Prism 6 software as outlined in the figure legends.

RESULTS

Mast Cells Influence Macrophage Phagocytosis During Resolution of Zymosan-Induced Inflammation

To study the time course of the inflammatory response to the TLR2 ligand zymosan, we determined the mechanical

hypersensitivity after subcutaneous injection of zymosan into the plantar side of one hind paw. Mechanical hypersensitivity increased significantly as early as 1 h after zymosan injection and was maintained for at least 8 h after injection. Afterwards hypersensitivity receded until it returned to baseline at day 5 (**Figure 1A**). The receding mechanical hypersensitivity is indicative for the resolution phase of the inflammation. To study the localization of mast cells and to determine their neighboring cells during resolution of inflammation, MELC analyses were performed with paws from naïve mice as well as

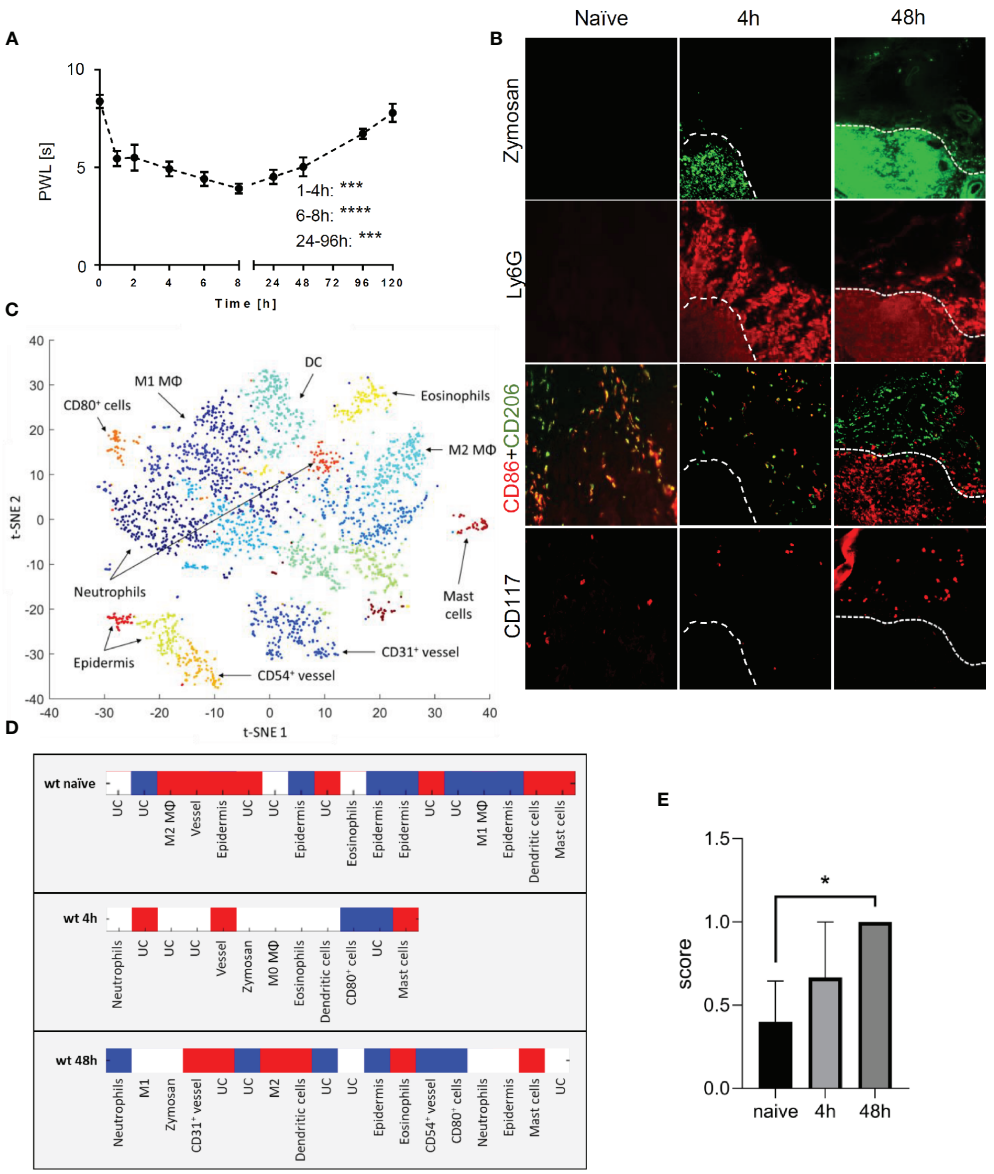

FIGURE 1 | Mast cells are located in antiinflammatory regions during resolution phase of zymosan-induced inflammation. **(A)** Mechanical paw withdrawal latencies in mice (n=10) at indicated time points after injection of zymosan (10 µl, 12 mg/ml in PBS). Data are mean ± S.E.M., one-way ANOVA, Dunnett's test vs. baseline, ***p<0.001, ****p<0.0001. **(B)** Representative images of immunohistological multi epitope ligand cartography (MELC) staining of paws form naïve mice or 4 h or 48 h after injection of zymosan. FITC-labeled zymosan, marker for pro-inflammatory cells (CD86), anti-inflammatory cells (CD206), mast cells (CD117) are shown in false colors. White dotted lines depict the outline of the zymosan-filled area in the paw. **(C)** Representative Barnes-Hut t-SNE (BH t-SNE) plot colored by cell clusters defined by PhenoGraph analysis. Underlying images originate from MELC analysis of mice paw 48 h after zymosan injection. The positions of some cell types are depicted in the plot. DC, dendritic cells; MΦ, macrophages. **(D)** Heat map showing a representative result of the neighborhood analysis for mast cells in naïve paw and 4 h or 48 h after zymosan injection (n=3–4). UC, unidentified cluster. Red depicts cells, which neighbor mast cells more frequently than they would in random permutations of cell cluster labels in each image set. Blue depicts cell clusters neighbor less frequently than with randomly permuted cell labels and white depicts cells cluster neighbors with random frequency. **(E)** Averaged score for mast cell neighborhood regarding antiinflammatory macrophages (M2 MΦ) based on neighborhood analysis of naïve paw or 4 h or 48 h after injection of zymosan (n=3-4). A score was assigned for red=1, white=0, blue=−1. Data are shown as mean ± S.E.M., one-way ANOVA test, *p<0.05.

4 and 48 h after injection of zymosan into the paw. Throughout the time-course there was no significant increase of the mast cell number (**Figures S2A, B**). The MELC technology is an automated system, allowing the sequential imaging of an unrestricted number of directly labeled antibodies on the same tissue sample. To enable visualization of zymosan in the paw FITC-labeled zymosan was used for injection. At peak inflammation 4 h after zymosan injection, a time point with early inflammation and hypersensitivity, neutrophils ($Ly6G^+$) were located in and around the zymosan-containing region (**Figure 1B**). In addition the appearance of $CD86^+/CD206^+$ macrophages outside of the zymosan-containing region was observed. Forty-eight hours after zymosan injection, a time point with declining mechanical hypersensitivity, neutrophils ($Ly6G^+$) were located mainly in the same region as zymosan (**Figure 1B**) and proinflammatory $CD86^+$ cells were located in or near the zymosan-containing area. Antiinflammatory $CD206^+$ cells surrounded the region containing the $CD86^+$ cells (18). Quantitative analysis of the MELC data was performed using a machine learning approach using HistoCAT software (20), to determine individual cell phenotypes and their cellular microenvironments. Single-cell segmentation was performed based on staining for CD45 and nuclei, which was followed by PhenoGraph analysis allowing the discrimination of the different immune cell types including mast cells (**Figure 1C**). PhenoGraph analysis of MELC images for the relative location of 21 antibodies showed expression of cytokines with certain antiinflammatory properties (IL-4, IL-13, and IL-33) as well as the proinflammatory cytokine IL-1β in mast cells (**Figure S3**). To determine the cellular neighborhood of mast cells, a neighborhood analysis for all identified mast cells was performed. This analysis aims to determine which cell types are neighboring mast cells more often as expected for a random distribution (20). The analysis revealed that 48 h after zymosan antiinflammatory M2-like macrophages ($CD206^+$) and to a lesser degree eosinophils (Siglec F^+) and dendritic cells ($CD11c^+$, MHC II^+) are found in the neighborhood of mast cells (**Figure 1D**). Quantitation of the presence of M2-like macrophages in the cellular neighborhood of mast cells was subsequently performed with independent MELC runs using a scoring system differentiating between random distribution (0) as well as more (1) or less (−1) often than expected for random distribution. Here, the presence of M2-like macrophages next to mast cells reached significance 48 h after zymosan injection (**Figure 1E**). Proinflammatory M1-like macrophages ($CD86^+$) or neutrophils ($Ly6G^+$) in the neighborhood of mast cells are found in numbers corresponding to a random distribution (**Figure 1D**).

To assess potential effects of mast cells on the immune response, we compared in a first approach the expression patterns of macrophage populations using a PhenoGraph analysis of MELC images with inflamed paw tissue 48 h after zymosan-injection in Mcpt5-DTA-Cre mice. In these mice Cre recombinase is under control of the mouse mast cell protease 5 (Mcpt5) promotor and activates a Cre-dependent expression of the catalytically active diphtheria toxin A (DTA) subunit causing constitutive mast cell deficiency (15). Accordingly, remaining numbers of mast cells in paws from Cre^+ mice were around 20% as compared to Cre^- mice (**Figure S2C**). The PhenoGraph analysis showed a striking reduction of the Ly6G marker for neutrophil granulocytes in M1-like macrophages of the mast cell-deficient mice (Cre^+), which is suggestive for decreased efferocytosis (**Figure 2**, **Figure S4**). Notably, neutrophils were more present 4 h than 48 h after zymosan injection, while Ly6G-positive macrophages were more prominent 48 h after zymosan injection (**Figure S5**) reflecting increased efferocytosis during the resolution phase.

The observed potential reduction of efferocytosis was not due to alterations in the recruitment of immune cells to the site of inflammation, since the number of neutrophils, macrophages, dendritic cells and eosinophils were not changed in mast cell-deficient mice 48 h after zymosan injection (**Figure 3A**, **Figure S6A**). Thus, mast cell-derived cytokines do not contribute to the recruitment of cells in that phase of the inflammatory reaction. Also, macrophage polarization toward M1-like or M2-like phenotypes was not altered by the absence of mast cells 48 h after zymosan injection (**Figure 3B**, **Figure S6B**). Finally, since mast cells are known to regulate the ability of macrophages to phagocytose apoptotic cells, such as neutrophils (30), we determined phagocytotic activity of macrophages and neutrophils by injecting pH-sensitive pHrodo Red zymosan bioparticles, which become fluorescent after phagocytosis inside of lysosomes. Forty-eight hours after injection of these pHrodo Red zymosan particles FACS analysis showed no difference in the percentage of for pHrodo Red $zymosan^+$ neutrophils or the mean fluorescence intensity (MFI) in these cells between Cre^- and Cre^+ Mcpt5-DTA mice (**Figures 3C, D**). Most importantly, the percentage and the MFI of pHrodo Red $zymosan^+/F4\ 80^+$ macrophages were significantly decreased in mast cell-deficient mice (**Figures 3C, E**). Likewise, the phagocytotic activity of macrophages toward neutrophils, as determined by the percentage of macrophages showing phagocytosis of neutrophils ($Ly6G^+$), was decreased in mast cell-deficient mice (**Figures 3F, G**). Notably, the observed decreased phagocytotic activity of macrophages in mast cell-deficient mice did not lead to significant changes in the mechanical hypersensitivity between Cre^- and Cre^+ Mcpt5-DTA mice (**Figure S7**), demonstrating that the decreased efferocytosis is not taking part in the nociceptive processes underlying mechanical hypersensitivity.

To identify mediators, that mediate mast cell-regulated efferocytosis, we determined the levels of 23 cytokines, chemokines and growth factors in Cre^- and Cre^+ Mcpt5-DTA mice. Out of 23 mediators included in the screen, 11 were significantly increased in the inflamed paws of Mcpt5-DTA-Cre- mice as compared to tissue from untreated mice (**Figure 4**). Out of these 11 mediators only IL-4 and CXCL1 showed a significant difference in zymosan-injected paws between Cre^- and Cre^+ mice. Both mediators were significantly lower in zymosan-injected paws of mast cell-deficient mice. Other cytokines, such as IL-6 and IL-9, were only significantly elevated in zymosan treated paws from Cre^- mice, but did not reach significance between Cre^- and Cre^+ mice (**Figure 4**). IL-4 is known for driving polarization of macrophages

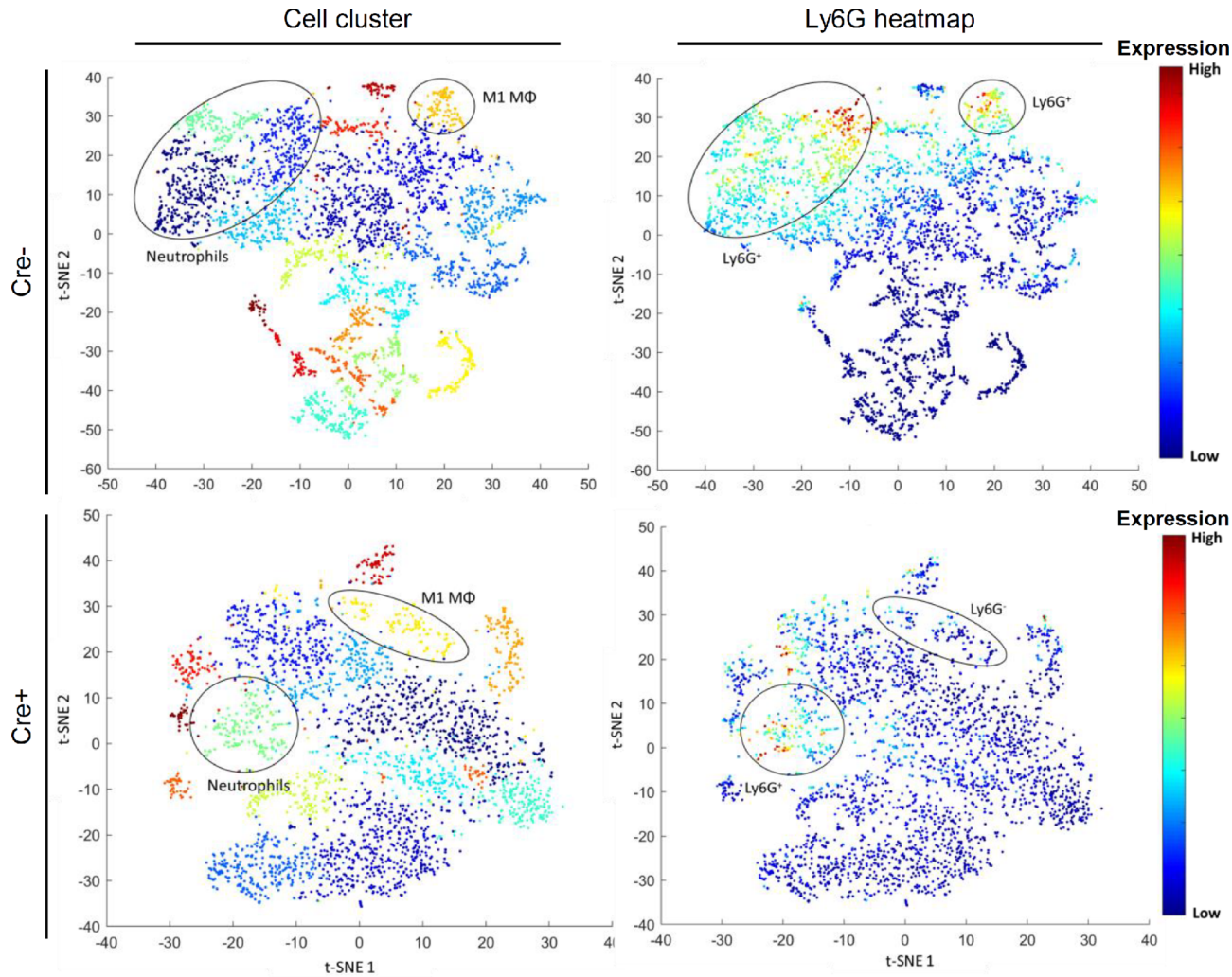

FIGURE 2 | M1 macrophage phagocytosis of neutrophils is reduced in mast cell-deficient Mcpt5-DTA Cre$^+$ mice compared to Cre$^-$ control mice. Images show representative BH t-SNE analysis from Mcpt5-DTA Cre$^+$ or Cre$^-$ mice 48 h after injection of zymosan. Plots on the left are colored by cell clusters defined by PhenoGraph analysis (**Figure S4**). Plots on the right are heatmaps for the expression of the neutrophil marker Ly6G. The position of cell phenotype clusters containing CD86$^+$ M1 macrophages (M1 MΦ) or neutrophils (Ly6G$^+$/F4 80$^-$) is indicated.

toward antiinflammatory (M2-like) phenotypes and CXCL1 for promoting chemotaxis of neutrophils. However, the decreased efferocytosis in mast cell-deficient mice cannot be explained by an increase of M1-like macrophages nor a decrease of neutrophil number, since neither of these effects was observed by flow cytometry analysis.

RNA Sequencing Shows Activation of Type I IFN Pathway in Zymosan-Induced Mast Cells

To better understand zymosan-induced changes in the gene expression of mast cells, we employed bone marrow-derived mast cells (BMMCs). First, we stimulated BMMCs with zymosan or LPS to determine the time course of their activation by determining the release of IL-10 and Il-1β. The levels of both cytokines reached a maximum after zymosan stimulation for 24–48 h (**Figure 5A**). A similar response was seen for LPS stimulation whereby the IL-10 release was markedly lower than during zymosan-stimulation (**Figure 5B**). Thus, to investigate the changes in gene expression induced by zymosan in mast cells in detail, we used untreated BMMCs as well as BMMCs stimulated for 24 or 48 h with zymosan, FACS-sorted them to homogeneity using antibodies against CD117 and FcεRIα (**Figure S8**) and performed the mRNA sequencing. The principal component analysis showed that the major differences in gene expression were seen between unstimulated and stimulated cells (**Figure 5C**). No significant differences in gene expression were detected between 24 and 48 h. Most of the significantly differentially expressed genes are upregulated at both time points when compared to unstimulated cells.

Gene ontology term enrichment analysis of the sequencing data showed that the most prominent response is the upregulation

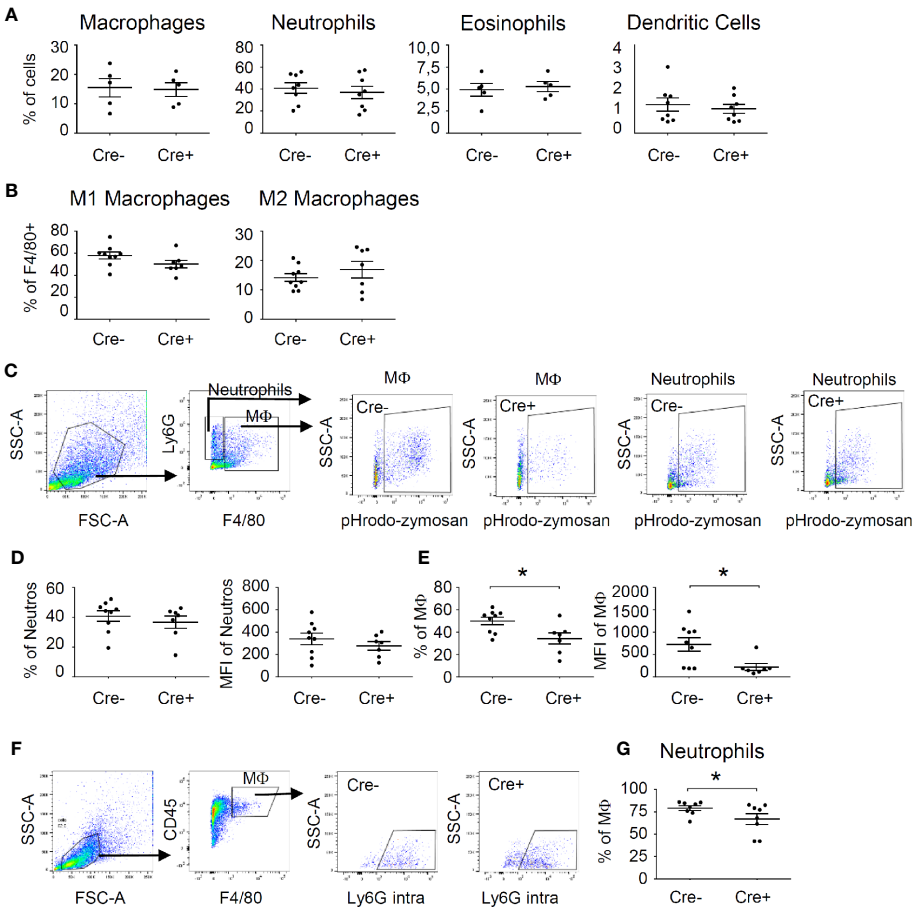

FIGURE 3 | Mast cells influence phagocytosing activity of macrophages during resolution phase of zymosan-induced inflammation. **(A)** FACS analysis for the number of neutrophils, macrophages, eosinophils and dendritic cells in Mcpt5-DTA-Cre$^-$ and Cre$^+$ mice 48 h after injection of zymosan (10 µl, 12 mg/ml in PBS). Data are shown in % of all cells as mean ± S.E.M. (n=5–9), unpaired two-tailed t-test. **(B)** Number of M1-like (CD86$^+$) macrophages and M2-like (CD206$^+$) macrophages 48 h after injection of zymosan (10 µl, 12 mg/ml in PBS). Data are shown in % of all F4 80$^+$ cells as mean ± S.E.M. (n=7–9), unpaired two-tailed t-test. **(C)** Gating strategy for flow cytometry analysis of phagocytosis of pHrodo Red zymosan by macrophages (F4 80$^+$) and neutrophils (F4 80$^-$/Ly6G$^+$). **(D, E)** Phagocytosis of pHrodo Red zymosan (10 µl, 12 mg/ml in PBS) by neutrophils (panel D) or macrophages (panel E) in Mcpt5-DTA-Cre$^-$ and Cre$^+$ mice 48 h after zymosan injection. Data are mean ± S.E.M. (n=7–9), unpaired two-tailed t-test, *p<0.05. **(F)** Gating strategy for flow cytometry analysis of phagocytosis of neutrophils by macrophages. Intracellular staining of Ly6G$^+$ neutrophils was performed. **(G)** Decreased phagocytosis of neutrophils (intracellular Ly6G) by macrophages (F4 80$^+$). Data are mean ± S.E.M. (n=7–9), unpaired two-tailed t-test, *p<0.05.

of the type I IFN pathway after 24 and 48 h incubation (**Figure 6A**, **Figure S9**). Eight and nine groups out of the top ten gene ontology terms were related to this response after 24 and 48 h, respectively. (**Figure 6A**, **Figure S9**). The type I IFN response is generally regarded as an anti-viral response, which explains why terms related to "response to virus" are assigned to some genes. Moreover, after 24 h the six strongest upregulated genes were all IFN-inducible genes (**Figure 6B**). One of the genes with the strongest increase (6,12 log2 fold change) after 24 h of zymosan stimulation is Interferon regulatory factor 7 (Irf7), a transcription factor, which mediates the induction of the type I IFN response by TLR ligands in macrophages (12). Likewise, Irf1 and Irf9 are upregulated, with a log2 fold increase of 1.45 and 2.18, respectively. Thus, so far the data show that in mast cells zymosan induces the release of several antiinflammatory cytokines, and additionally a type I IFN response is triggered. Either of the responses alone or in combination can serve to explain the altered efferocytosis by macrophages in mast cell-deficient mice. mRNA expression for the two mediators, IL-4 and CXCL1, which were at the protein level significantly lower in inflamed paws from mast cell-deficient mice, was also detected in the zymosan-stimulated BMMCs, although changes between untreated and treated cells did not reach significance due to variability of the expression levels.

Mast Cells Release of IFN-β in Response to Zymosan and LPS Requires Phagosome Maturation

Next, we aimed to validate the findings from the RNA sequencing approach by determining the concentration of type I IFNs released by BMMCs after induction with zymosan and LPS. The time course showed an early IFN-β increase in the medium (6 h after zymosan

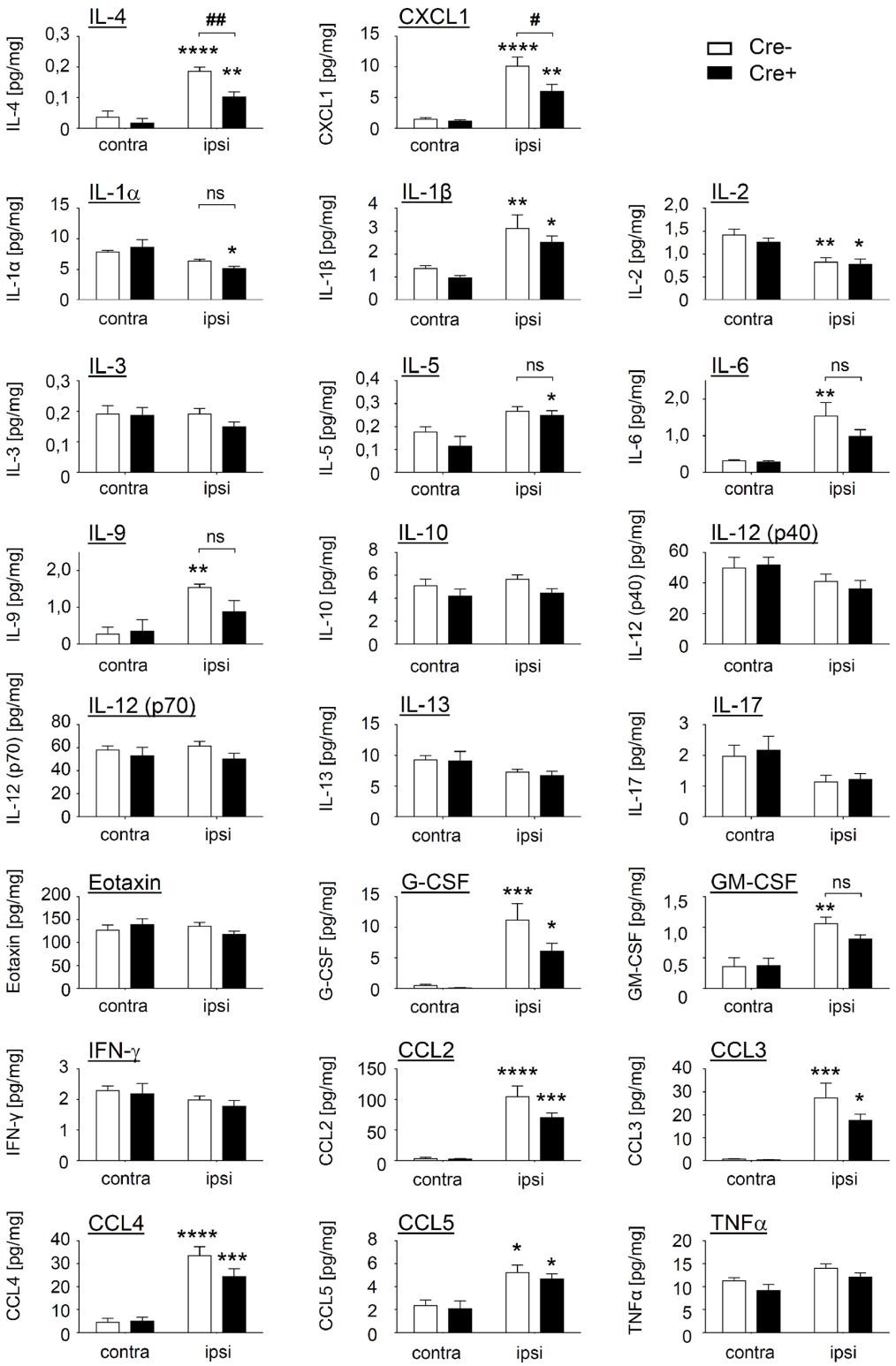

FIGURE 4 | Mast cells influence the level of IL-4 and CXCL1 in paws of zymosan-injected mice. Levels of 23 cytokines, chemokines and growth factors in contralateral paws (untreated) and ipsilateral paws 48 h after injection of zymosan (10 µl, 12 mg/ml in PBS) in Mcpt5-DTA Cre$^-$ and Cre$^+$ mice determined by multiplex cytokine assay. Data are mean ± S.E.M. (n=6). Two-way ANOVA, Tukey's multiple comparison test, significance between ipsi- and contralateral paws within one genotype is presented by *p<0.05, **p<0.01, ***p<0.001, ****p<0.0001, significance between genotypes is presented by $^{\#}$<0.05, $^{\#\#}$p<0.01.

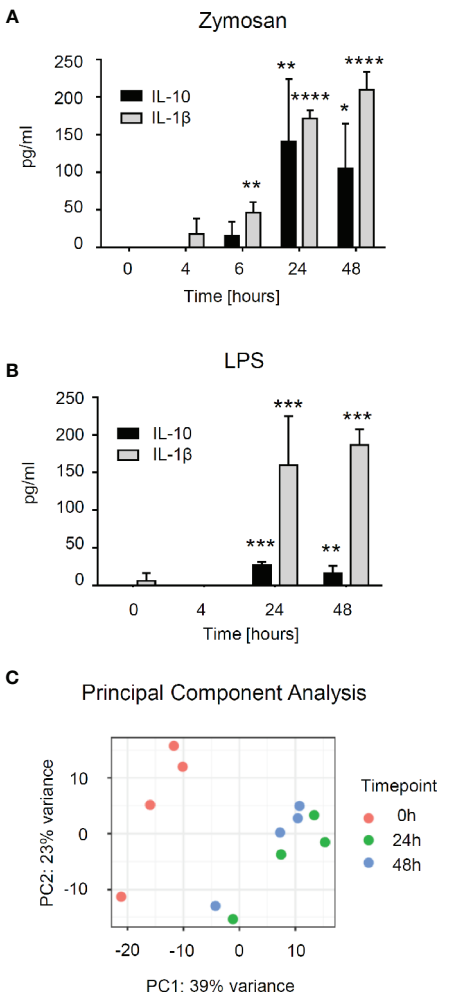

FIGURE 5 | RNA sequencing shows differential expression of genes in bone marrow-derived mast cells (BMMCs) after induction with zymosan. **(A, B)** Concentration of IL-10 and IL-1β in the supernatant of BMMCs induced with zymosan (10 µg/ml) (panel A) or lipopolysaccharides (LPS) (100 ng/ml) (panel B) at the indicated time points. Data are mean ± S.E.M. (n=4). One-way ANOVA, Dunnett's multiple comparison test for IL-10 and IL-1β, compared to 0 h control, *p<0.05, **p<0.01, ***p<0.001, ****p<0.0001. **(C)** The principal component analysis (PCA) was calculated on the 500 most variable genes across conditions in the RNA sequencing.

or LPS stimulation), which declined gradually afterwards (**Figures 7A, B**). In contrast, IFN-α, another member of the type I IFN-family, was not detected after stimulation of BMMCs (**Figure S10**). IFN-β concentrations in the mast cells themselves were not detectable in untreated BMMCs suggesting that IFN-β is newly synthesized (**Figure 7A**). It should be noted that the amount of IFN-β synthesized in BMMCs was in a similar range as the amount of IFN-β synthesized in bone marrow-derived macrophages, which served as positive control (**Figure 7C**). Importantly, immunohistological analysis showed that IFN-β is expressed in mast cells in paws from naïve mice as well as 4 and 48 h after zymosan injection into the paws of wild type mice (**Figure 7D**), suggesting that in contrast to BMMCs mast cells in paws show a basal IFN-β expression.

Since in macrophages TLR2- and TLR4-induced IFN-β release depends on the internalization of these receptors, we investigated if receptor internalization is also a prerequisite in mast cells (12, 13). First we tested whether or not IFN-β release depends in mast cells on the translocation of surface receptors to acidic endolysosomal compartments. We used Cytochalasin D (Cyt D) to prevent receptor internalization by inhibiting actin polymerization and Bafilomycin A (Baf A), a proton pump inhibitor, which interferes with endosomal acidification. Both inhibitors inhibited the release of IFN-β (**Figure 7E**), whereas the release of IL-1β in response to zymosan and LPS was not reduced (**Figure 7F**). Finally, zymosan has previously been demonstrated to activate various immune cells in an ERK-dependent matter through dectin-1 instead of TLR2 (31–33). However, inhibition of the ERK signaling pathway using the MEK inhibitor U0126 did not reduce zymosan-induced IFN-β release from BMMCs (**Figure 7G**).

DISCUSSION

Being located closely to host-environment interfaces, mast cells are among the first cells to come into contact with invading pathogens. They are equipped with a wide variety of receptors and an immense amount of preformed mediators and are thus able to respond quickly and specifically to diverse stimuli. Besides their role in initiating and promoting a proinflammatory immune response, they also have antiinflammatory and immunosuppressive functions. In this regard it has been proposed that mast cells are able to adjust their mode of action to the changing microenvironment during the different stages of an inflammation (34). Antiinflammatory immunomodulatory functions of mast cells have been so far mostly assigned to the cytokine IL-10 (35–38). It is well known that many cell types, including mast cells, respond to viral infections through TLR3, TLR7, and TLR9 initiating the type I IFN response as well as release of various proinflammatory cytokines (7, 8), which make them targets for antiinflammatory treatments including the use of cytokines of the IL-1 family with antiinflammatory properties (39, 40). RNA sequencing showed that mast cells are also able to initiate a strong type 1 IFN response in response to TLR2 and TLR4 activation. In this regard we observed a strong upregulation of genes associated with the type I IFN pathway in mast cells, stimulated with the TLR2 agonist zymosan as well as the release of IFN-β from these cells. This was surprising since mast cells were believed to be unable to internalize the receptor-pathogen complex necessary for IFN production and since TRIF signaling does not participate in LPS-mediated induction of TLR4 (13, 14). In contrast to TLR4, TLR2 is not associated with TRIF adaptor molecules and is known to be able to induce the type I IFN pathway in a MyD88-dependent way (10).

In our study we observed the release of IFN-β also after TLR4 induction by LPS, contradicting previous findings. A possible explanation for the induction of IFN-β by TLR4 despite the apparent absence of TRIF signaling might be that, similar to TLR2, TLR4 can mediate IFN-β induction in a MyD88-

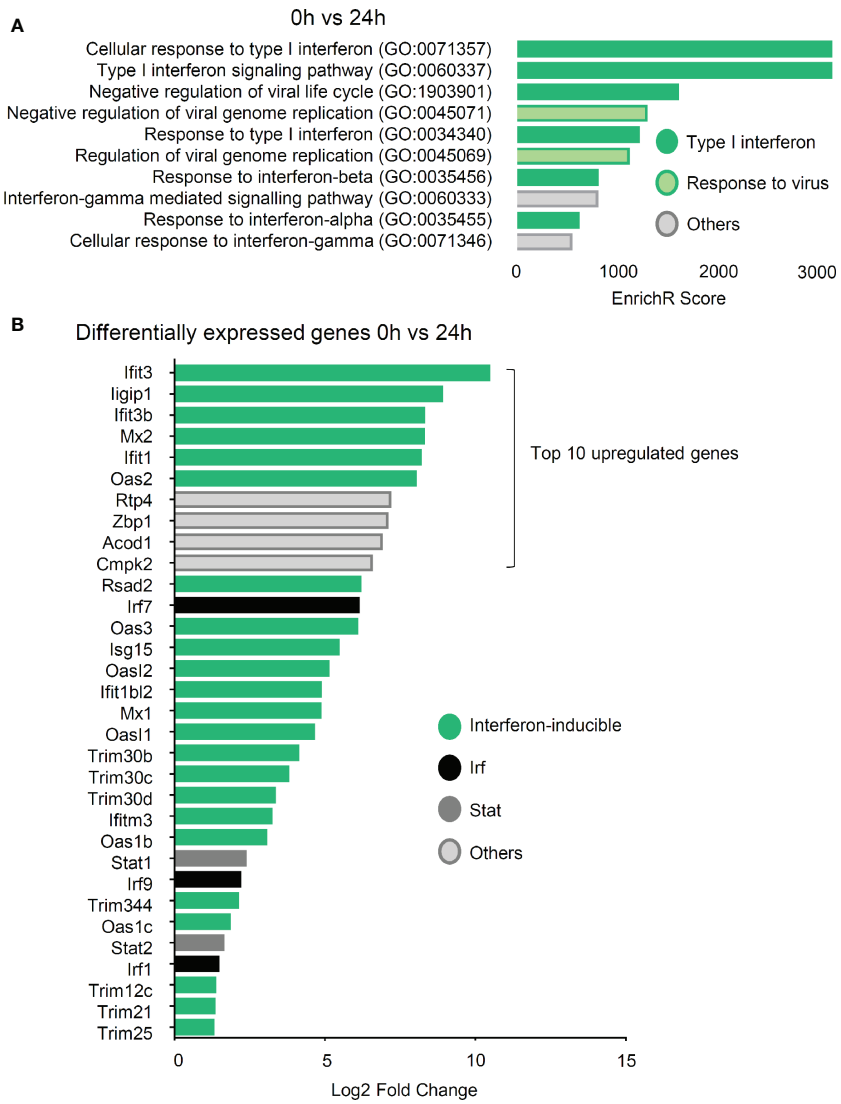

FIGURE 6 | IFN type I signaling is the dominant response in bone marrow-derived mast cells (BMMCs) after 24 h stimulation with zymosan. **(A)** Top ten upregulated gene ontology terms of RNA sequencing by EnrichR 24 h vs. 0 h after induction of BMMCs with 10 µg/ml zymosan. **(B)** List of the 32 genes with the strongest upregulation 24 h after induction with 10 µg/ml zymosan as compared to untreated BMMCs.

dependent way. The absence of detectable IFN-β in one previous study might be explained by the fact that IFN detection was not performed through a direct measurement, such as an ELISA assay, but through an indirect assay using IFN induced luciferase production in L929 cells transfected with an IFN-sensitive luciferase construct (14). Possibly this assay was not sensitive enough to detect IFN, since also viral activation of mast cells led not to IFN-β detection. In the study of Dietrich et al. (13), lack of TLR-induced IFN-β synthesis was proposed to be based on the inability of mast cells to actively internalize the pathogen-receptor complex. However, this is in contrast to several papers, which demonstrated the internalization of TLR4 receptor in mast cells. For example, LPS treatment of BMMCs induced the internalization of TLR4 receptor by a mechanism dependent on the activity of dynamin and the transport protein Huntingtin (41). Here, TLR4 internalization was necessary for LPS-induced ERK1/2 activation and TNFα production. Likewise, intracellular localization of TLR4 was shown for peripheral blood-derived mast cells, lung mast cells as well as in the human mast cell line HMC-1 (42, 43).

Previous studies demonstrated that endolysosomal trafficking is required for the successful induction of the type I IFN pathway for primarily cell surface-located TLRs. It was also shown that TRAF3 is necessary for induction of the type I IFN response and is not efficiently recruited to the TLR signaling complex at the plasma membrane. The intracellular localization together with potential conformational changes in the acidic environment are thought to facilitate the interaction with TRAF3 (11, 44, 45). In

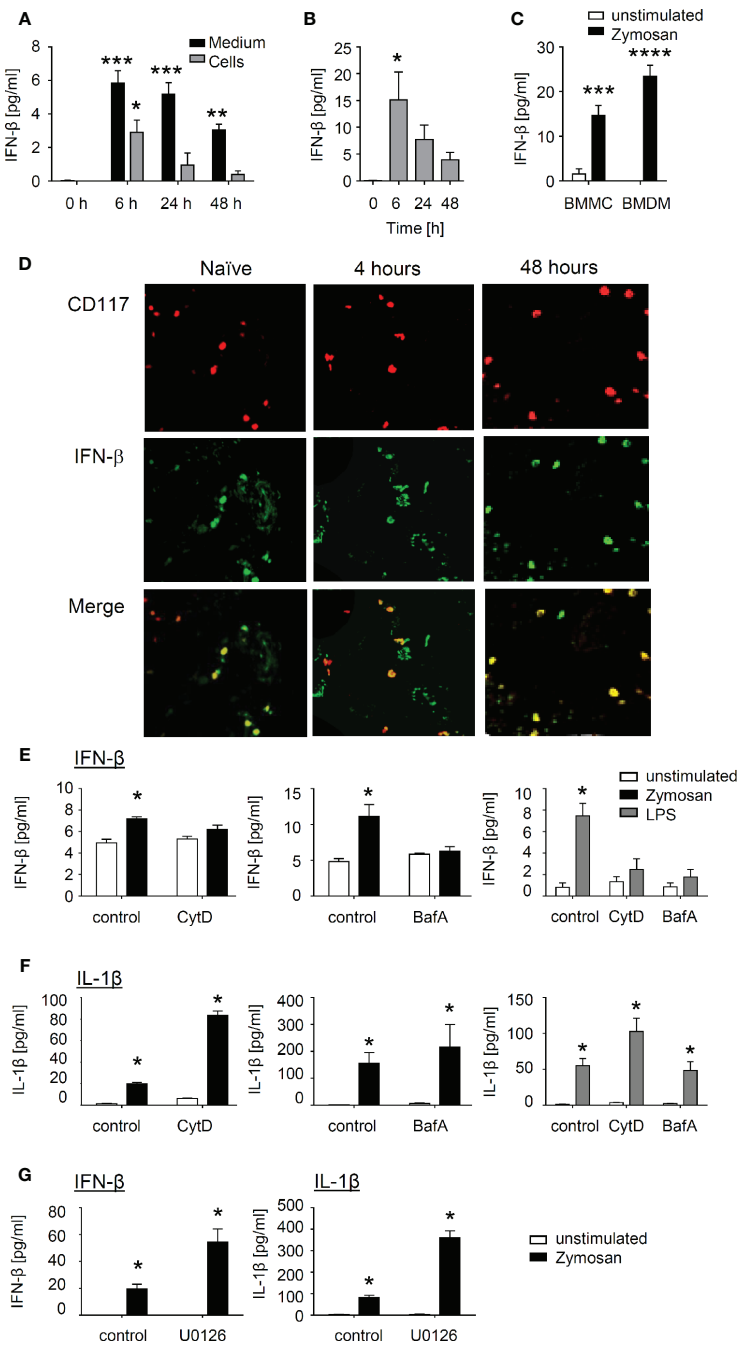

FIGURE 7 | Interferon (IFN)-β is produced by mast cells after induction with zymosan or LPS and requires receptor internalization. **(A)** IFN-β from bone marrow-derived mast cells (BMMCs) after induction with zymosan (10 µg/ml) at the indicated time points in cell pellet and supernatant. Data are shown as mean ± S.E.M. (n=3). One-way ANOVA, Dunnett's multiple comparison test compared to control, *p<0.05, **p<0.01, ***p<0.001. **(B)** Release of IFN-β from BMMCs after induction with lipopolysaccharides (LPS) (100 ng/ml) at the indicated time points. Data are shown as mean ± S.E.M. (n=3). One-way ANOVA, Dunnett's multiple comparison test compared to control, *p<0.05. **(C)** Release of IFN-β from BMMCs and BMDMs 24 h after induction with zymosan (10 µg/ml). Data are shown as mean ± S.E.M. (n=4). Two-way ANOVA, Sidak's multiple comparison test compared to unstimulated control, ***p<0.001, ****p<0.0001. **(D)** Representative stainings for CD117 and IFN-β of paws from naïve mice or 4 and 48 h after zymosan-injection. **(E, F)** BMMCs either untreated or pre-treated for 1 h with 25 µM Cytochalasin D or 50 µM Bafilomycin A were stimulated for 24 h with 10 µg/ml zymosan or 100 ng/ml LPS. The concentrations of IFN-β **(E)** or IL-1β **(F)** were determined in the medium. Data is shown as mean ± S.E.M. (n = 4). Multiple t-test comparing unstimulated and zymosan or LPS stimulated cells, Holm Sidak's multiple comparison test, *p<0.05. **(G)** BMMCs either untreated or pre-treated for 1 h with 10 µM MEK-inhibitor U0126 were stimulated for 24 h with 10 µg/ml zymosan. The concentrations of IFN-β and IL-1β were determined in the medium. Data are shown as mean ± S.E.M. (n = 4). Multiple t-test comparing control and zymosan treatment, Holm Sidak's multiple comparison test, *p<0.05.

accordance with this, pharmacological blockage of receptor internalization and endosome maturation in mast cells also inhibits the induction of type I IFNs, while the proinflammatory response is still active upon TLR2 and TLR4 activation.

The time course of the release of IFN-β from BMMCs showed that the IFN-β release peaks 6 h after zymosan stimulation, while significant amounts of IL-10 and IL-1β are only detected after 24 h of zymosan treatment. Since IFN-β was not detected in unstimulated mast cells, this early response demonstrates the induction of IFN-β synthesis. The induction of the expression of other mediators, which are able to induce IFN-β, would be also a possibility, although this scenario does not fit to the observed time frame. Taken together the data point toward a direct induction of IFN-β synthesis in BMMCs by zymosan. However, it should be noted that the situation *in vivo* differs from the findings in BMMCs, since we found mast cells expressing IFN-β not only in inflamed paws but also in naïve mice. The fact that mast cells in paws express IFN-β also under basal conditions points toward the storage of this mediator for its fast release in response to pathogens including zymosan or LPS. Thus, the specific *in vivo* microenvironment of mast cells in paw tissue apparently allows the basal expression and most likely the storage of IFN-β in mast cells. While IFN-β was seen in mast cells *in vivo* using immunohistochemistry, we did not detect IFN-β by ELISA in whole paw lysates. However, since relative few mast cells are localized in the paw, IFN-β levels might be locally increased but too low to be detected in the context of whole tissue analyses. Whether or not this IFN-β released by mast cells affects phagocytotic activity of macrophages during zymosan-induced inflammation is not clear. Also in case that IFN-β modulates the phagocytotic activity of macrophages in this model, it can only be speculated if this regulation is a direct effect or is mediated by secondary mechanisms, such as altering the release of other mediators from mast cells themselves or other immune cells is still an open question, which needs to be addressed in future studies.

The enhancing effect of IFN-β on efferocytosis by macrophages has been shown recently, demonstrating the pro-resolving functions of this cytokine (46). Here, we observed a decrease of the phagocytotic activity of macrophages in mast cell-deficient mice during resolution of inflammation, while no changes in the number of neutrophils, monocyte-derived macrophages, eosinophils or dendritic cells recruited to the zymosan-injected paw were observed. These findings show that mast cells do not play a dominant role in immune cell recruitment in the resolution phase of zymosan-induced inflammation. The screening for alterations in cytokine and chemokine levels in mast cell-deficient mice showed a decrease of IL-4 and CXCL1 in absence of mast cells. CXCL1 is best known for its ability to promote chemotaxis of neutrophils. The fact that CXCL1 levels are reduced in mast cell-deficient mice without that a change in neutrophil numbers occurs supports the notion that mast cells are not involved in immune cell recruitment in this phase of inflammation. Instead other CXCL1 functions, such as its role in wound healing (i.e. epithelialization and angiogenesis) (47), might explain its mast cell-dependent increase during the resolution phase of inflammation. IL-4 on the other hand is known to drive polarization of macrophages toward antiinflammatory (M2-like) phenotypes and fits to the localization of mast cells in the cellular neighborhood of M2-like macrophages. Other cytokines, which are released by mast cells, were not changed 48 h after zymosan injection in Cre^+ mast cell deficient mice as compared to Cre^- mice. In this regard, although IL-10 and PGE_2 synthesis in BMMCs was induced by zymosan there was no difference between their levels in inflamed paws from mast cell-deficient and control mice (**Figure 4**, **Figure S11**). On one hand this could reflect the differences between the phenotypes of BMMCs and mast cells located in the paw tissue. On the other hand IL-10 can also be produced by other immune cells in amounts, which could mask changes in mast cell-derived IL10 in the context of whole tissue analyses. Notably, this notion does not oppose possible local effects of mast cell-derived IL-10 in the defined area surrounding the zymosan-containing area. Another explanation could be based on IFN-β effects on mast cells themselves, which could influence the synthesis and release of mediators. In this regard also other mediators that can be produced by mast cells upon zymosan-stimulation, i.e. IL-1β, IL-4 and PGE_2, have been demonstrated to increase phagocytosis in macrophages as well (48–50). Therefore, the enhancing effect of mast cells on the phagocytosing activity of macrophages could be derived from one of these mediators, including IFN-β, or a combination of these (51).

Finally, the observed localization of mast cells during the resolution phase of local inflammation within an antiinflammatory cellular neighborhood suggests a reversal of the immunological function of mast cells. In this regard various mediators including cytokines (e.g. IL-10 and IL-4), chemokines (e.g. CXCL1) or lipids such as PGE_2, which all can mediate effects promoting antiinflammation and/or wound healing, have already been demonstrated to be synthesized in mast cells and to promote mast cell-dependent antiinflammatory effects (36, 52). Thus, the well-known proinflammatory role of mast cells in the beginning of an inflammation seems to be reversible allowing mast cells to gain an antiinflammatory phenotype and to expand its role in inflammation depending on the needs of the specific microenvironment.

DATA AVAILABILITY STATEMENT

The datasets presented in this study can be found in online repositories. The data are available in the GEO database with the accession number GSE165523.

ETHICS STATEMENT

The animal study was reviewed and approved by Regierungspräsidium Darmstadt. Written informed consent was

obtained from the owners for the participation of their animals in this study.

AUTHOR CONTRIBUTIONS

LK, SP, and JC did the *in vivo* experiments and performed FACS analyses. LK and TSchi performed mRNA sequencing. SE and IE processed and analyzed the mRNA sequencing data. NF and DT provided LC-MS/MS analysis data. AW, BB performed FACS sorting. TSchä and AK performed MELC analyses. KS and LK designed experiments and wrote the paper. All authors contributed to the article and approved the submitted version.

FUNDING

This work was supported by the DFG grants SCHO817/3-3, SFB1039 (TPA08, B04, B06 and Z01) and GRK2336 (TP01, TP06, TP07). The Else Kröner-Fresenius-Foundation (EKFS) funded JC as part of the Else-Kröner Graduateschool. This research was supported by the research funding program Landes-Offensive zur Entwicklung Wissenschaftlich-ökonomischer Exzellenz (LOEWE) of the State of Hessen, Research Center for Translational Medicine and Pharmacology TMP, and Research Center for Translational Biodiversity Genomics (TBG).

ACKNOWLEDGMENTS

Mcpt5-DTA-Cre mice were generously provided by Axel Roers, Technische Universität Dresden, Germany. The authors thank Yannick Schreiber, Praveen Mathoor, and Karin Schilling for excellent technical assistance.

SUPPLEMENTARY MATERIAL

The Supplementary Material for this article can be found online at: https://www.frontiersin.org/articles/10.3389/fimmu.2020.607048/full#supplementary-material

REFERENCES

1. Galli SJ, Gaudenzio N, Tsai M. Mast Cells in Inflammation and Disease: Recent Progress and Ongoing Concerns. *Annu Rev Immunol* (2020) 38:49–77. doi: 10.1146/annurev-immunol-071719-094903
2. Tarighi N, Menger D, Pierre S, Kornstädt L, Thomas D, Ferreirós N, et al. Thromboxane-Induced α-CGRP Release from Peripheral Neurons Is an Essential Positive Feedback Loop in Capsaicin-Induced Neurogenic Inflammation. *J Invest Dermatol* (2019) 139:656–64. doi: 10.1016/j.jid.2018.10.011
3. Lyons DO, Pullen NA. Beyond IgE: Alternative Mast Cell Activation Across Different Disease States. *Int J Mol Sci* (2020) 21:1498. doi: 10.3390/ijms21041498
4. Kawai T, Akira S. The role of pattern-recognition receptors in innate immunity: update on Toll-like receptors. *Nat Immunol* (2010) 11:373–84. doi: 10.1038/ni.1863
5. Kawai T, Akira S. Toll-like receptors and their crosstalk with other innate receptors in infection and immunity. *Immunity* (2011) 34:637–50. doi: 10.1016/j.immuni.2011.05.006
6. Shibata T, Motoi Y, Tanimura N, Yamakawa N, Akashi-Takamura S, Miyake K. Intracellular TLR4/MD-2 in macrophages senses Gram-negative bacteria and induces a unique set of LPS-dependent genes. *Int Immunol* (2011) 23:503–10. doi: 10.1093/intimm/dxr044
7. Conti P, Ronconi G, Caraffa A, Gallenga C, Ross R, Frydas I, et al. Induction of pro-inflammatory cytokines (IL-1 and IL-6) and lung inflammation by Coronavirus-19 (COVI-19 or SARS-CoV-2): anti-inflammatory strategies. *J Biol Regul Homeost Agents* (2020) 34:327–31. doi: 10.23812/CONTI-E
8. Conti P, Caraffa A, Tetè G, Gallenga CE, Ross R, Kritas SK, et al. Mast cells activated by SARS-CoV-2 release histamine which increases IL-1 levels causing cytokine storm and inflammatory reaction in COVID-19. *J Biol Regul Homeost Agents* (2020) 34:1629–32. doi: 10.23812/20-2EDIT
9. Boxx GM, Cheng G. The Roles of Type i Interferon in Bacterial Infection. *Cell Host Microbe* (2016) 19:760–9. doi: 10.1016/j.chom.2016.05.016
10. Barbalat R, Lau L, Locksley RM, Barton GM. Toll-like receptor 2 on inflammatory monocytes induces type I interferon in response to viral but not bacterial ligands. *Nat Immunol* (2009) 10:1200–7. doi: 10.1038/ni.1792
11. Bauernfeind F, Hornung V. TLR2 joins the interferon gang. *Nat Immunol* (2009) 10:1139–41. doi: 10.1038/ni1109-1139
12. Dietrich N, Lienenklaus S, Weiss S, Gekara NO. Murine Toll-Like Receptor 2 Activation Induces Type I Interferon Responses from Endolysosomal Compartments. *PLoS One* (2010) 5:e10250. doi: 10.1371/journal.pone.0010250
13. Dietrich N, Rohde M, Geffers R, Kroger A, Hauser H, Weiss S, et al. Mast cells elicit proinflammatory but not type I interferon responses upon activation of TLRs by bacteria. *Proc Natl Acad Sci* (2010) 107:8748–53. doi: 10.1073/pnas.0912551107
14. Keck S, Müller I, Fejer G, Savic I, Tchaptchet S, Nielsen PJ, et al. Absence of TRIF Signaling in Lipopolysaccharide-Stimulated Murine Mast Cells. *J Immunol* (2011) 186:5478–88. doi: 10.4049/jimmunol.1000458
15. Dudeck A, Dudeck J, Scholten J, Petzold A, Surianarayanan S, Kohler A, et al. Mast cells are key promoters of contact allergy that mediate the adjuvant effects of haptens. *Immunity* (2011) 34:973–84. doi: 10.1016/j.immuni.2011.03.028
16. Pierre S, Linke B, Suo J, Tarighi N, Del Turco D, Thomas D, et al. GPVI and Thromboxane Receptor on Platelets Promote Proinflammatory Macrophage Phenotypes during Cutaneous Inflammation. *J Invest Dermatol* (2017) 137:686–95. doi: 10.1016/j.jid.2016.09.036
17. Pierre S, Scholich K. Toponomics: studying protein-protein interactions and protein networks in intact tissue. *Mol Biosyst* (2010) 6:641–7. doi: 10.1039/b910653g
18. Kern K, Schäfer SMG, Cohnen J, Pierre S, Osthues T, Tarighi N, et al. The G2A Receptor Controls Polarization of Macrophage by Determining Their Localization Within the Inflamed Tissue. *Front Immunol* (2018) 9:2261. doi: 10.3389/fimmu.2018.02261
19. McQuin C, Goodman A, Chernyshev V, Kamentsky L, Cimini BA, Karhohs KW, et al. CellProfiler 3.0: Next-generation image processing for biology. *PLoS Biol* (2018) 16:e2005970. doi: 10.1371/journal.pbio.2005970
20. Schapiro D, Jackson HW, Raghuraman S, Fischer JR, Zanotelli VRT, Schulz D, et al. histoCAT: analysis of cell phenotypes and interactions in multiplex image cytometry data. *Nat Methods* (2017) 14:873–6. doi: 10.1038/nmeth.4391
21. Amir ED, Davis KL, Tadmor MD, Simonds EF, Levine JH, Bendall SC, et al. viSNE enables visualization of high dimensional single-cell data and reveals phenotypic heterogeneity of leukemia. *Nat Biotechnol* (2013) 31:545–52. doi: 10.1038/nbt.2594
22. Levine JH, Simonds EF, Bendall SC, Davis KL, Amir ED, Tadmor MD, et al. Data-Driven Phenotypic Dissection of AML Reveals Progenitor-like Cells that Correlate with Prognosis. *Cell* (2015) 162:184–97. doi: 10.1016/j.cell.2015.05.047
23. Suo J, Linke B, dos Santos SM, Pierre S, Stegner D, Zhang DD, et al. Neutrophils mediate edema formation but not mechanical allodynia during zymosan-induced inflammation. *J Leukoc Biol* (2014) 96:133–42. doi: 10.1189/jlb.3A1213-628R

24. Treutlein E-M, Kern K, Weigert A, Tarighi N, Schuh C-D, Nusing RM, et al. The prostaglandin E2 receptor EP3 controls CC-chemokine ligand 2-mediated neuropathic pain induced by mechanical nerve damage. *J Biol Chem* (2018) 293:9685–95. doi: 10.1074/jbc.RA118.002492
25. Dobin A, Davis CA, Schlesinger F, Drenkow J, Zaleski C, Jha S, et al. STAR: Ultrafast universal RNA-seq aligner. *Bioinformatics* (2013) 29:15–21. doi: 10.1093/bioinformatics/bts635
26. Liao Y, Smyth GK, Shi W. The R package Rsubread is easier, faster, cheaper and better for alignment and quantification of RNA sequencing reads. *Nucleic Acids Res* (2019) 47:e47. doi: 10.1093/nar/gkz114
27. Love MI, Huber W, Anders S. Moderated estimation of fold change and dispersion for RNA-seq data with DESeq2. *Genome Biol* (2014) 15:550. doi: 10.1186/s13059-014-0550-8
28. Chen EY, Tan CM, Kou Y, Duan Q, Wang Z, Meirelles G, et al. Enrichr: interactive and collaborative HTML5 gene list enrichment analysis tool. *BMC Bioinf* (2013) 14:128. doi: 10.1186/1471-2105-14-128
29. Kuleshov MV, Jones MR, Rouillard AD, Fernandez NF, Duan Q, Wang Z, et al. Enrichr: a comprehensive gene set enrichment analysis web server 2016 update. *Nucleic Acids Res* (2016) 44:W90–7. doi: 10.1093/nar/gkw377
30. Jachetti E, D'Incà F, Danelli L, Magris R, Dal Secco C, Vit F, et al. Frontline Science: Mast cells regulate neutrophil homeostasis by influencing macrophage clearance activity. *J Leukoc Biol* (2019) 105:633–44. doi: 10.1002/JLB.4HI1018-390R
31. Dillon S, Agrawal S, Banerjee K, Letterio J, Denning TL, Oswald-Richter K, et al. Yeast zymosan, a stimulus for TLR2 and dectin-1, induces regulatory antigen-presenting cells and immunological tolerance. *J Clin Invest* (2006) 116:916–28. doi: 10.1172/JCI27203
32. Baldwin KT, Carbajal KS, Segal BM, Giger RJ. Neuroinflammation triggered by β-glucan/dectin-1 signaling enables CNS axon regeneration. *Proc Natl Acad Sci USA* (2015) 112:2581–6. doi: 10.1073/pnas.1423221112
33. Slack EC, Robinson MJ, Hernanz-Falcón P, Brown GD, Williams DL, Schweighoffer E, et al. Syk-dependent ERK activation regulates IL-2 and IL-10 production by DC stimulated with zymosan. *Eur J Immunol* (2007) 37:1600–12. doi: 10.1002/eji.200636830
34. Galli SJ, Grimbaldeston M, Tsai M. Immunomodulatory mast cells: negative, as well as positive, regulators of immunity. *Nat Rev Immunol* (2008) 8:478–86. doi: 10.1038/nri2327
35. Depinay N, Hacini F, Beghdadi W, Peronet R, Mécheri S. Mast Cell-Dependent Down-Regulation of Antigen-Specific Immune Responses by Mosquito Bites. *J Immunol* (2006) 176:4141–6. doi: 10.4049/jimmunol.176.7.4141
36. Chan CY, St. John AL, Abraham SN. Mast Cell Interleukin-10 Drives Localized Tolerance in Chronic Bladder Infection. *Immunity* (2013) 38:349–59. doi: 10.1016/j.immuni.2012.10.019
37. Grimbaldeston MA, Nakae S, Kalesnikoff J, Tsai M, Galli SJ. Mast cell–derived interleukin 10 limits skin pathology in contact dermatitis and chronic irradiation with ultraviolet B. *Nat Immunol* (2007) 8:1095–104. doi: 10.1038/ni1503
38. Reber LL, Sibilano R, Starkl P, Roers A, Grimbaldeston MA, Tsai M, et al. Imaging protective mast cells in living mice during severe contact hypersensitivity. *JCI Insight* (2017) 2:e92900. doi: 10.1172/jci.insight.92900
39. Caraffa A, Gallenga CE, Kritas SK, Ronconi G, Di Emidio P, Conti P. CAR-T cell therapy causes inflammation by IL-1 which activates inflammatory cytokine mast cells: anti-inflammatory role of IL-37. *J Biol Regul Homeost Agents* (2019) 33:1981–5. doi: 10.23812/EditorialCaraffa
40. Kritas SK, Ronconi G, Caraffa A, Gallenga CE, Ross R, Conti P. Mast cells contribute to coronavirus-induced inflammation: new anti-inflammatory strategy. *J Biol Regul Homeost Agents* (2020) 34:9–14. doi: 10.23812/20-Editorial-Kritas
41. Pérez-Rodríguez MJ, Ibarra-Sánchez A, Román-Figueroa A, Pérez-Severiano F, González-Espinosa C. Mutant Huntingtin affects toll-like receptor 4 intracellular trafficking and cytokine production in mast cells. *J Neuroinflammation* (2020) 17:95. doi: 10.1186/s12974-020-01758-9
42. Okumura S, Kashiwakura J, Tomita H, Matsumoto K, Nakajima T, Saito H, et al. Identification of specific gene expression profiles in human mast cells mediated by Toll-like receptor 4 and FcepsilonRI. *Blood* (2003) 102:2547–54. doi: 10.1182/blood-2002-12-3929
43. Meng Z, Yan C, Deng Q, Dong X, Duan Z-M, Gao D-F, et al. Oxidized low-density lipoprotein induces inflammatory responses in cultured human mast cells via Toll-like receptor 4. *Cell Physiol Biochem Int J Exp Cell Physiol Biochem Pharmacol* (2013) 31:842–53. doi: 10.1159/000350102
44. Kagan JC, Su T, Horng T, Chow A, Akira S, Medzhitov R. TRAM couples endocytosis of Toll-like receptor 4 to the induction of interferon-β. *Nat Immunol* (2008) 9:361–8. doi: 10.1038/ni1569
45. Tanimura N, Saitoh S, Matsumoto F, Akashi-Takamura S, Miyake K. Roles for LPS-dependent interaction and relocation of TLR4 and TRAM in TRIF-signaling. *Biochem Biophys Res Commun* (2008) 368:94–9. doi: 10.1016/j.bbrc.2008.01.061
46. Kumaran Satyanarayanan S, El Kebir D, Soboh S, Butenko S, Sekheri M, Saadi J, et al. IFN-β is a macrophage-derived effector cytokine facilitating the resolution of bacterial inflammation. *Nat Commun* (2019) 10:3471. doi: 10.1038/s41467-019-10903-9
47. Castela M, Nassar D, Sbeih M, Jachiet M, Wang Z, Aractingi S. Ccl2/Ccr2 signalling recruits a distinct fetal microchimeric population that rescues delayed maternal wound healing. *Nat Commun* (2017) 8:15463. doi: 10.1038/ncomms15463
48. Wainszelbaum MJ, Proctor BM, Pontow SE, Stahl PD, Barbieri MA. IL4/PGE2 induction of an enlarged early endosomal compartment in mouse macrophages is Rab5-dependent. *Exp Cell Res* (2006) 312:2238–51. doi: 10.1016/j.yexcr.2006.03.025
49. Daseke MJ, Tenkorang-Impraim MAA, Ma Y, Chalise U, Konfrst SR, Garrett MR, et al. Exogenous IL-4 shuts off pro-inflammation in neutrophils while stimulating anti-inflammation in macrophages to induce neutrophil phagocytosis following myocardial infarction. *J Mol Cell Cardiol* (2020) 145:112–21. doi: 10.1016/j.yjmcc.2020.06.006
50. Schenk M, Fabri M, Krutzik SR, Lee DJ, Vu DM, Sieling PA, et al. Interleukin-1β triggers the differentiation of macrophages with enhanced capacity to present mycobacterial antigen to T cells. *Immunology* (2014) 174–80. doi: 10.1111/imm.12167
51. Dahdah A, Gautier G, Attout T, Fiore F, Lebourdais E, Msallam R, et al. Mast cells aggravate sepsis by inhibiting peritoneal macrophage phagocytosis. *J Clin Invest* (2014) 124:4577–89. doi: 10.1172/JCI75212
52. Lu L-F, Lind EF, Gondek DC, Bennett KA, Gleeson MW, Pino-Lagos K, et al. Mast cells are essential intermediaries in regulatory T-cell tolerance. *Nature* (2006) 442:997–1002. doi: 10.1038/nature05010

Conflict of Interest: SE was employed by Institute of Molecular Biology GmbH.

The remaining authors declare that the research was conducted in the absence of any commercial or financial relationships that could be construed as a potential conflict of interest.

Copyright © 2021 Kornstädt, Pierre, Weigert, Ebersberger, Schäufele, Kolbinger, Schmid, Cohnen, Thomas, Ferreirós, Brüne, Ebersberger and Scholich. This is an open-access article distributed under the terms of the Creative Commons Attribution License (CC BY). The use, distribution or reproduction in other forums is permitted, provided the original author(s) and the copyright owner(s) are credited and that the original publication in this journal is cited, in accordance with accepted academic practice. No use, distribution or reproduction is permitted which does not comply with these terms.

frontiers in Immunology

REVIEW
published: 12 February 2021
doi: 10.3389/fimmu.2020.607945

Modulation of Immune Responses by Particle Size and Shape

Maksim V. Baranov[1], Manoj Kumar[2], Stefano Sacanna[3], Shashi Thutupalli[2,4] and Geert van den Bogaart[1]**

[1] Department of Molecular Immunology and Microbiology, Groningen Biomolecular Sciences and Biotechnology Institute, University of Groningen, Groningen, Netherlands, [2] Simons Center for the Study of Living Machines, National Centre for Biological Sciences, Tata Institute for Fundamental Research, Bangalore, India, [3] Molecular Design Institute, Department of Chemistry, New York University, New York, NY, United States, [4] International Centre for Theoretical Sciences, Tata Institute for Fundamental Research, Bangalore, India

The immune system has to cope with a wide range of irregularly shaped pathogens that can actively move (e.g., by flagella) and also dynamically remodel their shape (e.g., transition from yeast-shaped to hyphal fungi). The goal of this review is to draw general conclusions of how the size and geometry of a pathogen affect its uptake and processing by phagocytes of the immune system. We compared both theoretical and experimental studies with different cells, model particles, and pathogenic microbes (particularly fungi) showing that particle size, shape, rigidity, and surface roughness are important parameters for cellular uptake and subsequent immune responses, particularly inflammasome activation and T cell activation. Understanding how the physical properties of particles affect immune responses can aid the design of better vaccines.

Keywords: phagocytosis, F-actin (filamentous actin), pathogens, vaccination, endocytosis

OPEN ACCESS

Edited by:
Valentin Jaumouillé, Simon Fraser University, Canada

Reviewed by:
Jason King, The University of Sheffield, United Kingdom
Mauricio Terebiznik, University of Toronto Scarborough, Canada

****Correspondence:***
Maksim V. Baranov
m.baranov@rug.nl
Geert van den Bogaart
g.van.den.bogaart@rug.nl

Specialty section:
This article was submitted to Antigen Presenting Cell Biology, a section of the journal Frontiers in Immunology

Received: *18 September 2020*
Accepted: *23 December 2020*
Published: *12 February 2021*

Citation:
Baranov MV, Kumar M, Sacanna S, Thutupalli S and van den Bogaart G (2021) Modulation of Immune Responses by Particle Size and Shape. Front. Immunol. 11:607945. doi: 10.3389/fimmu.2020.607945

INTRODUCTION

The cells of immune system can morphologically change their plasma membrane for uptake and clearance of foreign particles that enter the body, such as bacteria and fungi upon an infection, and particles from endogenous sources, such as apoptotic cell bodies (1). The cellular uptake of extracellular particles is essential for many cellular functions, and, among other things, plays important roles in the immune system and for tissue remodeling. Pathogens or particles entering the body are ingested by immune phagocytes by engaging receptors on their surface. This process is required for the clearance of infectious microbes (e.g., bacteria, fungi), senescent (cancer) cells and inorganic particles from the body by immune phagocytes (1). Endocytosis is an umbrella term for different types of uptake of smaller particles, while larger particles are taken up by a mechanistically different mechanism called phagocytosis. In this review we will define endocytosis as the uptake of particles < 0.5 μm in size and phagocytosis as the cellular uptake of particles larger than 0.5 μm. Endocytic vesicles can have vesicular, flask-like, or tubular morphologies (2). The best understood form of endocytosis is mediated by clathrin, a coat protein on the cytoplasmic side of the membrane, but other coat proteins (e.g., caveolin) also exist and endocytosis seems not always dependent on coat proteins (2). Due to size constrains of the clathrin lattice, clathrin has a preference for orchestrating uptake of small particles (<0.1 μm in diameter). Membrane invaginations, originating from membrane ruffles and from actin-rich membrane extensions called lamellipodia, form

phagocytic cups, which upon sealing lead to formation of large µm-sized membrane-bound vacuoles called phagosomes (receptor-mediated process) or macropinosomes (receptor-independent) (2, 3). Phagocytosis is generally mediated by the actin cytoskeleton that provides a substantial force for overcoming physical constrains necessary for the membrane wrapping of larger particles (**Figure 1**). Phagocytosis differs from the uptake of smaller particles by endocytosis, as it does not rely on coat proteins, such as clathrin and caveolin, and endocytosis has less involvement of the actin cytoskeleton (1, 2). For actin polymerization, phagocytosis requires activity of Rho-GTPases and phosphoinositide 3-kinase (PI3K)-family kinases (2), and this is especially necessary for phagocytosis of larger particles (> 5 µm) (4, 5). In this review, the focus is on µm-range model particles and fungal pathogens, as the effects of morphology on cellular uptake are best understood for these phagocytic cargoes.

The main immune phagocytes are macrophages, neutrophils and dendritic cells (DCs) (1). Neutrophils are the most abundant phagocytes in the body, capable of eliciting oxidative and non-oxidative microbicidal responses, such as by secretion of antibacterial proteins and trapping of pathogens in neutrophil extracellular traps (NETs) of released DNA (**Figure 1**) (6). Macrophages are found in all tissues and are able to clear infections by phagocytosis and trigger inflammatory responses. They are more equipped to phagocytose smaller morphological states of fungi; larger hyphae or spores sometimes cannot be taken up by macrophages (7–9). Macrophages can polarize into pro-inflammatory (M1) phenotypes if activated by pro-inflammatory stimuli such as interferon (IFN)-γ, granulocyte-macrophage colony-stimulating factor (GM-CSF), or microbial stimuli such as lipopolysaccharide (LPS) (10). Alternatively, macrophages can polarize into anti-inflammatory homeostatic (M2) phenotypes induced by anti-inflammatory cytokines interleukin (IL)-4 or IL-13 (10). The shift from M2 to M1-like phenotypes is associated with more microbicidal activity of macrophages (10). Similar to neutrophils and macrophages, dendritic cells (DCs) also sample the blood and peripheral tissues of the body for pathogens and apoptotic/necrotic cells (11). However, in contrast to neutrophils and macrophages, DCs can efficiently migrate to the lymph nodes after phagocytosis of pathogens. In the lymph nodes, the DCs can present antigenic peptides derived from the ingested pathogenic proteins on their cell surface in major histocompatibility complex (MHC) class II to naive CD4-positive "helper" T cells (Th) and, in a process called cross-presentation, in MHC class I to naive CD8-positive "killer" T cells (11, 12). Antigen (cross-)presentation by DCs is essential to activate naive T cells and elicit an adaptive immune response against invading pathogens and cancer.

Because clearance of different pathogens (fungi, bacteria, viruses, helminths) and malignant cells requires different immune responses, the immune system has evolved many receptors that recognize different pathogens, called pathogen recognition receptors (PRR). These PRRs recognize so-called microbial-associated molecular patterns (MAMPs), which are structures present on microbes but not host cells, and danger-associated

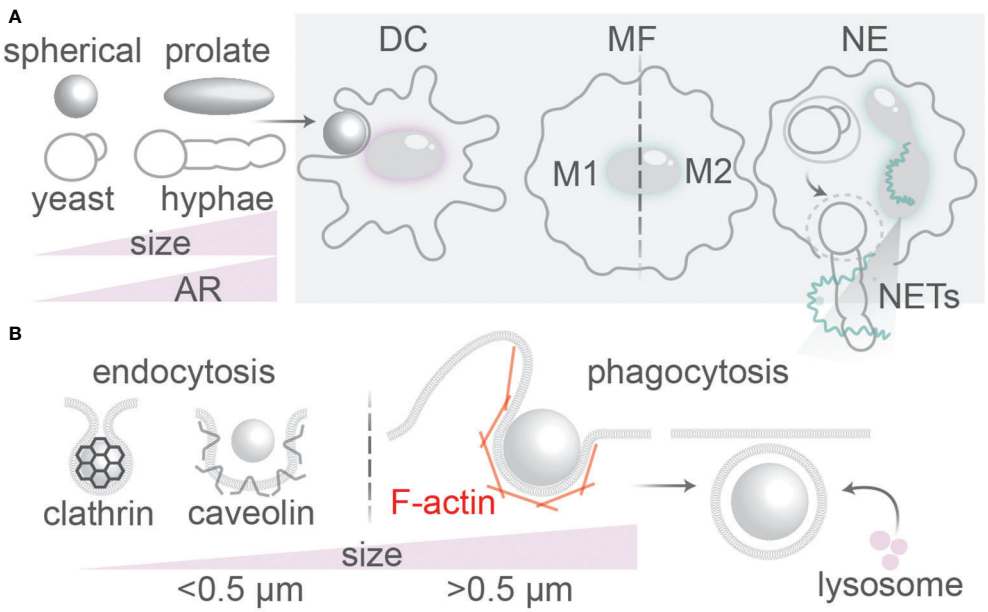

FIGURE 1 | Uptake of antigenic particles by immune phagocytes. **(A)** Dendritic cells (DC), macrophages (MF), and neutrophils (NE) of the immune system encounter particles with different physical properties (size, shape, rigidity, surface roughness). NE can release extracellular traps (NETs) for capturing large pathogens such as hyphal fungi. Macrophages can undergo reprogramming into pro-inflammatory (M1) or anti-inflammatory (M2) phenotypes. **(B)** Particles >0.5 µm are ingested by phagocytosis; smaller particles by endocytosis which can be clathrin or caveolin-mediated. The F-actin cytoskeleton is important for membrane wrapping at the phagocytic cup. Fusion with lysosomes containing lytic enzymes is the final step in endo/phagosomal maturation.

molecular patterns (DAMPs), which are present on damaged but not (or only in low amounts) on healthy host cells (13). Many PRRs, but not all, can also trigger endocytosis and/or phagocytosis. For example, the fungal cell wall β-glucans and chitins trigger both antigen recognition and phagocytosis by binding to the C-type lectins dectin-1 and the mannose receptor (CD206) on the surface of DCs and macrophages. A major class of PRRs are Toll-like receptors (TLR), which bind to many different MAMPs, such as TLR4 which binds to LPS. The engagement of different receptors, such as dectin-1 and TLRs, enables immune phagocytes to differentiate between different morphological states of fungi (14, 15). For example, compared to the hyphae, the swollen conidia form of the pathogenic fungus *Aspergillus fumigatus* has increased levels of surface-exposed β-glucans and triggers stronger inflammatory responses (16).

Likely because different pathogens have different sizes and engage different phagocytic PRRs, it can trigger different types of phagocytosis. For example, large hyphal forms of the mold *Aspergillus fumigatus* are ingested by Fc-receptor mediated phagocytosis, whereas smaller spores of the same mold are taken up *via* the mannose receptor (10). Phagocytosis mediated by the Fc-receptor triggers a so-called zipper model of uptake, characterized by a close-fitting zipper-like advance of membrane and the branched actin cytoskeleton over the particle surface; the efficiency of this process depends on the particle rigidity, size, the density of antibodies on the particle surface (17–19) and the distance between the phagocyte's membrane and the particle surface (limited by the size of the Fc-receptor-ligand complex) (20). Less stiff apoptotic cells are taken up through the zipper model as well (3), but with less efficiency than stiffer targets such as bacteria and yeasts (17). In contrast, phagocytosis by complement receptor 3 (CR3) occurs *via* flappy membrane ruffles orchestrated by linear actin, smaller membrane protrusions and phagosomal "sinking" into the cytoplasm (reviewed in (3)). Recent data shows that Fc- and complement-mediated uptake can be intertwined and both can rely on the anchoring of actin *via* integrin $\alpha_M\beta_2$ at the leading edge of pseudopods at the phagocytic cup (17, 21).

Particles that are too large for ingestion by immune phagocytes result in stalling of the phagocytic process and this is called frustrated phagocytosis (22, 23). Such frustrated phagocytosis can result in the so-called fiber paradigm that sets out the basis for the harmful effects of long (>15 μm), thin, non-biodegradable fibers such as asbestos in the lung (22). Here, the alveolar macrophages can only partially take up the fiber, resulting in the release of lytic enzymes and reactive oxygen species (ROS) in the extracellular environment (22). This release of these contents can lead to inflammation and tissue damage, and eventually can trigger chronic inflammation, fibrosis, and oncogenesis (22, 24).

Phagocytosis and endocytosis thus depend on the type of PRR and phagocytic receptor engaged, but also on the geometry and mechanical properties of the particle (23, 25–34). How the morphology of particles affects their uptake is well-understood from experimental (23, 25–33) and theoretical studies (34–41). The goal of this review is to draw general conclusions on how geometry and mechanical properties affect endocytosis and phagocytosis and the subsequent endo/phagosomal maturation and immune responses, and on how this knowledge can be used in particle-based vaccine design. We therefore compared both theoretical and experimental studies with differently sized and shaped model particles and pathogens. However, the conclusions from these comparisons have to be interpreted with care, because the modes of uptake can be very different among cells types and the direct comparison between endocytic and phagocytic cargoes and techniques might not always be warranted.

PARTICLE SIZE AND SHAPE: THEORETICAL STUDIES AND MODELING

Theoretical approaches have been extensively used to predict modes of uptake for different particles with different sizes and shapes (**Supplementary Table 1**) (35–37, 41). Spheroid particles can be described by their aspect ratio (AR), which is the ratio between its ellipsoid axis (axis a, see **Figure 2**) over its spherical axis (axis b): oblate disk-like particles (AR<1), spheres (AR=1), and prolate particles (AR>1). Prolate particles with high AR (AR>2) are also called ellipsoid or rod-shaped particles. Monte-Carlo (35) and coarse-grained (39) simulations compared three modes of uptake for oblate particles and ellipsoids: tip-first (membrane first faces highest curvature of prolate particles or lowest curvature faces of oblate particles), laying-down (membrane first faces lowest curvature of prolate particles or highest curvature faces of oblate particles), and tilted (principle axes are non-perpendicular relative to the membrane) (**Figure 2**). From these simulations, it was predicted that, at least for endocytosis of small particles with sizes between 25 and 100 nm, oblate particles with a low AR (AR<0.5) are likely to be ingested by tip-first uptake mode, e.g., facing the membrane with the lowest curvature side (35, 39) (**Figure 3**). Likewise, prolate particles are more likely to be ingested by laying-down mode, thus also facing the membrane with the lowest curvature side (39). Other computational studies also predicted that prolate particles are more likely to be ingested *via* the laying-down mode (35, 37) and that tip-first uptake for prolate particles will be slower than tip-first uptake for oblate particles (34). However, the wrapping can be accompanied by a reorientation of the particle. For instance, in several theoretical studies, it was predicted that while prolate particles become attached to the membrane in a laying-down mode, at higher adhesive strengths this state becomes unstable and the particle reorients toward a deeply wrapped tip-first uptake mechanism (42, 43).

The energy of uptake depends on the bending properties of the membrane and the strength of receptor interactions, and overall endocytosis is more efficient (lower free energy requirement) with a stronger adhesiveness and a larger contact area (44). Simulations of clathrin-mediated endocytosis of ~100 nm particles predicted that the efficiency of uptake is determined by the membrane bending rigidity, which is proportional to the stiffness of the plasma surface because this determines the formation of receptor-ligand bonds (37). Computational modelling also predicted that a membrane can completely wrap particles with 0.68<AR<2.3 (35). Compared to spherical

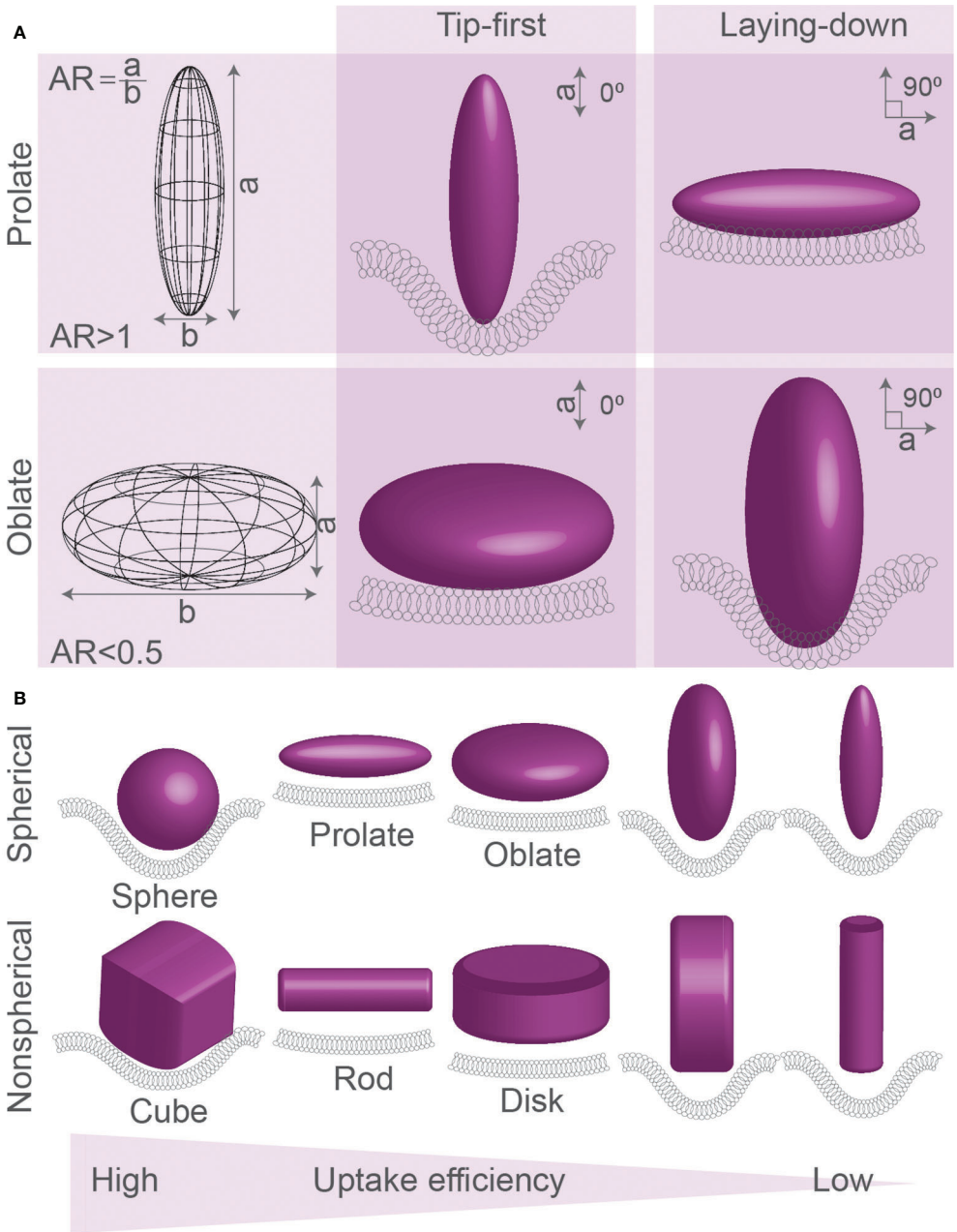

FIGURE 2 | Spherical, oblate, and prolate particles. **(A)** Spheroid particles can be described by their aspect ratio (AR), which is the ratio between the ellipsoid axis (axis a) over the spherical axis (axis b) of the particle: oblate disk-like particles (AR<1), spheres (AR=1), and prolate particles (AR>1). Particles can be ingested by different modes of uptake: tip-first (membrane first faces highest curvature of prolate particles or lowest curvature faces of oblate particles) or laying-down (membrane first faces lowest curvature of prolate particles or highest curvature faces of oblate particles). **(B)** Simulations of uptake of spherical, prolate, oblate, and corresponding non-spherical particles (cubic, rod-like, and disc-like) generally predict that spherical particles are ingested better than prolate and oblate particles. Prolate particles are generally predicted to be ingested most efficiently in laying-down mode, whereas oblate particles are ingested best in tip-first mode. Details; see text.

prolate particles, more stretched ellipsoid particles of the same volume can be less efficiently ingested because the reduced contact area facilitates less ligand-receptor interactions (35). Because of this, spheres are predicted to be engulfed more efficiently than prolate and oblate ellipsoids (**Figure 3**) (38), although particles with a bit of oblate shape, but close to spherical, might have an optimal contact area and therefore be engulfed faster than precisely round spheres (34). Thus, computational modelling predicts hindered uptake of particles with extreme shapes characterized by either high or low ARs, while more spherical particles are more permissive for uptake (**Figure 3**) (35, 38, 39).

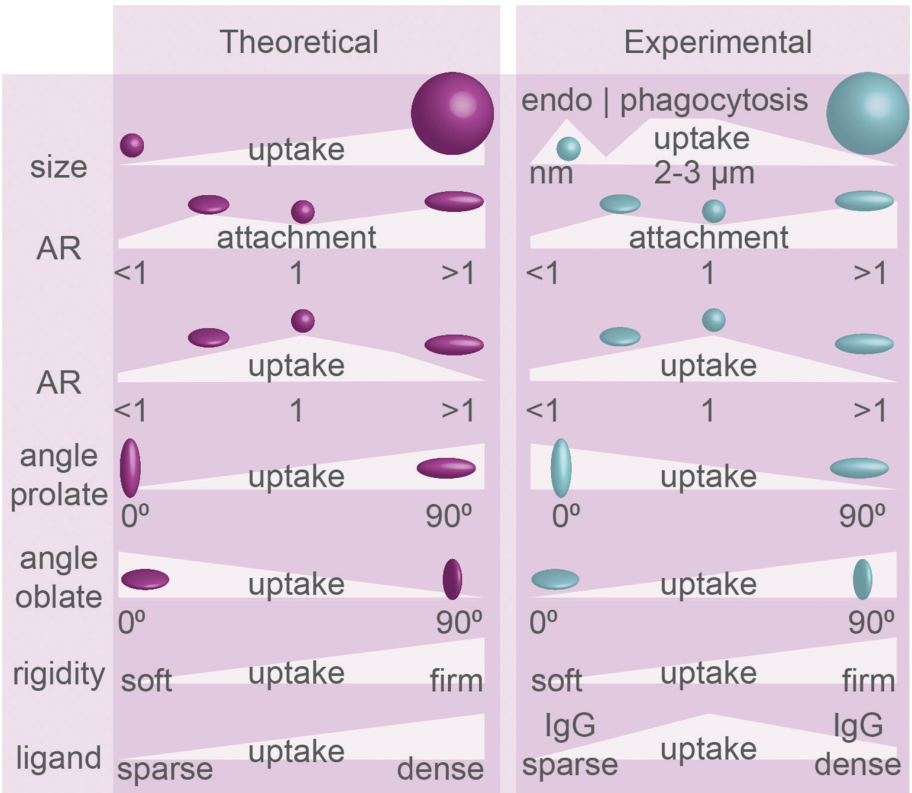

FIGURE 3 | Uptake efficiency determined by physical properties of particles: theoretical predictions and experimental evidence. Particle geometry in phagocytosis. Size, aspect ratio (AR), angle of initial contact between principle axis and membrane (see **Figure 2**), particle rigidity, and ligand density dictate the efficiency of endo/phagocytosis. Summary of theoretical predictions and experimental results. The experimental evidence for how particle rigidity affects uptake is controversial.

Simulations show that for particles of different shapes and volumes, the membrane has to overcome different free energy thresholds for particle wrapping (38, 45). Because of an increased energy cost for wrapping of the highly curved tips, ellipsoid particles are predicted to be ingested less efficiently than similarly sized spherical particles (45). Due to the lower local curvature of larger particles, smaller volume oblate particles are predicted to be taken up less efficiently than smaller volume prolate particles, but larger volume oblate particles are taken up more efficiently than larger volume prolate particles (38). For endocytosis, simulated clathrin-mediated uptake is predicted to be at maximum efficiency for larger spherical particles, with optimal sizes close to the size limit of the relatively rigid clathrin lattice (more efficient uptake for 80 nm, than for 40 nm or 160 nm-sized particles (37)), and this also depends on ligand coverage and rigidity for simulated particles (36, 37). Finally, a theoretical study predicted that the curvature of the tip of the particle matters, as particles with high aspect ratios and round tips were predicted to enter *via* laying-down mode, while particles with smaller aspect ratios and flat tips might be ingested more efficiently in tip-first mode (46). This seems to contradict another computational modelling study, where it was predicted that, given that the particle rigidity remains the same, the uptake rate and membrane bending are similar for cubes and spheres, discs and oblate particles, and rods and prolate particles (**Figure 2B**) (39). Overall, a single general rule seems to apply to the uptake of such differently shaped particles: particles with larger volumes might be taken up more efficiently than particles with smaller volumes but the same AR (**Figure 3**), because of lower membrane curvature and a higher number of receptor-ligand interactions (38).

Concerning the mechanical properties of particles, computer simulations predict that the uptake of elastic (soft) particles is less efficient than of more rigid particles, because particle deformations lead to higher energy barriers for membrane wrapping, and uptake of softer particles might need more receptors for overcoming this energy barrier (**Figure 3**) (39). Uptake of oblate particles is predicted to be least sensitive to this elasticity if the particles are positioned tip-first because they have a larger contact area with the membrane promoting the recruitment of receptors facilitating uptake. Similarly, when a prolate particle is in laying-down position at the cell membrane, its uptake could be more efficient due to a larger contact surface area with the membrane (39). This may well have consequences for phagocytosis as well, because for example cancer cells can be less rigid and softer than normal cells (47), and perhaps their rigidity is a determining factor for being phagocytosed by cells of the immune system.

Finally, asymmetry of the membrane (i.e., different composition of the membrane leaflets) is predicted to strongly affect phagocytosis, as this causes spontaneous membrane curvature which can aid or hinder membrane wrapping and can form a membrane area reservoir for providing additional membrane for engulfment of particles (48).

These theoretical predictions have several caveats. First, in real biological systems, the interaction between particles and membrane can be heavily influenced by a "corona" of proteins on the particle surface, leading to non-symmetrical engagement of uptake receptors (49). In addition, cellular uptake can be influenced by sugars on the particle surface (50), a so-called "glycocalyx" consisting of glycoproteins, glycolipids, and proteoglycans on the surface of target cells (51) and pathogens (52). Second, the plasma membrane of immune phagocytes is a highly crowded environment with different receptors and many other membrane proteins clustered and segregated in functional domains, and modelling showed that the membrane distribution of receptors can affect phagocytosis (35, 36, 39, 41). Third, most modelling approaches have as main assumption that the energy for membrane deformation is the bottleneck for uptake, and do not incorporate the role of the cytoskeleton nor do they include regulatory feedback. While the wrapping of membrane around a particle has been predicted to be strongly influenced by competing membrane-cytoskeleton interactions (53, 54), simulations do not account for the active remodelling of the cytoskeleton that can actively promote, and might even be the bottleneck for, particle invagination (see below). Fourth, biological membranes contain large numbers of different components that do not interact with the particle, such as membrane proteins and (glyco)lipids, which might affect the local membrane curvature and are predicted by statistical mechanical modelling and molecular dynamics simulations to dramatically influence cargo uptake even if the total spontaneous curvature of a membrane remains unchanged (55). Fifth, quantitative comparisons of simulation and experimental timescales associated with the phagocytic process are problematic and can only be done qualitatively. Because of these caveats, experimental findings sometimes contradict theoretical predictions as will be discussed below.

MODEL PARTICLE SIZE AND SHAPE: EXPERIMENTAL EVIDENCE

Experimental studies with synthetic model particles also show that shape, size and rigidity are important determinants for phagocytosis, but, likely due to the high complexity in cells, experimental findings are not always in agreement with the predictions from theoretical modeling. Moreover, as will be detailed below, experimental findings between studies do not always agree with each other, likely due to differences in the cell type, modes of uptake and properties of the phagocytic cargoes. Nevertheless, from a comparison of these different studies, some general conclusions can be drawn on how particle size and shape affect the endocytosis and phagocytosis of model particles.

Model particles can be ingested by the same PRRs and uptake mechanisms as microbes. In the circulation, soluble antibodies and/or proteins from the complement system can be deposited on the surface of pathogens, called opsonization, and this triggers phagocytosis by Fc-receptors and the complement receptor 3 (CR3/integrin $\alpha_M\beta_2$/Mac-1), respectively. Similarly, opsonization can mediate the uptake of model particles. For example, antibodies can also bind to the polyanionic surface of latex particles, which enhances their uptake by Fc-receptors, but the binding of antibodies (mainly IgG1 and IgM) may also trigger the classical complement pathway resulting in deposition of protein C3 cleavage products recognized by the complement receptors of host cells (56–58). Targets can also be recognized by a class of PRRs called scavenger receptors (SR), for example SCARB1 and MARCO, that recognize oxidized low-density lipoprotein (LDL) on the surface of apoptotic cells but also bind to polyanionic structures such as latex particles (56). Finally, integrins can mediate phagocytosis of particles (56, 59). Thus, naked polystyrene particles can be phagocytosed *via* four ways: i) direct binding to scavenger receptors, ii) opsonization by host-deposited IgG1 or IgM leading to iC3b binding followed by binding to complement receptor 3 (57), iii) opsonization by antibodies followed by recognition by Fc-receptors (FcR) (17), and iv) direct binding to integrins ($\alpha_V\beta_3$, $\alpha_5\beta_1$, and $\alpha_V\beta_5$) (59). Particles composed of other materials are also ingested by immune phagocytes. For example, silica particles are recognized by scavenger receptors SCARA1, SCARB1, and CD36, while monosodium urate (MSU) crystals can directly bind to cholesterol of cell membranes facilitating internalization. MSU and cholesterol crystals can also activate complement pathways through crystal opsonization by complement factor iC3b (60). The uptake routes of particles are not always understood, and for instance the mechanism of uptake of hydroxyapatite crystals by macrophages is still unclear (60).

Concerning particle size and phagocytosis, the available evidence seems to suggest there is an optimal size for spherical particles of about ~3 μm in diameter for most efficient phagocytosis. Both *in vivo* and *in vitro* studies showed that rat alveolar macrophages can efficiently clear particles in the range of 1–5 μm (**Figure 3**) (61–63), with an optimal particle size of ~2–3 μm (63). This is in line with another study addressing uptake of smaller (<1 μm) particles of different shapes made out of a polyethylene glycol diacrylate (PEGDA)-based hydrogel by endothelial cells, where it was found that the larger and more oblate particles were ingested more efficiently than smaller and prolate particles by endothelial cells (26).

There is an upper limit in the size of particles that cells can ingest, as particles exceeding the size of macrophages can halt phagocytosis (64), and larger sized particles result in frustrated phagocytosis (22). For needle-shaped particles, this limit is typically around 15 μM (22, 65), but this depends on the cell type: Although long (>20 μm) polystyrene worm-shaped particles with aspect ratios of about 22.5 could not be completely internalized by rat alveolar macrophages (27), 20 μm long calcium carbonate ($CaCO_3$) needles (aspect ratio >20) could be internalized by THP-1 macrophages and primary murine peritoneal macrophages (32). For spherical particles,

a study comparing differently sized of poly(lactic-co-glycolic acid) (PLGA) particles orally administrated to mice showed that 10 μm size was the largest size of particles that could be phagocytosed by gut phagocytes (66), although this finding might also be explained by a lower penetration of larger particles through the mucosal barrier. Likely, cells cannot phagocytose very large particles, because this requires more membrane and an increase in membrane surface area, which might be approximately equal to the surface area of the target, can thereby limit the size of particles that can be taken up (67). There is a limit up to which the plasma membrane can stretch without rupture (68, 69), about 3% for red blood cells (68), and in order to meet the need of substantial membrane for enveloping the target particles, there are two types of sources for membrane: i) folds in the plasma membrane, and ii) intracellular vesicles and granules (70–74). It is quite likely that phagocytosis of large particles requires a trigger to regulate the mobilization of these membrane reservoirs, and the plasma membrane itself might provide a mechano-chemical tuning mechanism by generating membrane tension during the uptake (75). Indeed, membrane tension could be released in a sequential manner where first the plasma membrane surface area increases by ~20 to 40% due to smoothening of the folded membrane and subsequently additional membrane was provided by exocytosis near the phagocytic cup (76). Such delivery of intracellular vesicles also plays a role during later stages of phagocytosis, an internal source of membrane derived from lysosomes was shown to be crucial to maintain the membrane integrity of phagosomes containing expanding hyphae of *Candida albicans* (74).

Although the surface density of ligands for phagocytic receptors improves uptake overall, this also seems to depend on the size of the particles. For phagocytosis, higher IgG opsonization only enhanced uptake of polystyrene spheres between 0.5 and 2 μm by RAW264.7 macrophage-like cells, but not for spheres > 2 μm (18). When uptake of differently sized liposomes by alveolar rat macrophages and RAW264.7 cells was compared, the largest tested liposomes of 650 nm – 2 um were ingested more efficiently than smaller liposomes (77, 78). For clathrin-mediated endocytosis, the uptake of particles seems restricted by the size (~100 nm) of the clathrin lattice, and larger particles are ingested less efficiently (**Figure 3**). Seventy nanometer sized flat hexagonally shaped or spherical particles were taken up with similar efficiency by mouse alveolar macrophages, but already a slight increase in size to 120 nm resulted in a reduced uptake of hexagonally shaped particles (79). Similarly, 150 nm silica spheres were ingested more efficiently by RAW264.7 cells compared to 250, 500 and 850 nm spheres (80) and round silica nanoparticles of 70 nm were ingested more efficiently than 300 nm and 1 μm sized particles by the murine XS52 epidermal Langerhans cell line (81). Thus, in general, phagocytosis might be most efficient for a particle size of about 3 μm, while clathrin-mediated endocytosis is optimal for particles around 100 nm.

Theoretical predictions that spheres are more efficiently ingested than more extremely shaped particles (35, 38, 39) are supported by experimental evidence (**Figure 3**). For both endocytosis and phagocytosis, a wide range of particles was tested to prove that shape rather than size has more effect on cellular uptake, and uptake of spheres was more efficient than uptake of any other stretched shapes (25, 29). Similarly, in comparison with spherical shapes, elongated particles (derived from 150 nm or 2 μm PLGA spheres) were ingested less efficiently by J774.A1 macrophages (82). HeLa cells more efficiently endocytosed spherical over rod-shaped nanometer-sized gold particles (83). Micrometer-sized spheres made out of CdTe quantum dot-cysteine micro-composites were phagocytosed with higher efficiency than rectangular disks and especially needle-shaped particles by RAW264.7 macrophages (84). Another study reports that although prolate micrometer-sized polystyrene particles showed the best attachment to RAW264.7 cells, they were less efficiently phagocytosed compared to spheres (**Figure 3**) (30). The same study showed that not spheres, but oblate disc-shaped ellipsoid particles are internalized with the highest efficiency, but this difference disappears with increasing particle size (30). Compared to other shapes and sizes, polystyrene prolate ellipsoid particles with 2-3 μm in their longest dimension also attached more to mouse J774 and rat alveolar NR8383 macrophage-like cells, but offered no advantage in actual uptake (25, 31). A similar preference for attachment of prolate particles was shown for nm-sized silica cylinders over spheres, although extremely long particles (worms) attached less well to RAW264.7 cells (85). Finally, prolate PLGA particles were inefficiently phagocytosed by J774 mouse macrophages, but were phagocytosed as soon as the shape of the particles was changed to more spherical (3 μm diameter) by pressure and temperature (86).

Evidence suggests that phagocytosis of differently shaped particles requires different signaling cascades. Experiments with the amoeba *Dictyostelium* showed that the coordinated activity of the small-GTPases Rac and Ras at the phagocytic cup by the multidomain protein RGBARG (RCC1, RhoGEF, BAR, and RasGAP-containing protein) is key for uptake of particles and microbes of different shapes (87). The authors propose that RGBARG promotes the protrusion of the cytoskeleton at the periphery of the phagocytic cup by expanding Rac activation in this region, while it suppresses Ras at more central regions of the nascent phagocytic cup (87). Although *Dictyostelium* without RGBARG showed improved phagocytosis of larger model particles and yeast, the spatial regulation of Ras by RGBARG was found to be important for phagocytosis of elongated cargoes (87).

Concerning the mode of uptake in phagocytosis, experimental findings seem to contradict most theoretical predictions (**Figure 3**). Tip-first phagocytosis by NR8383 and J774 cells was shown to be more efficient for μm-sized flattened prolate particles (*i.e.*, particles with three different primary axes) (25) and for long worm-shaped particles with high aspect ratios (~22.5) (27), showing that uptake is fostered by membrane interactions with high positive curvature regions. The same was observed for uptake of 2 × 10 μm cylinders made out of multiple silica spheres glued together with agarose by murine alveolar macrophages (33). Interestingly, the phagocytic cup membrane was found to move along the length of the orthogonally positioned cylinders, showing that phagocytes

were actively searching for high-curvature tips of the cylinders before uptake (33). Oblate μm-sized polystyrene particles were found to be phagocytosed inefficiently in tip-first mode by rat and mouse macrophage cell lines (25). A similar preference for uptake *via* high curvature (tip-first for prolate, or laying-down for oblate particles) over low curvature (laying down for prolate and tip-first for oblate particles) membrane contact was observed for rectangular disks composed of CdTe quantum dot–cystine microcomposites by RAW264.7 cells (84). Thus, all these findings show that phagocytosis is more efficient upon contact with higher membrane curved regions of particles and this seems to contradict most theoretical predictions (**Figure 3**) (35, 38).

Theoretical predictions that stiffer particles are generally better ingested by cells also do not always seem to hold true (39). A review of available experimental data reported on particle elasticity (39) showed that sometimes less rigid/softer particles are internalized with higher efficiency than more rigid particles. For example, phagocytosis of softer layer-by-layer (LBL) capsules by HeLa and SUM159 cells was found to be more efficient than more rigid counterparts (39). However, the opposite has also been reported and for instance antibody-opsonized deformable poly-AAm-co-AAc microparticles (DAAM-particles) with a relatively high rigidity of 7 kPa were phagocytosed by J774 murine macrophage-like cells with 6-fold higher efficiency than 1 kPa particles (19). This controversy is likely attributable to the different modes of uptake for different particles and cell types. For example, clathrin coats are relatively rigid and have a well-defined shape, and in some instances less-stiff particles might be easier to ingest because they can be deformed to better fit in clathrin-coated vesicles.

Particularly silica particles can be toxic to cells, although there does not seem to be consensus on the size dependency of this toxicity. In a study comparing uptake of 150–850 nm silica spheres by RAW264.7 cells, the larger particles caused higher toxicity as evident from higher membrane rupture, ROS and tumor necrosis factor (TNF)-α production (80). However, this contrasts findings in the mouse epidermal Langerhans cell line XS52, where 70 nm amorphous silica nanoparticles were more cytotoxic compared to 300 nm and 1 μm sized particles as assessed by acetate dehydrogenase (LDH) release (81). Moreover, crystalline 0.3 μm-sized silica particles caused more ROS and TNF-α production in RAW264.7 cells than larger 4.1 μm-sized particles (88). Also in non-phagocytic HeLa cells, spherical silica particles of 70 nm were proven to be more cytotoxic than 200 and 500 nm sized particles, and this was attributed to their higher tendency for lysosomal localization (89). The toxicity of silica is likely caused by inflammasome activation as will be discussed below.

PATHOGEN SIZE AND SHAPE: EXPERIMENTAL EVIDENCE

Findings from model particles might not always be directly applicable to real pathogens, as pathogens can engage different phagocytic receptors resulting in different modes of uptake. Moreover, pathogens can sometimes remodel their shape and express virulence factors that can affect the phagocytic process (90–93). In this section, we provide an overview of how the shape and size of pathogens affects phagocytosis. The phagocytosis of differentially shaped and sized pathogens is best understood for fungi, which are therefore the main focus of this section.

Different strains of the pathogenic fungi *C. albicans* can have different morphologies, ranging from a spherical yeast to an elongated hyphal cell (**Figure 4A**) (7, 8, 13, 93–97). As predicted by modeling of spherical *versus* elongated particles (see above), live *C. albicans* with spherical morphology were engulfed more efficiently than hyphal *C. albicans*, and hyphae of above 20 μm (but not below 20 μm) significantly hindered uptake by J774.1 macrophages (7). However, phagocytosis of live yeast-locked mutant strains of *C. albicans* that cannot form hyphae (and therefore have more spherical shapes) was significantly slower than for strains that formed hyphae (7). The phagocytosis efficiency was also dependent on the orientation of the pathogen, because hyphal cells of *C. albicans* that were positioned toward a phagocyte in a tip-first orientation were taken up more rapidly than those engulfed at an angle or where cell-cell contact was in laying-down mode (**Figure 4A**) (7). Also for bacteria, phagocytosis of

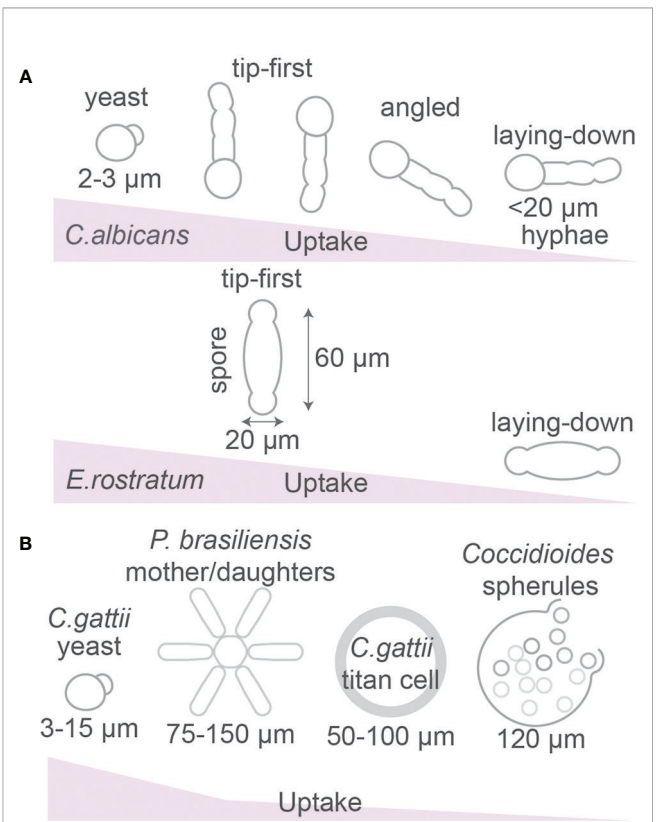

FIGURE 4 | Fungal morphology affects phagocytosis. **(A)** Uptake efficiency of yeast and hyphal forms of *Candida albicans* and *Exserohilum rostratum* by macrophages. **(B)** *Paracoccidioides brasiliensis* can form star-like mother-daughter shapes. *Cryptococcus gattii* forms large titan cells and *Coccidioides* spp. forms spherules which are larger than the size of phagocytic cells. Details; see text.

filamentous *Escherichia coli* bacteria by J774A.1 macrophages requires access to one of the terminal bacterial filament poles (tip-first), while a laying-down mode of uptake (with the longest axis of *E. coli* oriented parallel to the macrophage surface) was unsuccessful and no actin accumulation and phagocytic cup formation were observed (98). As discussed above, this contrasts previous theoretical predictions for the uptake of prolate ellipsoids, but is in agreement with experimental findings with model particles (**Figure 3**).

In contrast to elongated rods or filament shapes of bacteria that are taken up preferentially in a tip-first orientation, the phagocytosis of highly curved spiral-shaped bacterial species, for example *Campylobacter* and *Helicobacter*, might be stalled due to their shape (27, 99). Simulations have demonstrated inhibition in the uptake of such elongated particles in horizontal orientation due to the high energetic cost required for bending the plasma membrane around two different curvatures (99). Thus, the combination of a positive and negative curvature in spiral shaped particles may inhibit the membrane wrapping around the twisted surface and thereby prevent phagocytosis.

The hyphae of *C. albicans* are taken up more rapidly if phagocytosis of live fungi is initiated at the yeast-end than at the hyphae-end (7), perhaps because the round morphology of the yeast-end is more permissive for uptake. A similar observation was made for uptake of both live and heat-killed spindle-shaped spores of the fungus *Exserohilum rostratum* (~20 × 60 μm) (9). These are too large for uptake, but ~84% of macrophages attempted the uptake at the poles (reminiscent of tip-first uptake) and only ~16% positioned to the spore's middle section (laying-down mode of uptake) (9). However, this differential macrophage positioning might not be attributable to the shape of the spores, but rather to differences in the cell wall composition at the poles and in the middle of the microbes (9).

Some *C. albicans* strains can alter their shape after phagocytosis, because *C. albicans* can avoid its destruction and evade immune response by forming germ tubes and hyphen within the sealed phagosome, resulting in perforation of the phagosomal membrane (**Figure 4A**) (95, 100). The formation of hyphae is promoted by the conditions within phagosomes, such as nitric oxide (101–103), H_2O_2 (104, 105), and alkaline pH (106). *Candida albicans* actively alkalinizes the phagosomal lumen by utilizing amino acids as a carbon source and excreting ammonia (94).

The fungus *Blastomyces dermatitidis* can adopt a "Trojan Horse" method where it first is phagocytosed efficiently in a small spore form (2–5 μm) by alveolar macrophages and later survives intracellularly by increasing its size 10-fold and disseminate from the host cell as a larger yeast form (10–30 μm) (107). This large yeast form can also be taken up by phagocytes, but less efficiently compared to the smaller spore form (107). Not only fungi, but also some bacteria can adopt a filamentous morphology in order to escape phagocytosis (108–110), but how this affects phagosomal maturation is incompletely understood.

As already mentioned above, spores (~20 × 60 μm) or hyphae of *E. rostratum* are too large to be phagocytosed by RAW264.7 macrophages and primary mouse bone marrow-derived macrophages (**Figure 4A**) (9). Similarly, the fungal pathogen *Cryptococcus gattii* is capable to form titan cryptococcal cells of 50–100 μm in diameter, which is larger than most immune phagocytes and prevents phagocytosis (13, 111), whereas smaller sized (5–10 μm) *Cryptococcus neoformans* particles are efficiently phagocytosed (112, 113). Other fungi such as *Coccidioides immitis* and *Coccidioides posadasii* also form giant spherules of about 120 μm to avoid uptake by host phagocytes. Once reaching the host organism, the pathogenic fungi *Paracoccidioides brasiliensis* and *Paracoccidioides lutzii* can impede phagocytosis by creating so called asteroid bodies which are round colonies with radial symmetry of mother cells (~30 μm^2) surrounded by daughter cells reaching an area that ranges from 75 μm^2 to over 150 μm^2 diameter (**Figure 4B**) (114). Knock-down of the actin regulator Cdc42p in *P. brasiliensis* caused a size reduction of these asteroid bodies and promoted uptake by mouse bone marrow-derived macrophages and more efficient clearance from circulation after intravenous injection in mice, demonstrating that this pathogen increases its size to prevent host immune clearance (115).

Evidence suggests that neutrophils can sense microbial size. Phagocytosis of living small yeast-locked *C. albicans* mutant strains triggers ROS production and elastase recruitment to phagolysosomes, whereas uptake of the larger hyphal forms of *C. albicans* or the large aggregates of *Mycobacterium bovis* lead to elastase translocation to the nucleus of neutrophils (6). The latter nuclear translocation of elastase causes proteolytic cleavage of histones and chromatin decondensation which leads to the release of NETs targeting pathogens (**Figure 1A**) (6). Finally, budding yeasts can stall phagocytosis when the phagocytic cup reaches the negative curvature at the neck separating a mother and daughter cell, as shown for phagocytosis of living yeast by the amoeba *Dictyostelium* (116) and for paraformaldehyde-fixed and heat-killed yeast by RAW264.7 macrophages (117). This is in line with findings from theoretical modeling that hourglass-shaped particles can stall phagocytosis (**Figure 5A**) (34).

PHAGOCYTOSIS AND THE CYTOSKELETON

Phagocytosis is dependent on the actin cytoskeleton that aids in the protrusion of membrane for engulfment, forming a cup-shaped membrane fold around the particle (3, 17, 21) (**Figures 1** and **4B**). At the base of the phagocytic cup, F-actin is cleared thereby enabling the invagination of the membrane in a process driven by phosphoinositide remodeling (1, 2). At the rim of the phagocytic cup, F-actin rich pseudopodia continue to extent around the particle until they fully enwrap the particle and fuse, thereby sealing the particle into a phagosome (1, 2). The F-actin cytoskeleton exerts forces on the particles dragging them toward the center of the cell, and regulates membrane fusion events (118, 120–122). Moreover, the contractile activity of F-actin is necessary for phagocytic cup closure (17, 21). The role of F-actin in the phagocytic process has been extensively reviewed elsewhere (3, 17, 123–127), and we will limit our discussion to the role and organization of F-actin for uptake of differently shaped and sized phagocytic cargoes.

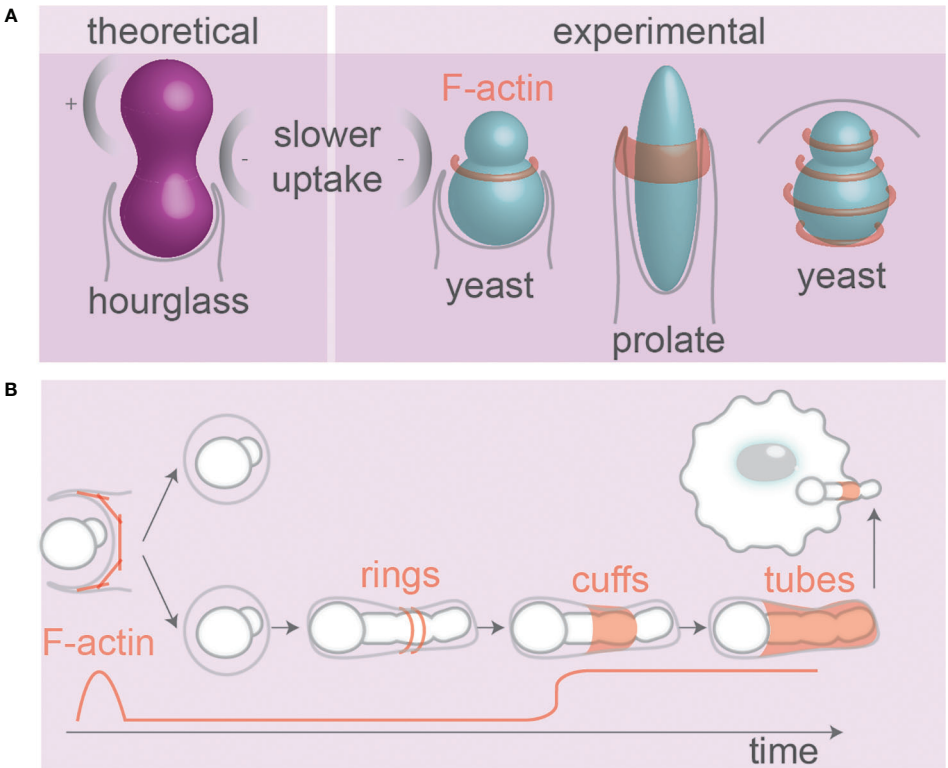

FIGURE 5 | Pathogen and particle shape affect phagosomal F-actin. **(A)** Theoretical modeling of receptor mediated uptake of hour-glass particles and experimental evidence from budding yeast. The local negative curvature at the neck can slow uptake. Ring(s) of F-actin present during uptake of yeast (117, 118) and prolate particles (64). **(B)** F-actin at phagosomes containing fungi that alter morphology inside host cells. F-actin forms wave-like dynamic rings and cuffs around hyphae during internalization. At later stages, tubes of dynamic F-actin cover hyphae (93, 97, 119). Hyphal tips protruding membranes also recruit F-actin. Details; see text.

The organization of F-actin on the surface of phagosomes might well be dependent on the shape of the ingested particle. Super-resolution microscopy revealed that F-actin aligns in concentric rings or parallel fibers on the surface of phagosomes containing (spherical) zymosan yeast particles (**Figure 5A**) (118). So far only a limited number of studies addressed the question of how the F-actin skeleton is organized at the subdiffractional level on phagosomes containing particles/pathogens with irregular shapes (128), but since many proteins and lipids involved in cytoskeletal anchoring (integrins, phosphoinositides, ERM proteins) are sensitive to curvature, phagosomes carrying irregularly shaped particles can be expected to have distinct cytoskeletal-anchoring sites (129, 130). Moreover, because of the persistence length of F-actin filaments, it might be expected that F-actin filaments tethered to phagosomes containing elongated particles would align along the long axis of such particles. In line with this, *in vitro* experiments with polymerization of actin encapsulated in artificial liposomes converted the morphology of the liposomes from spherical to tubular (131). The notion that F-actin formation is dependent on particle shape is supported by the finding that F-actin only formed a ring at the leading edge of the phagocytic cup in alveolar macrophages phagocytosing spheres or flattened prolate particles (~14 × 4 × 1 μm) provided they were phagocytosed orthogonal to their major axis (tip-first) (**Figure 5A**). In contrast, even though F-actin was assembled if the initial contact with the particles occurred orthogonal to their minor axis (laying-down), it failed to form cup-like membrane extensions or a F-actin ring, which stalled uptake (64). Similarly, uptake of filamentous *E. coli* bacteria by J774A.1 macrophages was unsuccessful and no actin accumulation and phagocytic cup formation was observed when the bacteria were positioned with their longest axis parallel to the macrophage surface (laying-down) (98).

A study utilizing DAAM-particles with stiffnesses comparable to biological objects showed that, during phagocytic uptake by murine macrophage-like cells J774A.1 cells, pseudopods of phagocytes exert ring-like compression on the DAAM particles (19). Interestingly, those rings were not round and contained dents and pits indicating that the pressure was not uniform over the perimeter of the ring (19). The dents might be caused by localized pressure exerted by podosome-like spots of F-actin at phagocytic cups (132). During the uptake of the DAAM-particles, also pits caused by compressive forces were observed at the base of the phagocytic cup and these pits were even observed during phagocytic cup closure (19). It seems unlikely that these compressive forces are exerted by the F-actin cytoskeleton, as F-actin is cleared from the cup base at this stage of phagocytosis (133).

The F-actin cytoskeleton not only mediates phagocytosis, but also plays a role later during the maturation of the phagosome and fungal pathogens sometimes express virulence factors that interfere with this. For instance, the intracellular pathogen *Cryptococcus neoformans* can block acidification of its phagosomes in a pathogen-driven process and disrupt the integrity of the phagosomal membrane to gain access to the cytosol (134). This phagosomal permeabilization is followed by transient appearance of F-actin on the phagosomal surface during fusion of the phagosome with the plasma membrane, leading to non-lytic escape of *C. neoformans* from the cell (vomocytosis) (135). In addition to virulence factors, the size, shape, and/or surface properties of *C. neoformans* might also contribute to these actin flashes, as they were not only observed in phagosomes with live pathogen, but also with heat-inactivated pathogen and they were more persistent than for latex beads (135). A point of discussion is whether this F-actin has a protective function against phagosomal membrane rupture. Such F-actin flashes have also been observed on phagocytosed latex beads and heat-inactivated *C. neoformans*, but these flashes occurred with lower frequency and such particles were not capable of the non-lytic expulsion (135). Moreover, F-actin removal from the phagosome could be a necessary step before the phagosome can fuse with endosomes and lysosomes (117, 135), although this is controversial because the F-actin tethering protein ezrin was shown to stabilize phagosomal F-actin promoting the recruitment of the lysosomal membrane protein LAMP2 (136).

There are indications that the recruitment of F-actin during later stages of phagosomal maturation depends on the shape of the ingested particle. The neck of budding yeasts creates negative curvature between mother and daughter cells, which stalls F-actin in that region during phagocytic uptake by RAW264.7 macrophages, leading to persistent F-actin flashes in that region (**Figure 5B**) (117). F-actin was only present during the early stages of phagocytic uptake of *C. albicans* mutants that were unable to form hyphae, whereas it was also present after phagocytosis of wildtype hyphae-forming *C. albicans*. In fact, different topologies of F-actin have been observed on phagosomes containing the hyphal form of *C. albicans*: cuffs of F-actin at entry points (sleeve-like extended phagocytic cups, also observed in (97)), tubes of F-actin lining fully internalized hyphae (unlike the yeast form that does not have F-actin), and F-actin at hyphal tips (93) (**Figure 5B**). However, it is arguable how much of these differences in F-actin localization is driven by the geometry of the pathogen and how much it depends on cell wall composition; F-actin was less recruited to phagosomes containing *C. albicans* mutants with dysfunctional O-mannosylation (and disrupted cell walls), even though this mutant formed hyphae comparable to wildtype fungi (93).

Moreover, *C. albicans* might express virulence factors that alter F-actin formation at the phagosomes. Using the class I PI3K inhibitor LY294002, the activity of PI3K was shown to be unnecessary for later tube-like F-actin polymerization around *C. albicans* hyphae (97). Since class I PI3K is known to play an essential role in cortical F-actin dynamics (2, 4, 137), this suggests that *C. albicans* might trigger signaling cascades to evade host defense responses, either by creating a F-actin barrier independent from class I PI3K kinases that prevents fusion with lysosomes, or by utilizing F-actin for repairing the membrane rupture caused by fast growing hyphae. Interestingly, the role of PI3K in endocytosis (138) seems to depend on particle shape, as the broad PI3K inhibitor wortmannin could block uptake of nm-sized silica worms by RAW264.7 and alveolar macrophages, but affected uptake of spheres to a lesser extent (85).

Although much less studied, not only the F-actin cytoskeleton, but also microtubules might affect phagocytosis. First, microtubules control RAW264.7 macrophage spreading and migration, thereby linking this to phagocytic capacity (139). The involvement of microtubules depends on the phagocytic cargo, as phagocytosis of spherical 3 μm-sized non-opsonized and complement-opsonized silica particles by the mouse alveolar macrophage cell line MH-S, but not antibody-opsonized silica particles, depends on the microtubular cytoskeleton (140). Second, after phagocytosis, ingested particles are moved from the cellular periphery toward the microtubule organizing center (MTOC) located at the center of the cell (139, 141). This retrograde intracellular transport is likely mediated by motor proteins of the dynein family (142). Microtubules are thus responsible for the intracellular transport of phagosomes (143, 144) and this facilitates the fusion of phagosomes with endocytic organelles (145). In Fc-receptor mediated phagocytosis by RAW264.7 macrophages, the microtubules also re-orient the MTOC toward the phagosomal cargo, and this is necessary for Golgi positioning next to the phagosome for subsequent antigen presentation to T cells (141).

Actin and microtubules are also important for clathrin-mediated endocytosis and this depends on particle shape. For instance, it was shown that small molecule inhibitors of F-actin or inhibitors of microtubule assembly in macrophages caused a reduced uptake of nm-sized particles with more complex shapes, such as worms and cylinders, but not of spherical particles which were more sensitive to inhibitors of clathrin (85).

Since particle shape would be expected to determine the resistance and drag forces a phagosome encounters within a cell, it is logical to assume that particles will be reoriented within the cell to minimize the forces required for intracellular transport. In line with this, it has been reported that the initial contact is not the only parameter determining the direction of phagocytosis, and (at least spherical) particles can be rotated following uptake (146).

PHAGOCYTOSIS AND ORGANELLAR TRAFFICKING

Most studies on cellular uptake of differently shaped and sized particles only focus on the uptake mechanism, and not on the maturation of phagocytic/endocytic organelles within host cells. After full particle engulfment by the plasma membrane, both endosomes and phagosomes undergo a process called endo/phagosomal maturation. This maturation is driven by membrane fusion events, where compartments of early endosomal and lysosomal nature fuse with the endo/phagosomes, and by

fission events characterized by vesicles budding-off from the endo/phagosome (1, 147–150). Cytosolic components, such as Rab proteins, their effectors, SNAREs, SNARE-interacting proteins, BAR-proteins, and phosphoinositide kinases, remodel the membrane of endo/phagosomes and thereby also drive maturation (1, 147, 148). After uptake of a microbial pathogen, the phagocyte attempts to kill the ingested pathogen by generating large amounts of reactive oxygen species (ROS) by the NADPH-oxidase NOX2 in the lumen of the phagosome (151). During endo/phagosomal maturation, the endo/phagosome becomes enriched in lipases, nucleases and proteases (126, 152). Among the proteases are cathepsins which play a role in antigen processing and MHC-class II chaperon chain pre-processing for antigen presentation to T cells (152). The resulting lysosome (endocytosis) or phagolysosome (phagocytosis) is a degradative compartment characterized by low pH, as a result of proton import by the vacuolar (v-)ATPase from the cytoplasm to the phagosomal lumen, and this enables the degradation of the ingested pathogen (1, 94, 108, 137).

The notion that membrane trafficking leads to asymmetry in phagosome maturation is well-established. This asymmetry can already occur early in the phagocytic process at the nascent phagocytic cup. For instance, it was observed that membrane fusion during phagocytosis of large spherical particles resulted in a displacement of the original membrane constituents at the base of the phagosomal cup, which thereby became more mature than peripheral regions and this heterogeneity was more apparent for larger particles (153). In line with this, a clear spatial gradient of phosphoinositide lipids and the proteins p85 and SHIP1 was observable early during phagocytosis of ellipsoid ~10 μm prolate polystyrene particles (154). In RAW264.7 macrophage-like cells, the uptake of PFA-inactivated filamentous *Legionella pneumophila*, *Salmonella typherium*, and *C. albicans* proceeded *via* long-lasting phagocytic cups and endosomes already fused with and released their contents along the surface of these nascent phagosomes (23, 155). However, despite acquiring late phagosomal markers (e.g., Rab7, LAMP1), the lumen of the nascent phagosomes did not acidify prior to sealing and low molecular compounds and lysosomal hydrolases could leak into the extracellular environment (23, 155). This shows that particle morphology affects phagocytic cup remodeling and closure, phagosomal acidification, and the integrity of the phagosomal membrane.

Also after sealing of the phagocytic cup, it can be expected that a maturation asymmetry is present on phagosomes carrying highly curved particles, since many phagosomal proteins (including BAR-domain proteins, vesicle coats) and lipids (phosphoinositides, phosphatidic acids) are responsive to membrane curvature (129, 130, 156, 157). Since these proteins and lipids regulate intracellular membrane fusion and fission, this raises the possibility that organellar trafficking events driving phagosomal maturation might predominantly occur at the highly curved membrane regions of phagosomes containing irregularly shaped particles. This might contribute to the pathogenicity of *C. albicans*, as it was found that phagosomes containing the hyphal form of the pathogen mature slower (93) and have prolonged presence of the small GTPase Rab14, which favors LAMP1 and cathepsin B recruitment compromising fungal survival and immune escape (119). In this study, the prolonged retention of Rab14 on phagosomes was found to be proportional to hyphal length, which supports the hypothesis that particle shape is a key parameter for phagosomal maturation.

INFLAMMASOME ACTIVATION

Several MAMPs and DAMPs can be sensed by an important class of PRRs: nucleotide-binding domain and leucine-rich-repeat proteins (NLRPs) (158). Within the cytosol, NLRPs can assemble into a large macromolecular complex called the inflammasome which triggers caspase-1 activity. Caspase-1 causes production of the inflammatory cytokines IL-1β and IL-18, leading to inflammation and inflammatory cell death (pyroptosis) (**Figure 6A**). In various pathological conditions, crystals of alum (e.g., in vaccine adjuvants), urate (in the disease gout), cholesterol (atherosclerotic lesions), calcium pyrophosphate (pseudogout), asbestos (asbestosis, meso thelioma), and silica (silicosis) can be ingested by phagocytes and trigger inflammasome activation (158–160), and this is the main explanation why crystalline silica particles are cytotoxic (see above). Inflammasome activation can be caused by destabilization of the membranes of lysosomes leading to the release of cathepsin B into the cytosol and/or efflux of potassium ions through K^+ channels (**Figures 6A, B**), which promote inflammasome activation and IL-1β and IL-18 production, but also can increase apoptosis due to cytochrome C release from mitochondria (158, 161–164).

The activation of the inflammasome by particles depends on their surface properties. Particles with reactive surface chemistry and/or particles with rough surface topologies (e.g., silica, carbon black, silver, polystyrene) can destabilize lysosomal and phagosomal membranes, thereby causing inflammasome activation, as has been extensively reviewed elsewhere (158, 165–168). Overall, for such particles with rough and/or reactive surfaces, smaller nanoparticles are more potent for inflammasome activation, because they have a larger surface area per mass, as also reviewed elsewhere (**Figure 7**) (166, 169). However, an inverse size-dependency has been reported for long particles with extreme AR. Such needle-like particles can also result in inflammasome activation, even if they are composed of biological inert material, and this is a hallmark of the fiber paradigm explaining the toxicity of long fiber like materials (asbestos, carbon nanoparticles) (22). For such particles with extreme NA, larger particles generally are more capable of inflammasome activation, as is well understood for needle-shaped particles of titanium rutile, poly(ethylene oxide), gold and carbon, and other materials (**Figure 7**) (161, 166). The activation of the inflammasome by needle-shaped particles depends on ROS production and cathepsin B (170), and although the precise mechanism and the contribution of membrane destabilization in this process are less clear (170, 171), it likely relates to frustrated phagocytosis and the leakage of ROS and lytic enzymes in the extracellular environment (the

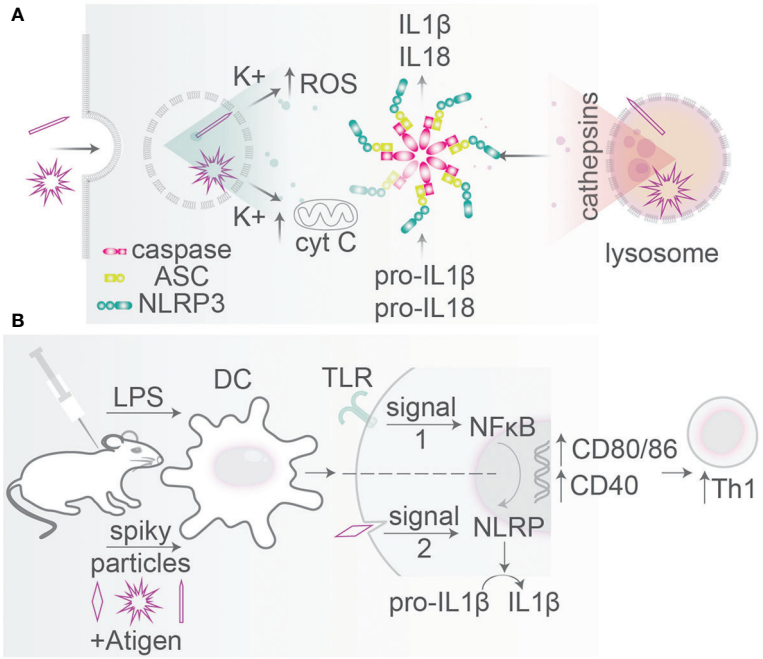

FIGURE 6 | Particle size and morphology: inflammasome activation. **(A)** Particles with spiky morphologies can disrupt endo/phagosomal membranes leading to K^+ and cathepsin leakage into the cytosol (so-called signal 2). Mitochondrial destabilization causes cytochrome C release leading to cytotoxicity. These stimuli activate inflammasome assembly from caspase-1, ASC, and NLRP3 which cleaves pro-IL-1β and pro-IL-18 into mature IL-1β and IL-18. Inflammasome activation can trigger cell death (pyroptosis). **(B)** Particle shape is an agonist in particle-based vaccination. Administration of TiO_2 spiky particles initiating mechanical rapture of phagosomes (signal 2) in mice together with a bacterial TLR ligand (signal 1). TLR signaling activates NF-κB relocation to the nucleus leading to pro-IL-1β and pro-IL-18 transcription and translation and upregulation of activation markers CD40, CD80, and CD86. Signal 2 initiates inflammasome-mediated proteolytic conversion into mature IL-1β and IL-18. Mice receiving a combination of spiky particles and a TLR-ligand thereby induce a potent Th1 response.

fiber paradigm) (22). Similar to needle-shaped particles, irregularly shaped particles with high curvatures can also induce the inflammasome and here larger particles are also more effective than smaller ones (161, 164, 166). For instance, 6 μm sized irregularly shaped CoCrMo particles were more potent for IL-1β production by human primary monocytes and human THP-1 monocytes than similarly sized smooth particles and 1 μm irregularly shaped particles (163).

The inflammasome can also be triggered following the uptake of certain pathogens. Here, the inflammasome can be activated following destabilization of endosomal or phagosomal membranes by virulence factors, but also certain topological cues such as the hyphae of fungi or some bacterial nanofeatures, such as flagella, pili, and fimbriae, might activate the inflammasome (74, 167, 168). For the pathogen *C. albicans*, this plays a role in its escape from phagocytes by lytic expulsion following pyroptosis (inflammasome-mediated cell death) (96). It is argued that the hyphae of *C. albicans* can trigger activation of the inflammasome which in turn triggers cytotoxicity of phagocytes (94), and that thereby the pathogen can escape from phagocytes. Whether filamentation is a sole trigger of such pyroptosis is debated, but it is agreed on that solely phagosomal rupture does not cause cell death, but rather a combination of NLRP3-activation, physical cell destruction, changes in pathogen morphology (96) and fungal cell wall remodeling (172) are required.

PARTICLE SIZE AND MORPHOLOGY IN THE IMMUNE SYSTEM

PRRs not only can mediate uptake but also signal intracellularly and IL-1β and IL-18 are critical for the immune system; it is therefore no surprise that particle size and shape can modulate immune activation as shown in both cultured immune cells and animal models (**Figure 8**). For example, compared to spherical particles composed of nucleic acids and cationic peptides, endocytosis by cultured mouse splenocytes of 10–100 nm sized fiber-shaped particles from the same material resulted in more expression of activation marker CD86 and the inflammatory cytokine IL-6, whereas expression of the co-stimulatory receptor CD40 and production of the inflammatory cytokine IFN-γ were reduced (173). In another study, the phagocytosis of 15–20 μm sized needle-shaped calcium carbonate particles by the THP-1 macrophage cell line resulted in more secretion of TNF-α and IL-8, thereby triggering a pro-inflammatory response (32). Finally, in mice injected with 7–8 μm-sized particles with complex geometries, neutrophil recruitment to the injection site was more rapid than with smooth particles, and phagocytosis, activation of the inflammasome and secretion of IL-1β were increased (174). The comparison of these *in vitro* and *in vivo* systems thus consistently shows that both endocytic and phagocytic cargoes with high NA induce more potent immune responses than more spherical particles.

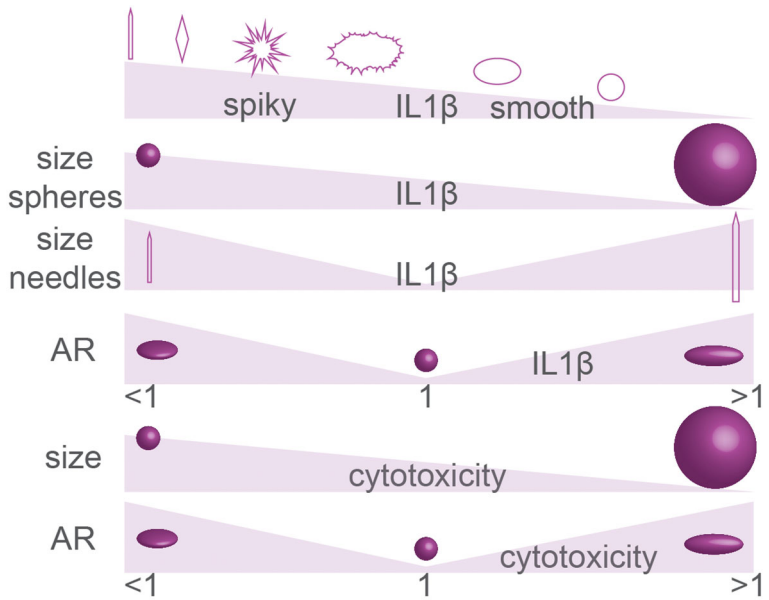

FIGURE 7 | Summary of particle geometry in inflammasome activation (IL-1β production) and cytotoxicity. The effect of particle size on inflammasome activation and cytotoxicity is controversial. Details; see text.

The size of the particles is also an important determinant for immune activation. Hydroxyapatite crystals smaller than 1–2 μm caused more TNF-α release by cultured human primary macrophages compared to 6 and 14 μm sized particles (175), likely because of more efficient activation of the inflammasome as discussed above (166). However, the particle size also influences the processing of the antigens for activation of T cells. Antigenic proteins conjugated to nanometer-sized PLGA particles were more efficient in eliciting MHC-I cross-presentation in comparison to micrometer-sized particles in cultured DCs (**Figure 8A**) (reviewed in (176)). Here, the differently sized particles were found to be differently processed by the antigen presenting DCs: the proteins bound to nanometer-range particles were processed by the proteasome for cross-presentation in cultured DCs, indicating that they escaped from the lumen of the endosome into the cytosol (177). In contrast, proteins bound to micrometer-sized particles were processed by endolysosomal proteases (177), indicating that these proteins did not escape into the cytosol.

The size of the endocytic particles also influences the immune response by determining the speed of endosomal maturation. Endosomes containing smaller silver particles of 200 nm acquired lysosomal markers, such as LAMP1, sooner than endosomes carrying larger particles of 500 nm in cultured mouse bone marrow-derived macrophages (178). Although MHC-II was recruited to endosomes containing both types of particles, antigen presentation occurred more efficiently with the larger particles and this fostered more efficient $CD4^+$ T cell activation (**Figure 8A**) (178). In this case, the efficient recruitment of lysosomes to endosomes containing smaller particles may result in a complete breakdown of the antigenic protein and thereby lower the efficiency of MHC-II presentation (179). Indeed, other studies found that not only the uptake but also the intracellular processing was determined by the particle size: 20–40 nm-sized particles composed of amphiphilic poly(gamma-glutamic acid) were not only more efficiently ingested by cultured murine bone marrow–derived DCs and RAW264.7 macrophage-like cells than larger 200–1,000 nm-sized particles (179, 180), but also underwent faster lysosomal degradation and were less likely to reside in earlier endosomal compartments (178, 179).

Because the shape and size of a particle can affect the immune system, it can affect the efficiency of particle-based vaccines (review (181)). First, the size of a particle is an important parameter for determining where a particle ends up in the body. Large particles (>1 μm) generally accumulate in small capillaries particularly in the lungs and can cause thrombosis (181). Partially due to uptake by macrophages and monocytes, which have an optimal particle size for endocytosis of about 100 nm as discussed above, particles with this size range are generally more readily cleared from circulation. For instance, one study reported that liposomal particles (bisphosphonates) carrying immune-activating molecules of ~80 nm size remained longer in circulation in animal models than 100 nm particles (**Figure 8A**) (78). However, the same study showed more potent immune responses for larger particles, as large liposomes (~200 nm) were more prone to cause cytokine production (IL-1β, TNF-α, IFN-γ, IL-6, IL-8, and IL-10) than small liposomes (~80 nm) both *in vitro* and *in vivo* (78). Finally, size is important for the efficacy of a vaccine, because large particles can simply contain more antigen than larger particles. PLGA particles of 40, 100, and 200 nm in size were administered subcutaneously in mice and, even although their uptake by lymphatic DCs showed a two-fold

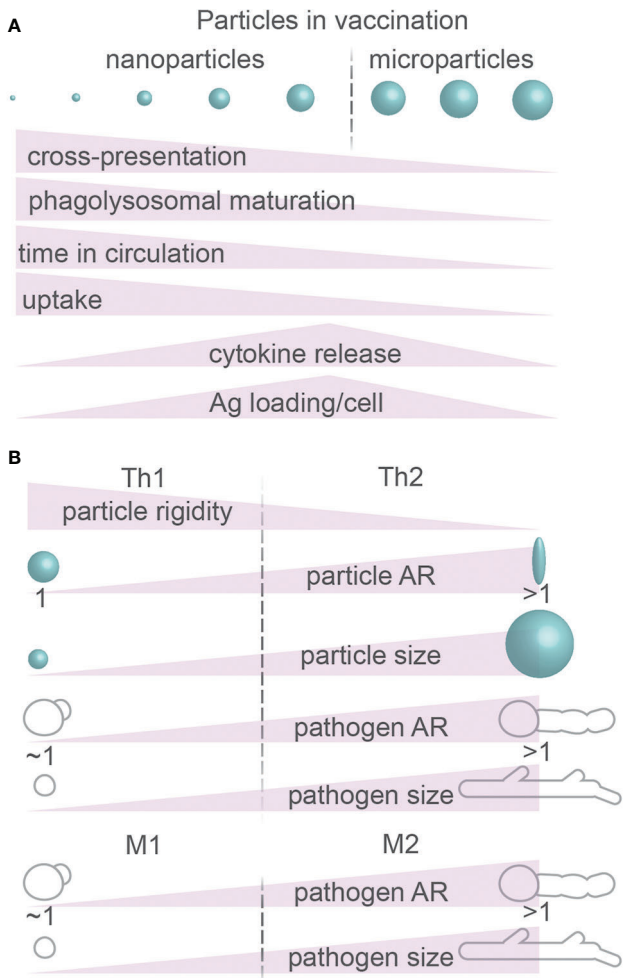

FIGURE 8 | Particle size and morphology: immune responses. **(A)** Summary of immunomodulatory effects of physical properties of particles. Ag, antigen. **(B)** Summary of effects of physical properties of particles on $CD4^+$ T cell differentiation (Th1 and Th2) and macrophage polarization (M1 and M2). Details; see text.

higher uptake for the smaller 40 nm particles, DCs carrying 200 nm particles showed a three-fold higher level of relative antigen content (180).

Based on different MAMP and DAMP signaling, DCs can discriminate between different pathogens and other immune challenges. This allows the DC to steer $CD4^+$ T cells toward different subsets: Th1 or Th2 (182). Th1 cells secrete pro-inflammatory cytokines, such as IFN-γ and TNF-α, for activating MHC expression and antimicrobial responses in phagocytes. Th2 cells secrete more anti-inflammatory cytokines including L-4, IL-5, IL-10, and IL-13 for activating responses against extracellular pathogens *via* class switching and antibody production by B-cells. Moreover, IL-10 produced by Th2 cells inhibits the function and development of Th1 cells and macrophages (182). Because of these different cytokines, Th1 cells promote immune responses that favor microbial and viral elimination (10), while Th2 responses are more directed to fending off large parasites such as helminths and worms (182). In addition to recognizing different pathogens based on MAMP and DAMP signaling, and as discussed above, immune phagocytes can discriminate between different pathogen types based on shape and size and this plays a role in T cell differentiation (**Figure 8B**) (182). Although very small gold particles (2 nm; the size of a protein) do not efficiently activate DCs because they diffuse into cells and end-up in a non-membranous compartments, 12 nm-sized particles can enter the DCs *via* some form of receptor-mediated endocytosis and promote Th1 differentiation by the DCs (181). Moreover, OVA-conjugated polystyrene particles in size ~50 nm are more likely to initiate Th1 activation in mice than micrometer-sized particles (183, 184), whereas micrometer-sized particles are more prone to trigger Th2 responses (185, 186). In line with these findings, the smaller sized round conidia of *Aspergillus fumigatus* or yeast form of *C. albicans* skew immune responses by monocytes toward Th1, while the larger hyphae forms of these pathogens trigger more Th2 responses (**Figure 8B**) (10). However, this also depends on the shape and topology of the particles, particularly whether the inflammasome is activated as discussed above, because for instance nano-spikes on the surface of TiO_2 particles resulted in Th1 responses in mice despite the large micrometer-range size of these particles (**Figure 8B**) (164).

FUTURE PROSPECTS

An apparent conclusion in this review is that predictions from simulations and theoretical modeling do not always agree with experimental findings, particularly concerning the uptake mode of elongated oblate or prolate particles. As discussed above, most theoretical studies predict that such elongated particles are ingested by maximizing the contact area between the plasma membrane and the particle (laying-down mode for prolate particles; tip-first mode for oblate particles) (34–41). However, as also discussed above, this seems to directly oppose experimental findings with model particles and hyphen-forming fungal pathogens and filamentous bacteria (7, 9, 10, 23, 25–33, 93, 94, 96–98, 119, 181). A reason for this discrepancy might be that most simulations and theoretical modeling only/mainly consider the plasma membrane, and are therefore based on the assumption that the energy required for the remodeling of the membrane is rate-limiting for uptake. However, as explained in this review, different forms of endocytosis and phagocytosis are far more complex and this assumption might not hold true. In the future, more sophisticated models should incorporate this complexity and for instance account for regional signaling by uptake receptors, localized activation of Rho-GTPases and the polarization and active remodeling of the actin cytoskeleton.

As discussed in this review, many proteins and lipids involved in signaling and cytoskeleton-anchoring are sensitive to membrane curvature (129, 130, 156, 157, 187–189). Therefore, regions on particles with high positive or negative curvature might well result in phagosomal domains of protein/lipid interactions and signaling.

These domains can be transient, given the highly dynamic nature of endocytosis and phagocytosis. In order to facilitate studying this, some approaches focus on creating stable membrane curvatures induced by surface topography that cells come in contact with (**Figure 9**) (188–192). Nano-topography-based methods such as electron-beam (E-beam) lithography can be used to create nanostructures as small as 50–100 nm, which enables high membrane curvatures (188–190). These approaches can be used for studying a wide range of questions related to curvature-induced distribution of clathrin-dependent endocytic proteins (187), polymerization of F-actin (188, 189) and nuclear membrane deformations affecting chromatin distribution and gene expression (190). Using this approach, it was found that nano-topographies of above 30 nm are sensed by macrophages and printed patterns above 71 nm in height induce higher endocytic activity (193). Moreover, microprinting allows creating adjacent structures with different sizes and topologies to compare these side-by-side using confocal or electron microscopy (**Figure 9B**) (187, 190). For example, one study using such a gradient of topologies showed that clathrin-related proteins prefer a positive curvature with a radius <200 nm (187). Moreover, an array of nanometer-sized bar-shaped structures with different diameters of the tips was used to show that only curvatures in the range of ~100–400 nm could trigger recruitment of the BAR protein FBP17 and the Arp2/3 complex required for F-actin assembly (188). An interesting modification of this method is the development of imprinted light-sensitive azobenzene-based polymer structures that can dynamically change their shape using light, thereby exerting forces and affecting the membrane curvature of cells interacting with these structures (**Figure 9C**) (189). Using this approach, it was

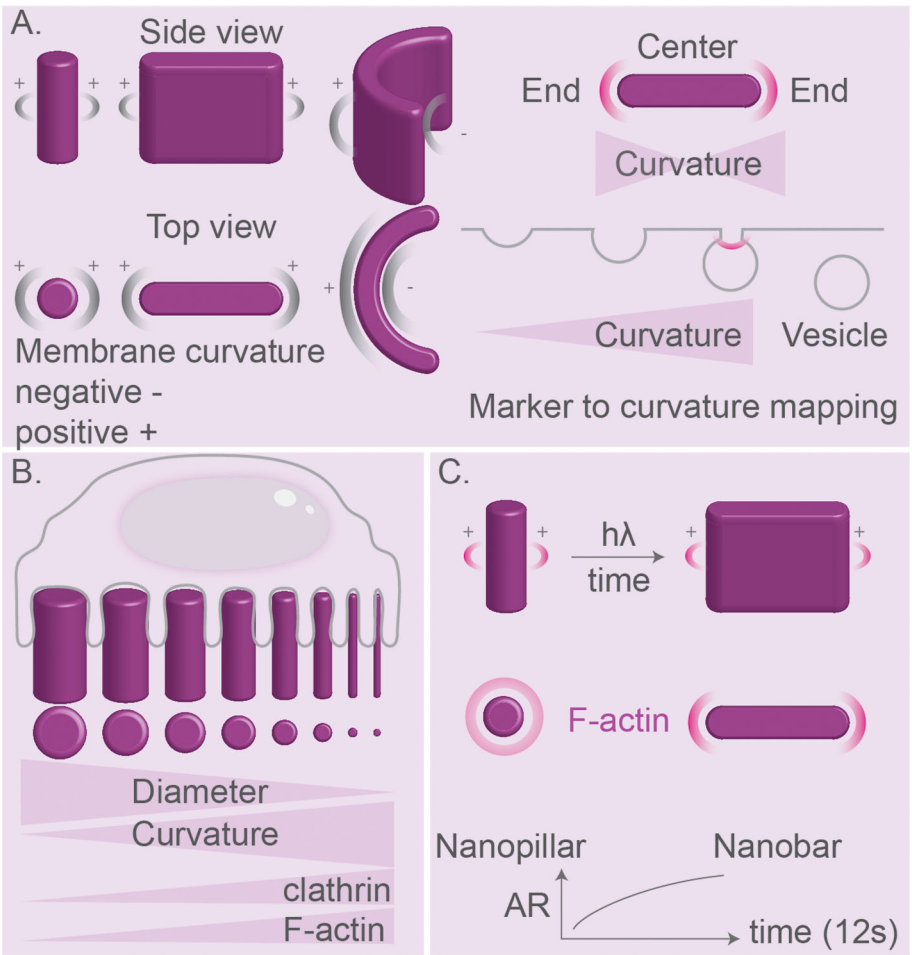

FIGURE 9 | Nanostructure topologies for studying effects of curvature on membrane. **(A)** Nanostructure fabrication using electron-beam (E-beam) lithography. Pillars, bars, and C-like patterns can be designed for generation of a library of positive and negative curvatures and flat surfaces. Curvature libraries such as nano-bars can be used of mapping proteins sensing curvature in clathrin-mediated endocytosis. End-to-center ratio is higher for markers localizing mainly to the regions of high curvature. Curvature signature can be used for mapping of curvature-dependent protein recruitment in time. **(B)** Cells can be cultured on patterned substrates for nanoscale manipulation of membrane curvature. A smaller pillar diameter results in a higher curvature. Positive curvature with a radius of <200 nm is preferred by components of clathrin-mediated endocytosis and F-actin. **(C)** Azopolymers can change shape from vertical pillar to stretched nano-bar under the influence of light and can be used for dynamic manipulation of membrane curvature. Membrane stretching at nano-bar ends triggered F-actin nucleation.

shown that the light-induced elongation of vertical pillars, which generated a higher cell membrane curvature on the tips of the pillars, promoted the local accumulation of the actin nucleator Arp2/3 complex and F-acting assembly (189). This method may inspire more future approaches to dynamically manipulate the membrane curvature and analyze protein responses in real-time.

Other advances in the material sciences and microscopy will also lead to the development of better tools to study how particle size and shape affect different forms of endocytosis and phagocytosis. Modern synthetic methods allow to create functional colloidal building blocks and define general self-assembly principles (194). Particle's shape, activity and patchiness can be engineered by combining classic sol-gel chemistry with a recently developed micro-emulsification methodology (195). These approaches will allow to design and fabricate biocompatible particles to serve as model phagocytic cargoes featuring tailored curvatures and symmetries. Designer cargos can be used for resolving particle reorientation within cells, heterogeneities of the phagosomal membrane, sites of membrane trafficking, and the arrangement of the cytoskeleton. Super-resolution stochastic optical reconstruction microscopy (STORM), stimulated emission depletion (STED) microscopy (128) and Förster resonance energy transfer-fluorescence lifetime imaging microscopy (FRET-FLIM) (196, 197) would be of benefit to determine membrane heterogeneities, the presence of maturation markers and cytoskeleton re-arrangements on the surface of irregularly shaped colloids engulfed by phagocytes. The combination of light sheet fluorescence microscopy with atomic force microscopy (AFM) enables to simultaneously visualize phagocytosis with force measurements (198) and hence will allow to answer the question of how particle size and shape affect the forces exerted by the cell. New image processing machine learning algorithms and digital holographic imaging techniques (128, 199) are gaining traction to visualize the positions and orientations of the colloids in 3D from 2D images. Phagosomes can be isolated from cells using density-gradient centrifugation or by using magnetic particles allowing for proteomic analysis. Such proteome analysis of different morphotypes of pathogenic fungi interacting with host immune cells may shed more light on the key curvature-sensing proteins that phagocytes rely on to interact with invaders (14).

In addition to these experiments with cells, experiments with artificial membranes can be of value and bridge the gap with modelling and theory. For instance, particles with a range of curvatures can be potentially encapsulated in artificial membranes for determining the organization of the membrane (*i.e.*, by encapsulating fluorescent lipid analogues, such as phospohoinositides, around the colloids for example by centrifugation of the colloids through a lipid/oil suspension on top of an aqueous buffer (200)). These artificial lipid membranes can be used for studying potential localized binding of recombinantly purified proteins that bind specific lipid species (e.g., pleckstrin-homology domains) or sense membrane curvature (e.g., BAR-domain proteins).

Current studies mostly employ either artificial colloids or killed microbial cells (by heat or chemicals) as models for phagocytosis, whereas the immune system encounters a wide range of pathogens in different shapes that actively move (e.g., by flagella) and can remodel their shape (13, 201). How pathogen motilities within phagosomes affect their degradation and whether the immune cell is somehow able to sense the movement of ingested pathogens is incompletely understood. As discussed above, various pathogens use shape to avoid clearance by the immune system, and the many pathogenic fungi can switch their morphology, for instance between small circular cells and extensive elongated hyphae (**Figure 5B**) (reviews (13, 201)). Moreover, bacteria of regular size (e.g., *Legionella pneumophila*, *Streptococcus pneumoniae*, uropathogenic *E. coli*) may undergo filamentation that slows down phagocytosis due to a higher AR (23, 98, 110). Size reduction is also used by some bacteria, as for example *Moraxella catarrhalis*, *Neisseria meningitidis*, *Salmonella typhimurium*, and *Streptococcus pneumoniae* convert from growing in longer chains to short chains, which results in a smaller surface area for complement deposition and reduced complement-dependent killing by phagocytes (110). These dynamic shape changes in the morphology of particles and the motion of particles in phagosomes can be studied using particles that can change their shape, for instance by light (189), and chemically powered micro- and nano-motors coupled to particles to induce self-propelled movements in fluids (202, 203) and by simulations (204). A particularly interesting class of model phagocytic cargoes are self-propelled colloids—synthetic particles equipped with a chemically powered nano-motor. The motor, typically platinum, catalyzes the decomposition of a suitable fuel generating a localized chemical gradient that propels the particle by either phoretic or bubble propulsion mechanisms (194, 205–211). Hematite or titania-based motors work in a similar manner, however, their activity can be controlled by light, thus allowing for a convenient on/off switch (212).

The H_2O_2 produced in phagosomes of neutrophils and dendritic cells by the NADPH oxidase NOX2 could be used as fuel to power active colloidal particles and generate forces in living cells (213, 214). More specifically, H_2O_2-fuelled particles might be engineered to utilize H_2O_2 produced in the phagosomal lumen by NOX2 for triggering particle motion, membrane rupture, and phagocytic escape (analogous to fungal pathogens). Moreover, membrane deformations by asymmetric forces exerted on the phagosome membrane by H_2O_2-fuelled active colloids might also result in polarized membrane trafficking. An alternative approach would be to create magnetic particles (*e.g.*, with Fe_2O_3 cores) to allow for external manipulation using magnetic fields (194, 205–211, 215).

Biocompatible particles with sizes in the nm range are of interest as carriers for drug-delivery or vaccination, therefore how their size, shape, rigidity, and surface composition affect cellular uptake is of particular interest (reviewed in (216)). Numerous studies attempt to use particles in the body to deliver drugs, vaccines, imaging agents or DNA or RNA for gene therapy (review (66, 164, 176, 181, 183, 184, 217)). Theoretical modeling and experiments addressing how particle shapes and sizes affect cellular uptake and (immune

responses) might help in the design of such particle-based clinical agents (35–41).

CONCLUDING REMARKS

-Theoretical simulations combined with experiments of pathogen shape, AR, and size may inspire particle design for vaccination for high antigen uptake or prolonged residence in circulation.

-Future theoretical studies should incorporate localized signaling of receptors and the cytoskeleton.

-The size and shape of pathogens affect the activation of antigen presenting cells and can skew T cell responses to Th1 and Th2 responses.

-Rough and spiky particles and particles with high AR can cause inflammasome activation and cell death.

-Pathogens change their shape to escape the immune system and this could be potentially used in vaccines.

-Molecular nanomotors can be used to study how pathogen mobility and shape-shifting affect phagocytosis and immune responses.

-Nano-topography-based methods of patterns printed on substrates can be used to gain a detailed understanding how curvature affects phagocytosis and different forms of endocytosis.

AUTHOR CONTRIBUTIONS

MB wrote the manuscript with support from MK, SS, ST, and GB. All authors contributed to the article and approved the submitted version.

FUNDING

ST, SS and GB are funded by a Young Investigator Grant from the Human Frontier Science Program (HFSP; RGY0080/2018). GB has received funding from the European Research Council (ERC) under the European Union's Horizon 2020 research and innovation program (grant agreement No. 862137) and the Netherlands Organization for Scientific Research (Vidi grant NWO-ALW VIDI 864.14.001). ST further acknowledges support from the Department of Atomic Energy, Government of India, under project no. 12-R&D-TFR-5.04-0800 and 12-D&D-TFR-5.10-1100, the Simons Foundation (Grant No. 287975) and the Max Planck Society through a Max-Planck Partner-Group.

SUPPLEMENTARY MATERIAL

The Supplementary Material for this article can be found online at: https://www.frontiersin.org/articles/10.3389/fimmu.2020.607945/full#supplementary-material

REFERENCES

1. Flannagan RS, Jaumouille V, Grinstein S. The cell biology of phagocytosis. *Annu Rev Pathol* (2012) 7:61–98. doi: 10.1146/annurev-pathol-011811-132445
2. Bohdanowicz M, Grinstein S. Role of Phospholipids in Endocytosis, Phagocytosis, and Macropinocytosis. *Physiol Rev* (2013) 93(1):69–106. doi: 10.1152/physrev.00002.2012
3. Swanson JA. Shaping cups into phagosomes and macropinosomes. *Nat Rev Mol Cell Biol* (2008) 9(8):639–49. doi: 10.1038/nrm2447
4. Cox D, Tseng CC, Bjekic G, Greenberg S. A requirement for phosphatidylinositol 3-kinase in pseudopod extension. *J Biol Chem* (1999) 274(3):1240–7. doi: 10.1074/jbc.274.3.1240
5. Schlam D, Bagshaw RD, Freeman SA, Collins RF, Pawson T, Fairn GD, et al. Phosphoinositide 3-kinase enables phagocytosis of large particles by terminating actin assembly through Rac/Cdc42 GTPase-activating proteins. *Nat Commun* (2015) 6(1):8623. doi: 10.1038/ncomms9623
6. Branzk N, Lubojemska A, Hardison SE, Wang Q, Gutierrez MG, Brown GD, et al. Neutrophils sense microbe size and selectively release neutrophil extracellular traps in response to large pathogens. *Nat Immunol* (2014) 15 (11):1017–25. doi: 10.1038/ni.2987
7. Lewis LE, Bain JM, Lowes C, Gillespie C, Rudkin FM, Gow NA, et al. Stage specific assessment of Candida albicans phagocytosis by macrophages identifies cell wall composition and morphogenesis as key determinants. *PloS Pathog* (2012) 8(3):e1002578. doi: 10.1371/journal.ppat.1002578
8. Duggan S, Essig F, Hünniger K, Mokhtari Z, Bauer L, Lehnert T, et al. Neutrophil activation by Candida glabrata but not Candida albicans promotes fungal uptake by monocytes. (2015) 17(9):1259–76. doi: 10.1111/cmi.12443
9. Reedy JL, Negoro PE, Feliu M, Lord AK, Khan NS, Lukason DP, et al. The Carbohydrate Lectin Receptor Dectin-1 Mediates the Immune Response to Exserohilum rostratum. *Infect Immun* (2017) 85(3):e00903-16. doi: 10.1128/IAI.00903-16
10. Heung LJ. Monocytes and the Host Response to Fungal Pathogens. *Front Cell Infect Microbiol* (2020) 10:34. doi: 10.3389/fcimb.2020.00034
11. Vyas JM, Van der Veen AG, Ploegh HL. The known unknowns of antigen processing and presentation. *Nat Rev Immunol* (2008) 8(8):607–18. doi: 10.1038/nri2368
12. Grotzke JE, Sengupta D, Lu Q, Cresswell P. The ongoing saga of the mechanism(s) of MHC class I-restricted cross-presentation. *Curr Opin Immunol* (2017) 46:89–96. doi: 10.1016/j.coi.2017.03.015
13. Erwig LP, Gow NA. Interactions of fungal pathogens with phagocytes. *Nat Rev Microbiol* (2016) 14(3):163–76. doi: 10.1038/nrmicro.2015.21
14. Kruger T, Luo T, Schmidt H, Shopova I, Kniemeyer O. Challenges and Strategies for Proteome Analysis of the Interaction of Human Pathogenic Fungi with Host Immune Cells. *Proteomes* (2015) 3(4):467–95. doi: 10.3390/proteomes3040467
15. Sukhithasri V, Nisha N, Biswas L, Anil Kumar V, Biswas R. Innate immune recognition of microbial cell wall components and microbial strategies to evade such recognitions. *Microbiol Res* (2013) 168(7):396–406. doi: 10.1016/j.micres.2013.02.005
16. Steele C, Rapaka RR, Metz A, Pop SM, Williams DL, Gordon S, et al. The beta-glucan receptor dectin-1 recognizes specific morphologies of Aspergillus fumigatus. *PloS Pathog* (2005) 1(4):e42. doi: 10.1371/journal.ppat.0010042
17. Freeman SA, Grinstein S. Phagocytosis: Mechanosensing, Traction Forces, and a Molecular Clutch. *Curr Biol* (2020) 30(1):R24–r26. doi: 10.1016/j.cub.2019.11.047
18. Pacheco P, White D, Sulchek T. Effects of microparticle size and Fc density on macrophage phagocytosis. *PloS One* (2013) 8(4):e60989. doi: 10.1371/journal.pone.0060989
19. Vorselen D, Wang Y, de Jesus MM, Shah PK, Footer MJ, Huse M, et al. Microparticle traction force microscopy reveals subcellular force exertion patterns in immune cell–target interactions. *Nat Commun* (2020) 11(1):20. doi: 10.1038/s41467-019-13804-z
20. Bakalar MH, Joffe AM, Schmid EM, Son S, Podolski M, Fletcher DA. Size-Dependent Segregation Controls Macrophage Phagocytosis of Antibody-Opsonized Targets. *Cell* (2018) 174(1):131–42.e13. doi: 10.1016/j.cell.2018.05.059

21. Jaumouille V, Cartagena-Rivera AX, Waterman CM. Coupling of beta2 integrins to actin by a mechanosensitive molecular clutch drives complement receptor-mediated phagocytosis. *Nat Cell Biol* (2019) 21 (11):1357–69. doi: 10.1038/s41556-019-0414-2
22. Donaldson K, Murphy FA, Duffin R, Poland CA. Asbestos, carbon nanotubes and the pleural mesothelium: a review of the hypothesis regarding the role of long fibre retention in the parietal pleura, inflammation and mesothelioma. *Part Fibre Toxicol* (2010) 7(1):5. doi: 10.1186/1743-8977-7-5
23. Prashar A, Bhatia S, Gigliozzi D, Martin T, Duncan C, Guyard C, et al. Filamentous morphology of bacteria delays the timing of phagosome morphogenesis in macrophages. *J Cell Biol* (2013) 203(6):1081–97. doi: 10.1083/jcb.201304095
24. Huang SX, Jaurand MC, Kamp DW, Whysner J, Hei TK. Role of mutagenicity in asbestos fiber-induced carcinogenicity and other diseases. *J Toxicol Environ Health B Crit Rev* (2011) 14(1-4):179–245. doi: 10.1080/10937404.2011.556051
25. Champion JA, Walker A, Mitragotri S. Role of particle size in phagocytosis of polymeric microspheres. *Pharm Res* (2008) 25(8):1815–21. doi: 10.1007/s11095-008-9562-y
26. Agarwal R, Singh V, Jurney P, Shi L, Sreenivasan SV, Roy K. Mammalian cells preferentially internalize hydrogel nanodiscs over nanorods and use shape-specific uptake mechanisms. *Proc Natl Acad Sci U.S.A.* (2013) 110(43):17247–52. doi: 10.1073/pnas.1305000110
27. Champion JA, Mitragotri S. Shape induced inhibition of phagocytosis of polymer particles. *Pharm Res* (2009) 26(1):244–9. doi: 10.1007/s11095-008-9626-z
28. Lu Z, Qiao Y, Zheng XT, Chan-Parka MB, Li CM. Effect of particle shape on phagocytosis of CdTe quantum dot–cystine composites. *Med Chem Commun* (2010) 1:84–6. doi: 10.1039/c0md00008f
29. Paul D, Achouri S, Yoon YZ, Herre J, Bryant CE, Cicuta P. Phagocytosis dynamics depends on target shape. *Biophys J* (2013) 105(5):1143–50. doi: 10.1016/j.bpj.2013.07.036
30. Sharma G, Valenta DT, Altman Y, Harvey S, Xie H, Mitragotri S, et al. Polymer particle shape independently influences binding and internalization by macrophages. *J Control Release* (2010) 147(3):408–12. doi: 10.1016/j.jconrel.2010.07.116
31. Doshi N, Mitragotri S. Macrophages recognize size and shape of their targets. *PLoS One* (2010) 5(4):e10051. doi: 10.1371/journal.pone.0010051
32. Tabei Y, Sugino S, Eguchi K, Tajika M, Abe H, Nakajima Y, et al. Effect of calcium carbonate particle shape on phagocytosis and pro-inflammatory response in differentiated THP-1 macrophages. *Biochem Biophys Res Commun* (2017) 490(2):499–505. doi: 10.1016/j.bbrc.2017.06.069
33. Tscheka C, Hittinger M, Lehr CM, Schneider-Daum N, Schneider M. Macrophage uptake of cylindrical microparticles investigated with correlative microscopy. *Eur J Pharm Biopharm* (2015) 95(Pt A):151–5. doi: 10.1016/j.ejpb.2015.03.010
34. Richards DM, Endres RG. Target shape dependence in a simple model of receptor-mediated endocytosis and phagocytosis. *Proc Natl Acad Sci USA* (2016) 113(22):6113–8. doi: 10.1073/pnas.1521974113
35. Deng H, Dutta P, Liu J. Entry modes of ellipsoidal nanoparticles on a membrane during clathrin-mediated endocytosis. *Soft Matter* (2019) 15 (25):5128–37. doi: 10.1039/C9SM00751B
36. Deng H, Dutta P, Liu J. Stochastic modeling of nanoparticle internalization and expulsion through receptor-mediated transcytosis. *Nanoscale* (2019) 11(23):11227–35. doi: 10.1039/C9NR02710F
37. Deng H, Dutta P, Liu J. Stochastic simulations of nanoparticle internalization through transferrin receptor dependent clathrin-mediated endocytosis. *Biochim Biophys Acta Gen Subj* (2018) 1862(9):2104–11. doi: 10.1016/j.bbagen.2018.06.018
38. Chen L, Xiao S, Zhu H, Wang L, Liang H. Shape-dependent internalization kinetics of nanoparticles by membranes. *Soft Matter* (2016) 12(9):2632–41. doi: 10.1039/C5SM01869B
39. Shen Z, Ye H. Membrane Wrapping Efficiency of Elastic Nanoparticles during Endocytosis: Size and Shape Matter. *ACS Nano* (2019) 13(1):215–28. doi: 10.1021/acsnano.8b05340
40. Xiong K, Zhao J, Yang D, Cheng Q, Wang J, Ji H. Cooperative wrapping of nanoparticles of various sizes and shapes by lipid membranes. *Soft Matter* (2017) 13(26):4644–52. doi: 10.1039/C7SM00345E
41. Bahrami AH, Raatz M, Agudo-Canalejo J, Michel R, Curtis EM, Hall CK, et al. Wrapping of nanoparticles by membranes. *Adv Colloid Interface Sci* (2014) 208:214–24. doi: 10.1016/j.cis.2014.02.012
42. Agudo-Canalejo J. Engulfment of ellipsoidal nanoparticles by membranes: full description of orientational changes. *J Phys Condens Matter* (2020) 32 (29):294001. doi: 10.1088/1361-648X/ab8034
43. Bahrami AH. Orientational changes and impaired internalization of ellipsoidal nanoparticles by vesicle membranes. *Soft Matter* (2013) 9 (36):8642–6. doi: 10.1039/c3sm50885d
44. Agudo-Canalejo J, Lipowsky R. Adhesive Nanoparticles as Local Probes of Membrane Curvature. *Nano Lett* (2015) 15(10):7168–73. doi: 10.1021/acs.nanolett.5b03475
45. Dasgupta S, Auth T, Gompper G. Wrapping of ellipsoidal nano-particles by fluid membranes. *Soft Matter* (2013) 9(22):5473–82. doi: 10.1039/C3SM50351H
46. Dasgupta S, Auth T, Gompper G. Shape and Orientation Matter for the Cellular Uptake of Nonspherical Particles. *Nano Lett* (2014) 14(2):687–93. doi: 10.1021/nl403949h
47. Alibert C, Goud B, Manneville JB. Are cancer cells really softer than normal cells? *Biol Cell* (2017) 109(5):167–89. doi: 10.1111/boc.201600078
48. Agudo-Canalejo J. Particle engulfment by strongly asymmetric membranes with area reservoirs. *Soft Matter* (2020) 17:298–307. doi: 10.1039/C9SM02367D
49. Ge C, Tian J, Zhao Y, Chen C, Zhou R, Chai Z. Towards understanding of nanoparticle-protein corona. *Arch Toxicol* (2015) 89(4):519–39. doi: 10.1007/s00204-015-1458-0
50. Wu L, Zhang Y, Li Z, Yang G, Kochovski Z, Chen G, et al. "Sweet" Architecture-Dependent Uptake of Glycocalyx-Mimicking Nanoparticles Based on Biodegradable Aliphatic Polyesters by Macrophages. *J Am Chem Soc* (2017) 139(41):14684–92. doi: 10.1021/jacs.7b07768
51. Kuo JC-H, Gandhi JG, Zia RN Paszek MJ. Physical biology of the cancer cell glycocalyx. *Nat Phys* (2018) 14(7):658–69. doi: 10.1038/s41567-018-0186-9
52. Möckl L. The Emerging Role of the Mammalian Glycocalyx in Functional Membrane Organization and Immune System Regulation. *Front Cell Dev Biol* (2020) 8:253. doi: 10.3389/fcell.2020.00253
53. Khosravanizadeh A, Sens P, Mohammad-Rafiee F. Wrapping of a nanowire by a supported lipid membrane. *Soft Matter* (2019) 15(37):7490–500. doi: 10.1039/C9SM00618D
54. Hashemi SM, Sens P, Mohammad-Rafiee F. Regulation of the membrane wrapping transition of a cylindrical target by cytoskeleton adhesion. *J R Soc Interface* (2014) 11(100):20140769. doi: 10.1098/rsif.2014.0769
55. Curk T, Wirnsberger P, Dobnikar J, Frenkel D, Šarić A. Controlling Cargo Trafficking in Multicomponent Membranes. *Nano Lett* (2018) 18(9):5350–6. doi: 10.1021/acs.nanolett.8b00786
56. Patel B, Gupta N, Ahsan F. Particle engineering to enhance or lessen particle uptake by alveolar macrophages and to influence the therapeutic outcome. *Eur J Pharm Biopharm* (2015) 89:163–74. doi: 10.1016/j.ejpb.2014.12.001
57. Dunkelberger JR, Song W-C. Complement and its role in innate and adaptive immune responses. *Cell Res* (2010) 20(1):34–50. doi: 10.1038/cr.2009.139
58. Jaumouillé V, Grinstein S. Molecular Mechanisms of Phagosome Formation. *Microbiol Spectr* (2016) 4(3):507–26. doi: 10.1128/9781555819194.ch27
59. Zaveri TD, Lewis JS, Dolgova NV, Clare-Salzler MJ, Keselowsky BG. Integrin-directed modulation of macrophage responses to biomaterials. *Biomaterials* (2014) 35(11):3504–15. doi: 10.1016/j.biomaterials.2014.01.007
60. Nakayama M. Macrophage Recognition of Crystals and Nanoparticles. *Front Immunol* (2018) 9:103. doi: 10.3389/fimmu.2018.00103
61. Edwards DA, Hanes J, Caponetti G, Hrkach J, Ben-Jebria A, Eskew ML, et al. Large porous particles for pulmonary drug delivery. *Science* (1997) 276 (5320):1868–71. doi: 10.1126/science.276.5320.1868
62. Makino K, Yamamoto N, Higuchi K, Harada N, Ohshima H, Terada H. Phagocytic uptake of polystyrene microspheres by alveolar macrophages: effects of the size and surface properties of the microspheres. *Colloids Surf B: Biointerfaces* (2003) 27(1):33–9. doi: 10.1016/S0927-7765(02)00042-5
63. Hirota K, Hasegawa T, Hinata H, Ito F, Inagawa H, Kochi C, et al. Optimum conditions for efficient phagocytosis of rifampicin-loaded PLGA microspheres by alveolar macrophages. *J Control Release* (2007) 119(1):69–76. doi: 10.1016/j.jconrel.2007.01.013
64. Champion JA, Mitragotri S. Role of target geometry in phagocytosis. *Proc Natl Acad Sci USA* (2006) 103(13):4930–4. doi: 10.1073/pnas.0600997103
65. Poland CA, Duffin R, Kinloch I, Maynard A, Wallace WAH, Seaton A, et al. Carbon nanotubes introduced into the abdominal cavity of mice show asbestos-like pathogenicity in a pilot study. *Nat Nanotechnol* (2008) 3 (7):423–8. doi: 10.1038/nnano.2008.111

66. Tabata Y, Inoue Y, Ikada Y. Size effect on systemic and mucosal immune responses induced by oral administration of biodegradable microspheres. *Vaccine* (1996) 14(17-18):1677–85. doi: 10.1016/S0264-410X(96)00149-1
67. Herant M, Heinrich V, Dembo M. Mechanics of neutrophil phagocytosis: behavior of the cortical tension. *J Cell Sci* (2005) 118(Pt 9):1789–97. doi: 10.1242/jcs.02275
68. Evans EA, Waugh R, Melnik L. Elastic area compressibility modulus of red cell membrane. *Biophys J* (1976) 16(6):585–95. doi: 10.1016/S0006-3495(76)85713-X
69. Zimmerberg J, Kozlov MM. How proteins produce cellular membrane curvature. *Nat Rev Mol Cell Biol* (2006) 7(1):9–19. doi: 10.1038/nrm1784
70. Petty HR, Hafeman DG, McConnell HM. Disappearance of macrophage surface folds after antibody-dependent phagocytosis. *J Cell Biol* (1981) 89(2):223–9. doi: 10.1083/jcb.89.2.223
71. Hirsch JG, Cohn ZA. Degranulation of polymorphonuclear leucocytes following phagocytosis of microorganisms. *J Exp Med* (1960) 112(6):1005–14. doi: 10.1084/jem.112.6.1005
72. Suzaki E, Kobayashi H, Kodama Y, Masujima T, Terakawa S. Video-rate dynamics of exocytotic events associated with phagocytosis in neutrophils. *Cell Motil Cytoskeleton* (1997) 38(3):215–28. doi: 10.1002/(SICI)1097-0169(1997)38:3<215::AID-CM1>3.0.CO;2-4
73. Jaumouillé V, Waterman CM. Physical Constraints and Forces Involved in Phagocytosis. *Front Immunol* (2020) 11:1097. doi: 10.3389/fimmu.2020.01097
74. Westman J, Walpole GFW, Kasper L, Xue BY, Elshafee O, Hube B, et al. Lysosome Fusion Maintains Phagosome Integrity during Fungal Infection. *Cell Host Microbe* (2020) 28(6):798–812.e6. doi: 10.1016/j.chom.2020.09.004
75. Hochmuth FM, Shao JY, Dai J, Sheetz MP. Deformation and flow of membrane into tethers extracted from neuronal growth cones. *Biophys J* (1996) 70(1):358–69. doi: 10.1016/S0006-3495(96)79577-2
76. Masters TA, Pontes B, Viasnoff V, Li Y, Gauthier NC. Plasma membrane tension orchestrates membrane trafficking, cytoskeletal remodeling, and biochemical signaling during phagocytosis. *Proc Natl Acad Sci U.S.A.* (2013) 110(29):11875–80. doi: 10.1073/pnas.1301766110
77. Chono S, Tanino T, Seki T, Morimoto K. Influence of particle size on drug delivery to rat alveolar macrophages following pulmonary administration of ciprofloxacin incorporated into liposomes. *J Drug Target* (2006) 14(8):557–66. doi: 10.1080/10611860600834375
78. Epstein-Barash H, Gutman D, Markovsky E, Mishan-Eisenberg G, Koroukhov N, Szebeni J, et al. Physicochemical parameters affecting liposomal bisphosphonates bioactivity for restenosis therapy: internalization, cell inhibition, activation of cytokines and complement, and mechanism of cell death. *J Control Release* (2010) 146(2):182–95. doi: 10.1016/j.jconrel.2010.03.011
79. Lin SY, Hsu WH, Lo JM, Tsai HC, Hsiue GH. Novel geometry type of nanocarriers mitigated the phagocytosis for drug delivery. *J Control Release* (2011) 154(1):84–92. doi: 10.1016/j.jconrel.2011.04.023
80. Leclerc L, Rima W, Boudard D, Pourchez J, Forest V, Bin V, et al. Size of submicrometric and nanometric particles affect cellular uptake and biological activity of macrophages in vitro. *Inhal Toxicol* (2012) 24(9):580–8. doi: 10.3109/08958378.2012.699984
81. Nabeshi H, Yoshikawa T, Matsuyama K, Nakazato Y, Arimori A, Isobe M, et al. Size-dependent cytotoxic effects of amorphous silica nanoparticles on Langerhans cells. *Pharmazie* (2010) 65(3):199–201.
82. Mathaes R, Winter G, Besheer A, Engert J. Influence of particle geometry and PEGylation on phagocytosis of particulate carriers. *Int J Pharm* (2014) 465(1-2):159–64. doi: 10.1016/j.ijpharm.2014.02.037
83. Chithrani BD, Ghazani AA, Chan WC. Determining the size and shape dependence of gold nanoparticle uptake into mammalian cells. *Nano Lett* (2006) 6(4):662–8. doi: 10.1021/nl052396o
84. Lu Z, Qiao Y, Zheng XT, Chan-Parka MB, Li CM. Effect of particle shape on phagocytosis of CdTe quantum dot–cystine composites. *Med Chem Commun* (2010) 1:84–6. doi: 10.1039/c0md00008f
85. Herd H, Daum N, Jones AT, Huwer H, Ghandehari H, Lehr CM. Nanoparticle geometry and surface orientation influence mode of cellular uptake. *ACS Nano* (2013) 7(3):1961–73. doi: 10.1021/nn304439f
86. Yoo JW, Mitragotri S. Polymer particles that switch shape in response to a stimulus. *Proc Natl Acad Sci USA* (2010) 107(25):11205–10. doi: 10.1073/pnas.1000346107
87. Buckley CM, Pots H, Gueho A, Vines JH, Munn CJ, Phillips BA, et al. Coordinated Ras and Rac Activity Shapes Macropinocytic Cups and Enables Phagocytosis of Geometrically Diverse Bacteria. *Curr Biol* (2020) 30(15):2912–26.e5. doi: 10.1016/j.cub.2020.05.049
88. Mischler SE, Cauda EG, Di Giuseppe M, McWilliams LJ, St Croix C, Sun M, et al. Differential activation of RAW 264.7 macrophages by size-segregated crystalline silica. *J Occup Med Toxicol* (2016) 11:57. doi: 10.1186/s12995-016-0145-2
89. Al-Rawi M, Diabate S, Weiss C. Uptake and intracellular localization of submicron and nano-sized SiO(2) particles in HeLa cells. *Arch Toxicol* (2011) 85(7):813–26. doi: 10.1007/s00204-010-0642-5
90. Höfs S, Mogavero S, Hube B. Interaction of Candida albicans with host cells: virulence factors, host defense, escape strategies, and the microbiota. *J Microbiol* (2016) 54(3):149–69. doi: 10.1007/s12275-016-5514-0
91. Douglas LM, Konopka JB. Plasma membrane organization promotes virulence of the human fungal pathogen Candida albicans. *J Microbiol (Seoul Korea)* (2016) 54(3):178–91. doi: 10.1007/s12275-016-5621-y
92. Ray SC, Rappleye CA. Flying under the radar: Histoplasma capsulatum avoidance of innate immune recognition. *Semin Cell Dev Biol* (2019) 89:91–8. doi: 10.1016/j.semcdb.2018.03.009
93. Bain JM, Louw J, Lewis LE, Okai B, Walls CA, Ballou ER, et al. Candida albicans hypha formation and mannan masking of beta-glucan inhibit macrophage phagosome maturation. *mBio* (2014) 5(6):e01874. doi: 10.1128/mBio.01874-14
94. Vylkova S, Lorenz MC. Phagosomal Neutralization by the Fungal Pathogen Candida albicans Induces Macrophage Pyroptosis. *Infect Immun* (2017) 85(2):e00832-16. doi: 10.1128/IAI.00832-16
95. Kornitzer D. Regulation of Candida albicans Hyphal Morphogenesis by Endogenous Signals. *J Fungi (Basel)* (2019) 5(1):21. doi: 10.3390/jof5010021
96. Wellington M, Koselny K, Sutterwala FS, Krysan DJ. Candida albicans triggers NLRP3-mediated pyroptosis in macrophages. *Eukaryot Cell* (2014) 13(2):329–40. doi: 10.1128/EC.00336-13
97. Heinsbroek SE, Kamen LA, Taylor PR, Brown GD, Swanson J, Gordon S. Actin and phosphoinositide recruitment to fully formed Candida albicans phagosomes in mouse macrophages. *J Innate Immun* (2009) 1(3):244–53. doi: 10.1159/000173694
98. Möller J, Luehmann T, Hall H, Vogel V. The Race to the Pole: How High-Aspect Ratio Shape and Heterogeneous Environments Limit Phagocytosis of Filamentous Escherichia coli Bacteria by Macrophages. *Nano Lett* (2012) 12(6):2901–5. doi: 10.1021/nl3004896
99. Tollis S, Dart AE, Tzircotis G, Endres RG. The zipper mechanism in phagocytosis: energetic requirements and variability in phagocytic cup shape. *BMC Syst Biol* (2010) 4:149. doi: 10.1186/1752-0509-4-149
100. McKenzie CG, Koser U, Lewis LE, Bain JM, Mora-Montes HM, Barker RN, et al. Contribution of Candida albicans cell wall components to recognition by and escape from murine macrophages. *Infect Immun* (2010) 78(4):1650–8. doi: 10.1128/IAI.00001-10
101. Hromatka BS, Noble SM, Johnson AD. Transcriptional response of Candida albicans to nitric oxide and the role of the YHB1 gene in nitrosative stress and virulence. *Mol Biol Cell* (2005) 16(10):4814–26. doi: 10.1091/mbc.e05-05-0435
102. Koch B, Barugahare AA, Lo TL, Huang C, Schittenhelm RB, Powell DR, et al. A Metabolic Checkpoint for the Yeast-to-Hyphae Developmental Switch Regulated by Endogenous Nitric Oxide Signaling. *Cell Rep* (2018) 25(8):2244–58.e7. doi: 10.1016/j.celrep.2018.10.080
103. Harcus D, Nantel A, Marcil A, Rigby T, Whiteway M. Transcription profiling of cyclic AMP signaling in Candida albicans. *Mol Biol Cell* (2004) 15(10):4490–9. doi: 10.1091/mbc.e04-02-0144
104. Nasution O, Srinivasa K, Kim M, Kim YJ, Kim W, Jeong W, et al. Hydrogen peroxide induces hyphal differentiation in Candida albicans. *Eukaryot Cell* (2008) 7(11):2008–11. doi: 10.1128/EC.00105-08
105. Rossi DCP, Gleason JE, Sanchez H, Schatzman SS, Culbertson EM, Johnson CJ, et al. Candida albicans FRE8 encodes a member of the NADPH oxidase family that produces a burst of ROS during fungal morphogenesis. *PloS Pathog* (2017) 13(12):e1006763. doi: 10.1371/journal.ppat.1006763
106. Davis D. Adaptation to environmental pH in Candida albicans and its relation to pathogenesis. *Curr Genet* (2003) 44(1):1–7. doi: 10.1007/s00294-003-0415-2

107. Sterkel AK, Mettelman R, Wuthrich M, Klein BS. The unappreciated intracellular lifestyle of Blastomyces dermatitidis. *J Immunol* (2015) 194 (4):1796–805. doi: 10.4049/jimmunol.1303089
108. Naufer A, Hipolito VEB, Ganesan S, Prashar A, Zaremberg V, Botelho RJ, et al. pH of endophagosomes controls association of their membranes with Vps34 and PtdIns(3)P levels. *J Cell Biol* (2018) 217(1):329–46. doi: 10.1083/jcb.201702179
109. Justice SS, Hunstad DA, Cegelski L, Hultgren SJ. Morphological plasticity as a bacterial survival strategy. *Nat Rev Microbiol* (2008) 6(2):162–8. doi: 10.1038/nrmicro1820
110. Yang DC, Blair KM, Salama NR. Staying in Shape: the Impact of Cell Shape on Bacterial Survival in Diverse Environments. *Microbiol Mol Biol Rev* (2016) 80(1):187–203. doi: 10.1128/MMBR.00031-15
111. Johnston SA, May RC. Cryptococcus interactions with macrophages: evasion and manipulation of the phagosome by a fungal pathogen. *Cell Microbiol* (2013) 15(3):403–11. doi: 10.1111/cmi.12067
112. Wozniak KL, Levitz SM. Cryptococcus neoformans enters the endolysosomal pathway of dendritic cells and is killed by lysosomal components. *Infect Immun* (2008) 76(10):4764–71. doi: 10.1128/IAI.00660-08
113. Huston SM, Li SS, Stack D, Timm-McCann M, Jones GJ, Islam A, et al. Cryptococcus gattii is killed by dendritic cells, but evades adaptive immunity by failing to induce dendritic cell maturation. *J Immunol* (2013) 191(1):249–61. doi: 10.4049/jimmunol.1202707
114. Hernandez-Chavez MJ, Perez-Garcia LA, Nino-Vega GA, Mora-Montes HM. Fungal Strategies to Evade the Host Immune Recognition. *J Fungi* (2017) 3(4):55. doi: 10.3390/jof3040051
115. Almeida AJ, Cunha C, Carmona JA, Sampaio-Marques B, Carvalho A, Malavazi I, et al. Cdc42p controls yeast-cell shape and virulence of Paracoccidioides brasiliensis. *Fungal Genet Biol* (2009) 46(12):919–26. doi: 10.1016/j.fgb.2009.08.004
116. Clarke M, Engel U, Giorgione J, Muller-Taubenberger A, Prassler J, Veltman D, et al. Curvature recognition and force generation in phagocytosis. *BMC Biol* (2010) 8:154. doi: 10.1186/1741-7007-8-154
117. Liebl D, Griffiths G. Transient assembly of F-actin by phagosomes delays phagosome fusion with lysosomes in cargo-overloaded macrophages. *J Cell Sci* (2009) 122(Pt 16):2935–45. doi: 10.1242/jcs.048355
118. Baranov MV, Revelo NH, Dingjan I, Maraspini R, Ter Beest M, Honigmann A, et al. SWAP70 Organizes the Actin Cytoskeleton and Is Essential for Phagocytosis. *Cell Rep* (2016) 17(6):1518–31. doi: 10.1016/j.celrep.2016.10.021
119. Okai B, Lyall N, Gow NA, Bain JM, Erwig LP. Rab14 regulates maturation of macrophage phagosomes containing the fungal pathogen Candida albicans and outcome of the host-pathogen interaction. *Infect Immun* (2015) 83 (4):1523–35. doi: 10.1128/IAI.02917-14
120. Greenberg S, el Khoury J, di Virgilio F, Kaplan EM, Silverstein SC. Ca(2+)-independent F-actin assembly and disassembly during Fc receptor-mediated phagocytosis in mouse macrophages. *J Cell Biol* (1991) 113 (4):757–67. doi: 10.1083/jcb.113.4.757
121. Kjeken R, Egeberg M, Habermann A, Kuehnel M, Peyron P, Floetenmeyer M, et al. Fusion between phagosomes, early and late endosomes: a role for actin in fusion between late, but not early endocytic organelles. *Mol Biol Cell* (2004) 15(1):345–58. doi: 10.1091/mbc.e03-05-0334
122. Yam PT, Theriot JA. Repeated cycles of rapid actin assembly and disassembly on epithelial cell phagosomes. *Mol Biol Cell* (2004) 15 (12):5647–58. doi: 10.1091/mbc.e04-06-0509
123. Barger SR, Gauthier NC, Krendel M. Squeezing in a Meal: Myosin Functions in Phagocytosis. *Trends Cell Biol* (2020) 30(2):157–67. doi: 10.1016/j.tcb.2019.11.002
124. Bain J, Gow NA, Erwig LP. Novel insights into host-fungal pathogen interactions derived from live-cell imaging. *Semin Immunopathol* (2015) 37(2):131–9. doi: 10.1007/s00281-014-0463-3
125. Feldman MB, Vyas JM, Mansour MK. It takes a village: Phagocytes play a central role in fungal immunity. *Semin Cell Dev Biol* (2019) 89:16–23. doi: 10.1016/j.semcdb.2018.04.008
126. Levin R, Grinstein S, Canton J. The life cycle of phagosomes: formation, maturation, and resolution. *Immunol Rev* (2016) 273(1):156–79. doi: 10.1111/imr.12439
127. Freeman SA, Grinstein S. Phagocytosis: receptors, signal integration, and the cytoskeleton. *Immunol Rev* (2014) 262(1):193–215. doi: 10.1111/imr.12212
128. Baranov MV, Olea RA, van den Bogaart G. Chasing Uptake: Super-Resolution Microscopy in Endocytosis and Phagocytosis. *Trends Cell Biol* (2019) 29(9):727–39. doi: 10.1016/j.tcb.2019.05.006
129. McMahon HT, Boucrot E. Membrane curvature at a glance. *J Cell Sci* (2015) 128(6):1065–70. doi: 10.1242/jcs.114454
130. Suetsugu S, Kurisu S, Takenawa T. Dynamic shaping of cellular membranes by phospholipids and membrane-deforming proteins. *Physiol Rev* (2014) 94 (4):1219–48. doi: 10.1152/physrev.00040.2013
131. Palmer AF, Wingert P, Nickels J. Atomic force microscopy and light scattering of small unilamellar actin-containing liposomes. *Biophys J* (2003) 85(2):1233–47. doi: 10.1016/S0006-3495(03)74559-7
132. Ostrowski PP, Freeman SA, Fairn G, Grinstein S. Dynamic Podosome-Like Structures in Nascent Phagosomes Are Coordinated by Phosphoinositides. *Dev Cell* (2019) 50(4):397–410.e3. doi: 10.1016/j.devcel.2019.05.028
133. Marion S, Mazzolini J, Herit F, Bourdoncle P, Kambou-Pene N, Hailfinger S, et al. The NF-κB Signaling Protein Bcl10 Regulates Actin Dynamics by Controlling AP1 and OCRL-Bearing Vesicles. *Dev Cell* (2012) 23(5):954–67. doi: 10.1016/j.devcel.2012.09.021
134. De Leon-Rodriguez CM, Fu MS, Corbali MO, Cordero RJB, Casadevall A. The Capsule of Cryptococcus neoformans Modulates Phagosomal pH through Its Acid-Base Properties. *mSphere* (2018) 3(5):e00437-18. doi: 10.1128/mSphere.00437-18
135. Johnston SA, May RC. The human fungal pathogen Cryptococcus neoformans escapes macrophages by a phagosome emptying mechanism that is inhibited by Arp2/3 complex-mediated actin polymerisation. *PloS Pathog* (2010) 6(8):e1001041. doi: 10.1371/journal.ppat.1001041
136. Marion S, Hoffmann E, Holzer D, Le Clainche C, Martin M, Sachse M, et al. Ezrin promotes actin assembly at the phagosome membrane and regulates phago-lysosomal fusion. *Traffic* (2011) 12(4):421–37. doi: 10.1111/j.1600-0854.2011.01158.x
137. Kasper L, Seider K, Hube B. Intracellular survival of Candida glabrata in macrophages: immune evasion and persistence. *FEMS Yeast Res* (2015) 15 (5):fov042. doi: 10.1093/femsyr/fov042
138. Jean S, Kiger AA. Classes of phosphoinositide 3-kinases at a glance. *J Cell Sci* (2014) 127(Pt 5):923–8. doi: 10.1242/jcs.093773
139. Binker MG, Zhao DY, Pang SJ, Harrison RE. Cytoplasmic linker protein-170 enhances spreading and phagocytosis in activated macrophages by stabilizing microtubules. *J Immunol* (2007) 179(6):3780–91. doi: 10.4049/jimmunol.179.6.3780
140. Gilberti RM, Knecht DA. Macrophages phagocytose nonopsonized silica particles using a unique microtubule-dependent pathway. *Mol Biol Cell* (2015) 26(3):518–29. doi: 10.1091/mbc.E14-08-1301
141. Eng EW, Bettio A, Ibrahim J, Harrison RE. MTOC reorientation occurs during FcgammaR-mediated phagocytosis in macrophages. *Mol Biol Cell* (2007) 18(7):2389–99. doi: 10.1091/mbc.e06-12-1128
142. Bonifacino JS, Neefjes J. Moving and positioning the endolysosomal system. *Curr Opin Cell Biol* (2017) 47:1–8. doi: 10.1016/j.ceb.2017.01.008
143. Blocker A, Griffiths G, Olivo JC, Hyman AA, Severin FF. A role for microtubule dynamics in phagosome movement. *J Cell Sci* (1998) 111(3):303.
144. Blocker A, Severin FF, Burkhardt JK, Bingham JB, Yu H, Olivo J-C, et al. Molecular Requirements for Bi-directional Movement of Phagosomes Along Microtubules. *J Cell Biol* (1997) 137(1):113–29. doi: 10.1083/jcb.137.1.113
145. Hart PD, Young MR, Jordan MM, Perkins WJ, Geisow MJ. Chemical inhibitors of phagosome-lysosome fusion in cultured macrophages also inhibit saltatory lysosomal movements. A combined microscopic and computer study. *J Exp Med* (1983) 158(2):477–92. doi: 10.1084/jem.158.2.477
146. Sanchez L, Patton P, Anthony SM, Yi Y, Yu Y. Tracking single-particle rotation during macrophage uptake. *Soft Matter* (2015) 11(26):5346–52. doi: 10.1039/C5SM00893J
147. Huotari J, Helenius A. Endosome maturation. *EMBO J* (2011) 30(17):3481–500. doi: 10.1038/emboj.2011.286
148. Fairn GD, Grinstein S. How nascent phagosomes mature to become phagolysosomes. *Trends Immunol* (2012) 33(8):397–405. doi: 10.1016/j.it.2012.03.003
149. Dingjan I, Paardekooper LM, Verboogen DRJ, von Mollard GF, Ter Beest M, van den Bogaart G. VAMP8-mediated NOX2 recruitment to endosomes is

necessary for antigen release. *Eur J Cell Biol* (2017) 96(7):705–14. doi: 10.1016/j.ejcb.2017.06.007
150. Dingjan I, Linders PT. Oxidized phagosomal NOX2 complex is replenished from lysosomes. *J Cell Sci* (2017) 130(7):1285–98. doi: 10.1242/jcs.196931
151. Vulcano M, Dusi S, Lissandrini D, Badolato R, Mazzi P, Riboldi E, et al. Toll receptor-mediated regulation of NADPH oxidase in human dendritic cells. *J Immunol* (2004) 173(9):5749–56. doi: 10.4049/jimmunol.173.9.5749
152. Turk V, Stoka V, Vasiljeva O, Renko M, Sun T, Turk B, et al. Cysteine cathepsins: from structure, function and regulation to new frontiers. *Biochim Biophys Acta* (2012) 1824(1):68–88. doi: 10.1016/j.bbapap.2011.10.002
153. Lee WL, Mason D, Schreiber AD, Grinstein S. Quantitative analysis of membrane remodeling at the phagocytic cup. *Mol Biol Cell* (2007) 18 (8):2883–92. doi: 10.1091/mbc.e06-05-0450
154. Kamen LA, Levinsohn J, Swanson JA. Differential association of phosphatidylinositol 3-kinase, SHIP-1, and PTEN with forming phagosomes. *Mol Biol Cell* (2007) 18(7):2463–72. doi: 10.1091/mbc.e07-01-0061
155. Maxson ME, Naj X, O'Meara TR, Plumb JD, Cowen LE, Grinstein S. Integrin-based diffusion barrier separates membrane domains enabling the formation of microbiostatic frustrated phagosomes. *eLife* (2018) 7:e34798. doi: 10.7554/eLife.34798
156. Kassas N, Tanguy E, Thahouly T, Fouillen L, Heintz D, Chasserot-Golaz S, et al. Comparative Characterization of Phosphatidic Acid Sensors and Their Localization during Frustrated Phagocytosis. *J Biol Chem* (2017) 292 (10):4266–79. doi: 10.1074/jbc.M116.742346
157. Cannon KS, Woods BL, Gladfelter AS. The Unsolved Problem of How Cells Sense Micron-Scale Curvature. *Trends Biochem Sci* (2017) 42(12):961–76. doi: 10.1016/j.tibs.2017.10.001
158. Sun B, Wang X, Ji Z, Li R, Xia T. NLRP3 inflammasome activation induced by engineered nanomaterials. *Small* (2013) 9(9-10):1595–607. doi: 10.1002/smll.201201962
159. Sayan M, Mossman BT. The NLRP3 inflammasome in pathogenic particle and fibre-associated lung inflammation and diseases. *Part Fibre Toxicol* (2016) 13(1):51. doi: 10.1186/s12989-016-0162-4
160. Desai J, Foresto-Neto O, Honarpisheh M, Steiger S, Nakazawa D, Popper B, et al. Particles of different sizes and shapes induce neutrophil necroptosis followed by the release of neutrophil extracellular trap-like chromatin. *Sci Rep* (2017) 7(1):15003. doi: 10.1038/s41598-017-15106-0
161. Lebre F, Sridharan R, Sawkins MJ, Kelly DJ, O'Brien FJ, Lavelle EC. The shape and size of hydroxyapatite particles dictate inflammatory responses following implantation. *Sci Rep* (2017) 7(1):2922. doi: 10.1038/s41598-017-03086-0
162. Rabolli V, Lison D, Huaux F. The complex cascade of cellular events governing inflammasome activation and IL-1beta processing in response to inhaled particles. *Part Fibre Toxicol* (2016) 13(1):40. doi: 10.1186/s12989-016-0150-8
163. Caicedo MS, Samelko L, McAllister K, Jacobs JJ, Hallab NJ, et al. Increasing both CoCrMo-alloy particle size and surface irregularity induces increased macrophage inflammasome activation in vitro potentially through lysosomal destabilization mechanisms. *J Orthop Res* (2013) 31(10):1633–42. doi: 10.1002/jor.22411
164. Wang J, Chen HJ, Hang T, Yu Y, Liu G, He G, et al. Physical activation of innate immunity by spiky particles. *Nat Nanotechnol* (2018) 13(11):1078–86. doi: 10.1038/s41565-018-0274-0
165. Chen L, Liu J, Zhang Y, Zhang G, Kang Y, Chen A, et al. The toxicity of silica nanoparticles to the immune system. *Nanomed (Lond)* (2018) 13(15):1939–62. doi: 10.2217/nnm-2018-0076
166. Rabolli V, Lison D, Huaux F. The complex cascade of cellular events governing inflammasome activation and IL-1β processing in response to inhaled particles. *Part Fibre Toxicol* (2016) 13(1):40–0. doi: 10.1186/s12989-016-0150-8
167. de Rivero Vaccari JP, Dietrich WD, Keane RW. Activation and regulation of cellular inflammasomes: gaps in our knowledge for central nervous system injury. *J Cereb Blood Flow Metab* (2014) 34(3):369–75. doi: 10.1038/jcbfm.2013.227
168. Johnson BM, Junkins RD, Ting JP. A spike in inflammation. *Nat Nanotechnol* (2018) 13(11):980–1. doi: 10.1038/s41565-018-0292-y
169. Kusaka T, Nakayama M, Nakamura K, Ishimiya M, Furusawa E, Ogasawara K. Effect of silica particle size on macrophage inflammatory responses. *PloS One* (2014) 9(3):e92634. doi: 10.1371/journal.pone.0092634
170. Palomäki J, Välimäki E, Sund J, Vippola M, Clausen PA, Jensen KA, et al. Long, Needle-like Carbon Nanotubes and Asbestos Activate the NLRP3 Inflammasome through a Similar Mechanism. *ACS Nano* (2011) 5(9):6861–70. doi: 10.1021/nn200595c
171. Hornung V, Bauernfeind F, Halle A, Samstad EO, Kono H, Rock KL, et al. Silica crystals and aluminum salts activate the NALP3 inflammasome through phagosomal destabilization. *Nat Immunol* (2008) 9(8):847–56. doi: 10.1038/ni.1631
172. O'Meara TR, Duah K, Guo CX, Maxson ME, Gaudet RG, Koselny K, et al. High-Throughput Screening Identifies Genes Required for Candida albicans Induction of Macrophage Pyroptosis. *mBio* (2018) 9(4):e01581-18. doi: 10.1128/mBio.01581-18
173. Mammadov R, Cinar G, Gunduz N, Goktas M, Kayhan H, Tohumeken S, et al. Virus-like nanostructures for tuning immune response. *Sci Rep* (2015) 5:16728. doi: 10.1038/srep16728
174. Vaine CA, Patel MK, Zhu J, Lee E, Finberg RW, Hayward RC, et al. Tuning innate immune activation by surface texturing of polymer microparticles: the role of shape in inflammasome activation. *J Immunol* (2013) 190(7):3525–32. doi: 10.4049/jimmunol.1200492
175. Nadra I, Boccaccini AR, Philippidis P, Whelan LC, McCarthy GM, Haskard DO, et al. Effect of particle size on hydroxyapatite crystal-induced tumor necrosis factor alpha secretion by macrophages. *Atherosclerosis* (2008) 196 (1):98–105. doi: 10.1016/j.atherosclerosis.2007.02.005
176. Silva AL, Soema PC, Slutter B, Ossendorp F, Jiskoot W. PLGA particulate delivery systems for subunit vaccines: Linking particle properties to immunogenicity. *Hum Vaccin Immunother* (2016) 12(4):1056–69. doi: 10.1080/21645515.2015.1117714
177. Mant A, Chinnery F, Elliott T, Williams AP. The pathway of cross-presentation is influenced by the particle size of phagocytosed antigen. *Immunology* (2012) 136(2):163–75. doi: 10.1111/j.1365-2567.2012.03558.x
178. Brewer JM, Pollock KG, Tetley L, Russell DG. Vesicle size influences the trafficking, processing, and presentation of antigens in lipid vesicles. *J Immunol* (2004) 173(10):6143–50. doi: 10.4049/jimmunol.173.10.6143
179. Seydoux E, Rothen-Rutishauser B, Nita IM, Balog S, Gazdhar A, Stumbles PA, et al. Size-dependent accumulation of particles in lysosomes modulates dendritic cell function through impaired antigen degradation. *Int J Nanomed* (2014) 9:3885–902. doi: 10.2147/IJN.S64353
180. Shima F, Uto T, Akagi T, Baba M, Akashi M. Size effect of amphiphilic poly (gamma-glutamic acid) nanoparticles on cellular uptake and maturation of dendritic cells in vivo. *Acta Biomater* (2013) 9(11):8894–901. doi: 10.1016/j.actbio.2013.06.010
181. Benne N, van Duijn J, Kuiper J, Jiskoot W, Slutter B. Orchestrating immune responses: How size, shape and rigidity affect the immunogenicity of particulate vaccines. *J Control Release* (2016) 234:124–34. doi: 10.1016/j.jconrel.2016.05.033
182. Ramirez-Ortiz ZG, Means TK. The role of dendritic cells in the innate recognition of pathogenic fungi (A. fumigatus, C. neoformans and C. albicans). *Virulence* (2012) 3(7):635–46. doi: 10.4161/viru.22295
183. Mottram PL, Leong D, Crimeen-Irwin B, Gloster S, Xiang SD, Meanger J, et al. Type 1 and 2 immunity following vaccination is influenced by nanoparticle size: formulation of a model vaccine for respiratory syncytial virus. *Mol Pharm* (2007) 4(1):73–84. doi: 10.1021/mp060096p
184. Fifis T, Gamvrellis A, Crimeen-Irwin B, Pietersz GA, Li J, Mottram PL, et al. Size-dependent immunogenicity: therapeutic and protective properties of nano-vaccines against tumors. *J Immunol* (2004) 173(5):3148–54. doi: 10.4049/jimmunol.173.5.3148
185. Kanchan V, Panda AK. Interactions of antigen-loaded polylactide particles with macrophages and their correlation with the immune response. *Biomaterials* (2007) 28(35):5344–57. doi: 10.1016/j.biomaterials.2007.08.015
186. Li X, Sloat BR, Yanasarn N, Cui Z. Relationship between the size of nanoparticles and their adjuvant activity: data from a study with an improved experimental design. *Eur J Pharm Biopharm* (2011) 78(1):107–16. doi: 10.1016/j.ejpb.2010.12.017
187. Zhao W, Hanson L, Lou HY, Akamatsu M, Chowdary PD, Santoro F, et al. Nanoscale manipulation of membrane curvature for probing endocytosis in live cells. *Nat Nanotechnol* (2017) 12(8):750–6. doi: 10.1038/nnano.2017.98
188. Lou HY, Zhao W, Li X, Duan L, Powers A, Akamatsu M, et al. Membrane curvature underlies actin reorganization in response to nanoscale surface

topography. *Proc Natl Acad Sci USA* (2019) 116(46):23143–51. doi: 10.1073/pnas.1910166116
189. De Martino S, Zhang W, Klausen L, Lou HY, Li X, Alfonso FS, et al. Dynamic Manipulation of Cell Membrane Curvature by Light-Driven Reshaping of Azopolymer. *Nano Lett* (2020) 20(1):577–84. doi: 10.1021/acs.nanolett.9b04307
190. Li X, Matino L, Zhang W, Klausen L, McGuire AF, Lubrano C, et al. A nanostructure platform for live-cell manipulation of membrane curvature. *Nat Protoc* (2019) 14(6):1772–802. doi: 10.1038/s41596-019-0161-7
191. Lou HY, Zhao W, Zeng Y, Cui B. The Role of Membrane Curvature in Nanoscale Topography-Induced Intracellular Signaling. *Acc Chem Res* (2018) 51(5):1046–53. doi: 10.1021/acs.accounts.7b00594
192. Singh AV, Patil R, Thombre DK, Gade WN. Micro-nanopatterning as tool to study the role of physicochemical properties on cell-surface interactions. *J BioMed Mater Res A* (2013) 101(10):3019–32. doi: 10.1002/jbm.a.34586
193. Yim EK, Leong KW. Significance of synthetic nanostructures in dictating cellular response. *Nanomedicine* (2005) 1(1):10–21. doi: 10.1016/j.nano.2004.11.008
194. Palacci J, Sacanna S, Steinberg AP, Pine DJ, Chaikin PM. Living crystals of light-activated colloidal surfers. *Science* (2013) 339(6122):936–40. doi: 10.1126/science.1230020
195. Youssef M, Hueckel T, Yi GR, Sacanna S. Shape-shifting colloids via stimulated dewetting. *Nat Commun* (2016) 7:12216. doi: 10.1038/ncomms12216
196. Verboogen DRJ, Baranov MV, Ter Beest M, van den Bogaart G. Visualizing Intracellular SNARE Trafficking by Fluorescence Lifetime Imaging Microscopy. *J Vis Exp* (2017) (130):e56745. doi: 10.3791/56745
197. Verboogen DRJ, Gonzalez Mancha N, Ter Beest M, van den Bogaart G. Fluorescence Lifetime Imaging Microscopy reveals rerouting of SNARE trafficking driving dendritic cell activation. *eLife* (2017) 6:e23525. doi: 10.7554/eLife.23525
198. Nelsen E, Hobson CM, Kern ME, Hsiao JP, O'Brien Iii ET, Watanabe T, et al. Combined Atomic Force Microscope and Volumetric Light Sheet System for Correlative Force and Fluorescence Mechanobiology Studies. *Sci Rep* (2020) 10(1):8133. doi: 10.1038/s41598-020-65205-8
199. Ozcan A, McLeod E. Lensless Imaging and Sensing. *Annu Rev BioMed Eng* (2016) 18:77–102. doi: 10.1146/annurev-bioeng-092515-010849
200. Noireaux V, Libchaber A. A vesicle bioreactor as a step toward an artificial cell assembly. *Proc Natl Acad Sci USA* (2004) 101(51):17669–74. doi: 10.1073/pnas.0408236101
201. Trevijano-Contador N, Rueda C, Zaragoza O. Fungal morphogenetic changes inside the mammalian host. *Semin Cell Dev Biol* (2016) 57:100–9. doi: 10.1016/j.semcdb.2016.04.008
202. Simmchen J, Katuri J, Uspal WE, Popescu MN, Tasinkevych M, Sanchez S. Topographical pathways guide chemical microswimmers. *Nat Commun* (2016) 7:10598. doi: 10.1038/ncomms10598
203. Sanchez S, Soler L, Katuri J. Chemically powered micro- and nanomotors. *Angew Chem Int Ed Engl* (2015) 54(5):1414–44. doi: 10.1002/anie.201406096
204. Chen P, Xu Z, Zhu G, Dai X, Yan LT. Cellular Uptake of Active Particles. *Phys Rev Lett* (2020) 124(19):198102. doi: 10.1103/PhysRevLett.124.198102
205. Howse JR, Jones RA, Ryan AJ, Gough T, Vafabakhsh R, Golestanian R, et al. Self-motile colloidal particles: from directed propulsion to random walk. *Phys Rev Lett* (2007) 99(4):048102. doi: 10.1103/PhysRevLett.99.048102
206. Gao W, Pei A, Wang J. Water-driven micromotors. *ACS Nano* (2012) 6(9):8432–8. doi: 10.1021/nn303309z
207. Wu Y, Wu Z, Lin X, He Q, Li J. Autonomous movement of controllable assembled Janus capsule motors. *ACS Nano* (2012) 6(12):10910–6. doi: 10.1021/nn304335x
208. Wang W, Chiang TY, Velegol D, Mallouk TE. Understanding the efficiency of autonomous nano- and microscale motors. *J Am Chem Soc* (2013) 135(28):10557–65. doi: 10.1021/ja405135f
209. Wang S, Wu N. Selecting the swimming mechanisms of colloidal particles: bubble propulsion versus self-diffusiophoresis. *Langmuir* (2014) 30(12):3477–86. doi: 10.1021/la500182f
210. Berthier L. Nonequilibrium glassy dynamics of self-propelled hard disks. *Phys Rev Lett* (2014) 112(22):220602. doi: 10.1103/PhysRevLett.112.220602
211. Golestanian R, Liverpool TB, Ajdari A. Propulsion of a molecular machine by asymmetric distribution of reaction products. *Phys Rev Lett* (2005) 94(22):220801. doi: 10.1103/PhysRevLett.94.220801
212. Palacci J, Sacanna S, Kim SH, Yi GR, Pine DJ, Chaikin PM. Light-activated self-propelled colloids. *Philos Trans A Math Phys Eng Sci* (2014) 372(2029):20130372. doi: 10.1098/rsta.2013.0372
213. Paardekooper LM, Dingjan I, Linders PTA, Staal AHJ, Cristescu SM, Verberk W, et al. Human Monocyte-Derived Dendritic Cells Produce Millimolar Concentrations of ROS in Phagosomes Per Second. *Front Immunol* (2019) 10:1216. doi: 10.3389/fimmu.2019.01216
214. Bedard K, Krause KH. The NOX family of ROS-generating NADPH oxidases: physiology and pathophysiology. *Physiol Rev* (2007) 87(1):245–313. doi: 10.1152/physrev.00044.2005
215. Mandal P, Patil G, Kakoty H, Ghosh A. Magnetic Active Matter Based on Helical Propulsion. *Acc Chem Res* (2018) 51(11):2689–98. doi: 10.1021/acs.accounts.8b00315
216. Francia V, Montizaan D. Interactions at the cell membrane and pathways of internalization of nano-sized materials for nanomedicine. *Beilstein J Nanotechnol* (2020) 11:338–53. doi: 10.3762/bjnano.11.25
217. Getts DR, Shea LD, Miller SD, King NJ. Harnessing nanoparticles for immune modulation. *Trends Immunol* (2015) 36(7):419–27. doi: 10.1016/j.it.2015.05.007

Conflict of Interest: The authors declare that the research was conducted in the absence of any commercial or financial relationships that could be construed as a potential conflict of interest.

Copyright © 2021 Baranov, Kumar, Sacanna, Thutupalli and van den Bogaart. This is an open-access article distributed under the terms of the Creative Commons Attribution License (CC BY). The use, distribution or reproduction in other forums is permitted, provided the original author(s) and the copyright owner(s) are credited and that the original publication in this journal is cited, in accordance with accepted academic practice. No use, distribution or reproduction is permitted which does not comply with these terms.

frontiers in Immunology

ORIGINAL RESEARCH
published: 15 February 2021
doi: 10.3389/fimmu.2020.617767

Check for updates

OPEN ACCESS

Edited by:
Valentin Jaumouillé, Simon Fraser University, Canada

Reviewed by:
Spencer Freeman, Hospital for Sick Children, Canada
Falk Nimmerjahn, University of Erlangen Nuremberg, Germany

***Correspondence:**
Adam D. Hoppe
Adam.Hoppe@sdstate.edu

†ORCID:
Elizabeth M. Bailey, orcid.org/0000-0002-0674-2182

‡Present address:
Elizabeth M. Bailey, Department of Pathology, University of New Mexico, Albuquerque, NM, United States

Specialty section:
This article was submitted to Molecular Innate Immunity, a section of the journal Frontiers in Immunology

Received: *15 October 2020*
Accepted: *24 December 2020*
Published: *15 February 2021*

Citation:
Bailey EM, Choudhury A, Vuppula H, Ortiz DF, Schaeck J, Manning AM, Bosques CJ and Hoppe AD (2021) Engineered IgG1-Fc Molecules Define Valency Control of Cell Surface Fcγ Receptor Inhibition and Activation in Endosomes. Front. Immunol. 11:617767. doi: 10.3389/fimmu.2020.617767

Engineered IgG1-Fc Molecules Define Valency Control of Cell Surface Fcγ Receptor Inhibition and Activation in Endosomes

Elizabeth M. Bailey[1,2†‡], Amit Choudhury[3], Harika Vuppula[1,2], Daniel F. Ortiz[3], John Schaeck[3], Anthony M. Manning[3], Carlos J. Bosques[3] and Adam D. Hoppe[1,2]*

[1] Department of Chemistry and Biochemistry, South Dakota State University, Brookings, SD, United States,
[2] BioSystems Networks and Translational Research, South Dakota State University, Brookings, SD, United States,
[3] Momenta Pharmaceuticals, Cambridge, MA, United States

The inhibition of Fcγ receptors (FcγR) is an attractive strategy for treating diseases driven by IgG immune complexes (IC). Previously, we demonstrated that an engineered tri-valent arrangement of IgG1 Fc domains (SIF1) potently inhibited FcγR activation by IC, whereas a penta-valent Fc molecule (PentX) activated FcγR, potentially mimicking ICs and leading to Syk phosphorylation. Thus, a precise balance exists between the number of engaged FcγRs for inhibition versus activation. Here, we demonstrate that Fc valency differentially controls FcγR activation and inhibition within distinct subcellular compartments. Large Fc multimer clusters consisting of 5-50 Fc domains predominately recruited Syk-mScarlet to patches on the plasma membrane, whereas PentX exclusively recruited Syk-mScarlet to endosomes in human monocytic cell line (THP-1 cells). In contrast, SIF1, similar to monomeric Fc, spent longer periods docked to FcγRs on the plasma membrane and did not accumulate and recruit Syk-mScarlet within large endosomes. Single particle tracking (SPT) of fluorescent engineered Fc molecules and Syk-mScarlet at the plasma membrane imaged by total internal reflection fluorescence microscopy (SPT-TIRF), revealed that Syk-mScarlet sampled the plasma membrane was not recruited to FcγR docked with any of the engineered Fc molecules at the plasma membrane. Furthermore, the motions of FcγRs docked with recombinant Fc (rFc), SIF1 or PentX, displayed similar motions with D ~ 0.15 $\mu m^2/s$, indicating that SIF1 and PentX did not induce reorganization or microclustering of FcγRs beyond the ligating valency.

Multicolor SPT-TIRF and brightness analysis of docked rFc, SIF1 and PentX also indicated that FcγRs were not pre-assembled into clusters. Taken together, activation on the plasma membrane requires assembly of more than 5 FcγRs. Unlike rFc or SIF1, PentX accumulated Syk-mScarlet on endosomes indicating that the threshold for FcγR activation on endosomes is lower than on the plasma membrane. We conclude that the inhibitory effects of SIF1 are mediated by stabilizing a ligated and inactive FcγR on the plasma membrane. Thus, FcγR inhibition can be achieved by low valency ligation with SIF1 that behaves similarly to FcγR docked with monomeric IgG.

Keywords: macrophage, Fcγ receptor, antibodies, immune complex, autoimmunity, monocyte, inhibitor, single molecule

INTRODUCTION

Immune complexes (IC) containing immunoglobulin G (IgG) are a hallmark of many autoimmune diseases and inflammatory reactions. The activation of Fcγ receptors (FcγR) on macrophages by IC-IgG contributes to cytokine signaling and inflammatory pathogenesis in autoimmunity including the recruitment of neutrophils, monocytes, T cells, natural killer cells (NK cells), and additional macrophages (1, 2). In systemic lupus erythematosus (SLE), a chronic autoimmune disease, IC-IgG deposits in organs and tissues (3) and are recognized by FcγRs on macrophages, monocytes and neutrophils (4). In SLE, macrophages are overwhelmed and unable to clear the ICs leading to continued macrophage activation, sustained secretion of pro-inflammatory cytokines, autoantibody production, tissue damage and acute phases of the disease (5). Macrophages also present antigen to T cells, which promotes their activation and additional tissue damage (5). Thus, inhibiting FcγR activation and disrupting this inflammatory circuit is an attractive therapeutic strategy for treating autoimmunity (6).

Immune reactions to IC-IgGs are governed by activating and inhibitory FcγRs. Activating FcγRs (FcγRI, FcγRIIa, FcγRIIc, and FcγRIIIa/b) signal *via* immunoreceptor tyrosine-based activation motifs (ITAMs) found in the cytoplasmic tail of FcγRIIa/c or within the 'common gamma chain' (FcRγ) associated with FcγRI and FcγRIIIa/b. FcγRIIb contains an immunoreceptor tyrosine-based inhibition motif (ITIM). IgG bound to ICs or pathogen surfaces bind FcγRs leading to clustering and phosphorylation of ITAM phosphotyrosines by the Src family kinases, including Lyn. Recruitment of Syk kinase to phosphorylated ITAM is the hallmark of FcγR activation (2, 7, 8), where it promotes phosphorylation of additional signaling molecules including phosphotidylinositiol-3-kinase and Bruton's tyrosine kinase (BTK) leading to signal amplification (9, 10). Phosphorylation of the ITIM within FcγRIIb allows docking of SHIP-1, a 5'-phophoinosital phosphatase that negatively regulates inflammatory responses triggered by ICs (2). Downstream effects of FcγR activation include antibody-dependent cell-mediated cytotoxicity (ADCC), and phagocytosis (ADCP) (1, 2, 11), as well as cytokine production promoting inflammation and autoimmunity in NFAT/NFkb dependent pathways (2).

FcγR inhibition is a therapeutic target for autoimmune diseases with demonstrated potential for treating IC-associated autoimmune diseases (6, 12–15). Monomeric IgG Fc fragments and IVIG are effective in treating rheumatoid arthritis models in mice and humans for various autoimmune diseases such as Kawasaki disease and acute immune thrombocytopenic purpura (ITP) (13–15). While this strategy can provide therapeutic benefit, it requires large doses as the Fc-FcγR binding is 1:1 and may be displaced by polyvalent ICs. An alternative strategy currently in clinical trial, is to create multivalent Fc molecules that have high affinity for the FcγR, but do not activate it, thereby preventing the IC-IgG binding and providing long-lived inhibition (6). Disruption of FcγR signaling in turn inhibits pro-inflammatory response and alleviates inflammation and tissue damage and limits B and T cell activation and autoantibody production (2, 5, 6). Previously, we demonstrated that the valency of engineered Fc molecules could potently inhibit or potently activate FcγRs (6). Specifically, pentameric Fc arranged in an X-geometry (PentX), was a strong agonist for FcγRs, mediating potent Syk phosphorylation, whereas the trimer, SIF1, inhibited FcγR activation by IC-IgG both *in vitro* as well as in animal autoimmune models (6). How these two constructs effect differential outcomes for FcγR signaling offers new mechanistic insights.

Understanding the biophysical mechanisms of FcγR activation is critical for elucidating robust strategies using engineered Fc molecules as inhibitors. In the context of phagocytosis, engagement of FcγR with hundreds to thousands of surface-associated IgG promotes FcγR clustering on the micrometer length scale driven by the macrophage cytoskeleton (16). For IC-IgG, recent superresolution experiments on fixed cells suggest that FcγRs exist as both monomers and in pre-formed clusters confined by the cytoskeleton and that IC-IgG prompts clustering of additional FcγRs (17, 18). Furthermore, IC-IgG immobilization of FcγR clusters is thought to promote internalization and degradation of the ICs in the lysosome (19), IC-mediated signaling from endosomes along the endocytic pathway have not been evaluated. Here, we defined the effect of Fcs with defined valency on the movements of FcγRs on the cell surface, endocytosis and Syk recruitment to the plasma membrane and FcγR bearing endosomes. Our findings shed new light on FcγR

inhibition at the plasma membrane and illustrate that endocytosis may lower thresholds for FcγR activation.

METHODS

Cell Culture

THP-1 cells were cultured in RPMI-1640 Medium (ATCC 30-2001) and maintained at 100,000–200,000 cells per milliliter. Differentiation of THP-1 cells into macrophage-like cells with high levels of FcγR was achieved in a 48-h incubation in RPMI containing 50 ng/ml Phorbol 12-myristate 13-acetate, 97% (PMA, Acros Organics, AC356150010) and rested for 24-h in RPMI without PMA. Lentiviral vectors were produced in 293T cells by transfection with Syk-mScarlet-pLJM1 (https://benchling.com/s/seq-VHzJFZG9UJ4vW2bJ2Rmp/edit), pPAX2 (Addgene plasmid # 12260), pVSVG (Addgene plasmid #8454), using polyethylenimine (PEI). After 48 h, lentivirus was harvested, centrifuged, and added to THP-1 cells. After the 48-h transduction, cells were selected with Blastidin (10 μg/ml) for 2 days.

PMA differentiated THP-1 cells were characterized using fluorescently conjugated Fab fragments (to exclude Fc-mediated binding to FcγRs) of anti-hCD64 (Santa Cruz Biotechnology sc1184) and anti-hCD32 (StemCell Technologies 60012). Fab fragments were generated using 62.5 μg of each antibody using the Pierce Fab micro preparation kit (Thermo Fisher 44685). The anti-CD64 and anti-CD32 Fab fragments were labeled with AF647 NHS ester and used to label THP-1 and differentiated THP-1 cells. Cells were blocked with dPBS+1% FBS for 15 min on ice before adding the Fab fragments diluted into dPBS with 1% FBS at a 1:8 dilution of 1.14 μM labeled Fab fragments (final concentration of approximately 0.18 μM), incubated 20 min on ice, spun down at 800 g for 3 min and resuspended in cold Hank's Balanced Salt Solution (HBSS, Corning™21023CV) and kept on ice until analyzed by the BD Accuri C6 flow cytometer (**Supplementary Figure 1**). We were unsuccessful in preparing anti-CD16 Fab fragments.

Differentiated THP-1 were evaluated for their phagocytic activity by dropping a 30:1 MOI of biotinylated and anti-IgG2a opsonized sRBCs (sheep red blood cells) on differentiated THP-1 cells. Phase contrast microscopy using an inverted fluorescent microscope was used for a qualitative analysis to observe phagocytosed sRBCs. PMA differentiated THP-1 cells had an elevated phagocytic capacity (data not shown).

Fetal liver macrophages expressing Cas9 (FLM^{Cas9}) cell cultures were generated from gestational day 15–19 mouse fetuses from B6J.129(Cg)-Igs2tm1.1(CAG-cas9*)Mmw/J mice (The Jackson Laboratory, Stock No. 028239, Bar Harbor, ME) (20) in accordance with South Dakota State University Institutional Animal Use and Care Committee. Liver tissue was mechanically dissociated using sterile fine-pointed forceps and a single-cell suspension was created by passing the tissue through a 1 ml pipette tip. Cells were plated on non-tissue culture treated dishes and kept in growth and differentiation medium containing the following: 20% heat-inactivated fetal bovine serum; 30% L-cell supernatant, a source of MCSF and 50% Dulbecco's modified growth medium containing 4.5 g/L glucose, 110 mg/L sodium pyruvate, 584 mg/L-glutamine, 1 IU/ml penicillin and 100 μg/ml streptomycin. FLM were cultured for at least 8 weeks prior to transduction and experiments.

Gene disruption of Syk in FLM^{Cas9} cells was conducted by lentiviral integration of an sgRNA and puromycin drug selection marker following the approach outlined above in 293T cells with the transfer plasmid replaced by plentiGuide-Puro (Addgene plasmid #52963) targeting an early exon (sgRNA targeting: ATTGCACTACCGCATTGACA). 293T supernatant was transferred onto the FLM^{Cas9} cells and puromycin selection of 1 μg/ml was carried out for 48h.

Multimeric Fc Molecules

All Fc molecules were prepared and labeled at Momenta Pharmaceutics using the methods described in (6). Size exclusion chromatography was used to validate the purity of the labeled molecules. **Supplementary Figure 1** provides the SEC data demonstrating that all molecules were of high purity and of the expected size.

Live Cell Imaging

For imaging cells on glass, cells were differentiated directly on ethanol flamed 25 mm coverslips (Number 1.5, Thermo Fisher) or onto 96-well glass bottom plates (Dot Scientific, MGB096-1-2-LG-L) for high content experiments. The 25 mm coverslips were imaged in AttoFluor chambers (Thermo Fisher). TIRF-based imaging which was conducted with an inverted microscope built around a Till iMIC (Till Photonics, Germany) equipped with a 60 × 1.49 N.A. oil immersion objective lens, enclosed in a custom environmental chamber to keep the samples at 35–37°C. The entire microscope setup and centering of the back focal plane was previously described in (21). Excitation for TIRF was provided by either a 561 nm laser, for DL594 labeled molecules or Syk-mScarlet, or a 488 nm laser for the AF488 labeled molecules. Single point TIRF was used for fast imaging of single particles while TIRF 360 was used to create uniform TIRF illumination for moderate speed particle tracking by steering the laser at the back-focal plane (22). The microscope was custom-built based on iMIC system (TILL Photonics, Munich, Germany) with 60x 1.49 oil immersion objective lens (Olympus, Tokyo, Japan).

For confocal experiments on undifferentiated THP-1 cells, cells were plated on 25mm coverslips that had been coated with 0.01% Poly-L-Lysine solution (Sigma, A-005-M) and imaging was performed on a TIL photonics Andromeda Spinning Disk Confocal, using a 60x oil 1.4 oil immersion objective lens. Cells were plated overnight and incubated with 100 μg/ml of either the FcM AF488 or the PentX AF488 for 5 min before imaging. As in the TIRF imaging, cells were maintained at 35–37°C in HBSS.

High content microscopy of FLM cell were plated into 96-well glass bottom plates (Dot Scientific, MGB096-1-2-LG-L) 2–4 h prior to imaging. Images were captured on an ImageXpress Micro XLS (Molecular Devices, Sunnyvale, CA) equipped with a 40 × 0.90 N.A. objective lens. Macrophages were marked with HCS NuclearMask™ Blue Stain (ThermoFisher scientific) for

identification and AF647 or DL647 fluorescence was collected using integrated filter cubes for far red and red respectively. For antibody dependent phagocytosis, sheep red blood cells (sRBC) were biotinlayted using a mixture of NHS-biotin and NHS-AF647 (Thermo Fisher scientific) and opsonized with murine IgG2a anti-biotin [3E6] (ab36406, Abcam). IgG-sRBCs were added at an MOI of 20 and incubated for 40 min prior to imaging.

Supported Lipid Bilayers

Supported lipid bilayers (SLB) were formed by spontaneous fusion of lipid vesicles. For the bilayers, small unilamellar vesicles were prepared by mixing DSPE-PEG(2000)-DBCO (Avanti Polar Lipids 880229) and POPC (850457 Avanti Polar Lipids) at a molar ratio of 1:1,000 with total lipid concentration of 500 μM (380 μg/ml), in chloroform and dried using vacuum centrifugation. The lipid film was resuspended in 1 milliliter PBS (without Ca^+ and Mg^+) by vortexing and then sonicating for 5 min using a bath sonicator, followed by extrusion (Avanti Polar Lipids 610000) through 100 nm filter at least 13 times (Whatman Nucleopore Track-Etch 100 nm membrane). The 500 uM stock of lipids were diluted 1:6 in 2 mM Mg^{2+} PBS. The bilayer was formed by pipetting the diluted lipids onto 25 mm Piranha acid [H_2SO_4 (30%, *v/v*):H_2O_2 (3:1, *v/v*)] cleaned coverslip (held in Leiden chambers) and incubated at 37°C for 20 min. Following incubation, bilayers were then submerged in water at 42°C to remove excess liposomes. The water was exchanged with PBS followed by HBSS for imaging.

The cRGD {Cyclo[Arg-Gly-Asp-D-Phe-Lys(Azide)]} was linked to liposomes *via* a copper free click chemistry reaction following resuspension of the dried lipids. Here, 1 μg cRGD-Azide (Peptides International RGD-3749-PI) was reacted to the 380 μg of liposomes, so that there was an excess (about 3 fold) of cRGD-Azide to liposomes. The cRGD-Azide was added to the liposome solution prior to vortexing. The lipids were then sonicated and extruded (to form the liposomes 100 nm in size as described above.

IgG-opsonized bilayers were prepared as described in but were instead comprised of DSPE-PEG(2000) Biotin (Avanti Polar Lipids 880129) mixed with POPC (850457 Avanti Polar Lipids) at a molar ratio of 1:1000 with total lipid concentration of 500 μM. Alexa Fluor 647 NHS ester (Thermo Fisher Invitrogen) was conjugated to anti-Biotin IgG (3E6) (Abcam ab36406) for antibody fluorescent labeling. The labeled antibody was incubated with the 0.1% PEG-biotin SLB at 37°C for 30 min in dPBS. Excess IgG was washed with HBSS.

Fc Inhibitor Treatments

For single particle assays on the cRGD bilayer, differentiated THP-1 cells were removed from the plastic dish using cold dPBS and then exposed to either 0.03 μg/ml rFc-DL594, 0.11 μg/ml SIF1-DL594, or 0.17 μg/ml PentX-DL594 (~0.7 nM each) in suspension at 4°C for 30 min. Cells were washed and resuspended in HBSS and dropped on the supported lipid bilayers at 37°C. For high dosage treatments on glass, Fc multimers labeled with AF488 were held at the same mass, 33 μg/ml, 66 μg/ml, or 100–110 μg/ml doses for the particle tracking data. These were treated at 37°C for 5 min and then washed with HBSS and imaged at times indicated. For brightness analysis, Fc multimers were all 0.4 μM for each to keep the total number of molecules the same for each.

For FcM-AF488 and PentX-AF488 treatment of undifferentiated THP-1 cells, plated on Poly-L-Lysine coated coverslips, 100 μg/ml for each was incubated for 5 min prior to imaging. Due to lack of cell adherence, cells were not washed, so cells were continuously exposed over the duration of imaging.

Image Processing

For fiducial data collection and image registration, single images were registered using calibration images acquired simultaneously on each of the four EMCCD detectors. A single image of 200 nm green beads (Life Technologies, Carlsbad, CA) immobilized on a glass coverslip were excited using 445 nm excitation. Coordinates for registration were determined using the MATLAB (The MathWorks, Inc., Natick MA) cpselect tool. A rigid affine transformation was used to transform all points onto the red channel. Image montages were generated using ImageJ, and due to unintended photobleaching in some data sets, the Bleach Correction tool was used.

U-track (Danuser Lab) was used for single particle tracking using the Gaussian detection (23). Motion of the Fc multimer tracks were classified by the divide-and-conquer moment scaling spectrum (DC-MSS) method (24). Syk detections per μm^2 per second were measured using Gaussian detection in U-track from a cropped region that excluded the cell edge to prevent anomalous detections from the transition between cell background and cell-free background regions. For the brightness analysis, point source detection in U-track was carried out from single frames.

RESULTS

Engagement of FcγRs by Large Complexes of Fc Recruit Syk to the Plasma Membrane, Whereas PentX Recruits Syk to Endosomes

To determine the location of FcγR activation in response to IC-IgG, fluorescently tagged polymeric multimers of Fc (uncontrolled multimer, UM (6), comprised predominately of 10–40 Fc domains similar to IC-IgG were added to THP-1 cells. Syk-mScarlet expressing THP-1 cells formed patches of UM clusters at the cell surface that recruited Syk-mScarlet within 30 min (**Figure 1A**, **Supplementary Video 1**). Intracellular vesicles bearing UM and Syk-mScarlet were also observed **(Figure 1A)**. This result was consistent with the conventional model in which clustering of FcγRs by binding IC-IgG or FcεRI binding IC-IgE, leads to phosphorylation of ITAMs, Syk recruitment and subsequent internalization (19, 25). We anticipated that PentX, which potently promoted Syk phosphorylation (6), would behave similarly. Surprisingly, PentX did not produce clusters at the plasma membrane (PM). Rather, PentX bound to the cell surface and then within 15 min

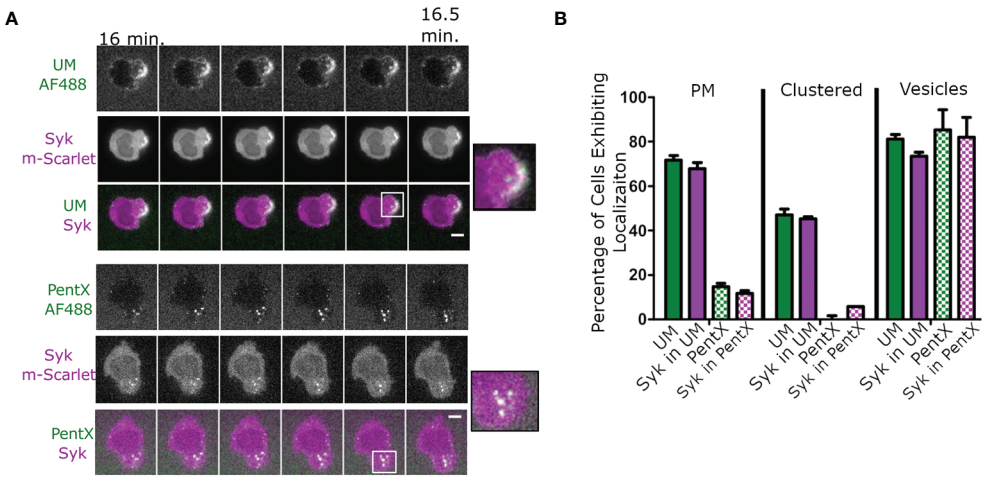

FIGURE 1 | PentX recruits Syk to endosomes, whereas multimeric Fc-FcγR complexes recruit Syk to the plasma membrane (PM). **(A)** Confocal imaging of Syk-mScarlet localization in THP-1 cells relative to fluorescently labeled PentX-AF488 or unconstrained Fc multimer (UM-AF488). By 15 min of incubation with Fc constructs, Syk-mScarlet localized to PM patches of UM-AF488 and occasionally on endosomes, whereas Syk-mScarlet localized only to endosomes PentX-AF488 (scale bar, 5μm). **(B)** The percentage of cells exhibiting localization of UM-AF488 or PentX-AF488 or Syk-mScarlet to PM, PM-clusters or intracellular vesicles following15 min of incubation (error bars are standard deviation, n= 34 and 53 cells for PentX and UM respectively, two independent experiments).

localized to small and large intracellular vesicles, where it recruited Syk-mScarlet (**Figure 1A**, **Supplementary Video 2**). Quantification of these confocal images indicated that Syk-mScarlet was weakly or not recruited to the PM of cells exposed to PentX, whereas UM readily accumulated Syk-mScarlet at the PM (**Figure 1B**). Thus, PentX did not significantly activate FcγRs on the cell surface, but rather selectively promoted FcγR activation and accumulation in endosomes. These results reveal that Fc valency controls the subcellular distribution and activation of FcγR.

SIF1 and rFc Linger on the Plasma Membrane and Do Not Recruit Syk

We next sought to compare the effects of monomeric, trimeric and pentameric Fc-molecules (**Figure 2A**) on the activation of FcγRs on subcellular membranes. Using HiLo microscopy, which allowed greater sensitivity than confocal microscopy, but with similar optical sectioning (26), we imaged the distributions of monomeric rFc, the inhibitory Fc trimer (SIF1), and PentX relative to Syk-mScarlet in THP-1 cells differentiated toward macrophages by 48 h exposure to PMA which increased expression of FcγR1 and adherence to glass coverslips (**Supplementary Figure 2**). Since PentX was internalized by ~15 min, the data were divided between early timepoints, below 15 min (**Figures 2B, C**), and later timepoints, 15–30 min (**Figures 2D, E**). In contrast to PentX which accumulated on endosomes, rFc and SIF1 were lingered on the PM, with a small fraction trafficking on small endosomes for at least 30 min and neither recruited Syk-mScarlet to the PM (**Figures 2B–E**) consistent with (6). The high sensitivity of the HiLo approach revealed many larger PentX containing endosomes that extensively recruited Syk-mScarlet with some variability between endosomes (**Figures 2B–E**). A basal level of endocytosis appeared to internalize rFc and SIF1 over time, but Syk-mScarlet did not colocalize with rFc or SIF1 in vesicles. These observations are consistent with the known inhibitory activity of SIF1 and indicate that it traps FcγR in a state mimicking monovalent Fc binding, whereas PentX either promotes FcγR internalization or prevents recycling of FcγRs to the PM by their activation on endosomes.

rFc, SIF1 and PentX Do Not Recruit Syk to the PM Unlike Surface Associated IgG During Frustrated Phagocytosis

Given that PentX recruited Syk to endosomes, we sought to determine if Syk was initially recruited to FcγRs at the PM and if there was any reversible recruitment of Syk to rFc or SIF1-engaged FcγRs. Total internal reflection fluorescence (TIRF) microscopy provides an exquisite view of single molecule movements at the PM while eliminating contaminating fluorescence from other regions of the cell (16). Differentiated THP-1 cells robustly engaged AF647-IgG docked on supported lipid bilayers (SLB) by spreading and recruiting many hundreds to thousands of Syk-mScarlet molecules per μm^2 to the advancing lamellipodia within ~–1–5 min of contacting the surface (**Figure 3A**, **Supplementary Video 3**). Notably, the patches of AF647-IgG, to which Syk-mScarlet was recruited, were reminiscent in structure to those created by UM molecules **(Figure 2**, compare with **Figure 1A**), suggesting the binding of surface associated IgG or high-valency IgG molecules such as UM, creates large patches of FcγRs on the PM to which Syk is recruited. Conversely, TIRF imaging of the adherent plasma membrane of Syk-mScarlet expressing THP-1 docked with saturating concentrations (100 μg/ml) of labeled AF488-rFc, SIF1 or PentX revealed a predominately uniform dim fluorescence emanating from Syk-mScarlet molecules diffusing in the cytoplasm. Syk-mScarlet

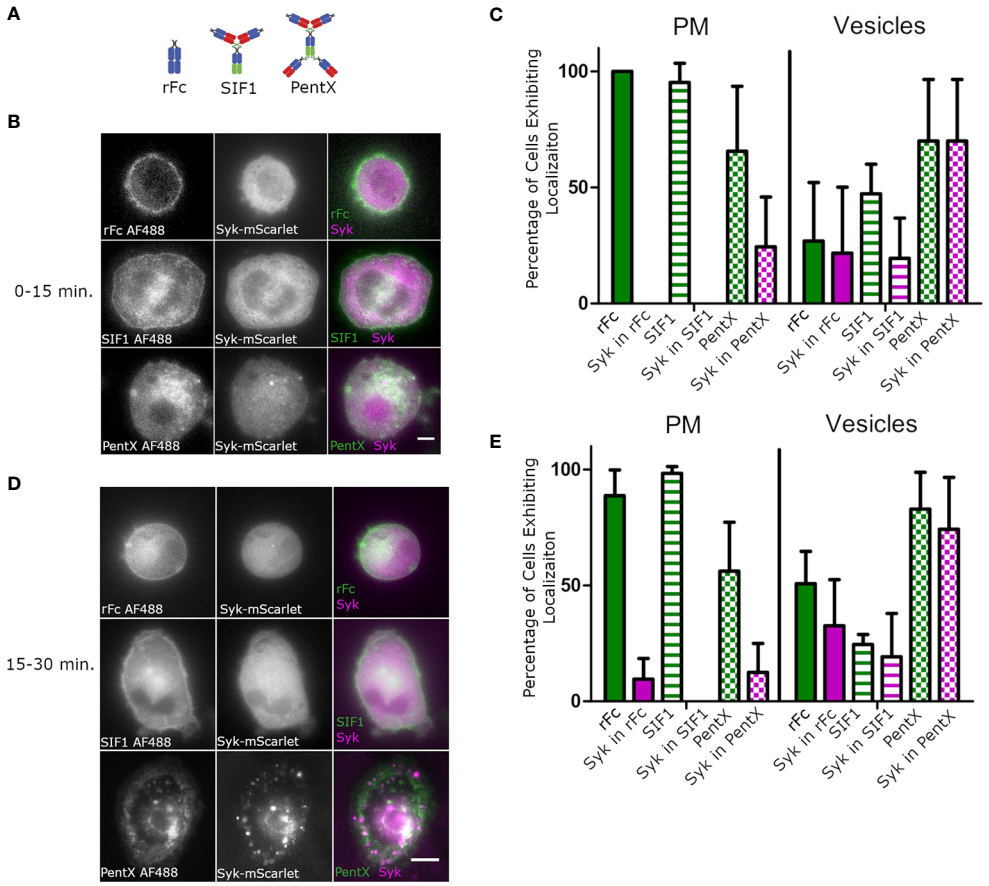

FIGURE 2 | SIF1 and rFc remain on PM and do not recruit Syk. **(A)** Molecular structure cartoons from (6). **(B)** Representative Hi-Lo images of Fc-AF488 constructs (100 μg/ml) and Syk-mScarlet distribution within 15 min. of exposure of differentiated THP-1 cells to Fc constructs (scale bar, 5μm). **(C)** Quantification of Fc-AF488 molecules and Syk-mScarlet localization within 15 min. post treatment (error bars = standard deviation, n=21 cells rFc, 16 cells SIF1, 14 cells across 3 experiments). Cells were categorized as exhibiting Fc and Syk localization at either the plasma membrane or intracellular, typically within distinct vesicles. Cells could show both localizations. **(D)** Representative Hi-Lo images of Fc-AF488 constructs (100 μg/ml) and Syk-mScarlet distribution between 16 min. and 30 min. of Fc treatment of differentiated THP-1 cells (scale bar, 5μm). **(E)** Data taken on cells within 16–30 min of Fc treatment were quantified in the same way as panel **(C)** (error bars = standard deviation, n=35 cells rFc, 35 cells SIF1, 33 cells across three experiments).

molecules transiently sampled the plasma membrane, as seen by localized bursts of fluorescence, however, the generally did not frequently colocalize with AF488-rFc, SIF1 or PentX docked to FcγRs (**Figure 3B** and **Supplementary Videos 4–6**). We quantified the number of Syk localizations to the plasma membrane, since their duration was too short to reliably track, and found only a slight, non-statistically significant trend toward more localizations for PentX and indistinguishable frequency for SIF1 and rFc (**Figure 3C**). Most of these localizations were fleeting, lasting around 1 s or less. Thus, unlike surface associated IgG, the soluble, multimeric molecules do not significantly recruit Syk to the PM.

Syk Contributes to the Endocytic Traffic of PentX

To determine if Syk was required for the accumulation of PentX in endosomes, we created murine fetal liver macrophages (FLMs) from Cas9 mice and knocked out Syk using lentiviral expression and selection for single guide RNA (sgRNA) targeting an early exon to produce Syk^{sgRNA} FLMs. Similar to differentiated THP-1 cells, DL594-rFc and DL594-SIF1 lingered on the PM and were small endosomes, whereas DL594-PentX was internalized and trafficked to large endosomes following 20 min of incubation (**Figure 3D**). Notably, more small endosomes containing DL594-rFc or DL594-SIF1 were observed than in THP-1 cells, potentially due to the elevated endocytic and macropinocytic activity of these cells relative to THP-1 cells (data not shown). Quantification by high content microscopy indicated that the failure of Syk^{sgRNA} FLMs to traffic DL594-PentX into large endosomes at 20 min post exposure (**Figures 3D, E**). Additionally, small vesicles were observed below the plasma membrane for DL594-rFc, DL594-SIF1 and DL594-PentX suggesting that Syk controls the endocytic traffic of the activating PentX and potentially recycling to the cell surface.

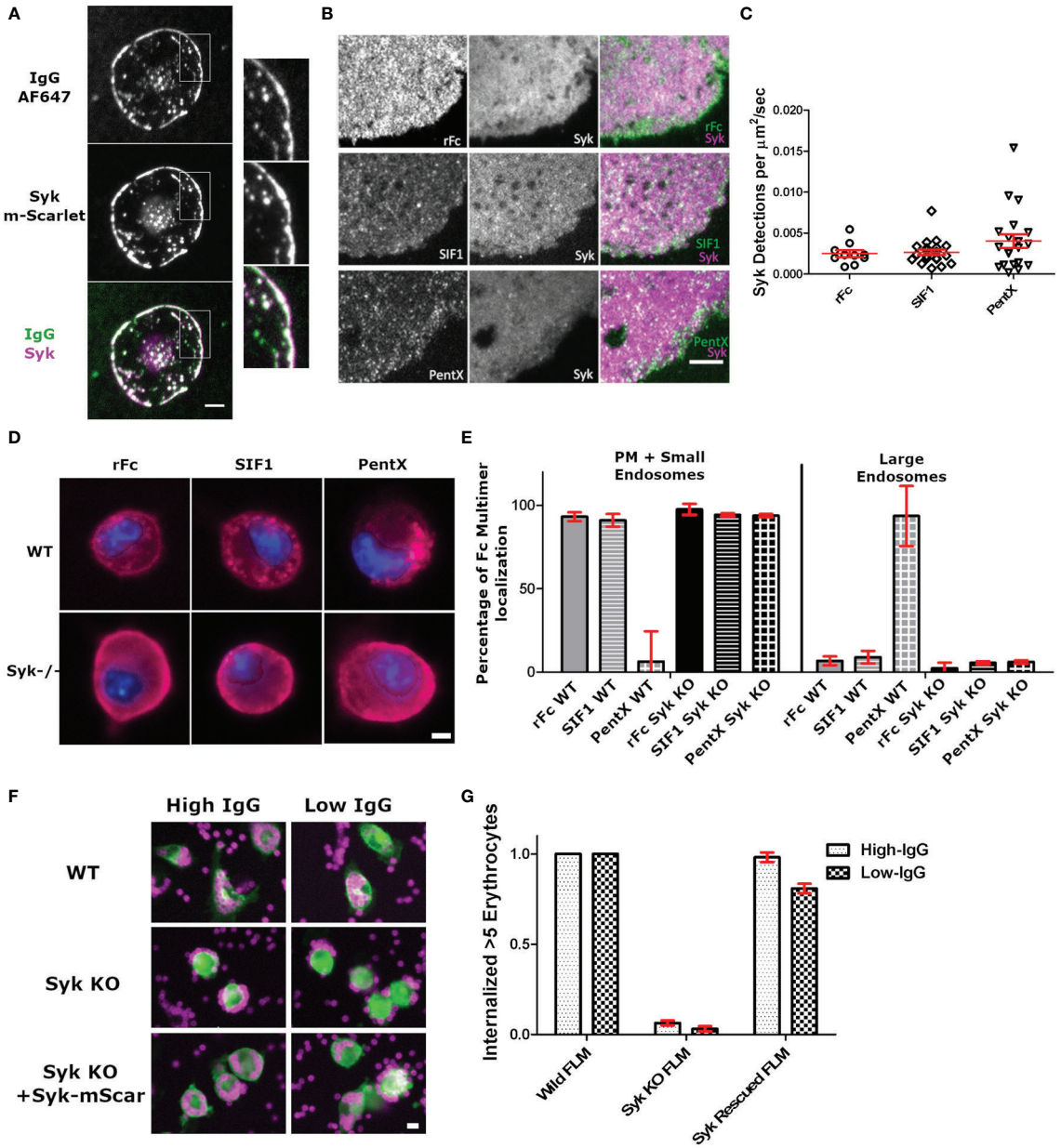

FIGURE 3 | Syk is recruited to surface associated IgG bound FcγR, but not those docked with low Fc valencies. **(A)** TIRF imaging of intense Syk-mScarlet recruitment during frustrated phagocytosis by a THP-1 cell of SLB presenting AF647-IgG. Note that too many Syk-mScarlet molecules are recruited for single molecule detection. Image is representative of 20+ cells. Scale bar is 5µm. **(B)** Single particle detections of Syk-mScarlet molecules on the surface of cells docked with AF488-Fc molecules (100 µg/ml rFc, SIF1, or PentX). Scale bar is 5µm. **(C)** The frequency of Syk-mScarlet detections observed. No statistical significant difference. Data represents 10 rFc-treated cells, 20 SIF1-treated cells, and 20 PentX-treated cells from a single day that represents results of two experiments. Bars are mean +/- standard error of the mean. **(D)** Wild-type and Syk-KO FLMs exposed to DL594-rFc, SIF1 or PentX. Scale bar is 5µm. **(E)** Quantification of localization frequencies of DL594-rFc, SIF1, or PentX in WT and Syk-KO FLMs. ~150 cells/condition from two independent experiments. Error bars are standard deviation. **(F)** Antibody dependent phagocytosis of IgG-sRBC labeled with AF647 by WT, Syk-KO, and Syk-KO+Syk-mScarlet expressing FLMs. Scale bar is 10µm. **(G)** Quantification of the frequency of macrophages internalizing 5 or more IgG-sRBC. ~120 cells/condition. Error bars are standard deviation.

To confirm the knockout phenotype of the Syk^{sgRNA} FLMs and functionality of the Syk-mScarlet probe we performed high content microscopy of WT, Syk-KO and Syk-KO/Syk-mScarlet rescued cells. WT FLMs robustly internalized IgG-opsonized sheep red blood cells (IgG-sRBC) whereas Syk-KO cells were incapable of engulfing sRBCs (**Figures 3F**, **G**). Expression of the Syk-mScarlet, followed by drug selection, showed a striking rescue of sRBC engulfment in Syk^{sgRNA} FLMs indicating that the Syk-mScarlet construct should not interfere with the function of the endogenous Syk molecules in the THP-1 cells and should

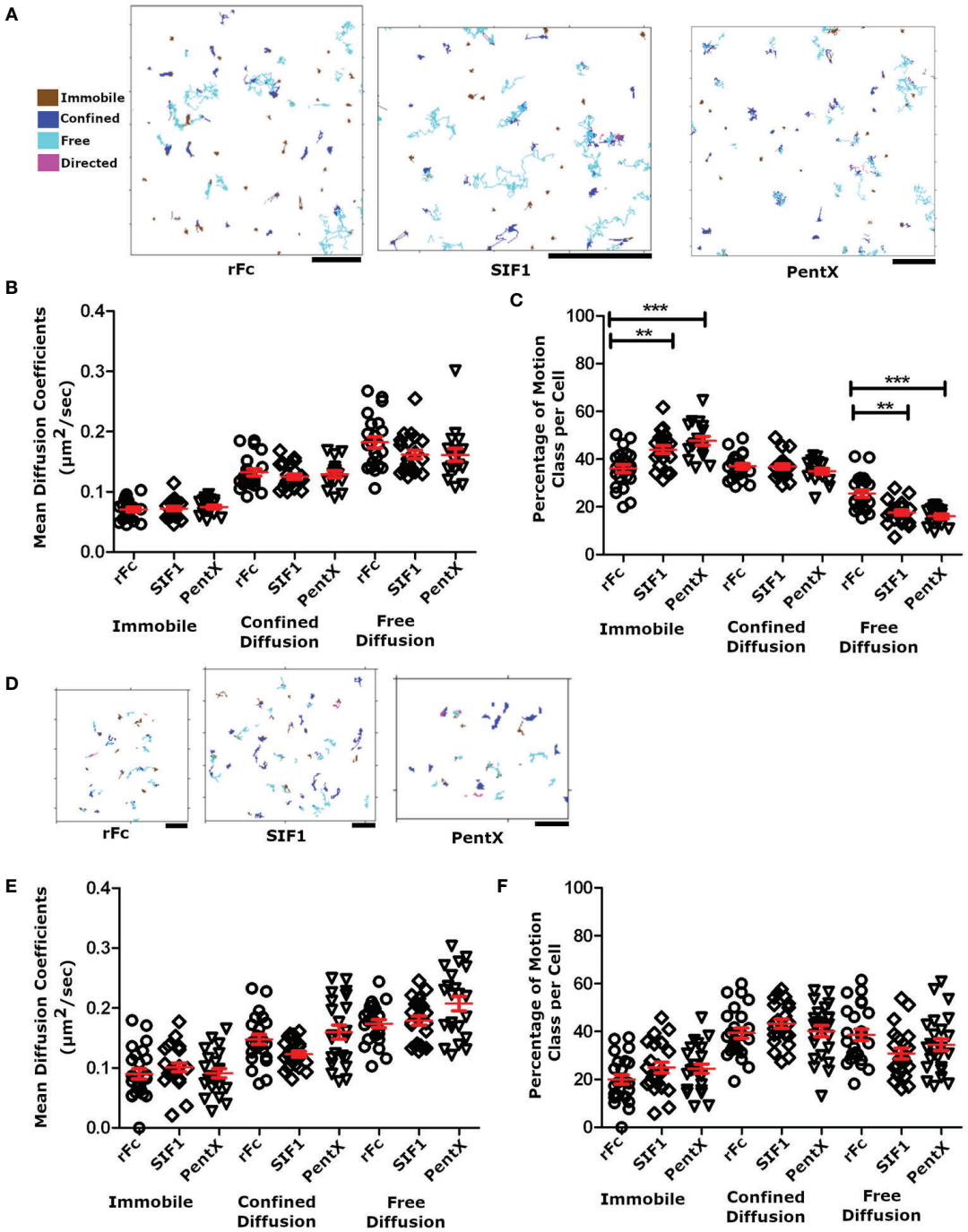

FIGURE 4 | Motion analysis of Fc molecules docked to FcγR. **(A)** SPT tracks following analysis with DC-MSS, from TIRF imaging of THP-1 cells treated with 100 μg/ml rFc, SIF1 or Pentx, color coded by motion class. Note that transitions in track classifications (e.g. confined to free) can be observed within single tracks. All scale bars represent 2μm. **(B)** The average diffusion coefficient for each cell by diffusion class. **(C)** The percentage of tracks for each diffusion class. Data in panels **A–C** are from 22 rFc treated cell, 21 SIF1 treated cells, and 17 PentX treated cells from a single day experiment but are representative of multiple replicates. **(D)** Representative SPT tracks of THP-1 cells treated with fluorescently labeled Fc molecules and attached to supported lipid bilayers displaying cycloRGD, at sub-activating/inhibiting doses of 0.7 nM (0.03 μg/ml rFc, 0.11 μg/ml SIF1, and 0.17 μg/ml PentX). All scale bars represent 2μm. **(E)** The average diffusion coefficient for each cell plotted by diffusion class at 0.7 nM. **(F)** The percentage of tracks for each diffusion at 0.7nM. Data from panels **(D–F)** are from 24 rFc treated cells, 22 SIF1 treated cells, and 22 PentX treated cells taken across three different experiments. Red bars are the mean +/- standard error of the mean. Significance was calculated using Tukey's one-way ANOVA where (*P < 0.05, **P < 0.005, *** < 0.0005).

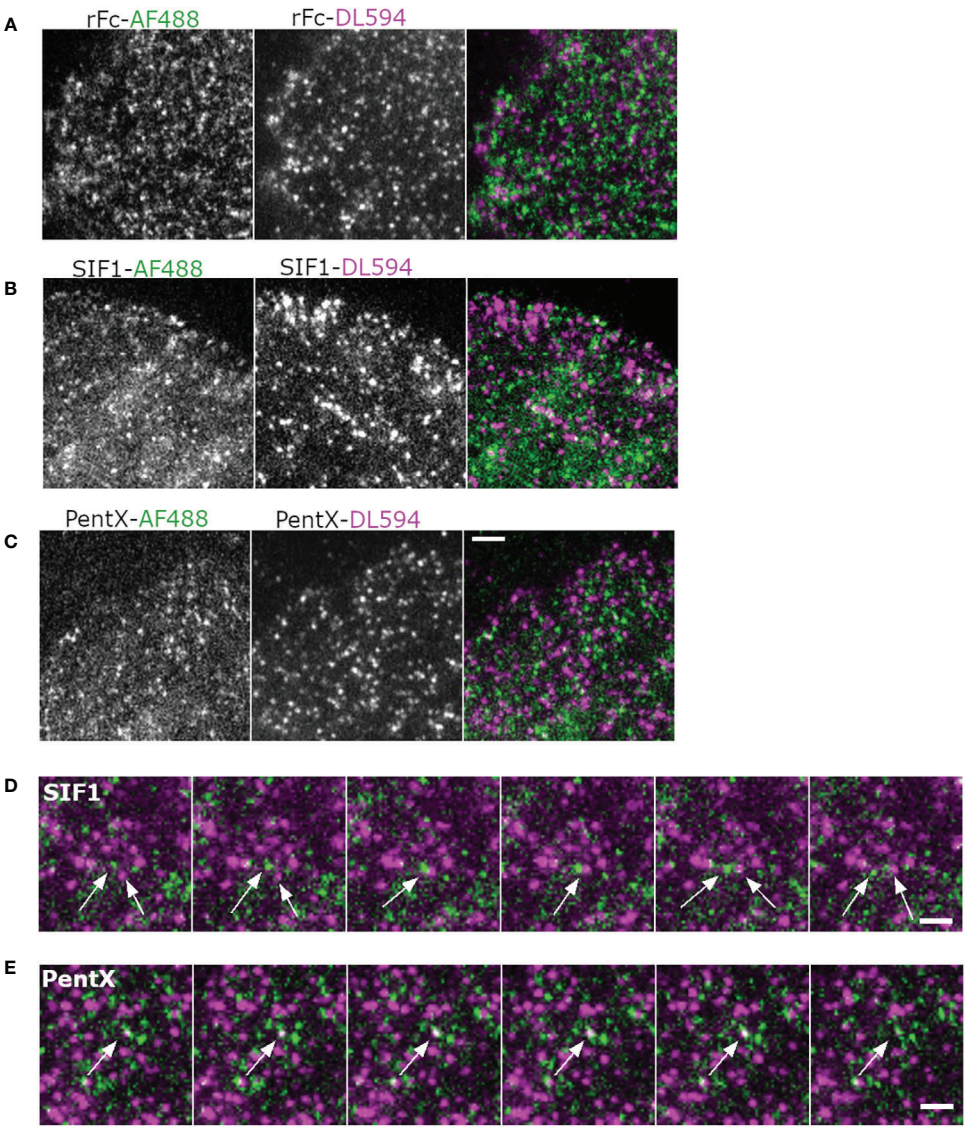

FIGURE 5 | Multicolor imaging of Fc molecules indicates an absence of FcγR superclustering. **(A, B)** Montages of cells treated with AF488 and DL594-labeled rFc **(A)**, SIF1 **(B)**, PentX **(C)** at 33 μg/ml and imaged with a time-lapse of 40 s. Scale bar is 5μm. **(D)** Montage illustrating path crossing of a green and red SIF1 molecules (arrows). Scale bar is 5 μm. **(E)** Co-association and disappearance of red and green PentX, indicating a putative endocytic event. Scale bar is 5 μm.

provide a functionally accurate view of Syk dynamics. We interpret these results to indicate that at the PM low valency (<5) Fcs may do not significantly recruit Syk or maintain it actively docked at the PM and that once internalized on endosomes. However, complexes of 5 FcγRs can robustly recruit Syk to endosomes where signaling unique from that encountered at the plasma membrane may occur (**Figure 2**).

rFc, SIF1, and PentX Display Similar Motions at the Plasma Membrane

Since Syk was not recruited to low valency Fc-FcγR complexes on the plasma membrane, we speculated that the SIF1- and PentX-FcγR complexes were not forming clusters and have similar diffusive motions on the PM. Conversely, decreased mobility of these complexes would be an indicator of FcγR clustering or the association with endosomal structures. To test this idea, THP-1 cells were treated with 100 μg/ml of DL594-Fc molecules at fully activating (PentX) or inhibiting (SIF1) concentrations (6) and plated onto coverslips. The adherent surface was imaged by TIRF microscopy at 18 frames per second for 200 frames. SPT trajectories from these movies were found using U-track (23) and classified by the divide-and-conquer moment scaling spectrum (DC-MSS) method (24) and color coded by the diffusion type as freely diffusing, confined diffusion and

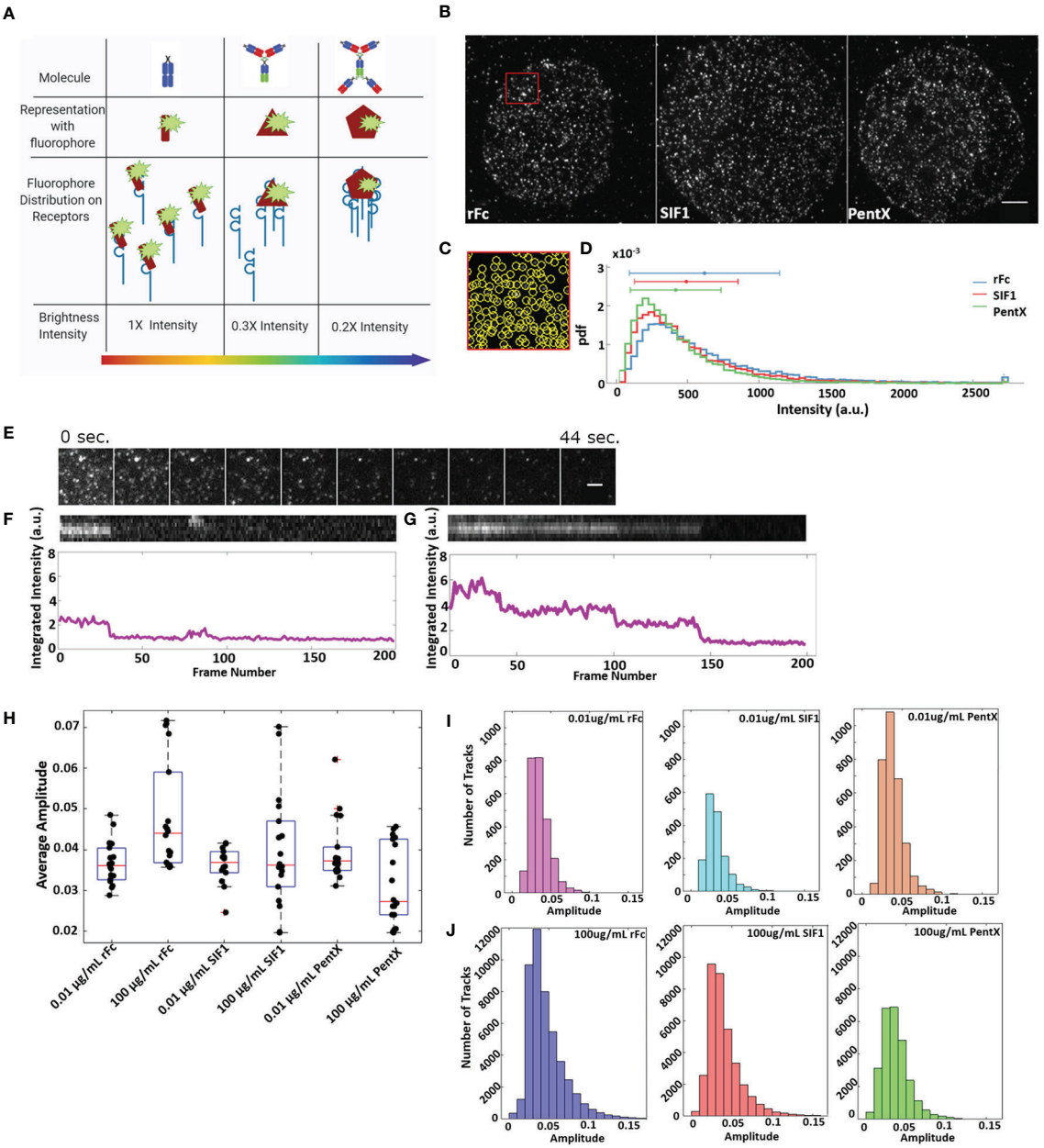

FIGURE 6 | Fc receptors are not substantially preclustered and remain in small, mobile clusters upon binding multivalent Fcs. **(A)** Schematic of Fc-FcγR groupings and the resulting intensities of sub-resolution clusters. **(B)** Representative images of cells treated with 0.4 µM Fc molecule (Scale bar, 5 µm). **(C)** Zoom of the red region in B displaying individual detections of fluorescence spots. **(D)** Frequency of fluorescence of Fc molecules at 0.4 µM. Data is taken from 14 cells treated with rFc, 14 cells treated with SIF1, and 13 cells treated with PentX. **(E)** Example of stepwise photobleaching of rFc-DL594 over 200 frames taken 0.22 s apart. The rFc-DL594 was kept at 10 µg/ml to be able to track while, the rFc-AF488 was at 100 µg/ml to ensure cells remained at saturating levels. Scale bar represents 2µm. **(F)** Top: chymograph of single fluorophore bleach event from **(E)** example. Bottom: Intensity over time (frames) of bleached track. **(G)** Top: chymograph of multistep/fluorophore bleach event. Bottom: Intensity over time (frames) of the above chymograph. **(H)** Average amplitude of individual spots per cell taken over the first four frames of 100 µg/ml and 0.01 µg/ml dose multivalent Fc SPT data. **(I–J)** Histograms of single spots amplitudes averaged over 4 frames for all tracks for 0.01 µg/ml **(I)** and 100 µg/ml conditions **(J)**.

immobile (**Figure 4A**). Here 'immobile' from the DC-MSS analysis may reflect highly confined trajectories at the noise/localization limit for the organic fluorophores used, and thus a diffusion coefficient is reported for this class, even though it likely reflects an upper bound. Overall, the quality of tracking was quite high indicating that the TIRF microscopy approach provided a sufficiently low background for imaging an organic fluorophore (DL594) rather than the more frequently used quantum dots.

The motions of the Fc constructs displayed similar proportions of each motion class and could be observed transitioning between classes (frequently between confined and free diffusion, dark blue to or from light blue, **Figure 3A**). These motion types are consistent with Fc-FcγR complexes interacting with actin corrals, lipid rafts, and protein islands (27–30). As predicted by the lack of Syk recruitment, only small differences in diffusion constants and types of motions were observed across rFc, SIF1 and PentX (**Figure 4B**). A small increase in the fraction of immobile complexes was observed for PentX and SIF1 over rFc along with a concomitant reduction in freely diffusing complexes (**Figure 4C**). We interpret these results to indicate that SIF1 and PentX do not assemble activated FcγR complexes at the PM. The small increase in immobile fractions of SIF1 and PentX likely reflects an increasing probability that one or more FcγR in the complex was trapped by a diffusion barrier.

We repeated these measurements using sub-activating and sub-inhibiting concentrations of Fc constructs to determine if the fractional occupancy of total FcγRs affected our SPT measurements. At low densities corresponding to ~1%–10% receptor occupancy, the tight adhesion of PMA differentiated THP-1 cells to glass appeared to result in more immobile Fc-FcγR complexes than expected. To overcome this limitation, we created SLBs displaying cyclo-RGD to allow integrin-mediated attachment. THP-1 cells were treated with the sub-activating or inhibiting concentrations (0.7 nM) multimeric Fcs at 4°C and then allowed to adhere to the cRGD-SLB at 37°C for 30 min prior to imaging by SPT-TIRF. TIRF imaging at 28 frames per second for 100 frames allowed clear resolution of low densities of DL594-Fc molecules as single particles (**Figure 4D**). As anticipated, the SLB increased the fraction of complexes undergoing free diffusion compared with cells plated on glass **(Figure 4F** vs. **Figure 4B**). Although we do not know the reasons for this, one possible explanation is that on glass, the integrin attachments may be quite static and create diffusion barriers (31), whereas on the SLB which was comprised of fluid lipids they may be free to move. Importantly, the diffusion coefficients for the rFc, SIF1 and PentX single complexes were statistically indistinguishable (**Figure 4E**), and similar to that observed on glass (**Figure 4B**), indicating that collisions with transmembrane proteins and cytosolic molecules dominated the diffusion coefficients as has been observed in apical surface SPT experiments (32, 33). Overall our diffusion coefficients measurements were nearly two times faster than those noted in literature, with the median rate of free receptors being 0.179 ± 0.012 μm^2 per second (median ± standard error of the mean), 0.192 ± 0.011 μm^2 per second, and 0.216 ± 0.010 μm^2 per second, for rFc, SIF1, and PentX, compared with 0.074 ± 0.004 $\mu m^2/s$ for FcγRIIa labeled with Cy3-Fab (32) or ~0.7 $\mu m^2/s$ for FcRIIa/b & III labeled with Qdot-Fab (24). These differences may reflect the smoothness of the adherent surface of the THP-1 cells observed in TIRF here, in contrast with the ostensibly rougher non-adherent surface imaged in these other studies. Thus, FcγRs ligated with low valency Fcs retain rapid diffusion on the PM, suggesting no additional binding or aggregation of FcγR occur, even when five FcγRs are bound by PentX.

FcγRs Move Autonomously in Preferential Sub-Domains of PM and Are Not Pre-Clustered

Previous studies using super-resolution imaging in fixed cells observed pre-clustering (18) or corralling of FcγR by actin or lipid rafts and these clusters expanded when IC-IgG were added (17). To determine if FcγR pre-clustering could be observed and was remodeled by low-valency Fc binding, we imaged mixtures of the engineered Fc constructs labeled with two different fluorophores. If pre-clustering of FcγR was present, rFc of both colors should frequently be observed within the same diffraction limited sites at diminishing frequency due to the increased valency of SIF1 and PentX. Moreover, if SIF1 or PentX induce clustering on the PM beyond their binding valencies, these structures should be evident as increased frequencies of co-localized colors. The SPT data (**Figure 4**), predicts that neither preclustering nor induced clustering occur with these molecules. To test these possibilities, THP-1 cells were treated with the rFc, SIF1, and PentX, tagged with AF488 or DL594 in a 1:1 mixture at FcγR saturating concentrations (33 μg/ml of each) and imaged by two-color TIRF-360 microscopy. TIRF movies revealed that the two-color rFc molecules generally moved independently of one another and only occasionally co-localized (**Figure 5A**, **Supplementary Video 7**). Similar behavior was observed for SIF1 and PentX, with an increase in the number of confined and immobile spots, consistent with the SPT analysis (**Figures 4**, **5B, C**). Overall, Fc-multimers appeared to predominately move independently from one another despite crossing paths (**Figure 5D**, **Supplementary Video 7**). Occasionally, green and red spots could be identified within these movies, often appearing to group at immobile sites followed by both colored molecules vanishing, suggesting endocytic events (**Figure 5E**). We were unable to quantify these data using dual color SPT as the SNR for the AF488-Fc multimers was simply too low relative to the background for reliable tracking of splitting and merging events. Our qualitative analysis indicated that, rFc, SIF1, and PentX largely maintained their autonomy on the cell surface, but only occasionally would group together on the cell surface. These observations are inconsistent with extensive FcγR preclustering and contrasts sharply with clusters that form in response to IgG-docked to the SLB (**Figure 3A**, **Supplementary Video 3**) and UM (**Figure 1**), which create large cluster of FcγRs that are rapidly remodeled (16).

With the findings that docked Fcs moved independently **(Figure 5**, **Supplementary Video 7**) and that preferential zones of plasma membrane occupancy were evident by SPT-TIRF (**Figure 2B**), we further explored the possibility that FcγRs are grouped within microdomains of the plasma membrane. Here, we performed an intensity analysis of our SPT data to count the number of molecules within single spots, limited by the resolution of the microscope (<250nm). Fluorescent Fc molecules binding to FcγRs within very small microdomains (<50 nm), should produce single spots with brightness that scales with the number of fluorescent Fc molecules docked (**Figures 6A–D**). Histograms of all Fc-spot detections at high, equimolar,

Fc concentrations on fixed cells had similar intensities, with the mean intensities of rFc>SIF1>PentX (**Figure 6D**), suggesting that Fcs could dock to microdomains containing multiple FcγRs. The differences in the means were less than a factor of two, much smaller than expected if pre-clustering was prominent amongst FcγRs. If pre-clustering of FcγRs was prevalent, the brightness of rFc spots should be maximal since multiple rFc molecules would dock within sub-resolution spots. The number of SIF1 or PentX molecules that could dock to microdomains containing a similar number of FcγRs would be reduced by ~1/3 for SIF1 and ~1/5 for PentX, resulting in a corresponding decrease in brightness. Previous work demonstrated full valency binding for these Fc multimers (6). The observed differences in intensity were much smaller, ~20% decrease from rFc to SIF1 and ~35% decrease from rFc to PentX. We conclude that the similar intensity histograms represent FcγRs generally dispersed over a larger ~ 50 nm corrals. This finding is consistent with the SPT tracks spanning hundreds of nanometers within 200 s (**Figures 2C**, **3B**), and thus, a chance of coincident occupation of FcγRs within a given microdomain is transient, consistent with the observations of the 2-color experiments (**Figure 5**). Thus, our data supports a model where corrals on the cell surface weakly constrain FcγR movements, but they do not trap them in pre-formed clusters in when bound with rFc, SIF1, or PentX.

Detailed analysis of fluorescent intensities from SPT data revealed that many tracked spots exhibited single stepwise photobleaching indicating a single fluorophore (**Figures 6E, F**). Occasionally multiple photobleaching steps indicative of multiple fluorophores could be observed (**Figure 6G**) indicating multiple Fcs or multiple dyes per Fc molecule. At low concentrations of Fc molecules (0.01 μg/ml) the spot intensities were indistinguishable across rFc, SIF1, and PentX (**Figure 6I**) indicating that they predominantly reflected single Fc molecules docked to FcγRs, supporting the notion that low valency Fcs did not create larger FcγR clusters. Moreover, at saturating doses (100 μg/ml) of rFc, SIF1 or PentX, the preponderance of spots in live cells displayed similar spot-intensity histograms (**Figure 6J**). For PentX, the histograms were nearly identical between low and saturating concentrations. For SIF1, and to a greater degree, rFc, the histograms displayed tails to the right, indicating that coincident detections were more common owing to more frequent labeling of multiple FcγR within a sub-resolution spot. Taken together, these results are consistent with a model in which FcγRs move independently within large corrals with some that are weakly trapped or immobilized in regions of the plasma membrane, yet changing their oligomerization states when docked with rFc, SIF1, or PentX had no impact on this trapping. Likely only activating valencies of Fcs such as encountered in IgG-IC (**Figure 1**) or surface associated IgG **(Figure 3A**) are able to remodel FcγR distributions on the cell surface.

DISCUSSION

The engineered multimeric Fc molecules, rFc, SIF1, and PentX, provided new insight into the minimal number of FcγRs that must be engaged for signaling and that this threshold depends on the subcellular environment. While the classical models for FcγR

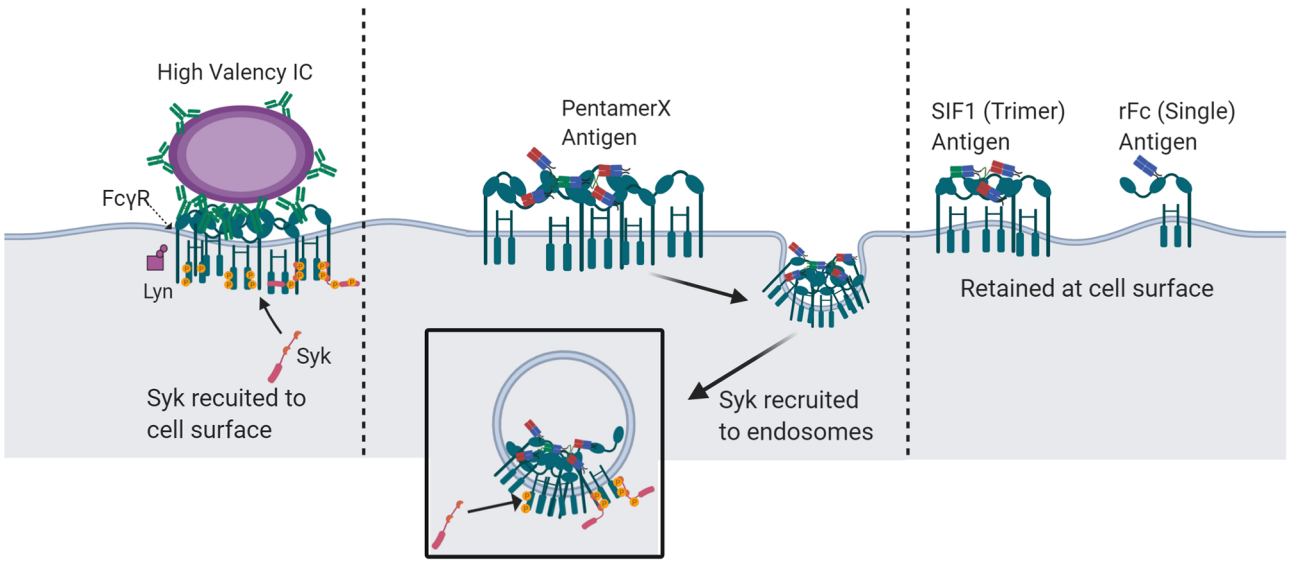

FIGURE 7 | Proposed mechanisms of spatio-temporal FcγR activation and Syk recruitment by multivalent-Fc molecules. IC-IgG : FcγR clusters at the plasma membrane with a valency of more than five Fc domains undergo Syk recruitment and activation at the cells surface. IC : FcγR clusters with a valency of five or fewer do not robustly recruit Syk to the plasma membrane and are unable to fully activate at the cell surface. However, at the valency of five, in a pentameric geometry, FcγR clusters are endocytosed and recruit Syk at the endosome. Molecules with less than 5 Fc domains can engage FcγRs at the cell surface but cannot recruit Syk. Created with BioRender.com.

activation predict a minimal number of ligated and clustered receptors is necessary for activation, our findings give the surprising result that endosomes may afford a lower threshold of activation for the minimum number of FcγRs than the plasma membrane. Specifically, we found that PentX, which potently drives Syk phosphorylation through the binding of five FcγRs (6), can only fully activate FcγRs within endosomes (**Figure 7**). This result could be explained by two potential mechanisms. First, endosomes may allow segregation of the FcγRs from plasma membrane associated phosphatases to allow full activation. Alternatively, sorting of PentX-FcγRs within endosome membrane may result in compartmental or sub-compartmental sorting that creates elevated concentrations of PentX-FcγRs enabling FcγR activation. A notable feature of these results was that PentX accumulated and was trafficked to large endosomes whereas SIF1 and rFc were only evident on small endosomes at similar times of incubation (**Figure 2**). Additionally, we found that Syk was required for the accumulation of PentX within large endosomes, and its absence resulted in PentX traffic that was similar to rFc and SIF1 (**Figure 3**). These observations support a model in which Syk recruitment to endosomal FcγRs may facilitate compartmental or sub-compartmental sorting by trapping PentX-FcγRs. Conversely, SIF1 and rFc do not recruit Syk to endosomes displayed slower internalization and endosomal traffic, which was faster in the likely more endocytic FLM than THP-1 cells. Another possibility, supported by the observation of vesicles bearing SIF1 and rFc but were dim and they did not recruit Syk, is that they are transient intermediate of membrane recycling. An implication of this finding is that IC-IgGs could preferentially activate FcγRs on endosomes, where FcγR signals may be unique from those generated at the PM. The PentX molecule provides a powerful new tool for studying the properties of endosomal FcγR-specific signaling that cannot be accessed as precisely with heterogenous IC-IgG preparations.

Our finding, that FcγRs on the PM are dynamically confined, but not preclustered on the PM, and that their threshold for activation requires more than five FcγRs sets a lower bound on the minimum number of FcγRs needed to form signaling competent clusters on the PM. While exactly how FcγR rearrangements generate productive signaling, our results are consistent with the actin cytoskeleton and potentially other transmembrane proteins acting as fences corralling FcγRs (29, 33, 34). These interactions are likely important for organizing FcγRs activation during engagement of particle associated IgG by sorting activated FcγRs into regions that have close spacing between the phagocyte membrane and target, allowing exclusion of bulky and glycosylated phosphatases such as CD45 (29, 35). More work will be needed to determine if initiation of FcγR phosphorylation by Src-family kinases, including Lyn, occurs on FcγRs docked with PentX or similar low valency molecules, but is insufficient to recruit Syk or is rapidly reversed at PM. Our finding here that large Fc oligomers (UM) were able to self-organize into patches at the PM suggests that this sorting process does not require an opposing target membrane for clustering FcγRs into PM patches, however it is possible that CD45 exclusion could occur by the molecular crowding of many Fc/FcγRs complexes. Moreover, super resolution imaging indicated that of IC-IgGs made up of 2,4-dinitrophenyl-bovine serum albumin bearing approximately 12-24 anti-DNP IgGs were sufficient to promote clustering and activation on human monocytes (17), implying that the number of ligated FcγRs required for signaling is between 6 and 12. In contrast to the work by Brandsma et al., in which pre-patching of FcγRs that were expanded by IC-IgG observed in fixed cells, we did not find evidence of pre-formed FcγR clusters or altered FcγR distributions for low-valency Fc molecules. Rather, our SPT traces in living cells showed zones of preferential dynamic occupancy and exclusion typically containing tracks from free and confined receptors with D ~ 0.15–0.2 $\mu m^2/s$ suggesting that rather than pre-formed clusters, the FcγRs are corralled by actin (29). Indeed, observed confined diffusion trajectories had dimensions similar to the cluster diameters (~ 50 nm) observed by Brandsma et al. (17). This distinction has important consequences for IC induced signaling and FcγR activation and inhibition, as both the number of ligated FcγRs and their spatial organization across membrane microdomains appears to be a critical for controlling their activation.

The mechanism of SIF1 inhibition of FcγR signaling elucidated here, indicates that FcγRs can be inhibited without activation or promoting degradation beyond membrane turnover. At the plasma membrane, SIF1-FcγR complexes had nearly indistinguishable motions as rFc-FcγR and none recruited Syk-mScarlet, indicating that SIF1 occupied the IgG binding sites while trapping the FcγR in a non-activatable state. Within endosomes, SIF1 and rFc docked FcγRs were few and transient indicating that they lingered on the PM, with a relatively slow internalization kinetic. We interpret these findings as SIF1 binds FcγRs but does not alter their native inactive state in any subcellular compartment, even with the lower activation thresholds as implied by the PentX results. SIF1 is an attractive inhibitor as it has significantly higher overall affinity than rFc or IVIG, arising from avidity by binding three FcγRs, leading to therapeutic effects at lower drug concentrations against immune complex mediated diseases (6). Moreover, SIF1 can likely engage with all FcγR types while maintaining the properties of a single receptor making it ideal to displace pathological IC-IgGs or to disrupt particle opsonized IgG responses such as antibody dependent cellular cytotoxicity or phagocytosis.

In contrast to conventional thinking, internalization from plasma membrane in this system does not appear to be a result of Syk recruitment to ligated FcγRs, but rather provides a microenvironment for FcγR signaling and Syk recruitment in subcellular membranes. A remaining question is do the multivalent Fcs promote Syk recruitment in endosomes or is internalization of the Fc/FcγR complexes a default pathway that through removal of the complex from the PM, facilitates FcγR activation? Our data suggest that in the case of SIF1 and rFc, no detectable Syk recruitment is observed on internal membranes or the PM, despite endocytic traffic of SIF1 and rFc. Furthermore, the long residence time of SIF1 and rFc on the cell surface,

suggests that these molecules docked to FcγRs are dynamically being internalized and recycled back to the cell surface.

DATA AVAILABILITY STATEMENT

The original contributions presented in the study are included in the article/**Supplementary Material**. Further inquiries can be directed to the corresponding author.

ETHICS STATEMENT

The animal study was reviewed and approved by South Dakota State University Institutional Animal Care and Use Committee.

AUTHOR CONTRIBUTIONS

AC, CB, EB, and AH designed the experimental plan and evaluated data. EB, DO, JS, AM, and AH conducted the experiments and analyzed the data. EB, AC, CB, and AH wrote the paper. All authors contributed to the article and approved the submitted version.

FUNDING

This work was supported by funds provided by Momenta Pharmaceuticals as well as the NSF/EPSCoR Cooperative Agreement #IIA-1355423, the South Dakota Research and Innovation Center, BioSNTR, and by the State of South Dakota BOR CRGP to AH. EB was supported through the ASERT-IRACDA program (K12GM088021).

ACKNOWLEDGMENTS

The authors thank Dr. Lu Huang for creating the Syk-mScarlet THP-1 cells and Ms. Seuly Akter for conducting the experiments on the CRISPR edited FLM cells.

SUPPLEMENTARY MATERIAL

The Supplementary Material for this article can be found online at: https://www.frontiersin.org/articles/10.3389/fimmu.2020.617767/full#supplementary-material

Supplementary Video 1 | Syk-mScarlet redistribution to patches of Uncontrolled Multimer (UM) AF488 (100 μg/ml). The confocal movies from left to right include the UM AF488, Syk-mScarlet, and the overlay of the two, with FcM pseudo-colored green and the Syk-mScarlet pseudo-colored magenta. Movies are 50 frames with time between frames being 0.292 s. Scale Bar represents 5μm.

upplementary Video 2 | Redistribution Syk-mScarlet, to internalized PentX-AF488 (100 μg/ml). The confocal movies from left to right include the PentX AF488, Syk-mScarlet, and the overlay of the two, with PentX pseudo-colored green and the Syk-mScarlet pseudo-colored magenta. Movies are 50 frames at 0.292 s between frames. Scale Bar represents 5μm.

Supplementary Video 3 | Syk-mScarlet is recruited to patches of FcγRs moving on an IgG opsonized bilayer. TIRF imaging show THP-1 cells engaging an IgG-AF647 opsonized bilayer, driving FcγR clustering, and Syk-mScarlet recruitment to clustering receptors. In the merge, green represents IgG-AF647 and the magenta represents Syk-mScarlet. 100 frames at 1 s between frames. Scale Bar represents 5μm.

upplementary Video 4 | TIRF imaging of Syk-mScarlet in THP-1 cells treated with 100 μg/ml rFc-AF488. In the merged movie, rFc is pseudo-colored green and Syk-mScarlet is pseudo-colored magenta. The movies are 100 frames with 0.120 s between frames. Scale bar represents 5μm.

Supplementary Video 5 | TIRF imaging of Syk-mScarlet in THP-1 cells treated with 100 μg/ml SIF1-AF488. In the merged movie, SIF1 is pseudo-colored green and Syk-mScarlet is pseudo-colored magenta. The movies are 100 frames with 0.120 s between frames. Scale bar represents 5μm.

Supplementary Video 6 | TIRF imaging of Syk-mScarlet in THP-1 cells treated with 100 μg/ml PentX-AF488. In the merged movie, PentX is pseudo-colored green and Syk is pseudo-colored magenta. The movies are 100 frames with 0.120 s between frames. Scale bar represents 5μm.

Supplementary Video 7 | THP-1 cells with a 1:1 mixtures of Fc multimers labeled with two different fluorophores. The molecules, rFc, SIF1, and PentX, were conjugated with either AF488 or DyL594 to investigate super clustering. The left panel shows THP-1 cells with docked rFc-AF88, pseudo-colored green, and rFc-DL594, pseudo-colored magenta. The middle panel shows THP-1 cells with docked SIF1-AF88, pseudo-colored green, and SIF1-DL594, pseudo-colored magenta. The right panel shows THP-1 cells with docked PentX-AF88, pseudo-colored green, and PentX-DL594, pseudo-colored magenta. The two-color movies are 50 frames with 0.220 s between frames, concentrations were 33 μg/ml for AF488- Fcs and 33μg/ml AF594-Fcs. The scale bar represents 5μm.

REFERENCES

1. Nimmerjahn F, Ravetch JV. Fcγ receptors as regulators of immune responses. *Nat Rev Immunol* (2008) 8:34. doi: 10.1038/nri2206
2. Li X, Kimberly RP. Targeting the Fc receptor in autoimmune disease. *Expert Opin Ther Targets* (2014) 18(3):335–50. doi: 10.1517/14728222.2014.877891
3. Cojocaru M, Cojocaru IM, Silosi I, Vrabie CD. Manifestations of systemic lupus erythematosus. *Maedica* (2011) 6(4):330–6.
4. Murphy KW. *Casey, Janeway"s Immunology. Vol. 9* Vol. 924. New York and London: Garland Science Taylor and Francis Group (2017).
5. Ushio A, Arakaki R, Yamada A, Saito M, Tsunematsu T, Kudo Y, et al. Crucial roles of macrophages in the pathogenesis of autoimmune disease. *World J Immunol* (2017) 7(1):1–8. doi: 10.5411/wji.v7.i1.1
6. Ortiz DF, Lansing JC, Rutitzky L, Kurtagic E, Prod'homme T, Choudhury A, et al. Elucidating the interplay between IgG-Fc valency and FcγR activation for the design of immune complex inhibitors. *Sci Trans Med* (2016) 8 (365):365ra158. doi: 10.1126/scitranslmed.aaf9418
7. Lowell CA. Src-family and Syk kinases in activating and inhibitory pathways in innate immune cells: signaling cross talk. *Cold Spring Harb Perspect Biol* (2011) 3(3). doi: 10.1101/cshperspect.a002352
8. Mocsai A, Ruland J, Tybulewicz VL. The SYK tyrosine kinase: a crucial player in diverse biological functions. *Nat Rev Immunol* (2010) 10(6):387–402. doi: 10.1038/nri2765
9. Flannagan RS, Jaumouille V, Grinstein S. The cell biology of phagocytosis. *Annu Rev Pathol* (2012) 7:61–98. doi: 10.1146/annurev-pathol-011811-132445
10. Goodridge HS, Reyes CN, Becker CA, Katsumoto TR, Ma J, Wolf AJ, et al. Activation of the innate immune receptor Dectin-1 upon formation of a 'phagocytic synapse'. *Nature* (2011) 472(7344):471–5. doi: 10.1038/nature10071

11. Zhang Y, Hoppe AD, Swanson JA. Coordination of Fc receptor signaling regulates cellular commitment to phagocytosis. *Proc Natl Acad Sci USA* (2010) 107(45):19332–7. doi: 10.1073/pnas.1008248107
12. Flaherty MM, MacLachlan TK, Troutt M, Magee T, Tuaillon N, Johnson S, et al. Nonclinical evaluation of GMA161–an antihuman CD16 (FcgammaRIII) monoclonal antibody for treatment of autoimmune disorders in CD16 transgenic mice. *Toxicol Sci* (2012) 125(1):299–309. doi: 10.1093/toxsci/kfr278
13. Debré M, Griscelli C, Bonnet MC, Carosella E, Philippe N, Reinert P, et al. Infusion of Fcγ fragments for treatment of children with acute immune thrombocytopenic purpura. *Lancet* (1993) 342(8877):945–9. doi: 10.1016/0140-6736(93)92000-J
14. Oates-Whitehead RM, Baumer JH, Haines L, Love S, Maconochie IK, Gupta A, et al. Intravenous immunoglobulin for the treatment of Kawasaki disease in children. *Cochrane Database Syst Rev* (2003) 4):CD004000. doi: 10.1002/14651858.CD004000
15. Anthony RM, Nimmerjahn F, Ashline DJ, Reinhold VN, Paulson JC, Ravetch JV. Recapitulation of IVIG Anti-Inflammatory Activity with a Recombinant IgG Fc. *Science* (2008) 320(5874):373–6. doi: 10.1126/science.1154315
16. Lin J, Kurilova S, Scott BL, Bosworth E, Iverson BE, Bailey EM, et al. TIRF imaging of Fc gamma receptor microclusters dynamics and signaling on macrophages during frustrated phagocytosis. *BMC Immunol* (2016) 17:5. doi: 10.1186/s12865-016-0143-2
17. Brandsma AM, Schwartz SL, Wester MJ, Valley CC, Blezer GLA, Vidarsson G, et al. Mechanisms of inside-out signaling of the high-affinity IgG receptor FcγRI. *Sci Signaling* (2018) 11(540):eaaq0891. doi: 10.1126/scisignal.aaq0891
18. Lopes FB, Balint S, Valvo S, Felce JH, Hessel EM, Dustin ML, et al. Membrane nanoclusters of FcgammaRI segregate from inhibitory SIRPalpha upon activation of human macrophages. *J Cell Biol* (2017) 216(4):1123–41. doi: 10.1083/jcb.201608094
19. Mellman I, Plutner H. Internalization and degradation of macrophage Fc receptors bound to polyvalent immune complexes. *J Cell Biol* (1984) 98 (4):1170–7. doi: 10.1083/jcb.98.4.1170
20. Chiou SH, Winters IP, Wang J, Naranjo S, Dudgeon C, Tamburini FB, et al. Pancreatic cancer modeling using retrograde viral vector delivery and in vivo CRISPR/Cas9-mediated somatic genome editing. *Genes Dev* (2015) 29 (14):1576–85. doi: 10.1101/gad.264861.115
21. Scott BL, Sochacki KA, Low-Nam ST, Bailey EM, Luu Q, Hor A, et al. Membrane bending occurs at all stages of clathrin-coat assembly and defines endocytic dynamics. *Nat Commun* (2018) 9(1):419. doi: 10.1038/s41467-018-02818-8
22. Lin J, Hoppe AD. Uniform total internal reflection fluorescence illumination enables live cell fluorescence resonance energy transfer microscopy. (2013) *Microsc Microanal* 19(2):350–9. doi: 10.1017/S1431927612014420
23. Jaqaman K, Loerke D, Mettlen M, Kuwata H, Grinstein S, Schmid SL, et al. Robust single-particle tracking in live-cell time-lapse sequences. *Nat Methods* (2008) 5(8):695–702. doi: 10.1038/nmeth.1237
24. Vega AR, Freeman SA, Grinstein S, Jaqaman K. Multistep Track Segmentation and Motion Classification for Transient Mobility Analysis. *Biophys J* (2018) 114(5):1018–25. doi: 10.1016/j.bpj.2018.01.012
25. Andrews NL, Pfeiffer JR, Martinez AM, Haaland DM, Davis RW, Kawakami T, et al. Small, mobile FcepsilonRI receptor aggregates are signaling competent. *Immunity* (2009) 31(3):469–79. doi: 10.1016/j.immuni.2009.06.026
26. Tokunaga M, Imamoto N Fau - Sakata-Sogawa K, Sakata-Sogawa K. Highly inclined thin illumination enables clear single-molecule imaging in cells. *Nat Methods* (2008) 5(2)(1548-7105: (2):159–61. doi: 10.1038/nmeth1171
27. Horejsi V, Hrdinka M. Membrane microdomains in immunoreceptor signaling. *FEBS Lett* (2014) 588(15):2392–7. doi: 10.1016/j.febslet.2014.05.047
28. Garcia-Parajo MF, Cambi A, Torreno-Pina JA, Thompson N, Jacobson K. Nanoclustering as a dominant feature of plasma membrane organization. *J Cell Sci* (2014) 127(23):4995–5005. doi: 10.1242/jcs.146340
29. Freeman SA, Goyette J, Furuya W, Woods EC, Bertozzi CR, Bergmeier W, et al. Integrins Form an Expanding Diffusional Barrier that Coordinates Phagocytosis. *Cell* (2016) 164(1-2):128–40. doi: 10.1016/j.cell.2015.11.048
30. Kara S, Amon L, Luhr JJ, Nimmerjahn F, Dudziak D, Lux A. Impact of Plasma Membrane Domains on IgG Fc Receptor Function. *Front Immunol* (2020) 11:1320. doi: 10.3389/fimmu.2020.01320
31. Freeman SA, Vega A, Riedl M, Collins RF, Ostrowski PP, Woods EC, et al. Transmembrane Pickets Connect Cyto- and Pericellular Skeletons Forming Barriers to Receptor Engagement. *Cell* (2018) 172(1-2):305–17.e10. doi: 10.1016/j.cell.2017.12.023
32. Jaumouille V, Farkash Y, Jaqaman K, Das R, Lowell CA, Grinstein S. Actin cytoskeleton reorganization by Syk regulates Fcgamma receptor responsiveness by increasing its lateral mobility and clustering. *Dev Cell* (2014) 29(5):534–46. doi: 10.1016/j.devcel.2014.04.031
33. Ostrowski PP, Grinstein S, Freeman SA. Diffusion Barriers, Mechanical Forces, and the Biophysics of Phagocytosis. *Dev Cell* (2016) 38(2):135–46. doi: 10.1016/j.devcel.2016.06.023
34. Grakoui A, Bromley SK, Sumen C, Davis MM, Shaw AS, Allen PM, et al. The Immunological Synapse: A Molecular Machine Controlling T Cell Activation. *Science* (1999) 285(5425):221. doi: 10.1126/science.285.5425.221
35. Bakalar MH, Joffe AM, Schmid EM, Son S, Podolski M, Fletcher DA. Size-Dependent Segregation Controls Macrophage Phagocytosis of Antibody-Opsonized Targets. *Cell* (2018) 174(1):131–42.e13. doi: 10.1016/j.cell.2018.05.059

Conflict of Interest: AC, DO, JS, AM, and CB were employed by Momenta Pharmaceuticals during the project and have equity interest. CB, AM, and DO are inventors on patent application PCT/US2015/028926 (WO/2015/168643) submitted by Momenta Pharmaceuticals that covers "Compositions and methods related to engineered Fc constructs".

The remaining authors declare that the research was conducted in the absence of any commercial or financial relationships that could be construed as a potential conflict of interest.

Copyright © 2021 Bailey, Choudhury, Vuppula, Ortiz, Schaeck, Manning, Bosques and Hoppe. This is an open-access article distributed under the terms of the Creative Commons Attribution License (CC BY). The use, distribution or reproduction in other forums is permitted, provided the original author(s) and the copyright owner(s) are credited and that the original publication in this journal is cited, in accordance with accepted academic practice. No use, distribution or reproduction is permitted which does not comply with these terms.

frontiers in Immunology

METHODS
published: 19 February 2021
doi: 10.3389/fimmu.2021.635825

Use of Flow Cytometry to Evaluate Phagocytosis of *Staphylococcus aureus* by Human Neutrophils

Elena Boero[1,2], *Iris Brinkman*[1], *Thessely Juliet*[1], *Eline van Yperen*[1], *Jos A. G. van Strijp*[1], *Suzan H. M. Rooijakkers*[1] *and Kok P. M. van Kessel*[1]*

[1] Medical Microbiology, University Medical Center Utrecht, Utrecht University, Utrecht, Netherlands, [2] GlaxoSmithKline Vaccines S.r.l., Siena, Italy

OPEN ACCESS

Edited by:
Johnathan Canton,
Francis Crick Institute,
United Kingdom

Reviewed by:
Victor J. Torres,
New York University, United States
Tomasz Prajsnar,
Jagiellonian University, Poland
Timothy J. Foster,
Trinity College Dublin, Ireland
Tomas Castro-Dopico,
Francis Crick Institute,
United Kingdom

***Correspondence:**
Kok P. M. van Kessel
K.kessel@umcutrecht.nl

Specialty section:
This article was submitted to Molecular Innate Immunity, a section of the journal Frontiers in Immunology

Received: 30 November 2020
Accepted: 04 January 2021
Published: 19 February 2021

Citation:
Boero E, Brinkman I, Juliet T, van Yperen E, van Strijp JAG, Rooijakkers SHM and van Kessel KPM (2021) Use of Flow Cytometry to Evaluate Phagocytosis of Staphylococcus aureus by Human Neutrophils. Front. Immunol. 12:635825. doi: 10.3389/fimmu.2021.635825

Neutrophils play a key role in the human immune response to *Staphylococcus aureus* infections. These professional phagocytes rapidly migrate to the site of infection to engulf bacteria and destroy them *via* specialized intracellular killing mechanisms. Here we describe a robust and relatively high-throughput flow cytometry assay to quantify phagocytosis of *S. aureus* by human neutrophils. We show that effective phagocytic uptake of *S. aureus* is greatly enhanced by opsonization, i.e. the tagging of microbial surfaces with plasma-derived host proteins like antibodies and complement. Our rapid assay to monitor phagocytosis can be used to study neutrophil deficiencies and bacterial evasion, but also provides a powerful tool to assess the opsonic capacity of antibodies, either in the context of natural immune responses or immune therapies.

Keywords: *Staphylococcus aureus*, human, neutrophils, phagocytosis, flow cytometry

INTRODUCTION

Staphylococcus aureus is a leading pathogen causing an array of serious and possibly fatal diseases in humans (1). Due to its fast acquisition of antibiotic resistance, treatment of *S. aureus* infections is becoming increasingly difficult (2). Alternative measures such as vaccine candidates tested so far were unsuccessful (3, 4), thus new research efforts are urgently required. Patients with compromised neutrophil function are more susceptible to *S. aureus* infections (5). This suggests that studying the role of neutrophils in the clearance of different clinical strains of this bacterium could provide us with clues to develop therapies.

Neutrophils are the most abundant professional phagocytes of the innate immune system. These terminally differentiated cells are regularly released in the bloodstream to patrol the body. When

Abbreviations: AUC, Area Under Curve; CH50, Classical Pathway Hemolytic Assay; CR, Complement Receptor; EC50, Half Maximal Effective Concentration; *FcRs, Fc receptors;* FITC, Fluorescein Isothiocyanate; FSC, Forward Scatter; GFP, Green Fluorescent Protein; HI-NHS, Heat-inactivated NHS; HSA, Human serum albumin; IgA, Immunoglobulin A; IgG, Immunoglobulin G; IgM, Immunoglobulin M; IVIg, Intravenous Immunoglobulin; PBS, Phosphate Buffer Saline; PMNs, *Polymorphonuclear* Leukocytes; LDS, Laser Dye Styryl; mAm, mAmetrine; MFL, Mean Fluorescence; MHB, Mueller-Hinton Broth; NHS, Normal Human Serum; RPMI, Roswell Park Memorial Institute Medium; Sbi, Second Immunoglobulin-Binding Protein; sGFP, Superfolder Green Fluorescent Protein; ShRBC, Sheep Red Blood Cells; SpA, Staphylococcal Protein A; SSC, Side Scatter; ΔIgGΔIgM serum, IgG and IgM-depleted Serum; THA, Todd Hewitt Agar; THB, Todd Hewitt Broth; TMB, 3,3',5,5'-Tetramethylbenzidine; WGA, Wheat Germ Agglutinin.

S. aureus invades tissues, neutrophils sense inflammatory signals released by local cells and extravasate, migrating towards the site of infection (5–8). The inflammatory milieu also primes neutrophils, boosting their capacity to recognize and clear bacteria (9). Neutrophils mainly kill pathogens through phagocytosis, a process in which bacteria are engulfed into intracellular vesicles called phagosomes. The phagosomes then mature into lytic vesicles: they become filled with antimicrobial substances stored into cytoplasmic granules and with toxic reactive oxygen species. These events, combined with the tuning of the vacuolar pH, finely regulates the enzymatic activity, ultimately leading to killing and digestion of the bacteria (10, 11).

Phagocytosis is an active process that requires the direct contact between *S. aureus* and the neutrophil. This process is typically aided by opsonins, host plasma proteins that mark bacterial surfaces increasing their probability of interacting with neutrophils phagocytic receptors. The main opsonins are immunoglobulins and complement proteins (12).

Immunoglobulins are adaptive immune molecules designed to specifically recognize an antigen, such as Staphylococcal surface proteins. Once bound to the bacteria, immunoglobulins of class G (IgG) and A (IgA) induce phagocytosis by direct interaction of their Fc with their specific phagocytic receptors FcγRs and FcαRs. Furthermore, IgGs and IgMs induce phagocytosis indirectly, by activating the complement cascade *via* the classical pathway (13).

The complement system also comprises proteins that label bacterial surfaces that enhance phagocytosis. Since complement deposition is aspecific its activation is guided by three recognition pathways, including the aforementioned classical complement pathway in which complement activation is triggered by the recognition of *S. aureus* by antibodies (14, 15). The three recognition pathways all converge to the cleavage of C3 into C3b, which deposits on and tags bacterial surfaces. C3b is further inactivated into iC3b, and together they are ligands of neutrophil phagocytic receptors CR1 and CR3 (16).

In this methodological paper we describe an *in vitro* assay to measure phagocytosis. Traditionally, bacterial phagocytosis by human neutrophils is analyzed by enumeration of viable bacteria on growth media or by counting particles under the microscope. This method is very time-consuming since for each condition serial dilutions of lysed neutrophils are needed. Therefore, we and others have developed several approaches to determine phagocytosis of bacteria by neutrophils (17–30), many of them in multi-well plates. Here, we describe a powerful flow cytometry method to quantify phagocytosis of *S. aureus* by freshly isolated human neutrophils *in vitro*. Although our phagocytosis assay is not novel, we here intend to provide an extensive overview of the methodology, pinpoint basic parameters and considerations for the proper interpretation of results. In particular, we apply the method to unravel the role of different opsonins in the phagocytosis process using primary human neutrophils. By taking these parameters into account, a flow cytometric phagocytosis assay becomes a powerful method for studying neutrophil activity, as well as bacterial phenotypes and antibody responses.

MATERIALS AND METHODS

Ethics Statement

Blood was obtained from healthy donors after informed consent was obtained from all subjects, in accordance with the Declaration of Helsinki. Approval from the Medical Ethics Committee of the University Medical Center Utrecht was obtained (METC protocol 07-125/C approved on March 1, 2010).

S. aureus Strains Choice, Labeling and Culture

S. aureus strains used in phagocytosis assays were selected to have low or no expression of staphylococcal protein A (SpA) and second immunoglobulin-binding protein (Sbi), the main immunoglobulin binding proteins of *S. aureus*, that could otherwise interfere with opsonization and lower the resolution of the assay. In a separate experiment, several wild type *S. aureus* strains were included for comparison (see **Table 1**). All *S. aureus* strains were fluorescently labelled to allow detection by flow cytometry. We used both genetically labelled bacteria (GFP and mAm) and surface-labelled bacteria (FITC).

To construct GFP-labelled *S. aureus* strains, bacteria were transformed with a GFP-expressing plasmid pCM29 that constitutively and robustly expresses the superfolder green fluorescent protein (sGFP) from the sarAP1 promoter (33). A codon optimized gene for the fluorescent protein mAmetrine (mAm; GenBank: KX759016) was also cloned into the pCM29 plasmid (34). Competent bacteria (~$5x10^9$) were electroporated with 10 µl plasmid with a Gene Pulser II (BioRad; 100 Ohm resistance, 25 µF capacitance at 2.5 kVolt) (35). After recovery, bacteria were plated on Todd Hewitt agar (THA) plates containing 10 µg/ml chloramphenicol. A colony was picked for propagation in liquid THB plus 10 µg/ml chloramphenicol, collected and stored in PBS + glycerol (final concentration 15%) at −80°C.

To prepare bacterial stocks for phagocytosis experiments, *S. aureus* was grown overnight in Todd Hewitt broth (THB)

TABLE 1 | *S. aureus* strains used.

S. aureus strains	Description	Reference or source	Notes
KV27	Clinical strain UMCU	Pleural effusion	Low SpA expression*
Newman *ΔSpA ΔSbi*	*spa sbi* knockout mutant	(31)	
Newman wt	Wild type strain	Tim Foster, Dublin	
MW2		Michael Otto, NIH	
8325-4		Tim Foster, Dublin	(32)
COL		Andreas Peschel, Germany	(32)
USA300		Frank Deleo, NIAID	(32)
Wood-46		ATCC10932	
SH1000		Tim Foster, Dublin	

**Determined by comparing isotype mouse IgG2a binding levels among several clinical S. aureus strains.*

with the necessary antibiotics, diluted to an OD^{660nm} of 0.05 in fresh THB and cultured until an OD^{660nm} of ~ 0.50, corresponding to an early exponential phase. Bacteria were then collected by centrifuging at 2,400 x g at 4°C, for 15 min, washed twice, resuspended in RPMI + 0.05% HSA (RPMI-HSA), and stored aliquoted at −20°C.

For the chemical surface labeling with FITC, bacteria were grown as described above and after centrifugation labelled for 1 h at 4°C in 0.1 M carbonate buffer (pH 9.0) or PBS containing 250 µg/ml FITC. Finally, bacteria were washed thoroughly from excessive dye and stored at −20°C. Since the FITC isothiocyanate group reacts with amino terminal and primary amines available on the surface of the bacteria, we checked whether this procedure would affect the opsonization capacity of the serum. We therefore compared the phagocytosis of *S. aureus* expressing a mAmetrine fluorescent protein, unlabelled or externally labelled with FITC. The additional FITC labeling did not change the opsonization profile of the bacteria and did not interfere with phagocytosis (**Figure S1**).

Isolation of Human Polymorphonuclear Leukocytes (PMNs)

PMNs were isolated from healthy donors' blood. Whole blood was obtained by venepuncture and collected in sodium heparin 9 mL tubes (Greiner). Dual Ficoll/Histopaque density gradients were prepared by slowly layering 10 mL Ficoll (GE Healthcare) over 12 mL Histopaque (density 1.119; Sigma) in 50 mL tubes. Finally, 20–25 mL of blood diluted 1:1 (v/v) with PBS were carefully layered on top of the gradient, which was then centrifuged at 22°C for 20 min at 390 x g in a swinging bucket rotor without brake. After centrifugation the upper plasma, PBMC ring and the transparent layer of Histopaque were discarded. The pink Histopaque layer on top of the packed erythrocytes containing the PMNs was collected and washed with RPMI-HSA at 4°C for 10 min at 249 x g. Residual erythrocytes in the pellet were lysed by hypotonic shock with 9 mL of cold sterile deionized H_2O. Osmolarity was restored with 1 mL of 10x PBS after exactly 30 s. Cells were washed again with RPMI-HSA at 4°C for 10 min at 249 x g and were suspended in RPMI-HSA. From 9 mL of blood the yield will range from 5 x 10^6 to 3 x 10^7, depending on the donor. For more details on the procedure see Surewaard et al. (30).

The isolated PMN fraction contains neutrophils, 1–5% non-phagocytosing eosinophils, other cell types and debris, with a viability of >97%.

Preparation of Serum From Blood

Fresh blood was collected in tubes with no anticoagulant (Greiner) and allowed to clot undisturbed for 30 min at room temperature. The blood tubes were then centrifuged at 4°C for 10 min at 2,075 x g, and the supernatant (serum) was collected. Sera from 20 healthy individuals were stored individually at −80°C and pooled to be aliquoted as normal human serum (NHS), to avoid donor to donor variability in anti-staphylococcal antibody repertoire and complement activity. It is important to process the serum rapidly at low temperature and avoid freeze-thaw cycles to preserve the activity of complement. Heat-inactivated serum was prepared by incubating serum at 56°C for 30 min to deactivate thermosensitive complement proteins.

Isolation of Antibodies From Serum and ΔIgGΔIgM NHS Production

The protocol is described in detail in by Zwarthoff (36). Briefly, part of the NHS was depleted from IgG and IgM (ΔIgGΔIgM NHS) by affinity chromatography, passing it through two affinity columns in tandem, a HiTrap Protein G High Performance column (GE Healthcare) and a Tricorn column filled with POROS CaptureSelect IgM Affinity Matrix (Thermo Scientific). The flow through fractions with serum-like appearance that also peaked in UV absorbance were pooled and stored aliquoted at −80°C. Roughly 70–80% of the original volume of serum was retrieved. Effectivity of the depletion of serum was determined by specific ELISAs leaving <1% of IgG and IgM. The residual complement activity of the ΔIgGΔIgM NHS was ~50%, evaluated by measuring the serum hemolytic activity of sheep erythrocytes (CH50).

IgG and IgM were separately recovered from their respective affinity columns using a 0.1 M glycine-HCl buffer at pH 2.7, runs pooled and dialyzed against PBS. Purified IgG and IgM were checked for purity on a size exclusion Superdex-200 column. NHS and ΔIgGΔIgM NHS were checked for the presence of IgG and IgM by ELISA using affinity purified Sheep-anti-Hu-IgG or anti-Hu-IgM respectively (ICN) as a capture and Peroxidase-labelled Goat-anti-Hu-IgG or anti-Hu-IgM (SouthernBiotech) as corresponding detection antibody. Purified IgG (Human Gamma Globulin; Jackson ImmunoResearch) or IgM (Sigma Aldrich) was used as reference.

Classical Pathway Hemolytic Assay (CH50)

Sheep blood (bioTRADING Benelux B.V.) was washed twice with PBS to obtain pelleted red blood cells (ShRBC). ShRBC carry the Forssman glycolid structure and most humans (considered to be a Forssman antigen-negative species) have naturally occurring anti-Forssman antibodies (IgG and IgM) that would induce ShRBC lysis without additional opsonization. Therefore, human serum was pre-absorbed with pelleted ShRBC for 15 min on ice to eliminate these antibodies.

For the lysis experiment, pelleted ShRBC were resuspended in Veronal buffer (727 mM NaCl, 9.1 mM sodium barbital, 10.2 mM diethyl barbituric acid, pH 7.5) containing 0.5 mM $CaCl_2$ and 0.25 mM $MgCl_2$ and sensitized with 1:2,000 diluted Rabbit-anti-ShRBC serum for 10 min, washed and resuspended again in Veronal buffer. In a round-bottom 96-well plate, 25 µl of anti-Forssman antibodies-depleted human serum (starting at 10% with 2-fold dilutions) were mixed with 25 µl opsonized ShRBC and incubated for 60 min at 37°C on a shaking plateau. After centrifugation, release of hemoglobin was measured at 415 nm after transferring 25 µl supernatant to a half-area flat-bottom plate containing 25 µl MQ per well. Data were normalized for plateau 4% serum value (after subtraction of background spontaneous lysis) and used to calculate the EC50 value (GraphPad version 8;

Sigmoidal dose–response with variable slope Least squares fit). EC50 is converted to titer using the formula 100/EC50.

Affinity Purification of Anti-*S. aureus* IgGs

As a source of anti-*S. aureus* IgGs, we chose a commercial human normal immunoglobulin preparation for intravenous use containing at least 95% polyclonal IgGs (Kiovig, Sanquin). We will refer to this product as intravenous immunoglobulin (IVIg). In order to isolate anti-*S. aureus* specific IgGs from IVIg, a column with coupled bacteria was prepared. For this purpose, we chose the *S. aureus* strain Newman *ΔSpA ΔSbi*, which lacks both main IgG-binding proteins of *S. aureus*, to avoid non-specific retaining of antibodies. Bacteria were grown overnight in Mueller-Hinton Broth (MHB), and subsequently diluted in fresh MHB and grown to OD^{660nm} 0.5. Bacteria were resuspended from growth medium in PBS, fixed with 1% formaldehyde in PBS for 30 min at 4°C with gentle mixing and washed again in PBS. Finally, bacteria were resuspended to OD^{660nm} of 1.0 in coupling buffer (0.2 M $NaCO_3$ and 0.5 M NaCl pH 8.0) and 7.5 mL recirculated over a 5 mL HiTrap NHS-column (GE healthcare). Column was washed alternating with 0.5 M ethanolamine in 0.5 M NaCl (pH 8.3) and 0.1 M acetate buffer in 0.5 M NaCl (pH 4.0) according to the manufacturer's instructions. Based on OD^{660nm}, 70% of the input was coated resulting in ± 43 x 10^9 coupled bacteria.

For the isolation of affinity-purified IgGs, the column was loaded at 2 mL/min with 1 g IVIg at 10 mg/mL. Column was washed with PBS, eluted with 100 mM Glycine-HCL (pH 2.7) and peak fractions for OD^{280nm} directly neutralized with 1 M Tris (pH 8.0). IgG eluate was dialyzed overnight against PBS. Finally, only 1.15 mg affinity purified IgG was recovered.

ELISA to Verify Enrichment of *S. aureus* Human IgGs From IVIg Preparation

To verify the enrichment of anti-*S. aureus* human IgG, the original and affinity purified IVIg were compared in an ELISA (detailed protocol in van den Berg et al., 2015). Briefly, logarithmic grown bacteria were coated at 5x106 per well (50 µl) in PBS overnight at 4°C in a high-binding microplate (Greiner). Plates were blocked with 4% BSA in PBS/Tween-20 (0.05%). Serial dilutions of IgG in PBS/Tween-20 with 1% BSA were added and bound IgG detected with F(ab')2-goat-anti-Hu-IgG (Fc-gamma)-HRP labelled (Jackson) and TMB as substrate. Reaction was stopped with H_2SO_4 and the absorbance was measured at 450nm.

Phagocytosis Assay

Phagocytosis was performed in phagocytosis buffer RPMI-HSA. In a round-bottom 96-well plate (Greiner), 20 µl of fluorescent bacteria (3.75 x 10^7 CFU/mL) were mixed with 20 µl of a concentration range of human serum and/or purified antibodies for opsonization, for 15 min at 37°C on a plate thermoshaker (750 rpm). Subsequently, 10 µl of PMNs (7.5 x 10^6 cells/mL) were added to reach a 10:1 bacteria-to-cell ratio in a final volume of 50 µl. The reaction was incubated for other 15 min at 37°C on a plate thermoshaker (750 rpm). Samples were then fixed for 30 min with 100 µL cold formaldehyde at a concentration of 1.5% (diluted from 10% aqueous methanol free, formaldehyde, Ultra pure; Polysciences, Inc.). Samples were either acquired immediately after 30 min of fixation at 4°C or after overnight fixation.

Standard Data Acquisition of Phagocytosis by Flow Cytometry

Samples were acquired on a FACSVerse flow cytometer with Universal Loader (Becton Dickinson) equipped with a three-laser system (405, 488, 633 nm), 8-color (4-2-2) configuration and BD FACSuite software version 1.06.

In our standard acquisition set up, only neutrophil-related parameters were analyzed. Although we used density gradient centrifugation to isolate highly pure PMNs, gating of cells is still required to eliminate cell debris and possible free or clumped bacteria. Neutrophils were therefore gated adjusting Forward scatter (FSC) and Side scatter (SSC) parameters to linear scale. A threshold at FSC signal was also set, so that free bacteria were excluded from the acquisition. The fluorescence of FITC-, GFP-, or mAm-labelled staphylococci associated with neutrophils was acquired in logarithmic scale. A total of 7,000 events were collected for each sample gated on neutrophils. All data were exported as Flow Cytometry Standard format 3.0 files (FCS files).

Analysis of Flow Cytometry Phagocytosis Data

FSC files were analyzed by FlowJo (Version 10; Treestar US, Ashland, OR). Our analysis of phagocytosis is based on the variation in the fluorescence intensity of neutrophils. This is easily visualized in histograms showing the number of cells distributed based on their fluorescence intensity (**Figures 1A, B**). The fluorescence intensity often results in two defined peaks: the GFP-negative cells that did not interact with fluorescent bacteria (left side), and of phagocytosing GFP-positive cells (right side). The main parameters of interest are: (1) the percentage of cells with a positive fluorescent signal (% positive cells), representing the part of the population that interacted with bacteria in our experimental conditions (2) the mean fluorescence (MFL) of all neutrophils. Because MFL values differ between experiments due to use of different batches of bacteria and labels, different Flow Cytometers with their respective instrument settings, and different donors, MFL data are preferably expressed relative to an optimal reference condition. To evaluate the different concentration curves in a single value, the Area Under the Curve (AUC) was calculated using GraphPad Prism (version 8). Therefore, serum concentration values were converted to their logarithmic number, and AUC was calculated using all serum concentrations with baseline correction for the % GFP+ Neutrophils of control samples (neutrophils and bacteria without serum).

Alternative Data Acquisition of Phagocytosis (Neutrophils and Bacteria)

We adapted the flow cytometry protocol to measure the percentage of bacteria taken up by the neutrophils, as usually

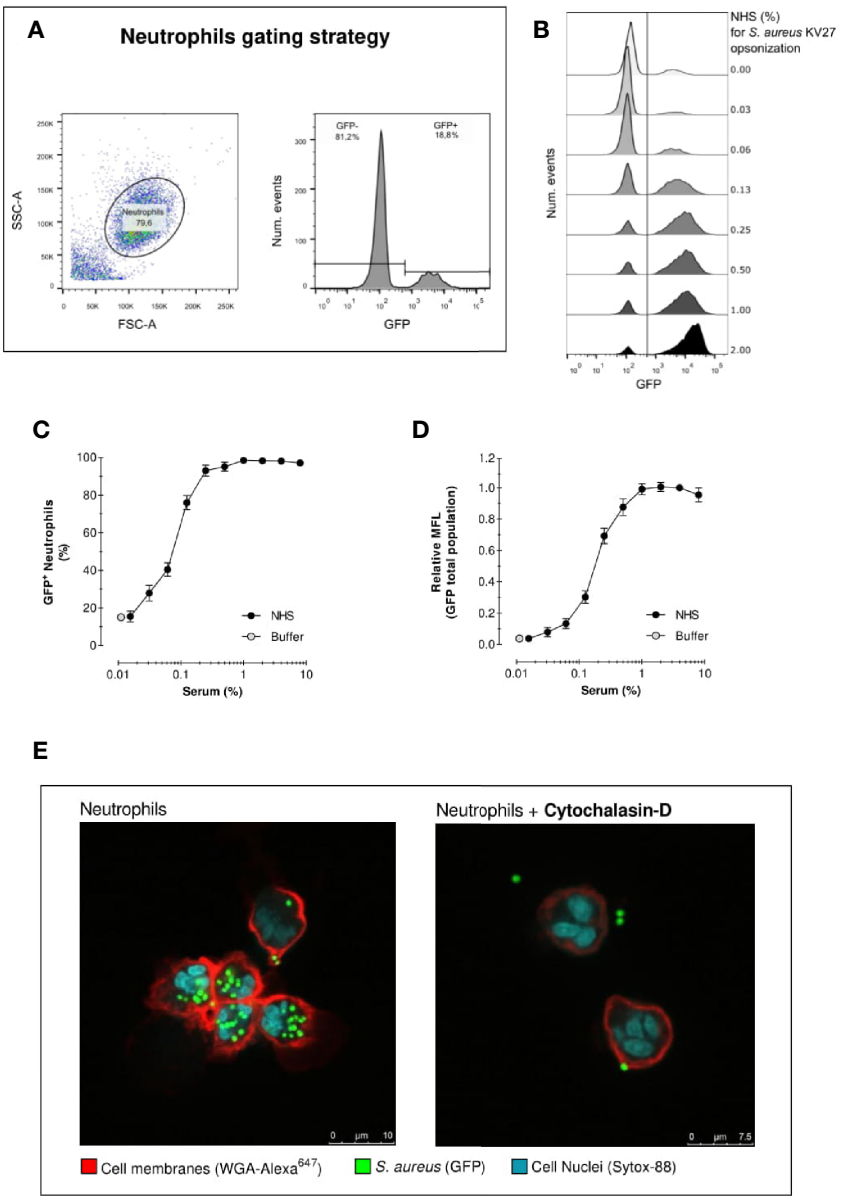

FIGURE 1 | Acquisition of phagocytosis assay by flow cytometry. Acquisition of neutrophil phagocytosis of *S. aureus* KV27 opsonized with normal human serum (NHS) at a 10:1 bacteria-to-cell ratio after 15 min incubation. **(A)** Gating of PMNs in the linear FSC and SSC, required to eliminate cell debris and possible free or clumped bacteria from the analysis (left graph). Representative histogram describing the GFP intensity per number of events. The total population is composed by a percentage of GFP- and GFP+ PMNs (right graph). **(B)** Typical histogram overlay of the GFP intensity distribution of the total neutrophil population per each concentration point of opsonizing NHS. **(C)** Phagocytosis expressed as the % of GFP+ neutrophils per increasing % of NHS. Mean ± SEM for n=8–25 **(D)** Phagocytosis expressed as the Mean Fluorescence (MFL) of neutrophils relative to the MFL obtained with opsonization with 4% NHS. Mean ± SD for n=8–25. **(E)** Confocal image of *S. aureus* KV27 (green, GFP) incubated with 4% NHS engulfed by human neutrophils (red, membrane stain WGA-Alexa647 and blue, nuclear stain SYTO-82), control (right image) or treated with actin-blocking agent cytochalasin-D (left image).

done in a classical phagocytosis assay. Samples pre- and post-phagocytosis were acquired on a FACSVerse flow cytometer. To acquire both bacteria (~1 μm diameter) and neutrophils (~12 μm), FSC and SSC parameters were set in logarithmic mode. To eliminate the substantial background events due to the full-scale log amplification for FSC and SSC, neutrophils were fluorescently labelled post-phagocytosis with 0.3 μg/ml LDS-751 nuclear stain (Thermofisher) for 5 min at 4°C without washing. GFP (*S. aureus*) and LDS-751 (PerCP channel setting) (neutrophils) signals were acquired on logarithmic scale and both used as threshold signals to collect only bacteria and neutrophils. A total of 50,000 events was acquired.

Setting quadrants in the GFP versus LDS-751 dot plot enables counting the number of free bacteria (GFP+/LDS-), neutrophils

(GFP-/LDS+) and neutrophils containing bacteria (LDS+/GFP+). Hereby both cell types are acquired with minimal noise, enabling to calculate the ratio of bacteria (GFP+) versus neutrophils (LDS+). This setup allows monitoring of the percentage of neutrophils that participate in phagocytosis (LDS+/GFP+ fraction of LDS+ events), as well as the MFL value of the neutrophil population, but also the percentage of bacterial uptake reflected by the drop-in ratio, as alternative for actual concentration determinations (**Figure S3**).

Microscopy Analysis of Phagocytosis

To analyse phagocytosis *via* light microscopy, samples were not fixed with formaldehyde, but immediately centrifugated onto glass slides using a cytospin-3 (Shandon), air dried and subsequently stained with the rapid Diff-Quick (Dade Behring) procedure. Pictures were taken with a Sony Nex-5 camera mounted without lens on an Olympus BX50 microscope.

For confocal microscopy, formaldehyde-fixed phagocytosis samples were mixed with Alexa Fluor^{647}-labelled WGA (3 μg/ml; Molecular Probes) and SYTO-82 Orange Fluorescent Nucleic Acid Stain (5 μM; Molecular Probes) for 5 min before cytospin preparation. Air-dried cytospin slides were mounted with Poly-Mount and a cover slip. For confocal microscopy, samples were viewed on a Leica TCS SP5 using the 488 Argon laser line, 543 and 633 Helium-Neon laser line with a TD 488/561/633 dichroic beam splitter. Samples were viewed with two successive sequential scans to eliminate spill-over signals.

RESULTS

Basic Parameters for the Acquisition of Neutrophils Phagocytosis of *S. aureus* by Flow Cytometry

Flow cytometry is a convenient high-throughput method for the evaluation of phagocytosis of fluorescently labelled *S. aureus* by neutrophils in suspension. In our standard assay set up we mix neutrophils with bacteria previously opsonized with pooled serum from healthy donors (normal human serum (NHS)), to enhance the engagement of cell surface receptors. By opsonizing bacteria with increasing concentrations of NHS, we can assess the impact of opsonization on phagocytosis.

As described in detail in the methods section, we evaluated the outcome of phagocytosis from cell-derived parameters. First, PMNs (containing >90% neutrophils) were gated to exclude cell debris and free bacteria from the analysis of internalized fluorescent *S. aureus*. **Figure 1A** shows an example of neutrophils gating, as well as the identification of the "GFP-" and "GFP+" cells in the GFP fluorescence histogram. The distinction between GFP negative and positive cells is defined by the autofluorescence signal of neutrophils in the absence of bacteria. **Figure 1B** shows the results in the form of overlaid histograms, representing the distribution of GFP fluorescence in the PMN population. With increasing serum concentrations, a marked increase of GFP-positive neutrophils is observed, together with the coherent increase of their fluorescence intensity, indicating that a larger number of cells was interacting with an increasing number of bacteria.

Figure 1C shows the percentage of GFP-positive neutrophils, thus the proportion of population that interacted with bacteria for each serum concentration. In the absence of serum, still 15% of PMNs interact with *S. aureus*. Conversely, when serum is introduced neutrophil engagement spikes rapidly. Already at a serum concentration of just 0.25%, more than >90% neutrophils are phagocytosing. Since isolated PMN fraction consists of ~95% neutrophils, 1–5% eosinophils (non-phagocytosing) and a few death cells, a non-phagocytosing fraction is always expected. We can reasonably conclude that >90% positive values indicate that virtually all neutrophils interacted with bacteria.

Figure 1D represents the mean fluorescence (MFL) of the neutrophil population, which summarizes the overall phagocytic activity of neutrophils considering both GFP- and GFP+ cells. This graph shows that, despite the percentage of neutrophils involved in phagocytosis reached a plateau after 0.25% opsonization, higher serum concentrations stimulate the cells to continue engulfing more bacteria.

One limitation of standard flow cytometry analysis is the inability to distinguish between bound or internalized bacteria within the GFP+ neutrophils. **Figure 1E** shows two representative confocal images of a phagocytosis experiment. The picture on the left clearly indicates that all bacteria are inside when opsonized with 4% NHS. The picture on the right shows a phagocytosis assay with neutrophils treated with actin-blocking agent Cytochalasin-D, which impairs phagocytosis. The confocal images thus demonstrate that despite the inability of flow cytometry to distinguish non-internalized bacteria, the number of bacteria attached to the cell surface is negligible, thus the results of flow cytometric analysis are attributable to the internalized bacteria. In addition, phagocytosis was performed on ice (with shaking) in parallel with 37°C, both conditions first opsonized for 15 min at 37°C. Keeping the conditions strictly cold, only background association was observed comparable with no serum (**Figure S2**).

Together our results confirm that, under these assay conditions, opsonization of bacteria with serum is essential for successful phagocytosis by neutrophils.

Incubation Time and Bacteria-To-Cell Ratio Dictate the Dynamics of the Phagocytosis Assay

The dynamics of phagocytosis *in vitro* depend on assay parameters that regulate the contact between cells and bacteria. Incubation time and bacteria-to-cell ratio are two main parameters that govern and influence the contact phase. In our standard phagocytosis assay, opsonized bacteria and cells are incubated together with vigorous shaking for 15 min at a 10:1 bacteria-to-cell ratio. To justify these choices, experiments are shown to evaluate the effect of varying the incubation time and ratio on the outcome of the phagocytosis assay.

To investigate how incubation time affects phagocytosis efficiency, we performed the same phagocytosis assay described in the previous section, with GFP-expressing *S. aureus* KV27

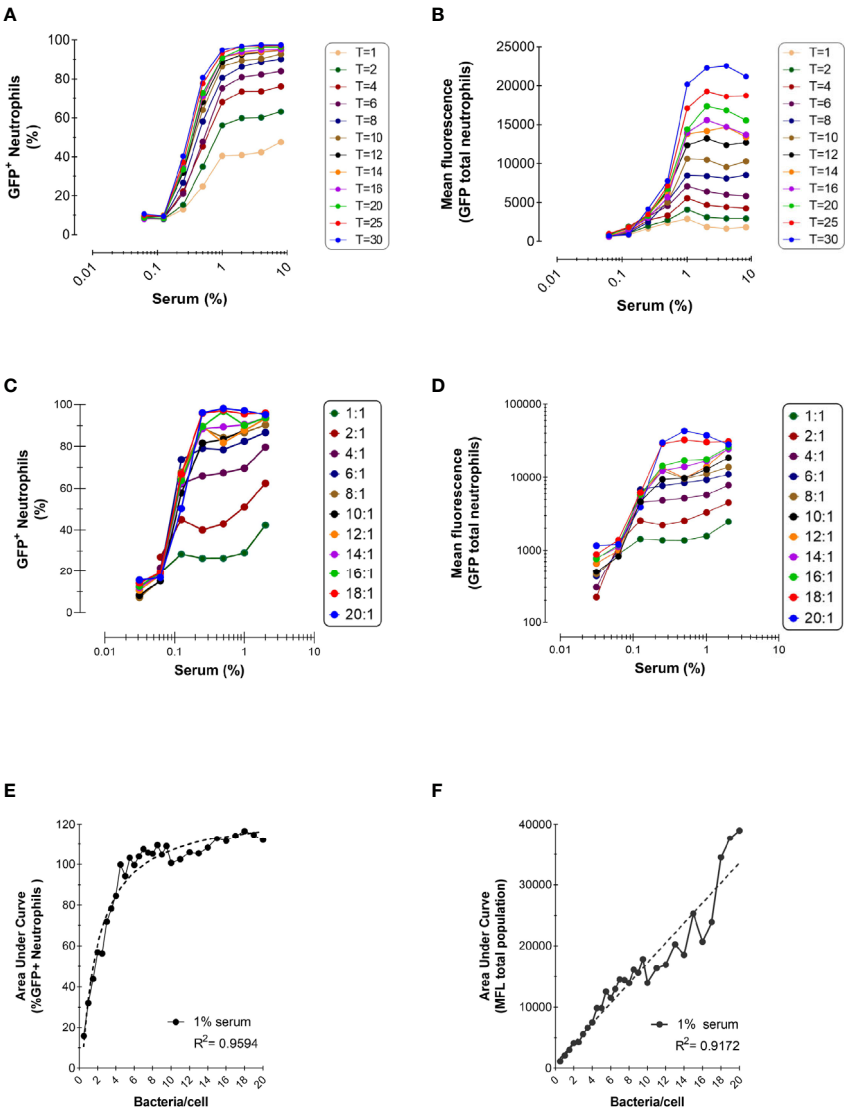

FIGURE 2 | Effect of Incubation Time and Bacteria-to-Cells Ratio on Opsonophagocytosis. **(A, B)** Time-dependent phagocytosis of KV27-GFP in the presence of pooled NHS. Bacteria and PMNs at a 10:1 ratio were incubated at 37°C in tubes and samples were withdrawn for each time point into ice cold formaldehyde to stop the reaction. Data are expressed as % GFP+ PMNs **(A)** and Mean fluorescence **(B)**. Representative experiment of n=2. **(C, D)** Phagocytosis of GFP-expressing Newman *ΔSpA ΔSbi* using different ratios bacteria to neutrophils. Phagocytosis of NHS opsonized bacteria expressed as % GFP+ neutrophils for depicted ratios **(C)** and as MFL of total neutrophils **(D)**. **(E, F)** For 1% serum at different ratios, data of % GFP+ neutrophils are fitted to a nonlinear regression curve [least squares fit; GraphPad, Agonist vs. response (three parameters)] **(E)** and data of total MFL are fitted to a linear regression curve **(F)**. Data pooled from n=2 experiments.

opsonized with increasing concentrations of NHS, but we stopped the incubation with cells between 1 to 30 min. **Figure 2A** shows that, as incubation time increases, so does the percentage of phagocytosing neutrophils, demonstrating that a longer incubation time increases the probability of a cell to encounter a bacterium. It is also clear that phagocytosis is a fast process; after only 1 min, more than 40% neutrophils phagocytosed bacteria, and by 8 min more than 90% neutrophils participated.

For all incubation times, we confirmed the observation from the previous section that a higher opsonization of bacteria enhanced phagocytosis. However, when bacteria were treated with 1% or more serum phagocytosis reached a plateau, suggesting that bacteria were saturated by opsonins and neutrophil stimulation reached its maximum.

Figure 2B represents the total mean fluorescence values, reflecting the mean number of phagocytosed bacteria per neutrophil. In accordance with **Figure 2A**, the MFL increased proportionally with incubation time, indicating that neutrophils engulf more bacteria when offered more time. When all neutrophils participated in the phagocytosis process, reaching their plateau after 8 min (**Figure 2A**), neutrophils kept engulfing more bacteria per cell the more the incubation time was extended (**Figure 2B**).

Next, we evaluated the outcome of phagocytosis when varying the bacteria-to-cell ratio. Low bacteria-to-cell ratios, from 0.5:1 to 20:1, were chosen to emulate the physiological ratios at the site of infection. **Figures 2C, D** show that both the percentage of positive neutrophils and total mean fluorescence are still dependent on the serum concentration for all ratios tested, and the percentage of neutrophil population involved reaches a plateau at ratio 8:1.

To better compare the serum-concentration curves for each ratio, the area under the curve (AUC) was calculated for both the percentage of positive neutrophils and their total MFL, as representative number for the phagocytic capacity of neutrophils for all serum concentrations. As already evident from **Figure 2C** (depicting a selected part of all ratios tested), with increasing ratios the AUC for neutrophils participating in phagocytosis reaches a plateau at a ratio of 6:1 (**Figure 2E**). Clearly, **Figure 2F** shows that, with increasing ratios, the ability to phagocytose more bacteria per neutrophil accumulates and under these conditions, does not reach a maximal plateau of phagocytic capacity.

Correlation of Microscopy and Flow Cytometry Analysis

A phagocytosis assay is typically evaluated by measuring engulfed bacteria inside cells, either by microscopy or flow cytometry. Here we compared the automated and more throughput flow cytometric analysis to the classical microscopic counting, to ensure that a higher MFL signal indeed reflects phagocytosis of more bacteria per neutrophil.

To provide two different phagocytosis conditions, bacteria were opsonized with either NHS or heat-inactivated serum (HI-NHS), in which key complement proteins are inactive. Due to the absence of complement activation, we expect a marked decrease in the efficiency of phagocytosis, since engulfment will be mainly mediated by the interaction of Fc receptors (FcRs) with opsonizing IgGs and a few IgAs. This will therefore give us the opportunity to compare two markedly different results with both techniques.

Figures 3A–C show the analysis of the assay *via* microscopy, where engulfment is typically evaluated by counting visually the number of bacteria per cell. The average number of bacteria per 50–100 cells is reported in **Figures 3B, C**. Phagocytosis is heterogeneous throughout the neutrophil population, as already evidenced in the relative broad fluorescence histograms shown in **Figure 1B**. As expected, the average number of bacteria per cell was higher with increasing concentrations of serum. In addition, a marked decrease in phagocytosis efficiency was observed when bacteria were opsonized with HI-NHS (**Figure 3C**), when compared with NHS (**Figure 3B**), showing that complement greatly contributes to enhance the phagocytic process.

Figures 3D–F show the analysis of the same experiments by flow cytometry. In contrast to the laborious microscopic analysis, the flow cytometer automatically evaluates the fluorescence of ~7000 neutrophils in a short time (exemplified in **Figure 3D**). This way of analysing the experiments clearly shows the presence of a significant portion of non-phagocytosing cells, which was also clear by microscopy analysis. However, for the evaluation by microscopy, only neutrophils containing bacteria were analyzed. The results of the experiments are presented in the standard format (explained in *Section 1*) as % of phagocytosing GFP+ neutrophils (**Figure 3E**) and relative GFP mean fluorescence of the total neutrophil population (**Figure 3F**).

To be able to compare the counted numbers with a representing fluorescence value, the mean fluorescence of the GFP+ neutrophil population alone was determined (**Figures 3D, G**). Plotting the bacteria/cell (microscopy) versus MFL/cell (flow cytometry) showed a linear regression with an $R^2 = 0.96$, indicating that the flow cytometric MFL reflects number of phagocytosed bacteria (**Figure 3H**).

Dissecting the Role of IgG, IgM, and Complement in Phagocytosis of *S. aureus*

In the previous section we showed that inactivating complement deposition on *S. aureus* severely impairs bacterial uptake. In this section we will elaborate more on the single contributions of serum opsonins in the phagocytosis of *S. aureus*.

First, we analyzed the contribution of complement proteins to opsonization. To obtain an antibody-free complement source (denoted as ΔIgGΔIgM NHS), we depleted pooled serum from all IgG and IgM antibodies. When bacteria were opsonized with ΔIgGΔIgM NHS, phagocytosis efficiency was scarce (**Figures 4A, B**). Only at the highest concentrations of 8 and 4% ΔIgGΔIgM NHS used, a small proportion of neutrophils were involved in phagocytosis. This result suggests that at lower concentrations of serum, antibodies are required to kick start complement deposition *via* the classical pathway.

Subsequently, we analyzed the phagocytic stimulus offered by monomeric IgGs and multimeric IgMs antibodies, which were recovered during the depletion of pooled serum. We used the equivalent concentrations of purified IgM and IgG present in 8% serum as 120 μg/ml for IgM (~1.5 mg/ml in serum) and 1,000 μg/ml for IgG (~12.5 mg/ml in serum) in Ig conditions only as well as reconstituted into ΔIgGΔIgM NHS. Additionally, we evaluated commercial IgGs for intravenous use (IVIg), which are usually offered to patients in need for a supplement of antibodies. As expected, purified IgMs alone did not stimulate any phagocytosis (**Figure 4A**). On the contrary, purified IgGs triggered phagocytosis, but reached a plateau of 40% cells involvement by ~60 μg/mL (shown as ~0.6% equivalent serum), suggesting a saturation of the bacterium and/or maximal engagement of FcγRs of neutrophils (**Figure 4B**). We also compared the phagocytic efficiency of the IgM or IgG antibody class from pooled serum recombined with their original complement source ΔIgGΔIgM NHS. In both cases, the percentage of phagocytosing neutrophils triplicated. We observed that when complement was present, IgM was slightly more efficient then IgG in stimulating phagocytosis (compare **Figure 4A** with **Figure 4B**). In fact, oligomeric IgM are strong complement activators, providing a preferential docking station for C1q deposition (37).

Also increasing concentrations of IVIg were used to opsonize bacteria, resulting in >70% phagocytosing neutrophils

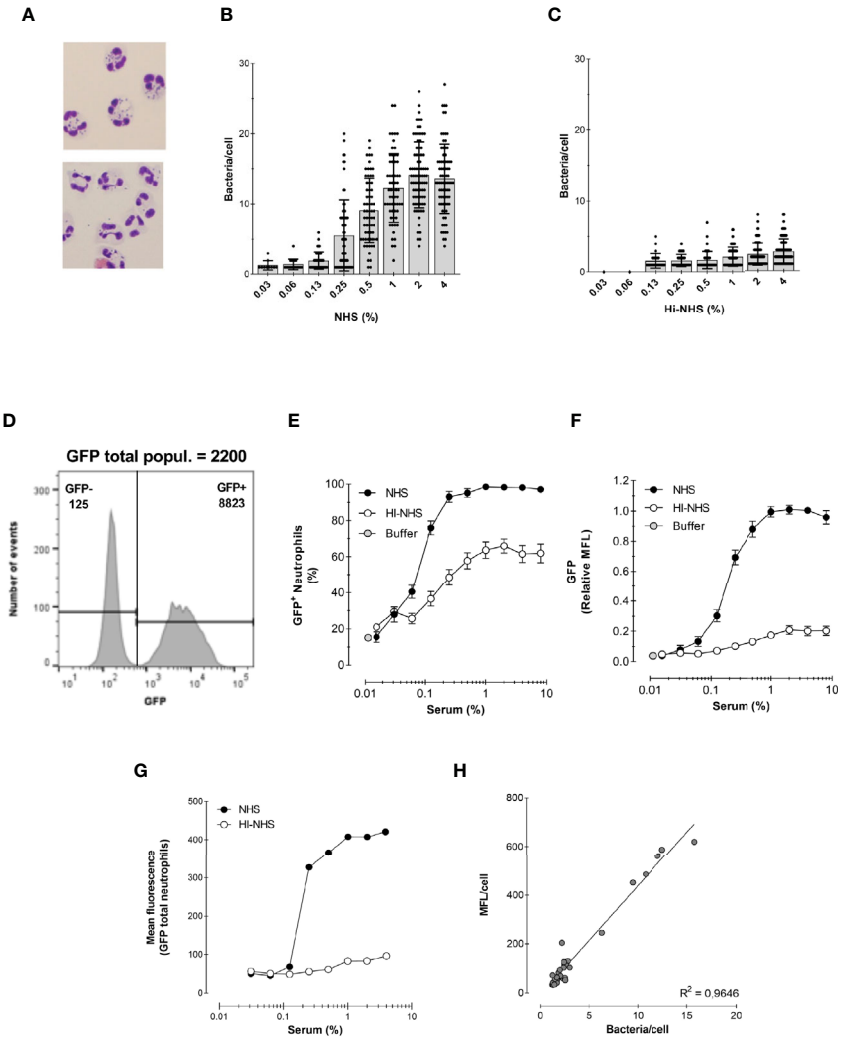

FIGURE 3 | Correlation between microscopy and flow cytometry. **(A)** Example of cytospin preparation after phagocytosis for 15 min with 1% NHS (top) and 1% HI-NHS (bottom). **(B, C)** Counting bacteria per neutrophil on cytospin preparations after phagocytosis with NHS **(B)** and HI-NHS **(C)**. Individual counts and means ± SD (n=25–100) for only neutrophils with bacteria. **(D)** Representative histogram to show GFP– and GFP+ population and their corresponding MFL value versus their total MFL. **(E, F)** Flow cytometry analysis of phagocytosis with NHS and HI-NHS shown as % GFP+ neutrophils **(E)** and relative MFL to 8% NHS **(F)** for total neutrophil population. **(G, H)** Representative figure for MFL of only the GFP+ neutrophil population **(G)** and correlation of that with microscopic counts per cell **(H)** for n=2 experiments.

(**Figures 4C, D**). The highest phagocytosis level was reached at IVIg concentrations of 200 μg/mL. This result confirms that commercial preparations also contain sufficient anti-Staphylococcal antibodies to efficiently stimulate *S. aureus* phagocytosis.

To show more directly the presence and capacity of specific anti-*S. aureus* antibodies within this pool of IgG, we enriched the IVIg solution by passing it over a column with sepharose-coupled formalin-fixed *S. aureus* Newman *ΔSpA ΔSbi* (Affi-IVIg). This strain was purposely chosen to prevent the aspecific capturing of antibodies by the IgG-binding proteins on the bacterial surface. The *S. aureus*-bound IgGs were then recovered and re-tested in the phagocytosis assay. To reach the same level of phagocytosis of the original IVIg, a 10-fold lower concentration of enriched IgGs was sufficient, in concordance with the 10-fold enrichment of anti-Staphylococcal antibodies measured by ELISA with coated bacteria (**Figure 4E**). The enrichment overall enhanced the percentage of phagocytosing neutrophils (**Figure 4C**), as well as the uptake of fluorescent bacteria at maximal concentrations used (**Figure 4D**).

In summary, purified IgGs provide a better phagocytic stimulus than IgM, but in combination with complement, their phagocytosis efficiency is comparable. We also observed that by enriching IgG preparations with *S. aureus*-specific antibodies, we can enhance phagocytosis and potentially aid the clearance of the bacterium in patients with lower amounts of specific antibodies.

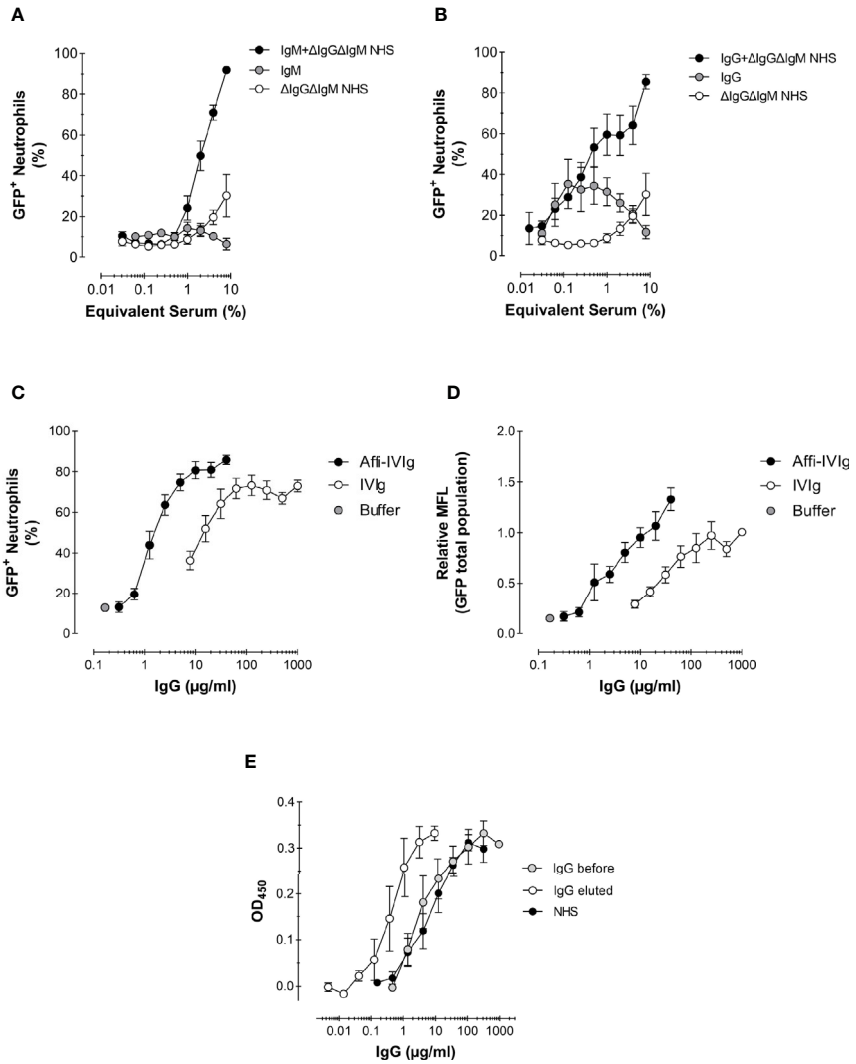

FIGURE 4 | Role of antibodies and complement in the phagocytosis of *S. aureus*. **(A, B)** Phagocytosis expressed as percentage of GFP+ neutrophils of Newman *ΔSpA ΔSbi* opsonized with a complement source depleted of antibodies (ΔIgGΔIgM NHS), NHS-purified IgM **(A)** or IgG **(B)**, or the combination of IgM **(A)** or IgG **(B)** reconstituted with complement. For purified IgM the equivalent concentration present in 8% serum is used, 120 µg/ml **(A)**, and for purified IgG that is 1,000 µg/ml **(B)**; these concentrations were also used to reconstitute into 8% ΔIgGΔIgM NHS. Data represent Mean ± SEM for n=2–8. **(C, D)** Phagocytosis of *S. aureus* KV27 opsonized with either commercial IgGs for intravenous use (IVIg), or the same IgGs affinity purified on a *S. aureus* Newman *ΔSpA ΔSbi* column (Affi-IVIg). Phagocytosis is expressed as the % of GFP+ neutrophils per increasing percentage of IVIgs or Affi-IVIgs. Mean ± SEM for n=7 **(C)** and as the Mean Fluorescence (MFL) of the total neutrophils engulfing GFP-expressing bacteria **(D)**. Mean ± SEM for n=6. **(E)** Binding specificity of NHS, IVIg (IgG total) and Affi-IVIg (IgG eluted) antibodies assessed by ELISA, using *S. aureus* strain Newman *ΔSpA ΔSbi*. Mean ± SD for n = 2.

Phagocytosis Efficiency of Single Serum Does Not Correlate With Its Antibody-Dependent Phagocytosis or Its Complement Activity

We observed in the previous section that pooled human serum, which is rich in anti-Staphylococcal antibodies, makes an excellent opsonic source for *S. aureus* phagocytosis. However, the humoral response differs in every individual, as well as complement activity. In this section we assess the ability of 24 sera from healthy donors to mediate phagocytosis of *S. aureus* strain Newman *ΔSpA ΔSbi* and we compare it to pooled serum (NHS).

Figure 5A shows the opsonic capacity of individual sera and their pooled NHS represented as the percentage of engulfing neutrophils. All sera succeeded in mediating phagocytosis, although they displayed some heterogeneity. **Figure 5B** represents the percentage of phagocytosis induced by the same sera after heat-inactivation, to eliminate complement activity. The same data were represented in **Figures 5C, D** where the areas under the curve (AUC) were related to NHS. We observed that the hierarchy observed in **Figure 5A** is not maintained in **Figure 5B**, exemplified by the colored individual sera. This suggests that the antibody repertoire mediating phagocytosis *via* FcγR is not the only determinant factor responsible for the

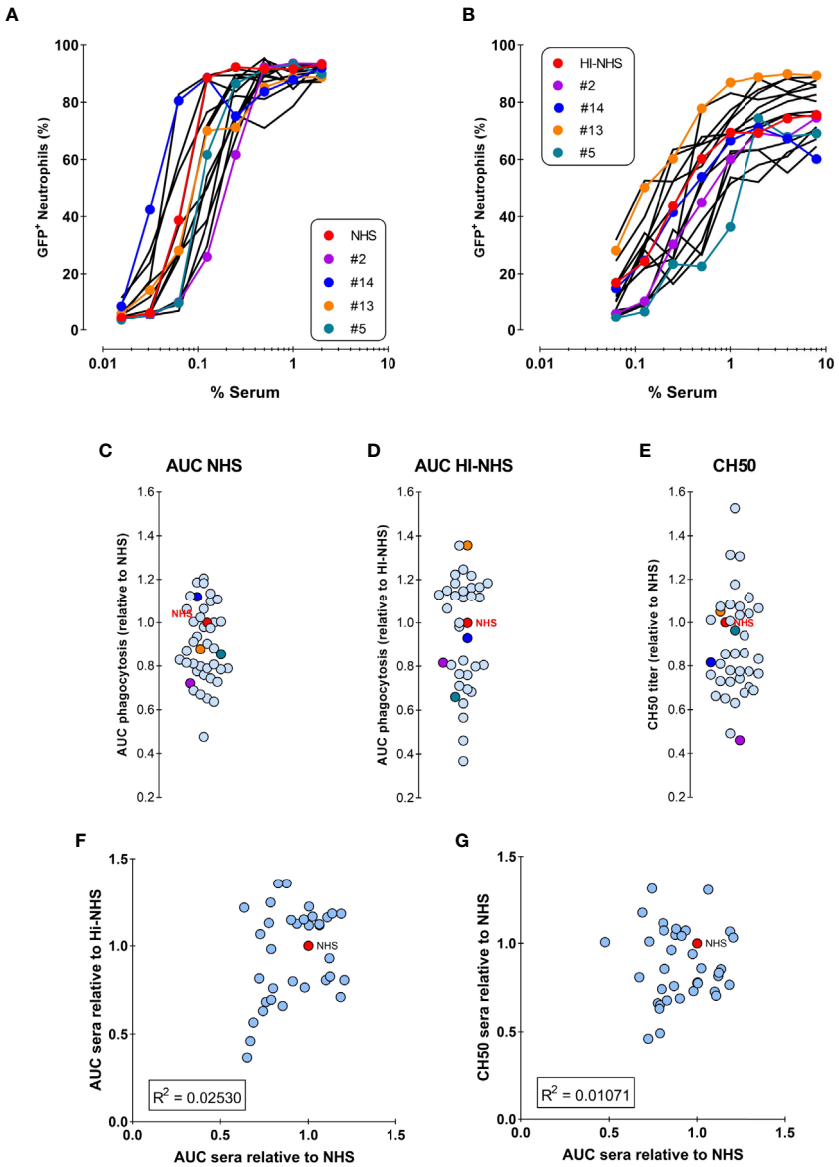

FIGURE 5 | No correlation between phagocytosis by NHS versus HI-NHS or complement activity. **(A, B)** Phagocytosis of individual sera as compared to the same sera present in the pooled NHS expressed as % GFP+ neutrophils for NHS **(A)** and Heat-Inactivated serum (HI-NHS), without complement activity **(B)**. Representative experiment for 16 individual sera and their pool (NHS) with some color coded for comparison. **C–E**) AUC value for each individual serum curve expressed relative to NHS phagocytosis (**C**; n=40), HI-NHS phagocytosis (**D**; n=37), and CH50 value relative to NHS (**E**; n=37). **(F, G)** No correlation between phagocytosis AUC for NHS versus HI-NHS **(F)** or for phagocytosis versus CH50 for NHS **(G)** with n=37.

final strength of the serum. In fact, no correlation was found between the potency of normal and heat inactivated sera (**Figure 5F**).

We then investigated whether complement could have a predominant role in the final efficacy of a serum in mediating *S. aureus* phagocytosis. To assess the complement activity of each serum independently from its antibody content, we performed a CH50 assay, which defines the percentage of serum that lyses 50% of sheep erythrocytes pre-sensitized by specific antibodies. When compared to NHS complement activity as a reference, sera still displayed heterogeneity (**Figure 5E**), however they also did not show any correlation with the potency of the related full sera (**Figure 5G**).

To further evaluate the competence of an individual donor serum for different *S. aureus* strains, we chose a "Low" (#15) and a "High" (#13) donor from the representative experiment shown in **Figure 5B**. These two donors were compared with the HI-NHS pool in opsonophagocytosis of 9 different *S. aureus* strains, including the KV27 and Newman *ΔSpA ΔSbi* strain as well as wild-type Newman. **Figures 6A, B** shows the phagocytosis curves for the different *S. aureus* strains opsonized by the "Low" and the "High" donor. There is a high variability among the tested *S. aureus* strains to be

phagocytosed. Conversion of the data to AUC and ranking the different strains for HI-NHS in ascending order (**Figure 6C**) clearly shows that the opsonic capacity of a serum is universal for different *S. aureus* strains, indicative for common epitope recognition.

In conclusion, the potency of a single donor serum to opsonize *S. aureus* for efficient phagocytosis by neutrophils is not solely determined by its anti-staphylococcal IgG or intrinsic complement activity, but is comparable for different strains.

Conditions to Clear All Bacteria Efficiently

Our standard phagocytosis assay provides efficient basic parameters to compare opsonization conditions, or factors that either inhibit or stimulate neutrophil phagocytic capacity. The former is exemplified by e.g. *S. aureus* immune evasion proteins that interfere with C3b deposition on bacteria (38) or IgG interaction with FcγRs (39). Modification of the assay also provides the opportunity to use flow cytometry to evaluate actual bacterial uptake; the percentage of phagocytosed bacteria. Using two fluorescent tags for neutrophils and bacteria during acquisition, both partners of the phagocytosis assay can be analyzed simultaneously. Phagocytosis was performed with a full serum opsonization range at different bacteria-to-cell ratios for both 15 and 60 min incubation time. The gating analysis strategy is depicted in **Figure S3** for samples with a starting ratio of 1:1 (**Figures S3A, B**) and 8:1 (**Figures S3 D, E**), in the presence of 4% NHS with immediate fixation. As phagocytosis proceeds with increasing serum concentrations and time, the percentage of free bacteria will decrease, which can be calculated from a decrease in bacteria-to-cell ratio, as compared to the starting situation. Representative example is shown in **Figure S3** for phagocytosis after 15 min in the presence of 4% NHS at a 1:1 (**Figure S3C**) and a 8:1 (**Figure S3F**) ratio. The multiple analysis of these data is depicted in heat-maps presented as percentage of GFP+ neutrophils (representing the % of all neutrophils that contain bacteria; *Section 2.11*) and percentage of bacterial phagocytosis (representing the % of all bacteria present that are taken up by the neutrophils; *Section 2.12*) (**Figure 7**). It is clear that at very low bacteria to neutrophil ratios (≤1:1), the percentage GFP+ cells remain low (**Figures 7A, C**; 15 min versus 60 min with NHS), but prolonging the incubation time enables efficient uptake of all available bacteria (**Figures 7B, D**). For the higher bacteria to neutrophil ratios (≥2:1), the percentage of GFP+

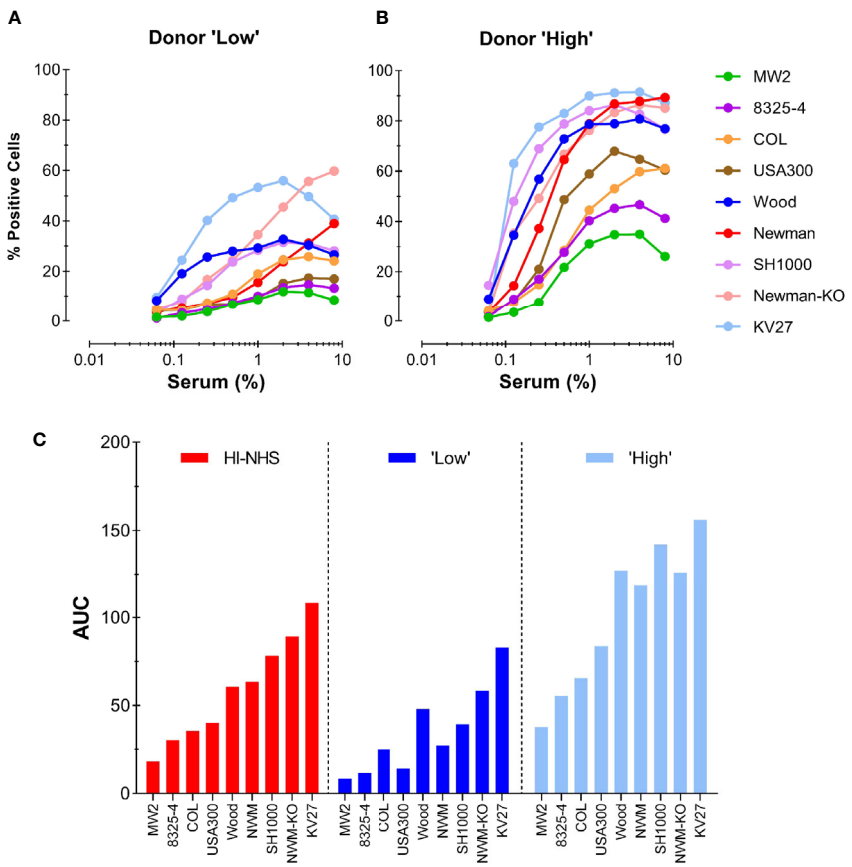

FIGURE 6 | Consistent donor opsonic capacity for multiple *S. aureus* strains. **(A, B)** Phagocytosis of different *S. aureus* strains opsonized with HI-serum of two individual donors chosen from the panel of 37 individual donors. Donor with "Low" **(A)** and donor with "High" **(B)** opsonic capacity as determined for Newman *ΔSpA ΔSbi* were compared with HI-NHS (graph not shown). **(C)** AUC values for each individual *S. aureus* curve were ranked in ascending order for HI-NHS as opsonic source. Data are from one experiment using standard 10:1 bacteria to neutrophil ratio and 15 min phagocytosis time and expressed as % GFP+ neutrophils.

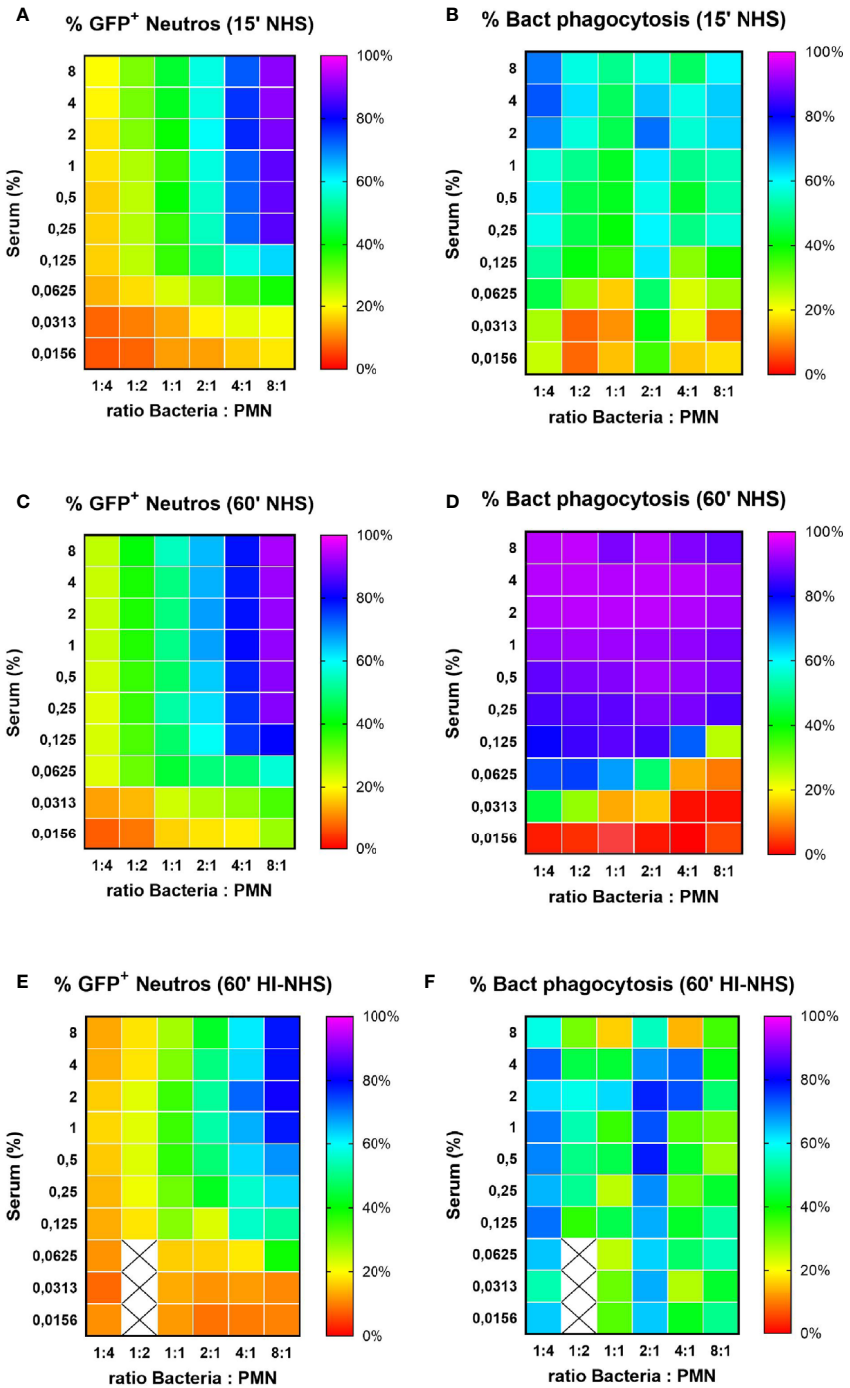

FIGURE 7 | Percentage of phagocytosing neutrophils vs. % phagocytosed bacteria. Heat map visualization of both % GFP+ neutrophils (left side panels) and % bacterial phagocytosis (right side panels) for increasing ratios of bacteria to neutrophils. Results for 15 **(A, B)** and 60 **(C, D)** min phagocytosis in the presence of increasing concentration NHS and for 60 min phagocytosis in the presence of HI-NHS **(E, F)**. Data are mean values of n=3 experiments, and X are missing data points.

neutrophils is much higher conform our previous data in **Figure 2**, but uptake of bacteria requires more opsonisation (**Figures 7A, B** for 15 min and **C, D** for 60 min). For all ratios, a prolonged incubation time is required to clear most of the bacteria from the incubation mixture. The same condition for heat-inactivated serum after 60 min incubation (**Figures 7E, F**) again stresses the requirement for active complement for proper opsonization to provide optimal uptake of all available bacteria.

General Conclusion

Our flow cytometric method for the determination of neutrophil mediated phagocytosis of *S. aureus* especially pinpoints to the role of different opsonins that steer the uptake. Basic characteristics of the method were evaluated that in general influence the dynamics of the assay, and maybe adapted for different research questions. The comparison of normal serum versus heat-inactivated serum (30 min at 56°C) is an easy way to study the contribution of the complement system in the opsonophagocytosis process. We also compared that with purified IgG, IgM and human serum depleted for naturally present IgG and IgM as an alternative complement source. Changing opsonisation conditions affects the phagocytosis capacity of neutrophils, not always reflected in the percentage of neutrophils that engulf bacteria, but usually more clear in the number of ingested bacteria (reflected by the total mean fluorescence value). This was verified by microscopic counting. In general, individual healthy donors possess sufficient opsonic capacity for proper phagocytosis of different *S. aureus* strains, but with variability that is consistent for the tested strains. Finally, we showed that under proper conditions of prolonged time and around a 1 to 1 bacteria to neutrophil ratio, almost all bacteria present can be engulfed. Although several well described flow cytometric assays were already known, this method adds some new considerations in comparing different opsonisation conditions.

DATA AVAILABILITY STATEMENT

The raw data supporting the conclusions of this article will be made available by the authors, without undue reservation.

ETHICS STATEMENT

The studies involving human participants were reviewed and approved by Blood was obtained from healthy donors after informed consent was obtained from all subjects, in accordance with the Declaration of Helsinki. Approval from the Medical Ethics Committee of the University Medical Center Utrecht was obtained (METC protocol 07-125/C approved on March 1, 2010). The patients/participants provided their written informed consent to participate in this study.

AUTHOR CONTRIBUTIONS

EB, IB, TJ, EV, and KV performed the experiments. EB, SR, and KV analyzed the data. EB, SR, and KK wrote the paper. JV, SR, and KV designed the research study and critically read the manuscript and provided constructive comments. All authors contributed to the article and approved the submitted version.

FUNDING

This work was supported by the European Union's Horizon 2020 research: H2020-MSCA-ITN (No. 675106 coordinated by Dr. Fabio Bagnoli, GSK Vaccines S.r.l., Siena, Italy) and ERC Starting grant (#639209, to SR).

ACKNOWLEDGMENTS

We thank Rita Cruz for the critical reading of the manuscript.

SUPPLEMENTARY MATERIAL

The Supplementary Material for this article can be found online at: https://www.frontiersin.org/articles/10.3389/fimmu.2021.635825/full#supplementary-material

Supplementary Figure 1 | Chemical surface labelling with FITC do not impact opsonization and phagocytosis. *S. aureus* Newman *ΔSpA ΔSbi* expressing the violet excitable yellow fluorescent protein mAmetrine was additionally externally labeled with fluorescein isothiocyanate (FITC) and compared with the mock treated bacteria in the phagocytosis assay with NHS and HI-NHS. Phagocytosis was measured as % of mAm+ PMNs **(A, B)** and mAmetrine MFL of the total population **(C, D)**. **(E, F)** Control graphs showing that FITC MFL of PMNs only increases when bacteria are FITC-labeled. Representative experiment.

Supplementary Figure 2 | On ice no phagocytosis occurs. *S. aureus* was opsonized with NHS at 37°C for 15 min, cooled on ice or kept on room temp for 10 min, and subsequently mixed with neutrophils (cold versus room temp) for a 15 min phagocytosis on ice or at 37°C. Phagocytosis is expressed as % GFP+ neutrophils **(A)** and GFP relative MFL (4% serum) of the total population **(B)**. Data are the mean of 2 experiments ± SD.

Supplementary Figure 3 | Gating strategies for the alternative phagocytosis assay using FITC (or GFP) and LDS-753 (PerCP signal) as threshold parameters for data aquisition. Shown are representative dot plots for a phagocytosis assays performed with putative bacteria to cell ratio 1:1 (upper panel) and 8:1 (lower panel). During the acquisition, bacteria to cell ratio was verified by gating both bacteria and PMNs by setting logarithmic scatter parameters (panel **A** for 1:1 and D for 8:1) or fluorescence parameters (panel **B** for 1:1 and **E** for 8:1). The actual observed ratio for the 1:1 appeared to be 1.1:1, and for the 8:1 ratio appeared to be 6.3:1, both in agreement for the scatter and the fluorescence based parameters. Dot plots are from the control samples before starting the experiments with 4% NHS, mixed on ice and immediately fixed with paraformaldehyde. Panels **C, F** are representative fluorescence dotplots for the 15 min phagocytosis timepoint with 4% NHS showing for the 1.1:1 ratio **(C)** 53.8% GFP+ neutrophils at a 0.45:1 ratio resulting in 59.8% bacterial phagocytosis, and for the 6.3:1 ratio **(F)** 96.6% GFP+ neutrophils and a 58.2% bacterial phagocytosis.

REFERENCES

1. Bagnoli F, Rappuoli R. *Staphylococcus aureus*. F Bagnoli, R Rappuoli, G Grandi, editors. Cham: Springer International Publishing (2017). doi: 10.1007/978-3-319-72063-0
2. David MZ, Daum RS. Treatment of Staphylococcus aureus infections. In: . *Current Topics in Microbiology and Immunology*. Switzerland: Springer Verlag (2017), p. 325–83. doi: 10.1007/82_2017_42
3. Missiakas D, Schneewind O. Staphylococcus aureus vaccines: Deviating from the carol. *J Exp Med* (2016) 213:1645–53. doi: 10.1084/jem.20160569

4. Redi D, Raffaelli CS, Rossetti B, De Luca A, Montagnani F. Staphylococcus aureus vaccine preclinical and clinical development: current state of the art. *New Microbiol* (2018) 41:208–13.
5. Rigby KM, DeLeo FR. Neutrophils in innate host defense against Staphylococcus aureus infections. *Semin Immunopathol* (2012) 34:237–59. doi: 10.1007/s00281-011-0295-3
6. Dale DC, Boxer L, Conrad Liles W. The phagocytes: Neutrophils and monocytes. *Blood* (2008) 112:935–45. doi: 10.1182/blood-2007-12-077917
7. Amulic B, Cazalet C, Hayes GL, Metzler KD, Zychlinsky A. Neutrophil Function: From Mechanisms to Disease. *Annu Rev Immunol* (2012) 30:459–89. doi: 10.1146/annurev-immunol-020711-074942
8. Spaan AN, Surewaard BGJ, Nijland R, van Strijp JAG. Neutrophils Versus *Staphylococcus aureus*: a biological tug of ear. *Annu Rev Microbiol* (2013) 67:629–50. doi: 10.1146/annurev-micro-092412-155746
9. Miralda I, Uriarte SM, McLeish KR. Multiple phenotypic changes define neutrophil priming. *Front Cell Infect Microbiol* (2017) 7:217:217. doi: 10.3389/fcimb.2017.00217
10. Foote JR, Patel AA, Yona S, Segal AW. Variations in the phagosomal environment of human neutrophils and mononuclear phagocyte subsets. *Front Immunol* (2019) 10:188:188. doi: 10.3389/fimmu.2019.00188
11. Nordenfelt P, Tapper H. Phagosome dynamics during phagocytosis by neutrophils. *J Leukoc Biol* (2011) 90:271–84. doi: 10.1189/jlb.0810457
12. Martinez-Pomares L. Phagocytes and Immunoglobulins. In: . *Antibody Fc: Linking Adaptive and Innate Immunity*. (2014) Elsevier Inc. p. 95–113. doi: 10.1016/B978-0-12-394802-1.00005-4
13. Vidarsson G, Dekkers G, Rispens T. IgG subclasses and allotypes: From structure to effector functions. *Front Immunol* (2014) 5:520:520. doi: 10.3389/fimmu.2014.00520
14. Ricklin D, Hajishengallis G, Yang K, Lambris JD. Complement: A key system for immune surveillance and homeostasis. *Nat Immunol* (2010) 11:785–97. doi: 10.1038/ni.1923
15. Morley BJ, Walport M. *The Complement FactsBook*. Academic Press (2017). doi: 10.1016/c2015-0-06595-9
16. Dustin ML. Complement Receptors in Myeloid Cell Adhesion and Phagocytosis. *Microbiol Spectr* (2016) 4:1–16. doi: 10.1128/microbiolspec.MCHD-0034-2016
17. Plested JS, Coull PA. Opsonophagocytosis assay using flow-cytometry. *Methods Mol Med* (2003) 71:263–75. doi: 10.1385/1-59259-321-6:263
18. Hasui M, Hirabayashi Y, Kobayashi Y. Simultaneous measurement by flow cytometry of phagocytosis and hydrogen peroxide production of neutrophils in whole blood. *J Immunol Methods* (1989) 117:53–8. doi: 10.1016/0022-1759(89)90118-X
19. Hartung S, Rauh C, Hoang TNM, Jahreis S, Wagner K, Macheleidt J, et al. Fast and Quantitative Evaluation of Human Leukocyte Interaction with Aspergillus fumigatus Conidia by Flow Cytometry. *Cytom Part A* (2019) 95:332–8. doi: 10.1002/cyto.a.23653
20. Smirnov A, Solga MD, Lannigan J, Criss AK. An improved method for differentiating cell-bound from internalized particles by imaging flow cytometry. *J Immunol Methods* (2015) 423:60–9. doi: 10.1016/j.jim.2015.04.028
21. Grasse M, Rosenkrands I, Olsen A, Follmann F, Dietrich J. A flow cytometry-based assay to determine the phagocytic activity of both clinical and nonclinical antibody samples against Chlamydia trachomatis. *Cytom Part A* (2018) 93:525–32. doi: 10.1002/cyto.a.23353
22. Nordenfelt P. Quantitative assessment of neutrophil phagocytosis using flow cytometry. *Methods Mol Biol* (2014) 1124:279–89. doi: 10.1007/978-1-62703-845-4_18
23. Fine N, Barzilay O, Glogauer M. Analysis of Human and Mouse Neutrophil Phagocytosis by Flow Cytometry. In: Phagocytosis and Phagosomes. Methods in Molecular Biology. *Methods in Molecular Biology*. New York, NY: Humana Press (2017), p. 17–24. doi: 10.1007/978-1-4939-6581-6_2
24. Lehmann AK, Sørnes S, Halstensen A. Phagocytosis: Measurement by flow cytometry. *J Immunol Methods* (2000) 243:229–42. doi: 10.1016/S0022-1759(00)00237-4
25. Rodríguez ME, Van Der Pol WL, Van De Winkel JGJ. Flow cytometry-based phagocytosis assay for sensitive detection of opsonic activity of pneumococcal capsular polysaccharide antibodies in human sera. *J Immunol Methods* (2001) 252:33–44. doi: 10.1016/S0022-1759(01)00329-5
26. Jansen WTM, Väkeväinen-Anttila M, Käyhty H, Nahm M, Bakker N, Verhoef J, et al. Comparison of a classical phagocytosis assay and a flow cytometry assay for assessment of the phagocytic capacity of sera from adults vaccinated with a pneumococcal conjugate vaccine. *Clin Diagn Lab Immunol* (2001) 8:245–50. doi: 10.1128/CDLI.8.2.245-250.2001
27. Van Amersfoort ES, Van Strijp JAG. Evaluation of a flow cytometric fluorescence quenching assay of phagocytosis of sensitized sheep erythrocytes by polymorphonuclear leukocytes. *Cytometry* (1994) 17:294–301. doi: 10.1002/cyto.990170404
28. Heinzelmann M, Gardner SA, Mercer-Jones M, Roll AJ, Polk HC. Quantification of phagocytosis in human neutrophils by flow cytometry. *Microbiol Immunol* (1999) 43:505–12. doi: 10.1111/j.1348-0421.1999.tb02435.x
29. Karsten CB, Mehta N, Shin SA, Diefenbach TJ, Slein MD, Karpinski W, et al. A versatile high-throughput assay to characterize antibody-mediated neutrophil phagocytosis. *J Immunol Methods* (2019) 471:46–56. doi: 10.1016/j.jim.2019.05.006
30. Surewaard BGJ, van Strijp JAG, Nijland R. Studying interactions of Staphylococcus aureus with neutrophils by flow cytometry and time lapse microscopy. *J Vis Exp* (2013) 77:e50788. doi: 10.3791/50788
31. Sibbald MJJB, Winter T, Van Der Kooi-Pol MM, Buist G, Tsompanidou E, Bosma T, et al. Synthetic effects of secG and secY2 mutations on exoproteome biogenesis in Staphylococcus aureus. *J Bacteriol* (2010) 192:3788–800. doi: 10.1128/JB.01452-09
32. Kuipers A, Stapels DAC, Weerwind LT, Ko YP, Ruyken M, Lee JC, et al. The Staphylococcus aureus polysaccharide capsule and Efb-dependent fibrinogen shield act in concert to protect against phagocytosis. *Microbiol (United Kingdom)* (2016) 162:1185–94. doi: 10.1099/mic.0.000293
33. Pang YY, Schwartz J, Thoendel M, Ackermann LW, Horswill AR, Nauseef WM. Agr-dependent interactions of Staphylococcus aureus USA300 with human polymorphonuclear neutrophils. *J Innate Immun* (2010) 2:546–59. doi: 10.1159/000319855
34. De Jong NWM, Van Der Horst T, Van Strijp JAG, Nijland R. Fluorescent reporters for markerless genomic integration in Staphylococcus aureus. *Sci Rep* (2017) 7:1–10. doi: 10.1038/srep43889
35. Schenk S, Laddaga RA. Improved method for electroporation of Staphylococcus aureus. *FEMS Microbiol Lett* (1992) 94:133–8. doi: 10.1016/0378-1097(92)90596-G
36. Zwarthoff SA, Magnoni S, Aerts PC, van Kessel KPM, Rooijakkers SHM. Method for Depletion of IgG and IgM from human serum as naive complement source. In: . *Methods in Molecular Biology - The Complement System, innovative diagnostic and research protocols*. (2021) Springer Nature, US. doi: 10.1007/978-1-0716-1016-9
37. Boes M. Role of natural and immune IgM antibodies in immune responses. *Mol Immunol* (2000) 37:1141–9. doi: 10.1016/S0161-5890(01)00025-6
38. Rooijakkers SHM, Ruyken M, Roos A, Daha MR, Presanis JS, Sim RB, et al. Immune evasion by a staphylococcal complement inhibitor that acts on C3 convertases. *Nat Immunol* (2005) 6:920–7. doi: 10.1038/ni1235
39. Stemerding AM, Köhl J, Pandey MK, Kuipers A, Leusen JH, Boross P, et al. Staphylococcus aureus Formyl Peptide Receptor–like 1 Inhibitor (FLIPr) and Its Homologue FLIPr-like Are Potent FcγR Antagonists That Inhibit IgG-Mediated Effector Functions. *J Immunol* (2013) 191:353–62. doi: 10.4049/jimmunol.1203243

Conflict of Interest: EB is participating in a post-graduate studentship program at GSK.

The remaining authors declare that the research was conducted in the absence of any commercial or financial relationships that could be construed as a potential conflict of interest.

Copyright © 2021 Boero, Brinkman, Juliet, van Yperen, van Strijp, Rooijakkers and van Kessel. This is an open-access article distributed under the terms of the Creative Commons Attribution License (CC BY). The use, distribution or reproduction in other forums is permitted, provided the original author(s) and the copyright owner(s) are credited and that the original publication in this journal is cited, in accordance with accepted academic practice. No use, distribution or reproduction is permitted which does not comply with these terms.

frontiers in Immunology

REVIEW
published: 25 February 2021
doi: 10.3389/fimmu.2021.636078

Better Together: Current Insights Into Phagosome-Lysosome Fusion

Jenny A. Nguyen[1] *and Robin M. Yates*[1,2,3]*

[1] Department of Biochemistry and Molecular Biology, Cumming School of Medicine, University of Calgary, Calgary, AB, Canada, [2] Department of Comparative Biology and Experimental Medicine, Faculty of Veterinary Medicine, University of Calgary, Calgary, AB, Canada, [3] Cumming School of Medicine, Snyder Institute of Chronic Disease, University of Calgary, Calgary, AB, Canada

Following phagocytosis, the nascent phagosome undergoes maturation to become a phagolysosome with an acidic, hydrolytic, and often oxidative lumen that can efficiently kill and digest engulfed microbes, cells, and debris. The fusion of phagosomes with lysosomes is a principal driver of phagosomal maturation and is targeted by several adapted intracellular pathogens. Impairment of this process has significant consequences for microbial infection, tissue inflammation, the onset of adaptive immunity, and disease. Given the importance of phagosome-lysosome fusion to phagocyte function and the many virulence factors that target it, it is unsurprising that multiple molecular pathways have evolved to mediate this essential process. While the full range of these pathways has yet to be fully characterized, several pathways involving proteins such as members of the Rab GTPases, tethering factors and SNAREs have been identified. Here, we summarize the current state of knowledge to clarify the ambiguities in the field and construct a more comprehensive phagolysosome formation model. Lastly, we discuss how other cellular pathways help support phagolysosome biogenesis and, consequently, phagocyte function.

Keywords: phagosome-lysosome fusion, phagosome, phagocyte, lysosome, membrane fusion, microbial clearance, homeostasis, phagosome maturation

OPEN ACCESS

Edited by:
Gregory D. Fairn,
St. Michael's Hospital, Canada

Reviewed by:
Johannes Westman,
Hospital for Sick Children, Canada
Albert Descoteaux,
Université du Québec, Canada

***Correspondence:**
Robin M. Yates
rmyates@ucalgary.ca

Specialty section:
This article was submitted to Molecular Innate Immunity, a section of the journal Frontiers in Immunology

Received: *30 November 2020*
Accepted: *18 January 2021*
Published: *25 February 2021*

Citation:
Nguyen JA and Yates RM (2021) Better Together: Current Insights Into Phagosome-Lysosome Fusion. Front. Immunol. 12:636078. doi: 10.3389/fimmu.2021.636078

INTRODUCTION

Professional phagocytes, such as macrophages, dendritic cells (DCs), and neutrophils, are critical to the innate immune response and the maintenance of homeostasis through their ability to ingest and degrade microbes, debris, and dying cells (1). The versatility of professional phagocytes stems from the expression of phagocytic receptors that can mediate the uptake of a vast array of cargoes *via* phagocytosis. Following uptake, the engulfed material is contained within the specialized vacuole called the phagosome, which initially has the lumenal characteristics of the extracellular space (2). The phagosome undergoes progressive maturation through multiple transient fusion-fission events with vesicles of the endolyososmal system leading to an increasingly acidic and hydrolytic environment within the phagosomal lumen (3, 4). The fusion of the phagosome with lysosomes forms the mature phagolysosome (PL) which has full degradative and microbicidal capacity. Heterotypic fusion between the phagosome and lysosome is imperative for phagocytes to carry out their functions in immunity and homeostasis and is a tightly regulated process. The importance of membrane fusion in

phagocyte function is further highlighted by the myriad of mechanisms various pathogens have developed which impede fusion machinery in order to prevent PL formation, and the microbicidal environment that is established. Indeed, gram-negative bacteria *Mycobacterium tuberculosis* and *Coxiella burnetii*, parasites of the *Leishmania* genus and the fungi *Aspergillus fumigatus* can inhibit PL fusion to avoid death in phagosomes, among many others (5–9).

PL fusion involves the stepwise recruitment and coordinated action of a number of proteins. To date, 30 soluble N-ethylmaleimide-sensitive fusion factor attachment protein (SNAP)-receptors (SNAREs), 20 Rab GTPases, six multi-subunit tethering complexes, and four tethering proteins of the Sec1/Munc18 (SM) family have been identified on phagosomes (10, 11). The extensive number of fusion proteins and promiscuity among interacting components creates mechanistic redundancy of this crucial function of phagocytes. Given the overwhelming number of fusion proteins and the even larger pool of potential binding partners, it is unsurprising that the identity and roles of the fusion machinery, their regulatory signals, and their spatiotemporal organizations in PL fusion have yet to be fully elucidated. These gaps in the literature continue to be active areas of investigation, and here we highlight the progress made on this topic in the context of phagocyte biology. This review aims to summarize current and recent developments in understanding the fusion machinery modulating PL fusion and the consequences to phagocyte function when this machinery is impaired. Finally, we discuss how phagocytes can employ the related engulfment process of autophagy, to support the phagocytic pathway during homeostasis and defense against pathogens.

Abbreviations: Arl, ADP-ribosylation factor-like protein; Arp2/3, actin-related protein 2/3; Atg, autophagy-related; CDC42, cell division control protein 42 homolog; DC, dendritic cell; ESAT6, early secretory antigenic target 6; Gabarap, γ-aminobutyric acid receptor-associated protein; GAP, GTPase-activating protein; GDI, guanine dissociation inhibitor; GEF, guanine exchange factor; HOPS, homotypic fusion and vacuole sorting; IFN-γ, interferon-γ; IKK2, inhibitor kappa B kinase 2; IL, interleukin; IRG, immunity-related GTPase; LAP, LC3-associated phagocytosis; LC3, microtubule-associated protein A1/B1-light chain 3; MAPK, p38α-mitogen-activated protein kinase; MHCII, major histocompatibility complex class II; MT, microtubule; N-WASP, Wiskott-Aldrich syndrome protein; NADPH, nicotinamide adenine dinucleotide phosphate; Ndk, nucleoside diphosphate kinase; Nox2, NADPH oxidase 2 complex; NRBF2, nuclear receptor binding factor 2; NSF, N-ethylmaleimide-sensitive factor; ORP1L, oxysterol-binding protein-related protein 1L; PI, phosphoinositide; PI3K, phosphoinositide 3-kinase; PI3KIA, class IA PI3K; PI3KIII, class III phosphoinositide 3-kinase; PI4KIIα, class II phosphatidylinositol 4-kinase α; PI4P, phospoinositide-4-phosphate; PL, phagolysosome; Plekhm1, pleckstrin homology domain-containing family M member 1; PtpA, protein phosphatase 2A; RILP, Rab7-interacting lysosomal protein; ROS, reactive oxygen species; SapM, secreted acid phosphatase M; SM, Sec1/Munc18; SNAP, soluble N-ethylmaleimide-sensitive fusion factor attachment protein; Snap23, synaptosomal-associated protein 23; Snapin, SNAP-associated protein; SNARE, soluble NSF attachment protein receptor; Snx10, sorting nexin 10; Stx, syntaxin; TIM4, T cell immunoglobin and mucin domain containing 4; TLR, toll-like receptor; V-ATPase, vacuolar-type ATPase; Vamp, vesicle associated membrane protein; Vps, vacuolar protein sorting; Vti1b, vesicle transport though interaction with T-SNAREs 1b.

PHAGOSOME-LYSOSOME MEMBRANE FUSION: AN OVERVIEW

Once the phagosome is formed and has undergone transient fusion-fission events with early and late endosomes, phagosomes migrate to the lysosome-rich perinuclear region of the phagocytic cell (12). Similar to many other types of cells, phagocytes employ a coordinated transport system consisting of the microtubule (MT) networks, the associated MT motors, and their effector/adaptor proteins to carry phagosomal vesicles to the perinuclear region (13, 14). Long-distance transport is initiated by the small Rab GTPases Rab5 and Rab7 which are recruited to early and late phagosomes, respectively. Rab5 and Rab7, in turn, coordinate the recruitment of necessary motor proteins required for the dynein-driven transport of phagosomes to the perinuclear region (13, 15). Once phagosomes and lysosomes are in close apposition, membrane fusion occurs through the concerted action of fusion proteins.

Membrane fusion is the process by which two separate lipid membranes combine to form one continuous bilayer (16). Within the endomembrane system, fusion requires the coordinated action between members of the Rab GTPase superfamily and their effectors, tethering factors, N-ethylmaleimide-sensitive factor (NSF), and SNAREs (17). Generally, these proteins are consecutively recruited during the following steps of membrane fusion: i) tethering; ii) SNARE assembly; iii) SNARE zippering and membrane fusion; and iv) SNARE disassembly and recycling (**Figure 1**). First, Rab GTPases are recruited to the membrane of vesicles pending fusion, to mark the position for fusion. Subsequently, Rabs, through the recruitment of their effectors bind to tethering factors from the cytosol (18, 19). Through this action, Rabs establish the site at which proteins assemble into membrane microdomains at the fusion site. Rab effector-mediated tethering brings adjacent membranes into proximity. Once tethered, SNARE proteins congregate at the fusion site and supply the energy necessary to overcome the electrostatic repulsion between two lipid membranes (20–22). Numerous SNAREs reside on endomembranes, yet only a finite number can form a stable SNARE complex in *trans* that consists of four SNARE domains (23). SNARE assembly is not a spontaneous process but requires SM proteins to form SNARE intermediates that await a missing cognate SNARE (24, 25). Once a *trans*-SNARE complex is formed, a conformational change brings the two membranes together, forming a *cis*-SNARE complex in a process called "zippering" (20–22, 26). The post-fusion *cis*-SNARE complex, where all SNARE proteins are located on the same membrane, is then disassembled by NSF along with its cofactor α-SNAP (27–29). The disassembly process is powered by NSF-mediated ATP hydrolysis which provides the energy for the dissociated SNARE proteins.

Early studies on pathogen clearance and efferocytosis in mice and *Caenorhabditis elegans* identified specific Rab GTPases and their corresponding tethering complexes in PL biogenesis and phagocyte function (30–33). Despite their lack in professional phagocytes, *C. elegans* have phagocytic-like cells that have been used in many early and current studies to study phagosome maturation after efferocytosis due to their genetic conservation

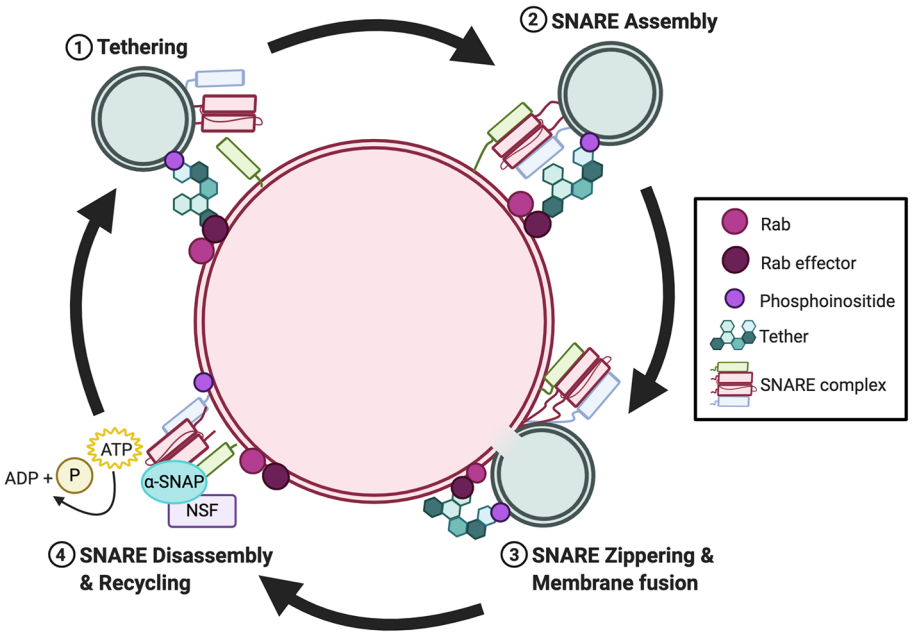

FIGURE 1 | Overview of the cyclical nature of membrane fusion. Rab GTPases and their effectors recruit tethers to the membrane fusion site during the tethering step. Subsequently, SNAREs are recruited to opposing membranes and assemble in *trans via* the catalyzing activity of a SM protein. Once assembled, SNARE zippering drives membrane fusion. Post-fusion, NSF and α-SNAP bind to the *cis*-SNARE and ATP-driven complex disassembly recycles the individual SNAREs intothe cytosol for recycling.

(34–36). Thus, *C. elegans* has been a powerful model to identify genes and mechanisms involved in PL fusion.

Identifying SNAREs involved in PL fusion has been more challenging due to their promiscuous nature and involvement in several cellular pathways crucial for cellular upkeep. Although, putative SNARE complexes have recently been identified using cell-free systems where subsequent investigations are beginning to unravel the functions of these proteins in PL fusion (37–40). Other insights into the proteins modulating PL fusion have been inferred from studies of the closely related process of endo-lysosome fusion in other cells. However, differences in the cargo and regulation between phagocytosis and endocytosis, maintain PL fusion as a distinct process compared to endosome-lysosome fusion (41). Given the large degree of heterogeneity in models and approaches to study this process, this review aims to consolidate the literature focusing on PL fusion proteins in phagocyte-specific studies, and where information is lacking in this context, identify potential candidate proteins and complexes, in order to generate a clearer picture of this fundamentally important aspect of phagocyte function. The key components of the PL fusion machinery are summarized in **Supplementary Table 1**.

MARKING THE MEMBRANES: SMALL RAB GTPASES

The Rab GTPases are peripheral membrane proteins that serve as molecular identifiers on membranes, and to regulate multiple steps during membrane fusion. Rab GTPases function as molecular switches that toggle between an inactive GDP-bound and an active GTP-bound state. Rabs are maintained in their inactive soluble GDP-bound state by a guanine dissociation inhibitor (GDI) (42, 43). At vesicular membranes, guanine exchange factors (GEFs) possess the dual capacity to recruit Rabs from the cytosol and catalyze the displacement of GDP with GTP, which both activates Rabs and displaces the GDI, thus allowing for Rabs to be inserted into the membrane (44, 45). Once activated, Rabs are able to bind to effector proteins on fusion targets in order to tether fusing vesicles, modulate the recruitment of fusion components, and mediate the process of PL biogenesis. Post-fusion, GTPase-activating proteins (GAPs) hydrolyze GTP to inactivate Rabs where they are solubilized by a GDI, returning them to the pool of inactive cytosolic Rabs (46). The numerous influences on GTPase regulation make Rabs a strong focal point for modulation of PL biogenesis.

It has long been established that small GTPase Rab7 is essential for the fusion between late-stage phagosomes and lysosomes, and consequently, for the function of phagocytes in both pathogen and apoptotic cell clearance (33, 47, 48). Several pathogens have been described to inhibit Rab7 recruitment in order to replicate and survive within phagosomes, and has been comprehensively reviewed (49). Early studies reported the inhibition of Rab7 recruitment to the phagosomes by *M. tuberculosis* and *M. bovis* J774 macrophages, preventing PL fusion (33). A more recent example describes the necessity of Rab7 in the clearance of *Pseudomonas aeruginosa* infection in J774A.1-derived macrophages (50). This study reported that

sialylated *P. aeruginosa* remained viable in phagosomes by preventing the recruitment of Rab7. In addition to the clearance of microbes, Rab7 is essential to the degradation of apoptotic cells following phagocytosis. In a *C. elegans* model of apoptotic cell removal, the siRNA-mediated knockdown of Rab7 contributed to the accumulation of apoptotic bodies in phagosomes (34). Similarly, in an *in vivo* model of murine ulcerative colitis, inflammation and disease severity was exacerbated when Rab7 activation and recruitment was impaired in macrophages, reportedly due to an accumulation of apoptotic epithelial cells in the colon (48).

The mechanism by which Rab7 is recruited to phagosomes in professional phagocytes is not fully elucidated. However, studies in *C. elegans* demonstrated that Rab7 recruitment to late endosomes/lysosomes was facilitated by the cytosolic SAND1-CCZ1 complex (51–53). The mammalian orthologues of SAND1 and CCZ1, namely, Mon1a/b and Ccz1 display GEF activity and were found to form a complex which displaces the GDI associated with the GDP-bound form of Rab7, allowing GTP switching and integration of Rab7 into phagosomal membranes (**Figure 2Ai**) in *C. elegans* which is believed to be evolutionary conserved in mammals (52).

Phosphatidylinositol-3-phosphates (PI3P) on early phagosomes have been proposed to both recruit Mon1-Ccz1 to early-to-late transitional phagosomes and activate the GEF activity of the complex (**Figure 2Ai**) (48, 53). Recently, nuclear receptor binding factor 2 (NRBF2), a component of the class III phosphoinositide 3-kinase (PI3KIII)/vacuolar sorting protein (Vps) 34 complex that generates PI3P on phagosomes, has been implicated to regulate the function of the Mon1-Ccz1 complex during apoptotic cell clearance in macrophages (48). NRBF2 is a binding partner of the catalytic subunit of the PI3KIII/Vps34 complex and can facilitate the interaction between PI3KIII/Vps34 and Mon1-Ccz1 (**Figure 2Ai**). Through this interaction, NRBF2 may bring the PI3KIII/Vps34 complex to phagosomes or support the activation of PI3KIII/Vps34, thereby generating PI3P to activate the GEF activity of the Mon1-Ccz1 complex. Further evidence that NRBF2 modulates the activity of the Mon1-Ccz1complex is provided by an observed loss of GTP-bound Rab7 around phagosomes as well as delayed Rab7 recruitment in NRBF2-knockout macrophages (48). Lou and colleagues (54) have proposed that another factor, sorting nexin 10 (Snx10), can promote the recruitment of Mon1-Ccz1 to early endosomes and phagosomes to mediate Rab7 recruitment (**Figure 2Ai**). Snx10 is upregulated in response to TLR signaling and phagocytosis of several different microbes, suggesting that Snx10 has an antimicrobial role (54). Indeed, depletion of Snx10 reduced Rab7 recruitment on bacteria-containing phagosomes. Taken together with the studies in *C. elegans*, Mon1-Ccz1 is likely a major Rab7 GEF on phagosomes in mammalian cells.

While there is ample evidence for the Mon1-Ccz1 complex as a Rab7 GEF on endosomes and phagosomes, it is potentially not the only one. Early insights from studies in yeast and *C. elegans* have implicated that the homotypic fusion and vacuole sorting (HOPS) complex can also act as a Rab7 GEF (**Figure 2Aii**) (52, 55). It was demonstrated by Barry and colleagues (56) that HOPS could function the same way in mammalian cells for Rab7 found

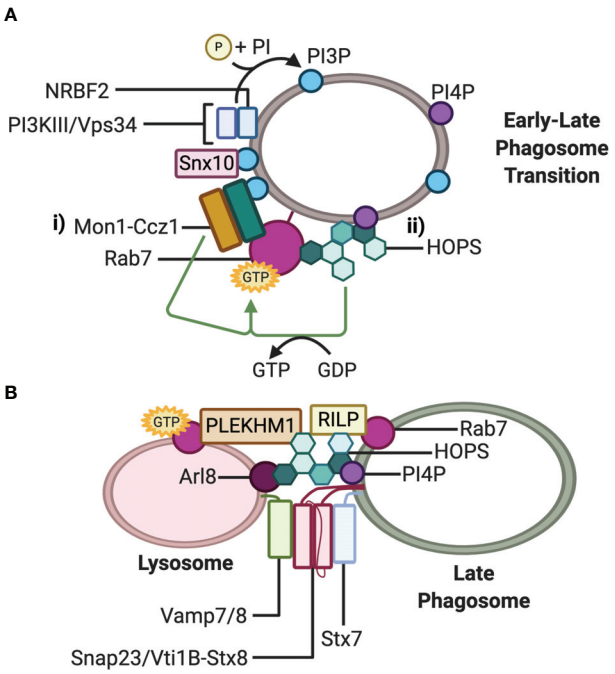

FIGURE 2 | Fusion machinery involved in phagosome maturation. **(A)** Working models for Rab7 recruitment and activation at the phagosome membrane during maturation: i) The Mon1-Ccz1 complex is recruited directly by PI3P and indirectly by Snx10 and NRBF2-PI3KIII/Vps34. PI3P activates the GEF activity of Mon1-Ccz1; ii) The GEF activity of PI4P-recruited HOPS activates Rab7. **(B)** Working model of the *trans*-SNARE complex mediating fusion between the late phagosome and lysosome. The small GTPase Rab7 recruits effectors RILP and Plekhm1, and concurrently with Arl8, additionally recruits the HOPS tethering complex. HOPS docks the late phagosome to the lysosome and stabilizes the *trans*-SNARE Stx7-Snap23-Vamp7/8 or Stx7-Vti1b-Stx8-Vamp7/8 complex at the point of membrane fusion. Note that either Plekhm1, Arl8, PI4P, or RILP on either lysosomes or phagosomes bind to HOPS Vps41 at one time, while RILP can also bind HOPS Vps39.

on phagosomes in macrophages containing *C. burnetii*. Macrophages phagocytosing an avirulent strain of *C. burnetti* induce p38α-mitogen-activated protein kinase (MAPK)-dependent phosphorylation of the HOPS Vps41 subunit which was demonstrated to be necessary for Rab7 recruitment to endosomal and phagosomal membranes (56). In contrast, the lipopolysaccharide produced by the virulent strain of *C. burnetti* prevented p38α- MAPK activation and phosphorylation of Vps41, allowing bacterial persistence in Rab7-deficient phagosomes. Why Mon1-Ccz1 was unable to act as the Rab7 GEF instead of HOPs in this model is unknown; however, it is possible that Mon1-Ccz1 and the HOPS complex act independently depending on the phagosomal cargo.

Rab7 is vital for PL fusion and therefore phagocytic function, but it is not the only GTPase involved in PL fusion: Rab2 and Rab14 have been shown to possibly function redundantly to each other or in parallel to recruit lysosomes to phagosomes during apoptotic cell degradation in *C. elegans* (31, 32). Rab2 and Rab14 are transiently recruited to phagosomes prior to Rab7, and it is postulated that like

Rab7, Rab2 and Rab14 may recruit tethering factors to initiate interaction between phagosomes and lysosomes (31). Interestingly, Rab2 is a direct binding partner of HOPS during autophagosome fusion with lysosomes in *Drosophila melanogaster* cells (57, 58), and thus, the HOPS complex may serve as the effector for both Rab2 and Rab14 to coordinate fusion of lysosomes to phagosomes. Additionally, proteomic studies in an oyster cell model of phagocytosis identified Rab2 and Rab14 in the phagosomal proteome (59). Although Rab2 has not been studied in a mammalian model, the role of Rab14 in PL fusion was partially elucidated in Raw264.7 and J774 murine macrophages infected with the fungal pathogen *Candida albicans*. Knockdown of Rab14 disrupted fusion of lysosomes to phagosomes which both delayed the acquisition and activation of hydrolytic proteases in PLs. This defect in lysosome fusion and protease activation resulted in increased susceptibility of macrophages to *C. albicans* (60).

Taken together, Rab2 and Rab14 may function redundantly in an early tethering step prior to Rab7 recruitment and the docking/fusion of lysosomes with phagosomes. The presence of Rab7 on the phagosome membrane sets the stage for PL fusion; however, the mere presence of Rab7 on phagosomes is not sufficient to enact PL fusion (61). Rather, it requires further interaction with effector proteins to tether the vesicles together to facilitate fusion.

SECURING THE PHAGOSOMES TO LYSOSOMES: TETHERING EFFECTORS

Tethering effectors, in the form of proteins and protein complexes, are recruited from the cytoplasm to specific membranes designated by small GTPases such as Rab or ADP-ribosylation factor-like protein (Arl) proteins (17). During the tethering step prior to fusion, tethering factors bind to Rab GTPases on the adjacent vesicles to provide an initial physical interaction (62). In addition to their function as linkages between two vicinal membranes, tethers can recruit SNARES as well as the proteins that catalyze the formation of the SNARE complex. Moreover, tethers can strengthen the association amongst fusion-relevant factors at the fusion site. Altogether, tethers ensure fusion fidelity and increase the efficiency of SNARE formation at the docking site.

Rab GTPases modulate fusion of vesicular membranes through their effector proteins. One of the most well-characterized Rab7 effectors is the Rab7-interacting lysosomal protein (RILP) which is found on endosomes, lysosomes, and phagosomes (47, 63). The role of RILP in PL formation lies in its interaction with the dynein-dynactin complex during centripetal migration of phagosomes (47). Further, RILP recruits other Rab effectors involved in vesicle tethering and Rab7 activation. Thus, RILP recruitment is an attractive target for intracellular pathogens to exploit. Indeed, live *Mycobacteria* were found to secrete a Rab7 deactivating factor that could disrupt the interaction between RILP and membrane-bound Rab7 in macrophages (30). This was later determined to be nucleoside diphosphate kinase (Ndk), which enacts GAP activity to lock Rab7 in a GDP-bound state, and permitted survival of *Mycobacteria* within the phagosome (64). While this effect is likely not specific to RILP-Rab7 interactions, it does highlight the importance of maintaining Rab7 in a GTP-bound state to facilitate effector protein function.

Pleckstrin homology domain-containing family M member 1 (Plekhm1) is another Rab7 adaptor that is implicated in modulating PL formation. After the uptake of *Salmonella* by macrophages, Plekhm1 has been shown to bind the multi-subunit HOPS complex which facilitates the delivery of late endosome and lysosomes to *Salmonella*-containing vacuoles, and this is essential to maintain the integrity of these phagosomes for bacterial persistence (65, 66).

The multi-subunit complex HOPS is a Rab7 effector that can function as an upstream Rab7 GEF and a downstream tethering effector (56, 67, 68). Mammalian HOPS is a well-characterized tethering complex that facilitates vesicle-lysosome fusion of multiple degradative pathways, including PL fusion. The complex consists of seven proteins: Vps11, Vps16, Vps18, Vps33A, Vps39, and Vps41 (56, 69, 70). Two subunits appear to be particularly crucial for tethering. Vps39 and Vps41, which are respectively recruited to the HOPs complex by Vps11 and Vps18, can each interact with RILP and this may bridge two RILP molecules on opposing vesicles (**Figure 2B**) (71). Vps41 can also bind directly to Plekhm1 on either lysosomes or phagosomes (66), lysosomal Arl8 (70, 72) and phospoinositide-4-phosphates (PI4P) on phagosomes (73). The capacity for HOPS to bind to multiple partners likely increases the efficiency of HOPS acquisition to the fusion site, improves tethering between vesicles and maintains fusion fidelity (73).

In addition to its function in vesicle tethering, the HOPS complex can promote *trans*-SNARE docking at the PL fusion site and guide the formation of SNARE complexes to promote SNARE-mediated PL fusion (73). The HOPS Vps33 subunit is a member of the SM-family of proteins (74, 75) that can interact directly with SNAREs (76) and is proposed to catalyze SNARE complex assembly. Insights from yeast models suggest a dual-binding capacity of Vps33, where it binds two SNAREs, each from a different membrane, and serve as a base for generating partially-formed SNARE intermediates (24, 25). Bach et al. (77) provided evidence that mammalian Vps33 has a similar function during PL fusion through host-pathogen studies in *Mycobacterium*-infected THP-1-derived macrophages. Protein phosphatase 2A (PtpA), produced by *M. tuberculosis*, can dephosphorylate and inactivate Vps33b, one of the two Vps33 proteins in higher eukaryotes, as evidenced by a reduction in PL fusion after the uptake of PtpA-coated experimental particles by macrophages (77). PL biogenesis was similarly abrogated in Vps33b-silenced macrophages with or without PtpA-coated experimental particles and re-introduction of active Vps33b to the Vps33b-silenced macrophages restored PL fusion. The observation that functional Vps33b is important in PL biogenesis and bacterial clearance is even further supported by the observation that the loss of Vps33b or its binding partner

Vps16b in the *Drosophila* Oregon-R phagocytic cell line leads to defects in PL formation (78). Taken together, all seven HOPs subunits are necessary for phagosome maturation.

The HOPS complex is the most extensively characterized Rab7 tethering effector facilitating PL fusion. Since other Rabs have been implicated in PL biogenesis, such as, Rab2 and Rab14, non-Rab7-facilitated HOPS recruitment is possible, or other tethering factors are involved in PL biogenesis, which warrants further investigation. Additional Rab7 adaptors including oxysterol-binding protein-related protein 1L (ORP1L) (79), Vps34/p150 (80) and Rubicon (81) have been characterized in endosome maturation but have yet to be explored in the context of phagosome maturation. Overall, the multifunctional HOPS complex provides a base at the PL fusion site that allows for local SNARE assembly, stabilizing the intermediate complex as the SM protein activity of HOPS chaperones SNARE assembly.

FUSING THE PHAGOSOME AND LYSOSOME MEMBRANES: SNARES

SNARE proteins compose the core machinery required to fuse phagosomes with lysosomes efficiently. Based on the contributing amino acid to the hydrophobic core in the assembled SNARE complex, SNAREs can be structurally categorized into R-SNAREs or Q-SNAREs (of which can be subclassified into Q_a-, Q_b-, and Q_c-SNAREs) (82). During membrane fusion, an R-SNARE on one membrane forms a transient *trans*-SNARE complex with three Q-SNARES located on the partner membrane (82). The resulting complex consists of an R, Q_a-, Q_b-, and Q_c-SNARE that aligns in a parallel four-helix bundle and fuses the juxtaposed membranes *via* a zipper model (22). Post-fusion, all of the SNAREs are located on the same membrane in a fully assembled *cis*-SNARE complex. The post-fusion *cis*-SNARE complex is then recognized and disassembled by NSF along with its cofactor α-SNAP (27).

Early studies performed in J774 macrophages and cell-free systems demonstrated that PL fusion is dependent on NSF, providing first experimental evidence that this process employs SNARE proteins (83, 84). According to several quantitative proteomic studies, the presence and abundance of different SNAREs found at the phagosome changes depending on the cell-type, stage of maturation and the phagocytosed cargo (11, 85–88). As many as 30 of the 38 known human SNARE proteins have been identified on phagosomes (10), but which of these members function in coordinating late-stage phagosome-lysosome fusion is not well described. Rather, there is a greater understanding of their involvement in phagocytosis, phagosomal trafficking and early phagosome maturation, than during the final stages of maturation. The SNAREs that have thus far been implicated in PL fusion and found to be enriched in lysosomes and phagosomes, include, Syntaxin (Stx) 7, Stx8, vesicle transport through interaction with T-SNAREs 1b (Vti1b), vesicle associated membrane protein 7 (Vamp7) and Vamp8 (37, 39, 89, 90). Initial evidence of the involvement of these SNAREs in PL fusion was provided in a cell-free study wherein SNARE function was inhibited by the addition of the soluble cytosolic domain of various SNAREs (37). These truncated SNARE fragments outcompete their endogenous counterparts for binding with their membrane-bound cognate partners and form a stable SNARE complex that cannot mediate fusion because they lack transmembrane anchors. In the presence of the truncated form of the Q_{abc}-SNAREs Stx7, Vti1b and Stx8, and the R-SNAREs Vamp7 and Vamp8, PL fusion was reduced, as evidenced by decreased lumenal mixing between lysosomes and phagosomes (37). Stx7-Vti1b-Stx8 were found to form a stable quaternary complex with the lysosomal R-SNARE Vamp7 or Vamp8, suggesting these may constitute a possible SNARE complex in PL fusion (37). In summary, Stx7-Vti1b-Stx8 may form a ternary Q_{abc}-SNARE intermediate on the late phagosome that can then mediate PL fusion together with Vamp7 or Vamp8 on the lysosome, although evidence is lacking to support that these particular SNARE complexes are occurring within living cells to facilitate the fusion of phagosomes with lysosomes.

Interestingly, several investigations into the molecular mechanism underlying $gp91^{phox}$ recruitment to phagosomes have provided insight into PL fusion, and identified synaptosomal-associated protein 23 (Snap23) as a potential Q_{bc}-SNARE acting in this process (38, 39, 91). $gp91^{phox}$ is the integral membrane component of nicotinamide adenine dinucleotide phosphate (NADPH) oxidase 2 complex (Nox2) which is responsible for generating the reactive oxygen species (ROS) that facilitate pathogen killing and the modulation of phagosomal proteolysis for antigen processing (92–94). The phagosome accumulates $gp91^{phox}$ predominantly through its fusion with lysosomes (95–97). siRNA-mediated knockdown of Snap23, Stx7, and Vamp8 decreased phagosomal $gp91^{phox}$ recruitment and subsequent ROS production in J774 macrophages, presumably from inhibited PL fusion (39). In corroboration with this observation, silencing Snap23 in primary neutrophils (91) and DCs (38) also inhibited $gp91^{phox}$ trafficking to phagosomes for subsequent ROS production. Whether Snap23 can act as the Q_{bc}-SNARE instead of Vti1b-Stx8 in the Stx7-Vti1b-Stx8-Vamp7/8 model described above was supported by immunofluorescence and cellular fractionation experiments which found that Snap23 colocalizes with Stx7 and Vamp8 and can interact with Stx7 in J774 macrophages (38, 39). Moreover, Snap23, Stx7, and Vamp8 can form a stable SNARE complex *in vitro* (39) and knockdown of any of these SNAREs decreases phagosomal acquisition of $gp91^{phox}$ (38, 98). In another study, Vamp8 contributed to the regulation of phagosomal oxidative activity *via* PL fusion in *Leishmania*-infected primary macrophages (99). It is worth noting that Snap23 can also pair with Vamp7 (39), thus Vamp7 and Vamp8 may have redundant roles as a cognate R-SNARE on lysosomes.

Further insight into the function of Snap23 in PL formation was generated from a recent study by Sakurai et al. (40) that reported Snap23 could regulate PL formation based on its phosphorylation status. It was found that the phosphorylation of Snap23 at Ser95 by the protein kinase inhibitor kappa B kinase 2 (IKK2), in response to interferon-γ (IFN-γ) treatment, decreased fusion between

phagosomes and late-endosomes/lysosomes in J774 macrophages. Thus, Snap23 is implicated to have an important physiologic role in activated macrophages by delaying phagosome fusion with acidic lysosomes, thereby contributing to the development of a phagosomal environment that favors antigen processing in pro-inflammatory environments (40, 100).

Current evidence suggests that Vamp7/8 on lysosomes, paired with Stx7 and Snap23/Vti1B-Stx8 on late phagosomes, act as the R-, Q_a- and Q_{bc}-SNAREs respectively, to facilitate fusion of these vesicles (**Figure 2B**). However, the promiscuous nature of SNARE proteins likely allows multiple SNARE complex permutations to facilitate the fusion of phagosomes and lysosomes and is reflected in the studies examined (10, 37, 39, 40). Similarly, multiple levels of posttranslational regulation of SNARE proteins beyond Snap23 phosphorylation likely exist to prevent erroneous fusion of these vesicles yet remain to be characterized (40).

OTHER FACTORS INVOLVED IN PL FUSION

It is clear from the number of fusion proteins discussed thus far that PL fusion is a complex process. However, Rabs, tethers and SNAREs are not the only factors involved in this process. The lipid composition of phagosomes, the actin cytoskeleton, the vacuolar-type ATPase (V-ATPase) and calcium signaling play important roles during phagosome maturation. Here, we will only discuss the phosphoinositide lipids and the controversial role of actin and the V-ATPase in PL biogenesis, as calcium signaling has been extensively reviewed elsewhere (101).

Phosphoinositide Lipids and Their Kinases

Phosphoinositides (PIs) play a critical role in PL formation. These are a family of mono-, bi-, or tri- phosphorylated derivatives of the glycerophospholipid phosphatidylinositol. Phosphorylation of the third, fourth or fifth position of the PI inositol headgroup by their specific lipid kinases generates different PI variants that regulate the actin cytoskeleton, signal transduction and membrane fusion/fission through interactions with their respective effector proteins (102, 103). In the context of PL biogenesis, PI3P and PI4P together with their lipid kinases are the most well-characterized in the fusion of phagosomes and lysosomes (73).

P13P is enriched on early phagosomes and is necessary to bind Rab5 for fusion with early endosomes (5, 104). As the phagosome progresses to the early-to-late-stage transition, PI3P is lost while both PI4P and PI3,5P2 are acquired in tandem with Rab7 (105, 106). PI4P is associated with the recruitment of the HOPS complex (73), whereas the role of PI3,5P2 remains less understood and there is conflicting reports on whether this lipid is essential for PL fusion and the full activation of the phagosomal V-ATPase (107, 108). Reduced PI3,5P2 synthesis in Raw264.7 macrophages abrogated both PL fusion and degradative capacity but had little effect on phagosome acidification, and at least on lysosomes, the V-ATPase was still active (107, 109). However, in lower eukaryotic models and mammalian epithelial cells, PI3,5P2 was required for V-ATPase activity, efficient phagosome fusion with lysosomes and acquisition of a microbicidal phagosomal lumen (108, 110–112). Thus, these discrepancies are likely due to physiological differences between macrophages and other cell models/types. Interestingly, PI3,5P2 has also been implicated in regulating lysosome/phagosome calcium channels in Raw264.7 macrophages (113).

Deciphering the roles of PIs during each step of PL formation within phagocytes is challenging as PIs function in the early steps of phagocytosis, and interference of PIs also affects the maturation of the phagosome upstream of PL fusion (114). Thus, reconstitution of PL fusion in cell-free *in vitro* assays in this scenario provides an advantage over *in vitro* systems since each fusion "subreaction" in PL formation can be manipulated and studied in isolation, without interfering with the early maturation of the phagosome (73, 114). In particular, work by Jeschke and colleagues have shed additional light on the role of PI3P, PI4P and their lipid kinases. As found by Jeschke et al. (114), phagosomes containing opsonized latex beads isolated from J774 macrophages contained PI3P, PI4P, and the class II phosphatidylinositol 4-kinase α (PI4KIIα), one of the four lipid kinases that catalyze the formation of PIs to PI4P (114). Sequestration of PI3P by the mouse hepatocyte growth factor-regulated tyrosine kinase substrate 2xFYVE domain or PI4P by the P4C fragment of *Legionella pneumophila* protein SidC blocked PL formation (115, 116). Further, chemical inhibition of either PI4KIIα or PI3KIII/Vps34 respectively reduced the levels of PI4P or PI3P generated on phagosomes, also impeding PL formation. This corroborates earlier studies, wherein inhibition of PI3KIII/Vps34 in J774 and Raw264.7 macrophages precluded the acquisition of the late endosome/lysosome makers, LAMP1 and lysobisphosphatidic acid, by phagosomes due to a defect in PL fusion (5, 104). Hence, PI3P and PI4P are required for PL fusion in a cell-free system, and this process can be regulated by PI lipid kinases that modulate the levels of PI3P and PI4P generated on phagosomes (114).

Further investigation by Jeschke and Haas (73) into the role of PI3P and PI4P in the steps leading to PL fusion observed that these PIs were involved during the tethering step of membrane fusion. Both PI3P and PI4P were present on phagosomes bound to lysosomes and sequestration of PI4P with P4C inhibited phagosome-to-lysosome binding and hemi-fusion of vesicles, while sequestration of PI3P by the 2xFYVE domain inhibited PL fusion after vesicles had docked (73). Since PIs exert their functions by anchoring PI effector proteins to membranes, it was postulated that PI3P and PI4P were recruiting PL-fusion-relevant proteins to phagosomes and lysosomes (73, 117). Indeed, a lack of available PI3P due to sequestration decreased the presence of the HOPS component Vps41 on phagosomes and lysosomes, and similarly, PI4P sequestration decreased both Vps41 and Arl8 levels. Further, when P4C and 2xFYVE were added to fusion sub-reactions containing isolated phagosomes and lysosomes but in the absence of cytosol, (which contains free PIs), membrane-bound Vps41 and Arl8 were absent, thereby

supporting the observation that PI3P and PI4P are required to anchor tethering effectors. In addition to tethering, PI3P and PI4P have an impact on the fusion step of PL biogenesis, and thus may directly or indirectly recruit SNARE proteins (73). Interestingly, Vamp8 can bind directly to PI3P on *Salmonella*-containing vacuoles (118). It is known that Vamp8 binds PI3P to support phagocytosis of *Salmonella* (118), but whether the Vamp8-PI3P interaction is required or able to facilitate SNARE complex formation or PL membrane fusion requires further investigation. PI4P is also a substrate for the formation of PI4,5P2 on late endosomes/phagosomes and lysosomes (119). PI4,5P2 is required for the nucleation of actin around phagosomes, wherein this process has been postulated to promote PL fusion by interacting with SNARE proteins and will be discussed below (119, 120).

The class IA PI3K (PI3KIA), a kinase commonly associated with phagocytosis of large particles (>4 μm) and early endosome-phagosome fusion, has also been implicated in PL fusion (121). Thi and colleagues (121) used THP-1-derived macrophages to report a novel role for the class IA PI3K in PL fusion that depended on its catalytic subunit p110α (121). In p110α knockdown cells, phagocytosis of *M. smegmatis* or experimental particles occurred normally, however, phagosomes displayed impaired procurement of LAMP1 and lysosomal hydrolases due to defective fusion with lysosomes. Interestingly, p110α knockdown did not prevent Rab7 recruitment to phagosomes, nor its subsequent activation, as the recruitment of the Rab7 effectors HOPS and RILP were unaffected. This suggests recruitment of Rab7 and its effectors is insufficient to drive PL fusion alone, and requires the additional action of PI3KIA to mediate the formation of the PL. Moreover, cellular and phagosomal levels of the SNAREs Vamp7 and Vti1b in p110α-silenced macrophages were similar to the control. Hence, in this experimental system, the blockage of PL fusion is not due to a lack of membrane fusion machinery, but an undetermined mechanism. PIK3IA generates PI3,4,5P3 by the phosphorylation of PI4,5P2 (122). PI3,4,5P3 is transiently enriched at the phagocytic cup and is known for its role in actin polymerization upon Fc-γ receptor and complement receptor-mediated phagocytosis (123). With the exception of Fc-γ receptor phagocytosis, PI3,4,5P3 reappears on the maturing phagosome and is implicated in activating a second wave of actin formation important for PL biogenesis (124, 125). Since PI3,4,5P3 levels are decreased upon depletion of p110α (121), it is plausible that this may interfere with PI3,4,5P3-regulated actin polymerization around phagosomes (124).

Overall, host-pathogen studies have unveiled the consequences to bacterial clearance when certain PIs are unavailable for PL fusion while cell-free assays have allowed us better to understand where and when certain PIs are involved in the formation of PLs. From these studies, PI3KIII/Vps34, PI4KIIα and their respective lipid products PI3P and PI4P, as well as PI3KIA, regulate the development of PLs.

The Actin Cytoskeleton

The actin cytoskeleton is a major player in regulating phagocytosis (126, 127) and the fusion/fission of endolysosomes with phagosomes (120, 125, 128–130). Filamentous actin (hereafter referred to as actin) has been observed to transiently polymerize around phagosomes in a process called "actin-flashing". The function of this phenomena is unclear but has been proposed to prevent PL fusion (125). Numerous reports using phagocytes and cell-free systems have demonstrated that actin coats a subset of purified phagosomes and acts as a physical barrier to PL biogenesis (**Figure 3A**) (125, 131–133). Furthermore, when internalized, certain pathogens, including *Legionella*, *Leishmania*, *and Mycobacteria*, induce the assembly of actin on the early phagosome to prevent phagosomal maturation (133–136). However, conflicting reports propose that actin can have a stimulatory role in membrane fusion, thus lending uncertainty to the role of actin in PL fusion (**Figure 3B**) (120, 128). A plausible explanation is that actin has dual roles in membrane fusion whereby it can both inhibit and induce phagosome-lysosome fusion depending on the maturation state of the phagosome (120). Most studies reporting the inhibitory role of actin limited their investigation to early-stage phagosomes. In particular, transient accumulations of actin were observed to surround a subpopulation of purified immature phagosomes which prevented association with endolysosomal vesicles (125, 137). It was also demonstrated that *de novo* actin assembly on nascent phagosomes increases under cell stress conditions when the phagocytic or endocytic pathway is overloaded with digestive cargo (125). These actin "flashes" repeat in waves to physically block phagosome-lysosome fusion.

Not only can actin act as a physical barrier to fusion, it can also compete with dynein-dynactin-based binding to microtubules at the cellular periphery (**Figure 3A**). Phagosomes can bind to actin, in an ATP-dependent manner, through association with the actin motor protein myosin Va (131). Myosin Va interactions occur at defined regions of the phagosomal membrane, which dissociates the interactions with MT-associated proteins. It has been postulated that transient actin assembly on endolysosomal and phagosomal systems slows phagosome-lysosome fusion when these vesicles contain more cargo than they have the capacity to digest (125). Actomyosin association is a possible complimentary mechanism that can either delay phagosome migration to the perinuclear region to allow them extra time to preprocess internalized phagosomal content, and to not outpace the availability of lysosomes for fusion (131, 137).

In contrast, late-stage phagosomes and endolysosomes have been shown to nucleate actin locally around the phagosome-to-lysosome docking sites (128). Interestingly, numerous actin cytoskeleton-associated machinery regulating actin nucleation were localized around latex bead-containing late-phagosomes, such as ezrin, neural Wiskott-Aldrich syndrome protein (N-WASP) and the actin-related protein 2/3 (Arp2/3) complex (**Figure 3C**). Ezrin binds to PI4,5P2 on the phagosomal membrane, although it is unclear whether PI4,5P2 is sufficient to recruit ezrin (119, 138). Ezrin has been proposed to recruit N-WASP to the phagosome membrane, which subsequently activates Arp2/3 to initiate actin nucleation. The idea that actin promotes late-stage phagosome maturation was further supported by the observation that downregulating ezrin

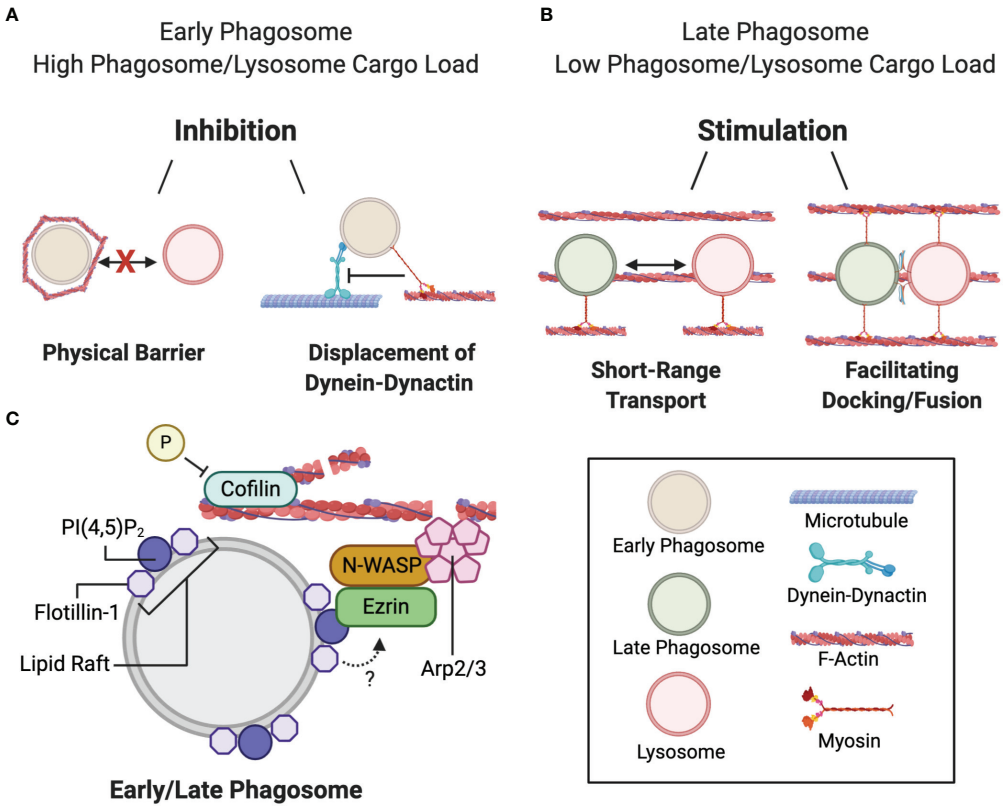

FIGURE 3 | Duality of filamentous actin during phagosome maturation. **(A)** Actin delays phagolysosome biogenesis at the early phagosome maturation stage by: i) transiently assembling around nascent phagosomes when the early phagosome and/or lysosome system is overloaded with cargo thereby blocking phagosome-lysosome contact, or ii) by facilitating myosin-mediated displacement of the dynein-dynactin microtubule motor and preventing minus-end transport. **(B)** Actin stimulates phagolysosome biogenesis by: i) bringing the fusing organelles closer together, or ii) facilitating docking and fusion. **(C)** Actin polymerization at the phagosome is mediated by the ezrin-N-WASP-Arp2/3 complex binding to phagosomal PI(4,5)P_2 at flotillin-1-associated lipid rafts. Cyclic actin polymerization and depolymerization is mediated by the respective phosphorylation and dephosphorylation of cofilin.

hindered PL fusion (120). In later studies, cell division control protein 42 homolog (CDC42) of the Rho-family of GTPases was found to be required for the activation of N-WASP (139, 140). The dynamic phosphorylation and dephosphorylation of actin-binding protein cofilin is also required to mediate cyclic actin polymerization and depolymerization that promotes PL fusion (141). Furthermore, flotillin-1, a membrane protein that associates with lipid rafts on late phagosomes is also implicated in actin nucleation since actin predominantly accumulates and polymerizes at these sites (142, 143). Dermine et al. (142) observed decreased flotillin-1 association with phagosomes containing *Leishmania* in J774 macrophages. *Leishmania* expresses a surface glycolipid lipophosphoglycan that impedes PL fusion. Since lipophosphoglycan preferentially anchors to phagosomal lipid rafts, it was proposed that this process may interfere with lipid raft formation, and subsequent flotillin-1 association and actin assembly (142). However, the molecular interactions between flotillin-1 and the other actin polymerizing machinery at phagosomal lipid microdomains were not addressed and remain largely obscure. How actin functions in tandem with membrane fusion machinery—whether by bringing fusing vesicles together *via* myosin motor proteins, or by facilitating the docking and tethering of lysosomes to the phagosome membrane (**Figure 3B**) (120, 128)—is unclear and warrants further investigation.

Interestingly, the same actin nucleation machinery is recruited to early and late phagosomes to exert dualistic stimulatory and inhibitory effects. *Leishmania donovani* promastigotes promote CDC42 retention at phagosomes thereby prolonging phagosomal actin accumulation to evade the host endomembrane system in Raw264.7 macrophages (135). It was recently found that CDC42 is unable to associate with its GAP and GDI in this context, thereby locking it in a GTP-bound state (144, 145). One of these studies demonstrated that *Shigella flexneri* exploits N-WASP and Arp2/3 recruitment to the nascent bacteria-containing vesicles to impede lysosomal fusion. Molecularly, the acyltransferase activity of the type 3 secretion system effector IcsB on CDC42 disrupts its association with its GDI (144), locking CDC42 in a GTP-bound state which retains CDC42 at phagosomes (145). Through this, IcsB clusters

N-WASP and Arp2/3 around vesicles to nucleate thick actin coats, which both block the recruitment of fusion machinery and shield the bacterium from the endolysosomes. It is important to note that the studies by Liu et al. (144) and Kühn et al. (145) were conducted in epithelial cells that although are capable of phagocytosis, do not possess the repertoire of surface receptors of professional phagocytes.

In summary, actin networks are thought to have a dual role in phagosome-lysosome fusion depending on how far the phagosome has matured and the cargo load of phagosomes and lysosomes. Actin networks are inhibitory when phagosomes and lysosomes are saturated with digestive cargo by physically preventing early phagosomes from contacting endolysosomes. Actomyosin could potentially compete with dynein-dynactin motor proteins for binding to the phagosome to delay phagosome maturation. In contrast, actin networks can support late phagosome-lysosome fusion, either by bringing vesicles closer together or by facilitating vesicle docking—although the mechanisms by which actin achieves these functions and whether the involvement of actin is cargo-dependent is unclear. Moreover, the spatiotemporal control of actin that enables it to either block or enhance PL fusion remains uncharacterized. Indeed, the role of the actin-myosin network during phagosome maturation is only beginning to be understood, and further work in the area will help garner appreciation of such complex interactions.

The Vacuolar ATPase

Phagocytes acidify the phagosomal lumen by recruiting the V-ATPase, a multiprotein complex that consists of 14 different subunits (146). The cytosolic V1 domain mediates ATP hydrolysis, whereas the transmembrane V0 domain forms the proton channel (146). Phagosomal V-ATPase is largely considered to be derived from lysosomes; however, other data suggests that phagosomes acquire V-ATPases from multiple sources, including, the trans-Golgi, early endosomes, lysosomes and the plasma membrane (147–149).

Although it is well-known that V-ATPase-mediated phagosomal acidification is essential for antimicrobial defense and efficient digestion/processing of phagocytosed cargo, there is controversy surrounding the role of the V-ATPase in membrane fusion. The first evidence to demonstrate the requirement of the V-ATPase in homotypic vesicle fusion was from a study in yeast (150). Following *trans*-SNARE formation, the V0 domains from apposing vesicles were proposed to complex, leading to a conformational change which allows for lipid mixing and the formation of a fusion pore (150). An acidification-independent role of the V-ATPase in membrane fusion was observed in higher eukaryotes in subsequent studies (151–153).

The role of the V-ATPase in PL fusion was first observed in a zebrafish model, wherein knockdown of the V0 A1 subunit prevented PL fusion in microglial cells (154). Further, inhibiting the macrophage-specific V0 subunit D2 in murine bone marrow-derived macrophages impaired PL fusion and *Salmonella* clearance (155). Interestingly, by immunoprecipitation and glutathione S-transferase affinity isolation assays, subunit D2 was found to form a complex with the SNAREs Stx17 and Vamp8 important in autophagosome-lysosome fusion (155). Whether the V-ATPase could associate with fusion machinery involved in PL fusion was demonstrated in an earlier study in *Mycobacterium*-infected THP-1 macrophages (156). As mentioned above, the *M. tuberculosis* effector PtpA dephosphorylates the SM protein Vps33B to prevent PL fusion (77). Wong et al. (156) demonstrated that PtpA directly binds to the V1 subunit H to: i) block the trafficking of this subunit to the mycobacterial phagosome and ii) block its interaction with Vps33B (156). Moreover, this binding step is a prerequisite to dephosphorylate Vps33B. When macrophages were challenged with *ptpA* knockout strains, subunit H could localize to phagosomes and recruit Vps33B. Contrary to these findings implicating the V-ATPase in PL biogenesis, other reports dispute this contribution.

In mouse peritoneal macrophages, the loss of the V0 subunit A3 did not block PL formation during Fc-γ receptor phagocytosis of IgG-opsonized latex beads—phagosomes could acquire lysosomal characteristics including the mature forms of lysosomal cathepsins, and late-phagosome/lysosome markers Rab7 and Lamp2 (157). In corroboration with these findings, mouse bone marrow-derived macrophages deficient in the V0 subunits A1-3 had unaltered microbicidal activity since these cells could clear avirulent strains of *Escherichia coli* and *Listeria innocua* as efficiently as the control (158). Interestingly, through pulse-chase experiments with latex beads, the rate of PL fusion was elevated upon the loss of the V0 subunits A1-3.

Thus, whether the V-ATPase enhances PL fusion is still being debated. Different phagocytic cargoes and/or cell models leading to slightly altered maturation pathways may explain discrepancies in the works described. Moreover, it appears that specific subunits of the V-ATPase (V0 subunit D2 and V1 subunit H) have more important roles in supporting PL fusion than others (V0 subunits A1-3).

AUTOPHAGY TO THE RESCUE: SUPPORTING PHAGOCYTE FUNCTION IN THE CONTEXT OF PL FUSION

As noted earlier, several pathogens have evolved mechanisms to subvert canonical maturation of the phagosome. In response, alternative mechanisms to facilitate PL fusion have coevolved in professional phagocytes. Macroautophagy, or bulk degradation autophagy (herein referred to as autophagy), has been established as a fundamental homeostatic pathway that affects innate and adaptive immunity (159, 160). Similar to the phagocytic pathway for exogenous cargoes, autophagy delivers endogenous material to lysosomes for degradation. Low levels of basal autophagy is essential for all cells to clear unwanted cytosolic material and maintain cellular homeostasis (161–163). In phagocytes, autophagy is upregulated by several stress signals, including pro-inflammatory cytokines (164), TLR signaling (165), starvation (166), and microbial infection (167). The role of autophagy in infection, inflammation, and adaptive immunity has received increasing attention over the past 2 decades. Germane to this review, components of the autophagic pathway have been implicated in PL fusion—proposed

as an alternate pathway to overcome pathogen inhibition of canonical phagosomal maturation and enhancing the presentation of exogenous antigens. In the following section, we will discuss how the autophagic pathway complements the phagocytic pathway with an emphasis on PL fusion.

Microbial Clearance

The best-understood pathways by which autophagy augments microbicidal capabilities of phagocytes are xenophagy (168) and microtubule-associated protein A1/B1-light chain 3 (LC3)-associated phagocytosis (LAP) (169–171). Xenophagy is the selective degradation of cytosolic pathogens or pathogen-containing vesicles that have been marked with ubiquitin through autophagic mechanisms (172–174). In contrast, LAP is a non-canonical form of autophagy that involves phagocytosis and uses some components of the autophagic pathway to create a more robust phagolysosome (169–171).

Xenophagy

Several intracellular pathogens have developed mechanisms to avoid PL-mediated destruction, and autophagy can be deployed to assist in their elimination (**Figure 4**). *M. tuberculosis* is well known to inhibit phagosomal maturation, but induction of autophagy is sufficient to eliminate the pathogen *via* autophagic consumption of the arrested bacteria-containing phagosome (175). The parasite *Toxoplasma gondii* can survive within macrophages by residing in vacuoles that avoid fusion with lysosomes (176). However, when macrophages are activated by a T cell ligand, cluster of differentiation 40 (CD40), xenophagy is induced to restrict *T. gondii* growth (177, 178). Alternatively, when activated by IFN-γ, macrophages use some components of the autophagic machinery to recruit members of the immunity-related GTPase (IRG) family to mediate the elimination of these parasites in a process that is not fully understood (179, 180). However, evidence from *Mycobacteria*-containing macrophages suggests that IRGs may promote the fusion of phagosomes to lysosomes since Irgm1 has been observed to interact with SNAP-associated protein (Snapin), which binds to SNAREs to mediate vesicular fusion (181, 182).

Although xenophagy functions as a second line of defense against pathogens that overcome PL-mediated killing in phagocytes, some pathogens have further evolved to evade xenophagic activity by inhibiting the autophagic response. For example, the virulence factors of *M. tuberculosis* early secretory antigenic target 6 (ESAT6) and secreted acid phosphatase M (SapM), block autophagosome-lysosome fusion in Raw264.7 macrophage-like cells; ESAT6 stimulates the negative regulator of autophagy mammalian target of rapamycin (MTOR), and SapM hydrolyzes PI3P to prevent Rab7 recruitment to phagosomes and autophagosomes (183–186). In another study using Raw264.7 cells, *L. monocytogenes* was found to hide from autophagic recognition through its virulence factor Inlk (187).

In summary, while xenophagy often serves as an effective second defense to pathogen PL arrest or escape in many cases, some well-adapted pathogens have evolved virulence factors that target these autophagic pathways.

LC3-Associated Phagocytosis

Autophagy can also augment the antimicrobial activity of phagocytes by supporting increased PL fusion through LAP (**Figure 4**). The process of LAP requires several members of the canonical autophagic machinery, namely autophagy-related (Atg) 5, Atg7, Atg12, Atg16L, Beclin1, and Vps34 (169), as well as Rubicon and ROS production by Nox2 (171, 188). Despite sharing components, LAP and autophagy are functionally distinct processes that are differentially regulated. For example, Rubicon inhibits autophagy but is required for efficient LAP (189). LAP can be stimulated when internalized particles activate certain surface receptors of phagocytes, including TLRs, Fc receptors, Dectin-1, and the apoptotic cell receptor T cell immunoglobin and mucin domain containing 4 (TIM4) (169–171). When these receptors are engaged, phagosomes recruit LC3 (now referred to as LAPosomes) which promotes rapid fusion with lysosomes and enhances cargo degradation (169, 188). Through LAP, phagocytes are better equipped to deal with microbial infection by bacteria and fungi. For example, PL fusion with phagosomes containing the bacteria *L. monocytogenes* (190) and *Legionella dumoffi* (191), and the fungi *S. cerevisiae* (169) and *A. fumigatus* (188) is promoted by LAP [reviewed by (192)]. In the absence of LC3 recruitment to phagosomes, macrophages could not efficiently kill these pathogens and were more susceptible to sustained infection.

It is unsurprising then that pathogens have also evolved strategies to avoid targeting by LAP. Some prominent examples are CpsA production by *M. tuberculosis* (193), surface metalloprotease GP63 production by *Leishmania major* (194), and melanin production by *A. fumigatus* (195), which all function to evade LAP by preventing the Nox2-mediated ROS production crucial for LC3-recruitment [reviewed by (192)].

It is worth noting that LAP is not the only process that can enhance PL fusion. Enhanced PL fusion was observed despite the absence of Nox2-mediated LC3 recruitment to phagosomes containing IgG-opsonized zymosan and sheep erythrocytes in macrophages (196). This suggests that under certain conditions, proteins other than those belonging to the autophagic pathway such as members of the IRG family mentioned above (181, 182), can also enhance membrane fusion. Alternatively, it has been recently demonstrated that the mechanical stress caused by the growth of some intraphagosomal pathogens can induce lysosome recruitment and fusion with the phagosome as a means to increase phagosomal surface area and maintain membrane integrity (197). Further, LAP has a dual function in antigen presentation depending on the cell type. LAP stimulates rapid PL fusion in murine macrophages, favoring cargo degradation over antigen presentation (169). In contrast, LAP delays recruitment of lysosomes in human macrophages and DCs to stabilize substrates for major histocompatibility complex class II (MHCII)-mediated presentation to the adaptive immunity (198). Thus, LC3-mediated phagosome maturation is host- and condition-dependent and is a dynamic process that is influenced by the activation of phagocytes.

How LAP promotes or inhibits PL fusion at the molecular level is only beginning to be discerned. One plausible mechanism

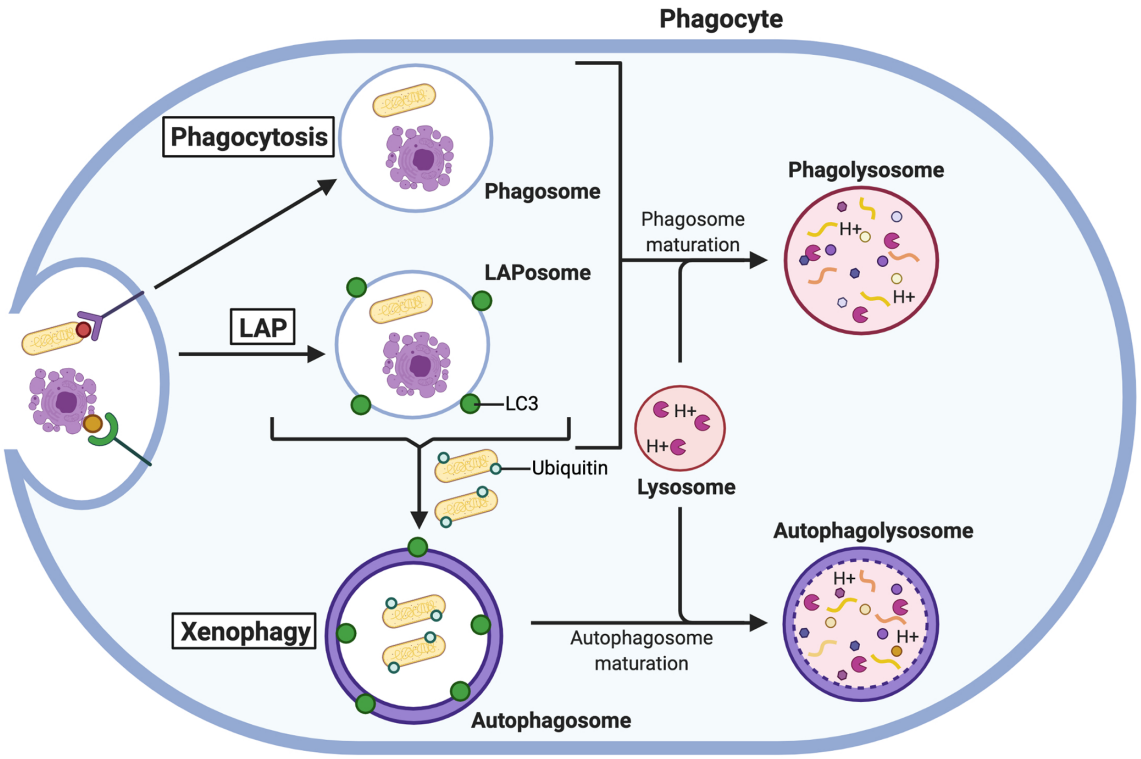

FIGURE 4 | The autophagic response aids the phagocytic pathway. Phagocytosed microbes and apoptotic cells are degraded in PLs formed from the fusion of lysosomes with phagosomes. Under certain conditions, LC3 is recruited to phagosomes for LAP to create more robust PLs. Microbes that escape PL-mediated degradation are ubiquitinated in the cytosol and degraded in autophagolysosomes *via* xenophagy.

was seen in neuronal cells, where LC3 binding of RILP to autophagosomes facilitated the recruitment of the dynein-dynactin motor complex for subsequent centripetal movement to the lysosome-rich perinuclear region (199). It would be interesting to investigate whether phagosomal LC3 can recruit RILP-dynein-dynactin to facilitate phagosome trafficking in a similar manner in phagocytes, particularly in the context of LAP. Another possibility is that LC3 plays a role in recruiting machinery to the phagosome that can assist in tethering lysosomes to phagosomes (192). Plekhm1 can be recruited by LC3 to autophagosomes in HeLa cells (200). By extension, LC3-recruited Plekhm1 on phagosomes could serve to tether HOPS- and RILP-containing vesicles during PL formation. Additionally, the LC3 isoforms γ-aminobutyric acid receptor-associated protein (Gabarap) and Gabarap-like 2 can recruit PI4KIIα (201), which generates PI4P on phagosomes and lysosomes to promote HOPS recruitment (114, 202). However, direct evidence to support these hypotheses in phagocyte LAPosomes has yet to be substantiated and awaits further investigation.

Homeostasis and Inflammation Dampening

Rapid and efficient clearance of apoptotic cells by phagocytes is critical for the regulation of tissue and immune homeostasis. Professional phagocytes are recruited by chemo-attractants released by apoptotic cells, and the "eat-me" cell-surface ligands on the dying cells mark them for phagocytotic engulfment by efferocytosis. It is now well-established that autophagy has a complex relationship with apoptosis in that autophagy can either be preventative or facilitative in programmed cell death [discussed comprehensively by (203)]. Most recently, LAP has been established as a crucial process in efferocytosis (**Figure 4**). Disrupting LAP in macrophages during TIM4-mediated engulfment delays degradation of apoptotic and necrotic cells in phagosomes (204). In the absence of LAP (created by deleting key autophagic genes), apoptotic bodies accumulate in phagosomes but are not digested due to a decrease in lysosomal fusion (205). Moreover, the accumulation in apoptotic cargo leads to secondary necrosis in macrophages. This was also observed in another study by Zhou et al. (206) in which autophagy had a cytoprotective effect on macrophages that phagocytosed apoptotic cells. Silencing a key autophagic protein, Beclin1, in macrophages displayed increased apoptotic cell cargo resulting in decreased viability and survival, and macrophage rupturing (206). When stimulated with apoptotic cells, macrophages deficient in LAP due to genetic knockout of Rubicon or Nox2 produced higher levels of pro-inflammatory cytokines (interleukin-(IL)-1β, IL-6, CXCL10) and lower levels

of anti-inflammatory cytokines (IL-10) compared to LAP-sufficient cells (205). This increase in pro-inflammatory signals translates to autoimmunity and the development of systemic lupus erythematosus-like disease in *in vivo* mouse models when LAP is not functioning to clear apoptotic cells (205). Hence, LAP-enhanced PL fusion is fundamental to regulate pro-inflammatory and pro-death signals.

In summary, autophagy and phagocytosis are two complementary pathways that cooperate in PL-mediated elimination of dangerous exogenous and endogenous material to regulate infection and homeostasis. Canonical autophagic machinery is employed to either supplement or support phagosome maturation or to conduct microbicidal and homeostatic functions. Induction of the autophagic machinery enhances PL biogenesis *via* LAP, although the molecular mechanism has not yet been fully characterized. Current evidence suggests LC3-recruitment of phagosome trafficking and fusion machinery, yet this warrants further investigation.

CONCLUDING REMARKS

Here we have summarized recent findings regarding phagosome-lysosome fusion. The Rab GTPases Rab7, Rab2 and Rab14 participate in tethering phagosomes and lysosomes albeit through mechanisms that are less known for Rab2 and Rab14. Rab7 recruits tethering effectors, whereby the individual subunits of the HOPS complex give it the multifunctional capacity to serve as a Rab GEF, a tether and an SM protein that catalyzes SNARE assembly. The SNAREs Snap23, Stx7, Vamp8, Vti1b, and Stx8 have been shown to assemble into specific complexes to execute PL fusion. While the Rabs, tethering factors and SNAREs involved in PL biogenesis are best known, we know less about how phagosomal lipids, the actin network and the V-ATPase regulate PL fusion. PI3P and PI4P have been implicated to interact with fusion machinery, whereas PI4,5P2 is involved in actin nucleation, which exhibits dual function to either support or inhibit PL fusion. PI3,5P2 is required for V-ATPase activation and PL fusion in lower eukaryotes but this has yet to be shown in mammalian phagocytes. Acidification-independent roles of the V-ATPase in fusion is still under contention but some evidence suggests the involvement of specific subunits. Lastly, the autophagic pathway can bolster the phagocytic pathway through LAP-enhanced PL fusion, or xenophagy-mediated protection of phagocyte integrity.

Although there have been great advances in understanding the proceedings of the molecular events that mediate PL biogenesis, we have only scratched the surface in delineating the full extent of all the participating molecules and modulating signals. For those that have been identified, little is known regarding their spatiotemporal regulation. The greatest caveat to the existing studies that have furthered our understanding of the aforementioned fusion machinery is that they have been performed extensively in *in vitro* cell-free models or phagocyte-like cell lines which limits our ability to confidently extrapolate to primary phagocytes. To this degree, few studies have investigated the molecules that control phagosome-lysosome fusion in live primary phagocytes, generating a gap between experimental evidence and functional relevance to the management of infection and disease. For studies that have employed primary cell models, it is unclear whether the fusion molecules recruited to phagosomes is consistent for all cargo types. Phagocytic uptake of macromolecular cargos can be mediated by several cell-surface receptors that activate different signaling pathways based on the type of cargo. The activation/inflammation status of these cells can influence the rate and magnitude of the dynamic recruitment of fusion-mediating proteins. Even the type of phagocyte and particular species from which cells are sourced can influence which particular fusion proteins are involved. Thus, further studies are required to more comprehensively characterize this critical and often underappreciated aspect of phagocyte biology.

Phagosome fusion with lysosomes is crucial to the functional outcome of phagocytosis and efferocytosis. Impaired lysosome fusion—and by extension, cargo degradation—disrupts the immune response to microbial and apoptotic cell clearance, and can underlie autoimmune and inflammatory disorders, and persistence of infection. Deciphering the mechanisms that drive and regulate the fusion of phagosomes with lysosomes will not only contribute to the greater knowledge of the pathogenesis of many diseases, but also contribute to our understanding of health, growth, and homeostasis.

AUTHOR CONTRIBUTIONS

JN wrote the manuscript with support from RY. All authors contributed to the article and approved the submitted version.

ACKNOWLEDGMENTS

We are grateful to Dr. Catherine Greene and Dr. Corey Arnold and thank them for their critical review of the manuscript. The figures used in this review were created with BioRender.com. This work was supported by the Canadian Institutes of Health Research and Natural Sciences and Engineering Research Council of Canada.

SUPPLEMENTARY MATERIAL

The Supplementary Material for this article can be found online at: https://www.frontiersin.org/articles/10.3389/fimmu.2021.636078/full#supplementary-material

REFERENCES

1. Turvey SE, Broide DH. Innate immunity. *J Allergy Clin Immunol* (2010) 125 (2 Suppl 2):S24–32. doi: 10.1016/j.jaci.2009.07.016
2. Vieira OV, Botelho RJ, Grinstein S. Phagosome maturation: aging gracefully. *Biochem J* (2002) 366(Pt 3):689–704. doi: 10.1042/BJ20020691
3. Desjardins M. Biogenesis of phagolysosomes: the 'kiss and run' hypothesis. *Trends Cell Biol* (1995) 5(5):183–6. doi: 10.1016/s0962-8924(00)88989-8
4. Desjardins M, Huber LA, Parton RG, Griffiths G. Biogenesis of phagolysosomes proceeds through a sequential series of interactions with the endocytic apparatus. *J Cell Biol* (1994) 124(5):677–88. doi: 10.1083/jcb.124.5.677
5. Fratti RA, Backer JM, Gruenberg J, Corvera S, Deretic V. Role of phosphatidylinositol 3-kinase and Rab5 effectors in phagosomal biogenesis and mycobacterial phagosome maturation arrest. *J Cell Biol* (2001) 154(3):631–44. doi: 10.1083/jcb.200106049
6. Vergne I, Fratti RA, Hill PJ, Chua J, Belisle J, Deretic V. Mycobacterium tuberculosis phagosome maturation arrest: mycobacterial phosphatidylinositol analog phosphatidylinositol mannoside stimulates early endosomal fusion. *Mol Biol Cell* (2004) 15(2):751–60. doi: 10.1091/mbc.e03-05-0307
7. Desjardins M, Descoteaux A. Inhibition of phagolysosomal biogenesis by the Leishmania lipophosphoglycan. *J Exp Med* (1997) 185(12):2061–8. doi: 10.1084/jem.185.12.2061
8. Graham JG, MacDonald LJ, Hussain SK, Sharma UM, Kurten RC, Voth DE. Virulent Coxiella burnetii pathotypes productively infect primary human alveolar macrophages. *Cell Microbiol* (2013) 15(6):1012–25. doi: 10.1111/cmi.12096
9. Thywissen A, Heinekamp T, Dahse HM, Schmaler-Ripcke J, Nietzsche S, Zipfel PF, et al. Conidial Dihydroxynaphthalene Melanin of the Human Pathogenic Fungus Aspergillus fumigatus Interferes with the Host Endocytosis Pathway. *Front Microbiol* (2011) 2:96. doi: 10.3389/fmicb.2011.00096
10. Dingjan I, Linders PTA, Verboogen DRJ, Revelo NH, Ter Beest M, van den Bogaart G. Endosomal and Phagosomal SNAREs. *Physiol Rev* (2018) 98 (3):1465–92. doi: 10.1152/physrev.00037.2017
11. Rogers LD, Foster LJ. The dynamic phagosomal proteome and the contribution of the endoplasmic reticulum. *Proc Natl Acad Sci U S A* (2007) 104(47):18520–5. doi: 10.1073/pnas.0705801104
12. Knapp PE, Swanson JA. Plasticity of the tubular lysosomal compartment in macrophages. *J Cell Sci* (1990) 95(Pt 3):433–9.
13. Keller S, Berghoff K, Kress H. Phagosomal transport depends strongly on phagosome size. *Sci Rep* (2017) 7(1):17068. doi: 10.1038/s41598-017-17183-7
14. Li X, Rydzewski N, Hider A, Zhang X, Yang J, Wang W, et al. A molecular mechanism to regulate lysosome motility for lysosome positioning and tubulation. *Nat Cell Biol* (2016) 18(4):404–17. doi: 10.1038/ncb3324
15. Rai A, Pathak D, Thakur S, Singh S, Dubey AK, Mallik R. Dynein Clusters into Lipid Microdomains on Phagosomes to Drive Rapid Transport toward Lysosomes. *Cell* (2016) 164(4):722–34. doi: 10.1016/j.cell.2015.12.054
16. Jahn R, Lang T, Sudhof TC. Membrane fusion. *Cell* (2003) 112(4):519–33. doi: 10.1016/s0092-8674(03)00112-0
17. Lurick A, Kummel D, Ungermann C. Multisubunit tethers in membrane fusion. *Curr Biol* (2018) 28(8):R417–R20. doi: 10.1016/j.cub.2017.12.012
18. Ali BR, Wasmeier C, Lamoreux L, Strom M, Seabra MC. Multiple regions contribute to membrane targeting of Rab GTPases. *J Cell Sci* (2004) 117(Pt 26):6401–12. doi: 10.1242/jcs.01542
19. Conibear E, Cleck JN, Stevens TH. Vps51p mediates the association of the GARP (Vps52/53/54) complex with the late Golgi t-SNARE Tlg1p. *Mol Biol Cell* (2003) 14(4):1610–23. doi: 10.1091/mbc.e02-10-0654
20. Fiebig KM, Rice LM, Pollock E, Brunger AT. Folding intermediates of SNARE complex assembly. *Nat Struct Biol* (1999) 6(2):117–23. doi: 10.1038/5803
21. Chen YA, Scales SJ, Scheller RH. Sequential SNARE assembly underlies priming and triggering of exocytosis. *Neuron* (2001) 30(1):161–70. doi: 10.1016/s0896-6273(01)00270-7
22. Melia TJ, Weber T, McNew JA, Fisher LE, Johnston RJ, Parlati F, et al. Regulation of membrane fusion by the membrane-proximal coil of the t-SNARE during zippering of SNAREpins. *J Cell Biol* (2002) 158(5):929–40. doi: 10.1083/jcb.200112081
23. Poirier MA, Xiao W, Macosko JC, Chan C, Shin YK, Bennett MK. The synaptic SNARE complex is a parallel four-stranded helical bundle. *Nat Struct Biol* (1998) 5(9):765–9. doi: 10.1038/1799
24. Baker RW, Jeffrey PD, Zick M, Phillips BP, Wickner WT, Hughson FM. A direct role for the Sec1/Munc18-family protein Vps33 as a template for SNARE assembly. *Science* (2015) 349(6252):1111–4. doi: 10.1126/science.aac7906
25. Song H, Orr AS, Lee M, Harner ME, Wickner WT. HOPS recognizes each SNARE, assembling ternary trans-complexes for rapid fusion upon engagement with the 4th SNARE. *Elife* (2020) 9. doi: 10.7554/eLife.53559
26. Ellena JF, Liang B, Wiktor M, Stein A, Cafiso DS, Jahn R, et al. Dynamic structure of lipid-bound synaptobrevin suggests a nucleation-propagation mechanism for trans-SNARE complex formation. *Proc Natl Acad Sci U S A* (2009) 106(48):20306–11. doi: 10.1073/pnas.0908317106
27. Sollner T, Bennett MK, Whiteheart SW, Scheller RH, Rothman JE. A protein assembly-disassembly pathway in vitro that may correspond to sequential steps of synaptic vesicle docking, activation, and fusion. *Cell* (1993) 75 (3):409–18. doi: 10.1016/0092-8674(93)90376-2
28. Hanson PI, Otto H, Barton N, Jahn R. The N-ethylmaleimide-sensitive fusion protein and alpha-SNAP induce a conformational change in syntaxin. *J Biol Chem* (1995) 270(28):16955–61. doi: 10.1074/jbc.270.28.16955
29. Ungermann C, Nichols BJ, Pelham HR, Wickner W. A vacuolar v-t-SNARE complex, the predominant form in vivo and on isolated vacuoles, is disassembled and activated for docking and fusion. *J Cell Biol* (1998) 140 (1):61–9. doi: 10.1083/jcb.140.1.61
30. Sun J, Deghmane AE, Soualhine H, Hong T, Bucci C, Solodkin A, et al. Mycobacterium bovis BCG disrupts the interaction of Rab7 with RILP contributing to inhibition of phagosome maturation. *J Leukoc Biol* (2007) 82 (6):1437–45. doi: 10.1189/jlb.10.1189
31. Guo P, Hu T, Zhang J, Jiang S, Wang X. Sequential action of Caenorhabditis elegans Rab GTPases regulates phagolysosome formation during apoptotic cell degradation. *Proc Natl Acad Sci U S A* (2010) 107(42):18016–21. doi: 10.1073/pnas.1008946107
32. Mangahas PM, Yu X, Miller KG, Zhou Z. The small GTPase Rab2 functions in the removal of apoptotic cells in Caenorhabditis elegans. *J Cell Biol* (2008) 180(2):357–73. doi: 10.1083/jcb.200708130
33. Via LE, Deretic D, Ulmer RJ, Hibler NS, Huber LA, Deretic V. Arrest of mycobacterial phagosome maturation is caused by a block in vesicle fusion between stages controlled by rab5 and rab7. *J Biol Chem* (1997) 272 (20):13326–31. doi: 10.1074/jbc.272.20.13326
34. Kinchen JM, Doukoumetzidis K, Almendinger J, Stergiou L, Tosello-Trampont A, Sifri CD, et al. A pathway for phagosome maturation during engulfment of apoptotic cells. *Nat Cell Biol* (2008) 10(5):556–66. doi: 10.1038/ncb1718
35. Gumienny TL, Hengartner MO. How the worm removes corpses: the nematode C. elegans as a model system to study engulfment. *Cell Death Differ* (2001) 8(6):564–8. doi: 10.1038/sj.cdd.4400850
36. Zhou Z, Yu X. Phagosome maturation during the removal of apoptotic cells: receptors lead the way. *Trends Cell Biol* (2008) 18(10):474–85. doi: 10.1016/j.tcb.2008.08.002
37. Becken U, Jeschke A, Veltman K, Haas A. Cell-free fusion of bacteria-containing phagosomes with endocytic compartments. *Proc Natl Acad Sci U S A* (2010) 107(48):20726–31. doi: 10.1073/pnas.1007295107
38. Dingjan I, Linders PT, van den Bekerom L, Baranov MV, Halder P, Ter Beest M, et al. Oxidized phagosomal NOX2 complex is replenished from lysosomes. *J Cell Sci* (2017) 130(7):1285–98. doi: 10.1242/jcs.196931
39. Sakurai C, Hashimoto H, Nakanishi H, Arai S, Wada Y, Sun-Wada GH, et al. SNAP-23 regulates phagosome formation and maturation in macrophages. *Mol Biol Cell* (2012) 23(24):4849–63. doi: 10.1091/mbc.E12-01-0069
40. Sakurai C, Itakura M, Kinoshita D, Arai S, Hashimoto H, Wada I, et al. Phosphorylation of SNAP-23 at Ser95 causes a structural alteration and negatively regulates Fc receptor-mediated phagosome formation and maturation in macrophages. *Mol Biol Cell* (2018) 29(13):1753–62. doi: 10.1091/mbc.E17-08-0523
41. Fairn GD, Grinstein S. How nascent phagosomes mature to become phagolysosomes. *Trends Immunol* (2012) 33(8):397–405. doi: 10.1016/j.it.2012.03.003

42. Pfeffer SR, Dirac-Svejstrup AB, Soldati T. Rab GDP dissociation inhibitor: putting rab GTPases in the right place. *J Biol Chem* (1995) 270(29):17057–9. doi: 10.1074/jbc.270.29.17057
43. Sivars U, Aivazian D, Pfeffer SR. Yip3 catalyses the dissociation of endosomal Rab-GDI complexes. *Nature* (2003) 425(6960):856–9. doi: 10.1038/nature02057
44. Rybin V, Ullrich O, Rubino M, Alexandrov K, Simon I, Seabra MC, et al. GTPase activity of Rab5 acts as a timer for endocytic membrane fusion. *Nature* (1996) 383(6597):266–9. doi: 10.1038/383266a0
45. Blumer J, Rey J, Dehmelt L, Mazel T, Wu YW, Bastiaens P, et al. RabGEFs are a major determinant for specific Rab membrane targeting. *J Cell Biol* (2013) 200(3):287–300. doi: 10.1083/jcb.201209113
46. Rivera-Molina FE, Novick PJ. A Rab GAP cascade defines the boundary between two Rab GTPases on the secretory pathway. *Proc Natl Acad Sci U S A* (2009) 106(34):14408–13. doi: 10.1073/pnas.0906536106
47. Harrison RE, Bucci C, Vieira OV, Schroer TA, Grinstein S. Phagosomes fuse with late endosomes and/or lysosomes by extension of membrane protrusions along microtubules: role of Rab7 and RILP. *Mol Cell Biol* (2003) 23(18):6494–506. doi: 10.1128/mcb.23.18.6494-6506.2003
48. Wu MY, Liu L, Wang EJ, Xiao HT, Cai CZ, Wang J, et al. PI3KC3 complex subunit NRBF2 is required for apoptotic cell clearance to restrict intestinal inflammation. *Autophagy* (2020), 19:1–16. doi: 10.1080/15548627.2020.1741332
49. Mottola G. The complexity of Rab5 to Rab7 transition guarantees specificity of pathogen subversion mechanisms. *Front Cell Infect Microbiol* (2014) 4:180. doi: 10.3389/fcimb.2014.00180
50. Mukherjee K, Khatua B, Mandal C. Sialic Acid-Siglec-E Interactions During Pseudomonas aeruginosa Infection of Macrophages Interferes With Phagosome Maturation by Altering Intracellular Calcium Concentrations. *Front Immunol* (2020) 11:332. doi: 10.3389/fimmu.2020.00332
51. Nieto C, Almendinger J, Gysi S, Gomez-Orte E, Kaech A, Hengartner MO, et al. ccz-1 mediates the digestion of apoptotic corpses in C. elegans. *J Cell Sci* (2010) 123(Pt 12):2001–7. doi: 10.1242/jcs.062331
52. Kinchen JM, Ravichandran KS. Identification of two evolutionarily conserved genes regulating processing of engulfed apoptotic cells. *Nature* (2010) 464(7289):778–82. doi: 10.1038/nature08853
53. Poteryaev D, Datta S, Ackema K, Zerial M, Spang A. Identification of the switch in early-to-late endosome transition. *Cell* (2010) 141(3):497–508. doi: 10.1016/j.cell.2010.03.011
54. Lou J, Li X, Huang W, Liang J, Zheng M, Xu T, et al. SNX10 promotes phagosome maturation in macrophages and protects mice against Listeria monocytogenes infection. *Oncotarget* (2017) 8(33):53935–47. doi: 10.18632/oncotarget.19644
55. Wurmser AE, Sato TK, Emr SD. New component of the vacuolar class C-Vps complex couples nucleotide exchange on the Ypt7 GTPase to SNARE-dependent docking and fusion. *J Cell Biol* (2000) 151(3):551–62. doi: 10.1083/jcb.151.3.551
56. Barry AO, Boucherit N, Mottola G, Vadovic P, Trouplin V, Soubeyran P, et al. Impaired stimulation of p38alpha-MAPK/Vps41-HOPS by LPS from pathogenic Coxiella burnetii prevents trafficking to microbicidal phagolysosomes. *Cell Host Microbe* (2012) 12(6):751–63. doi: 10.1016/j.chom.2012.10.015
57. Lorincz P, Toth S, Benko P, Lakatos Z, Boda A, Glatz G, et al. Rab2 promotes autophagic and endocytic lysosomal degradation. *J Cell Biol* (2017) 216 (7):1937–47. doi: 10.1083/jcb.201611027
58. Gillingham AK, Sinka R, Torres IL, Lilley KS, Munro S. Toward a comprehensive map of the effectors of rab GTPases. *Dev Cell* (2014) 31 (3):358–73. doi: 10.1016/j.devcel.2014.10.007
59. Mao F, Mu H, Wong NK, Liu K, Song J, Qiu J, et al. Hemocyte phagosomal proteome is dynamically shaped by cytoskeleton remodeling and interorganellar communication with endoplasmic reticulum during phagocytosis in a marine invertebrate, Crassostrea gigas. *Sci Rep* (2020) 10 (1):6577. doi: 10.1038/s41598-020-63676-3
60. Okai B, Lyall N, Gow NA, Bain JM, Erwig LP. Rab14 regulates maturation of macrophage phagosomes containing the fungal pathogen Candida albicans and outcome of the host-pathogen interaction. *Infect Immun* (2015) 83 (4):1523–35. doi: 10.1128/IAI.02917-14
61. Vieira OV, Bucci C, Harrison RE, Trimble WS, Lanzetti L, Gruenberg J, et al. Modulation of Rab5 and Rab7 recruitment to phagosomes by phosphatidylinositol 3-kinase. *Mol Cell Biol* (2003) 23(7):2501–14. doi: 10.1128/mcb.23.7.2501-2514.2003
62. Wickner W, Rizo J. A cascade of multiple proteins and lipids catalyzes membrane fusion. *Mol Biol Cell* (2017) 28(6):707–11. doi: 10.1091/mbc.E16-07-0517
63. Wu M, Wang T, Loh E, Hong W, Song H. Structural basis for recruitment of RILP by small GTPase Rab7. *EMBO J* (2005) 24(8):1491–501. doi: 10.1038/sj.emboj.7600643
64. Sun J, Wang X, Lau A, Liao TY, Bucci C, Hmama Z. Mycobacterial nucleoside diphosphate kinase blocks phagosome maturation in murine RAW 264.7 macrophages. *PloS One* (2010) 5(1):e8769. doi: 10.1371/journal.pone.0008769
65. Sindhwani A, Arya SB, Kaur H, Jagga D, Tuli A, Sharma M. Salmonella exploits the host endolysosomal tethering factor HOPS complex to promote its intravacuolar replication. *PloS Pathog* (2017) 13(10):e1006700. doi: 10.1371/journal.ppat.1006700
66. McEwan DG, Richter B, Claudi B, Wigge C, Wild P, Farhan H, et al. PLEKHM1 regulates Salmonella-containing vacuole biogenesis and infection. *Cell Host Microbe* (2015) 17(1):58–71. doi: 10.1016/j.chom.2014.11.011
67. van der Kant R, Fish A, Janssen L, Janssen H, Krom S, Ho N, et al. Late endosomal transport and tethering are coupled processes controlled by RILP and the cholesterol sensor ORP1L. *J Cell Sci* (2013) 126(Pt 15):3462–74. doi: 10.1242/jcs.129270
68. Lin X, Yang T, Wang S, Wang Z, Yun Y, Sun L, et al. RILP interacts with HOPS complex via VPS41 subunit to regulate endocytic trafficking. *Sci Rep* (2014) 4:7282. doi: 10.1038/srep07282
69. Jiang P, Nishimura T, Sakamaki Y, Itakura E, Hatta T, Natsume T, et al. The HOPS complex mediates autophagosome-lysosome fusion through interaction with syntaxin 17. *Mol Biol Cell* (2014) 25(8):1327–37. doi: 10.1091/mbc.E13-08-0447
70. Khatter D, Raina VB, Dwivedi D, Sindhwani A, Bahl S, Sharma M. The small GTPase Arl8b regulates assembly of the mammalian HOPS complex on lysosomes. *J Cell Sci* (2015) 128(9):1746–61. doi: 10.1242/jcs.162651
71. van der Kant R, Jonker CT, Wijdeven RH, Bakker J, Janssen L, Klumperman J, et al. Characterization of the Mammalian CORVET and HOPS Complexes and Their Modular Restructuring for Endosome Specificity. *J Biol Chem* (2015) 290(51):30280–90. doi: 10.1074/jbc.M115.688440
72. Garg S, Sharma M, Ung C, Tuli A, Barral DC, Hava DL, et al. Lysosomal trafficking, antigen presentation, and microbial killing are controlled by the Arf-like GTPase Arl8b. *Immunity* (2011) 35(2):182–93. doi: 10.1016/j.immuni.2011.06.009
73. Jeschke A, Haas A. Sequential actions of phosphatidylinositol phosphates regulate phagosome-lysosome fusion. *Mol Biol Cell* (2018) 29(4):452–65. doi: 10.1091/mbc.E17-07-0464
74. Seals DF, Eitzen G, Margolis N, Wickner WT, Price A. A Ypt/Rab effector complex containing the Sec1 homolog Vps33p is required for homotypic vacuole fusion. *Proc Natl Acad Sci U S A* (2000) 97(17):9402–7. doi: 10.1073/pnas.97.17.9402
75. Subramanian S, Woolford CA, Jones EW. The Sec1/Munc18 protein, Vps33p, functions at the endosome and the vacuole of Saccharomyces cerevisiae. *Mol Biol Cell* (2004) 15(6):2593–605. doi: 10.1091/mbc.e03-10-0767
76. Brocker C, Kuhlee A, Gatsogiannis C, Balderhaar HJ, Honscher C, Engelbrecht-Vandre S, et al. Molecular architecture of the multisubunit homotypic fusion and vacuole protein sorting (HOPS) tethering complex. *Proc Natl Acad Sci U S A* (2012) 109(6):1991–6. doi: 10.1073/pnas.1117797109
77. Bach H, Papavinasasundaram KG, Wong D, Hmama Z, Av-Gay Y. Mycobacterium tuberculosis virulence is mediated by PtpA dephosphorylation of human vacuolar protein sorting 33B. *Cell Host Microbe* (2008) 3(5):316–22. doi: 10.1016/j.chom.2008.03.008
78. Akbar MA, Tracy C, Kahr WH, Kramer H. The full-of-bacteria gene is required for phagosome maturation during immune defense in Drosophila. *J Cell Biol* (2011) 192(3):383–90. doi: 10.1083/jcb.201008119
79. Johansson M, Rocha N, Zwart W, Jordens I, Janssen L, Kuijl C, et al. Activation of endosomal dynein motors by stepwise assembly of Rab7-RILP-p150Glued, ORP1L, and the receptor betalll spectrin. *J Cell Biol* (2007) 176 (4):459–71. doi: 10.1083/jcb.200606077

80. Stein MP, Feng Y, Cooper KL, Welford AM, Wandinger-Ness A. Human VPS34 and p150 are Rab7 interacting partners. *Traffic* (2003) 4(11):754–71. doi: 10.1034/j.1600-0854.2003.00133.x
81. Sun Q, Westphal W, Wong KN, Tan I, Zhong Q. Rubicon controls endosome maturation as a Rab7 effector. *Proc Natl Acad Sci U S A* (2010) 107(45):19338–43. doi: 10.1073/pnas.1010554107
82. Fasshauer D, Sutton RB, Brunger AT, Jahn R. Conserved structural features of the synaptic fusion complex: SNARE proteins reclassified as Q- and R-SNAREs. *Proc Natl Acad Sci U S A* (1998) 95(26):15781–6. doi: 10.1073/pnas.95.26.15781
83. Mayorga LS, Bertini F, Stahl PD. Fusion of newly formed phagosomes with endosomes in intact cells and in a cell-free system. *J Biol Chem* (1991) 266 (10):6511–7.
84. Funato K, Beron W, Yang CZ, Mukhopadhyay A, Stahl PD. Reconstitution of phagosome-lysosome fusion in streptolysin O-permeabilized cells. *J Biol Chem* (1997) 272(26):16147–51. doi: 10.1074/jbc.272.26.16147
85. Dill BD, Gierlinski M, Hartlova A, Arandilla AG, Guo M, Clarke RG, et al. Quantitative proteome analysis of temporally resolved phagosomes following uptake via key phagocytic receptors. *Mol Cell Proteomics* (2015) 14(5):1334–49. doi: 10.1074/mcp.M114.044594
86. Campbell-Valois FX, Trost M, Chemali M, Dill BD, Laplante A, Duclos S, et al. Quantitative proteomics reveals that only a subset of the endoplasmic reticulum contributes to the phagosome. *Mol Cell Proteomics* (2012) 11(7): M111 016378. doi: 10.1074/mcp.M111.016378
87. Duclos S, Clavarino G, Rousserie G, Goyette G, Boulais J, Camossetto V, et al. The endosomal proteome of macrophage and dendritic cells. *Proteomics* (2011) 11(5):854–64. doi: 10.1002/pmic.201000577
88. Goyette G, Boulais J, Carruthers NJ, Landry CR, Jutras I, Duclos S, et al. Proteomic characterization of phagosomal membrane microdomains during phagolysosome biogenesis and evolution. *Mol Cell Proteomics* (2012) 11 (11):1365–77. doi: 10.1074/mcp.M112.021048
89. Collins RF, Schreiber AD, Grinstein S, Trimble WS. Syntaxins 13 and 7 function at distinct steps during phagocytosis. *J Immunol* (2002) 169 (6):3250–6. doi: 10.4049/jimmunol.169.6.3250
90. Buschow SI, Lasonder E, Szklarczyk R, Oud MM, de Vries IJ, Figdor CG. Unraveling the human dendritic cell phagosome proteome by organellar enrichment ranking. *J Proteomics* (2012) 75(5):1547–62. doi: 10.1016/j.jprot.2011.11.024
91. Uriarte SM, Rane MJ, Luerman GC, Barati MT, Ward RA, Nauseef WM, et al. Granule exocytosis contributes to priming and activation of the human neutrophil respiratory burst. *J Immunol* (2011) 187(1):391–400. doi: 10.4049/jimmunol.1003112
92. Rybicka JM, Balce DR, Khan MF, Krohn RM, Yates RM. NADPH oxidase activity controls phagosomal proteolysis in macrophages through modulation of the lumenal redox environment of phagosomes. *Proc Natl Acad Sci U S A* (2010) 107(23):10496–501. doi: 10.1073/pnas.0914867107
93. Mantegazza AR, Savina A, Vermeulen M, Perez L, Geffner J, Hermine O, et al. NADPH oxidase controls phagosomal pH and antigen cross-presentation in human dendritic cells. *Blood* (2008) 112(12):4712–22. doi: 10.1182/blood-2008-01-134791
94. Savina A, Jancic C, Hugues S, Guermonprez P, Vargas P, Moura IC, et al. NOX2 controls phagosomal pH to regulate antigen processing during crosspresentation by dendritic cells. *Cell* (2006) 126(1):205–18. doi: 10.1016/j.cell.2006.05.035
95. Arango Duque G, Fukuda M, Descoteaux A. Synaptotagmin XI regulates phagocytosis and cytokine secretion in macrophages. *J Immunol* (2013) 190 (4):1737–45. doi: 10.4049/jimmunol.1202500
96. Casbon AJ, Allen LA, Dunn KW, Dinauer MC. Macrophage NADPH oxidase flavocytochrome B localizes to the plasma membrane and Rab11-positive recycling endosomes. *J Immunol* (2009) 182(4):2325–39. doi: 10.4049/jimmunol.0803476
97. Jancic C, Savina A, Wasmeier C, Tolmachova T, El-Benna J, Dang PM, et al. Rab27a regulates phagosomal pH and NADPH oxidase recruitment to dendritic cell phagosomes. *Nat Cell Biol* (2007) 9(4):367–78. doi: 10.1038/ncb1552
98. Dingjan I, Paardekooper LM, Verboogen DRJ, von Mollard GF, Ter Beest M, van den Bogaart G. VAMP8-mediated NOX2 recruitment to endosomes is necessary for antigen release. *Eur J Cell Biol* (2017) 96(7):705–14. doi: 10.1016/j.ejcb.2017.06.007
99. Matheoud D, Moradin N, Bellemare-Pelletier A, Shio MT, Hong WJ, Olivier M, et al. Leishmania evades host immunity by inhibiting antigen cross-presentation through direct cleavage of the SNARE VAMP8. *Cell Host Microbe* (2013) 14(1):15–25. doi: 10.1016/j.chom.2013.06.003
100. Yates RM, Hermetter A, Taylor GA, Russell DG. Macrophage activation downregulates the degradative capacity of the phagosome. *Traffic* (2007) 8 (3):241–50. doi: 10.1111/j.1600-0854.2006.00528.x
101. Westman J, Grinstein S, Maxson ME. Revisiting the role of calcium in phagosome formation and maturation. *J Leukoc Biol* (2019) 106(4):837–51. doi: 10.1002/JLB.MR1118-444R
102. Balla T. Phosphoinositides: tiny lipids with giant impact on cell regulation. *Physiol Rev* (2013) 93(3):1019–137. doi: 10.1152/physrev.00028.2012
103. Rusten TE, Stenmark H. Analyzing phosphoinositides and their interacting proteins. *Nat Methods* (2006) 3(4):251–8. doi: 10.1038/nmeth867
104. Vieira OV, Botelho RJ, Rameh L, Brachmann SM, Matsuo T, Davidson HW, et al. Distinct roles of class I and class III phosphatidylinositol 3-kinases in phagosome formation and maturation. *J Cell Biol* (2001) 155(1):19–25. doi: 10.1083/jcb.200107069
105. Samie M, Wang X, Zhang X, Goschka A, Li X, Cheng X, et al. A TRP channel in the lysosome regulates large particle phagocytosis via focal exocytosis. *Dev Cell* (2013) 26(5):511–24. doi: 10.1016/j.devcel.2013.08.003
106. Levin R, Hammond GR, Balla T, De Camilli P, Fairn GD, Grinstein S. Multiphasic dynamics of phosphatidylinositol 4-phosphate during phagocytosis. *Mol Biol Cell* (2017) 28(1):128–40. doi: 10.1091/mbc.E16-06-0451
107. Kim GH, Dayam RM, Prashar A, Terebiznik M, Botelho RJ. PIKfyve inhibition interferes with phagosome and endosome maturation in macrophages. *Traffic* (2014) 15(10):1143–63. doi: 10.1111/tra.12199
108. Buckley CM, Heath VL, Gueho A, Bosmani C, Knobloch P, Sikakana P, et al. PIKfyve/Fab1 is required for efficient V-ATPase and hydrolase delivery to phagosomes, phagosomal killing, and restriction of Legionella infection. *PloS Pathog* (2019) 15(2):e1007551. doi: 10.1371/journal.ppat.1007551
109. Ho CY, Choy CH, Wattson CA, Johnson DE, Botelho RJ. The Fab1/PIKfyve phosphoinositide phosphate kinase is not necessary to maintain the pH of lysosomes and of the yeast vacuole. *J Biol Chem* (2015) 290(15):9919–28. doi: 10.1074/jbc.M114.613984
110. Gary JD, Wurmser AE, Bonangelino CJ, Weisman LS, Emr SD. Fab1p is essential for PtdIns(3)P 5-kinase activity and the maintenance of vacuolar size and membrane homeostasis. *J Cell Biol* (1998) 143(1):65–79. doi: 10.1083/jcb.143.1.65
111. Li SC, Diakov TT, Xu T, Tarsio M, Zhu W, Couoh-Cardel S, et al. The signaling lipid PI(3,5)P(2) stabilizes V(1)-V(o) sector interactions and activates the V-ATPase. *Mol Biol Cell* (2014) 25(8):1251–62. doi: 10.1091/mbc.E13-10-0563
112. Kerr MC, Wang JT, Castro NA, Hamilton NA, Town L, Brown DL, et al. Inhibition of the PtdIns(5) kinase PIKfyve disrupts intracellular replication of Salmonella. *EMBO J* (2010) 29(8):1331–47. doi: 10.1038/emboj.2010.28
113. Dayam RM, Saric A, Shilliday RE, Botelho RJ. The Phosphoinositide-Gated Lysosomal Ca(2+) Channel, TRPML1, Is Required for Phagosome Maturation. *Traffic* (2015) 16(9):1010–26. doi: 10.1111/tra.12303
114. Jeschke A, Zehethofer N, Lindner B, Krupp J, Schwudke D, Haneburger I, et al. Phosphatidylinositol 4-phosphate and phosphatidylinositol 3-phosphate regulate phagolysosome biogenesis. *Proc Natl Acad Sci U S A* (2015) 112(15):4636–41. doi: 10.1073/pnas.1423456112
115. Ragaz C, Pietsch H, Urwyler S, Tiaden A, Weber SS, Hilbi H. The Legionella pneumophila phosphatidylinositol-4 phosphate-binding type IV substrate SidC recruits endoplasmic reticulum vesicles to a replication-permissive vacuole. *Cell Microbiol* (2008) 10(12):2416–33. doi: 10.1111/j.1462-5822.2008.01219.x
116. Gillooly DJ, Morrow IC, Lindsay M, Gould R, Bryant NJ, Gaullier JM, et al. Localization of phosphatidylinositol 3-phosphate in yeast and mammalian cells. *EMBO J* (2000) 19(17):4577–88. doi: 10.1093/emboj/19.17.4577
117. Jeschke A, Haas A. Deciphering the roles of phosphoinositide lipids in phagolysosome biogenesis. *Commun Integr Biol* (2016) 9(3):e1174798. doi: 10.1080/19420889.2016.1174798
118. Dai S, Zhang Y, Weimbs T, Yaffe MB, Zhou D. Bacteria-generated PtdIns(3) P recruits VAMP8 to facilitate phagocytosis. *Traffic* (2007) 8(10):1365–74. doi: 10.1111/j.1600-0854.2007.00613.x
119. Defacque H, Bos E, Garvalov B, Barret C, Roy C, Mangeat P, et al. Phosphoinositides regulate membrane-dependent actin assembly by latex

bead phagosomes. *Mol Biol Cell* (2002) 13(4):1190–202. doi: 10.1091/mbc.01-06-0314
120. Marion S, Hoffmann E, Holzer D, Le Clainche C, Martin M, Sachse M, et al. Ezrin promotes actin assembly at the phagosome membrane and regulates phago-lysosomal fusion. *Traffic* (2011) 12(4):421–37. doi: 10.1111/j.1600-0854.2011.01158.x
121. Thi EP, Lambertz U, Reiner NE. Class IA phosphatidylinositol 3-kinase p110alpha regulates phagosome maturation. *PloS One* (2012) 7(8):e43668. doi: 10.1371/journal.pone.0043668
122. Hinchliffe KA. Cellular signalling: stressing the importance of PIP3. *Curr Biol* (2001) 11(9):R371–2. doi: 10.1016/s0960-9822(01)00197-x
123. Marshall JG, Booth JW, Stambolic V, Mak T, Balla T, Schreiber AD, et al. Restricted accumulation of phosphatidylinositol 3-kinase products in a plasmalemmal subdomain during Fc gamma receptor-mediated phagocytosis. *J Cell Biol* (2001) 153(7):1369–80. doi: 10.1083/jcb.153.7.1369
124. Bohdanowicz M, Cosio G, Backer JM, Grinstein S. Class I and class III phosphoinositide 3-kinases are required for actin polymerization that propels phagosomes. *J Cell Biol* (2010) 191(5):999–1012. doi: 10.1083/jcb.201004005
125. Liebl D, Griffiths G. Transient assembly of F-actin by phagosomes delays phagosome fusion with lysosomes in cargo-overloaded macrophages. *J Cell Sci* (2009) 122(Pt 16):2935–45. doi: 10.1242/jcs.048355
126. Schlam D, Bagshaw RD, Freeman SA, Collins RF, Pawson T, Fairn GD, et al. Phosphoinositide 3-kinase enables phagocytosis of large particles by terminating actin assembly through Rac/Cdc42 GTPase-activating proteins. *Nat Commun* (2015) 6:8623. doi: 10.1038/ncomms9623
127. Dewitt S, Tian W, Hallett MB. Localised PtdIns(3,4,5)P3 or PtdIns(3,4)P2 at the phagocytic cup is required for both phagosome closure and Ca2+ signalling in HL60 neutrophils. *J Cell Sci* (2006) 119(Pt 3):443–51. doi: 10.1242/jcs.02756
128. Kjeken R, Egeberg M, Habermann A, Kuehnel M, Peyron P, Floetenmeyer M, et al. Fusion between phagosomes, early and late endosomes: a role for actin in fusion between late, but not early endocytic organelles. *Mol Biol Cell* (2004) 15 (1):345–58. doi: 10.1091/mbc.e03-05-0334
129. Gopaldass N, Patel D, Kratzke R, Dieckmann R, Hausherr S, Hagedorn M, et al. Dynamin A, Myosin IB and Abp1 couple phagosome maturation to F-actin binding. *Traffic* (2012) 13(1):120–30. doi: 10.1111/j.1600-0854.2011.01296.x
130. Jahraus A, Egeberg M, Hinner B, Habermann A, Sackman E, Pralle A, et al. ATP-dependent membrane assembly of F-actin facilitates membrane fusion. *Mol Biol Cell* (2001) 12(1):155–70. doi: 10.1091/mbc.12.1.155
131. Al-Haddad A, Shonn MA, Redlich B, Blocker A, Burkhardt JK, Yu H, et al. Myosin Va bound to phagosomes binds to F-actin and delays microtubule-dependent motility. *Mol Biol Cell* (2001) 12(9):2742–55. doi: 10.1091/mbc.12.9.2742
132. Lerm M, Brodin VP, Ruishalme I, Stendahl O, Sarndahl E. Inactivation of Cdc42 is necessary for depolymerization of phagosomal F-actin and subsequent phagosomal maturation. *J Immunol* (2007) 178(11):7357–65. doi: 10.4049/jimmunol.178.11.7357
133. Kolonko M, Geffken AC, Blumer T, Hagens K, Schaible UE, Hagedorn M. WASH-driven actin polymerization is required for efficient mycobacterial phagosome maturation arrest. *Cell Microbiol* (2014) 16(2):232–46. doi: 10.1111/cmi.12217
134. Franco IS, Shohdy N, Shuman HA. The Legionella pneumophila effector VipA is an actin nucleator that alters host cell organelle trafficking. *PloS Pathog* (2012) 8(2):e1002546. doi: 10.1371/journal.ppat.1002546
135. Lodge R, Descoteaux A. Leishmania donovani promastigotes induce periphagosomal F-actin accumulation through retention of the GTPase Cdc42. *Cell Microbiol* (2005) 7(11):1647–58. doi: 10.1111/j.1462-5822.2005.00582.x
136. Ghosh A, Tousif S, Bhattacharya D, Samuchiwal SK, Bhalla K, Tharad M, et al. Expression of the ARPC4 subunit of human Arp2/3 severely affects mycobacterium tuberculosis growth and suppresses immunogenic response in murine macrophages. *PloS One* (2013) 8(7):e69949. doi: 10.1371/journal.pone.0069949
137. Poirier MB, Fiorino C, Rajasekar TK, Harrison RE. F-actin flashes on phagosomes mechanically deform contents for efficient digestion in macrophages. *J Cell Sci* (2020) 133(12). doi: 10.1242/jcs.239384
138. Defacque H, Egeberg M, Habermann A, Diakonova M, Roy C, Mangeat P, et al. Involvement of ezrin/moesin in de novo actin assembly on phagosomal membranes. *EMBO J* (2000) 19(2):199–212. doi: 10.1093/emboj/19.2.199
139. Ho HY, Rohatgi R, Lebensohn AM, Le M, Li J, Gygi SP, et al. Toca-1 mediates Cdc42-dependent actin nucleation by activating the N-WASP-WIP complex. *Cell* (2004) 118(2):203–16. doi: 10.1016/j.cell.2004.06.027
140. Park H, Cox D. Cdc42 regulates Fc gamma receptor-mediated phagocytosis through the activation and phosphorylation of Wiskott-Aldrich syndrome protein (WASP) and neural-WASP. *Mol Biol Cell* (2009) 20(21):4500–8. doi: 10.1091/mbc.E09-03-0230
141. Akhter A, Caution K, Abu Khweek A, Tazi M, Abdulrahman BA, Abdelaziz DH, et al. Caspase-11 promotes the fusion of phagosomes harboring pathogenic bacteria with lysosomes by modulating actin polymerization. *Immunity* (2012) 37(1):35–47. doi: 10.1016/j.immuni.2012.05.001
142. Dermine JF, Duclos S, Garin J, St-Louis F, Rea S, Parton RG, et al. Flotillin-1-enriched lipid raft domains accumulate on maturing phagosomes. *J Biol Chem* (2001) 276(21):18507–12. doi: 10.1074/jbc.M101113200
143. Rozelle AL, Machesky LM, Yamamoto M, Driessens MH, Insall RH, Roth MG, et al. Phosphatidylinositol 4,5-bisphosphate induces actin-based movement of raft-enriched vesicles through WASP-Arp2/3. *Curr Biol* (2000) 10(6):311–20. doi: 10.1016/s0960-9822(00)00384-5
144. Liu W, Zhou Y, Peng T, Zhou P, Ding X, Li Z, et al. N(epsilon)-fatty acylation of multiple membrane-associated proteins by Shigella IcsB effector to modulate host function. *Nat Microbiol* (2018) 3(9):996–1009. doi: 10.1038/s41564-018-0215-6
145. Kuhn S, Bergqvist J, Gil M, Valenzuela C, Barrio L, Lebreton S, et al. Actin Assembly around the Shigella-Containing Vacuole Promotes Successful Infection. *Cell Rep* (2020) 31(6):107638. doi: 10.1016/j.celrep.2020.107638
146. Forgac M. Vacuolar ATPases: rotary proton pumps in physiology and pathophysiology. *Nat Rev Mol Cell Biol* (2007) 8(11):917–29. doi: 10.1038/nrm2272
147. Fratti RA, Chua J, Vergne I, Deretic V. Mycobacterium tuberculosis glycosylated phosphatidylinositol causes phagosome maturation arrest. *Proc Natl Acad Sci U S A* (2003) 100(9):5437–42. doi: 10.1073/pnas.0737613100
148. Maxson ME, Grinstein S. The vacuolar-type H(+)-ATPase at a glance - more than a proton pump. *J Cell Sci* (2014) 127(Pt 23):4987–93. doi: 10.1242/jcs.158550
149. Kinchen JM, Ravichandran KS. Phagosome maturation: going through the acid test. *Nat Rev Mol Cell Biol* (2008) 9(10):781–95. doi: 10.1038/nrm2515
150. Peters C, Bayer MJ, Buhler S, Andersen JS, Mann M, Mayer A. Trans-complex formation by proteolipid channels in the terminal phase of membrane fusion. *Nature* (2001) 409(6820):581–8. doi: 10.1038/35054500
151. Liegeois S, Benedetto A, Garnier JM, Schwab Y, Labouesse M. The V0-ATPase mediates apical secretion of exosomes containing Hedgehog-related proteins in Caenorhabditis elegans. *J Cell Biol* (2006) 173(6):949–61. doi: 10.1083/jcb.200511072
152. Di Giovanni J, Boudkkazi S, Mochida S, Bialowas A, Samari N, Leveque C, et al. V-ATPase membrane sector associates with synaptobrevin to modulate neurotransmitter release. *Neuron* (2010) 67(2):268–79. doi: 10.1016/j.neuron.2010.06.024
153. Hiesinger PR, Fayyazuddin A, Mehta SQ, Rosenmund T, Schulze KL, Zhai RG, et al. The v-ATPase V0 subunit a1 is required for a late step in synaptic vesicle exocytosis in Drosophila. *Cell* (2005) 121(4):607–20. doi: 10.1016/j.cell.2005.03.012
154. Peri F, Nusslein-Volhard C. Live imaging of neuronal degradation by microglia reveals a role for v0-ATPase a1 in phagosomal fusion in vivo. *Cell* (2008) 133(5):916–27. doi: 10.1016/j.cell.2008.04.037
155. Xia Y, Liu N, Xie X, Bi G, Ba H, Li L, et al. The macrophage-specific V-ATPase subunit ATP6V0D2 restricts inflammasome activation and bacterial infection by facilitating autophagosome-lysosome fusion. *Autophagy* (2019) 15(6):960–75. doi: 10.1080/15548627.2019.1569916
156. Wong D, Bach H, Sun J, Hmama Z, Av-Gay Y. Mycobacterium tuberculosis protein tyrosine phosphatase (PtpA) excludes host vacuolar-H+-ATPase to inhibit phagosome acidification. *Proc Natl Acad Sci U S A* (2011) 108 (48):19371–6. doi: 10.1073/pnas.1109201108

157. Sun-Wada GH, Tabata H, Kawamura N, Aoyama M, Wada Y. Direct recruitment of H+-ATPase from lysosomes for phagosomal acidification. *J Cell Sci* (2009) 122(Pt 14):2504–13. doi: 10.1242/jcs.050443
158. Kissing S, Hermsen C, Repnik U, Nesset CK, von Bargen K, Griffiths G, et al. Vacuolar ATPase in phagosome-lysosome fusion. *J Biol Chem* (2015) 290 (22):14166–80. doi: 10.1074/jbc.M114.628891
159. Levine B, Mizushima N, Virgin HW. Autophagy in immunity and inflammation. *Nature* (2011) 469(7330):323–35. doi: 10.1038/nature09782
160. Deretic V, Saitoh T, Akira S. Autophagy in infection, inflammation and immunity. *Nat Rev Immunol* (2013) 13(10):722–37. doi: 10.1038/nri3532
161. Hara T, Nakamura K, Matsui M, Yamamoto A, Nakahara Y, Suzuki-Migishima R, et al. Suppression of basal autophagy in neural cells causes neurodegenerative disease in mice. *Nature* (2006) 441(7095):885–9. doi: 10.1038/nature04724
162. Komatsu M, Waguri S, Chiba T, Murata S, Iwata J, Tanida I, et al. Loss of autophagy in the central nervous system causes neurodegeneration in mice. *Nature* (2006) 441(7095):880–4. doi: 10.1038/nature04723
163. Nakai A, Yamaguchi O, Takeda T, Higuchi Y, Hikoso S, Taniike M, et al. The role of autophagy in cardiomyocytes in the basal state and in response to hemodynamic stress. *Nat Med* (2007) 13(5):619–24. doi: 10.1038/nm1574
164. Matsuzawa T, Kim BH, Shenoy AR, Kamitani S, Miyake M, Macmicking JD. IFN-gamma elicits macrophage autophagy via the p38 MAPK signaling pathway. *J Immunol* (2012) 189(2):813–8. doi: 10.4049/jimmunol.1102041
165. Delgado MA, Elmaoued RA, Davis AS, Kyei G, Deretic V. Toll-like receptors control autophagy. *EMBO J* (2008) 27(7):1110–21. doi: 10.1038/emboj.2008.31
166. Shang L, Chen S, Du F, Li S, Zhao L, Wang X. Nutrient starvation elicits an acute autophagic response mediated by Ulk1 dephosphorylation and its subsequent dissociation from AMPK. *Proc Natl Acad Sci U S A* (2011) 108 (12):4788–93. doi: 10.1073/pnas.1100844108
167. Deretic V, Levine B. Autophagy, immunity, and microbial adaptations. *Cell Host Microbe* (2009) 5(6):527–49. doi: 10.1016/j.chom.2009.05.016
168. Gatica D, Lahiri V, Klionsky DJ. Cargo recognition and degradation by selective autophagy. *Nat Cell Biol* (2018) 20(3):233–42. doi: 10.1038/s41556-018-0037-z
169. Sanjuan MA, Dillon CP, Tait SW, Moshiach S, Dorsey F, Connell S, et al. Toll-like receptor signalling in macrophages links the autophagy pathway to phagocytosis. *Nature* (2007) 450(7173):1253–7. doi: 10.1038/nature06421
170. Tam JM, Mansour MK, Khan NS, Seward M, Puranam S, Tanne A, et al. Dectin-1-dependent LC3 recruitment to phagosomes enhances fungicidal activity in macrophages. *J Infect Dis* (2014) 210(11):1844–54. doi: 10.1093/infdis/jiu290
171. Huang J, Canadien V, Lam GY, Steinberg BE, Dinauer MC, Magalhaes MA, et al. Activation of antibacterial autophagy by NADPH oxidases. *Proc Natl Acad Sci U S A* (2009) 106(15):6226–31. doi: 10.1073/pnas.0811045106
172. Watson RO, Bell SL, MacDuff DA, Kimmey JM, Diner EJ, Olivas J, et al. The Cytosolic Sensor cGAS Detects Mycobacterium tuberculosis DNA to Induce Type I Interferons and Activate Autophagy. *Cell Host Microbe* (2015) 17 (6):811–9. doi: 10.1016/j.chom.2015.05.004
173. Manzanillo PS, Ayres JS, Watson RO, Collins AC, Souza G, Rae CS, et al. The ubiquitin ligase parkin mediates resistance to intracellular pathogens. *Nature* (2013) 501(7468):512–6. doi: 10.1038/nature12566
174. Franco LH, Nair VR, Scharn CR, Xavier RJ, Torrealba JR, Shiloh MU, et al. The Ubiquitin Ligase Smurf1 Functions in Selective Autophagy of Mycobacterium tuberculosis and Anti-tuberculous Host Defense. *Cell Host Microbe* (2017) 22(3):421–3. doi: 10.1016/j.chom.2017.08.005
175. Gutierrez MG, Master SS, Singh SB, Taylor GA, Colombo MI, Deretic V. Autophagy is a defense mechanism inhibiting BCG and Mycobacterium tuberculosis survival in infected macrophages. *Cell* (2004) 119(6):753–66. doi: 10.1016/j.cell.2004.11.038
176. Besteiro S. The role of host autophagy machinery in controlling Toxoplasma infection. *Virulence* (2019) 10(1):438–47. doi: 10.1080/21505594.2018.1518102
177. Andrade RM, Wessendarp M, Gubbels MJ, Striepen B, Subauste CS. CD40 induces macrophage anti-Toxoplasma gondii activity by triggering autophagy-dependent fusion of pathogen-containing vacuoles and lysosomes. *J Clin Invest* (2006) 116(9):2366–77. doi: 10.1172/JCI28796
178. Muniz-Feliciano L, Van Grol J, Portillo JA, Liew L, Liu B, Carlin CR, et al. Toxoplasma gondii-induced activation of EGFR prevents autophagy protein-mediated killing of the parasite. *PloS Pathog* (2013) 9(12):e1003809. doi: 10.1371/journal.ppat.1003809
179. Choi J, Park S, Biering SB, Selleck E, Liu CY, Zhang X, et al. The parasitophorous vacuole membrane of Toxoplasma gondii is targeted for disruption by ubiquitin-like conjugation systems of autophagy. *Immunity* (2014) 40(6):924–35. doi: 10.1016/j.immuni.2014.05.006
180. Sasai M, Sakaguchi N, Ma JS, Nakamura S, Kawabata T, Bando H, et al. Essential role for GABARAP autophagy proteins in interferon-inducible GTPase-mediated host defense. *Nat Immunol* (2017) 18(8):899–910. doi: 10.1038/ni.3767
181. Tiwari S, Choi HP, Matsuzawa T, Pypaert M, MacMicking JD. Targeting of the GTPase Irgm1 to the phagosomal membrane via PtdIns(3,4)P(2) and PtdIns(3,4,5)P(3) promotes immunity to mycobacteria. *Nat Immunol* (2009) 10(8):907–17. doi: 10.1038/ni.1759
182. MacMicking JD, Taylor GA, McKinney JD. Immune control of tuberculosis by IFN-gamma-inducible LRG-47. *Science* (2003) 302(5645):654–9. doi: 10.1126/science.1088063
183. Dong H, Jing W, Runpeng Z, Xuewei X, Min M, Ru C, et al. ESAT6 inhibits autophagy flux and promotes BCG proliferation through MTOR. *Biochem Biophys Res Commun* (2016) 477(2):195–201. doi: 10.1016/j.bbrc.2016.06.042
184. Hu D, Wu J, Wang W, Mu M, Zhao R, Xu X, et al. Autophagy regulation revealed by SapM-induced block of autophagosome-lysosome fusion via binding RAB7. *Biochem Biophys Res Commun* (2015) 461(2):401–7. doi: 10.1016/j.bbrc.2015.04.051
185. Zulauf KE, Sullivan JT, Braunstein M. The SecA2 pathway of Mycobacterium tuberculosis exports effectors that work in concert to arrest phagosome and autophagosome maturation. *PloS Pathog* (2018) 14(4):e1007011. doi: 10.1371/journal.ppat.1007011
186. Vergne I, Chua J, Lee HH, Lucas M, Belisle J, Deretic V. Mechanism of phagolysosome biogenesis block by viable Mycobacterium tuberculosis. *Proc Natl Acad Sci U S A* (2005) 102(11):4033–8. doi: 10.1073/pnas.0409716102
187. Dortet L, Mostowy S, Samba-Louaka A, Gouin E, Nahori MA, Wiemer EA, et al. Recruitment of the major vault protein by InlK: a Listeria monocytogenes strategy to avoid autophagy. *PloS Pathog* (2011) 7(8): e1002168. doi: 10.1371/journal.ppat.1002168
188. Martinez J, Malireddi RK, Lu Q, Cunha LD, Pelletier S, Gingras S, et al. Molecular characterization of LC3-associated phagocytosis reveals distinct roles for Rubicon, NOX2 and autophagy proteins. *Nat Cell Biol* (2015) 17 (7):893–906. doi: 10.1038/ncb3192
189. Wong SW, Sil P, Martinez J. Rubicon: LC3-associated phagocytosis and beyond. *FEBS J* (2018) 285(8):1379–88. doi: 10.1111/febs.14354
190. Gluschko A, Herb M, Wiegmann K, Krut O, Neiss WF, Utermohlen O, et al. The beta2 Integrin Mac-1 Induces Protective LC3-Associated Phagocytosis of Listeria monocytogenes. *Cell Host Microbe* (2018) 23(3):324–37 e5. doi: 10.1016/j.chom.2018.01.018
191. Hubber A, Kubori T, Coban C, Matsuzawa T, Ogawa M, Kawabata T, et al. Bacterial secretion system skews the fate of Legionella-containing vacuoles towards LC3-associated phagocytosis. *Sci Rep* (2017) 7:44795. doi: 10.1038/srep44795
192. Herb M, Gluschko A, Schramm M. LC3-associated phagocytosis - The highway to hell for phagocytosed microbes. *Semin Cell Dev Biol* (2020) 101:68–76. doi: 10.1016/j.semcdb.2019.04.016
193. Koster S, Upadhyay S, Chandra P, Papavinasasundaram K, Yang G, Hassan A, et al. Mycobacterium tuberculosis is protected from NADPH oxidase and LC3-associated phagocytosis by the LCP protein CpsA. *Proc Natl Acad Sci U S A* (2017) 114(41):E8711–E20. doi: 10.1073/pnas.1707792114
194. Matte C, Casgrain PA, Seguin O, Moradin N, Hong WJ, Descoteaux A. Leishmania major Promastigotes Evade LC3-Associated Phagocytosis through the Action of GP63. *PloS Pathog* (2016) 12(6):e1005690. doi: 10.1371/journal.ppat.1005690
195. Kyrmizi I, Ferreira H, Carvalho A, Figueroa JAL, Zarmpas P, Cunha C, et al. Calcium sequestration by fungal melanin inhibits calcium-calmodulin signalling to prevent LC3-associated phagocytosis. *Nat Microbiol* (2018) 3 (7):791–803. doi: 10.1038/s41564-018-0167-x

196. Cemma M, Grinstein S, Brumell JH. Autophagy proteins are not universally required for phagosome maturation. *Autophagy* (2016) 12(9):1440–6. doi: 10.1080/15548627.2016.1191724
197. Westman J, Walpole GFW, Kasper L, Xue BY, Elshafee O, Hube B, et al. Lysosome Fusion Maintains Phagosome Integrity during Fungal Infection. *Cell Host Microbe* (2020) 28(6):798–812 e6. doi: 10.1016/j.chom.2020.09.004
198. Romao S, Gasser N, Becker AC, Guhl B, Bajagic M, Vanoaica D, et al. Autophagy proteins stabilize pathogen-containing phagosomes for prolonged MHC II antigen processing. *J Cell Biol* (2013) 203(5):757–66. doi: 10.1083/jcb.201308173
199. Khobrekar NV, Quintremil S, Dantas TJ, Vallee RB. The Dynein Adaptor RILP Controls Neuronal Autophagosome Biogenesis, Transport, and Clearance. *Dev Cell* (2020) 53(2):141–53 e4. doi: 10.1016/j.devcel.2020.03.011
200. McEwan DG, Popovic D, Gubas A, Terawaki S, Suzuki H, Stadel D, et al. PLEKHM1 regulates autophagosome-lysosome fusion through HOPS complex and LC3/GABARAP proteins. *Mol Cell* (2015) 57(1):39–54. doi: 10.1016/j.molcel.2014.11.006
201. Wang H, Sun HQ, Zhu X, Zhang L, Albanesi J, Levine B, et al. GABARAPs regulate PI4P-dependent autophagosome:lysosome fusion. *Proc Natl Acad Sci U S A* (2015) 112(22):7015–20. doi: 10.1073/pnas.1507263112
202. Lopez-Haber C, Levin-Konigsberg R, Zhu Y, Bi-Karchin J, Balla T, Grinstein S, et al. Phosphatidylinositol-4-kinase IIalpha licenses phagosomes for TLR4 signaling and MHC-II presentation in dendritic cells. *Proc Natl Acad Sci U S A* (2020). 117(45):28251–28262. doi: 10.1073/pnas.2001948117
203. Marino G, Niso-Santano M, Baehrecke EH, Kroemer G. Self-consumption: the interplay of autophagy and apoptosis. *Nat Rev Mol Cell Biol* (2014) 15 (2):81–94. doi: 10.1038/nrm3735
204. Martinez J, Almendinger J, Oberst A, Ness R, Dillon CP, Fitzgerald P, et al. Microtubule-associated protein 1 light chain 3 alpha (LC3)-associated phagocytosis is required for the efficient clearance of dead cells. *Proc Natl Acad Sci U S A* (2011) 108(42):17396–401. doi: 10.1073/pnas.1113421108
205. Martinez J, Cunha LD, Park S, Yang M, Lu Q, Orchard R, et al. Noncanonical autophagy inhibits the autoinflammatory, lupus-like response to dying cells. *Nature* (2016) 533(7601):115–9. doi: 10.1038/nature17950
206. Zhou P, Tan YZ, Wang HJ, Li T, He T, Yu Y, et al. Cytoprotective effect of autophagy on phagocytosis of apoptotic cells by macrophages. *Exp Cell Res* (2016) 348(2):165–76. doi: 10.1016/j.yexcr.2016.09.011

Conflict of Interest: The authors declare that the research was conducted in the absence of any commercial or financial relationships that could be construed as a potential conflict of interest.

Copyright © 2021 Nguyen and Yates. This is an open-access article distributed under the terms of the Creative Commons Attribution License (CC BY). The use, distribution or reproduction in other forums is permitted, provided the original author(s) and the copyright owner(s) are credited and that the original publication in this journal is cited, in accordance with accepted academic practice. No use, distribution or reproduction is permitted which does not comply with these terms.

frontiers in Immunology

REVIEW
published: 10 March 2021
doi: 10.3389/fimmu.2021.635173

Harnessing and Enhancing Macrophage Phagocytosis for Cancer Therapy

Siqi Chen[1*†], *Seigmund W. T. Lai*[1†], *Christine E. Brown*[1,2] *and Mingye Feng*[1*]

[1] Department of Immuno-Oncology, Beckman Research Institute, City of Hope Comprehensive Cancer Center, Duarte, CA, United States, [2] Department of Hematology and Hematopoietic Cell Transplantation, City of Hope National Medical Center, Duarte, CA, United States

Cancer immunotherapy has revolutionized the paradigm for the clinical management of cancer. While FDA-approved cancer immunotherapies thus far mainly exploit the adaptive immunity for therapeutic efficacy, there is a growing appreciation for the importance of innate immunity in tumor cell surveillance and eradication. The past decade has witnessed macrophages being thrust into the spotlight as critical effectors of an innate anti-tumor response. Promising evidence from preclinical and clinical studies have established targeting macrophage phagocytosis as an effective therapeutic strategy, either alone or in combination with other therapeutic moieties. Here, we review the recent translational advances in harnessing macrophage phagocytosis as a pivotal therapeutic effort in cancer treatment. In addition, this review emphasizes phagocytosis checkpoint blockade and the use of nanoparticles as effective strategies to potentiate macrophages for phagocytosis. We also highlight chimeric antigen receptor macrophages as a next-generation therapeutic modality linking the closely intertwined innate and adaptive immunity to induce efficacious anti-tumor immune responses.

Keywords: macrophage, cancer immunotherapy, phagocytosis, antibody, chimeric antigen receptor (CAR), nanoparticle

OPEN ACCESS

Edited by:
Johnathan Canton, Francis Crick Institute, United Kingdom

Reviewed by:
Meghan Morrissey, University of California, Santa Barbara, United States
Edwin Bremer, University Medical Center Groningen, Netherlands

***Correspondence:**
Siqi Chen
siqchen@coh.org
Mingye Feng
mfeng@coh.org

[†]*These authors have contributed equally to this work*

Specialty section:
This article was submitted to Molecular Innate Immunity, a section of the journal Frontiers in Immunology

Received: *29 November 2020*
Accepted: *18 January 2021*
Published: *10 March 2021*

Citation:
Chen S, Lai SWT, Brown CE and Feng M (2021) Harnessing and Enhancing Macrophage Phagocytosis for Cancer Therapy. Front. Immunol. 12:635173. doi: 10.3389/fimmu.2021.635173

INTRODUCTION

Immunotherapy has had a long-standing history in the fight against cancer, with its early beginnings in the 19th century with Coley's toxin (1). Up until now, about 40 biologics have been approved by the U.S. Food and Drug Administration (FDA) for patient use, with approximately 4,000 being actively investigated in clinical trials globally (2, 3). These modalities include immunomodulators (e.g., antibodies, antibody conjugates, cytokines, and immune agonists), vaccines, oncolytic viruses, and cell-based therapies (e.g., chimeric antigen receptor (CAR) T cell therapy) (2). As the exploration of novel immunotherapeutic targets and tumor-immunity interactions continue (4, 5), there is a growing interest in harnessing innate immunity to drive the development of effective immunotherapies for cancer.

The innate immune system, a major component of the body's defense system, stands as the first line of defense against infectious pathogens and malignancies to maintain the body's homeostasis (6). Innate immune cells are a diverse group consisting of effector cells such as natural killer (NK)

cells and professional antigen-presenting cells like monocytes, macrophages, and dendritic cells (DCs). These cells rely on germline-encoded pattern recognition receptors (PRRs) and other cell-surface molecules to detect pathogen-associated molecular patterns (PAMPs) on invading microbes and tumor cells to orchestrate downstream responses (7). Furthermore, the innate immune system also cross-primes the adaptive immune system, during which antigen-presenting cells (APCs) process and present antigens to naive T and B cells, resulting in their activation (6). A precursor to this bridging of innate and adaptive immunity is APC antigen capture *via* phagocytosis, a multistep process closely regulated by the interaction of phagocytes and target cells (8). To evade detection and phagocytosis by the innate immune system, tumor cells exploit techniques normal cells use to label themselves as self-cells or counteract signals that can be detected by the innate immune system (9, 10). Thus, understanding the mechanism behind phagocytosis regulation could provide a new avenue for the development of next-generation therapeutic modalities, unleashing the power of innate immune system, especially macrophages, the most prominent tumor-infiltrating innate immune cell (11, 12).

Macrophages are highly efficient phagocytes capable of engulfing materials such as debris, dead cells, or pathogens (13). Tumor associated macrophages (TAMs) are a subset of macrophages that are abundant within the tumor microenvironment (14). They have demonstrated clinical significance in that they have been shown to contribute highly to tumor progression (15), resistance to therapies (16), and tumor metastases (17). M2 polarized TAMs are generally considered to have an anti-inflammatory phenotype and foster an immunosuppressive environment and produce anti-inflammatory cytokines and chemokines to benefit tumor growth (18, 19). M1 polarized TAMs have a pro-inflammatory phenotype and maintains an environment unfavorable for the tumor via pro-inflammatory cytokines to help hamper tumor growth. Both M1 and M2 polarized TAMs are capable of phagocytosing cancer cells (20), with the former being arguably superior (21). This function is largely mediated by the recognition of foreign materials mediated by the engagement of PRRs, scavenger receptors, and Fc receptors (22). For example, ligation of Fc gamma receptors (FcγRs) on macrophages with antibody Fc fragments initiates the process of antibody-dependent cellular phagocytosis (ADCP), an important mechanism linking innate and adaptive immunity.

In this review, we highlight recent advances made in enhancing macrophage by phagocytosis by targeting different stages of this process based on distinct principles. We first summarize the effects of therapeutic antibodies in inducing anti-cancer ADCP, followed by a discussion of strategies to promote ADCP-independent phagocytosis by macrophages, including nanoparticles and phagocytosis checkpoint blockade. Lastly, we will discuss recent breakthroughs in utilizing macrophages equipped with CARs for enhanced targeting and attacking of cancer cells. We aim to elucidate strategies ligating the closely intertwined innate and adaptive immune systems to elicit a superior anti-tumor response as a pivotal and modern effort to solve an age-old disease. Furthermore, we examine the implications this has on driving forward the field of immuno-oncology by challenging the status quo of standard cancer treatment and care.

ANTIBODY-DEPENDENT CELLULAR PHAGOCYTOSIS *VIA* THERAPEUTIC ANTIBODIES

Monoclonal antibodies are an established paradigm for cancer treatment (23), achieving therapeutic efficacy not only by the antigen binding variable domains, but also the fragment crystallizable (Fc) domains. The Fc domain is bound by its corresponding immunoglobulin Fc receptor (FcR), a cell surface receptor family expressed by several hematopoietic cells, which includes IgG (FcγRI/CD64, FcγRII/CD32, and FcγRIII/CD16), IgE (FcεRI), IgA (FcαRI/CD89), IgM (FcμR), and IgA/IgM (Fcα/μR) (24, 25). Within the human FcγR family, all but FcγRIIB are immunoreceptor tyrosine-based activation motif (ITAM) bearing activating FcRs that activate upon binding to IgGs *via* multimerization of intracellular ITAM domains (24, 26). FcγRIIB, on the other hand, is an immunoreceptor tyrosine-based inhibition motif (ITIM) bearing inhibitory FcR that dampens the activation of ITAM-bearing immune receptors (25), producing an immunosuppressive effect.

ADCP is tumoricidal, as macrophages have been shown to phagocytose antibody-opsonized tumors across various preclinical models (**Figure 1A**). For example, ADCP is a critical and clinically relevant mechanism of action for daratumumab, a human monoclonal antibody targeting CD38, a glycoprotein found on immune cells, in multiple myeloma (27). Furthermore, ADCP is one of the cytotoxic mechanisms used by rituximab, ofatumumab, ocaratuzumab, and obinutuzumab, which are human monoclonal antibodies targeting CD20, a B cell surface protein, in chronic lymphocytic leukemia (28), as well as trastuzumab, an anti-HER2 monoclonal antibody that triggers phagocytic cytotoxicity of $HER2^+$ cancer cells both *in vitro* and *in vivo* (29).

ADCP has also shown to be markedly dependent on FcγR. When transplanted with human breast tumor and B cell lymphoma xenografts, mice deficient in FcγRIIB exhibit a superior antibody-dependent cytotoxicity to tumor cells. That is, in the absence of the ITIM-bearing inhibitory Fc receptors, there is significantly more immune activation and cytotoxic effects exerted on target cells. This is in direct contrast to mice deficient in ITAM-bearing activating Fc receptors (FcγRI and FcγRIII), which results in impaired and overall inferior tumor growth inhibition upon treatment with the same antibody *in vivo* (30). This dependency on FcγR is further supported by *in vivo* experiments that demonstrate that macrophage depletion abrogates the ability for anti-CD20 antibodies to deplete B cells (31). Furthermore, colony-stimulating factor 1 (CSF-1) deficient mice with impaired macrophage development exhibit incomplete depletion of B cells upon treatment with anti-CD20

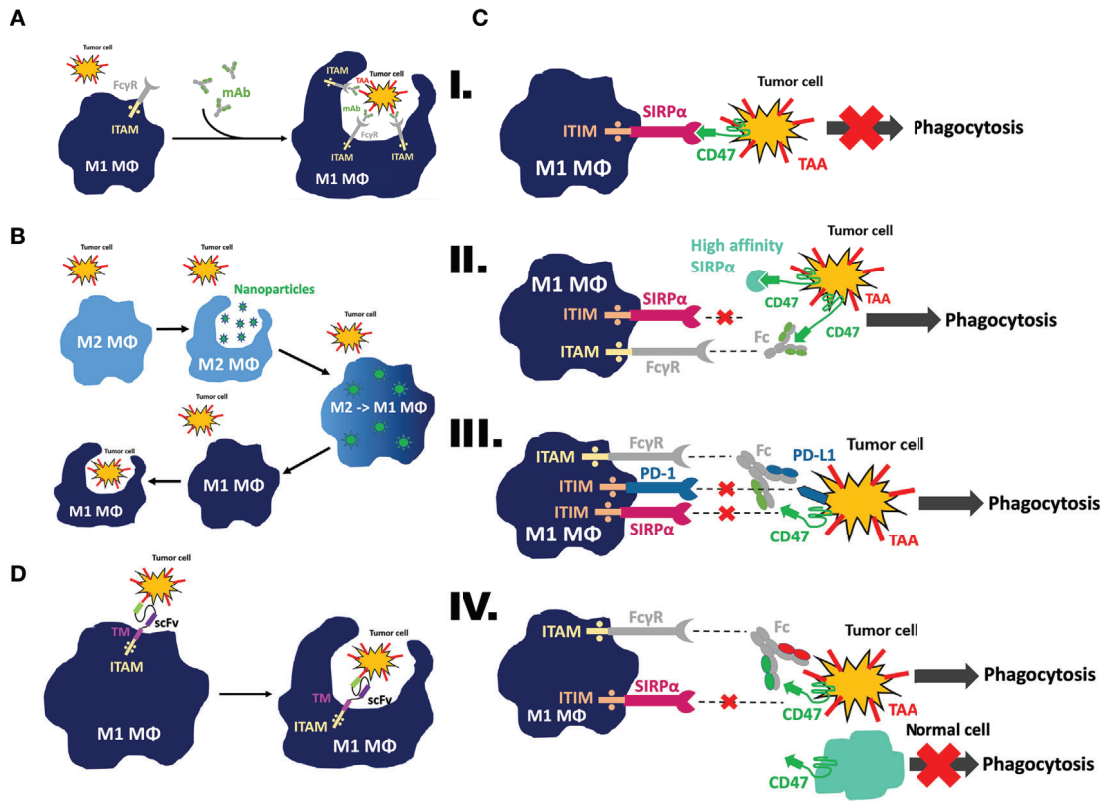

FIGURE 1 | Mechanism of action to mobilize macrophages as effector cells against tumor cells. **(A)** Antibody-dependent cellular phagocytosis (ADCP). Following treatment with mAbs targeting tumor-associated antigens, Fc gamma receptors on macrophages will recognize the Fc domain of the antibody and trigger downstream activation of the immunoreceptor tyrosine-based activation motif (ITAM) to cause phagocytosis of the tumor cell. **(B)** Nanoparticle-mediated reeducation of M2 tumor associated macrophages (TAMs) into M1 TAMs. Nanoparticles will be recognized as foreign material and engulfed by M2 TAMs. Once this occurs, their contents will be released into the cytosol and trigger polarization of the macrophage away from the M2 pro-tumor phenotype toward the M1 anti-tumor phenotype. This process retrains the macrophage to perform phagocytosis on tumor cells. **(C)** CD47/SIRPα phagocytosis checkpoint blockade. I. Upon binding of CD47 on the tumor cell to SIRPα on the macrophage, an immunoreceptor tyrosine-based inhibition motif (ITIM) becomes activated, sparing the tumor cell from phagocytosis. II. Upon binding of the high affinity SIRPα fusion protein or anti-CD47 mAbs to CD47 on the tumor cells, or binding of anti-SIRPα mAbs to SIRPα on macrophages, the CD47/SIRPα axis is blocked and phagocytosis is restored. III. When a bispecific antibody is used, macrophage SIRPα and PD-1 ITIM activation is inhibited by a bispecific anti-CD47/PD-L1 antibody targeting the tumor cells, preventing the ligands from binding to its receptors; IV. In another scenario, the specificity of CD47 blockade is reinforced by dual-targeting of CD47 and tumor-associated antigen *via* a CD47/TAA bispecific antibody, therefore sparing normal tissue cells expressing CD47 but not TAA; the Fc region on the antibody is recognized by the FcγR on the macrophage, activating its immunoreceptor tyrosine-based activation motif (ITAM) and subsequently triggering phagocytosis of the tumor cell. **(D)** CAR-macrophages demonstrate enhanced phagocytic ability and tumor targeting specificity. When fitted with a CAR construct, macrophages are able to recognize tumor cells *via* their scFv region and trigger phagocytosis of the tumor cell. This occurs at a higher specificity and efficacy due to the CAR construct conferring increased tumor recognition capability to the macrophage.

antibodies, while T or natural killer (NK) cells depletion had no impact on B cell clearance (31), emphasizing the importance of FcγR to propagate macrophage mediated ADCP.

Not only are macrophages professional phagocytes, they are antigen presenting cells as well. Thus, following ADCP of target cells, phagosomes containing tumor cells fuse with lysosomes for degradation, and tumor-derived antigen peptides are trafficked to major histocompatibility complexes (MHCs). This allows for the cross-presentation, activation, and priming of T cells (32). The breakdown of phagocytosed target cells within the phagosome often releases a significant amount of PAMPs. Nucleic acid sensors toll-like receptor 7 (TLR7), toll-like receptor 9 (TLR9), absent in melanoma 2 inflammasome (AIM2), and cyclic GMP-AMP synthase (cGAS) have been implicated in PAMP detection, subsequently activating inflammatory pathway cascades and causing the production and release of pro-inflammatory cytokines such as type I interferons, IL-1β, IL-6, and IL-12 (33–35).

Multiple lines of evidence have suggested that the inflammatory biological events in macrophages occur following ADCP. Interestingly, a recent study demonstrated that ADCP did not lead to an inflamed tumor microenvironment, but an immunosuppressive one for NK cells and CD8+ cytotoxic T cells *via* upregulation of PD-L1 and IDO expression by tumor-associated macrophages (34). Admittedly, this phenomenon has thus far only been reported in breast cancers opsonized by Trastuzumab, and therefore warrants further investigation. Beyond this, it has also been reported that upon phagocytosis

of Herceptin-opsonized HER2+ breast cancer tumor cells, AIM2 in tumor-associated macrophages is recruited and activated upon detection of tumoral DNA. This results in the cleavage of the IL-1β precursor and the release of bioactive IL-1β, stimulating the upregulation of PD-L1 and IDO in macrophages. Essentially, this phenomenon effectively inhibits antibody-dependent cellular cytotoxicity (ADCC) *via* NK cells and CD8+ cytotoxic T cells, but is rescued *via* PD-L1 and IDO blockade in addition to an anti-HER2 antibody (34).

Ultimately, the conclusion of these studies support the rationale of utilizing therapeutic strategies developed from a deeper understanding of macrophage immunology, either alone or in combination with standard of care therapeutic modalities, to create a more efficacious and favorable anti-tumor outcome. There is a dynamic interaction between macrophages and cancer cells during which macrophages detect and target cancer cells *via* the recognition of "eat me" signals which in many cases are exposed on cancer cells due to their intrinsic oncogenic stresses (36–38). On the other hand, tumor cells could utilize additional layers of "don't eat me" signals, passing as self-cells, deceiving phagocytes to evade phagocytosis (36–38). Priming macrophages to enhance their ability in recognizing and targeting cancer cells, and/or blocking negative checkpoints or their ligands that transduce inhibitory signaling for phagocytosis have become attractive strategies for inducing the robust tumoricidal functions of macrophages (39). Moreover, the adoptive transfer of macrophages, especially *in vitro* tailored macrophages, to replenish tumor-infiltrating effector cells emerges as a novel avenue to boost tumor phagocytosis (40).

PHAGOCYTOSIS CHECKPOINT BLOCKADE

Although the tumoricidal impact of ADCP is well-established, the complex relationship between tumors and macrophages has obscured the potential for harnessing tumor-associated macrophages as effector cells (18). Recent breakthroughs have highlighted phagocytosis checkpoint axes which can be targeted to induce the anti-cancer functions of macrophages, such as the CD47-SIRPα phagocytosis axis (41), PD1-PDL1 axis (10), MHC I–LILRB1 axis (42), and CD24–Siglec-10 axis (43). While antagonizing these phagocytosis checkpoints induces phagocytosis, the CD47-SIRPα axis is not only the best studied phagocytosis checkpoint, but also the only one with multiple therapeutic biologics entering clinical phase investigations with promising early-stage results.

CD47, also known as integrin-associated protein (IAP), is a ubiquitously expressed surface protein comprised of a long N-terminal extracellular domain, five transmembrane domains, and a short cytosolic tail (44). CD47 interacts with its binding partner, signal regulatory protein α (SIRPα), *via* its IgV-like domain with the N-terminal IgV-like domain of SIRPα (36). The CD47-SIRPα binding leads to the phosphorylation of two SIRPα intracellular ITIMs (45). Phosphorylated tyrosines in ITIMs recruit and activate SHP-1 and SHP-2, leading to the dephosphorylation of many proteins, including myosin IIA and paxillin (46). Activated SHP-1 and SHP-2, following CD47/SIRPα ligation at the phagocytosis synaptic interface, prevent integrin activation, as demonstrated by a recent study (47). As a result, cytoskeleton rearrangement is subsequently inhibited, and phagocytosis of target cells fails as well (**Figure 1C–I**). Antagonistic monoclonal antibodies are able to disrupt the binding of tumoral CD47 with SIRPα expressed on myeloid lineage cells, such as macrophages, dendritic cells, and neutrophils (41). Upon this blockade, the phagocytosis inhibition signal conferred by SIRPα is reversed, restoring phagocytic ability.

By exploiting this unique feature of CD47, it thus is an attractive therapeutic target to be used in clinical practice. As the most well-known anti-phagocytic signal, there have been and currently are a plethora of studies into using anti-CD47 targeting either as a standalone therapy, in combination with chemotherapy or to augment existing ADCP-inducing antibodies for example (48–50). Single agent therapies involving CD47-SIRPα axis blockade have been extensively discussed below. Studies have demonstrated that CD47 blockade synergizes with chemotherapy, radiotherapy (51), or ADCP, such as when in combination with Azacitidine (52), with anti-HER2 Trastuzumab (53), or with anti-CD20 Rituximab (54). It has also been reported that CD47 blockade not only mobilizes macrophages, but also activates dendritic cells, triggering phagocytosis of target cells and cross-presentation to the adaptive immune system (55, 56). Taken together, a wide array *in vitro* and *in vivo* studies have reinforced and supported the appealing therapeutic promise of exploiting CD47 blockade as a meaningful clinical practice to look toward.

Currently, the CD47-SIRPα axis is one of the most sought-after phagocytosis checkpoints in anti-tumor therapeutic development (**Figure 1C–II**) (57, 58). Multiple therapeutic biologicals designed to target CD47-SIRPα axis are now under extensive investigation in different developmental phases (36). A selection of such therapeutics targeting the CD47-SIRPα checkpoint currently in clinical trials has been summarized and compiled in **Table 1**. As of writing, the most advanced biologic is magrolimab, a humanized anti-CD47 monoclonal antibody (59), formally known as hu5F9-G4 (60–62). Magrolimab was the first-in-class therapeutic antibody, followed by many, to demonstrate that tumor-associated macrophages can be weaponized against tumor cells by blocking a phagocytosis checkpoint. Although magrolimab is generally well-tolerated in human clinical trials, anemia caused by on-target off-tumor binding of CD47 expressed on erythrocytes was a common treatment-related side effect (63). Given the wide therapeutic potential of anti-CD47 monoclonal antibody, one that effectively block the CD47 on tumor cells while sparing erythrocytes would be desirable (64). It is worth noting that the blockade of tumoral CD47 *via* a functional monoclonal antibody does not necessarily bring about hemagglutination, suggesting that anemia is not an unavoidable toxicity (65). To resolve this, a "priming dose"

TABLE 1 | Current clinical trials involving CD47 blockade.

NCT Trial Identifier*	Drug Name	Target Disease(s)	Treatment Type	Current Phase	Status
NCT04435691	Magrolimab (Hu5F9-G4)	Recurrent acute myeloid leukemia Refractory acute myeloid leukemia	With azacitidine With venetoclax	Phase 1 Phase 2	Recruiting
NCT04541017		T-cell lymphoma	With mogamulizumab	Phase 1	Not yet recruiting
NCT02953509		Relapsed/Refractory B-cell Non-Hodgkin's Lymphoma	With rituximab or with rituximab and chemotherapy	Phase 1/2	Recruiting
NCT03248479		Hematological Malignancies	Alone and with azacitidine	Phase 1	Recruiting
NCT04599634		Relapsed and Refractory Indolent B-cell Malignancies	With obinutuzumab and venetoclax	Phase 1	Not yet recruiting
NCT04435691		Acute myeloid leukemia	With azacitidine and venetoclax	Phase 1/2	Recruiting
NCT03869190		Advanced/Metastatic ureothelial carcinoma	With multiple different immunotherapies	Phase 1/2	Recruiting
NCT04313881		Myelodysplastic syndrome (MDS)	With azacitidine	Phase 3	Recruiting
NCT02663518	TTI-621	Hematological malignancies and solid tumors	Alone or with either rituximab or nivolumab	Phase 1	Recruiting
NCT03530683	TTI-622	Advanced relapsed/refractory lymphoma or myeloma	Alone or with either rituximab, PD-1 inhibitors, or proteasome inhibitors	Phase 1	Recruiting
NCT02367196	CC-90002	Advanced solid and hematological cancers	Alone and with rituximab	Phase 1	Active, not recruiting
NCT04485052	IBI-188	Acute myeloid leukemia	With azacitidine	Phase 1/2	Recruiting
NCT03763149		Advanced malignancies	Alone	Phase 1	Active, not recruiting
NCT04485065		High risk myelodysplastic syndrome (MDS)	With azacitidine	Phase 1	Not yet recruiting
NCT03717103		Advanced malignancies	Alone and with rituximab	Phase 1	Recruiting
NCT03834948	AO-176	Advanced solid tumors	Alone and with paclitaxel	Phase 1/2	Recruiting
NCT04445701		Relapsed/refractory multiple myeloma	Alone and with either dexamethasone or both dexamethasone and bortezomib	Phase 1/2	Recruiting
NCT04653142	BI 765063 BI 765064	Advanced solid tumors	Alone or with BI 765064 Alone or with BI 765063	Phase 1	Recruiting
NCT03990233	BI 765063	Advanced solid tumors	Alone or with BI 754091	Phase 1	Recruiting
NCT04417517	ALX-148	High risk myelodysplastic syndrome (MDS)	Alone and with azacitidine	Phase 1/2	Recruiting
NCT04675294		Advanced head/neck squamous cell carcinoma	Alone and with pembrolizumab	Phase 2	Recruiting
NCT04675333			Alone or with pembrolizumab or with pembrolizumab and chemotherapy	Phase 2	Recruiting
NCT03013218		Advanced solid tumors and lymphoma	Alone or with either pembrolizumab, trastuzumab, rituximab, pembrolizumab and 5FU and platinum, or trastuzumab and ramucirumab and paclitaxel	Phase 1	Recruiting
NCT04097769	HX009	Advanced malignant tumors	Alone	Phase 1	Recruiting
NCT04202003	TJ011133	Relapsed/refractory AML or MDS	Alone	Phase 1/2	Recruiting
NCT03934814		Relapsed/refractory advanced solid tumors and lymphoma	Alone or with either pembrolizumab or rituximab	Phase 1	Recruiting

**Information adapted from clinicaltrials.gov is current as of 10 January 2021.*

strategy was proposed and put to practice in clinics to mitigate the anemic side effects. 1 mg/kg of body weight magrolimab delivered intravenously eliminated aging red blood cells selectively while sparing 'younger' red blood cells, followed by a therapeutic dose of antibody treatment up to 45mg/kg one week later (63). In addition, tailored antibody screening and engineering was used when later anti-CD47 monoclonal antibodies were developed, such as Lemzoparlimab (TJC4), SRF231, and AO-176 (65–67), in which candidates causing hemagglutination or red blood cell (RBC) phagocytosis were pre-excluded alongside the characterization and ranking of their anti-tumor activity. As a result, these anti-CD47 antibodies maintain favorable phagocytosis of tumor cells facilitated by CD47 blocking, but exhibit a minimal to negligible amount of RBC related on-target off-tumor effect in preclinical *in vitro* and *in vivo* development (65–67). Currently, all three aforementioned anti-CD47 antibodies are in phase I clinical investigation. Interim analysis of lemzoparlimab in phase I clinical trial (NCT03934814) showed improved safety profile, escalated to 30 mg/kg without dose-limiting toxicity while achieved one confirmed PR in 30 mg/kg cohort (68).

Beyond employing antibodies to block CD47, another effective and popular approach is by using recombinant proteins (**Figure 1C–II**). These CD47 antagonist recombinant proteins are designed by first fusing an engineered fragment derived from the N-terminal V-set Ig domain of SIRPα's extracellular domain with a Fc region of an antibody. As of writing, the most advanced fusion products developed are TTI-621 (69), TTI-622 (70), and ALX-148, previously known as CV1 (60, 61). TTI-621 and TTI-622 are derived from the natural human SIRPα allelic variant V2, harboring a 12 amino-acid mutation to the allelic variant V1 commonly referred to the SIRPα. TTI-621 and TTI-622 preferably bind with tumoral CD47 with high affinity, but minimally to CD47 expressed on erythrocytes. Taking advantage of this selectivity, the two SIRPα-Fc fusion proteins achieved a biased CD47 binding selectivity, thereby facilitating phagocytosis of tumor cells while avoiding hemagglutination in patients (62, 70). It is

also worth noting that TTI-621 and TTI-622 vary only in their Fc isotype. TTI-621 is fused to a human IgG1 Fc domain, whereas TTI-622 to a human IgG4 Fc domain, therefore, differential activating signals through Fcγ receptors in addition to CD47 blockade can be generated from these two fusion proteins. However, because the overall safety profile of the effector functions of Fc fragment in conjugation to CD47 blockade was not fully determined at the time, both therapeutic biologics were developed preclinically. Both TTI-621 and TTI-622 are currently undergoing clinical trial investigation against hematologic malignancies (NCT03530683, NCT02663518)

On the other hand, ALX-148 is able to saturate CD47 receptors and easily outcompete endogenous wildtype SIRPα due to its extraordinarily high binding affinity. However, because ALX-148 is engineered based on the natural SIRPα allelic variant V1, it does not differentiate between CD47 expressed on tumor cells and RBCs, therefore anemia is still observed in clincial trials (71). The approach of using fusion proteins is largely similar to using anti-CD47 monoclonal antibodies with regard to their mechanism of action. Both arms result in a blockade of the CD47-SIRPα axis, but the fusion protein strategy may have certain advantages over the monoclonal antibody approach, such as superior binding affinity and biodistribution. Taking ALX-148 for example, generated *via* yeast display and directed evolution, its binding affinity has been enhanced to 11 pM (72), whereas hu5F9-G4, generated from hybridomas, binds with CD47 at an affinity of 8 nM, 2 magnitudes lower than ALX-148 (73). Fusion proteins weigh roughly half the molecular weight of a monoclonal antibody, therefore it is putative to be easier for fusion proteins to penetrate into solid tumors, as it has been shown that smaller molecules can infiltrate solid tumors easier through leaky capillary vessels *via* simple diffusion (74, 75). However, no evidence thus far has supported an improved biodistribution profile for ALX-148 to the best of our knowledge

However, therapeutic strategies targeting the CD47-SIRPα axis do not stop at just blocking CD47. Several functional anti-SIRPα monoclonal antibodies have been reported, serving as an antagonist for the CD47-SIRPα signal (59, 76–78). For example, the anti-SIRPα mouse antibody KWAR23 demonstrated enhanced neutrophil and macrophage anti-tumor abilities in human SIRPα knocked-in mice. When synergized with rituximab, the growth of human Burkitt's lymphoma xenograft models were profoundly inhibited (76). Humanized anti-SIRPα antibody 1H9 is the latest reported therapeutic antibody, showing broad-spectrum binding to several SIRPα variants without cross-reacting with other SIRP family members. When synergized with other therapeutic antibodies in various preclinical *in vivo* models, 1H9 demonstrates a good safety profile in non-human primates with less antigen sink compared to anti-CD47 antibody 5F9 (78). Unlike ubiquitously expressed CD47, SIRPα expression is largely restricted to cells of myeloid lineages. Because of this, specifically targeting SIRPα, as opposed to CD47, could bring about differentiated safety and efficacy of therapeutic models, therefore allowing for an improved therapeutic index.

CD47-SIRPα "don't eat me" axis blockade has been proved so far to be a great success in mobilizing tumor-associated macrophages for tumor cell eradication (57). Various improvements for therapeutic monoclonal antibodies were implemented in pursuit of better therapeutic profiles. However, monoclonal antibodies are sometimes handicapped by their mechanism of action, in that their biodistribution could lead to an unfavorable pharmacokinetic profile, bottlenecking clinical efficacy. Indeed, though CD47 blockade therapies have achieved early therapeutic efficacy in acute myeloid leukemia (AML) and myelodysplastic syndrome (MDS) patients in clinical trials (79, 80), this strategy has so far struggled in coping with solid tumors. Furthermore, it is possible that monotherapy acting on a single target is simply insufficient to overcoming the heterogeneous tumor microenvironment (81).

SYSTEMATIC ENGAGEMENT OF MACROPHAGES BY BISPECIFIC ANTIBODY

Given the increasing awareness and interest in tumor heterogeneity, bispecific antibodies have become a promising strategy to combat cancer and other diseases. In contrast to targeting T cells or NK cells through a bispecific antibody (82, 83), this principle has remained understudied in macrophages. To the best of our knowledge, the concept of approaching macrophages as tumoricidal effectors by bispecific antibody was first proposed in 2015 (13). As of writing, only a handful of bispecific antibodies designed to exploit macrophages have been reported, with even less validated in clinical trials.

Unlike T cell engagers, which require a specific antibody variable domain arm for engagement (84), macrophages can recognize and bind to the Fc fragment of an antibody *via* FcγR recognition, followed by the phagocytosis of opsonized target cells (13). This unique feature licenses bispecific antibodies adopting IgG-like formats to recruit macrophages without variable domain engagement. Therefore, variable domains of bispecific antibodies in this category can be exploited to target tumor-associated antigens and "don't eat me" signals on target cells simultaneously, harnessing the power of ADCP and phagocytosis checkpoint blockade at the same time to enhance phagocytosis of tumor cells.

The role of CD47 in immune evasion as well as therapeutic potential of CD47 blockade was first described in an AML model (9, 41). Following this study, HMBD004, an anti-CD47/CD33 bispecific antibody, was developed based on a humanized anti-CD47 antibody and anti-CD33 gemtuzumab, adapting a 1 + 1 IgG format (85). This bispecific antibody maintained CD47-SIRPα axis blockade as well as phagocytosis induction with negligible hemagglutination of erythrocytes *in vitro*. Furthermore, HMBD004 treatment of AML xenograft mice models resulted in a significant decrease in tumor burden and increased progression-free survival (85). Another notable example of a bispecific engager was noted in NI-1701, a CD47/

CD19 bispecific antibody constructed with the IgG1 isotype to elicit an ADCP response. This bispecific antibody demonstrated potent *in vitro* and *in vivo* activity across a plethora of B cell malignancy models, which rely on the co-engagement of CD47 and CD19 on B cells simultaneously to induce potent ADCP of target cells (86, 87).

With the success of the anti-CD47 antibody Magrolimab (hu5F9-G4) in combination with Rituximab in clinical trials treating B-cell non-Hodgkin's lymphoma (54, 88), a logical bispecific antibody design strategy is to combine the anti-CD47 arm with another arm targeting a B-cell specific antigen, such as CD20 (89, 90) or CD19 (86, 87, 91) (**Figure 1C–IV**). Two bispecific antibodies were recently reported adapting this strategy: one fused an anti-CD20 variable domains at the N-terminal of the variable domains of an anti-CD47 antibody (89); the other fused with the N-terminal V-set Ig domain (residues 1-118) of SIRPα to the N-terminal of the heavy-chain variable domain of an anti-CD20 antibody (90). Both bispecific antibodies exhibited improved tumor cell targeting while avoiding any on-target off-tumor effect. Furthermore, both bispecific antibodies resulted in superior *in-vivo* efficacy in Raji xenograft, conferring improved tumor growth inhibition and prolonged survival in comparison to parental antibody monotherapy and combination therapy. Furthermore, a recent study in 2017 engineered a novel bispecific antibody known as RTX-CD47 with the ability to target both CD47 signaling as well as CD20-positive cells. To accomplish this, the CD20-targeting scFV antibody fragment from rituximab was fused to a CD47-blocking scFv. *In vitro* examinations conducted in various CD20 expressing cell lines demonstrated superior macrophage-mediated phagocytosis, particularly when used in synergy with therapeutic antibodies such as cetuximab, daratumumab, alemtuzumb, rituximab, or obinutuzumab (92).

In addition to targeting tumor antigens, it is also of interest to target multiple immune checkpoints, such as CD47 and PD-L1. PD-L1 is generally overexpressed on tumor lesions, and thus targeting it could help to improve the retention of CD47/PD-L1 bispecific antibody in tumor tissue (**Figure 1C–III**). Not only is PD-L1 a canonical T cell checkpoint (93), it has also been recently identified as a macrophage "don't eat me" signal. Therefore, its blockade has been shown to reinvigorate the anti-tumor function of TAMs (10). Because of this, a CD47/PD-L1 bispecific antibody could unleash more potent macrophage phagocytosis ability. In a recent proof-of-principle study (94, 95), the pre-clinical anti-tumor efficacy of such a bispecific antibody was tested in multiple synergistic mouse models. In comparison to anti-CD47 or anti-PDL1 monotherapy or anti-CD47 + anti-PDL1 combinational therapy, simultaneously targeting both CD47 and PDL1 on tumor cells with a CD47/PDL1 bispecific antibody delivered the best tumor growth inhibition and prolonged recipient survival (94, 95). Mechanistically, the systemic delivery of the dual-targeting agent significantly increased DNA sensing, dendritic cell cross-presentation, and an anti-tumor T cell response (94, 95).

Another notable example of a bispecific antibody was constructed by researchers at Stanford University to target CD70 and SIRPα by fusing the variable domain of Vorsetuzumab, an antibody targeting CD70, a protein expressed on activated lymphocytes, to the N-terminal of corresponding variable domain of KWAR23, an anti-SIRPα antibody. The CD70/SIRPα bispecific antibody was able to target CD70-expressing cells including NHL and renal cell carcinoma and facilitate the engagement of macrophages. When compared to Vorsetuzumab + KWAR23 treatment, the CD70/SIRPα bispecific antibody demonstrated an enhanced *in-vitro* phagocytosis of target tumor cells, but there was no apparent difference in *in vivo* efficacy observed (76). This demonstrates that the bispecific antibody is able to function on a par with a combinatory treatment of both arms of the antibody separately (Vorsetuzumab + KWAR23). Given that this only requires the administration of a single biologic, it eliminates the possible confounding variable associated with balancing the administration and controlling for interactions between two separate biologics. Pharmacokinetically speaking, this would have implications warranting further study into the dosing and safety profile of such an antibody.

IMMUNO-QUIESCENT BISPECIFIC ANTIBODY

Phagocytosis is crucial for maintaining homeostasis. A bispecific antibody to bring together macrophages and phagocytosis targets would be of particular interest in cases where tissue homeostasis restoration is key, without inciting an inflammatory response. Such scenarios include but are not limited to degenerative central nervous system diseases, autoimmune diseases, and pandemics like severe acute respiratory syndrome coronavirus 2 (SARS-CoV-2).

Recently, a team at Genentech performed a proof-of-principle validation of a MerTK-agonist bispecific antibody (96). MerTK is a part of the Tyro3-Axl-MerTK family of receptor tyrosine kinases and are indispensable for maintaining tissue homeostasis. Guided phagocytosis through agonism of MerTK was shown to be inflammation-quiescent, in sharp contrast to the inflammatory nature of FcγRs-mediated phagocytosis, namely ADCP (96–98). By exploiting LALAPG mutations in Fc fragments (L234A, L235A, and P329G) to completely abolish Fc mediated effector function (99, 100), the CD20/MerTK bispecific antibody (CD20/18G7-LALAPG) has been shown to induce antigen-specific target cell phagocytosis through activation of MerTK in human macrophages with negligible production of pro-inflammatory cytokines (96). This bispecific antibody model was further engrafted with an anti-Aβ amyloid plaque arm. The Aβ/MerTK bispecific antibody, 3D6/20F5-LALAPG, elicited improved Aβ aggregate clearance by microglial cells, but not the production of inflammatory cytokines (96).

FACILITATING PHAGOCYTOSIS USING NANOPARTICLES

Seeing as ADCP is in some cases insufficient to mount an effective anti-tumor response, a potential method of invigorating the phagocytic response is using nanoparticles. The use of different nanoparticles, such as silica, carbon, iron oxide, or gold to drive macrophage polarization states has been extensively studied in literature (101). When TAMs recognize the nanoparticles as foreign, they will engulf them *via* phagocytosis, releasing the contents of the nanoparticle within the TAMs (102). Therefore, nanoparticles can be packed with drugs or contents designed to induce macrophage polarization toward a more phagocytic phenotype to reprogram them with an affinity for phagocytosis, thus making them an attractive vehicle for therapy delivery (**Figure 1B**) (101, 103, 104).

Nanoparticles are an appealing therapeutic vehicle largely due to their physical characteristics and small size (105, 106). Their appeal is further reinforced by the phenomenon of Enhanced Permeability and Retention (EPR) effect, which in tumor tissue helps to promote the accumulation and persistence of nanomedicines at the site of the tumor (107, 108). The leaky nature of the tumor vasculature allows for nanomedicines to penetrate into tumors, where the minimal lymphatic drainage and filtration facilitates their accumulation and persistence (109, 110). As of writing, there are over 200 clinical trials currently underway globally investigating the use of different nanoparticles against different cancers, primarily solid tumors (111). Patient use of several nanoparticles has already been validated and approved by the FDA (112).

However, the prospect of nanoparticles delivering drugs to specific subsets of macrophage phenotypes has been relatively understudied (113). A recently published study was among the first to engineer nanoparticles capable of preferentially targeting M2 TAMs through the delivery of nanoparticles carrying M1-polarizing transcription factors and mRNAs for interferon regulatory factor 5 (IRF5) as well as IKKB, its activating kinase (114). The delivery of both IRF5 and IKKB were able to force M2 TAMs to polarize to a pro-inflammatory state and convert to a M1 cytotoxic phenotype (114). A unique quality of this method is its method of administration *via* injection that does not trigger an immune reaction or lead to systemic toxicity in the recipient. Another innovative aspect about this study is how the authors generated the targeted mRNA delivery system to target mannose receptors on M2 macrophages. When tested *in vivo*, treatment with IRF5/IKKB NPs led to a significant regression of ovarian cancer and was able to be cleared and prolonged the lifespan of the mice (114).

This finding was supported by a later study in which researchers loaded IMD-0354, a TAM repolarization agent, into mannose-modified cationic lipid-based nanoparticles (M-IMD-CLN), and sorafenib, a kinase inhibitor used to treat cancer, into cationic lipid-based nanoparticles (SF-CLN) (115). Mannose is selectively taken up by M2 TAMs, which are characterized as highly expressing mannose receptors. Therefore, the mannose present on the nanoparticles become the ligand for M2 mannose receptors and thus enhance its active uptake by M2 TAMs, as demonstrated by the *in vivo* experiments exhibited a superior biodistribution profile and localization to the site of the tumor, eliciting TAM potent anti-tumor properties in Hepa1-6 tumor bearing mice (115). In addition to this, when M-IMD-CLN and SF-CLN are used together in junction, there appears to be a synergistic augmented anti-tumor efficacy and TAM re-polarization compared to mice treated with SF-CLN alone (115).

Later, Chen et al. further reinforced the potential for using mannose as a ligand for targeted delivery of nanoparticles to M2 TAMs by conjugating bivalent ligands for mannose receptors onto nanoparticles, effectively driving their uptake by M2 TAMs (113). This was accomplished by differentiating rat peritoneal macrophages into M1 *via* IFN-y and M2 *via* IL-4/IL-13 treatment. Markers distinguishing between resting, M1, and M2 macrophages were assessed to confirm their phenotypes. These groups of macrophages were then treated with the bivalent mannose nanoparticles and their uptake was quantified. These nanoparticles were found to have a significantly higher level of uptake in M2 macrophages, especially when compared to M1 or resting macrophages (113).

It is important to note that nanoparticles are not limited to containing only a single drug or compound to be delivered (116). Multivalent nanoparticles have been studied extensively for their potential to carry multiple drugs or compounds, thus hitting multiple targets (117, 118). For example, albumin-based nanoparticles expressing transferrin receptor binding peptide T12 and mannose were capable of not only polarizing M2 TAMs to become M1, but also remodeling the tumor microenvironment to allow for an enhanced anti-tumor response (119). Gliomas highly express transferrin receptor and albumin-binding receptor SPARC, while M2 TAMs also highly express SPARC and mannose, therefore facilitating the dual-targeting role of these nanoparticles for both gliomas and M2 TAMs. When these nanoparticles are loaded with both disulfiram/copper complex, a treatment for glioma, and regorafenib, a kinase inhibitor that repolarizes TAMs to M1, glioma proliferation was inhibited and M2 TAMs were re-programmed toward a M1 phenotype (119, 120). Thus, these studies and others provide a proof-of-principle that nanomedicines can be designed to preferentially target M2 TAMs. Future investigations could study arming these nanoparticles with drug payload with a final destination of M2 TAMs to either inactivate or reprogram them. Therefore, when considering the use of nanoparticles to facilitate and enhance macrophage-mediated phagocytosis, the following main approaches are of interest: 1) inactivating or eliminating M2 TAMs, and 2) reprogramming M2 TAMs to acquire a M1 pro-inflammatory phenotype to enhance phagocytosis.

Furthermore, a multi-functional protein calreticulin has been demonstrated as an important pro-phagocytic "eat me" signals for apoptotic cells and many types of cancer cells. In cancer cells with apoptosis induced by chemotherapeutic agents such as anthracyclines and oxliplatin, calreticulin trafficks to the cell surface, dictating a process of immunogenic cell death

(ICD) (121). ICD is characterized as an immunostimulatory process that triggers an adaptive immune response against certain epitopes of antigens, including tumor neo-epitopes (122). In addition, macrophages have been shown to be an important resource for calreticulin (123–127). Macrophages present calreticulin on their cell surface or secrete it to the extracellular media to directly label unwanted cells such as aging or malignant cells for subsequent phagocytosis. Interaction between calreticulin and asialoglycans on unwanted cells enables their recognition by macrophages and initiation of phagocytosis. A recent study demonstrated that macrophage-mediated anti-tumor immunity was found to be enhanced upon intratumoral injection of nanoparticles containing calreticulin (128). Yuan et al. designed dual-function colloidal nanoparticles capable of 1) targeting HER2, a receptor commonly expressed on cancers, and 2) promoting anti-tumor phagocytosis *via* calreticulin (129). In this case, calreticulin promotes phagocytosis of target cells by enhancing APC recognition of target cells. In junction with the HER2 targeting, engagement of this dual-function nanoparticle with APCs augments the anti-tumor response by activating both the innate and adaptive immune system with one particle (129). Effectively, these allow for a synergistic effect achieved through a combinatory therapy being delivered within a single particle that may be superior to either therapy alone. Particularly, this allows for the selective targeting of M2 TAMs to either inactivate them to remove their immunosuppression or reprogram them into a M1 phenotype to elicit anti-tumor immunity.

However, a significant barrier for using nanoparticles is the fact that despite being able extravasate and persist due to EPR, only a very small percentage (less than 1%) of injected nanoparticles are actually able to traffic and be delivered to their intended destination (130, 131). As such, this remains a critical handicap to the efficacy of using nanoparticle-based treatments in patients. It remains a challenge for the nanoparticles to be homed and actively directed to the site of the tumor, rather than rely on passive targeting (132).

A study conducted in 2019 highlighted the potential for using exosomes derived from effector CAR-T cells as they retain their anti-tumor capabilities with minimal toxicity or cytokine storm (133). This method could thus be used to mitigate the problem of poor trafficking and localization of nanoparticles to their destination. That is, the "CAR exosomes" retain the CAR expressed on their host cells, allowing these nanoparticles to maintain their parental cells' unique targeting feature (133). Conversely, rather than taking exosomes from CAR-T cells, another recent study demonstrated this phenomenon in nanoparticles coated with the cell membrane of CAR-T cells, therefore conferring them target antigen specificity similar to CAR-T cells (134). In this study, the CAR-T cell membrane coated nanoparticles demonstrated a superior tumor targeting ability compared to uncoated nanoparticles (134). Both of these findings open the door to future investigation into how to maximize nanoparticle infiltration, persistence, and targeting to overcome these barriers in order to enhance their therapeutic efficacy.

CHIMERIC ANTIGEN RECEPTOR ENGINEERED MACROPHAGES

Despite the increasing interest in CAR-T cell therapies, there has been a struggle in reproducing its therapeutic efficacy observed in hematological malignancies in solid tumors (135–137). This is heavily related to the biology of how T cells fight tumor cells, as they need to be presented with antigens, primed, trafficked to the tumor, infiltrate tumor tissue, and recognize and kill malignant cells (81, 138). However, due to the heterogeneous nature of tumor tissue and the complex immunoinhibitory tumor microenvironment, not all of these critical events can occur successfully (74, 136, 139–142).

To address these roadblocks, CAR T cell therapy has recently turned to macrophages. Macrophages are known to be abundant and actively recruited to various types of solid tumor tissue (17, 143, 144). Recruited by macrophage chemo-attractants (i.e, CCL2, MCP1, CSF-1), tumor-associated macrophages represent up to 50% of tumor-infiltrating cells, as seen in melanoma, renal cancer, and colonic carcinoma (145, 146), suggesting they may be able to efficiently infiltrate into solid tumors upon adoptive transfer. Not only this, but macrophages have a unique quality in that they have a high degree of versatility and plasticity (147), and are thus able to adapt and change in response to external stimuli or the environment (148). The abundance and plasticity of tumor associated macrophages corroborate the idea of fitting macrophages with CAR constructs, therefore conferring target antigen specificity, and promoting engineered macrophages to efficaciously target solid tumors (**Figure 1D**). However, it is worth noting here that although their plasticity may provide therapeutic versatility, it may also act as a potential pitfall. In particular, although plasticity can be a desired trait, it is only so if they skewed toward a M1 pro-inflammatory phenotype that will target the tumor. Furthermore, macrophage activation has been associated with the development of macrophage activation syndrome (MAS), characterized by a surge in pro-inflammatory cytokines, resulting in a cytokine storm (149, 150). Ultimately, this warrants further investigation to see how to prevent or mitigate these phenotypes *in vivo* to minimize unwanted side effects and enhance treatment efficacy and most importantly, patient safety.

The construction of CARs for macrophages requires similar components to that of T cells: a target binding extracellular domain adapted from an antibody, followed by a hinge sequence, a transmembrane domain connecting the extracellular domain and intracellular signaling domain (136). It is worth to keep in mind the differences of signal pathway required for T cell activation and macrophage phagocytosis when designing a CAR for macrophages. The intracellular domains of CAR-macrophages reported so far have varied from that of CAR-T cells. CD3ζ is a common intracellular domain being studied in both, while CD147, FcγR, and Megf10 have been studied more exclusively in CAR-macrophages (CAR-Ms) only, for example (40, 151, 152). Phagocytosis-oriented CAR constructs are capable of rewiring macrophages and jumpstarting phagocytosis.

Theoretically, CAR expression by macrophages would not only help the effectors to target cells, but also to circumvent the need of an "eat me" signal, to initiate phagocytosis signaling.

CURRENT STUDIES OF CAR-MACROPHAGES

Up until now, the study of utilizing CAR-Ms, has been relatively limited. A recent study by Morrissey and colleagues was among the first to provide initial evidence that CAR-engineered macrophages can promote phagocytosis. By utilizing an extracellular antibody variable fragment (ScFv) targeting CD19 as well as the CD8 transmembrane domain present in a traditional CD19 CAR-T construct, researchers were able to generate chimeric antigen receptors for phagocytosis (CAR-Ps) on murine macrophage cell line J774A.1 that successfully drove the phagocytosis of antigen-coated decoy particles in an *ex vivo* setting (151). In this study, the authors were able to test phagocytosis specificity guided only by the antigen recognition feature of the ScFv domain of the CAR construct. The authors were also able to compare the capacity of driving phagocytosis by various intracellular domains in a relatively simplified *ex vivo* assay (151).

The potential for engineering macrophages with CAR constructs was further reinforced by another study that elected to generate murine CAR-Ms specifically targeting the solid tumor antigen HER2 that utilized the intracellular signaling domain of CD147 to drive expression of matrix metalloproteinases (MMPs) in a HER2-dependent manner. To accomplish this, the authors first forced HER2 expression on 4T1 tumor cells and transduced murine macrophage cell line Raw264.7 with the HER2-147-CAR (152). From this, they were able to induce matrix MMP3 and MMP13 expression specifically upon ligation of the CAR and its antigen to remodel tumor microenvironment, increase T cell infiltration, and reduce tumor growth *in vivo* (152).

A study published earlier this year was the first to successfully generate human CAR-Ms with demonstrated functionality in both *in vitro* and *in vivo* models (40). CAR-expressing human macrophages were generated with a chimeric Ad5/F35 adenovirus (40, 153). Using CAR constructs with the CD3-ζ intracellular signaling domain and ScFvs targeting CD19, HER2, and mesothelin, the authors showed that antigen specific tumor cell killing was triggered by the CAR-transduced human macrophage line THP-1. Importantly, the authors establish that primary human macrophages can also be engineered to express a CAR to promote phagocytosis, and showed that HER2-CAR Ms exhibited dramatic *in vivo* therapeutic efficacy in various preclinical xenograft models. Interesting, transduction using Ad5/F35 adenovirus polarized human macrophages to a pro-inflammatory M1 state independent of CAR expression. Furthermore, CAR-Ms recognition of tumor cells shifted the tumor microenvironment from an anti-inflammatory one to a pro-inflammatory one, activating several interferon genes and inflammatory pathways along the way (40). Taken together, these findings suggest that CAR-Ms can both induce tumor phagocytosis, as well as reshape the tumor microenvironment to promote anti-tumor T cell responses. A Phase 1 preclinical trial (NCT04660929) investigating the safety and early-stage efficacy of HER-2 CAR-Ms is underway.

Collectively, these studies represent the first proof-of-principle validation of using CAR-M as an immunotherapeutic. CAR-Ms not only function *via* direct target cell phagocytosis, but also through vaccinal antigen cross-presentation and T cell co-stimulation (40). Macrophages have been shown to reside and persist within tissues, and certain tissue-resident macrophages are able to survive quiescently for relatively long period of time until challenged (154–156). This very feature makes CAR-Ms the ideal local sentinels for metastatic tumor cells, thus preventing tumor relapse at early metastasis stage. It is worth noting that the plasticity of macrophages endows itself the potential for application beyond tumors where inflammation is dispensable. With the proper design of CAR constructs, macrophages can be converted into immunoquiescent CAR-Ms while preserving their capacity to phagocytose, thus addressing other unmet medical challenges such as pathogen infection, autoimmune diseases, and degenerative neural diseases. Given the vast potential, CAR-Ms can transform the current landscape of cancer care and become a next-generation therapy for cancers and beyond.

CONCLUSION

The mechanisms of macrophage phagocytosis and subsequent adaptive immune cross-priming have been increasingly appreciated and studied as a crucial effector function complementing adaptive anti-tumor immune responses. Antibody-dependent cellular phagocytosis has long been extensively studied and applied in clinical settings for at least 20 years. For example, ritxuimab was the first-in class monoclonal antibody approved by the FDA in 1997. Since then, this list has expanded to include a plethora of novel antibodies of varying designs that are now approved or undergoing clinical trial evaluation. Although this exciting field of study first began with the initiation of ADCP *via* therapeutic antibodies, it has now gone on to expand into exploiting phagocytosis checkpoints and beyond to enhance therapeutic efficacy, leading to novel fields of study including: 1) using nanoparticles to engineer macrophages with enhanced phagocytic ability, 2) strategies to block self-protective signals on cancer cells, and 3) fitting CAR constructs on macrophages to confer target antigen specificity. These exciting breakthroughs have marked an important step forward as macrophage-mediated phagocytosis of cancer has begun to enter the spotlight as a promising novel cell-based therapy.

The CD47–SIRPα axis was the first phagocytosis checkpoint discovered in cancer (41), and new phagocytosis checkpoints have since been identified, such as PD1-PDL1 (10), MHC I–LILRB1 (42), and CD24–Siglec-10 (43). Phagocytosis checkpoint blockade therapies have thus far resulted in promising human trial data, such as CD47 blocking therapeutics Magrolimab in NHL and AML, or TTI-622 in lymphoma (52, 70). By the nature of different yet complementary immunological pathways mobilized upon phagocytosis checkpoint blockade, macrophage phagocytosis

proves itself as a novel and promising therapeutic tool on par with many approved treatments, such as PD-1 checkpoint blockade (157). Given the heterogeneity of solid tumor cells, and the suppressive and often immune exclusive tumor microenvironment, phagocytosis checkpoint blockade appears to be a promising starting place for effective anti-tumor innate immune responses. Whether phagocytosis checkpoint blockades can serve as a vehicle, either in the form of monoclonal antibody or bispecific antibody, to conquer solid tumors, especially hard-to-treat metastatic tumors, warrants further intense investigation.

There are also several clinical trials underway to evaluate therapies specifically targeting TAMs *via* nanoparticles. These trials and other original research studies have yielded promising data that can hopefully be applied to patients soon (158, 159). However, in order for these therapies to be optimally translated into patient use, there is much work that still needs to be done to prove TAM targeting *via* nanomedicine is feasible. Thus far, promising preliminary results suggests there is vast potential in which these nanoparticles can be applied, even beyond just targeting TAMs (116). Despite this, more proof-of-principle and validation studies need to be conducted before its use can be optimized and integrated into standard practice for cancer patient care. For example, a critical question that remains to be answered is how to optimize and maximize the number of nanoparticles that will actually traffic and localize to the tumor. As demonstrated in countless studies, despite being bolstered by EPR to enhance nanoparticle accumulation *via* leaky vasculature, only around 1% of the nanoparticles will actually make it to the site of the tumor (130, 131). This is an important first roadblock that critically needs to be overcome before expanding into the plethora of possibilities surrounding nanomedicines. Furthermore, another question of interest is how to facilitate the persistence of these nanoparticles *in vivo* such that they are not rapidly eliminated by the immune system. Even if the particles are able to overcome the low trafficking and tumor localization rate, another factor to consider is the body's immune system perceiving them as foreign threats and eliminating them before they are able to exert their therapeutic effect. To address this, it would be interesting to apply a principle studied in Deuse et al. in generating hypoimmunogenic nanoparticles that evade immune detection and elimination to allow them to persist and ensure drug delivery through the suppression of MHC I and MHC II while overexpressing anti-phagocytic signal CD47 (160). Seeing as these are major handicaps dampening the full potential and efficacy of nanomedicine-based approaches to elicit potent M1 TAM activity, there ultimately remains much work to be done to study this exciting and novel form of immunotherapy.

Last but not least, the prospect of CAR-M based immunotherapy was propelled forward by previous findings by Morrissey et al. and Zhang et al. (151, 152). The Klichinsky et al. study marked a critical breakthrough in reinforcing the efficacy of macrophage-based therapeutics against cancer (40). By fitting macrophages with a CAR construct, they leveraged the potency of macrophage-mediated phagocytosis in conjunction with target antigen specificity to elicit potent anti-cancer effects that appear to be on par with their CAR-T counterparts. Not only were they able to successfully overcome the difficulties with transducing primary macrophages, they were also able to exploit their plasticity to drive them toward a M1 phenotype while simultaneously remodeling the tumor microenvironment to be pro-inflammatory. These exciting findings are now beginning to be put to the test clinically, beginning with a CAR-M against HER2. Though the use of CAR-Ms holds great promise as an innovative immuno-oncology therapeutic avenue, there is still a need for the development of a pipeline investigating its efficacy and safety profile. As many studies have demonstrated in their CAR-T counterparts, cytokine release syndrome remains one of the main obstacles to overcome. Cytokine release syndrome is largely mediated by the activation of macrophages, triggering an overwhelming sudden release of pro-inflammatory cytokines (161). As such, investigations into the safety profile of CAR-Ms would be particularly interesting to delve into. In addition to this, another question of interest is how to design CAR constructs and strike a balance between maximizing phagocytosis signals and enhancing the CAR-M's specificity while minimizing unwanted toxicity. Collectively, this could be an emerging direction of study in this promising field.

Ultimately, recent breakthroughs in the exciting field of harnessing macrophage-mediated phagocytosis have highlighted their potential for clinical use to improve patient outcomes. With an estimated 1.8 million new cancer cases to be diagnosed and 600,000 cancer-related deaths to occur in the United States in 2020, the development of effective and innovative therapeutics is urgently needed more than ever (162). The up and coming field of immunotherapeutics has yielded a vast array of promising data and approaches for the treatment of different cancers. However, there remains much work to be done to continue the momentum and push forward the hopeful progress that has been established in preliminary work in this exciting avenue. This would be crucial for developing further therapies that bridge the innate and adaptive immune systems to benefit patients with cancer in a clinical setting. We hope this review inspires more studies to advance the work done and continue challenging the status quo of standard cancer care and treatment in order to improve patient outcomes.

AUTHOR CONTRIBUTIONS

SL, SC, and MF researched data for the article. All authors contributed to the article and approved the submitted version.

FUNDING

This work was supported by the National Cancer Institute of the National Institutes of Health K99/R00 Pathway to Independence Award K99CA201075/R00CA201075 (to MF), the Damon Runyon-Dale F. Frey Award for Breakthrough Scientists DFS-22-16 (to MF), the Margaret E. Early Medical Research Trust Grant (to MF), the V Foundation for Cancer Research V Scholar Award (V2018-012) (to MF), and the startup research funding from City of Hope (to MF).

REFERENCES

1. Coley WB. The Treatment of Malignat Tumors by Repeated Inoculations of Erysipelas. *Am J Med Sci* (1893) 105:487–510. doi: 10.1097/00000441-189305000-00001
2. Xin Yu J, Hubbard-Lucey VM, Tang J. Immuno-oncology drug development goes global. *Nat Rev Drug Discov* (2019) 18:899–900. doi: 10.1038/d41573-019-00167-9
3. Yu JX, Upadhaya S, Tatake R, Barkalow F, Hubbard-Lucey VM. Cancer cell therapies: the clinical trial landscape. *Nat Rev Drug Discov* (2020) 19:583–4. doi: 10.1038/d41573-020-00099-9
4. Wei SC, Levine JH, Cogdill AP, Zhao Y, Anang NAAS, Andrews MC, et al. Distinct Cellular Mechanisms Underlie Anti-CTLA-4 and Anti-PD-1 Checkpoint Blockade. *Cell* (2017) 170:1120–1133.e17. doi: 10.1016/j.cell.2017.07.024
5. Pardoll DM. The blockade of immune checkpoints in cancer immunotherapy. *Nat Rev Cancer* (2012) 12:252–64. doi: 10.1038/nrc3239
6. Iwasaki A, Medzhitov R. Regulation of adaptive immunity by the innate immune system. *Science (80-)* (2010) 327:291–5. doi: 10.1126/science.1183021
7. Dranoff G. Cytokines in cancer pathogenesis and cancer therapy. *Nat Rev Cancer* (2004) 4:11–22. doi: 10.1038/nrc1252
8. Jutras I, Desjardins M. Phagocytosis: At the crossroads of innate and adaptive immunity. *Annu Rev Cell Dev Biol* (2005) 21:511–27. doi: 10.1146/annurev.cellbio.20.010403.102755
9. Jaiswal S, Jamieson CHM, Pang WW, Park CY, Chao MP, Majeti R, et al. CD47 Is Upregulated on Circulating Hematopoietic Stem Cells and Leukemia Cells to Avoid Phagocytosis. *Cell* (2009) 138:271–85. doi: 10.1016/j.cell.2009.05.046
10. Gordon SR, Maute RL, Dulken BW, Hutter G, George BM, McCracken MN, et al. PD-1 expression by tumour-associated macrophages inhibits phagocytosis and tumour immunity. *Nature* (2017) 545:495–9. doi: 10.1038/nature22396
11. Noy R, Pollard JW. Tumor-Associated Macrophages: From Mechanisms to Therapy. *Immunity* (2014) 41:49–61. doi: 10.1016/j.immuni.2014.06.010
12. Cassetta L, Pollard JW. Targeting macrophages: Therapeutic approaches in cancer. *Nat Rev Drug Discov* (2018) 17:887–904. doi: 10.1038/nrd.2018.169
13. Weiskopf K, Weissman IL. Macrophages are critical effectors of antibody therapies for cancer. *MAbs* (2015) 7:303–10. doi: 10.1080/19420862.2015.1011450
14. Zhu J, Zhi Q, Zhou BP, Tao M, Liu J, Li W. The Role of Tumor Associated Macrophages in the Tumor Microenvironment: Mechanism and Functions. *Anticancer Agents Med Chem* (2016) 16:1133–41. doi: 10.2174/1871520616666160520112622
15. Komohara Y, Jinushi M, Takeya M. Clinical significance of macrophage heterogeneity in human malignant tumors. *Cancer Sci* (2014) 105:1–8. doi: 10.1111/cas.12314
16. Vitale I, Manic G, Coussens LM, Kroemer G, Galluzzi L. Macrophages and Metabolism in the Tumor Microenvironment. *Cell Metab* (2019) 30:36–50. doi: 10.1016/j.cmet.2019.06.001
17. Ruffell B, Coussens LM. Macrophages and therapeutic resistance in cancer. *Cancer Cell* (2015) 27:462–72. doi: 10.1016/j.ccell.2015.02.015
18. Guerriero JL. Macrophages: The Road Less Traveled, Changing Anticancer Therapy. *Trends Mol Med* (2018) 24:472–89. doi: 10.1016/j.molmed.2018.03.006
19. Lin Y, Xu J, Lan H. Tumor-associated macrophages in tumor metastasis: biological roles and clinical therapeutic applications. *J Hematol Oncol* (2019) 12:76. doi: 10.1186/s13045-019-0760-3
20. Atri C, Guerfali FZ, Laouini D. Role of human macrophage polarization in inflammation during infectious diseases. *Int J Mol Sci* (2018) 19:1801. doi: 10.3390/ijms19061801
21. Tarique AA, Logan J, Thomas E, Holt PG, Sly PD, Fantino E. Phenotypic, functional, and plasticity features of classical and alternatively activated human macrophages. *Am J Respir Cell Mol Biol* (2015) 53:676–88. doi: 10.1165/rcmb.2015-0012OC
22. Gordon S. Pattern recognition receptors: Doubling up for the innate immune response. *Cell* (2002) 111:927–30. doi: 10.1016/S0092-8674(02)01201-1
23. Scott AM, Wolchok JD, Old LJ. Antibody therapy of cancer. *Nat Rev Cancer* (2012) 12:278–87. doi: 10.1038/nrc3236
24. Nimmerjahn F, Ravetch JV. Fcγ receptors as regulators of immune responses. *Nat Rev Immunol* (2008) 8:34–47. doi: 10.1038/nri2206
25. Mkaddem SB, Benhamou M, Monteiro RC. Understanding Fc receptor involvement in inflammatory diseases: From mechanisms to new therapeutic tools. *Front Immunol* (2019) 10:811. doi: 10.3389/fimmu.2019.00811
26. Daëron M. Fc receptor biology. *Annu Rev Immunol* (1997) 15:203–34. doi: 10.1146/annurev.immunol.15.1.203
27. Overdijk MB, Verploegen S, Bögels M, Van Egmond M, Lammerts Van Bueren JJ, Mutis T, et al. Antibody-mediated phagocytosis contributes to the anti-tumor activity of the therapeutic antibody daratumumab in lymphoma and multiple myeloma. *MAbs* (2015) 7:311–20. doi: 10.1080/19420862.2015.1007813
28. VanDerMeid KR, Elliott MR, Baran AM, Barr PM, Chu CC, Zent CS. Cellular cytotoxicity of next-generation CD20 monoclonal antibodies. *Cancer Immunol Res* (2018) 6:1150–60. doi: 10.1158/2326-6066.CIR-18-0319
29. Shi Y, Fan X, Deng H, Brezski RJ, Rycyzyn M, Jordan RE, et al. Trastuzumab Triggers Phagocytic Killing of High HER2 Cancer Cells In Vitro and In Vivo by Interaction with Fcγ Receptors on Macrophages. *J Immunol* (2015) 194:4379–86. doi: 10.4049/jimmunol.1402891
30. Clynes RA, Towers TL, Presta LG, Ravetch JV. Inhibitory Fc receptors modulate in vivo cytoxicity against tumor targets. *Nat Med* (2000) 6:443–6. doi: 10.1038/74704
31. Uchida J, Hamaguchi Y, Oliver JA, Ravetch JV, Poe JC, Haas KM, et al. The innate mononuclear phagocyte network depletes B lymphocytes through Fc receptor-dependent mechanisms during anti-CD20 antibody immunotherapy. *J Exp Med* (2004) 199:1659–69. doi: 10.1084/jem.20040119
32. Tseng D, Volkmer JP, Willingham SB, Contreras-Trujillo H, Fathman JW, Fernhoff NB, et al. Anti-CD47 antibody-mediated phagocytosis of cancer by macrophages primes an effective antitumor T-cell response. *Proc Natl Acad Sci USA* (2013) 110:11103–8. doi: 10.1073/pnas.1305569110
33. Aderem A, Underhill DM. Mechanisms of phagocytosis in macrophages. *Annu Rev Immunol* (1999) 17:593–623. doi: 10.1146/annurev.immunol.17.1.593
34. Su S, Zhao J, Xing Y, Zhang X, Liu J, Ouyang Q, et al. Immune Checkpoint Inhibition Overcomes ADCP-Induced Immunosuppression by Macrophages. *Cell* (2018) 175:442–457.e23. doi: 10.1016/j.cell.2018.09.007
35. MacKenzie KJ, Carroll P, Martin CA, Murina O, Fluteau A, Simpson DJ, et al. CGAS surveillance of micronuclei links genome instability to innate immunity. *Nature* (2017) 548:461–5. doi: 10.1038/nature23449
36. Feng M, Jiang W, Kim BYSS, Zhang CC, Fu Y-XX, Weissman IL. Phagocytosis checkpoints as new targets for cancer immunotherapy. *Nat Rev Cancer* (2019) 19:568–86. doi: 10.1038/s41568-019-0183-z
37. Chao MP, Majeti R, Weissman IL. Programmed cell removal: A new obstacle in the road to developing cancer. *Nat Rev Cancer* (2012) 12:58–67. doi: 10.1038/nrc3171
38. Jaiswal S, Chao MP, Majeti R, Weissman IL. Macrophages as mediators of tumor immunosurveillance. *Trends Immunol* (2010) 31:212–9. doi: 10.1016/j.it.2010.04.001
39. Mantovani A, Longo DL. Macrophage checkpoint blockade in cancer ' Back to the future. *N Engl J Med* (2018) 379:1780–2. doi: 10.1056/NEJMe1811699
40. Klichinsky M, Ruella M, Shestova O, Lu XM, Best A, Zeeman M, et al. Human chimeric antigen receptor macrophages for cancer immunotherapy. *Nat Biotechnol* (2020) 38:947–53. doi: 10.1038/s41587-020-0462-y
41. Majeti R, Chao MP, Alizadeh AA, Pang WW, Jaiswal S, Gibbs KD, et al. CD47 Is an Adverse Prognostic Factor and Therapeutic Antibody Target on Human Acute Myeloid Leukemia Stem Cells. *Cell* (2009) 138:286–99. doi: 10.1016/j.cell.2009.05.045
42. Barkal AA, Weiskopf K, Kao KS, Gordon SR, Rosental B, Yiu YY, et al. Engagement of MHC class i by the inhibitory receptor LILRB1 suppresses macrophages and is a target of cancer immunotherapy article. *Nat Immunol* (2018) 19:76–84. doi: 10.1038/s41590-017-0004-z
43. Barkal AA, Brewer RE, Markovic M, Kowarsky M, Barkal SA, Zaro BW, et al. CD24 signalling through macrophage Siglec-10 is a target for cancer immunotherapy. *Nature* (2019) 572:392–6. doi: 10.1038/s41586-019-1456-0
44. Brown EJ, Frazier WA. Integrin-associated protein (CD47) and its ligands. *Trends Cell Biol* (2001) 11:130–5. doi: 10.1016/S0962-8924(00)01906-1

45. Kharitonenkov A, Chen Z, Sures I, Wang H, Schilling J. Ullrich A. A family of proteins that inhibit signalling through tyrosine kinase receptors. *Nature* (1997) 386:181–6. doi: 10.1038/386181a0
46. Tsai RK, Discher DE. Inhibition of "self" engulfment through deactivation of myosin-II at the phagocytic synapse between human cells. *J Cell Biol* (2008) 180:989–1003. doi: 10.1083/jcb.200708043
47. Morrissey MA, Kern N, Vale RD. CD47 Ligation Repositions the Inhibitory Receptor SIRPA to Suppress Integrin Activation and Phagocytosis. *Immunity* (2020) 53:290–302.e6. doi: 10.1016/j.immuni.2020.07.008
48. Pietsch EC, Dong J, Cardoso R, Zhang X, Chin D, Hawkins R, et al. Anti-leukemic activity and tolerability of anti-human CD47 monoclonal antibodies. *Blood Cancer J* (2017) 7:e536. doi: 10.1038/bcj.2017.7
49. Lo J, Lau EYT, So FTY, Lu P, Chan VSF, Cheung VCH, et al. Anti-CD47 antibody suppresses tumour growth and augments the effect of chemotherapy treatment in hepatocellular carcinoma. *Liver Int* (2016) 36:737–45. doi: 10.1111/liv.12963
50. Gallagher S, Turman S, Lekstrom K, Wilson S, Herbst R, Wang Y. CD47 limits antibody dependent phagocytosis against non-malignant B cells. *Mol Immunol* (2017) 85:57–65. doi: 10.1016/j.molimm.2017.01.022
51. Golden EB, Apetoh L. Radiotherapy and Immunogenic Cell Death. *Semin Radiat Oncol* (2015) 25:11–7. doi: 10.1016/j.semradonc.2014.07.005
52. Sallman DA, Asch AS, Al Malki MM, Lee DJ, Donnellan WB, Marcucci G, et al. The First-in-Class Anti-CD47 Antibody Magrolimab (5F9) in Combination with Azacitidine Is Effective in MDS and AML Patients: Ongoing Phase 1b Results. *Blood* (2019) 134:569–9. doi: 10.1182/blood-2019-126271
53. Tsao LC, Crosby EJ, Trotter TN, Agarwal P, Hwang BJ, Acharya C, et al. CD47 blockade augmentation of trastuzumab antitumor efficacy dependent on antibody-dependent cellular phagocytosis. *JCI Insight* (2019) 4(24): e131882. doi: 10.1172/jci.insight.131882
54. Maute RL, Chen JY, Marjon KD, Duan J, Choi T, Chao M, et al. Translational Study of Cell Surface Proteins in Non-Hodgkin Lymphoma Patients Treated with the First-in-Class Anti-CD47 Antibody Magrolimab (5F9) in Combination with Rituximab. *Blood* (2019) 134:5229–9. doi: 10.1182/blood-2019-127526
55. Liu X, Jiang S, Fang C, Yang S, Olalere D, Pequignot EC, et al. Affinity-tuned ErbB2 or EGFR chimeric antigen receptor T cells exhibit an increased therapeutic index against tumors in mice. *Cancer Res* (2015) 75:3596–607. doi: 10.1158/0008-5472.CAN-15-0159
56. Yi T, Li J, Chen H, Wu J, An J, Xu Y, et al. Splenic Dendritic Cells Survey Red Blood Cells for Missing Self-CD47 to Trigger Adaptive Immune Responses. *Immunity* (2015) 43:764–75. doi: 10.1016/j.immuni.2015.08.021
57. Jalil AR, Andrechak JC, Discher DE. Macrophage checkpoint blockade: results from initial clinical trials, binding analyses, and CD47-SIRPα structure–function. *Antib Ther* (2020) 3:80–94. doi: 10.1093/abt/tbaa006
58. Russ A, Hua AB, Montfort WR, Rahman B, Riaz IB, Khalid MU, et al. Blocking "don't eat me" signal of CD47-SIRPα in hematological malignancies, an in-depth review. *Blood Rev* (2018) 32:480–9. doi: 10.1016/j.blre.2018.04.005
59. Voets E, Paradé M, Lutje Hulsik D, Spijkers S, Janssen W, Rens J, et al. Functional characterization of the selective pan-allele anti-SIRPα antibody ADU-1805 that blocks the SIRPα-CD47 innate immune checkpoint. *J Immunother Cancer* (2019) 7:340. doi: 10.1186/s40425-019-0772-0
60. Kauder SE, Kuo TC, Harrabi O, Chen A, Sangalang E, Doyle L, et al. ALX148 blocks CD47 and enhances innate and adaptive antitumor immunity with a favorable safety profile. *PloS One* (2018) 13:e0201832. doi: 10.1371/journal.pone.0201832
61. Weiskopf K, Ring AM, Ho CCM, Volkmer JP, Levin AM, Volkmer AK, et al. Engineered SIRPα variants as immunotherapeutic adjuvants to anticancer antibodies. *Science (80-)* (2013) 341:88–91. doi: 10.1126/science.1238856
62. Ansell S, Chen RW, Flinn IW, Maris MB, O'Connor OA, Johnson LD, et al. A Phase 1 Study of TTI-621, a Novel Immune Checkpoint Inhibitor Targeting CD47, in Patients with Relapsed or Refractory Hematologic Malignancies. *Blood* (2016) 128:1812–2. doi: 10.1182/blood.v128.22.1812.1812
63. Advani R, Flinn I, Popplewell L, Forero A, Bartlett NL, Ghosh N, et al. CD47 Blockade by Hu5F9-G4 and Rituximab in Non-Hodgkin's Lymphoma. *N Engl J Med* (2018) 379:1711–21. doi: 10.1056/NEJMoa1807315
64. Chao MP, Takimoto CH, Feng DD, McKenna K, Gip P, Liu J, et al. Therapeutic Targeting of the Macrophage Immune Checkpoint CD47 in Myeloid Malignancies. *Front Oncol* (2019) 9:1380. doi: 10.3389/fonc.2019.01380
65. Puro RJ, Bouchlaka MN, Hiebsch RR, Capoccia BJ, Donio MJ, Manning PT, et al. Development of AO-176, a next-generation humanized anti-CD47 antibody with novel anticancer properties and negligible red blood cell binding. *Mol Cancer Ther* (2020) 19:835–46. doi: 10.1158/1535-7163.MCT-19-1079
66. Peluso MO, Adam A, Armet CM, Zhang L, O'Connor RW, Lee BH, et al. The Fully human anti-CD47 antibody SRF231 exerts dual-mechanism antitumor activity via engagement of the activating receptor CD32a. *J Immunother Cancer* (2020) 8:413. doi: 10.1136/jitc-2019-000413
67. Meng Z, Wang Z, Guo B, Cao W, Shen H. TJC4, a Differentiated Anti-CD47 Antibody with Novel Epitope and RBC Sparing Properties. *Blood* (2019) 134:4063–3. doi: 10.1182/blood-2019-122793
68. Berlin J, Harb W, Adjei A, Xing Y, Swiecicki P, Seetharam M, et al. 385 A first-in-human study of lemzoparlimab, a differentiated anti-CD47 antibody, in subjects with relapsed/refractory malignancy: initial monotherapy results. *J Immunother Cancer* (2020) 8:A410–0. doi: 10.1136/jitc-2020-SITC2020.0385
69. Petrova PS, Viller NN, Wong M, Pang X, Lin GHY, Dodge K, et al. TTI-621 (SIRPaFc): A CD47-Blocking Innate Immune Checkpoint Inhibitor with Broad Antitumor Activity and Minimal Erythrocyte Binding. *Clin Cancer Res* (2016) 23:1068–79. doi: 10.1158/1078-0432.CCR-16-1700
70. Lin GHY, Viller NN, Chabonneau M, Brinen L, Mutukura T, Dodge K, et al. Abstract 2709: TTI-622 (SIRPα-IgG4 Fc), a CD47-blocking innate immune checkpoint inhibitor, suppresses tumor growth and demonstrates enhanced efficacy in combination with antitumor antibodies in both hematologic and solid tumor models. *Cancer Res* (2018) 78(13 Supplement):2709. doi: 10.1158/1538-7445.am2018-2709
71. Kim TM, Lakhani N, Gainor J, Kamdar M, Fanning P, Squifflet P, et al. A Phase 1 Study of ALX148, a CD47 Blocker, in Combination with Rituximab in Patients with Non-Hodgkin Lymphoma. *Blood* (2019) 134:1953–3. doi: 10.1182/blood-2019-123219
72. Maute RL, Gordon SR, Mayer AT, McCracken MN, Natarajan A, Ring NG, et al. Engineering high-affinity PD-1 variants for optimized immunotherapy and immuno-PET imaging. *Proc Natl Acad Sci U S A* (2015) 112:E6506–14. doi: 10.1073/pnas.1519623112
73. Liu J, Wang L, Zhao F, Tseng S, Narayanan C, Shura L, et al. Pre-Clinical Development of a Humanized Anti-CD47 Antibody with Anti-Cancer Therapeutic Potential. *PloS One* (2015) 10:e0137345. doi: 10.1371/journal.pone.0137345
74. Hanahan D, Weinberg RA. Hallmarks of cancer: The next generation. *Cell* (2011) 144:646–74. doi: 10.1016/j.cell.2011.02.013
75. Chen W, Zhu Z, Feng Y, Xiao X, Dimitrov DS. Construction of a Large Phage-Displayed Human Antibody Domain Library with a Scaffold Based On a Newly Identified Highly Soluble, Stable Heavy Chain Variable Domain. *J Mol Biol* (2008) 382:779–89. doi: 10.1016/j.jmb.2008.07.054
76. Ring NG, Herndler-Brandstetter D, Weiskopf K, Shan L, Volkmer JP, George BM, et al. Anti-SIRPα antibody immunotherapy enhances neutrophil and macrophage antitumor activity. *Proc Natl Acad Sci U S A* (2017) 114:E10578–85. doi: 10.1073/pnas.1710877114
77. Sim J, Sockolosky JT, Sangalang E, Izquierdo S, Pedersen D, Harriman W, et al. Discovery of high affinity, pan-allelic, and pan-mammalian reactive antibodies against the myeloid checkpoint receptor SIRPα. *MAbs* (2019) 11:1036–52. doi: 10.1080/19420862.2019.1624123
78. Liu J, Xavy S, Mihardja S, Chen S, Sompalli K, Feng D, et al. Targeting macrophage checkpoint inhibitor SIRPα for anticancer therapy. *JCI Insight* (2020) 5(12):e134278. doi: 10.1172/jci.insight.134728
79. Sallman DA, Donnellan WB, Asch AS, Lee DJ, Al Malki M, Marcucci G, et al. The first-in-class anti-CD47 antibody Hu5F9-G4 is active and well tolerated alone or with azacitidine in AML and MDS patients: Initial phase 1b results. *J Clin Oncol* (2019) 37:7009–9. doi: 10.1200/jco.2019.37.15_suppl.7009
80. Sallman DA, Al Malki M, Asch AS, Lee DJ, Kambhampati S, Donnellan WB, et al. Tolerability and efficacy of the first-in-class anti-CD47 antibody magrolimab combined with azacitidine in MDS and AML patients: Phase

Ib results. *J Clin Oncol* (2020) 38:7507–7. doi: 10.1200/jco.2020.38.15_suppl.7507
81. Chen DS, Mellman I. Elements of cancer immunity and the cancer-immune set point. *Nature* (2017) 541:321–30. doi: 10.1038/nature21349
82. Waite JC, Wang B, Haber L, Hermann A, Ullman E, Ye X, et al. Tumor-targeted CD28 bispecific antibodies enhance the antitumor efficacy of PD-1 immunotherapy. *Sci Transl Med* (2020) 12:eaba2325. doi: 10.1126/scitranslmed.aba2325
83. Wu L, Seung E, Xu L, Rao E, Lord DM, Wei RR, et al. Trispecific antibodies enhance the therapeutic efficacy of tumor-directed T cells through T cell receptor co-stimulation. *Nat Cancer* (2020) 1:86–98. doi: 10.1038/s43018-019-0004-z
84. Chen S, Li J, Li Q, Wang Z. Bispecific antibodies in cancer immunotherapy. *Hum Vaccines Immunother* (2016) 12:2491–500. doi: 10.1080/21645515.2016.1187802
85. Boyd-Kirkup J, Thakkar D, Brauer P, Zhou J, Chng W-J, Ingram PJ. HMBD004, a Novel Anti-CD47xCD33 Bispecific Antibody Displays Potent Anti-Tumor Effects in Pre-Clinical Models of AML. *Blood* (2017) 130:1378–8. doi: 10.1182/BLOOD.V130.SUPPL_1.1378.1378
86. Buatois V, Johnson Z, Salgado-Pires S, Papaioannou A, Hatterer E, Chauchet X, et al. Preclinical development of a bispecific antibody that safely and effectively targets CD19 and CD47 for the treatment of B-cell lymphoma and leukemia. *Mol Cancer Ther* (2018) 17:1739–51. doi: 10.1158/1535-7163.MCT-17-1095
87. Hatterer E, Barba L, Noraz N, Daubeuf B, Aubry-Lachainaye JP, von der Weid B, et al. Co-engaging CD47 and CD19 with a bispecific antibody abrogates B-cell receptor/CD19 association leading to impaired B-cell proliferation. *MAbs* (2019) 11:322–34. doi: 10.1080/19420862.2018.1558698
88. Chao MP, Alizadeh AA, Tang C, Myklebust JH, Varghese B, Gill S, et al. Anti-CD47 Antibody Synergizes with Rituximab to Promote Phagocytosis and Eradicate Non-Hodgkin Lymphoma. *Cell* (2010) 142:699–713. doi: 10.1016/j.cell.2010.07.044
89. Piccione EC, Juarez S, Liu J, Tseng S, Ryan CE, Narayanan C, et al. A bispecific antibody targeting CD47 and CD20 selectively binds and eliminates dual antigen expressing lymphoma cells. *MAbs* (2015) 7:946–56. doi: 10.1080/19420862.2015.1062192
90. Piccione EC, Juarez S, Tseng S, Liu J, Stafford M, Narayanan C, et al. SIRPα-antibody fusion proteins selectively bind and eliminate dual antigen-expressing tumor cells. *Clin Cancer Res* (2016) 22:5109–19. doi: 10.1158/1078-0432.CCR-15-2503
91. Dheilly E, Moine V, Broyer L, Salgado-Pires S, Johnson Z, Papaioannou A, et al. Selective Blockade of the Ubiquitous Checkpoint Receptor CD47 Is Enabled by Dual-Targeting Bispecific Antibodies. *Mol Ther* (2017) 25:523–33. doi: 10.1016/j.ymthe.2016.11.006
92. van Bommel PE, He Y, Schepel I, Hendriks MAJM, Wiersma VR, van Ginkel RJ, et al. CD20-selective inhibition of CD47-SIRPα "don't eat me" signaling with a bispecific antibody-derivative enhances the anticancer activity of daratumumab, alemtuzumab and obinutuzumab. *Oncoimmunology* (2018) 7:e1386361. doi: 10.1080/2162402X.2017.1386361
93. Ishida Y, Agata Y, Shibahara K, Honjo T. Induced expression of PD-1, a novel member of the immunoglobulin gene superfamily, upon programmed cell death. *EMBO J* (1992) 11:3887–95. doi: 10.1002/j.1460-2075.1992.tb05481.x
94. Liu B, Guo H, Xu J, Qin T, Guo Q, Gu N, et al. Elimination of tumor by CD47/PD-L1 dual-targeting fusion protein that engages innate and adaptive immune responses. *MAbs* (2018) 10:315–24. doi: 10.1080/19420862.2017.1409319
95. Liu X, Liu L, Ren Z, Peng H, Zhu M, Fu Y-X. Dual Targeting of Innate and Adaptive Checkpoints on Tumor Cells Limits Immune Evasion. *Cell Reports* (2018) 24:2101–11. doi: 10.1016/j.celrep.2018.07.062
96. Kedage V, Ellerman D, Chen Y, Liang W-C, Borneo J, Wu Y, et al. Harnessing MerTK agonism for targeted therapeutics. *MAbs* (2020) 12:1685832. doi: 10.1080/19420862.2019.1685832
97. Cai B, Kasikara C, Doran AC, Ramakrishnan R, Birge RB, Tabas I. MerTK signaling in macrophages promotes the synthesis of inflammation resolution mediators by suppressing CaMKII activity. *Sci Signal* (2018) 11:eaar3721. doi: 10.1126/scisignal.aar3721
98. Zhou Y, Fei M, Zhang G, Liang WC, Lin WY, Wu Y, et al. Blockade of the Phagocytic Receptor MerTK on Tumor-Associated Macrophages Enhances P2X7R-Dependent STING Activation by Tumor-Derived cGAMP. *Immunity* (2020) 52:357–373.e9. doi: 10.1016/j.immuni.2020.01.014
99. Schlothauer T, Herter S, Koller CF, Grau-Richards S, Steinhart V, Spick C, et al. Novel human IgG1 and IgG4 Fc-engineered antibodies with completely abolished immune effector functions. *Protein Eng Des Sel* (2016) 29:457–66. doi: 10.1093/protein/gzw040
100. Lo M, Kim HS, Tong RK, Bainbridge TW, Vernes JM, Zhang Y, et al. Effector-attenuating substitutions that maintain antibody stability and reduce toxicity in mice. *J Biol Chem* (2017) 292:3900–8. doi: 10.1074/jbc.M116.767749
101. Reichel D, Tripathi M, Perez JM. Biological Effects of Nanoparticles on Macrophage Polarization in the Tumor Microenvironment. *Nanotheranostics* (2019) 3:66–88. doi: 10.7150/ntno.30052
102. Walkey CD, Olsen JB, Guo H, Emili A, Chan WCW. Nanoparticle size and surface chemistry determine serum protein adsorption and macrophage uptake. *J Am Chem Soc* (2012) 134:2139–47. doi: 10.1021/ja2084338
103. Miao X, Leng X, Zhang Q. The Current State of Nanoparticle-Induced Macrophage Polarization and Reprogramming Research. *Int J Mol Sci* (2017) 18(2):336. doi: 10.3390/ijms18020336
104. Gao S, Yang D, Fang Y, Lin X, Jin X, Wang Q, et al. Engineering Nanoparticles for Targeted Remodeling of the Tumor Microenvironment to Improve Cancer Immunotherapy. *Theranostics* (2019) 9:126–51. doi: 10.7150/thno.29431
105. Tang L, Gabrielson NP, Uckun FM, Fan TM, Cheng J. Size-dependent tumor penetration and in vivo efficacy of monodisperse drug-silica nanoconjugates. *Mol Pharm* (2013) 10:883–92. doi: 10.1021/mp300684a
106. Su Y-L, Hu S-H. Functional Nanoparticles for Tumor Penetration of Therapeutics. *Pharmaceutics* (2018) 10:193. doi: 10.3390/pharmaceutics10040193
107. Torchilin V. Tumor delivery of macromolecular drugs based on the EPR effect. *Adv Drug Deliv Rev* (2011) 63:131–5. doi: 10.1016/j.addr.2010.03.011
108. Golombek SK, May J-N, Theek B, Appold L, Drude N, Kiessling F, et al. Tumor targeting via EPR: Strategies to enhance patient responses. *Adv Drug Deliv Rev* (2018) 130:17–38. doi: 10.1016/j.addr.2018.07.007
109. Prabhakar U, Maeda H, Jain RK, Sevick-Muraca EM, Zamboni W, Farokhzad OC, et al. Challenges and key considerations of the enhanced permeability and retention effect for nanomedicine drug delivery in oncology. *Cancer Res* (2013) 73:2412–7. doi: 10.1158/0008-5472.CAN-12-4561
110. Maeda H, Nakamura H, Fang J. The EPR effect for macromolecular drug delivery to solid tumors: Improvement of tumor uptake, lowering of systemic toxicity, and distinct tumor imaging in vivo. *Adv Drug Deliv Rev* (2013) 65:71–9. doi: 10.1016/j.addr.2012.10.002
111. Anselmo AC, Mitragotri S. Nanoparticles in the clinic: An update. *Bioeng Transl Med* (2019) 4:e10143. doi: 10.1002/btm2.10143
112. Bobo D, Robinson KJ, Islam J, Thurecht KJ, Corrie SR. Nanoparticle-Based Medicines: A Review of FDA-Approved Materials and Clinical Trials to Date. *Pharm Res* (2016) 33:2373–87. doi: 10.1007/s11095-016-1958-5
113. Chen P, Zhang X, Venosa A, Lee IH, Myers D, Holloway JA, et al. A Novel Bivalent Mannosylated Targeting Ligand Displayed on Nanoparticles Selectively Targets Anti-Inflammatory M2 Macrophages. *Pharmaceutics* (2020) 12:243. doi: 10.3390/pharmaceutics12030243
114. Zhang F, Parayath NN, Ene CI, Stephan SB, Koehne AL, Coon ME, et al. Genetic programming of macrophages to perform anti-tumor functions using targeted mRNA nanocarriers. *Nat Commun* (2019) 10:3974. doi: 10.1038/s41467-019-11911-5
115. Wang T, Zhang J, Hou T, Yin X, Zhang N. Selective targeting of tumor cells and tumor associated macrophages separately by twin-like core-shell nanoparticles for enhanced tumor-localized chemoimmunotherapy. *Nanoscale* (2019) 11:13934–46. doi: 10.1039/c9nr03374b
116. Hu G, Guo M, Xu J, Wu F, Fan J, Huang Q, et al. Nanoparticles Targeting Macrophages as Potential Clinical Therapeutic Agents Against Cancer and Inflammation. *Front Immunol* (2019) 10:1998. doi: 10.3389/fimmu.2019.01998
117. Poupot R, Goursat C, Fruchon S. Multivalent nanosystems: targeting monocytes/macrophages. *Int J Nanomedicine* (2018) 13:5511–21. doi: 10.2147/IJN.S146192
118. Rodell CB, Arlauckas SP, Cuccarese MF, Garris CS, Li R, Ahmed MS, et al. TLR7/8-agonist-loaded nanoparticles promote the polarization of tumour-associated macrophages to enhance cancer immunotherapy. *Nat BioMed Eng* (2018) 2:578–88. doi: 10.1038/s41551-018-0236-8

119. Zhao P, Wang Y, Kang X, Wu A, Yin W, Tang Y, et al. Dual-targeting biomimetic delivery for anti-glioma activity via remodeling the tumor microenvironment and directing macrophage-mediated immunotherapy. *Chem Sci* (2018) 9:2674–89. doi: 10.1039/c7sc04853j
120. Lun X, Wells JC, Grinshtein N, King JC, Hao X, Dang NH, et al. Disulfiram when combined with copper enhances the therapeutic effects of temozolomide for the treatment of glioblastoma. *Clin Cancer Res* (2016) 22:3860–75. doi: 10.1158/1078-0432.CCR-15-1798
121. Obeid M, Tesniere A, Ghiringhelli F, Fimia GM, Apetoh L, Perfettini JL, et al. Calreticulin exposure dictates the immunogenicity of cancer cell death. *Nat Med* (2007) 13:54–61. doi: 10.1038/nm1523
122. Serrano-del Valle A, Anel A, Naval J, Marzo I. Immunogenic cell death and immunotherapy of multiple myeloma. *Front Cell Dev Biol* (2019) 7:50. doi: 10.3389/fcell.2019.00050
123. Feng M, Chen JY, Weissman-Tsukamoto R, Volkmer JP, Ho PY, McKenna KM, et al. Macrophages eat cancer cells using their own calreticulin as a guide: Roles of TLR and Btk. *Proc Natl Acad Sci U S A* (2015) 112:2145–50. doi: 10.1073/pnas.1424907112
124. Feng M, Marjon KD, Zhu F, Weissman-Tsukamoto R, Levett A, Sullivan K, et al. Programmed cell removal by calreticulin in tissue homeostasis and cancer. *Nat Commun* (2018) 9:1–15. doi: 10.1038/s41467-018-05211-7
125. Ogden CA, DeCathelineau A, Hoffmann PR, Bratton D, Fadok B, Ghebrehiwet VA, et al. C1q and mannose binding lectin engagement of cell surface calreticulin and CD91 initiates macropinocytosis and uptake of apoptotic cells. *J Exp Med* (2001) 194:781–95. doi: 10.1084/jem.194.6.781
126. Vandivier RW, Ogden CA, Fadok VA, Hoffmann PR, Brown KK, Botto M, et al. Role of Surfactant Proteins A, D, and C1q in the Clearance of Apoptotic Cells In Vivo and In Vitro: Calreticulin and CD91 as a Common Collectin Receptor Complex. *J Immunol* (2002) 169:3978–86. doi: 10.4049/jimmunol.169.7.3978
127. Byrne JC, Ní Gabhann J, Stacey KB, Coffey BM, McCarthy E, Thomas W, et al. Bruton's Tyrosine Kinase Is Required for Apoptotic Cell Uptake via Regulating the Phosphorylation and Localization of Calreticulin. *J Immunol* (2013) 190:5207–15. doi: 10.4049/jimmunol.1300057
128. Sethuraman SN, Singh MP, Patil G, Li S, Fiering S, Hoopes PJ, et al. Novel calreticulin-nanoparticle in combination with focused ultrasound induces immunogenic cell death in melanoma to enhance antitumor immunity. *Theranostics* (2020) 10:3397–412. doi: 10.7150/thno.42243
129. Yuan H, Jiang W, von Roemeling CA, Qie Y, Liu X, Chen Y, et al. Multivalent bi-specific nanobioconjugate engager for targeted cancer immunotherapy. *Nat Nanotechnol* (2017) 12:763–9. doi: 10.1038/nnano.2017.69
130. Wilhelm S, Tavares AJ, Dai Q, Ohta S, Audet J, Dvorak HF, et al. Analysis of nanoparticle delivery to tumours. *Nat Rev Mater* (2016) 1:1–12. doi: 10.1038/natrevmats.2016.14
131. Blanco E, Shen H, Ferrari M. Principles of nanoparticle design for overcoming biological barriers to drug delivery. *Nat Biotechnol* (2015) 33:941–51. doi: 10.1038/nbt.3330
132. Clemons TD, Singh R, Sorolla A, Chaudhari N, Hubbard A, Iyer KS. Distinction between Active and Passive Targeting of Nanoparticles Dictate Their Overall Therapeutic Efficacy. *Langmuir* (2018) 34:15343–9. doi: 10.1021/acs.langmuir.8b02946
133. Fu W, Lei C, Liu S, Cui Y, Wang C, Qian K, et al. CAR exosomes derived from effector CAR-T cells have potent antitumour effects and low toxicity. *Nat Commun* (2019) 10:4355. doi: 10.1038/s41467-019-12321-3
134. Ma W, Zhu D, Li J, Chen X, Xie W, Jiang X, et al. Coating biomimetic nanoparticles with chimeric antigen receptor T cell-membrane provides high specificity for hepatocellular carcinoma photothermal therapy treatment. *Theranostics* (2020) 10:1281–95. doi: 10.7150/thno.40291
135. Gill S, June CH. Going viral: Chimeric antigen receptor T-cell therapy for hematological malignancies. *Immunol Rev* (2015) 263:68–89. doi: 10.1111/imr.12243
136. June CH, O'Connor RS, Kawalekar OU, Ghassemi S, Milone MC. CAR T cell immunotherapy for human cancer. *Science (80-)* (2018) 359:1361–5. doi: 10.1126/science.aar6711
137. Jackson HJ, Rafiq S, Brentjens RJ. Driving CAR T-cells forward. *Nat Rev Clin Oncol* (2016) 13:370–83. doi: 10.1038/nrclinonc.2016.36
138. Chen DS, Mellman I. Oncology meets immunology: The cancer-immunity cycle. *Immunity* (2013) 39:1–10. doi: 10.1016/j.immuni.2013.07.012
139. Gabrilovich DI, Nagaraj S. Myeloid-derived suppressor cells as regulators of the immune system. *Nat Rev Immunol* (2009) 9:162–74. doi: 10.1038/nri2506
140. Sakaguchi S, Yamaguchi T, Nomura T, Ono M. Regulatory T Cells and Immune Tolerance. *Cell* (2008) 133:775–87. doi: 10.1016/j.cell.2008.05.009
141. Lynn RC, Weber EW, Sotillo E, Gennert D, Xu P, Good Z, et al. c-Jun overexpression in CAR T cells induces exhaustion resistance. *Nature* (2019) 576:293–300. doi: 10.1038/s41586-019-1805-z
142. Martinez M, Moon EK. CAR T cells for solid tumors: New strategies for finding, infiltrating, and surviving in the tumor microenvironment. *Front Immunol* (2019) 10:128. doi: 10.3389/fimmu.2019.00128
143. Poh AR, Ernst M. Targeting macrophages in cancer: From bench to bedside. *Front Oncol* (2018) 8:1. doi: 10.3389/fonc.2018.00049
144. Yang M, McKay D, Pollard JW, Lewis CE. Diverse functions of macrophages in different tumor microenvironments. *Cancer Res* (2018) 78:5492–503. doi: 10.1158/0008-5472.CAN-18-1367
145. Genard G, Lucas S, Michiels C. Reprogramming of Tumor-Associated Macrophages with Anticancer Therapies: Radiotherapy versus Chemo- and Immunotherapies. *Front Immunol* (2017) 8:828. doi: 10.3389/fimmu.2017.00828
146. van Ravenswaay Claasen HH, Kluin PM, Fleuren GJ. Tumor infiltrating cells in human cancer. On the possible role of CD16+ macrophages in antitumor cytotoxicity. *Lab Invest* (1992) 67:166–74.
147. Das A, Sinha M, Datta S, Abas M, Chaffee S, Sen CK, et al. Monocyte and macrophage plasticity in tissue repair and regeneration. *Am J Pathol* (2015) 185:2596–606. doi: 10.1016/j.ajpath.2015.06.001
148. Murray PJ, Wynn TA. Protective and pathogenic functions of macrophage subsets. *Nat Rev Immunol* (2011) 11:723–37. doi: 10.1038/nri3073
149. Crayne CB, Albeituni S, Nichols KE, Cron RQ. The immunology of macrophage activation syndrome. *Front Immunol* (2019) 10:119:119. doi: 10.3389/fimmu.2019.00119
150. Schulert GS, Grom AA. Pathogenesis of Macrophage Activation Syndrome and Potential for Cytokine- Directed Therapies. *Annu Rev Med* (2015) 66:145–59. doi: 10.1146/annurev-med-061813-012806
151. Morrissey MA, Williamson AP, Steinbach AM, Roberts EW, Kern N, Headley MB, et al. Chimeric antigen receptors that trigger phagocytosis. *Elife* (2018) 7:e36688. doi: 10.7554/eLife.36688
152. Zhang W, Liu L, Su HF, Liu Q, Shen J, Dai H, et al. Chimeric antigen receptor macrophage therapy for breast tumours mediated by targeting the tumour extracellular matrix. *Br J Cancer* (2019) 121:837–45. doi: 10.1038/s41416-019-0578-3
153. Miller MR, Blystone SD. Reliable and inexpensive expression of large, tagged, exogenous proteins in murine bone marrow-derived macrophages using a second generation lentiviral system. *J Biol Methods* (2015) 2:e23. doi: 10.14440/jbm.2015.66
154. Shaw TN, Houston SA, Wemyss K, Bridgeman HM, Barbera TA, Zangerle-Murray T, et al. Tissue-resident macrophages in the intestine are long lived and defined by Tim-4 and CD4 expression. *J Exp Med* (2018) 215:1507–18. doi: 10.1084/jem.20180019
155. Davies LC, Jenkins SJ, Allen JE, Taylor PR. Tissue-resident macrophages. *Nat Immunol* (2013) 14:986–95. doi: 10.1038/ni.2705
156. Hashimoto D, Chow A, Noizat C, Teo P, Beasley MB, Leboeuf M, et al. Tissue-resident macrophages self-maintain locally throughout adult life with minimal contribution from circulating monocytes. *Immunity* (2013) 38:792–804. doi: 10.1016/j.immuni.2013.04.004
157. Sockolosky JT, Dougan M, Ingram JR, Ho CCM, Kauke MJ, Almo SC, et al. Durable antitumor responses to CD47 blockade require adaptive immune stimulation. *Proc Natl Acad Sci U S A* (2016) 113:E2646–54. doi: 10.1073/pnas.1604268113
158. Bercovici N, Guérin MV, Trautmann A, Donnadieu E. The Remarkable Plasticity of Macrophages: A Chance to Fight Cancer. *Front Immunol* (2019) 10:1563. doi: 10.3389/fimmu.2019.01563
159. Grégoire H, Roncali L, Rousseau A, Chérel M, Delneste Y, Jeannin P, et al. Targeting Tumor Associated Macrophages to Overcome Conventional Treatment Resistance in Glioblastoma. *Front Pharmacol* (2020) 11:368. doi: 10.3389/fphar.2020.00368
160. Deuse T, Hu X, Gravina A, Wang D, Tediashvili G, De C, et al. Hypoimmunogenic derivatives of induced pluripotent stem cells evade immune rejection in fully immunocompetent allogeneic recipients. *Nat Biotechnol* (2019) 37:252–8. doi: 10.1038/s41587-019-0016-3

161. Giavridis T, Van Der Stegen SJC, Eyquem J, Hamieh M, Piersigilli A, Sadelain M. CAR T cell-induced cytokine release syndrome is mediated by macrophages and abated by IL-1 blockade letter. *Nat Med* (2018) 24:731–8. doi: 10.1038/s41591-018-0041-7
162. Siegel RL, Miller KD, Jemal A. Cancer statistics, 2020. *CA Cancer J Clin* (2020) 70:7–30. doi: 10.3322/caac.21590

Conflict of Interest: MF declares patent applications pertaining to stimulating TLR/BTK signaling to promote CRT in macrophages assigned to the Stanford University and equity and/or consulting with Forty Seven, Inc.

The remaining authors declare that the research was conducted in the absence of any commercial or financial relationships that could be construed as a potential conflict of interest.

Copyright © 2021 Chen, Lai, Brown and Feng. This is an open-access article distributed under the terms of the Creative Commons Attribution License (CC BY). The use, distribution or reproduction in other forums is permitted, provided the original author(s) and the copyright owner(s) are credited and that the original publication in this journal is cited, in accordance with accepted academic practice. No use, distribution or reproduction is permitted which does not comply with these terms.

frontiers in Immunology

MINI REVIEW
published: 31 March 2021
doi: 10.3389/fimmu.2021.633639

The Activation and Regulation of β2 Integrins in Phagocytes and Phagocytosis

Hao Sun[1†], *Kangkang Zhi*[2†], *Liang Hu*[3] *and Zhichao Fan*[4*]

[1] Department of Medicine, University of California, San Diego, La Jolla, CA, United States, [2] Department of Vascular Surgery, Changzheng Hospital, Shanghai, China, [3] Department of Cardiology, Cardiovascular Institute of Zhengzhou University, The First Affiliated Hospital of Zhengzhou University, Zhengzhou, China, [4] Department of Immunology, School of Medicine, UConn Health, Farmington, CT, United States

Phagocytes, which include neutrophils, monocytes, macrophages, and dendritic cells, protect the body by removing foreign particles, bacteria, and dead or dying cells. Phagocytic integrins are greatly involved in the recognition of and adhesion to specific antigens on cells and pathogens during phagocytosis as well as the recruitment of immune cells. β2 integrins, including αLβ2, αMβ2, αXβ2, and αDβ2, are the major integrins presented on the phagocyte surface. The activation of β2 integrins is essential to the recruitment and phagocytic function of these phagocytes and is critical for the regulation of inflammation and immune defense. However, aberrant activation of β2 integrins aggravates auto-immune diseases, such as psoriasis, arthritis, and multiple sclerosis, and facilitates tumor metastasis, making them double-edged swords as candidates for therapeutic intervention. Therefore, precise regulation of phagocyte activities by targeting β2 integrins should promote their host defense functions with minimal side effects on other cells. Here, we reviewed advances in the regulatory mechanisms underlying β2 integrin inside-out signaling, as well as the roles of β2 integrin activation in phagocyte functions.

Keywords: β2 integrins, integrin activation, integrin adaptors, phagocytes, phagocytosis

OPEN ACCESS

Edited by:
Valentin Jaumouillé, Simon Fraser University, Canada

Reviewed by:
Esther M. Lafuente, Complutense University of Madrid, Spain
Pontus Nordenfelt, Lund University, Sweden
Mehmet Sen, University of Houston, United States

***Correspondence:**
Zhichao Fan
zfan@uchc.edu

[†]*These authors have contributed equally to this work*

Specialty section:
This article was submitted to Molecular Innate Immunity, a section of the journal Frontiers in Immunology

Received: *25 November 2020*
Accepted: *11 March 2021*
Published: *31 March 2021*

Citation:
Sun H, Zhi K, Hu L and Fan Z (2021) The Activation and Regulation of β2 Integrins in Phagocytes and Phagocytosis. Front. Immunol. 12:633639. doi: 10.3389/fimmu.2021.633639

INTRODUCTION

Phagocytosis is the mechanism by which microorganisms are engulfed and killed, and it is the main process by which immune cells disassemble pathogens to present antigens. This is important for the innate immune response and initiating adaptive immune responses. Phagocytosis is a special form of cell endocytosis, whereby cells ingest solid particles through vesicles, including microbial pathogens (1–3). While most cells are capable of phagocytosis, the professional phagocytes of the immune system, such as macrophages, monocytes, neutrophils, and dendritic cells, excel in this process (4). During phagocytic uptake, phagocytes use receptors to interact with particles and mediate signals that encapsulate the particle within the membrane, leading to complete engulfment (5, 6). Particle recognition and uptake are conducted by a receptor ligation zipper-like process that involves several types of receptors, such as integrins, Fcγ receptors (FcγRs), and scavenger receptors (1, 7).

Integrins are essential cell-surface adhesion molecules that are widely expressed on cell membranes. As cell adhesion receptors, integrins transduce intracellular and bidirectional intercellular signals (8, 9), and are crucial for immune system functions (10, 11). In recent years, great progress has been made in elucidating integrin signal transduction mechanisms in phagocytes. β2 integrins, such as complement receptor 3 (CR3, also known as integrin αMβ2, CD11b/CD18, macrophage-1 antigen, or Mac-1) and complement receptor 4 (CR4, also known as integrin αXβ2, CD11c/CD18, or p150/95), are highly expressed in phagocytes and are important for phagocytosis. This review focuses on the role of β2 integrin activation and signaling during both adhesion and phagocytosis. We highlight the inside-out signaling basis of β2 integrin function during adhesion and phagocytosis and propose that β2 integrin-mediated phagocytosis is a great model to understand functional regulation of integrins.

β2 INTEGRINS EXPRESSED BY PHAGOCYTES

β2 integrins play a major role in regulating phagocyte adhesion and migration to inflamed organs and other immunological processes, such as phagocytosis (12, 13) (**Table 1**). In mammals, professional phagocytes express complement receptors, some of which are β2 integrins, such as CR3 and CR4, which are critical for anti-pathogen defense and inflammation regulation. Phagocytes like monocytes and macrophages express all four β2 integrin family members: CR3, CR4, αLβ2 (also known as CD11a/CD18, lymphocyte function-associated antigen 1, or LFA-1), and αDβ2 (CD11d/CD18) (23). The activation of β2 integrins is involved in multiple functions of phagocytes, such as cell adhesion, locomotion, exocytosis, and phagocytosis (14, 24–26). The central role of β2 integrins in immunity is highlighted by the fact that patients with leukocyte adhesion deficiency type I (LAD-I) syndrome, who lack β2 integrin expression, are particularly prone to bacterial infections (27). LAD-III (leukocyte adhesion deficiency type III) patients have mutations in kindlin-3 (an integrin binding protein) and show a deficiency in integrin β2 activation, leading to an adhesion defect of phagocytes similar to LAD-I (28). These patients end up suffering from recurrent life-threatening infections (29). Overaggressive β2 integrin activation leads to excessive inflammation and associated tissue damage (30).

Integrin αLβ2 is critical for the adhesion of blood phagocytes (such as neutrophils and monocytes) to the vascular endothelium (31–35), as well as intravascular patrolling of monocytes (36, 37) and transendothelial migration of neutrophils (38, 39). Integrin αMβ2 is involved in cell adhesion, cell migration, phagocytosis, and degranulation of phagocytes (14, 24–26, 37, 40). Integrin αMβ2 recognizes various structurally and functionally different ligands, including extracellular matrix (ECM)-associated ligands that are released from damaged cells during inflammatory responses, such as intercellular adhesion molecule 1 (ICAM-1), glycoprotein Ib-IX, and junctional adhesion molecule 3 (JAM-3) (41–45). Both αMβ2 and αXβ2 can bind to complement component iC3b and are crucial for RhoA-dependent phagocytosis in phagocytes (46–48). The differences between these two integrins have been studied in αM and αX knockout mice (**Table 1**). αMβ2 plays a major role in recruitment of polymorphonuclear neutrophil (PMN) to bacterial and fungal pathogens. αXβ2 plays a central role in monocyte- and macrophage-mediated inflammatory functions, as shown by αXβ2 deficiency that abrogated the recruitment of monocytes and macrophages to sites of inflammation or infection and reduced the ability of these cells to kill/phagocytose pathogens (17). Integrin αDβ2 is rarely expressed on peripheral blood phagocytes but is significantly up-regulated on macrophages during inflammation (e.g., atherosclerosis) (19). Integrin αDβ2 and αMβ2 show some similarities in many functions and share some ligands, such as ICAM-1, ICAM-2, ICAM-4, fibrinogen, collagen, iC3b, heparin, GPIbα, Thy-1, and plasminogen (49, 50). Recently, it was shown that β2 integrins are required for both monocyte and hematopoietic functions, and lower β2 integrin expression is associated with more severe schistosomiasis in mice (51).

β2 integrins are important for the fusion of human (52) but not mouse (53) macrophages; Macrophage fusion happens during chronic infection of persistent pathogens or encounters with nondegradable foreign objects, and results in the formation of multinucleated giant cells. Human monocyte-derived

TABLE 1 | Distribution of β2 integrins and phenotypes of engineered gene knockout mice.

	Distribution	Phenotypes of knockout mice	
αLβ2	All leukocytes but predominates on lymphocytes	Defective adhesion and migration of neutrophils, monocytes, and macrophages; impaired neutrophil chemotaxis; a defect in TNF-α-induced neutrophil and monocyte extravasation from blood vessels; a defect in the induction of peripheral immune responses; reduced NK cytotoxicity.	(14–16)
αMβ2	Abundant on myeloid cells, monocytes/macrophages, neutrophils, NK cells, fibrocytes, mast cells, B cells, CD8+ T cells, and CD4+ γδ T cells	Defective recruitment of neutrophils and mast cells to bacterial and fungal pathogens; a defect in neutrophil binding to fibrinogen and degranulation; impaired mast cell development and innate immunity; a defect in macrophage egression from the peritoneal cavity.	(14, 15)
αXβ2	Abundant on myeloid dendritic cells, monocytes/macrophages; expressed on human NK cells and lymphocyte subpopulations	Defect in intraperitoneal recruitment and adhesive functions of monocytes and macrophages and their ability to kill/phagocytose pathogens.	(17, 18)
αDβ2	Abundant on myeloid cells, macrophages, neutrophils, and monocytes; highly expressed on human NK cells, B cells, and γδT cells	Defective macrophage retention and reduced neutrophil accumulation in the atherosclerotic lesions; defective accumulation of mononuclear cells and neutrophils in the peritoneal cavities of mice infected by *S. typhimurium*; reduced lung macrophages and increased blood neutrophils in mice with cecal ligation and puncture sepsis or LPS-induced endotoxemia.	(19–22)

macrophage fusion was decreased ~66% upon treatment with β2 integrin-blocking antibody (52). In mouse studies, thioglycollate-elicited peritoneal macrophages from Mac-1 knockout mice showed a significant ~50% decrease in fusion compared to those from wild-type controls (53). However, thioglycollate-elicited peritoneal macrophages from wild-type mice treated with β2 integrin-blocking antibody showed a slight (~35%) but non-significant decrease of fusion compared to those without antibody treatment (53).

INTEGRIN ACTIVATION BY INSIDE-OUT SIGNALING

Both integrin α and β subunits have long ectodomains with a headpiece and tailpiece, a transmembrane domain (TMD), and a flexible cytoplasmic tail (54–59) (**Figure 1A**). β2 integrins form at least three conformational states (58, 61–66): inactive (bent ectodomain with closed headpiece, bent-closed), intermediate (extended ectodomain with closed headpiece, extended-closed), and active state (extended ectodomain with open headpiece, extended-closed extended-open). The conformational change in the extracellular domains enables rapid modulation of cell adhesion and migration (58, 67, 68). The extended-open conformation in α5β1 exhibits a 4,000 to 6,000-fold increase in ligand-binding affinity over the bent-closed and extended-closed conformations (69). On human peripheral T lymphocytes or K562 cells, most of the integrin αLβ2 are inactive. After stimulation, αLβ2 integrins on T lymphocytes are activated and show an ICAM-1 binding K_D of ~26 μM (~1.5-3-fold affinity increase, phorbol 12-myristate 13-acetate or stromal cell-derived factor 1 stimulation) or ~460 nM (~87-174-fold affinity increase, manganese stimulation) (65). These results indicated that only a small amount of αLβ2 integrins were activated upon leukocyte activation.

Recently, a bent-open (bent ectodomain with open headpiece) conformation was described for β2 integrins (70, 71). By introducing αX N920C and β2 V674C mutations

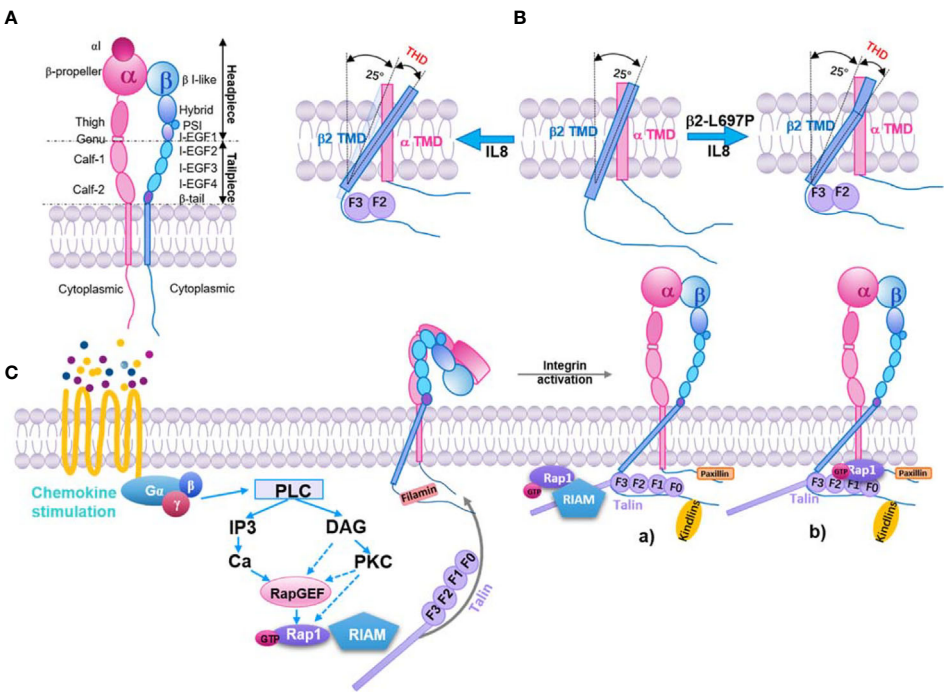

FIGURE 1 | Inside-out pathway of integrin β2 activation. **(A)** Structure model of integrin β2. Subdomains and headpiece/tailpiece portions labeled. **(B)** In resting β2 integrin (middle), the beta subunit (blue) crosses the membrane at a 25° angle, whereas the α subunit (pink) crosses vertically (0 degrees). Upon exposure to IL-8 (left), talin-1 binds to the beta subunit and forces the transmembrane angle to be >25°. This change is transmitted to the extracellular domain through the stiff transmembrane domain (TMD), resulting in extended β2 integrin with an open headpiece. If the β2 TMD is mutated (β2 L697P, right), talin-1 will still bind the intracellular domain and align the beginning of the TMD to an angle >25°, but the kink prevents this from being transmitted to the extracellular domain. The integrin stays bent, but the headpiece opens (60). Talin head domain (THD). **(C)** Key signaling events that occur downstream of chemokine and lead to integrin activation. Inactive integrins exist in a bent conformation, and the α and β cytoplasmic tails are held in close proximity by a salt bridge between residues found in the membrane-proximal region of the tail. Activation of a variety of signaling pathways results in the recruitment of GTP-bound Rap1 and activated talin to the integrin, leading to tail separation. The conformational change in the cytoplasmic region is transmitted through the integrin transmembrane domains that result in structural changes in the extracellular region, leading to an open conformation that can bind ligand with high affinity. Part of this signaling pathway is shown here. **a)** The Rap1/RIAM/talin-1 axis. Rap1-GTP binds to RIAM, which leads to RIAM binding to talin-1 and recruiting of talin-1 to integrin β tails, consequently activating the integrin. **b)** The direct association of Rap1 and talin-1. Rap1-GTP binds to talin-1 through talin-F0 and F1 domains, recruiting talin-1 to interact with integrin β tails and activation of integrin.

to form a disulfide, a structure of the bent αXβ2 with an internal ligand-bound headpiece has been shown (72). The internal ligand has residues on the αI domain that can bind to the βI-like domain during activation. The binding of internal ligands is correlated to the headpiece opening in the transition from extended-closed to extended-open structure (73). The bent internal ligand-bound structure was considered a bent-open conformation of αXβ2 in this study by reviewing the structure detail of αI metal-ion-dependent adhesion site (72). There is no direct ligand-binding result of this bent internal ligand-bound integrin αXβ2. However, other mutations were introduced that are functionally relevant to the internal ligand. After Mn^{2+} treatment, the αX K313I, F315E, and I317H mutations exhibited increased monoclonal antibody 24 (mAb24) binding, which indicates headpiece opening, but unchanged KIM127 antibody binding, which indicates extension. A previous electron microscopy study showed that mAb24 exclusively binds to extended but not bent αXβ2 integrins (61). This can be explained by the different methods of expressing αXβ2 integrin protein in these two studies: Chen et al. fused αX (1-1084) and β2 (1-677) ectodomains, respectively, to a C-terminal 54-residue pepetide, which contains an acidic coiled-coil region and a cysteine for disulfide bond formation; Sen et al. introduced a disulfide bond by αX N920C and β2 V674C mutations. The difference in disulfide bond position might result in these different conformations. Thus, knowing whether bent-open β2 integrins exist on physiologically relevant cells is important.

The mAb24 and KIM127 antibodies combined with total internal reflection fluorescence microscopy or super-resolution stochastic optical reconstruction microscopy indicates the existence of the bent-open β2 integrins on primary human neutrophils (70, 71). It has been shown that β2 integrins with this conformation can bind ligands (ICAM-1, ICAM-2, ICAM-3, or Fcγ receptor IIA) expressed on the same neutrophils in *cis* and auto-inhibit neutrophil adhesion and aggregation (70, 71, 74). The cis interaction between FcγRIIA and the αI domain of bent αMβ2 (74) reduces the binding of FcγRIIA to IgG and inhibits FcγRIIA-mediated neutrophil recruitment under flow, which indicates a new anti-inflammatory function for sialylation in immune responses and benefits for auto-immune disease. Thus, cis interactions may more broadly serve as an important regulatory mechanism for calibrating both the activity of the integrin and, in turn, the heterologous receptor(s) with which it interacts. However, details of this activation mechanism need further investigation.

Intracellular proteins bind to integrin α or β subunits, lead to the separation of integrin cytoplasmic tails, and stabilize the extended-open conformation (50, 75). This can be initiated by signaling from other receptors (inside-out signaling) or ligand-binding of integrins themselves (outside-in signaling) (76). One model of integrin inside-out signaling suggests that talin (a major cytoskeletal protein; see below) binds to the β subunit cytoplasmic tail and disrupts the stabilization of the inner membrane association of α and β TMDs. This alters the membrane-crossing angle of β TMD, thereby disrupting the outer membrane association of α and β TMDs, which is important for αIIbβ3 integrin activation (77). Studies showed that these transmitting conformation changes across the cell membrane are also important for both β7 (78) and β2 integrins (60). Blocking TMD topology transmission by introducing a TMD kink (L697P mutation) impairs chemokine-induced cell adhesion and β2 integrin extension, but not chemokine-induced β2 integrin high-affinity confirmation and manganese-induced cell spreading (60). As expected, talin-1 knockout cells showed a dramatic defect in chemokine-induced β2 integrin extension and high-affinity confirmation as well as manganese-induced cell spreading (**Figure 1B**). These results indicate that talin-1 interaction with the cytoplasmic tail of β2 subunits may be involved in two signaling pathways: one includes the TMD topology transmission and β2 integrin extension, the other is irrelevant to the TMD topology transmission and regulates β2 integrin high-affinity confirmation.

ADAPTOR PROTEINS/REGULATORS OF INTEGRIN ACTIVATION

Integrin inside-out signaling is regulated by intracellular signaling cascades initiated from several receptors (79). In phagocytes, these receptors are mostly G-protein-coupled receptors (GPCRs) for chemokines (such as interleukin 8, monocyte chemoattractant protein-1, stromal cell-derived factor 1), cytokines (such as tumor necrosis factor α), and inflammatory factors (such as N-formylmethionyl-leucyl-phenylalanine and leukotriene B4). The canonical inside-out signaling pathway of integrin activation (50) involves the dissociation of guanine nucleotide-binding protein, the activation of Rho GTPases and phospholipases, the elevation of intracellular calcium and diacylglycerol, the activation of Ras-related protein 1 guanine nucleotide exchange factors (Rap1-GEFs) or protein kinase C, and the activation of Ras-related protein 1 (Rap-1, from GDP-bound form to GTP-bound form). Rap1-GTP can bind with Rap1-GTP-interacting-adaptor molecule (RIAM, also known as Amyloid Beta Precursor Protein Binding Family B Member 1 Interacting Protein, *APBB1IP*) and recruit talin-1 to the plasma membrane to interact with the β2 cytoplasmic tail (**Figure 1C**). Kindlin-3 is also involved in this process (80).

Rap1 is a small GTPase that functions as the hub in integrin inside-out signaling (81, 82). Rap1-dependent αMβ2 activation is critical for complement-mediated phagocytosis of red blood cells (83). Rap1 continuously circulates between inactivated (GDP-bound) and activated (GTP-bound) forms. It is activated by Rap1-GEFs from the GDP-bound form to the GTP-bound form downstream of GPCR signaling, resulting in β2 integrin activation (81, 82). Calcium and diacylglycerol regulated guanine nucleotide exchange factor I (CalDAG–GEFI) (84, 85), RapGEF1, RapGEF3, and RapGEF6 (79) have been identified as Rap1-GEFs that can activate Rap-1 and integrins. Activated Rap-1 then goes through a conformational change, allowing both recruitment and binding to its effectors.

Talin-1 is an adaptor protein linking β2 integrins to the cytoskeleton. Talin-1 has a head domain and a rod domain. The talin-1 head domain (THD) is a FERM (band 4.1, ezrin, radixin,

and moesin) domain with four subdomains: F0, F1, F2, and F3. Structural studies revealed that the F3 subdomain binds to the cytoplasmic tail of β2 integrins, leading to integrin conformational change, the critical final step of integrin activation (86–90). There are two F3 subdomain binding sites in the cytoplasmic tail of β2 integrins (88): the membrane-distal binding site is the membrane-proximal NPXY motif of the β2 tail, which contains two NPXY motifs; The membrane-proximal binding site might be Y713 and F716 in β2 (corresponding to F727 and F730 in β3). Talin-1 W359A and L325R mutations cause a deficiency in binding to these two sites, respectively, and affect β2 integrin activation and neutrophil adhesion (91). The rod domain has 13 subdomains (R1-R13), including a dimerization domain and binding sites for integrin, F-actin, vinculin, and RIAM (87, 92).

In the phagocytosis of red blood cells by macrophages, talin-1 is recruited to the phagocytic cups and is essential for red blood cell capturing and phagocytosis during αMβ2-dependent uptake. Mutation of the membrane-proximal NPXY motif of the β2 tail prevents the recruitment of talin-1 to phagocytic cups as well as red blood cell phagocytosis (93). The mechanism of talin-1 activation remains unclear. A study showed that phosphatidylinositol-4-phosphate 5-kinase type 1 γ (PIP5K1γ) interacts with THD *via* a short amino acid sequence present in its 28 amino acid tail (94, 95). This interaction increases the activity of PIP5K1γ (95). Phosphatidylinositol-4,5-bisphosphate (PI(4,5)P2) is the product of PIP5K1γ and strengthens the binding of talin-1 to integrins (96). Additionally, the RIAM-talin-1 interaction is considered important for the activation and integrin tail recruitment of talin-1 (97) (**Figure 1C**). In a study using the fibroblast-like COS-7 cell line, Rap1 was found co-immunoprecipitated with talin-1 and regulated the recruitment of talin-1 to phagocytic cups. Disrupting the interaction between talin-1 and the β2 tail also inhibits the recruitment of Rap1 to phagocytic cups. Thus, Rap1 and talin-1 influence each other's recruitment to phagocytic cups (98). Recently, a direct interaction binding site of Rap1 was found in F0 and F1 subdomains of THD (99). Synergistic interaction between these two domains and an F1 lipid-interacting helix facilitates talin-1 recognition and activation of integrins (100). This pathway could be relevant to rapid immune cell responses. Blocking direct binding between Rap1 and talin-1 inhibits neutrophil adhesion and phagocytosis but not macrophage adhesion and spreading (101, 102).

The connection between the Rap proteins and talin-1 is not fully investigated. One model suggests that activated Rap1 can recruit RIAM, which relays Rap1 signaling to talin-1 and targets talin-1 to the integrin (80); RIAM is another critical intracellular protein for integrin activation. RIAM recruits talin-1 to the cytoplasmic membrane and facilitates the binding of talin-1 and the integrin β chain (80). Deletion of RIAM results in β2 integrin inactivation, which disables β2-mediated cell migration and adhesion (103). Loss of RIAM in leukocytes prevents antigen-dependent autoimmunity by disrupting cell-cell conjugation between effector T-cells and dendritic cells (104). Recent work shows that RIAM is necessary for leukocyte integrin activation in conventional T cells. Surprisingly, it is dispensable for integrin activation in regulatory T cells, which is because lamellipodin (Lpd), a RIAM paralogue (105), compensates for RIAM deficiency (106). Lpd also contains talin binding sites and can drive integrin activation in a Rap1- and talin-dependent manner (97, 107). Interestingly, RIAM was also shown to associate with kindlin-3, even before it bound to talin-1 (108). However, whether RIAM directly interacts with kindlin-3 is unknown.

The cytoplasmic tail of β2 integrins interacts with both talin-1 and kindlin-3 (109), both important for phagocyte function. As mentioned above, talin-1 is critical for β2 integrin activation, thus essential for phagocyte adhesion and trafficking (91, 110, 111). Kindlin-3 binds to the membrane-distal NPXY motif of the β2 tail and is also vital for β2 integrin activation (112), especially the headpiece-open conformation and phagocyte adhesion (111, 113, 114). The migration and phagocytosis of macrophages are regulated by the kindlin-3 association with the cytoskeleton (115). In contrast to other known kindlin binding partners, interactions between kindlin-3 and paxillin negatively regulate integrin-dependent functions of myeloid cells and limit myeloid cell motility and phagocytosis (115). However, talin-1 and kindlin-3 play distinct roles. Talin-1 is essential for both integrin extension and headpiece-open conformation, which mediates cell slow-rolling and firm adhesion. In contrast, kindlin-3 is necessary for headpiece-open activation, which mediates firm cell adhesion (90, 111, 116). However, although both talin-1 and kindlin-3 are essential for integrin inside-out signaling, it is unclear whether they bind sequentially or simultaneously. The signaling pathway guiding kindlin-3 to integrins requires further investigation.

Additionally, many other direct or indirect integrin-tail-binding proteins, such as vinculin, filamin A, paxillin, coronin 1A, or Dok1 might be important for integrin activation regulation (76, 79, 106). Filamin A is a cytoskeletal protein that occupies the same site as talin; therefore, it negatively regulates integrin activation by blocking talin-1 binding to β integrin tails (117–119). The kindlin binding protein, migfilin, binds to filamin A. It is possible that kindlin-3 binding to migfilin releases filamin A from this binding site, leaving it free for talin (119). Thus, the shuttling on and off of filamin A from integrins may have the ability of kindlins to coactivate integrins. Several other FERM domain-containing proteins block integrin activation, such as docking protein 1 (Dok1) (120) and integrin cytoplasmic domain associated protein 1 (ICAP1), which compete for talin binding, thus blocking integrin activation (121). The talin rod domain includes actin and vinculin binding sites. It binds to the actin cytoskeleton both directly and indirectly through vinculin (122). An alternative mechanism of the Rap1/RIAM/talin1 axis was reported in lymphocytes, in which WASP family verprolin homologous 2 (WAVE2) recruited vinculin to the immunological synapse, thereby recruiting talin-1 (123). Paxillin binding to the α4 cytoplasmic tail benefits cell migration but reduces cell spreading. Phosphorylation of the integrin α4 subunit releases paxillin and the GTPase ARF6 from the membrane, leading to the accumulation of active Rac at the leading edge (124). It is worth studying these integrin-binding proteins in phagocytes to

identify their roles in integrin activation and particle engulfment during phagocytosis.

INTEGRIN MODULATION DURING PHAGOCYTOSIS

Phagocytosis is a multi-step process. Firstly, particles are recognized and adhered to the surface of phagocytes, followed by the formation of a phagocytic cup (125), internalization, and formation of an intracellular-membrane-enclosed organelle – a phagosome (126, 127). The phagocytic cup and particle internalization is dependent on the dynamic rearrangement of F-actin, which is controlled by the Rho GTPase family (46, 128), in all forms of phagocytosis (125–127). Distinct Rho GTPases regulate several types of phagocytosis. In FcγR-dependent phagocytosis, activation of Rac1, Rac2, Cdc42, and RhoG is thought to play important roles in forming local pseudopods and membrane ruffles during particle engulfment (129, 130). Dectin-1-dependent phagocytosis involves activation of Rac1 and Cdc42, but not RhoA (131). In the FcγR and dectin-1 mediated "zipper model" mechanism of internalization, the F-actin first forms a bona fide phagocytic cup, then matures to first completely surround the bound particles and eventually fuse to complete phagocytosis (132).

αMβ2 integrin (CR3)-dependent phagocytosis exhibit distinct characteristic. The activation of αMβ2 prior to challenge with particles is required for αMβ2-mediated phagocytosis. The engulfment process in αMβ2-dependent phagocytosis is initiated by surface-tethering of particles, that then induces an invagination in the phagocyte plasma membrane into which the particle sinks, drawn by F-actin cytoskeletal forces (133). Obvious membrane ruffles were shown during αMβ2-mediated phagocytosis after integrin activation (134). These membrane ruffles differ from the membrane extensions of the zipper mechanism: They extend only from one side across the bound phagocytic particle, whereas the membrane tightly surrounds the entire surface of the particle in FcR-dependent zipper phagocytosis. Different from FcR-dependent phagocytosis, αMβ2-dependent phagocytosis requires activation of RhoA, Vav, and RhoG, but not Rac1 or Cdc42 (135, 136). However, this opinion is still controversial. Recent studies have shown that the formation of protrusions during particle engulfment is triggered by αMβ2-dependent phagocytosis (134, 137). A genetic ablation study demonstrated that Rac1 and Rac2 double-knockout macrophages are defective in both FcγR and αMβ2-mediated phagocytosis (138). This suggests that these two types of phagocytosis share common elements. Moreover, small GTPase Rap1 activation, mediated by a variety of growth factor receptors or other factors, plays an important role in αMβ2 activation and phagocytic uptake (83).

As mentioned above, talin-1 and kindlin-3 bind to the integrin β cytoplasmic tail, which activates integrins (139). Talin-1 bridges integrin with the actin cytoskeleton, stabilizes integrin activation, and transmits forces (140, 141). In the phagocytosis of red blood cells by macrophages, talin-1 is recruited to the phagocytic cups by a talin-based "molecular clutch" (142) and is essential for red blood cell capturing and phagocytosis during αMβ2-dependent uptake. Mutation of the membrane-proximal NPXY motif of the β2 tail prevents the recruitment of talin-1 to phagocytic cups as well as red blood cell phagocytosis (93). A recent study reported that β2 integrins could be coupled to actin and drive phagocytosis by a mechanosensitive molecular clutch that is mediated by talin, vinculin, and Arp2/3 (143). Thus, talin and vinculin promote phagosome formation by coupling actin to αMβ2 to drive phagocytosis. Previous studies have shown talin is transiently recruited to different types of particles during phagocytosis; however, talin is essential for αMβ2-mediated but not FcγR-mediated phagocytosis (93, 98). Kindlins are another family of integrin intracellular binding proteins that mediate integrin activation by inside-out signaling. A recent study found that kindlin-3 directly interacts with paxillin and leupaxin through its F0 domain in the macrophage-like RAW 264.7 cell line; inhibition of kindlin-3 and paxillin/leupaxin interactions promoted cell motility and augmented phagocytosis (115). Another recent work reported that kindlin-3 was essential for patrolling function and cancer particle uptake of nonclassical monocytes during tumor metastasis to the lung (144).

RIAM has been shown to play an important role in complement-dependent phagocytosis (145). Suppressing RIAM expression in neutrophil-like HL-60 cells, monocyte-like THP-1 cells, or human monocyte-derived macrophages inhibits the recruitment of talin-1 to phagocytic cups, the activation of integrin αMβ2, and complement-dependent phagocytosis (145). In RIAM knockout mice, macrophages and neutrophils show deficiencies in cell adhesion, αMβ2-mediated phagocytosis, and reactive oxygen species production (103). Recently, VASP was reported to work together with RIAM as a module regulating β2 integrin-dependent phagocytosis (146). VASP (vasodilator-stimulated phosphoprotein) is the binding partner of RIAM. This study showed that RIAM-deficient HL-60 cells presented impaired particle internalization and altered integrin downstream signaling during complement-dependent phagocytosis. Similarly, VASP deficiency completely blocked phagocytosis, while VASP overexpression increased the random movement of phagocytic particles at the cell surface, with reduced internalization. These results suggest that RIAM regulates αMβ2 activation and the cytoskeleton *via* its interaction with VASP.

DISCUSSION

Integrins are well-established mediators of cell adhesion and migration, yet underlying mechanisms and signaling pathways continue to be revealed (147). Further investigation is required into the role of integrins in mediating multiple phagocytic process in physiological and pathological conditions and whether integrin activation signaling pathways during cell movement and trafficking are also involved in particle engulfment.

Critical gaps remain in our knowledge of phagocytic integrin signaling. Several alternative mechanisms regulate talin-1

recruitment, but their contributions and significance are obscure. The Rap1-talin-1 interaction is evolutionarily conserved and may contribute to short-term adhesions (148), whereas the Rap1-RIAM-talin-1 axis may have longer and faster recruitment of effector proteins. Phagocytosis occurs in various cell types and is mediated by many integrin types. Several phagocytosis studies have shown that integrins need adaptor proteins or co-receptors to exert full functionality. All integrins have a common characteristic of signaling *via* Rho GTPases to modulate actin cytoskeleton dynamics. During integrin-dependent uptake, signaling involves either RhoA (for αMβ2-mediated phagocytosis) or Rac1/Cdc42 activity. This suggests that the particle engulfment in integrin-dependent phagocytosis may share similar actin-regulating pathways with general Fc-receptor-dependent phagocytosis modes.

Studies on β2 integrins indicate that integrin-mediated phagocytosis is an extension capacity of integrin-mediated cell adhesion. Besides β2 integrins, other integrins may also be involved in phagocytosis, including those in non-leukocytes. Integrins bind to ECM components, such as fibrinogen (ligand of integrin αIIbβ3, αVβ3, and others), fibronectin (ligand of α5β1, α8β1, αVβ1, αVβ3, αIIbβ3, and others), vitronectin (ligand of αvβ1, αvβ3, αvβ5, αvβ6, αvβ8, and others), or collagen (ligand of integrin α1β1, α2β1, α10β1, and α11β1). However, it is not clear which integrins are involved in phagocytosis. Those integrins known to induce actin remodeling might support particle uptake but need to be further evaluated. As far as we know, integrins αVβ3 and αVβ5 are involved in apoptotic-cell (AC) uptake (149). RGD (arginine-glycine-aspartate) peptides severely inhibit AC uptake of human macrophages (150). The remodeling of collagen is essential to the progression of a number of diseases and depends on the degradation and phagocytosis process, in which the uptake of collagen fibrils is mediated by α2β1 integrin (151).

An improved understanding of phagocytosis is important since it is involved in bacterial clearance, antigen presentation, inflammation resolution, and progression of chronic inflammatory or auto-immune diseases. β2 integrins are clearly important in phagocytosis, although their general role is just emerging. Investigating the detailed molecular mechanism of integrin functions in the complex phagocytotic process is a fascinating challenge. β2 integrins are a valuable clinical target (152). However, side effects of β2 integrin-targeting drugs include immune deficiency and infections. This may be due to the important roles that β2 integrins play in regulating the function of all kinds of immune cells, and they may exert contrary functions in a cell type-specific manner. For example, β2 integrins could limit T cell activation when expressed on antigen-presenting cells (153), but be necessary for T cell activation when expressed on T cells (154); infiltration of β2 T cells prevents tumor progression in early tumor development (155), but β2 integrins increase tumor migration and angiogenesis (156). Thus, insight into how the function of β2 integrins can be inhibited in a cell type-specific manner can avoid potential mechanism-based toxicities. This might be achieved by targeting specific integrin conformations or signaling pathways, such as if only the Rap1/talin-1 interaction pathway regulates integrin activation in platelets, the Rap1/RIAM/talin-1 axis might be dominant in lymphocytes. It is worth understanding the regulatory mechanism of β2 integrin activation in phagocytes and other cell types, since this difference can be therapeutically exploited in auto-immune diseases and cancer.

AUTHOR CONTRIBUTIONS

HS and KZ contributed equally to this work. HS prepared figures. HS and KZ drafted the manuscript. HS, KZ, LH, and ZF edited and revised the manuscript. ZF approved the final version of the manuscript. All authors contributed to the article and approved the submitted version.

FUNDING

This research was supported by funding from the National Institutes of Health, USA (NIH, R01HL145454) and a startup fund from UConn Health.

ACKNOWLEDGMENTS

We acknowledge Dr. Christopher "Kit" Bonin and Dr. Geneva Hargis from UConn School of Medicine for their help in the scientific writing and editing of this manuscript.

REFERENCES

1. Aderem A, Underhill DM. Mechanisms of phagocytosis in macrophages. *Annu Rev Immunol* (1999) 17:593–623. doi: 10.1146/annurev.immunol.17.1.593
2. Greenberg S, Grinstein S. Phagocytosis and innate immunity. *Curr Opin Immunol* (2002) 14:136–45. doi: 10.1016/s0952-7915(01)00309-0
3. Kourtzelis I, Hajishengallis G, Chavakis T. Phagocytosis of Apoptotic Cells in Resolution of Inflammation. *Front Immunol* (2020) 11:553. doi: 10.3389/fimmu.2020.00553
4. Rabinovitch M. Professional and non-professional phagocytes: an introduction. *Trends Cell Biol* (1995) 5:85–7. doi: 10.1016/s0962-8924(00)88955-2
5. Griffin FM Jr. Activation of macrophage complement receptors for phagocytosis. *Contemp Top Immunobiol* (1984) 13:57–70. doi: 10.1007/978-1-4757-1445-6_3
6. Richards DM, Endres RG. The mechanism of phagocytosis: two stages of engulfment. *Biophys J* (2014) 107:1542–53. doi: 10.1016/j.bpj.2014.07.070
7. Underhill DM, Ozinsky A. Phagocytosis of microbes: complexity in action. *Annu Rev Immunol* (2002) 20:825–52. doi: 10.1146/annurev.immunol.20.103001.114744
8. Huttenlocher A, Sandborg RR, Horwitz AF. Adhesion in cell migration. *Curr Opin Cell Biol* (1995) 7:697–706. doi: 10.1016/0955-0674(95)80112-x
9. Huttenlocher A, Ginsberg MH, Horwitz AF. Modulation of cell migration by integrin-mediated cytoskeletal linkages and ligand-binding affinity. *J Cell Biol* (1996) 134:1551–62. doi: 10.1083/jcb.134.6.1551
10. Thelen M, Stein JV. How chemokines invite leukocytes to dance. *Nat Immunol* (2008) 9:953–9. doi: 10.1038/ni.f.207

11. Alon R, Ley K. Cells on the run: shear-regulated integrin activation in leukocyte rolling and arrest on endothelial cells. *Curr Opin Cell Biol* (2008) 20:525–32. doi: 10.1016/j.ceb.2008.04.003
12. Torres-Gomez A, Cabanas C, Lafuente EM. Phagocytic Integrins: Activation and Signaling. *Front Immunol* (2020) 11:738. doi: 10.3389/fimmu.2020.00738
13. Bednarczyk M, Stege H, Grabbe S, Bros M. beta2 Integrins-Multi-Functional Leukocyte Receptors in Health and Disease. *Int J Mol Sci* (2020) 21(4). doi: 10.3390/ijms21041402
14. Lu H, Smith CW, Perrard J, Bullard D, Tang L, Shappell SB, et al. LFA-1 is sufficient in mediating neutrophil emigration in Mac-1-deficient mice. *J Clin Invest* (1997) 99:1340–50. doi: 10.1172/JCI119293
15. Ding ZM, Babensee JE, Simon SI, Lu H, Perrard JL, Bullard DC, et al. Relative contribution of LFA-1 and Mac-1 to neutrophil adhesion and migration. *J Immunol* (1999) 163:5029–38.
16. Schmits R, Kundig TM, Baker DM, Shumaker G, Simard JJ, Duncan G, et al. LFA-1-deficient mice show normal CTL responses to virus but fail to reject immunogenic tumor. *J Exp Med* (1996) 183:1415–26. doi: 10.1084/jem.183.4.1415
17. Jawhara S, Pluskota E, Cao W, Plow EF, Soloviev DA. Distinct Effects of Integrins alphaXbeta2 and alphaMbeta2 on Leukocyte Subpopulations during Inflammation and Antimicrobial Responses. *Infect Immun* (2017) 85(1). doi: 10.1128/IAI.00644-16
18. Wu J, Wu H, An J, Ballantyne CM, Cyster JG. Critical role of integrin CD11c in splenic dendritic cell capture of missing-self CD47 cells to induce adaptive immunity. *Proc Natl Acad Sci USA* (2018) 115:6786–91. doi: 10.1073/pnas.1805542115
19. Aziz MH, Cui K, Das M, Brown KE, Ardell CL, Febbraio M, et al. The Upregulation of Integrin alphaDbeta2 (CD11d/CD18) on Inflammatory Macrophages Promotes Macrophage Retention in Vascular Lesions and Development of Atherosclerosis. *J Immunol* (2017) 198:4855–67. doi: 10.4049/jimmunol.1602175
20. Wu H, Rodgers JR, Perrard XY, Perrard JL, Prince JE, Abe Y, et al. Deficiency of CD11b or CD11d results in reduced staphylococcal enterotoxin-induced T cell response and T cell phenotypic changes. *J Immunol* (2004) 173:297–306. doi: 10.4049/jimmunol.173.1.297
21. Bailey WP, Cui K, Ardell CL, Keever KR, Singh S, Rodriguez-Gil DJ, et al. The expression of integrin alphaD beta2 (CD11d/CD18) on neutrophils orchestrates the defense mechanism against endotoxemia and sepsis. *J Leukoc Biol* (2021). doi: 10.1002/JLB.3HI0820-529RR
22. Nascimento DO, Vieira-de-Abreu A, Arcanjo AF, Bozza PT, Zimmerman GA, Castro-Faria-Neto HC. Integrin alphaDbeta2 (CD11d/CD18) Modulates Leukocyte Accumulation, Pathogen Clearance, and Pyroptosis in Experimental Salmonella Typhimurium Infection. *Front Immunol* (2018) 9:1128. doi: 10.3389/fimmu.2018.01128
23. Schittenhelm L, Hilkens CM, Morrison VL. beta2 Integrins As Regulators of Dendritic Cell, Monocyte, and Macrophage Function. *Front Immunol* (2017) 8:1866. doi: 10.3389/fimmu.2017.01866
24. Coxon A, Rieu P, Barkalow FJ, Askari S, Sharpe AH, von Andrian UH, et al. A novel role for the beta 2 integrin CD11b/CD18 in neutrophil apoptosis: a homeostatic mechanism in inflammation. *Immunity* (1996) 5:653–66. doi: 10.1016/s1074-7613(00)80278-2
25. van Spriel AB, Leusen JH, van Egmond M, Dijkman HB, Assmann KJ, Mayadas TN, et al. Mac-1 (CD11b/CD18) is essential for Fc receptor-mediated neutrophil cytotoxicity and immunologic synapse formation. *Blood* (2001) 97:2478–86. doi: 10.1182/blood.v97.8.2478
26. Podolnikova NP, Kushchayeva YS, Wu Y, Faust J, Ugarova TP. The Role of Integrins alphaMbeta2 (Mac-1, CD11b/CD18) and alphaDbeta2 (CD11d/CD18) in Macrophage Fusion. *Am J Pathol* (2016) 186:2105–16. doi: 10.1016/j.ajpath.2016.04.001
27. Bunting M, Harris ES, McIntyre TM, Prescott SM, Zimmerman GA. Leukocyte adhesion deficiency syndromes: adhesion and tethering defects involving beta 2 integrins and selectin ligands. *Curr Opin Hematol* (2002) 9:30–5. doi: 10.1097/00062752-200201000-00006
28. McDowall A, Svensson L, Stanley P, Patzak I, Chakravarty P, Howarth K, et al. Two mutations in the KINDLIN3 gene of a new leukocyte adhesion deficiency III patient reveal distinct effects on leukocyte function in vitro. *Blood* (2010) 115:4834–42. doi: 10.1182/blood-2009-08-238709
29. Etzioni A. Leukocyte adhesion deficiency III - when integrins activation fails. *J Clin Immunol* (2014) 34:900–3. doi: 10.1007/s10875-014-0094-4
30. Mitroulis I, Alexaki VI, Kourtzelis I, Ziogas A, Hajishengallis G, Chavakis T. Leukocyte integrins: role in leukocyte recruitment and as therapeutic targets in inflammatory disease. *Pharmacol Ther* (2015) 147:123–35. doi: 10.1016/j.pharmthera.2014.11.008
31. Lefort CT, Ley K. Neutrophil arrest by LFA-1 activation. *Front Immunol* (2012) 3:157. doi: 10.3389/fimmu.2012.00157
32. Neelamegham S, Taylor AD, Burns AR, Smith CW, Simon SI, et al. Hydrodynamic shear shows distinct roles for LFA-1 and Mac-1 in neutrophil adhesion to intercellular adhesion molecule-1. *Blood* (1998) 92:1626–38.
33. Gopalan PK, Smith CW, Lu H, Berg EL, McIntire LV, Simon SI. Neutrophil CD18-dependent arrest on intercellular adhesion molecule 1 (ICAM-1) in shear flow can be activated through L-selectin. *J Immunol* (1997) 158:367–75.
34. Thomson W, Frame W. Prevention of accidental poisoning in children. *Health Bull* (1979) 37:221–4.
35. Gerhardt T, Ley K. Monocyte trafficking across the vessel wall. *Cardiovasc Res* (2015) 107:321–30. doi: 10.1093/cvr/cvv147
36. Quintar A, McArdle S, Wolf D, Marki A, Ehinger E, Vassallo M, et al. Endothelial Protective Monocyte Patrolling in Large Arteries Intensified by Western Diet and Atherosclerosis. *Circ Res* (2017) 120:1789–99. doi: 10.1161/CIRCRESAHA.117.310739
37. Finsterbusch M, Hall P, Li A, Devi S, Westhorpe CL, Kitching AR, et al. Patrolling monocytes promote intravascular neutrophil activation and glomerular injury in the acutely inflamed glomerulus. *Proc Natl Acad Sci USA* (2016) 113:E5172–5181. doi: 10.1073/pnas.1606253113
38. Hyun YM, Choe YH, Park SA, Kim M. LFA-1 (CD11a/CD18) and Mac-1 (CD11b/CD18) distinctly regulate neutrophil extravasation through hotspots I and II. *Exp Mol Med* (2019) 51:1–13. doi: 10.1038/s12276-019-0227-1
39. Ostermann G, Weber KS, Zernecke A, Schroder A, Weber C. JAM-1 is a ligand of the beta(2) integrin LFA-1 involved in transendothelial migration of leukocytes. *Nat Immunol* (2002) 3:151–8. doi: 10.1038/ni755
40. Weber C, Springer TA. Neutrophil accumulation on activated, surface-adherent platelets in flow is mediated by interaction of Mac-1 with fibrinogen bound to alphaIIbbeta3 and stimulated by platelet-activating factor. *J Clin Invest* (1997) 100:2085–93. doi: 10.1172/JCI119742
41. Diamond MS, Staunton DE, de Fougerolles AR, Stacker SA, Garcia-Aguilar J, Hibbs ML, et al. ICAM-1 (CD54): a counter-receptor for Mac-1 (CD11b/CD18). *J Cell Biol* (1990) 111:3129–39. doi: 10.1083/jcb.111.6.3129
42. Simon DI, Chen Z, Xu H, Li CQ, Dong J, McIntire LV, et al. Platelet glycoprotein ibalpha is a counterreceptor for the leukocyte integrin Mac-1 (CD11b/CD18). *J Exp Med* (2000) 192:193–204. doi: 10.1084/jem.192.2.193
43. Santoso S, Sachs UJ, Kroll H, Linder M, Ruf A, Preissner KT, et al. The junctional adhesion molecule 3 (JAM-3) on human platelets is a counterreceptor for the leukocyte integrin Mac-1. *J Exp Med* (2002) 196:679–91. doi: 10.1084/jem.20020267
44. Podolnikova NP, Podolnikov AV, Haas TA, Lishko VK, Ugarova TP. Ligand recognition specificity of leukocyte integrin alphaMbeta2 (Mac-1, CD11b/CD18) and its functional consequences. *Biochemistry* (2015) 54:1408–20. doi: 10.1021/bi5013782
45. Yakubenko VP, Lishko VK, Lam SC, Ugarova TP. A molecular basis for integrin alphaMbeta 2 ligand binding promiscuity. *J Biol Chem* (2002) 277:48635–42. doi: 10.1074/jbc.M208877200
46. Dupuy AG, Caron E. Integrin-dependent phagocytosis: spreading from microadhesion to new concepts. *J Cell Sci* (2008) 121:1773–83. doi: 10.1242/jcs.018036
47. Underhill DM, Goodridge HS. Information processing during phagocytosis. *Nat Rev Immunol* (2012) 12:492–502. doi: 10.1038/nri3244
48. Rosales C, Uribe-Querol E. Phagocytosis: A Fundamental Process in Immunity. *BioMed Res Int* (2017) 2017:9042851. doi: 10.1155/2017/9042851
49. Yakubenko VP, Yadav SP, Ugarova TP. Integrin alphaDbeta2, an adhesion receptor up-regulated on macrophage foam cells, exhibits multiligand-binding properties. *Blood* (2006) 107:1643–50. doi: 10.1182/blood-2005-06-2509
50. Fan Z, Ley K. Leukocyte arrest: Biomechanics and molecular mechanisms of beta2 integrin activation. *Biorheology* (2015) 52:353–77. doi: 10.3233/BIR-15085

51. Souza COS, Espindola MS, Fontanari C, Prado MKB, Frantz FG, Rodrigues V, et al. CD18 Regulates Monocyte Hematopoiesis and Promotes Resistance to Experimental Schistosomiasis. *Front Immunol* (2018) 9:1970. doi: 10.3389/fimmu.2018.01970
52. McNally AK, Anderson JM. Beta1 and beta2 integrins mediate adhesion during macrophage fusion and multinucleated foreign body giant cell formation. *Am J Pathol* (2002) 160:621–30. doi: 10.1016/s0002-9440(10)64882-1
53. Helming L, Tomasello E, Kyriakides TR, Martinez FO, Takai T, Gordon S, et al. Essential role of DAP12 signaling in macrophage programming into a fusion-competent state. *Sci Signaling* (2008) 1:ra11. doi: 10.1126/scisignal.1159665
54. Xiong J-P, Stehle T, Diefenbach B, Zhang R, Dunker R, Scott DL, et al. Crystal structure of the extracellular segment of integrin aVb3. *Science* (2001) 294:339–45. doi: 10.1126/science.1064535
55. Xiong JP, Stehle T, Zhang R, Joachimiak A, Frech M, Goodman SL, et al. Crystal structure of the extracellular segment of integrin aVb3 in complex with an Arg-Gly-Asp ligand. *Science* (2002) 296:151–5. doi: 10.1126/science.1069040
56. Xiong JP, Mahalingham B, Alonso JL, Borrelli LA, Rui X, Anand S, et al. Crystal structure of the complete integrin alphaVbeta3 ectodomain plus an alpha/beta transmembrane fragment. *J Cell Biol* (2009) 186:589–600. doi: 10.1083/jcb.200905085
57. Xie C, Zhu J, Chen X, Mi L, Nishida N, Springer TA. Structure of an integrin with an alphaI domain, complement receptor type 4. *EMBO J* (2010) 29:666–79. doi: 10.1038/emboj.2009.367
58. Zhu J, Luo BH, Xiao T, Zhang C, Nishida N, Springer TA. Structure of a complete integrin ectodomain in a physiologic resting state and activation and deactivation by applied forces. *Mol Cell* (2008) 32:849–61. doi: 10.1016/j.molcel.2008.11.018
59. Springer TA, Zhu J, Xiao T. Structural basis for distinctive recognition of fibrinogen gammaC peptide by the platelet integrin alphaIIbbeta3. *J Cell Biol* (2008) 182:791–800. doi: 10.1083/jcb.200801146
60. Sun H, Fan Z, Gingras AR, Lopez-Ramirez MA, Ginsberg MH, Ley K. Frontline Science: A flexible kink in the transmembrane domain impairs beta2 integrin extension and cell arrest from rolling. *J Leukoc Biol* (2020) 107:175–83. doi: 10.1002/JLB.1HI0219-073RR
61. Chen X, Xie C, Nishida N, Li Z, Walz T, Springer TA. Requirement of open headpiece conformation for activation of leukocyte integrin alphaXbeta2. *Proc Natl Acad Sci USA* (2010) 107:14727–32. doi: 10.1073/pnas.1008663107
62. Takagi J, Petre BM, Walz T, Springer TA. Global conformational rearrangements in integrin extracellular domains in outside-in and inside-out signaling. *Cell* (2002) 110:599–11. doi: 10.1016/s0092-8674(02)00935-2
63. Springer TA, Dustin ML. Integrin inside-out signaling and the immunological synapse. *Curr Opin Cell Biol* (2012) 24:107–15. doi: 10.1016/j.ceb.2011.10.004
64. Luo BH, Carman CV, Springer TA. Structural basis of integrin regulation and signaling. *Annu Rev Immunol* (2007) 25:619–47. doi: 10.1146/annurev.immunol.25.022106.141618
65. Schurpf T, Springer TA. Regulation of integrin affinity on cell surfaces. *EMBO J* (2011) 30:4712–27. doi: 10.1038/emboj.2011.333
66. Salas A, Shimaoka M, Kogan AN, Harwood C, von Andrian UH, Springer TA. Rolling adhesion through an extended conformation of integrin alphaLbeta2 and relation to alpha I and beta I-like domain interaction. *Immunity* (2004) 20:393–406. doi: 10.1016/s1074-7613(04)00082-2
67. Nordenfelt P, Moore TI, Mehta SB, Kalappurakkal JM, Swaminathan V, Koga N, et al. Direction of actin flow dictates integrin LFA-1 orientation during leukocyte migration. *Nat Commun* (2017) 8:2047. doi: 10.1038/s41467-017-01848-y
68. Nordenfelt P, Elliott HL, Springer TA. Coordinated integrin activation by actin-dependent force during T-cell migration. *Nat Commun* (2016) 7:13119. doi: 10.1038/ncomms13119
69. Li J, Su Y, Xia W, Qin Y, Humphries MJ, Vestweber D, et al. Conformational equilibria and intrinsic affinities define integrin activation. *EMBO J* (2017) 36:629–45. doi: 10.15252/embj.201695803
70. Fan Z, Kiosses WB, Sun H, Orecchioni M, Ghosheh Y, Zajonc DM, et al. High-Affinity Bent beta2-Integrin Molecules in Arresting Neutrophils Face Each Other through Binding to ICAMs In cis. *Cell Rep* (2019) 26:119–30.e115. doi: 10.1016/j.celrep.2018.12.038
71. Fan Z, McArdle S, Marki A, Mikulski Z, Gutierrez E, Engelhardt B, et al. Neutrophil recruitment limited by high-affinity bent beta2 integrin binding ligand in cis. *Nat Commun* (2016) 7:12658. doi: 10.1038/ncomms12658
72. Sen M, Yuki K, Springer TA. An internal ligand-bound, metastable state of a leukocyte integrin, alphaXbeta2. *J Cell Biol* (2013) 203:629–42. doi: 10.1083/jcb.201308083
73. Carman CV, Springer TA. Integrin avidity regulation: are changes in affinity and conformation underemphasized? *Curr Opin Cell Biol* (2003) 15:547–56. doi: 10.1016/j.ceb.2003.08.003
74. Saggu G, Okubo K, Chen Y, Vattepu R, Tsuboi N, Rosetti F, et al. Cis interaction between sialylated FcgammaRIIA and the alphaI-domain of Mac-1 limits antibody-mediated neutrophil recruitment. *Nat Commun* (2018) 9:5058. doi: 10.1038/s41467-018-07506-1
75. Calderwood DA, Yan B, de Pereda JM, Alvarez BG, Fujioka Y, Liddington RC, et al. The phosphotyrosine binding-like domain of talin activates integrins. *J Biol Chem* (2002) 277:21749–58. doi: 10.1074/jbc.M111996200
76. Harburger DS, Calderwood DA. Integrin signalling at a glance. *J Cell Sci* (2009) 122:159–63. doi: 10.1242/jcs.018093
77. Kim C, Schmidt T, Cho EG, Ye F, Ulmer TS, Ginsberg MH. Basic amino-acid side chains regulate transmembrane integrin signalling. *Nature* (2012) 481:209–13. doi: 10.1038/nature10697
78. Sun H, Lagarrigue F, Gingras AR, Fan Z, Ley K, Ginsberg MH. Transmission of integrin beta7 transmembrane domain topology enables gut lymphoid tissue development. *J Cell Biol* (2018). doi: 10.1083/jcb.201707055
79. Abram CL, Lowell CA. The ins and outs of leukocyte integrin signaling. *Annu Rev Immunol* (2009) 27:339–62. doi: 10.1146/annurev.immunol.021908.132554
80. Lagarrigue F, Kim C, Ginsberg MH. The Rap1-RIAM-talin axis of integrin activation and blood cell function. *Blood* (2016) 128:479–87. doi: 10.1182/blood-2015-12-638700
81. Franke B, Akkerman JW, Bos JL. Rapid Ca2+-mediated activation of Rap1 in human platelets. *EMBO J* (1997) 16:252–9. doi: 10.1093/emboj/16.2.252
82. Jeon TJ, Lee DJ, Lee S, Weeks G, Firtel RA. Regulation of Rap1 activity by RapGAP1 controls cell adhesion at the front of chemotaxing cells. *J Cell Biol* (2007) 179:833–43. doi: 10.1083/jcb.200705068
83. Caron E, Self AJ, Hall A. The GTPase Rap1 controls functional activation of macrophage integrin alphaMbeta2 by LPS and other inflammatory mediators. *Curr Biol CB* (2000) 10:974–8. doi: 10.1016/s0960-9822(00)00641-2
84. Stadtmann A, Brinkhaus L, Mueller H, Rossaint J, Bolomini-Vittori M, Bergmeier W, et al. Rap1a activation by CalDAG-GEFI and p38 MAPK is involved in E-selectin-dependent slow leukocyte rolling. *Eur J Immunol* (2011) 41:2074–85. doi: 10.1002/eji.201041196
85. Lozano ML, Cook A, Bastida JM, Paul DS, Iruin G, Cid AR, et al. Novel mutations in RASGRP2, which encodes CalDAG-GEFI, abrogate Rap1 activation, causing platelet dysfunction. *Blood* (2016) 128:1282–9. doi: 10.1182/blood-2015-11-683102
86. Kim C, Ye F, Ginsberg MH. Regulation of integrin activation. *Annu Rev Cell Dev Biol* (2011) 27:321–45. doi: 10.1146/annurev-cellbio-100109-104104
87. Hemmings L, Rees DJ, Ohanian V, Bolton SJ, Gilmore AP, Patel B, et al. Talin contains three actin-binding sites each of which is adjacent to a vinculin-binding site. *J Cell Sci* (1996) 109(Pt 11):2715–26.
88. Wegener KL, Partridge AW, Han J, Pickford AR, Liddington RC, Ginsberg MH, et al. Structural basis of integrin activation by talin. *Cell* (2007) 128:171–82. doi: 10.1016/j.cell.2006.10.048
89. Garcia-Alvarez B, de Pereda JM, Calderwood DA, Ulmer TS, Critchley D, Campbell ID, et al. Structural determinants of integrin recognition by talin. *Mol Cell* (2003) 11:49–58. doi: 10.1016/s1097-2765(02)00823-7
90. Shattil SJ, Kim C, Ginsberg MH. The final steps of integrin activation: the end game. *Nat Rev Mol Cell Biol* (2010) 11:288–300. doi: 10.1038/nrm2871
91. Yago T, Petrich BG, Zhang N, Liu Z, Shao B, Ginsberg MH, et al. Blocking neutrophil integrin activation prevents ischemia-reperfusion injury. *J Exp Med* (2015) 212:1267–81. doi: 10.1084/jem.20142358
92. Goult BT, Zacharchenko T, Bate N, Tsang R, Hey F, Gingras AR, et al. RIAM and vinculin binding to talin are mutually exclusive and regulate adhesion assembly and turnover. *J Biol Chem* (2013) 288:8238–49. doi: 10.1074/jbc.M112.438119

93. Lim J, Wiedemann A, Tzircotis G, Monkley SJ, Critchley DR, Caron E. An essential role for talin during alpha(M)beta(2)-mediated phagocytosis. *Mol Biol Cell* (2007) 18:976–85. doi: 10.1091/mbc.e06-09-0813
94. Ling K, Doughman RL, Firestone AJ, Bunce MW, Anderson RA. Type I gamma phosphatidylinositol phosphate kinase targets and regulates focal adhesions. *Nature* (2002) 420:89–93. doi: 10.1038/nature01082
95. Di Paolo G, Pellegrini L, Letinic K, Cestra G, Zoncu R, Voronov S, et al. Recruitment and regulation of phosphatidylinositol phosphate kinase type 1 gamma by the FERM domain of talin. *Nature* (2002) 420:85–9. doi: 10.1038/nature01147
96. Martel V, Racaud-Sultan C, Dupe S, Marie C, Paulhe F, Galmiche A, et al. Conformation, localization, and integrin binding of talin depend on its interaction with phosphoinositides. *J Biol Chem* (2001) 276:21217–27. doi: 10.1074/jbc.M102373200
97. Lee HS, Lim CJ, Puzon-McLaughlin W, Shattil SJ, Ginsberg MH. RIAM activates integrins by linking talin to ras GTPase membrane-targeting sequences. *J Biol Chem* (2009) 284:5119–27. doi: 10.1074/jbc.M807117200
98. Lim J, Dupuy AG, Critchley DR, Caron E. Rap1 controls activation of the alpha(M)beta(2) integrin in a talin-dependent manner. *J Cell Biochem* (2010) 111:999–1009. doi: 10.1002/jcb.22788
99. Lagarrigue F, Gingras AR, Paul DS, Valadez AJ, Cuevas MN, Sun H, et al. Rap1 binding to the talin 1 F0 domain makes a minimal contribution to murine platelet GPIIb-IIIa activation. *Blood Adv* (2018) 2:2358–68. doi: 10.1182/bloodadvances.2018020487
100. Gingras AR, Lagarrigue F, Cuevas MN, Valadez AJ, Zorovich M, McLaughlin W, et al. Rap1 binding and a lipid-dependent helix in talin F1 domain promote integrin activation in tandem. *J Cell Biol* (2019) 218:1799–809. doi: 10.1083/jcb.201810061
101. Bromberger T, Klapproth S, Rohwedder I, Zhu L, Mittmann L, Reichel CA, et al. Direct Rap1/Talin1 interaction regulates platelet and neutrophil integrin activity in mice. *Blood* (2018) 132:2754–62. doi: 10.1182/blood-2018-04-846766
102. Lagarrigue F, Paul DS, Gingras AR, Valadez AJ, Sun H, Lin J, et al. Talin-1 is the principal platelet Rap1 effector of integrin activation. *Blood* (2020) 136:1180–90. doi: 10.1182/blood.2020005348
103. Klapproth S, Sperandio M, Pinheiro EM, Prunster M, Soehnlein O, Gertler FB, et al. Loss of the Rap1 effector RIAM results in leukocyte adhesion deficiency due to impaired beta2 integrin function in mice. *Blood* (2015) 126:2704–12. doi: 10.1182/blood-2015-05-647453
104. Lagarrigue F, Gertler FB, Ginsberg MH, Cantor JM. Cutting Edge: Loss of T Cell RIAM Precludes Conjugate Formation with APC and Prevents Immune-Mediated Diabetes. *J Immunol* (2017) 198:3410–5. doi: 10.4049/jimmunol.1601743
105. Lafuente EM, van Puijenbroek AA, Krause M, Carman CV, Freeman GJ, Berezovskaya A, et al. RIAM, an Ena/VASP and Profilin ligand, interacts with Rap1-GTP and mediates Rap1-induced adhesion. *DevCell* (2004) 7:585. doi: 10.1016/j.devcel.2004.07.021
106. Sun H, Lagarrigue F, Wang H, Fan Z, Lopez-Ramirez MA, Chang JT, et al. Distinct integrin activation pathways for effector and regulatory T cell trafficking and function. *J Exp Med* (2021) 218(2). doi: 10.1084/jem.20201524
107. Watanabe N, Bodin L, Pandey M, Krause M, Coughlin S, Boussiotis VA, et al. Mechanisms and consequences of agonist-induced talin recruitment to platelet integrin alphaIIbbeta3. *J Cell Biol* (2008) 181:1211–22. doi: 10.1083/jcb.200803094
108. Kliche S, Worbs T, Wang X, Degen J, Patzak I, Meineke B, et al. CCR7-mediated LFA-1 functions in T cells are regulated by 2 independent ADAP/SKAP55 modules. *Blood* (2012) 119:777–85. doi: 10.1182/blood-2011-06-362269
109. Moser M, Legate KR, Zent R, Fassler R. The tail of integrins, talin, and kindlins. *Science* (2009) 324:895–9. doi: 10.1126/science.1163865
110. Manevich-Mendelson E, Grabovsky V, Feigelson SW, Cinamon G, Gore Y, Goverse G, et al. Talin1 is required for integrin-dependent B lymphocyte homing to lymph nodes and the bone marrow but not for follicular B-cell maturation in the spleen. *Blood* (2010) 116:5907–18. doi: 10.1182/blood-2010-06-293506
111. Lefort CT, Rossaint J, Moser M, Petrich BG, Zarbock A, Monkley SJ, et al. Distinct roles for talin-1 and kindlin-3 in LFA-1 extension and affinity regulation. *Blood* (2012) 119:4275–82. doi: 10.1182/blood-2011-08-373118
112. Hart R, Stanley P, Chakravarty P, Hogg N. The kindlin 3 pleckstrin homology domain has an essential role in lymphocyte function-associated antigen 1 (LFA-1) integrin-mediated B cell adhesion and migration. *J Biol Chem* (2013) 288:14852–62. doi: 10.1074/jbc.M112.434621
113. Morrison VL, MacPherson M, Savinko T, Lek HS, Prescott A, Fagerholm SC. The beta2 integrin-kindlin-3 interaction is essential for T-cell homing but dispensable for T-cell activation in vivo. *Blood* (2013) 122:1428–36. doi: 10.1182/blood-2013-02-484998
114. Wen L, Marki A, Roy P, McArdle S, Sun H, Fan Z, et al. Kindlin-3 recruitment to the plasma membrane precedes high affinity beta2 integrin and neutrophil arrest from rolling. *Blood* (2020). doi: 10.1182/blood.2019003446
115. Liu H, Zhu L, Dudiki T, Gabanic B, Good L, Podrez EA, et al. Macrophage Migration and Phagocytosis Are Controlled by Kindlin-3's Link to the Cytoskeleton. *J Immunol* (2020) 204:1954–67. doi: 10.4049/jimmunol.1901134
116. Tadokoro S, Shattil SJ, Eto K, Tai V, Liddington RC, de Pereda JM, et al. Talin binding to integrin beta tails: a final common step in integrin activation. *Science* (2003) 302:103–6. doi: 10.1126/science.1086652
117. Kiema T, Lad Y, Jiang P, Oxley CL, Baldassarre M, Wegener KL, et al. The molecular basis of filamin binding to integrins and competition with talin. *Mol Cell* (2006) 21:337–47. doi: 10.1016/j.molcel.2006.01.011
118. Ithychanda SS, Das M, Ma YQ, Ding K, Wang X, Gupta S, et al. Migfilin, a molecular switch in regulation of integrin activation. *J Biol Chem* (2009) 284:4713–22. doi: 10.1074/jbc.M807719200
119. Lad Y, Jiang P, Ruskamo S, Harburger DS, Ylanne J, Campbell ID, et al. Structural basis of the migfilin-filamin interaction and competition with integrin beta tails. *J Biol Chem* (2008) 283:35154–63. doi: 10.1074/jbc.M802592200
120. Oxley CL, Anthis NJ, Lowe ED, Vakonakis I, Campbell ID, Wegener KL. An integrin phosphorylation switch: the effect of beta3 integrin tail phosphorylation on Dok1 and talin binding. *J Biol Chem* (2008) 283:5420–6. doi: 10.1074/jbc.M709435200
121. Millon-Fremillon A, Bouvard D, Grichine A, Manet-Dupe S, Block MR, Albiges-Rizo C. Cell adaptive response to extracellular matrix density is controlled by ICAP-1-dependent beta1-integrin affinity. *J Cell Biol* (2008) 180:427–41. doi: 10.1083/jcb.200707142
122. Boujemaa-Paterski R, Martins B, Eibauer M, Beales CT, Geiger B, Medalia O. Talin-activated vinculin interacts with branched actin networks to initiate bundles. *Elife* (2020) 9. doi: 10.7554/eLife.53990
123. Nolz JC, Medeiros RB, Mitchell JS, Zhu P, Freedman BD, Shimizu Y, et al. WAVE2 regulates high-affinity integrin binding by recruiting vinculin and talin to the immunological synapse. *Mol Cell Biol* (2007) 27:5986–6000. doi: 10.1128/MCB.00136-07
124. Nishiya N, Kiosses WB, Han J, Ginsberg MH. An alpha4 integrin-paxillin-Arf-GAP complex restricts Rac activation to the leading edge of migrating cells. *Nat Cell Biol* (2005) 7:343–52. doi: 10.1038/ncb1234
125. Swanson JA. Shaping cups into phagosomes and macropinosomes. *Nat Rev Mol Cell Biol* (2008) 9:639–49. doi: 10.1038/nrm2447
126. Mao Y, Finnemann SC. Regulation of phagocytosis by Rho GTPases. *Small GTPases* (2015) 6:89–99. doi: 10.4161/21541248.2014.989785
127. Freeman SA, Grinstein S. Phagocytosis: receptors, signal integration, and the cytoskeleton. *Immunol Rev* (2014) 262:193–215. doi: 10.1111/imr.12212
128. Ridley AJ, Schwartz MA, Burridge K, Firtel RA, Ginsberg MH, Borisy G, et al. Cell migration: integrating signals from front to back. *Science* (2003) 302:1704–9. doi: 10.1126/science.1092053
129. Sindrilaru A, Peters T, Schymeinsky J, Oreshkova T, Wang H, Gompf A, et al. Wound healing defect of Vav3-/- mice due to impaired {beta}2-integrin-dependent macrophage phagocytosis of apoptotic neutrophils. *Blood* (2009) 113:5266–76. doi: 10.1182/blood-2008-07-166702
130. Tzircotis G, Braga VM, Caron E. RhoG is required for both FcgammaR- and CR3-mediated phagocytosis. *J Cell Sci* (2011) 124:2897–902. doi: 10.1242/jcs.084269
131. Goodridge HS, Reyes CN, Becker CA, Katsumoto TR, Ma J, Wolf AJ, et al. Activation of the innate immune receptor Dectin-1 upon formation of a 'phagocytic synapse'. *Nature* (2011) 472:471–5. doi: 10.1038/nature10071
132. Griffin FM Jr, Griffin JA, Leider JE, Silverstein SC. Studies on the mechanism of phagocytosis. I. Requirements for circumferential attachment of particle-

bound ligands to specific receptors on the macrophage plasma membrane. *J Exp Med* (1975) 142:1263–82. doi: 10.1084/jem.142.5.1263
133. Lee CY, Herant M, Heinrich V. Target-specific mechanics of phagocytosis: protrusive neutrophil response to zymosan differs from the uptake of antibody-tagged pathogens. *J Cell Sci* (2011) 124:1106–14. doi: 10.1242/jcs.078592
134. Patel PC, Harrison RE. Membrane ruffles capture C3bi-opsonized particles in activated macrophages. *Mol Biol Cell* (2008) 19:4628–39. doi: 10.1091/mbc.E08-02-0223
135. Allen LA, Aderem A. Molecular definition of distinct cytoskeletal structures involved in complement- and Fc receptor-mediated phagocytosis in macrophages. *J Exp Med* (1996) 184:627–37. doi: 10.1084/jem.184.2.627
136. Caron E, Hall A. Identification of two distinct mechanisms of phagocytosis controlled by different Rho GTPases. *Science* (1998) 282:1717–21. doi: 10.1126/science.282.5394.1717
137. Bohdanowicz M, Cosio G, Backer JM, Grinstein S. Class I and class III phosphoinositide 3-kinases are required for actin polymerization that propels phagosomes. *J Cell Biol* (2010) 191:999–1012. doi: 10.1083/jcb.201004005
138. Hall AB, Gakidis MA, Glogauer M, Wilsbacher JL, Gao S, Swat W, et al. Requirements for Vav guanine nucleotide exchange factors and Rho GTPases in FcgammaR- and complement-mediated phagocytosis. *Immunity* (2006) 24:305–16. doi: 10.1016/j.immuni.2006.02.005
139. Ye F, Kim C, Ginsberg MH. Reconstruction of integrin activation. *Blood* (2012) 119:26–33. doi: 10.1182/blood-2011-04-292128
140. Ye F, Snider AK, Ginsberg MH. Talin and kindlin: the one-two punch in integrin activation. *Front Med* (2014) 8:6–16. doi: 10.1007/s11684-014-0317-3
141. Calderwood DA, Campbell ID, Critchley DR. Talins and kindlins: partners in integrin-mediated adhesion. *Nat Rev Mol Cell Biol* (2013) 14:503–17. doi: 10.1038/nrm3624
142. Jaumouille V, Waterman CM. Physical Constraints and Forces Involved in Phagocytosis. *Front Immunol* (2020) 11:1097. doi: 10.3389/fimmu.2020.01097
143. Jaumouille V, Cartagena-Rivera AX, Waterman CM. Coupling of beta2 integrins to actin by a mechanosensitive molecular clutch drives complement receptor-mediated phagocytosis. *Nat Cell Biol* (2019) 21:1357–69. doi: 10.1038/s41556-019-0414-2
144. Marcovecchio PM, Zhu YP, Hanna RN, Dinh HQ, Tacke R, Wu R, et al. Frontline Science: Kindlin-3 is essential for patrolling and phagocytosis functions of nonclassical monocytes during metastatic cancer surveillance. *J Leukoc Biol* (2020) 107:883–92. doi: 10.1002/JLB.4HI0420-098R
145. Medrano-Fernandez I, Reyes R, Olazabal I, Rodriguez E, Sanchez-Madrid F, Boussiotis VA, et al. RIAM (Rap1-interacting adaptor molecule) regulates complement-dependent phagocytosis. *Cell Mol Life Sci* (2013) 70:2395–410. doi: 10.1007/s00018-013-1268-6
146. Torres-Gomez A, Sanchez-Trincado JL, Toribio V, Torres-Ruiz R, Rodriguez-Perales S, Yanez-Mo M, et al. RIAM-VASP Module Relays Integrin Complement Receptors in Outside-In Signaling Driving Particle Engulfment. *Cells* (2020) 9(5). doi: 10.3390/cells9051166
147. Margadant C, Monsuur HN, Norman JC, Sonnenberg A. Mechanisms of integrin activation and trafficking. *Curr Opin Cell Biol* (2011) 23:607–14. doi: 10.1016/j.ceb.2011.08.005
148. Bromberger T, Zhu L, Klapproth S, Qin J, Moser M. Rap1 and membrane lipids cooperatively recruit talin to trigger integrin activation. *J Cell Sci* (2019) 132(21). doi: 10.1242/jcs.235531
149. Taverna D, Moher H, Crowley D, Borsig L, Varki A, Hynes RO. Increased primary tumor growth in mice null for beta3- or beta3/beta5-integrins or selectins. *Proc Natl Acad Sci USA* (2004) 101:763–8. doi: 10.1073/pnas.0307289101
150. Savill J, Dransfield I, Hogg N, Haslett C. Vitronectin receptor-mediated phagocytosis of cells undergoing apoptosis. *Nature* (1990) 343:170–3. doi: 10.1038/343170a0
151. Lee W, Sodek J, McCulloch CA. Role of integrins in regulation of collagen phagocytosis by human fibroblasts. *J Cell Physiol* (1996) 168:695–704. doi: 10.1002/(SICI)1097-4652(199609)168:3<695::AID-JCP22>3.0.CO;2-X
152. Ley K, Rivera-Nieves J, Sandborn WJ, Shattil S. Integrin-based therapeutics: biological basis, clinical use and new drugs. *Nat Rev Drug Discov* (2016) 15:173–83. doi: 10.1038/nrd.2015.10
153. Pettmann J, Santos AM, Dushek O, Davis SJ. Membrane Ultrastructure and T Cell Activation. *Front Immunol* (2018) 9:2152. doi: 10.3389/fimmu.2018.02152
154. Varga G, Nippe N, Balkow S, Peters T, Wild MK, Seeliger S, et al. LFA-1 contributes to signal I of T-cell activation and to the production of T(h)1 cytokines. *J Invest Dermatol* (2010) 130:1005–12. doi: 10.1038/jid.2009.398
155. Harjunpaa H, Llort Asens M, Guenther C, Fagerholm SC. Cell Adhesion Molecules and Their Roles and Regulation in the Immune and Tumor Microenvironment. *Front Immunol* (2019) 10:1078. doi: 10.3389/fimmu.2019.01078
156. Soloviev DA, Hazen SL, Szpak D, Bledzka KM, Ballantyne CM, Plow EF, et al. Dual role of the leukocyte integrin alphaMbeta2 in angiogenesis. *J Immunol* (2014) 193:4712–21. doi: 10.4049/jimmunol.1400202

Conflict of Interest: The authors declare that the research was conducted in the absence of any commercial or financial relationships that could be construed as a potential conflict of interest.

Copyright © 2021 Sun, Zhi, Hu and Fan. This is an open-access article distributed under the terms of the Creative Commons Attribution License (CC BY). The use, distribution or reproduction in other forums is permitted, provided the original author(s) and the copyright owner(s) are credited and that the original publication in this journal is cited, in accordance with accepted academic practice. No use, distribution or reproduction is permitted which does not comply with these terms.

frontiers in Immunology

REVIEW
published: 01 April 2021
doi: 10.3389/fimmu.2021.659533

Examining the Underappreciated Role of *S*-Acylated Proteins as Critical Regulators of Phagocytosis and Phagosome Maturation in Macrophages

Charneal L. Dixon[1,2], *Katrina Mekhail*[1,2] *and Gregory D. Fairn*[1,2,3,4]*

[1] Keenan Research Centre for Biomedical Science, St. Michael's Hospital, Unity Health Toronto, Toronto, ON, Canada, [2] Department of Biochemistry, University of Toronto, Toronto, ON, Canada, [3] Department of Surgery, University of Toronto, Toronto, ON, Canada, [4] Department of Laboratory Medicine and Pathobiology, Toronto, ON, Canada

Phagocytosis is a receptor-mediated process used by cells to engulf a wide variety of particulates, including microorganisms and apoptotic cells. Many of the proteins involved in this highly orchestrated process are post-translationally modified with lipids as a means of regulating signal transduction, membrane remodeling, phagosome maturation and other immunomodulatory functions of phagocytes. *S*-acylation, generally referred to as *S*-palmitoylation, is the post-translational attachment of fatty acids to a cysteine residue exposed topologically to the cytosol. This modification is reversible due to the intrinsically labile thioester bond between the lipid and sulfur atom of cysteine, and thus lends itself to a variety of regulatory scenarios. Here we present an overview of a growing number of *S*-acylated proteins known to regulate phagocytosis and phagosome biology in macrophages.

Keywords: phagocytosis, phagosome, macrophage, palmitoylation, acylation, lipidation

OPEN ACCESS

Edited by:
Junji Xing,
Houston Methodist Research Institute, United States

Reviewed by:
Nobukazu Araki,
Kagawa University, Japan
Adriana Mantegazza,
Children's Hospital of Philadelphia, United States

***Correspondence:**
Gregory D. Fairn
greg.fairn@unityhealth.to

Specialty section:
This article was submitted to Molecular Innate Immunity, a section of the journal Frontiers in Immunology

Received: *27 January 2021*
Accepted: *15 March 2021*
Published: *01 April 2021*

Citation:
Dixon CL, Mekhail K and Fairn GD (2021) Examining the Underappreciated Role of S-Acylated Proteins as Critical Regulators of Phagocytosis and Phagosome Maturation in Macrophages. Front. Immunol. 12:659533. doi: 10.3389/fimmu.2021.659533

INTRODUCTION

The functionality of many peripheral and membrane proteins depends on the co- or post-translational addition of lipids. Covalent attachment of fatty acids to proteins is one of the more prominent types of lipidation. The type of fatty acylation depends on the fatty acid species and resulting linkage. *N*-terminal glycine myristoylation (*N*-acylation) and cysteine palmitoylation (*S*-acylation) are amongst the most common acylation reactions in mammalian cells; each reaction involves different enzymes, fatty acyl-CoA, and occur in different intracellular locations (1). In either case, the addition of fatty acids markedly increases the hydrophobicity of targeted proteins and modulates function by affecting, binding affinity to biological membranes, subcellular localization and trafficking, folding and stability, and binding interactions with other proteins and co-factors (1, 2).

S-palmitoylation is a reversible, post-translational modification of proteins in which palmitic acid (C16:0), is attached to the cysteine residue of a protein substrate *via* a thioester linkage. Nearly all palmitoylated proteins are modified *via* a thioester linkage to cysteine. There are also rare

instances of palmitate attached to serine residues (*O*-acylation) and the *N*-terminal of a protein (*N*-acylation) (**Table 1**). The transfer of palmitate from palmitoyl-CoA to the sulfhydryl group of a cysteine residue is catalyzed by a family of protein acyltransferases (PATs) that possess a zinc finger Asp-His-His-Cys (zDHHC) domain (3). Notably, many of the studies cited in this review generally assume that palmitate is the acyl group attached. Although palmitoyl-CoA is the preferred substrate for members of the zDHHC family, other acyl-CoAs such as myristoyl-CoA (C14) and stearoyl-CoA (C18) are also utilized as donors (4); as such a more encompassing and accurate term for this modification is *S*-acylation.

In contrast to other types of acylation, *S*-acylation is a highly reversible post-translational modification (**Figure 1**). Due to the labile nature of the thioester bond, *S*-acylated proteins can undergo a cycle of acylation and deacylation mediated by the opposing activities of PATs and thioesterases, respectively. There are at least 3 classes of enzymes capable of de-acylation: cytosolic acyl protein thioesterases (APT1 and APT2) (5); α/β hydrolase domain-containing (ABHD) proteins (6, 7); and palmitoyl-protein thioesterase 1 (PPT1) that remove palmitate from proteins in the lysosome prior to their degradation (8). The extent to which *S*-acylation is regulated by enzymatic de-acylation is unknown. Still, it is clear that within the cellular context, the cycle of acylation and de-acylation provides an important mechanism for dynamically regulating the localization and function of proteins within a cell. In particular, cell signaling, and membrane trafficking require that secreted proteins are able to reversibly associate with membranes. In this review, we focus on *S*-acylated proteins as regulators of phagocytosis and phagosome maturation.

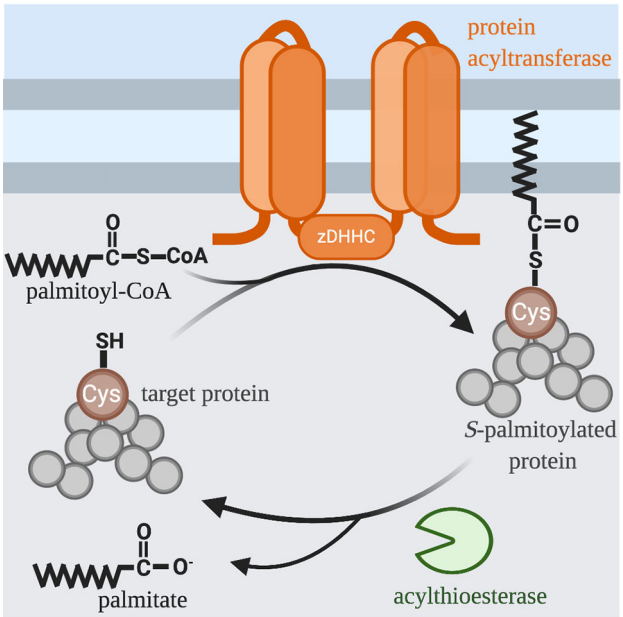

FIGURE 1 | *S*-acylation Cycle. The palmitoyl group is transferred to the free thiol of cysteine from palmitoyl-CoA by a family of integral membrane zinc-dependent DHHC protein acyltransferases. The hydrophobicity of palmitate allows modified proteins to associate with the membranes of various organelles and facilitates trafficking between these organelles. Acyl-protein thioesterases remove thioester-linked fatty acids and thus regenerate a free thiol group.

TABLE 1 | Fatty acylation of proteins.

Modification	Lipid	Amino acid modified	Linkage
S-acylation	C16:0 palmitic acid C18:0 stearic acid C16:1 palmitoleic acid C18:1 oleic acid C20:4 arachidonic acid	Cysteine	Thioester (R-SH)
N-acylation	C14:0 myristic acid C16:0 palmitic acid	Glycine	Amide (R-NH2)
	C16:0 palmitic acid	Cysteine	Amide (R-NH2)
N-acylation	C14:0 myristic acid C16:0 palmitic acid	Lysine	Amide (R-NH2)
O-acylation	C16:0 palmitic acid C8:0 octanoic acid C16:1 palmitoleic acid	Serine or threonine	Oxyester (R-OH)

PHAGOCYTOSIS

Phagocytosis is a critical component of both the innate and adaptive immune responses to microbial pathogens (9). It is a specialized form of endocytosis that involves receptor-mediated recognition and ingestion of particles larger than 0.5μm into plasma membrane derived vacuoles called phagosomes. Most cell types are capable of phagocytosis, however only a few immune cells, namely macrophages, neutrophils and dendritic cells are adept at it. These professional phagocytes (10) play a critical role in innate immunity – the first line of defense against infection – by eliminating microorganisms. In addition to their roles in the innate immune response, phagocytes contribute to tissue homeostasis and remodeling by removing apoptotic bodies (11, 12).

Phagocytosis is initiated when a plasma membrane bound receptor engages its cognate ligand on the surface of a particle. Receptor engagement initiates complex signaling cascades that lead to particle internalization by inducing localized membrane remodeling of the plasma membrane, and the formation of actin-driven pseudopods which engulf the target particle to form a nascent phagosome (13). The nascent phagosome then follows a

highly choreographed pathway of successive fusion and fission events with early endosomes, late endosomes and finally lysosomes, whereby it matures into a microbiocidal vacuole called a phagolysosome (**Figure 2**) (14, 15). At the conclusion of maturation, the lumen of the mature phagolysosome is a highly oxidative environment, rich in hydrolytic enzymes that function at a low pH to destroy the internalized particle. Once the prey within the phagolysosome has been degraded, a tubulovesicular process mediates the dissolution of the vacuole to reform lysosomes which support subsequent rounds of phagocytosis.

The importance of *S*-acylation in cellular processes like phagocytosis has only recently been recognized, owing in large part to the development of methods that allow high throughput analysis of *S*-acylated proteins. The first acyl-biotin exchange proteomic analysis of RAW 264.7 macrophage-like cells identified ~80 *S*-acylated proteins, nearly half of which partition into detergent resistant membrane (DRM) fractions (16). Many of the proteins identified have known roles in signal transduction (Src family kinases (SFKs)) and vesicular transport (soluble NSF attachment proteins (SNAP) receptor (SNARE) proteins (e.g., VAMP3, 4, 5, 7 and Syntaxin6, 7, 8, 12). The identification of these specific proteins highlights the potential importance of *S*-acylation for signaling, optimal completion of particle internalization during phagocytosis, as well as the overall ability of macrophages to perform their functions as sentinels of the immune system.

In addition to the elimination of microorganisms and effete cells *via* phagocytosis, macrophages must also sense and respond to bacterial products such as lipopolysaccharide (LPS) or peptidoglycan (PGN) and mount an effective inflammatory response. Analysis of macrophages, using metabolic labeling

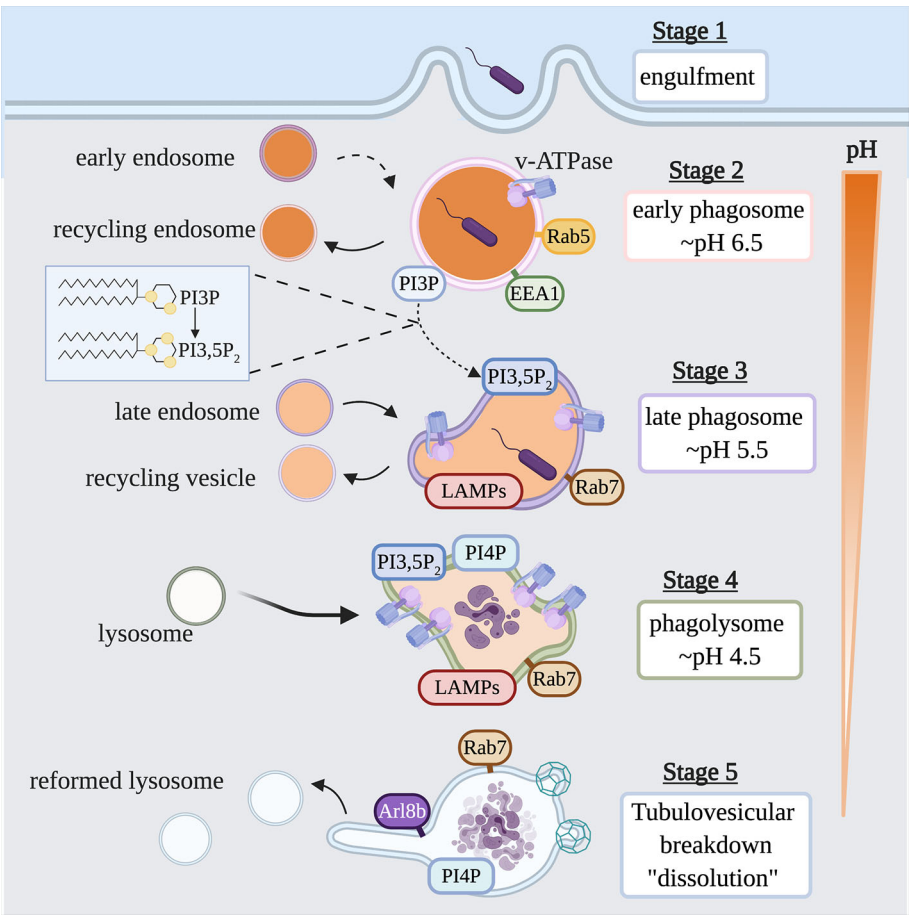

FIGURE 2 | Life Cycle of the Phagosome. Phagosomes are formed on demand when professional phagocytes encounter target particles such as, opsonized bacteria or apoptotic cells. Following internalization of a phagocytic target, the nascent phagosome is transformed into a microbiocidal vacuole through successive fusion and fission events within the endocytic pathway. During this maturation process, the lumen of the phagosome is acidified by the action of v-ATPase, and also acquires hydrolases and other antimicrobial proteins. Key steps in the maturation process include the conversion from a Rab5-positive early phagosome to a Rab7-positive late phagosome; the acquisition of LAMP and v-ATPase; the conversion of PI3P to $PI3,5P_2$; and the appearance of PI4P. Once the particle within the phagolysosome has been degraded, PI4P- and Arl8b-dependent membrane tubulation and budding events breakdown the organelle, reforming lysosomes consumed in the maturation process. EEA1, early endosomal antigen 1; LAMP, lysosome-associated membrane protein; PI3P, phosphatidylinositol 3-phosphate; $PI3,5P_2$, phosphatidylinositol 3,5- bisphosphate; PI4P, phosphatidylinositol 4-phosphate; Arl8b, ADP-ribosylation factor-like protein 8B.

with a lipid analog, revealed that when the cells are stimulation with LPS, the *S*-acylated proteome is extensively remodeled, with 154 proteins upregulated and 186 downregulated (17). This study further demonstrated that the cellular pool of phosphatidylinositol 4-kinase IIβ (PI4KIIβ) displays enhanced levels of *S*-acylation following the addition of LPS, and that this lipid kinase is required for the proper production of inflammatory cytokines. The inducible *S*-acylation of the cytosolic PGN sensors NOD1 and NOD2 was recently revealed as a novel regulatory mechanism. Treating primary bone marrow derived macrophage cells with PGN resulted in a zDHHC5-dependent increase in *S*-acylation of NOD1 and NOD2 required for their localization to the plasma membrane or phagosomes and to initiate a signal transduction cascade and NF-kB activation (18). Taken together, these examples demonstrate that dynamic control of protein *S*-acylation in macrophages, and likely most cell types, is a key regulatory mechanism.

S-Acylation of Immune Receptors and SFKs

Internalization of immunoglobulin G (IgG) opsonized particles by Fcγ receptors (FcγRs) on the surface of macrophages is the most widely used model of phagocytosis. FcγRs bind to bivalent or multivalent ligands to elicit downstream signaling (13). Recognition and binding of complementary IgG on the surface of a particle results in receptor clustering, which brings the cytosolic domain of each FcγR into close apposition and triggers signaling cascades. The first signaling event to occur after receptor-ligand binding is phosphorylation of tyrosine residues within conserved immunoreceptor tyrosine-based activation motifs (ITAMs) on the cytosolic tail of the FcγRs, mediated by Src family kinases (SFKs) (**Figure 3**). Inhibition of SFKs or overexpression of their negative regulator, C-terminal Src kinase (Csk), eliminates particle engulfment, but not binding (19–21). Conversely, the heterologous expression of FcγRs in many non-phagocytic cells is able to elicit SFK signaling cascade and the engulfment of IgG-opsonized particles highlighting the robustness and this system.

Many immunoreceptors including FcγRs are found to reside in DRMs that also contain SFKs (22). The amino acid constituents of transmembrane domains and the *S*-acylation of juxtamembrane regions can partition proteins into liquid ordered regions of the plasma membrane (23). The current evidence suggests that FcγRIIa signaling is only partially dependent on *S*-acylation of Cys208; its absence prevents the intracellular mobilization of calcium without directly impairing the phosphorylation of the ITAMs (24). Additionally, mutations in the transmembrane domain, which ablate its localization to

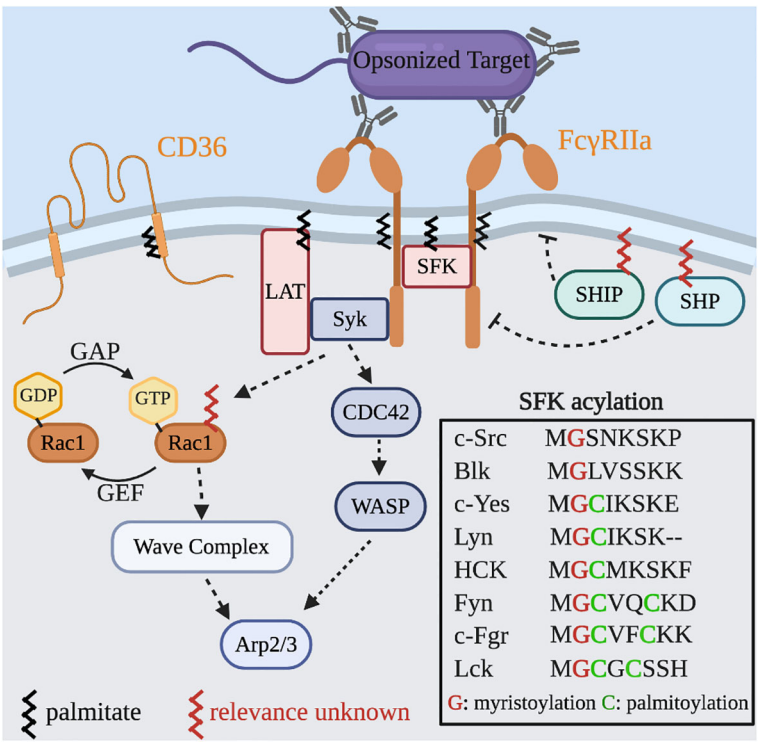

FIGURE 3 | *S*-acylated proteins in Fcγ receptor signaling and actin dynamics. Binding of IgG to the FcγR leads to localized clustering and signal transduction. Phosphorylation of the ITAM motifs and SFKs generates binding sites for Syk and the recruitment of LAT which together amplify the signal intensity. Additional downstream signaling leads to GTP-loading of both Cdc42 and Rac1 that results in Wiskott–Aldrich syndrome protein (WASP) and WASP-family verprolin homologous protein (WAVE) complex mediated actin rearrangements to drive particle engulfment. Two phosphatases, SHP and SHIP, serve as negative regulators of phagocytosis and are recruited by binding the inhibitor FcγRIIb and may also require *S*-acylation for their activity. Inset: All SFKs are myristoylated and most are S-acylated.

DRMs, prevent the activation of NF-kB downstream of FcγRIIa activation (25). Together these studies demonstrate that both the *S*-acylation and the composition of the transmembrane domain support proper receptor function.

It is possible that multiple activated FcγRs and SFKs associate in an ordered domain to support maximal signal output, and that this depends on the membrane lipids, the transmembrane domain of the receptor, and the recruitment of SFKs. We suspect that under suboptimal conditions the size of this domain could be restricted thereby limiting the overall strength and duration of signals. Similar observations have been seen with another phagocytic receptor, the scavenger receptor CD36 (26). In resting cells, CD36 resides in small clusters associated with the SFK Fyn. Upon activation the clusters increase in size recruiting more Fyn, leading to stronger signaling. Since CD36 is *S*-acylated by zDHHC4 and zDHHC5 (27), and Fyn is dually acylated with myristate and palmitate, it is possible that these modifications assist in lateral segregation and cluster density. Whether this mechanism explains the observations of FcγRIIa remains to be directly tested.

S-Acylated Proteins That Regulate Actin Dynamics and Pseudopod Extension

The role of these initial signaling events is to drive particle internalization through extensive remodeling of the actin cytoskeleton. In FcγR mediated phagocytosis, the small Rho-family GTPases Cdc42 and Rac, key regulators of actin dynamics, are activated and recruited to the site of phagocytosis (28, 29). GTPases function as molecular switches alternating between an active (GTP-bound) state and an inactive (GDP-bound) state (30), through the action of guanine nucleotide exchange factors (GEFs) and GTPase-activating proteins (GAPs), respectively. GEFs stimulate GDP dissociation to allow its replacement by GTP, while GAPs are essential to prompt GTP hydrolysis. The eventual outcome of cytoskeletal reorganization is the formation of pseudopod extensions and phagocytic cups that engulf the particle. Soon after sealing the phagocytic cup, the newly formed phagosome participates in successive fission and fusion interactions with endosomes and lysosomes to mature into a highly degradative phagolysosome.

Rac1 stimulates actin polymerization to promote the internalization of attached particles and microorganisms during phagocytosis (31). In its active GTP-bound state, Rac1 is targeted to membranes by prenylation (geranylgeranylation) and a *C*-terminal polybasic region (KKRKRK) (32, 33). Metabolic labeling in fibroblasts with tritiated palmitate revealed that Rac1 is modified on Cys178 (34, 35). This modification requires Rac1 to already be localized to the membrane as both prenylation and an intact *C*-terminal polybasic region was required to support *S*-acylation. Preventing the *S*-acylation of Rac1 by treatment with 2-bromopalmitate or mutation of the Cys178 residue results in a reduction in both plasma membrane localization and GTP loading of Rac1, which leads to a reduced activation of p21 activated kinase. Ultimately, cells with impaired Rac1 acylation display impaired spreading and defects in migration suggesting defects in the ability to polymerize actin. Whether the *S*-acylation of Rac1 occurs in macrophage or is important for pseudopod extension during phagocytosis is currently unknown. The identity of the of the zDHHC isoform(s) modifying Rac1 also needs to be determined.

S-Acylated Membrane Fusion Machinery Required for Focal Exocytosis During Particle Engulfment

Video-microscopy of phagocytosing macrophages has revealed that these cells have the ability to consume large volumes of particles without a noticeable diminution of their surface area or alteration in shape. Indeed, through the use of fluorescent spectroscopic and electrophysiological techniques (e.g., membrane capacitance) it was determined that the surface area of the cell actually increases immediately following phagocytosis (36, 37). Endocytic vesicles serve as the primary donor of this "extra" membrane used to support particle engulfment (38). This localized delivery at the site of phagocytosis is referred to as "focal exocytosis" (39). Fusion of endocytic vesicles with the base of the phagocytic cup is mediated by the soluble *N*-ethylmaleimide–sensitive factor attachment protein (SNAP) receptors (SNAREs). SNAREs are classified as Qa-, Qb-, Qc-, Qbc- (which contain two SNARE motifs) or R-SNAREs (40, 41). Specific Q-SNAREs in the target membrane bind, *via* their SNARE motifs, to a partner R-SNARE on vesicles to form a trans-SNARE complex (42). This brings the two membranes into close proximity allowing fusion and delivery of cargo. On the plasma membrane and base of the phagocytic cup SNAP-23 (a Qbc) is in complex with a Qa SNARE such as Syntaxin2, 3 or 4. Unlike the Qa SNAREs, SNAP-23 does not have a transmembrane and instead associates with cellular membranes through acylation of a cysteine-rich domain present in the linker region connecting its Qb and Qc motifs (43, 44). SNAP-23 has five acylated cysteines and is found to partition into DRMs (45) which may also explain its preference for the plasma membrane and endosomes over the endoplasmic reticulum. Silencing of SNAP-23 in J774 macrophage cells results in impaired phagocytosis and a reduction in the delivery of NADPH oxidase 2 complex required to generate superoxide at the site of phagocytosis/nascent phagosome (46).

During phagocytosis recycling endosomes, early endosomes and late endosomes/phagosomes can all fuse at the base of the phagocytic cup. The R-SNAREs vesicle-associated membrane protein (VAMP) 3 (recycling endosomes) and VAMP7 (late endosomes/lysosomes) have been shown to be important for membrane fusion. VAMP3 has been identified in proteomics screens as an *S*-acylated protein in macrophages (16, 17). VAMP3 contains a sole cysteine residue, Cys76, located in the cytosol and adjacent to its transmembrane domain. To our knowledge direct examination of this acylation and any potential role has not been examined. Proteomic studies have also identified VAMP7 as an *S*-acylated protein in macrophages (17). Recent studies using Jurkat T cells have demonstrated that Cys183 can be acylated by zDHHC18 and zDHHC20 and that the fraction of VAMP7 that is acylated increases following T cell

receptor stimulation (47). In T cells wild-type VAMP7 has a perinuclear localization which partly overlaps with the Golgi marker Giantin and possibly recycling endosomes. Conversely, the Cys183Ala mutant displays a more diffuse cytoplasmic signal demonstrating that *S*-acylation is critical for the proper subcellular distribution. To date the importance of *S*-acylation in macrophage or to phagocytosis has not been examined. However, given the similarity between T cell receptor and FcγR signaling and the role of VAMP7 in phagocytosis it is tempting to speculate that this modification will also support the process.

PHAGOSOME MATURATION

The nascent phagosome lacks the microbicidal and degradative capacity required to destroy an engulfed particle. Through a sequential process known as maturation, it amasses an arsenal of oxidative, acidifying and hydrolytic enzymes (14, 48). Phagosome maturation, particularly the process of phagolysosome formation, shares some features with the progression of endosomes to lysosomes, a complex process that is orchestrated by Rab GTPases. Soon after sealing the phagocytic cup, the newly formed phagosome fuses with early endosomes and acquires Rab5 and phosphatidylinositol 3-phosphate. Eventually, the early phagosome transitions to a late phagosome that is defined by the acquisition of distinct biochemical markers, such as Rab7; Rab7 acquisition is concomitant with the loss of early markers such as Rab5 (49). Active GTP-bound Rab7 recruits Rab-interacting lysosomal protein (RILP) to the maturing phagosome and, together, they regulate the assembly and activation of the vacuolar ATPase (v-ATPase) leading to further luminal acidification (50, 51). As the phagosome matures it also receives newly synthesized pro-enzymes from the Golgi. Many of these pro-enzymes are packaged in the vesicles arising from the *trans*-Golgi network (TGN) *via* cargo receptors such as mannose 6-phosphate receptor (M6PR) and sortillin (**Figure 4**) (52, 53). These receptors must be actively retrieved from the late phagosome and returned to the Golgi for subsequent rounds of cargo delivery or will otherwise be degraded and the pro-enzymes secreted. The retrograde transport of material from the late phagosomes to the Golgi is incompletely understood but likely involves clathrin machinery and the retromer complex and is possibly regulated by Rab7 (52, 54).

S-Acylated SNAREs Involved in Phagosome Maturation

In addition to supporting focal exocytosis SNAP23 is also critical for mediating membrane fusion events during phagosome maturation. The activity of SNAP23 is necessary for the for the recruitment of several proteins essential for phagosome maturation including v-ATPase (46), MHCI (55) and NOX2 (46, 56, 57) from recycling endosomes and lysosomes. Focal exocytosis of recycling and late endosomes during particle engulfment results in the delivery of a variety of membrane proteins found on these compartments including Syntaxin7 and 13 (also referred to as Syntaxin12) (58). This delivery of endocytic Q-SNAREs to the nascent phagosome allows for further fusions events with recycling and late endosomes/lysosomes containing the appropriate R-SNAREs.

In RAW macrophage, Syntaxin13 colocalizes with the transferrin receptor on recycling endosomes (58). Expression of the cytosolic domain of Syntaxin13, which is known to act as a dominant negative mutant, did not have any impact of the uptake of particles. However, this dominant negative construct impaired the ability of the phagosome to mature to a late phagosome/phagolysosome stage. Syntaxin13 is not reported to be *S*-acylated and it does not contain any juxtamembrane cysteine residues. However, its cognate partner Syntaxin4 has been found to be *S*-acylated (59). The presence of Syntaxin7 and 8 on maturing phagosomes supports the fusion with late endosomes and lysosomes *via* interactions with their cognate pattern VAMP7. Syntaxin7 and 8 are modified with palmitate on Cys239 and Cys214, respectively, adjacent to their transmembrane domains (60). In HeLa cells the Syntaxin 8 is partly colocalized with both CD63 and LAMP1 consistent with a late endosome/lysosome distribution. The Cys214Ala mutant that lacks *S*-acylation has the same subcellular localization. In contrast in HeLa cells Syntaxin7 localizes primarily with the early endosomal marker EEA1 while the Cys239Ala mutant is retained on the plasma membrane of HeLa. This suggests that *S*-acylation is needed for partitioning into an endocytic carrier. Whether this mode of regulation is important in macrophage is yet to be examined.

S-Acylation Regulates Delivery of v-ATPase to Lysosomes and Possibly Phagosomes

Fusion with late endosomes, lysosomes and carriers derived from the TGN lead to the accumulation of v-ATPases in the membrane of the late phagosome that results in the acidification of the phagosomal lumen. Fusion of the maturing phagosome with these compartments also delivers a variety of hydrolytic enzymes to the lumen of the phagolysosome to facilitate destruction of the internalized prey. The v-ATPase is a large multimeric protein complex consisting of two functional subcomplexes, V_1 and V_0, that together control the import of protons into the lumen of endosomes and phagosomes (61). The cytosolic V_1 subcomplex mediates ATP hydrolysis, while the V_0 subcomplex, integral to the membrane, constitutes the pore through which protons are pumped at the expense of ATP (62). The phagosomal acquisition of the membrane embedded V_0 subcomplex requires membrane trafficking either from pre-existing active complex (i.e., fusion with lysosomes) or the delivery of newly synthesized V_0 from the ER *via* the Golgi (**Figure 4**).

Batten disease is a group of rare, fatal, genetically inherited disorders that impact the nervous system which all manifest as neuronal ceroid lipofuscinoses (63). Infantile Batten disease, or ceroid lipofuscinosis, neuronal, 1 (*CLN1*) is a severe form of the disease caused by mutations in the thioesterase PPT1 (64). PPT1 is a soluble protein thioesterase enzyme that resides in the lumen

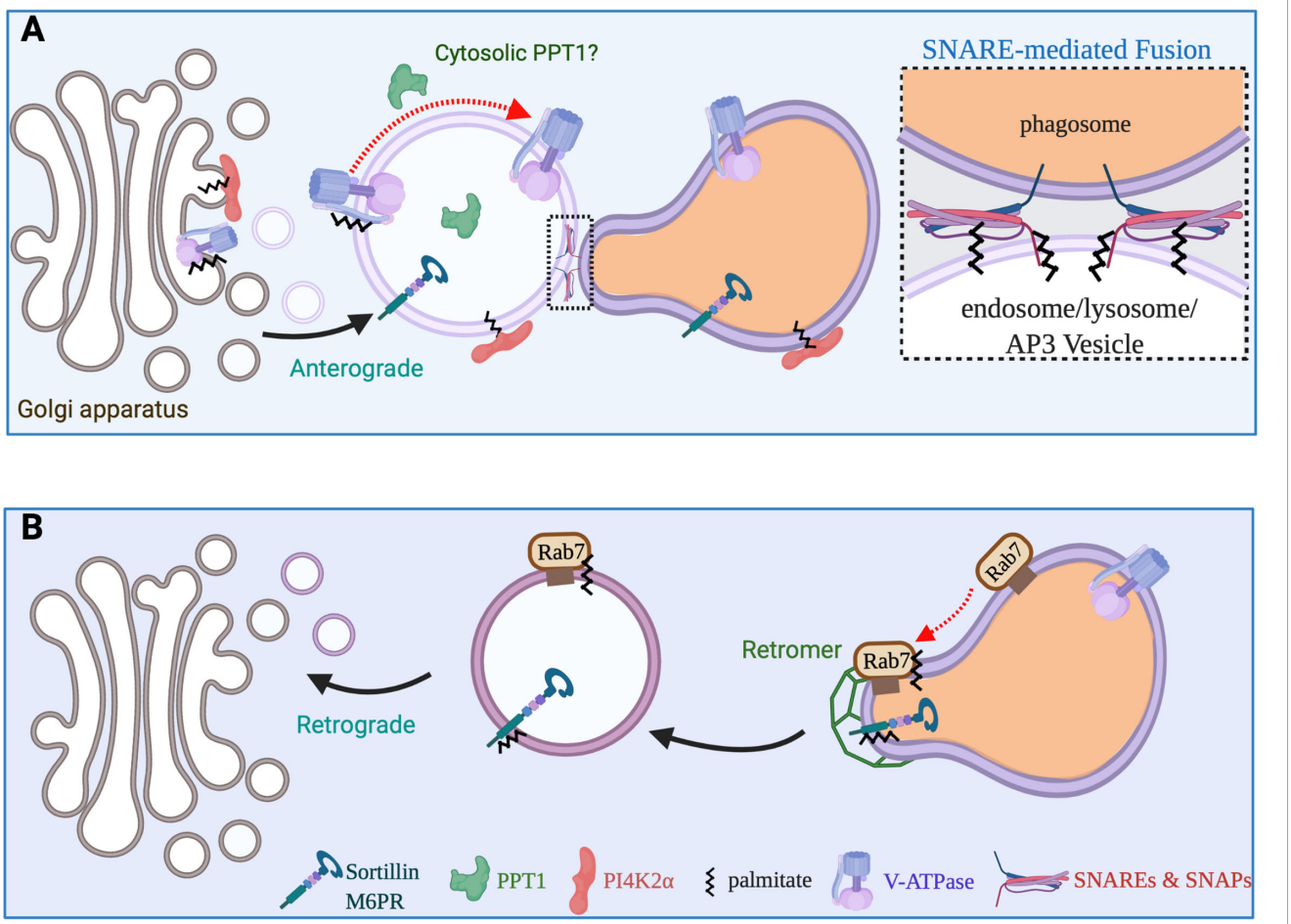

FIGURE 4 | Vesicular transport pathways required for phagosome maturation. **(A)** The maturing phagosome undergoes numerous SNARE-mediated fusion events during the course of its maturation. SNAP23 and SNAP25 are *S*-acylated, while a subset of SNARE proteins also require acylation for proper function and stability. Newly synthesized v-ATPase transits from the Golgi to late endosomes/lysosomes or directly to maturing phagosomes. The clathrin adaptor complex 3 aids in the sorting and delivery of a variety of proteins including the PI4KIIα and cargo receptors such as sortillin to the (phago)lysosome. *S*-acylation of the PI4KIIα and v-ATPase is critical to deliver these enzymes to (phago)lyosomes. **(B)** Cargo receptors M6PR and sortillin must constantly traffic back and forth between the Golgi apparatus and (phago)lysosomes to ensure that pro-hydrolytic enzymes are properly delivered to the lumen of (phago)lysosomes. Both the cation independent M6PR and Sortillin can be *S*-acylated and modification aids in interactions with the retromer complex. Additionally, *S*-acylation of Rab7 also promotes its interactions with the retromer complex and the retrieval cargo receptors.

of lysosomes involved in the degradation of lipid-modified proteins by removing thioester-linked fatty acyl groups from cysteine residues (65). Delivery of recombinant PPT1 *via* fluid phase endocytosis is able to reverse the accumulation of proteinaceous deposits in the lysosomes lacking PPT1 function. Paradoxically, recent evidence suggests that the activity of the v-ATPase also requires PPT1 to directly remove an acyl chain from the v-ATPase in the cytosol.

Neurons, macrophage and microglia express the V_0a1 isoform as part of the membrane embedded V_0 complex of the v-ATPase. A recent study has demonstrated that the V_0a1 containing Vo complex requires S-acylation for proper trafficking from the Golgi to lysosomes (66). This feature is unique to the a1 isoform compared to the other tissue-selective isoforms (a2-a4). Cys25 of the a1 subunit was shown to be *S*-acylated by acyl-biotin exchange and that this modification is important for the recognition of the V_0 complex by the adaptor complex 3 in the *trans*-Golgi and its subsequent delivery to lysosomes. Curiously, despite its role in trafficking, the modification itself impairs maximal proton translocation activity (66). Mutations in PPT1 result in a significantly higher lysosomal pH in neurons compared to those from littermate controls. It is currently unclear how lysosomal PPT1 can remove fatty acids attached to a cytosolically modified Cys residue. One possibility is that a small fraction of the PPT1 also resides in the cytosol (66). Whether this is through inefficient insertion into the ER during biosynthesis or escape *via* some sort of transient "leak" in limiting membrane of the lysosome is unclear. Since some bacterial pathogens and inert particles can rupture phagolysosomes it would be worth investigating to determine

if the release of PPT1 into the cytosol impacts the *S*-acylome of macrophages.

S-Acylation of PI4KIIα and Its Delivery and Activity Are Required for Optimal Phagolysosome Acidification

Phosphatidylinositol 4-kinase IIa (PI4KIIα) resides primarily in the *trans*-Golgi network (TGN) and endosomes/lysosomes and plays essential roles in membrane transport including: cargo trafficking between the TGN and endosomes *via* direct interactions with adaptor protein complexes, AP-1 and AP-3 (67–69). Importantly both the activity and the presence of PI4KIIα supports the formation of vesicular carriers (68). PI4KIIα is a peripheral membrane protein that is *S*-acylated within its catalytic core (70). All four cysteine residues within its CCPCC motif are capable of being *S*-acylated by zDHHC3 and/or zDHHC7 (71). However, mutational analysis indicates that the first two are the preferred sites of this modification (70).

Recently it was also demonstrated that following the acquisition of Rab7, the maturing late phagosome, acquires PI4KIIα by fusion with lysosomes or vesicles from the TGN. This leads to the appearance of PI4P on this late stage phagosome and is required for the maximal acidification of the now phagolysosome (72). Additionally, in dendritic cells PI4K2a and PI4P have been shown to be critical for the localization and activity of toll-like receptor 4 (73). Following the digestion of the prey within the phagolysosome, the organelle is eliminated by a tubulovesicular dissolution process, which concomitantly regenerates lysosomes. The precise mechanisms of this phagolysosomal dissolution or resolution are unclear, however, it is known that if the phagolysosome fails to acquire PI4P its dissolution in inhibited (74). Moreover, similar PI4P/PI4K2a positive tubules in dendritic cells may account for the requirement for PI4K2a to support optimal presentation of antigens by the major histocompatibility complex II (73). Thus, we would predict that loss of both zDHHC3 and zDHHC7 would result in an inability of phagolysosomes to degrade prey and be broken down into lysosomes.

A Potential Role for *S*-Acylation of Rab7 in Retrograde Transport From the Phagolysosome to Trans-Golgi Network

In non-myeloid cells, Rab7 is *S*-acylated on Cys83 and Cys84 and this regulates the ability of Rab7 to interact with and recruit the retromer complex to late endosomes (75). Prevention of Rab7 acylation results in the aberrant secretion of lysosomal pro-enzyme to the extracellular medium. Although the *S*-acylation of these two residues has now been demonstrated, it is still not fully understood how this regulates the retromer. While the role of Rab7 acylation has not been investigated in phagosome maturation, it is tempting to speculate that it will also be required for retrograde transport of cargo receptors such as the mannose 6-phosphate receptor or sortillin back to the Golgi. In a separate investigation identified zDHHC15 as a protein required for optimal retrograde lysosome to Golgi transport of sortillin and the cation-independent M6PR (76). This study also demonstrated that acylation was required for these two cargo proteins to associate with the retromer complex. This raises the possibility that zDHHC15 may directly modify Rab7 to mediate retrograde transport from lysosomes/phagosomes to the *trans*-Golgi Network.

WHY DO MACROPHAGES THAT LACK ZDHHC5 EAT FASTER?

Using the human myeloid cell line U937, a recent CRISPR screen identified numerous genes that either positively or negatively regulated phagocytosis of numerous phagocytic prey (77). The authors demonstrated that loss of zDHHC5 resulted in a substantial increase in phagocytosis mediated by a variety of receptors including FcγR, complement, dectin and phosphatidylserine (apoptotic body). This finding was substantiated by another study using murine bone marrow derived macrophage cells lacking zDHHC5 (18). Together, these studies reveal that key negative regulator(s) of phagocytosis require zDHHC5-mediated *S*-acylation for their proper function and that in the absence of this post-translational modification, phagocytic signaling is either enhanced and/or accelerated.

In addition to ITAM containing receptors, there exist comparable receptors which contain immunoreceptor tyrosine-based inhibitory motifs (ITIMs). These include FcγIIb and the phosphatidylserine receptor CD300a (78, 79). Two key molecules which associate with the inhibitory ITIM motifs are Src homology 2 (SH2)-containing tyrosine phosphatase (SHP) and SH2 domain containing inositol phosphatase (SHIP) (80) both of which inhibit phagocytosis by directly dephosphorylating phosphotyrosine and phosphatidylinositol 3,4,5-trisphosphate, respectively, essential for phagocytosis. Proteomics screens for *S*-acylated proteins in RAW264.7 macrophage-like cells have identified both SHP (17, 81) and SHIP (81). We speculate that the plasmalemmal localized zDHHC5 acylates one or both of these proteins which is required for their optimal function. In the absence of lipidation, these phosphatases would have impaired targeting to the sites of receptor activation leading to enhanced signaling and faster rates of phagocytosis.

CONCLUSIONS AND PERSPECTIVES

In this review, we have focused on the role of experimentally validated *S*-acylated proteins as regulators of phagocytosis and phagosome maturation in macrophages. It is clear from these examples that protein acylation can contribute to membrane binding, trafficking and targeting. All of which can be explained, at least in part, by two molecular mechanisms: the hydrophobic insertion of an acyl chain into a lipid bilayer enhances membrane binding, and saturated fatty acids prefer to insert into liquid ordered raft domains rather than the bulk plasma membrane. It is intriguing to speculate whether the function of *S*-acylated proteins is directly associated with the acylation process or is a

consequence of correct trafficking or localization of the target protein. *S*-acylation of FcγRIIa and Rac1 exemplify the versatility of *S*-acylation in modifying protein function beyond membrane binding and targeting. In both instances' acylation is essential for downstream signaling pathways. However, the relationship between *S*-acylation and protein function isn't always so transparent as we see for many of the proteins reviewed here. As more *S*-acylated proteins and PATs are identified, knockdown, knockout and knockin techniques will complement the biochemical studies to help elucidate the functions of *S*-acylation.

Finally, our collective understanding of the cellular roles of protein *S*-acylation has lagged behind other post-translational modifications such as phosphorylation, ubiquitination and prenylation. Although in the past few years the identification of several palmitoyl transferases as well as their protein substrates has brought major advances to the protein palmitoylation field many central questions remain. Part of the challenge historically has been the limited number of tools, techniques and reagents to study *S*-palmitoylation. However, the development of new methods using bioorthogonal chemical reporters, ABE and the closely related acyl PEG and acyl-RAC assays, have accelerated both proteomic and directed studies. Additionally, the recent cryo-EM structures of zDHHC15 and zDHHC20 will no doubt help bolster the development of better ligands for *in vitro* studies and inhibitors for cell and animal studies. As the field continues to grow, we believe that the macrophage and the process of phagocytosis and phagosome maturation will be excellent paradigms to study the role of zDHHC PATs, thioesterases and their modified substrates.

AUTHOR CONTRIBUTIONS

CD and GF wrote the paper. KM prepared the figures. All authors contributed to the article and approved the submitted version.

FUNDING

This work is supported by the Canadian Institutes of Health Research Project Grants PJT166010 and PJT165968 to GF.

ACKNOWLEDGMENTS

Figures were generated using BioRender.com.

SUPPLEMENTARY MATERIAL

The Supplementary Material for this article can be found online at: https://www.frontiersin.org/articles/10.3389/fimmu.2021.659533/full#supplementary-material

REFERENCES

1. Resh MD. Fatty acylation of proteins: The long and the short of it. *Prog Lipid Res* (2016) 63:120–31. doi: 10.1016/j.plipres.2016.05.002
2. Chen B, Sun Y, Niu J, Jarugumilli GK, Wu X. Protein Lipidation in Cell Signaling and Diseases: Function, Regulation, and Therapeutic Opportunities. *Cell Chem Biol* (2018) 25(7):817–31. doi: 10.1016/j.chembiol.2018.05.003
3. Mitchell DA, Vasudevan A, Linder ME, Deschenes RJ. Thematic review series: Lipid Posttranslational Modifications.Protein palmitoylation by a family of DHHC proteinS-acyltransferases: Fig. 1. *J Lipid Res* (2006) 47(6):1118–27. doi: 10.1194/jlr.r600007-jlr200
4. Fukata M, Fukata Y, Adesnik H, Nicoll RA, Bredt DS. Identification of PSD-95 Palmitoylating Enzymes. *Neuron* (2004) 44(6):987–96. doi: 10.1016/j.neuron.2004.12.005
5. Hernandez JL, Majmudar JD, Martin BR. Profiling and inhibiting reversible palmitoylation. *Curr Opin Chem Biol* (2013) 17(1):20–6. doi: 10.1016/j.cbpa.2012.11.023
6. Lin DT, Conibear E. ABHD17 proteins are novel protein depalmitoylases that regulate N-Ras palmitate turnover and subcellular localization. *Elife* (2015) 4: e11306. doi: 10.7554/eLife.11306
7. Yokoi N, Fukata Y, Sekiya A, Murakami T, Kobayashi K, Fukata M. Identification of PSD-95 Depalmitoylating Enzymes. *J Neurosci* (2016) 36 (24):6431–44. doi: 10.1523/JNEUROSCI.0419-16.2016
8. Lu J-Y, Hofmann SL. Thematic review series: Lipid Posttranslational Modifications.Lysosomal metabolism of lipid-modified proteins. *J Lipid Res* (2006) 47(7):1352–7. doi: 10.1194/jlr.r600010-jlr200
9. Gordon S. Phagocytosis: An Immunobiologic Process. *Immun Rev* (2016) 44 (3):13. doi: 10.1016/j.immuni.2016.02.026
10. Rabinovitch M. Professional and non-professional phagocytes: an introduction. *Trends Cell Biol* (1995) 5(3):85–7. doi: 10.1016/s0962-8924(00)88955-2
11. Arandjelovic S, Ravichandran KS. Phagocytosis of apoptotic cells in homeostasis. *Nat Immunol* (2015) 16(9):907–17. doi: 10.1038/ni.3253
12. Lim JJ, Grinstein S, Roth Z. Diversity and Versatility of Phagocytosis: Roles in Innate Immunity, Tissue Remodeling, and Homeostasis. *Front Cell Infect Microbiol* (2017) 7:191. doi: 10.3389/fcimb.2017.00191
13. Freeman SA, Grinstein S. Phagocytosis: receptors, signal integration, and the cytoskeleton. *Immunol Rev* (2014) 262(1):193–215. doi: 10.1111/imr.12212
14. Kinchen JM, Ravichandran KS. Phagosome maturation: going through the acid test. *Nat Rev Mol Cell Biol* (2008) 9(10):781–95. doi: 10.1038/nrm2515
15. Pauwels A-M, Trost M, Beyaert R, Hoffmann E. Patterns, Receptors, and Signals: Regulation of Phagosome Maturation. *Trends Immunol* (2017) 38 (6):407–22. doi: 10.1016/j.it.2017.03.006
16. Merrick BA, Dhungana S, Williams JG, Aloor JJ, Peddada S, Tomer KB, et al. Proteomic Profiling of S-acylated Macrophage Proteins Identifies a Role for Palmitoylation in Mitochondrial Targeting of Phospholipid Scramblase 3. *Mol Cell Proteomics* (2011) 10(10):M110.006007. doi: 10.1074/mcp.m110.006007
17. Sobocińska J, Roszczenko-Jasińska P, Zaręba-Kozioł M, Hromada-Judycka A, Matveichuk OV, Traczyk G, et al. Lipopolysaccharide Upregulates Palmitoylated Enzymes of the Phosphatidylinositol Cycle: An Insight from Proteomic Studies. *Mol Cell Proteomics* (2018) 17(2):233–54. doi: 10.1074/mcp.ra117.000050
18. Lu Y, Zheng Y, Coyaud É, Zhang C, Selvabaskaran A, Yu Y, et al. Palmitoylation of NOD1 and NOD2 is required for bacterial sensing. *Science* (2019) 366(6464):7. doi: 10.1126/science.aau6391
19. Fitzer-Attas CJ, Lowry M, Crowley MT, Finn AJ, Meng F, DeFranco AL, et al. Fcgamma receptor-mediated phagocytosis in macrophages lacking the Src family tyrosine kinases Hck, Fgr, and Lyn. *J Exp Med* (2000) 191(4):669–82. doi: 10.1084/jem.191.4.669
20. Suzuki T, Kono H, Hirose N, Okada M, Yamamoto T, Yamamoto K, et al. Differential involvement of Src family kinases in Fc gamma receptor-mediated phagocytosis. *J Immunol* (2000) 165(1):473–82. doi: 10.4049/jimmunol.165.1.473
21. Abram CL, Lowell CA. The diverse functions of Src family kinases in macrophages. *Front Biosci* (2008) 13:4426–50. doi: 10.2741/3015

22. Kwiatkowska K, Sobota A. The clustered Fcγ receptor II is recruited to Lyn-containing membrane domains and undergoes phosphorylation in a cholesterol-dependent manner. *Eur J Immunol* (2001) 31(4):989–98. doi: 10.1002/1521-4141(200104)31:4<989::aid-immu989>3.0.co;2-v
23. Sezgin E, Levental I, Mayor S, Eggeling C. The mystery of membrane organization: composition, regulation and roles of lipid rafts. *Nat Rev Mol Cell Biol* (2017) 18(6):361–74. doi: 10.1038/nrm.2017.16
24. Barnes NC, Powell MS, Trist HM, Gavin AL, Wines BD, Hogarth PM. Raft localisation of FcγRIIa and efficient signaling are dependent on palmitoylation of cysteine 208. *Immunol Lett* (2006) 104(1-2):118–23. doi: 10.1016/j.imlet.2005.11.007
25. Garcia-Garcia E, Brown EJ, Rosales C. Transmembrane Mutations to Fc RIIA Alter Its Association with Lipid Rafts: Implications for Receptor Signaling. *J Immunol* (2007) 178(5):3048–58. doi: 10.4049/jimmunol.178.5.3048
26. Githaka JM, Vega AR, Baird MA, Davidson MW, Jaqaman K, Touret N. Ligand-induced growth and compaction of CD36 nanoclusters enriched in Fyn induces Fyn signaling. *J Cell Sci* (2016) 129(22):4175–89. doi: 10.1242/jcs.188946
27. Wang J, Hao J-W, Wang X, Guo H, Sun H-H, Lai X-Y, et al. DHHC4 and DHHC5 Facilitate Fatty Acid Uptake by Palmitoylating and Targeting CD36 to the Plasma Membrane. *Cell Rep* (2019) 26(1):209–21.e205. doi: 10.1016/j.celrep.2018.12.022
28. Hoppe AD, Swanson JA. Cdc42, Rac1, and Rac2 Display Distinct Patterns of Activation during Phagocytosis. *Mol Biol Cell* (2004) 15(8):3509–19. doi: 10.1091/mbc.e03-11-0847
29. Sit ST, Manser E. Rho GTPases and their role in organizing the actin cytoskeleton. *J Cell Sci* (2011) 124(5):679–83. doi: 10.1242/jcs.064964
30. Biro M, Munoz MA, Weninger W. Targeting Rho-GTPases in immune cell migration and inflammation. *Br J Pharmacol* (2014) 171(24):5491–506. doi: 10.1111/bph.12658
31. Bosco EE, Mulloy JC, Zheng Y. Rac1 GTPase: A "Rac" of All Trades. *Cell Mol Life Sci* (2009) 66(3):370–4. doi: 10.1007/s00018-008-8552-x
32. Michaelson D, Silletti J, Murphy G, D'Eustachio P, Rush M, Philips MR. Differential Localization of Rho Gtpases in Live Cells. *J Cell Biol* (2001) 152 (1):111–26. doi: 10.1083/jcb.152.1.111
33. Abdrabou A, Wang Z. Post-Translational Modification and Subcellular Distribution of Rac1: An Update. *Cells* (2018) 7(12):263. doi: 10.3390/cells7120263
34. Navarro-Lérida I, Sánchez-Perales S, Calvo M, Rentero C, Zheng Y, Enrich C, et al. A palmitoylation switch mechanism regulates Rac1 function and membrane organization. *EMBO J* (2012) 31(3):534–51. doi: 10.1038/emboj.2011.446
35. Tsai FD, Philips MR. Rac1 gets fattier. *EMBO J* (2012) 31(3):517–8. doi: 10.1038/emboj.2011.481
36. Hackam DJ, Rotstein OD, Sjolin C, Schreiber AD, Trimble WS, Grinstein S. v-SNARE-dependent secretion is required for phagocytosis. *Proc Natl Acad Sci* (1998) 95(20):11691–6. doi: 10.1073/pnas.95.20.11691
37. Holevinsky KO, Nelson DJ. Membrane Capacitance Changes Associated with Particle Uptake during Phagocytosis in Macrophages. *Biophys J* (1998) 75 (5):2577–86. doi: 10.1016/s0006-3495(98)77703-3
38. Touret N, Paroutis P, Terebiznik M, Harrison RE, Trombetta S, Pypaert M, et al. Quantitative and Dynamic Assessment of the Contribution of the ER to Phagosome Formation. *Cell* (2005) 123(1):157–70. doi: 10.1016/j.cell.2005.08.018
39. Booth JW, Trimble WS, Grinstein S. Membrane dynamics in phagocytosis. *Semin Immunol* (2001) 13(6):357–64. doi: 10.1006/smim.2001.0332
40. Fasshauer D, Sutton RB, Brunger AT, Jahn R. Conserved structural features of the synaptic fusion complex: SNARE proteins reclassified as Q- and R-SNAREs. *Proc Natl Acad Sci* (1998) 95(26):15781–6. doi: 10.1073/pnas.95.26.15781
41. Kloepper TH, Kienle CN, Fasshauer D. An Elaborate Classification of SNARE Proteins Sheds Light on the Conservation of the Eukaryotic Endomembrane System. *Mol Biol Cell* (2007) 18(9):3463–71. doi: 10.1091/mbc.e07-03-0193
42. Ungermann C, Sato K, Wickner W. Defining the functions of trans-SNARE pairs. *Nature* (1998) 396(6711):543–8. doi: 10.1038/25069
43. Lane SR, Liu Y. Characterization of the Palmitoylation Domain of SNAP-25. *J Neurochem* (2002) 69(5):1864–9. doi: 10.1046/j.1471-4159.1997.69051864.x
44. Greaves J, Gorleku OA, Salaun C, Chamberlain LH. Palmitoylation of the SNAP25 Protein Family. *J Biol Chem* (2010) 285(32):24629–38. doi: 10.1074/jbc.m110.119289
45. Salaün C, Gould GW, Chamberlain LH. The SNARE Proteins SNAP-25 and SNAP-23 Display Different Affinities for Lipid Rafts in PC12 Cells. *J Biol Chem* (2005) 280(2):1236–40. doi: 10.1074/jbc.m410674200
46. Sakurai C, Hashimoto H, Nakanishi H, Arai S, Wada Y, Sun-Wada G-H, et al. SNAP-23 regulates phagosome formation and maturation in macrophages. *Mol Biol Cell* (2012) 23(24):4849–63. doi: 10.1091/mbc.e12-01-0069
47. Morrison E, Wegner T, Zucchetti AE, Álvaro-Benito M, Zheng A, Kliche S, et al. Dynamic palmitoylation events following T-cell receptor signaling. *Commun Biol* (2020) 3(1). doi: 10.1038/s42003-020-1063-5
48. Fairn GD, Grinstein S. How nascent phagosomes mature to become phagolysosomes. *Trends Immunol* (2012) 33(8):397–405. doi: 10.1016/j.it.2012.03.003
49. Harrison RE, Bucci C, Vieira OV, Schroer TA, Grinstein S. Phagosomes Fuse with Late Endosomes and/or Lysosomes by Extension of Membrane Protrusions along Microtubules: Role of Rab7 and RILP. *Mol Cell Biol* (2003) 23(18):6494–506. doi: 10.1128/mcb.23.18.6494-6506.2003
50. Cantalupo G. Rab-interacting lysosomal protein (RILP): the Rab7 effector required for transport to lysosomes. *EMBO J* (2001) 20(4):683–93. doi: 10.1093/emboj/20.4.683
51. De Luca M, Cogli L, Progida C, Nisi V, Pascolutti R, Sigismund S, et al. RILP regulates vacuolar ATPase through interaction with the V1G1 subunit. *J Cell Sci* (2014) 127(12):2697–708. doi: 10.1242/jcs.142604
52. Wahe A, Kasmapour B, Schmaderer C, Liebl D, Sandhoff K, Nykjaer A, et al. Golgi-to-phagosome transport of acid sphingomyelinase and prosaposin is mediated by sortilin. *J Cell Sci* (2010) 123(Pt 14):2502–11. doi: 10.1242/jcs.067686
53. Barry AO, Mege JL, Ghigo E. Hijacked phagosomes and leukocyte activation: an intimate relationship. *J Leukoc Biol* (2011) 89(3):373–82. doi: 10.1189/jlb.0510270
54. Chen D, Xiao H, Zhang K, Wang B, Gao Z, Jian Y, et al. Retromer is required for apoptotic cell clearance by phagocytic receptor recycling. *Science* (2010) 327(5970):1261–4. doi: 10.1126/science.1184840
55. Nair-Gupta P, Baccarini A, Tung N, Seyffer F, Florey O, Huang Y, et al. TLR Signals Induce Phagosomal MHC-I Delivery from the Endosomal Recycling Compartment to Allow Cross-Presentation. *Cell* (2014) 158: (3):506–21. doi: 10.1016/j.cell.2014.04.054
56. Uriarte SM, Rane MJ, Luerman GC, Barati MT, Ward RA, Nauseef WM, et al. Granule Exocytosis Contributes to Priming and Activation of the Human Neutrophil Respiratory Burst. *J Immunol* (2011) 187(1):391–400. doi: 10.4049/jimmunol.1003112
57. Dingjan I, Linders PTA, Van Den Bekerom L, Baranov MV, Halder P, Ter Beest M, et al. Oxidized phagosomal NOX2 is replenished from lysosomes. *J Cell Sci* (2017) 31:1285–98. doi: 10.1242/jcs.196931
58. Collins RF, Schreiber AD, Grinstein S, Trimble WS. Syntaxins 13 and 7 Function at Distinct Steps During Phagocytosis. *J Immunol* (2002) 169 (6):3250–6. doi: 10.4049/jimmunol.169.6.3250
59. Wedegaertner PB, Bourne HR. Activation and depalmitoylation of Gsα. *Cell* (1994) 77(7):1063–70. doi: 10.1016/0092-8674(94)90445-6
60. He Y, Linder ME. Differential palmitoylation of the endosomal SNAREs syntaxin 7 and syntaxin 8. *J Lipid Res* (2008) 50(3):398–404. doi: 10.1194/jlr.m800360-jlr200
61. Kissing S, Saftig P, Haas A. Vacuolar ATPase in phago(lyso)some biology. *Int J Med Microbiol* (2018) 308(1):58–67. doi: 10.1016/j.ijmm.2017.08.007
62. Grinstein S, Nanda A, Lukacs G, Rotstein O. V-ATPases in phagocytic cells. *J Exp Biol* (1992) 172(1):179–92.
63. Haltia M. The neuronal ceroid-lipofuscinoses: From past to present. *Biochim Biophys Acta (BBA) - Mol Basis Dis* (2006) 1762(10):850–6. doi: 10.1016/j.bbadis.2006.06.010
64. Vesa J, Hellsten E, Verkruyse LA, Camp LA, Rapola J, Santavuori P, et al. Mutations in the palmitoyl protein thioesterase gene causing infantile neuronal ceroid lipofuscinosis. *Nature* (1995) 376(6541):584–7. doi: 10.1038/376584a0
65. Lu JY, Verkruyse LA, Hofmann SL. Lipid thioesters derived from acylated proteins accumulate in infantile neuronal ceroid lipofuscinosis: correction of the defect in lymphoblasts by recombinant palmitoyl-protein thioesterase. *Proc Natl Acad Sci* (1996) 93(19):10046–50. doi: 10.1073/pnas.93.19.10046
66. Bagh MB, Peng S, Chandra G, Zhang Z, Singh SP, Pattabiraman N, et al. Misrouting of v-ATPase subunit V0a1 dysregulates lysosomal acidification in a neurodegenerative lysosomal storage disease model. *Nat Commun* (2017) 8 (1):14612. doi: 10.1038/ncomms14612

67. Wang YJ, Wang J, Sun HQ, Martinez M, Sun YX, Macia E, et al. Phosphatidylinositol 4 Phosphate Regulates Targeting of Clathrin Adaptor AP-1 Complexes to the Golgi. *Cell* (2003) 114(3):299–310. doi: 10.1016/s0092-8674(03)00603-2
68. Salazar G, Craige B, Wainer BH, Guo J, De Camilli P, Faundez V. Phosphatidylinositol-4-Kinase Type II α Is a Component of Adaptor Protein-3-derived Vesicles. *Mol Biol Cell* (2005) 16(8):3692–704. doi: 10.1091/mbc.e05-01-0020
69. Wieffer M, Cibrián Uhalte E, Posor Y, Otten C, Branz K, Schütz I, et al. PI4K2β/AP-1-Based TGN-Endosomal Sorting Regulates Wnt Signaling. *Curr Biol* (2013) 23(21):2185–90. doi: 10.1016/j.cub.2013.09.017
70. Barylko B, Mao YS, Wlodarski P, Jung G, Binns DD, Sun HQ, et al. Palmitoylation Controls the Catalytic Activity and Subcellular Distribution of Phosphatidylinositol 4-Kinase II. *J Biol Chem* (2009) 284(15):9994–10003. doi: 10.1074/jbc.m900724200
71. Lu D, Sun H-Q, Wang H, Barylko B, Fukata Y, Fukata M, et al. Phosphatidylinositol 4-Kinase IIα Is Palmitoylated by Golgi-localized Palmitoyltransferases in Cholesterol-dependent Manner. *J Biol Chem* (2012) 287(26):21856–65. doi: 10.1074/jbc.m112.348094
72. Levin R, Hammond GRV, Balla T, De Camilli P, Fairn GD, Grinstein S. Multiphasic dynamics of phosphatidylinositol 4-phosphate during phagocytosis. *Mol Biol Cell* (2017) 28:128–40. doi: 10.1091/mbc.e16-06-0451
73. López-Haber C, Levin-Konigsberg R, Zhu Y, Bi-Karchin J, Balla T, Grinstein S, et al. Phosphatidylinositol-4-kinase IIα licenses phagosomes for TLR4 signaling and MHC-II presentation in dendritic cells. *Proc Natl Acad Sci* (2020) 117(45):28251–62. doi: 10.1073/pnas.2001948117
74. Levin-Konigsberg R, Montano-Rendon F, Keren-Kaplan T, Li R, Ego B, Mylvaganam S, et al. Phagolysosome resolution requires contacts with the endoplasmic reticulum and phosphatidylinositol-4-phosphate signalling. *Nat Cell Biol* (2019) 21(10):1234–47. doi: 10.1038/s41556-019-0394-2
75. Modica G, Skorobogata O, Sauvageau E, Vissa A, Yip CM, Kim PK, et al. Rab7 palmitoylation is required for efficient endosome-to-TGN trafficking. *J Cell Sci* (2017) 130(15):2579–90. doi: 10.1242/jcs.199729
76. McCormick PJ, Dumaresq-Doiron K, Pluviose AS, Pichette V, Tosato G, Lefrancois S. Palmitoylation controls recycling in lysosomal sorting and trafficking. *Traffic* (2008) 9(11):1984–97. doi: 10.1111/j.1600-0854.2008.00814.x
77. Haney MS, Bohlen CJ, Morgens DW, Ousey JA, Barkal AA, Tsui CK, et al. Identification of phagocytosis regulators using magnetic genome-wide CRISPR screens. *Nat Genet* (2018) 50(12):1716–27. doi: 10.1038/s41588-018-0254-1
78. Smith KGC, Clatworthy MR. FcγRIIB in autoimmunity and infection: evolutionary and therapeutic implications. *Nat Rev Immunol* (2010) 10 (5):328–43. doi: 10.1038/nri2762
79. Zenarruzabeitia O, Vitallé J, Eguizabal C, Simhadri VR, Borrego F. The Biology and Disease Relevance of CD300a, an Inhibitory Receptor for Phosphatidylserine and Phosphatidylethanolamine. *J Immunol* (2015) 194 (11):5053–60. doi: 10.4049/jimmunol.1500304
80. Huang Z-Y, Hunter S, Kim M-K, Indik ZK, Schreiber AD. The effect of phosphatases SHP-1 and SHIP-1 on signaling by the ITIM- and ITAM-containing Fcγ receptors FcγRIIB and FcγRIIA. *J Leukocyte Biol* (2003) 73 (6):823–9. doi: 10.1189/jlb.0902454
81. Thinon E, Fernandez JP, Molina H, Hang HC. Selective Enrichment and Direct Analysis of Protein S-Palmitoylation Sites. *J Proteome Res* (2018) 17 (5):1907–22. doi: 10.1021/acs.jproteome.8b00002

Conflict of Interest: The authors declare that the research was conducted in the absence of any commercial or financial relationships that could be construed as a potential conflict of interest.

Copyright © 2021 Dixon, Mekhail and Fairn. This is an open-access article distributed under the terms of the Creative Commons Attribution License (CC BY). The use, distribution or reproduction in other forums is permitted, provided the original author(s) and the copyright owner(s) are credited and that the original publication in this journal is cited, in accordance with accepted academic practice. No use, distribution or reproduction is permitted which does not comply with these terms.

frontiers in Immunology

MINI REVIEW
published: 19 April 2021
doi: 10.3389/fimmu.2021.661974

Modular Organization of Engulfment Receptors and Proximal Signaling Networks: Avenues to Reprogram Phagocytosis

Emily A. Britt[†], *Vanessa Gitau*[†], *Amara Saha*[†] *and Adam P. Williamson*[*]

Department of Biology, Bryn Mawr College, Bryn Mawr, PA, United States

Transmembrane protein engulfment receptors expressed on the surface of phagocytes engage ligands on apoptotic cells and debris to initiate a sequence of events culminating in material internalization and immunologically beneficial outcomes. Engulfment receptors are modular, comprised of functionally independent extracellular ligation domains and cytosolic signaling motifs. Cognate kinases, adaptors, and phosphatases regulate engulfment by controlling the degree of receptor activation in phagocyte plasma membranes, thus acting as receptor-proximal signaling modules. Here, we review recent efforts to reprogram phagocytes using modular synthetic receptors composed of antibody-based extracellular domains fused to engulfment receptor signaling domains. To aid the development of new phagocyte reprogramming methods, we then define the kinases, adaptors, and phosphatases that regulate a conserved family of engulfment receptors. Finally, we discuss current challenges and opportunities for the field.

Keywords: phagocytosis, engulfment, immune receptor, signal transduction, macrophage reprogramming, chimeric antigen receptor, immunotherapy

OPEN ACCESS

Edited by:
Valentin Jaumouillé, Simon Fraser University, Canada

Reviewed by:
Nicolas Touret, University of Alberta, Canada
Carlos Rosales, Universidad Nacional Autónoma de México, Mexico

***Correspondence:**
Adam P. Williamson
awilliams6@brynmawr.edu

[†]*These authors have contributed equally to this work*

Specialty section:
This article was submitted to Molecular Innate Immunity, a section of the journal Frontiers in Immunology

Received: *31 January 2021*
Accepted: *22 March 2021*
Published: *19 April 2021*

Citation:
Britt EA, Gitau V, Saha A and Williamson AP (2021) Modular Organization of Engulfment Receptors and Proximal Signaling Networks: Avenues to Reprogram Phagocytosis. Front. Immunol. 12:661974. doi: 10.3389/fimmu.2021.661974

INTRODUCTION

The Megf10/Draper/CED-1 receptors, an ancient family of single-pass transmembrane proteins, enable phagocytes across phyla to initiate the internalization of apoptotic cells, synapses, and cell debris (1–3). Ligation of engulfment receptor extracellular domains to "eat me" signals on the target, including the complement protein C1q and the lipid phosphatidylserine (PS), induces receptor phosphorylation by "writer" kinases. Phosphorylation recruits "reader" proteins that initiate a series of cytoskeletal and membrane-remodeling events that enable the phagocytes to ingest large targets and digest internalized material in intracellular compartments. "Eraser" phosphatases then dephosphorylate engulfment receptors to return the receptor to its unphosphorylated resting state (4). Writer-reader-eraser modules that regulate receptor activation are common components of vertebrate immune cell signaling pathways (**Figure 1A**). Notable examples include the Src-Syk-CD45 writer-reader-eraser network that controls Fc-receptor signaling and the Lck-ZAP70-CD45 module that tunes activation the T cell receptor (TCR) (5).

The Megf10/Draper/CED-1 receptors are composed of functionally separable extracellular ligation and intracellular signaling modules. The modularity of engulfment receptors enables phagocyte reprogramming, as replacement of the extracellular domain with a new recognition element directs

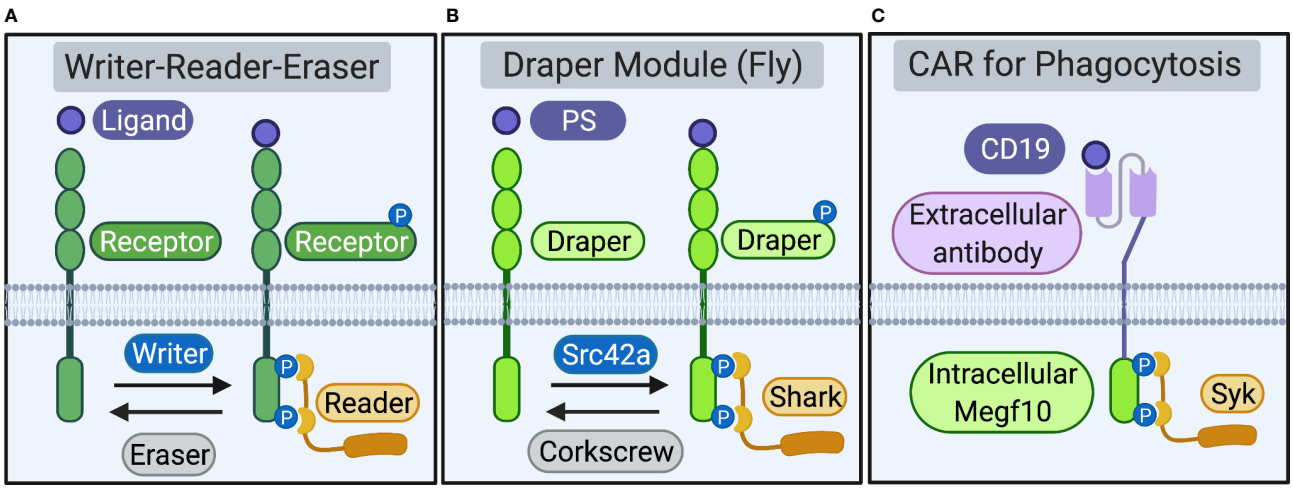

FIGURE 1 | Receptors and proximal writer-reader-eraser modules. **(A)** Schematic of a generalized receptor and writer-reader-eraser module. Receptor ligation induces phosphorylation of a receptor intracellular signaling domain by a writer kinase. The phosphorylated receptor recruits a reader adaptor protein. An eraser phosphatase removes phosphorylation marks on the receptor intracellular domain, returning the system to its resting state. **(B)** A writer-reader-eraser module regulates signal transduction through the Draper receptor. Draper, expressed on fruit fly phagocytes, recognizes phosphatidylserine (PS) or other ligands. Phosphorylation of the Draper intracellular domain by the kinase Src42a induces recruitment of the adaptor kinase Shark. The phosphatase Corkscrew erases phosphorylation marks on the intracellular domain of Draper. **(C)** Chimeric Antigen Receptor for Phagocytosis (CAR-P). Synthetic CAR-Ps bind cancer antigens (e.g. the B cell antigen CD19) *via* an extracellular single-chain antibody fragment (scFv). Extracellular antibody ligation induces phosphorylation of engulfment receptor signaling domains (e.g. the intracellular domain of mouse Megf10). Phosphorylation of the Megf10 receptor signaling domain on CAR-P recruits the Syk adaptor, a cognate reader for murine Megf10. Schematic created in BioRender (biorender.com).

phagocytes to identify and ingest new targets (6–8). The organization of engulfment signaling is also modular at the level of the receptor proximal signaling networks. Engulfment receptors function in concert with effector modules comprised of kinases, adaptors, and phosphatases that initiate the engulfment signaling program. Here, we review recent work that highlights the promise of reprogramming phagocytosis to understand basic immunology in pre-clinical settings. We then use the modular structure of synthetic engulfment receptors as an inlet to define and compare the writers, readers, and erasers that regulate initiation of the engulfment signaling program through the Megf10/Draper/CED-1 receptors (**Figure 1B**).

REPROGRAMMING PHAGOCYTOSIS USING CHIMERIC ANTIGEN RECEPTORS

In multiple immune cell types, including T cells, phagocytes, and natural killer cells, replacement of an extracellular domain with a single-chain antibody fragment (scFv) can reprogram an immune cell towards the cognate antigen of a specific scFv (7, 9, 10). Reprogramming immune cell signaling has ushered in a new suite of methods to engineer the immune response to target cancer (11). Analogous to Chimeric Antigen Receptors in T cells (CAR-T), the modular organization of engulfment receptors enables investigators to reprogram phagocytes to identify and eliminate targets of therapeutic interest.

The modular organization of the T cell, Fc-, and phagocyte receptors enables the reprogramming of immune cells to recognize and respond to non-native targets of therapeutic interest, including cancer antigens (6, 7, 9). Multiple groups have successfully reprogrammed macrophages to recognize cancer antigens by introducing synthetic Chimeric Antigen Receptors for Phagocytosis (CAR-Ps) (6, 7). Fusing the Megf10 or Fc-receptor signaling domains to an scFv recognizing the B-lymphocyte antigen CD19 programmed mouse macrophages to ingest antigen-coated beads and cancer cells (**Figure 1C**) (7). Surprisingly, chimeric receptors expressed in macrophages composed of extracellular scFvs fused to the T cell receptor signaling domain CD3ζ also drive engulfment (6, 7). Importantly, Klichinsky et al. also demonstrated the following: anti-cancer activity in humanized mouse models; induction of a pro-inflammatory tumor microenvironment; and antigen cross presentation to boost anti-tumor T cell responses (6). Collectively, coupling scFv-based extracellular modules to ITAM-based intracellular signaling domains from Megf10, Fc-receptor, and the TCR, presents an attractive strategy to reprogram macrophages towards therapeutically relevant targets linked to both hematopoietic malignancies and solid tumors (6, 7).

At present, methods primarily rely on extracellular antibody-based modules that recognize antigens with high affinity. However, high-affinity CAR-Ps may signal in a manner that does not reflect endogenous receptor mechanisms. Recent work demonstrates that T cells transduce signals through CAR-T independently of a key T cell signaling protein required by physiological T cells called Linker of Activated T cells (LAT) (12). Future work for the field will require engineering molecules

that more closely reflect the biology of native engulfment receptors, perhaps by developing new CARs that combine multiple signaling modules to orient cellular responses towards desired immunological outcomes. To learn how engulfment receptors interface with proximal signaling modules, we systematically defined the writer, reader, and erasers that regulate the Megf10/Draper/CED-1 family.

MODULAR ORGANIZATION OF ENGULFMENT SIGNALING NETWORKS ACROSS PHYLA

Application of the writer-reader-eraser framework enables conserved rules and regulatory principles underlying engulfment to emerge from this complex collection of receptors and their proximal signaling networks. Here, writers refer to protein tyrosine kinases that create reversible binding sites for readers. The readers, SH2- and PTB-domain-containing proteins, initiate the engulfment program by activating "downstream" signaling modules that remodel the actin cytoskeleton and cell membranes (13). The cycle is completed by erasers, protein tyrosine phosphatases that return the system to its deactivated state.

Megf10: Clearing Corpses and Shaping Synapses in the Mouse Brain

Megf10, a receptor expressed on phagocytic astrocytes in the mouse brain, promotes synapse elimination (14) and apoptotic cell clearance (1). Megf10 also plays roles in retinal patterning (15) and elimination of amyloid-β (16). After recognition of its ligand, the complement protein C1q (1), Src-family kinase writers phosphorylate Tyrosine (Tyr) residues within the Megf10 Immunoreceptor Tyrosine-based Activation Motif (ITAM) (17). In addition to its ITAM, the cytosolic tail of Megf10 encodes an NPxY motif (18), a domain capable of recruiting cytosolic signaling proteins *via* direct interaction with phosphotyrosine binding (PTB) domains. Consistent with a writer function for Src-family kinases, treating HeLa cells that overexpress Megf10 with the Src-family kinase inhibitor PP2 decreases engulfment of microspheres by HeLa cells transfected with Megf10 (17). Thus, multiple Src-family kinases can create binding sites for readers on the cytosolic tail of Megf10.

The tandem SH2-domain-containing kinase Syk is a Megf10 reader that interacts with phosphorylated ITAM residues on the cytosolic domain of Megf10 (17). Though the specific actions of Syk that enable phagocytosis in glia are unclear, Syk is an important engulfment effector in macrophages and plays a role in remodeling the actin cytoskeleton when bound to the Fc-receptor (19). The PTB-containing protein GULP is upregulated in reactive astrocytes after transient ischemic injury, an expression pattern similar to Megf10 (20). Thus, in addition to Syk, GULP is a candidate to interact with the intracellular domain of Megf10 *via* an NPxY motif.

A specific eraser for Megf10 is not reported, though mouse astrocytes express SHP-2 (PTPN11) mRNA (21). SHP-2 is a cytosolic protein tyrosine phosphatase that dephosphorylates the ITAM-bearing C-type lectin receptor that governs anti-fungal immunity (22). In sum, Megf10 is an invariant single-pass transmembrane engulfment receptor. A module comprised of multiple Src-family kinases and Syk enables Megf10 to initiate the clearance of apoptotic cells and synapses.

Draper and a Proximal Writer-Reader-Eraser Module Initiate Engulfment by Fly Phagocytes

Phagocytes in the fruit fly *Drosophila melanogaster* clear apoptotic corpses and axonal debris to maintain tissue homeostasis and repair the nervous system after injury. Engulfment in flies is carried out by an array of cell types including hemocytes (23), epithelial cells (24), and glia (2, 25). The Draper receptor, expressed in each of these cell types, is comprised of an extracellular emlin (EMI) domain that facilitates protein-protein interactions (26) and nimrod (NIM) repeats, EGF-like domains found on multiple fruit fly innate immune receptors (27). The intracellular signaling domain of Draper contains two phosphotyrosine-based signaling sequences that serve as candidate sites for phosphorylation by Src-family kinase writers: an NPxY and an ITAM.

Ligation of Draper to phosphatidylserine induces phosphorylation of the cytosolic signaling domain of Draper (8, 28). Intriguingly, Draper recognizes a diverse array of additional ligands in other contexts including the proteins Pretaporter (29) and DmCaBP1 (30) and the bacterial surface molecule Lipoteichoic acid (31). Once ligand-receptor binding occurs, clustered Draper is rapidly phosphorylated in phagocyte plasma membranes (8). At least 5 residues on the cytoplasmic signaling domain of Draper, including at least 4 outside the ITAM, are phosphorylated by the kinase Src42a (8, 32). The kinase Src42a is the writer in this system, creating a binding site for the tandem SH2-domain kinase Shark (32) (**Figure 1B**).

The cytosolic protein tyrosine phosphatase Corkscrew, which binds an alternatively spliced isoform of Draper called Draper-II *via* an Immunoreceptor Tyrosine-based Inhibitory Motif (ITIM), is the eraser for Draper (33). Corkscrew is capable of dephosphorylating Draper and, intriguingly, loss of Corkscrew *in vivo* inhibits the ability of glia to respond to secondary injury (33). The interdependence of the writer, reader, and eraser in the fly system underscores the importance of returning this immune cell signaling system to its ground state to respond to future insults.

Collectively, a wealth of genetic, biochemical, and cell biological evidence supports the model that engulfment through Draper is carried out by a writer-reader-eraser module comprised of a writer kinase Src42a, an SH2-domain-containing reader Shark, and an eraser Corkscrew. As writers, readers, and erasers remain to be determined in other organisms, the fruit fly represents an exceptional model system for defining the mechanisms underlying engulfment through the Megf10/Draper/CED-1 receptors.

CED-1 in the Worm: A Divergent Engulfment Receptor

Genetic work in the nematode *Caenorhabditis elegans*, including the discovery of the CED-1 receptor (3), founded the engulfment

field. *C. elegans* phagocytes clear dead and dying cells using two pathways governed by engulfment factors expressed by ced genes. One pathway includes ced-2, ced-5, and ced-12 while the other pathway includes ced-1, ced-6, and ced-7 (34). These pathways converge on actin to facilitate rearrangements that enable engulfment (35).

Corpse clearance by phagocytic cells in the worm is initiated when cells neighboring the apoptotic cell release the secretory protein Transthyretin-related 52 (TTR-52) (36). TTR-52 binds PS on the corpse and serves as a bridging molecule to the receptor CED-1. CED-1 ligation to TTR-52 induces activation of the CED-6 and CED-7 signaling pathway. Like Draper and Megf10, the extracellular domain of CED-1 contains EMI and EGF-like domains (3, 26). The cytosolic signaling tail on CED-1 contains a possible Tyrosine phosphorylation site on a single YxxL motif (3). The tail also contains an NPxY motif with a Tyr residue. However, *in vitro* evidence indicates that NPxY motifs may bind PTB-domain-containing proteins such as CED-6 in the absence of Tyr phosphorylation (37). Thus, our application of the writer-reader-eraser framework to the *C. elegans* CED-1/CED-6/CED-7 engulfment module reveals that while worms do encode candidate writer kinases and eraser phosphatases, the CED-1 receptor may perform engulfment in the absence of Tyr phosphorylation.

CONCLUSIONS, CURRENT CHALLENGES, AND NEW OPPORTUNITIES

Comparison of Writer-Reader-Eraser Modules Used by Phagocytes Across Phyla

Our application of the writer-reader-eraser framework to define the proximal signaling networks that regulate the Megf10/Draper/CED-1 receptor family revealed broad mechanistic similarities and intriguing differences (**Table 1**). All three receptors contain at least one cytoplasmic Tyr residue in an ITAM or NPxY motif, potential phosphorylation sites for kinase writers. At least one reader protein interacts with Megf10, Draper, or CED-1 to initiate the complex series of cytoskeletal and membrane-remodeling events that power material internalization. Megf10 and Draper recruit a Syk-family kinase reader and CED-6/GULP adaptor proteins. CED-1 binds the reader CED-6. Collectively, the proximal writers and readers governing Megf10 and Draper function are highly similar to one another. Because the CED-6 adaptor protein may bind CED-1 independently of Tyr phosphorylation, CED-1 may function *via* a distinct activation mechanism that does not require a writer kinase. Less is known about the eraser phosphatases that negatively regulate the Megf10/Draper/CED-1 receptors. The eraser for Draper, a SHP-2 tyrosine phosphatase ortholog called Corkscrew, works by binding an inhibitory splice isoform of Draper (33). The cognate phosphatases for Megf10 and CED-1, though presumably expressed by the relevant phagocytes, remain unreported.

Megf10, Draper, and CED-1 differ remarkably in their ligand specificities, perhaps a result of their evolutionary divergence and the large number of different "eat me" signals presented on the surface of apoptotic cells and other targets (41). Megf10 binds the complement protein C1q to initiate the engulfment of apoptotic cells (1). Draper initiates engulfment by interacting with diverse ligands including the lipid PS and the proteins DmCaBP1 and Pretaporter (8, 28–30). Finally, CED-1 recognizes the secreted protein TTR-52 that serves as A bridge between CED-1 and PS (36). Perhaps the diversity of ligands that the Megf10/Draper/CED-1 receptors recognize provides the mechanistic basis for reprogramming the receptors using synthetic extracellular domains. We hope that further study of engulfment receptors and their proximal signaling modules will enable researchers to design a new generation of synthetic signaling systems comprised of CARs that interact with engineered intracellular signaling modules.

Reprogramming Phagocytes Toward New Targets

In theory, new CAR-Ps that enable phagocytes to bind any extracellular cell surface protein or secreted molecule should program phagocytes to ingest non-native targets. At present, however, implementing CAR-Ps in a clinical context requires laborious editing protocols to manipulate autologous cells. Thus, the use of CAR-Ps as therapies to treat human disease remains a goal for the future. For now, CAR-Ps are emerging as important tools to define basic immunology by elucidating the mechanisms used by receptors expressed across diverse phagocyte populations.

TABLE 1 | Summary of receptors and writer-reader-eraser modules used across biological processes and organisms.

Biological Process (Organism)	Receptor	Ligand(s)	Writer	Reader	Eraser	References
Phagocytosis of opsonized targets (Mouse)	Fc-receptor	Antibody fragment crystallizable (Fc) region	Src-family kinases	Syk	CD45	(38, 39)
T-cell receptor activation (Mouse)	T-cell receptor	Peptide-MHC	Lck	ZAP70	CD45	(40)
Targeting hematologic malignancies (Mouse)	Antibody-based Chimeric Receptors	CD19, CD22	Not reported	Syk	Not reported	(6, 7)
Targeting solid tumors (Mouse)	Antibody-based Chimeric Receptors	Mesothelin, HER2	Not reported	Syk	Not reported	(6)
Engulfment of apoptotic cells and synapses (Mouse)	Megf10	C1q	Src-family kinases	Syk	Not reported	(1, 17)
Engulfment of apoptotic cells and axonal debris (Fly)	Draper	Phosphatidylserine, Lipoteichoic acid, Pretaporter, DmCaBP1	Src42a	Shark	Corkscrew	(8, 28–33)
Engulfment of apoptotic cells (Worm)	CED-1	TTR-52	Not reported	CED-6	Not reported	(3, 35, 36)

As investigators continue to design and express new receptors, it will be critical to move beyond internalization to learn how engulfed material is targeted to promote specific immunological outcomes. For example, recent work linking the receptor DNGR-1 to antigen cross-presentation suggests that expression of a DNGR-1-based CAR-P in Dendritic Cells may drive the efficient cross-presentation of cancer antigens (42). In the long term, replacing cell-based CAR-Ps with bi- or tri-specific antibodies that couple desired phagocyte populations exposing known cell surface molecules to disease-associated antigens may prove to be viable, inexpensive strategies that could democratize access to new therapies.

Reprogrammed Phagocytes That Facilitate Nondestructive Immune Responses

In conclusion, further study of engineered phagocytes could spur the development of therapeutic interventions that cover a broad array of "accommodation" immune archetypes: active, nondestructive responses that, among other outcomes, promote wound healing and tissue repair (43). Phagocytes are particularly well suited to promote nondestructive responses because their endogenous functions include clearing apoptotic cells without inducing local inflammatory responses. In this review, we focused on modular receptor signaling systems that offer opportunities to reprogram phagocytes to ingest cancer cells. A key future challenge for the field is to develop phagocyte engineering strategies targeted at a broader range of diseases and cell populations. We anticipate that the development of new chimeric receptors that connect extracellular ligation to synthetic intracellular signaling modules will lead to exciting discoveries at the frontier of this nascent, expanding field.

AUTHOR CONTRIBUTIONS

EB, VG, and AS contributed equally to this work and are listed alphabetically. EB completed an analysis of the Megf10 primary literature and drafted and edited the article. VG completed an analysis of the CED-1 primary literature and drafted and edited the article. AS completed an analysis of the Draper primary literature and drafted and edited the article. AW drafted and edited the article. All authors contributed to the article and approved the submitted version.

FUNDING

EB, VG, AS – Undergraduate Summer Science Research Funding, Bryn Mawr College. AW – Research Startup Funds, Bryn Mawr College.

ACKNOWLEDGMENTS

EB, VG, and AS thank the Bryn Mawr Undergraduate Summer Science Research program for financial support. Work in the Williamson Lab is supported by research startup funds from Bryn Mawr College. We thank Ani Dixit, Ellen Luecke, Vanessa Shehu, and Katrina Sparks for productive discussions and comments on the manuscript. We also acknowledge the efforts of two reviewers who provided helpful feedback during peer-review.

REFERENCES

1. Iram T, Ramirez-Ortiz Z, Byrne MH, Coleman UA, Kingery ND, Means TK, et al. Megf10 Is a Receptor for C1Q That Mediates Clearance of Apoptotic Cells by Astrocytes. *J Neurosci* (2016) 36(19):5185–92. doi: 10.1523/JNEUROSCI.3850-15.2016
2. MacDonald JM, Beach MG, Porpiglia E, Sheehan AE, Watts RJ, Freeman MR. The Drosophila Cell Corpse Engulfment Receptor Draper Mediates Glial Clearance of Severed Axons. *Neuron* (2006) 50(6):869–81. doi: 10.1016/j.neuron.2006.04.028
3. Zhou Z, Hartwieg E, Horvitz HR. CED-1 Is a Transmembrane Receptor that Mediates Cell Corpse Engulfment in *C. elegans*. *Cell* (2001) 104(1):43–56. doi: 10.1016/S0092-8674(01)00190-8
4. Lim WA, Pawson T. Phosphotyrosine Signaling: Evolving a New Cellular Communication System. *Cell* (2010) 142(5):661–7. doi: 10.1016/j.cell.2010.08.023
5. Niedergang F, Di Bartolo V, Alcover A. Comparative Anatomy of Phagocytic and Immunological Synapses. *Front Immunol* (2016) 7:18. doi: 10.3389/fimmu.2016.00018
6. Klichinsky M, Ruella M, Shestova O, Lu XM, Best A, Zeeman M, et al. Human chimeric antigen receptor macrophages for cancer immunotherapy. *Nat Biotechnol* (2020) 38:947–53. doi: 10.1038/s41587-020-0462-y
7. Morrissey MA, Williamson AP, Steinbach AM, Roberts EW, Kern N, Headley MB, et al. Chimeric antigen receptors that trigger phagocytosis. *eLife* (2018) 7: e36688. doi: 10.7554/eLife.36688
8. Williamson AP, Vale RD. Spatial control of Draper receptor signaling initiates apoptotic cell engulfment. *J Cell Biol* (2018) 217(11):3977–92. doi: 10.1083/jcb.201711175
9. Grupp SA, Kalos M, Barrett D, Aplenc R, Porter DL, Rheingold SR, et al. Chimeric Antigen Receptor–Modified T Cells for Acute Lymphoid Leukemia. *New Engl J Med* (2013) 368(16):1509–18. doi: 10.1056/NEJMoa1215134
10. Töpfer K, Cartellieri M, Michen S, Wiedemuth R, Müller N, Lindemann D, et al. DAP12-Based Activating Chimeric Antigen Receptor for NK Cell Tumor Immunotherapy. *J Immunol* (2015) 194(7):3201–12. doi: 10.4049/jimmunol.1400330
11. Lim WA, June CH. The Principles of Engineering Immune Cells to Treat Cancer. *Cell* (2017) 168(4):724–40. doi: 10.1016/j.cell.2017.01.016
12. Dong R, Libby KA, Blaeschke F, Fuchs W, Marson A, Vale RD, et al. Rewired signaling network in T cells expressing the chimeric antigen receptor (CAR). *EMBO J* (2020) 39(16):e104730. doi: 10.15252/embj.2020104730
13. Zhang Y, Hoppe AD, Swanson JA. Coordination of Fc receptor signaling regulates cellular commitment to phagocytosis. *Proc Natl Acad Sci* (2010) 107 (45):19332–7. doi: 10.1073/pnas.1008248107
14. Chung W-S, Clarke LE, Wang GX, Stafford BK, Sher A, Chakraborty C, et al. Astrocytes mediate synapse elimination through MEGF10 and MERTK pathways. *Nature* (2013) 504(7480):394–400. doi: 10.1038/nature12776
15. Kay JN, Chu MW, Sanes JR. MEGF10 and MEGF11 mediate homotypic interactions required for mosaic spacing of retinal neurons. *Nature* (2012) 483 (7390):465–9. doi: 10.1038/nature10877
16. Singh TD, Park S-Y, Bae J, Yun Y, Bae Y-C, Park R-W, et al. MEGF10 functions as a receptor for the uptake of amyloid-β. *FEBS Lett* (2010) 584 (18):3936–42. doi: 10.1016/j.febslet.2010.08.050
17. Scheib JL, Sullivan CS, Carter BD. Jedi-1 and MEGF10 Signal Engulfment of Apoptotic Neurons through the Tyrosine Kinase Syk. *J Neurosci* (2012) 32 (38):13022–31. doi: 10.1523/JNEUROSCI.6350-11.2012
18. Wu H-H, Bellmunt E, Scheib JL, Venegas V, Burkert C, Reichardt LF, et al. Glial precursors clear sensory neuron corpses during development via Jedi-1, an engulfment receptor. *Nat Neurosci* (2009) 12(12):1534–41. doi: 10.1038/nn.2446
19. Jaumouillé V, Farkash Y, Jaqaman K, Das R, Lowell CA, Grinstein S. Actin Cytoskeleton Reorganization by Syk Regulates Fcγ Receptor Responsiveness

by Increasing Its Lateral Mobility and Clustering. *Dev Cell* (2014) 29(5):534–46. doi: 10.1016/j.devcel.2014.04.031
20. Morizawa YM, Hirayama Y, Ohno N, Shibata S, Shigetomi E, Sui Y, et al. Reactive astrocytes function as phagocytes after brain ischemia via ABCA1-mediated pathway. *Nat Commun* (2017) 8(28). doi: 10.1038/s41467-017-00037-1
21. Zhang Y, Chen K, Sloan SA, Bennett ML, Scholze AR, O'Keeffe S, et al. An RNA-Sequencing Transcriptome and Splicing Database of Glia, Neurons, and Vascular Cells of the Cerebral Cortex. *J Neurosci* (2014) 34(36):11929–47. doi: 10.1523/JNEUROSCI.1860-14.2014
22. Deng Z, Ma S, Zhou H, Zang A, Fang Y, Li T, et al. Tyrosine phosphatase SHP-2 mediates C-type lectin receptor–induced activation of the kinase Syk and anti-fungal TH17 responses. *Nat Immunol* (2015) 16(6):642–52. doi: 10.1038/ni.3155
23. Wood W, Martin P. Macrophage Functions in Tissue Patterning and Disease: New Insights from the Fly. *Dev Cell* (2017) 40(3):221–33. doi: 10.1016/j.devcel.2017.01.001
24. Etchegaray JI, Timmons AK, Klein AP, Pritchett TL, Welch E, Meehan TL, et al. Draper acts through the JNK pathway to control synchronous engulfment of dying germline cells by follicular epithelial cells. *Development* (2012) 139(21):4029–39. doi: 10.1242/dev.082776
25. Sonnenfeld MJ, Jacobs JR. Macrophages and glia participate in the removal of apoptotic neurons from theDrosophila embryonic nervous system. *J Comp Neurol* (1995) 359(4):644–52. doi: 10.1002/cne.903590410
26. Callebaut I, Mignotte V, Souchet M, Mornon J-P. EMI domains are widespread and reveal the probable orthologs of the *Caenorhabditis elegans* CED-1 protein. *Biochem Biophys Res Commun* (2003) 300(3):619–23. doi: 10.1016/S0006-291X(02)02904-2
27. Somogyi K, Sipos B, Penzes Z, Kurucz E, Zsamboki J, Hultmark D, et al. Evolution of Genes and Repeats in the Nimrod Superfamily. *Mol Biol Evol* (2008) 25(11):2337–47. doi: 10.1093/molbev/msn180
28. Tung TT, Nagaosa K, Fujita Y, Kita A, Mori H, Okada R, et al. Phosphatidylserine recognition and induction of apoptotic cell clearance by Drosophila engulfment receptor Draper. *J Biochem* (2013) 153(5):483–91. doi: 10.1093/jb/mvt014
29. Kuraishi T, Nakagawa Y, Nagaosa K, Hashimoto Y, Ishimoto T, Moki T, et al. Pretaporter, a Drosophila protein serving as a ligand for Draper in the phagocytosis of apoptotic cells. *EMBO J* (2009) 28(24):3868–78. doi: 10.1038/emboj.2009.343
30. Okada R, Nagaosa K, Kuraishi T, Nakayama H, Yamamoto N, Nakagawa Y, et al. Apoptosis-dependent Externalization and Involvement in Apoptotic Cell Clearance of DmCaBP1, an Endoplasmic Reticulum Protein of Drosophila*. *J Biol Chem* (2012) 287(5):3138–46. doi: 10.1074/jbc.M111.277921
31. Hashimoto Y, Tabuchi Y, Sakurai K, Kutsuna M, Kurokawa K, Awasaki T, et al. Identification of Lipoteichoic Acid as a Ligand for Draper in the Phagocytosis of *Staphylococcus aureus* by *Drosophila* Hemocytes. *J Immunol* (2009) 183(11):7451–60. doi: 10.4049/jimmunol.0901032
32. Ziegenfuss JS, Biswas R, Avery MA, Hong K, Sheehan AE, Yeung Y-G, et al. Draper-dependent glial phagocytic activity is mediated by Src and Syk family kinase signalling. *Nature* (2008) 453(7197):935–9. doi: 10.1038/nature06901
33. Logan MA, Hackett R, Doherty J, Sheehan A, Speese SD, Freeman MR. Negative regulation of glial engulfment activity by Draper terminates glial responses to axon injury. *Nat Neurosci* (2012) 15(5):722–30. doi: 10.1038/nn.3066
34. Gumienny TL, Brugnera E, Tosello-Trampont A-C, Kinchen JM, Haney LB, Nishiwaki K, et al. CED-12/ELMO, a Novel Member of the CrkII/Dock180/Rac Pathway, Is Required for Phagocytosis and Cell Migration. *Cell* (2001) 107(1):27–41. doi: 10.1016/S0092-8674(01)00520-7
35. Kinchen JM, Cabello J, Klingele D, Wong K, Feichtinger R, Schnabel H, et al. Two pathways converge at CED-10 to mediate actin rearrangement and corpse removal in *C. elegans*. *Nature* (2005) 434(7029):93–9. doi: 10.1038/nature03263
36. Wang X, Li W, Zhao D, Liu B, Shi Y, Chen B, et al. *Caenorhabditis elegans* transthyretin-like protein TTR-52 mediates recognition of apoptotic cells by the CED-1 phagocyte receptor. *Nat Cell Biol* (2010) 12(7):655–64. doi: 10.1038/ncb2068
37. Su HP, Nakada-Tsukui K, Tosello-Trampont A-C, Li Y, Bu G, Henson PM, et al. Interaction of CED-6/GULP, an Adapter Protein Involved in Engulfment of Apoptotic Cells with CED-1 and CD91/Low Density Lipoprotein Receptor-related Protein (LRP). *J Biol Chem* (2002) 277(14):11772–9. doi: 10.1074/jbc.M109336200
38. Freeman SA, Goyette J, Furuya W, Woods EC, Bertozzi CR, Bergmeier W, et al. Integrins Form an Expanding Diffusional Barrier that Coordinates Phagocytosis. *Cell* (2016) 164(1–2):128–40. doi: 10.1016/j.cell.2015.11.048
39. Greenberg S, Chang P, Wang DC, Xavier R, Seed B. Clustered syk tyrosine kinase domains trigger phagocytosis. *Proc Natl Acad Sci* (1996) 93(3):1103–7. doi: 10.1073/pnas.93.3.1103
40. Davis SJ, van der Merwe PA. The kinetic-segregation model: TCR triggering and beyond. *Nat Immunol* (2006) 7(8):803–9. doi: 10.1038/ni1369
41. Ravichandran KS. Find-me and eat-me signals in apoptotic cell clearance: progress and conundrums. *J Exp Med* (2010) 207(9):1807–17. doi: 10.1084/jem.20101157
42. Canton J, Blees H, Henry CM, Buck MD, Schulz O, Rogers NC, et al. The receptor DNGR-1 signals for phagosomal rupture to promote cross-presentation of dead-cell-associated antigens. *Nat Immunol* (2021) 22140–53. doi: 10.1038/s41590-020-00824-x
43. Mujal AM, Krummel MF. Immunity as a continuum of archetypes. *Science* (2019) 364(6435):28–9. doi: 10.1126/science.aau8694

Conflict of Interest: AW is an inventor on U.S. patent application WO2020097193 "Chimeric antigen receptors for phagocytosis" and receives licensing fees for the work described in this article.

The remaining authors declare that the research was conducted in the absence of any commercial or financial relationships that could be construed as a potential conflict of interest.

Copyright © 2021 Britt, Gitau, Saha and Williamson. This is an open-access article distributed under the terms of the Creative Commons Attribution License (CC BY). The use, distribution or reproduction in other forums is permitted, provided the original author(s) and the copyright owner(s) are credited and that the original publication in this journal is cited, in accordance with accepted academic practice. No use, distribution or reproduction is permitted which does not comply with these terms.

frontiers in Immunology

REVIEW
published: 20 April 2021
doi: 10.3389/fimmu.2021.662944

Intravacuolar Pathogens Hijack Host Extracellular Vesicle Biogenesis to Secrete Virulence Factors

*Anna Gioseffi, Mariola J. Edelmann and Peter E. Kima**

Department of Microbiology and Cell Science, Institute of Food and Agricultural Sciences, University of Florida, Gainesville, FL, United States

Extracellular vesicles (EVs) have garnered significant interest in recent years due to their contributions to cell-to-cell communication and disease processes. EVs are composed of a complex profile of bioactive molecules, which include lipids, nucleic acids, metabolites, and proteins. Although the biogenesis of EVs released by cells under various normal and abnormal conditions has been well-studied, there is incomplete knowledge about how infection influences EV biogenesis. EVs from infected cells contain specific molecules of both host and pathogen origin that may contribute to pathogenesis and the elicitation of the host immune response. Intracellular pathogens exhibit diverse lifestyles that undoubtedly dictate the mechanisms by which their molecules enter the cell's exosome biogenesis schemes. We will discuss the current understanding of the mechanisms used during infection to traffic molecules from their vacuolar niche to host EVs by selected intravacuolar pathogens. We initially review general exosome biogenesis schemes and then discuss what is known about EV biogenesis in *Mycobacterium, Plasmodium, Toxoplasma*, and *Leishmania* infections, which are pathogens that reside within membrane delimited compartments in phagocytes at some time in their life cycle within mammalian hosts. The review includes discussion of the need for further studies into the biogenesis of EVs to better understand the contributions of these vesicles to host-pathogen interactions, and to uncover potential therapeutic targets to control these pathogens.

Keywords: extracellular vesicles, exosomes, infections, Leishmania, Mycobacterium, Plasmodium, Toxoplasma

OPEN ACCESS

Edited by:
Johnathan Canton, University of Calgary, Canada

Reviewed by:
Fernando Real, Centre National de la Recherche Scientifique (CNRS), France
Patricia Xander, Federal University of São Paulo, Brazil

***Correspondence:**
Peter E. Kima
pkima@ufl.edu

Specialty section:
This article was submitted to Molecular Innate Immunity, a section of the journal Frontiers in Immunology

Received: *01 February 2021*
Accepted: *30 March 2021*
Published: *20 April 2021*

Citation:
Gioseffi A, Edelmann MJ and Kima PE (2021) Intravacuolar Pathogens Hijack Host Extracellular Vesicle Biogenesis to Secrete Virulence Factors. Front. Immunol. 12:662944. doi: 10.3389/fimmu.2021.662944

INTRODUCTION

There are myriad facets of host–pathogen interactions that contribute to infection outcomes. Such is the case with intracellular pathogenesis, which includes organisms that use the host biosynthetic machinery to propagate themselves, organisms that reside in the cell cytoplasm and organisms that reside within vacuolar compartments in host cells. Progress in our understanding of mechanisms deployed by pathogens to exploit or subvert host mechanisms is uneven. It should therefore be enlightening to consider current knowledge of pathogen-host interactions by pathogens that share important characteristics. Our focus will be on pathogens that reside within membrane delimited vacuolar compartments in the cell. Even among this relatively small subset of pathogens, there is

great diversity in pathogen strategies to interface with the cell, including differences in the composition and interactions of the pathogen-containing vacuolar compartments. Each pathogen elaborates unique strategies to translocate molecules from their intravacuolar niche into the cell cytosol or to other host cell organelles where they target host cell processes. It is presumed that some of the molecules that are released into the cell cytosol may access the exosome biogenesis machinery of host cells. The intravacuolar pathogens that we will discuss infect phagocytes at some point in their life cycle. Phagocytes are residents of tissues where they play important roles in tissue homeostasis and disease [reviewed in (1)]. Phagocytes are also recruited to sites of tissue damage from infection or other insults, where they proceed to limit the infection by various strategies, including ingesting and destroying any intruders, elaboration of molecular mediators to recruit and activate cells, removal of damaged host cells, or attempts to wall off the site. Paradoxically, phagocytes are unwitting hosts of a wide range of pathogens, including viruses, bacteria, and eukaryotic parasites. Infection of phagocytes and other host cells by the intravacuolar pathogens discussed here results in diseases that cause tremendous human suffering.

Numerous studies have shown that extracellular vesicles (EVs) released by phagocytic cells infected with intracellular pathogens hold infection-specific molecular cargo that may contribute to pathogenesis and host immune responses [reviewed in (2–4)]. Despite the abundance of proteomic and functional data, the process of EV biogenesis during infection and mechanisms by which pathogen-derived molecules are packaged into host exosomes are poorly understood. Insightful studies of EV biogenesis in the context of infection have focused on viral pathogens, revealing that many viruses utilize the endosomal sorting complex required for transport (ESCRT) machinery for viral egress. However, the biogenesis of EVs from infection by intracellular bacteria or intracellular eukaryotic pathogens remains poorly understood. The purpose of this review is to discuss the current understanding of the mechanisms of EV biogenesis in the context of intravacuolar pathogen infection to highlight each pathogen's strategies to exploit host EV biogenesis schemes. We initially discuss universal characteristics and EV biogenesis schemes, after which the situation in the context of infection is considered.

EXOSOME COMPOSITION AND BIOGENESIS

Extracellular vesicles are secreted by all mammalian cells and can be isolated from various bodily fluids, including blood, urine, breast milk, tears, and cerebrospinal fluid (5). Extracellular vesicles have garnered significant interest in recent years because of their ability to transfer potentially important intercellular communication mediators, including proteins (6). This function is of particular interest in the context of host-pathogen interactions, as EVs may be critical mediators of host-pathogen communication and contribute to pathogenesis. Exosomes may be classified by their size, cell of origin, biogenesis, or proposed function (7–9). Apoptotic bodies are membrane-enveloped vesicles that range in diameter between 50 - 5000nm released *via* the blebbing of cells undergoing apoptosis (5, 8, 10). The existence of apoptotic bodies has been long known and studied. Healthy cells also shed extracellular vesicles, including microvesicles and exosomes (11). Microvesicles are membrane-bound vesicles released through outward budding and fission of the plasma (11, 12). Microvesicles are a heterogeneous group of vesicles that have been referred to by various terms including, ectosomes, shedding vesicles, microparticles, or platelet dust; that range in size from 100 - >1000nm in diameter (12, 13). Lastly, exosomes are membrane-enclosed vesicles between 50-150 nm in diameter that are secreted when multivesicular bodies (MVBs) in the endosomal pathway fuse with the plasma membrane and release intraluminal vesicles (ILVs) into the extracellular space (13). Together, these three classes of vesicles whose minimal characteristics and nomenclature have been standardized (14), are set apart in significant ways by both their biogenesis and biological functions.

Exosomes were first described in 1987 (15) and have since been found to be secreted by nearly all eukaryotic cells except for mature red blood cells, which do not possess endocytic capacities (16). Exosomes are secreted by healthy cells continuously, and their cargo and pattern of release can be altered by conditions of stress or infection (17). These nanosized vesicles contain thousands of cell-specific molecules, including proteins, nucleic acids, and lipids, enclosed within a single lipid bilayer membrane (18). Some of these molecules are conserved across exosomes from different origins, including tetraspanins (CD9, CD63, and CD81), proteins involved in intracellular trafficking (Rab GTPases, annexins), chaperones (Hsc70), biogenesis factors (ALIX), and proteins associated with signal transduction (14-3-3 proteins) (11). However, the exact composition of exosomes is dynamic and reflective of cellular context and the health of its cell of origin. Because the composition of exosomes is adaptive and reflective of the cell environment and condition, they are intriguing candidates for disease biomarker discovery through the isolation and screening of exosomes from patient bodily fluids (19).

Exosomes are of endosomal origin and are created when intraluminal vesicles (ILVs) form by inward budding of the early endosome (EE) (20). Early endosomes containing ILVs then mature into MVBs and are directed either to the lysosome for degradation or fuse with the plasma membrane to release the ILVs to the extracellular space as exosomes (20). Exosomes contain an assortment of molecular cargo, including membrane proteins with exposed extracellular domains on the exosomal surface and cytosolic proteins enclosed within their lumen (21). The protein composition of exosomes is specific and not reflective of the total cell, indicating that there are specific mechanisms to control the loading of select molecules into exosomes (22). Exosome biogenesis and the process of selective protein loading remain poorly understood phenomena. It is known, however, that the process of exosome biogenesis is driven by at least two general mechanisms:

endosomal sorting complexes required for transport (ESCRT)-dependent and ESCRT-independent (tetraspanin or lipid-dependent) processes (22).

ESCRT-Dependent Pathway

The ESCRT machinery was first shown to play a role in sorting proteins into MVBs in yeast in 2001 (23). The ESCRT complex comprises nearly 30 proteins assembled into five coordinating subcomplexes that function in a stepwise fashion (24): ESCRT-0, -I, -II, and -III, and associated AAA ATPase Vps4 complex (25). The primary function of ESCRT in ancestral organisms was to constrict and sever narrow membrane necks by a currently unknown mechanism of membrane scission (26). The ESCRT machinery is involved in many eukaryotic cellular processes, including the sorting of ubiquitinated proteins into ILVs for lysosomal degradation, viral egress, and membrane scission during cytokinesis (27). More recently, ESCRT components such as Tsg101 and Alix have been identified in exosome preparations from different sources, which suggested the involvement of ESCRT in the biogenesis of these vesicles (25).

The ESCRT subcomplexes perform a series of synchronized tasks to drive both cargo loading and physical membrane-remodeling and scission, leading to the production of ILVs: ESCRT-0 sequesters ubiquitinated cargo, ESCRT-I, -II, and -III control ILV budding, and Vps4 regulates membrane scission (28). ESCRT-0 consists of two subunits, hepatocyte growth factor-regulated tyrosine kinase substrate (Hrs) and signal-transducing adaptor molecule 1/2 (STAM1/2), and can bind both phosphatidylinositol 3-phosphate (PtdIns3P) and ubiquitin, providing membrane recruitment, endosomal specificity, and interaction with ubiquitinated target proteins (29). ESCRT-0, ESCRT-I, and ESCRT-II all contain ubiquitin-binding domains, suggesting that ubiquitination is important for the selective loading of cargo proteins into exosomes (30). ESCRT-I consists of tumor susceptibility gene 101 (Tsg101), Vps28, Vps37, and multivesicular body 12 (hMvb12) and interacts with both ESCRT-0 and ESCRT-II using domains located on opposite ends of the complex (31). ESCRT-I then recruits ESCRT-II, a Y-shaped subcomplex consisting of EAP30, EAP45, and two subunits of EAP20, which cooperates with ESCRT-0 to provide further endosomal specificity and recruits ESCRT-III (32). ESCRT-III is composed of four main subunits-charged multivesicular body proteins (CHMPs) CHMP2A, B, CHMP6, CHMP3, and CHMP4A,B,C- and several adaptors and accessory proteins such as ALIX, which can recruit a deubiquitinating enzyme and is essential for cargo loading (33, 34), Deubiquitylation appears to be involved in loading cargo into ILVs, which are destined for degradation, while exosomal proteins remain ubiquitinated (25). The multimeric mechanoenzyme class I AAA (ATPase associated with various cellular activities) ATPase Vps4 is required to remove assembled ESCRT-III from the membrane before vesicle formation (35).

The PDZ (postsynaptic density protein, disc large, and zonula occludens) domain-containing protein syntenin is important for the biogenesis of a specific subclass of CD63-positive ILVs. Syntenin interacts with ALIX, pieces of the ESCRT machinery, and membrane receptors such as syndecans to produce ILVs using an alternative ESCRT pathway of cargo recruitment and vesicle budding (36), suggesting that ESCRT-dependent exosome production may be a flexible process resulting in a heterogeneous population of vesicles (9).

ESCRT-Independent Pathway

Depletion of all four ESCRT subcomplexes is insufficient to block exosome secretion entirely in eukaryotic cell lines but does result in drastic changes in cell morphology, such as enlarged, empty MVBs and irregularly shaped ILVs (37). Therefore, these larger, heterogeneous vesicles are produced by ESCRT-independent mechanisms that rely on other lipids and proteins for the loading and budding of exosomes (25).

Lipidomic analysis of EVs reveals that exosomes contain an overall low concentration of lipids, resulting in a high protein/lipid ratio (38). The lipid composition of exosomes is reminiscent of detergent-resistant lipid rafts, and it is enriched in cholesterol, ceramide, and sphingolipids essential for the ESCRT-independent sorting of cargo into ILVs (39). Inhibition of ceramide production using the neutral sphingomyelinase (nSMase) inhibitor GW4869 showed a marked reduction in exosome release, which appeared to be specific and independent from ESCRT-dependent mechanisms rather than a derangement of the entire endosomal system (39). Furthermore, ILVs destined to be secreted as exosomes contain ceramide while ILVs intended for lysosomal degradation contain another related lipid, lysobisphosphatidic acid (LBPA), which is absent in exosomes, suggesting that lipid composition is involved in the determination of vesicle fate (40, 41).

However, depletion of ceramide has no effect on MVB biogenesis or exosome secretion in human melanoma cells (42). In these cells, the tetraspanin CD63 was involved in the ESCRT-independent sorting of cargo into ILVs (42). Other tetraspanins, including CD82 and CD9, have also been shown to participate in the ceramide-dependent biogenesis of exosomes in healthy primary cells (43). Tetraspanin-enriched microdomains (TEMs) may act as sorting platforms for cargo molecules during the ESCRT-independent biogenesis of ILVs (**Figure 1C**). However, the exact mechanisms by which tetraspanins facilitate exosomal cargo sorting are unknown (44).

Cargo Sorting: Post-Translational Modification of Target Proteins

Exosomal protein composition is selective and dynamic, suggesting that there are regulated mechanisms involved in loading specific target molecules during vesicle biogenesis. Mass spectrometry analysis of exosomes reveals that post-translational modifications (PTMs) such as ubiquitination (mono-ubiquitination and poly-ubiquitination), the addition of small ubiquitin-related modifier (SUMOylation), phosphorylation, and glycosylation are all common modifications of exosome proteins and may be involved in the selective sorting of cargo molecules (45).

Ubiquitin can be bound to a target protein at numerous positions *via* the isopeptide bond of C-terminal glycine of ubiquitin with the ϵ-amino group of a lysine residue present in the target protein, resulting in a complex network of

modifications (45). The relationship between ubiquitination and cargo sorting is unclear as protein sorting can also occur through ESCRT and ubiquitin- independent mechanisms (22). SUMO, another ubiquitin-like modifier, has also been shown to modify exosomal proteins and influence miRNAs packaging into exosomes (46). Also, phosphorylation has been found to work in conjunction with ubiquitination and lipid rafts to regulate the sorting of some specific subsets of proteins into the exosomes (47). Despite these observations, current studies are so far unable to unravel the complicated network of PTMs and their involvement in selective cargo trafficking and vesicle fate.

The Potential of EVs in Infectious Disease

Extracellular vesicles are known to carry cargo whose composition is unique to the cell of origin and is modulated by the cell's environment and growth conditions. This implies that the profile of cargo molecules in EVs from cells experiencing stressful growth conditions, including infection, will differ somewhat from the molecular profile of EVs released under non-stressful growth conditions. EVs therefore carry biomarkers that can inform on the staging of a disease process. It is no surprise therefore that exosomes are being touted as a source for promising biomarkers for cancer diagnosis and that they represent new targets for cancer therapy (48). In infectious diseases as well, knowledge of EV composition modulated by infection could similarly be exploited for development of biomarkers for diagnosis of infection and identification of immune targets. Exosomes released by macrophages infected with several intracellular pathogens, including *Salmonella enterica* and *Mycobacterium tuberculosis*, have been demonstrated to include pathogen antigens, stimulate a pro-inflammatory response in naïve cells (49) and protect against subsequent infection challenges (50), suggesting that exosomes may also be useful as cell-free vaccines against infectious pathogens.

INTRAVACUOLAR PROKARYOTIC PATHOGEN

Roles of Exosomes in Infections Caused by *Mycobacteria*

Mycobacteria are acid-fast bacteria that prefer an intracellular lifestyle. *Mycobacterium tuberculosis* is a human pathogen that causes tuberculosis, and *M. avium* complex bacteria also lead to lung infection, although primarily in immunocompromised individuals. Finally, *M. bovis* bacillus Calmette-Guérin (BCG) is a vaccine strain of *Mycobacterium*. *Mycobacteria* can infect several cell types, such as neutrophils, macrophages, and monocytes, although alveolar macrophages appear to be the preferred host of *Mycobacterium tuberculosis* in the early phases of infection (51). During the host cell infection, *Mycobacterium* binds to the macrophage surface, followed by internalization of the bacteria into *Mycobacterium* containing vacuoles (MCV) that do not fuse with lysosomes, which ensures that the bacterium survives in the vacuole (52). This bacterium recruits several host proteins to the MCV surface, including rab5, to prevent phagolysosomal fusion at the early endosome stage. This phenomenon is reflected by the fact that MCVs have a low abundance of lysosomal markers, such as CD63, LAMP-1 and -2, or rab7 (53, 54). *Mycobacterium* uses the SecA2 pathway to secrete SapM and PknG effector proteins that affect phagosome and autophagosome maturation (55).

While surviving in the MCV, *Mycobacterium* components, pathogen-associated molecular patterns (PAMPs) appear to be translocated from the vacuole *via* secretion systems. It has been shown that cell wall constituents of *M. avium*, glycopeptidolipids, are released by infected macrophages (56). These glycopeptidolipids are trafficked from the MCV to multivesicular bodies (MVBs), and the trafficking process is enabled by the endocytic network. After the MVBs fuse with the plasma membrane, the released exosomes still contain the glycopeptidolipids, which are transferred from infected to uninfected macrophages where they stimulate proinflammatory mediators *via* Toll-like receptors (TLRs) -2, -4, that are dependent on the MyD88 pathway (56). Other studies showed that exosomes isolated from the bronchoalveolar lavage fluid (BALF) of *M. bovis* BCG–infected mice also stimulated proinflammatory responses in macrophages, resulting in TNF-α production (57). These vesicles contained the *Mycobacteria* components lipoarabinomannan and the 19-kDa lipoprotein. Intranasal vaccination with exosomes isolated from macrophages previously infected with *M. bovis* BCG and *M. tuberculosis* stimulated TNF-α or IL-12 production and aided in neutrophil and macrophage recruitment to the lung of mice (57). A similar experiment was performed with exosomes isolated from *Mycobacterium*-infected macrophages, which were used to treat naïve bone marrow-derived macrophages, revealing that these exosomes also stimulate other cytokines, such as GCSF, sICAM1, IL-1ra, MIP-1a, MIP-1b, MIP-2, RANTES, and MCP-5. In addition to inducing the release of cytokines, exosomes from *Mycobacteria*-infected cells have been shown to induce migration of macrophages. This phenomenon has been demonstrated *in vivo*, based on the fact that the intranasally injected exosomes resulted in the recruitment of CD11b+ cells into the lung (58).

Apart from exosomes' effect on innate immune cells, exosomes derived from *Mycobacteria*-infected cells also stimulate adaptive immunity in the *M. tuberculosis* model. Exosomes derived from macrophages exposed to culture filtrate proteins (CFP) of *M. tuberculosis* induced pathogen-specific IFN-γ and IL-2-expressing CD4+ and CD8+ T cells. This Th1-biased immune response was specific to mice vaccinated with exosomes obtained from CFP-treated macrophages, while the BCG vaccine boosted the Th2 response. Those exosomes were also shown to prime a protective immune response at a level comparable to BCG and provided a booster to a previous BCG immunization, leading to a decrease in mycobacterial count in lung and spleen of mice challenged with aerosolized *M. tuberculosis* (50). Exosomes released *in vivo* during infection with *M. tuberculosis* also contribute to T cell response, which was shown by using rab27a-deficient mice (59), which have a defect in the exosome generation (60). The deletion of rab27a was correlated with an increased bacterial burden and decreased T cell activation, indicating the importance of exosomes in the T cell function (59).

Trafficking of Mycobacterial Proteins to Exosomes

Mycobacterial proteins are trafficked to exosomes, shown first for the 19-kDa lipoprotein (57). A proteomic study conducted on exosomes derived from *M. tuberculosis*-infected J774 cells identified 41 mycobacterial proteins, mostly predicted or known to be secreted proteins, including previously known immunogenic proteins ESAT-6, Ag85 complex proteins, MPT64, or MPT63 (61). Interestingly, some of the mycobacterial proteins in exosomes released from macrophages treated with *M. tuberculosis* CFP were identical to the ones contained in exosomes isolated from infected cells. This observation implies that mycobacterial proteins may have a signal for trafficking into exosomes upon entry into the cell *via* phagocytosis or endocytosis-based mechanisms (61). Similarly, exosomes obtained from sera of active TB patients also include *M. tuberculosis* proteins. This observation suggested that exosomes can serve as a source of peptide biomarkers for TB. In comparison to the exosomes isolated from the bronchoalveolar lavage (BAL) fluid from *M. tuberculosis*-infected BALB/c mice and infected J774 macrophages (61), five of these proteins were in common, including DnaK, PstS2, GlcB, HspX, and AcpM (62). The mycobacterial proteins contained within the host exosomes appear to be secreted *via* the SecA and type VII secretion system, although at least one of these proteins is not expected to be secreted (GabD1). This might mean that several different mechanisms, including bacterial lysis, are responsible for the release of mycobacterial proteins prior to their incorporation into exosomes (61).

The mechanisms that control the trafficking of these soluble bacterial antigens to the exosomal compartments are not currently known. For *M. tuberculosis* several pathways have been shown to be important in the antigen trafficking to exosomes. In addition to rab27a discussed above, they also showed reduced trafficking of *M. tuberculosis* 19 kDa lipoprotein, which were (59). This observation suggested the importance of rab27a pathway in the trafficking of mycobacterial proteins to exosomes.

The pathway that is crucial for the trafficking of proteins into macrophages is ESCRT dependent pathway. Knockdown of Tsg101 and Hrs, which are the ubiquitin-binding domains of ESCRT-1 and ESCRT-0, respectively, resulted in the reduction of exosomes produced in RAW 264.7 macrophages, which indicated that ubiquitin might be one of the mechanisms involved in the trafficking of proteins to MVBs and exosomes (63). Schorey et al. examined whether ubiquitination is a post-translational modification necessary for the trafficking of soluble mycobacterial antigens into the exosomes. Toward this goal, exosomes were purified from *Mycobacterium*-infected RAW264.7 macrophages, followed by pull-down of mono-ubiquitinated proteins. The western blotting of such mono-ubiquitinated proteins was done using an antibody that recognizes culture filtrate proteins of *M. tuberculosis*, and the results indicated that several mycobacterial proteins are ubiquitinated. Moreover, specific mycobacterial proteins KatG, HspX, and GroES were shown to be ubiquitinated by using this western blot technique (63). An inhibitor PYR-41 was used to treat cells prior to the exosome purification since this molecule inhibits the thioester bond formation between ubiquitin and E1. This compound treatment leads to a complete depletion of mycobacterial proteins in the collected exosomes. Further, mutation of a specific lysine residue in the mycobacterial protein HspX diminished its trafficking into the exosomes that was dependent on the clathrin-mediated endocytosis. Mono-ubiquitination is required for the trafficking of some proteins into the endosomes. Indeed, the trafficking of HspX was shown to be dependent on clathrin-mediated endocytosis, based on the treatment with Dynasore, which is an inhibitor of this uptake mechanism (63). In addition, expression of a C-terminal fusion of ubiquitin to EGFP and *M. tuberculosis* proteins Ag85B and ESAT-6 in HEK 293 cells enhanced the delivery of these proteins into exosomes by ten-fold when they were coupled to ubiquitin (**Figure 1**). These exosomes were able to elicit a T cell response by stimulating the production of INFγ-secreting T lymphocytes in the lung and spleen (64).

These results collectively suggested that mono-ubiquitination could serve as a mechanism for the trafficking of bacterial proteins into the exosomes *via* clathrin-mediated endocytosis. The ubiquitin E3 ligases responsible for the ubiquitination of these bacterial proteins have not yet been identified, but it is likely that multiple E3 ligases exist that play this function in sorting of proteins to exosomes. Furthermore, apart from a better characterization of ubiquitination in this context, it would be interesting to investigate additional mechanisms that might guide mycobacterial proteins to vesicular compartments. Moreover, the fate of the mycobacterial proteins that are carried in exosomes to target cells is also unknown. It would be important to track the bacterial proteins carried to target cells *via* exosomes, in order to identify the colocalization of these proteins with intracellular compartments, such as endocytic vesicles and lysosomes. Furthermore, since exosomes can carry these mycobacterial proteins to the antigen-presenting cells, and because exosomes formed during the Mtb infection stimulate protective immunity against Mtb (50, 59), it is possible that the Mtb antigens are either loaded on MHC molecules or the entire exosomal complex containing MHC and Mtb antigenic peptide are exposed on the cell surface. The trafficking of the exosomal content within the target cell clearly deserves further mechanistic studies.

Small Extracellular Vesicles From Mycobacterium-Infected Macrophages Carry RNA

Apart from proteins, exosomes can also transmit other molecules from infected cells. In the case of *M. tuberculosis* infection, exosomes carry a smaller amount of microRNA (miRNA) than uninfected cells. However, transcripts regulating immune response are more abundant in exosomes derived from *M. tuberculosis*-infected macrophages. Apart from the host RNA, the vesicles are also capable of carrying mycobacterial RNA. Similar to proteins, the RNA cargo is transferred between cells *via* exosomes (65). Currently, a mechanism responsible for the trafficking of bacterial transcripts to the exosomes remains uncharacterized, although RNA-binding protein hnRNPA2B1 has been shown to bind specific miRNAs (46). This and other RNA-binding proteins are, therefore, likely capable of sorting relevant miRNAs into the vesicles.

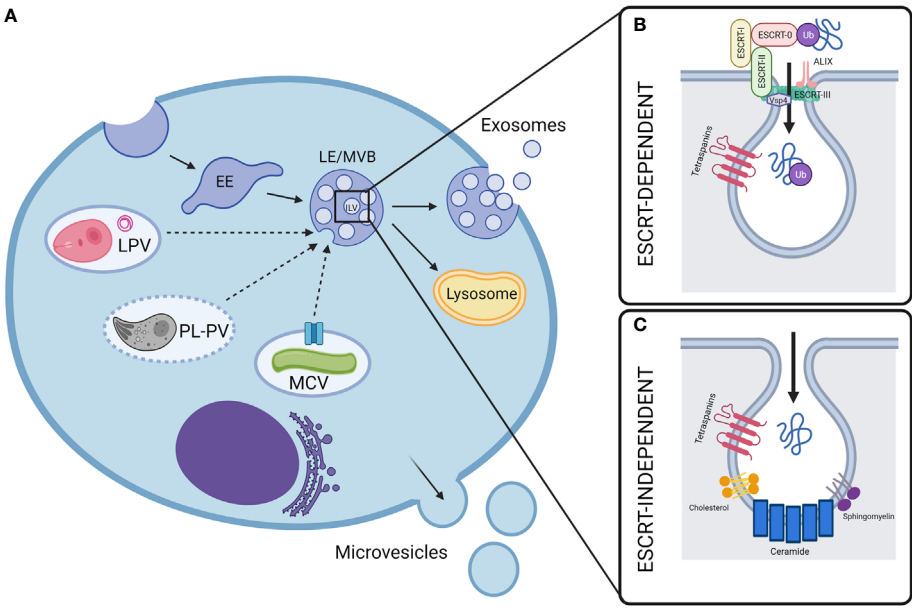

FIGURE 1 | Biogenesis of extracellular vesicles in intravacuolar pathogen infections. **(A)** Mammalian cell-derived extracellular vesicles include exosomes and microvesicles, which can be characterized by their biogenesis, size, and composition. While microvesicles are generated by the direct outward budding of the cell's outer membrane, exosomes are derived from an endocytic origin. First, early endosomes (EE) undergo inward budding. This forms intralumenal vesicles (ILVs) inside what is then called the late endosomal vesicle (LE) or multivesicular body (MVB). Depending on molecular signals, the MVB may then be destined for degradation by fusing with lysosomes or will fuse with the plasma membrane, releasing the ILVs to the extracellular space where they are then called exosomes. In the context of intravacuolar pathogens, exosomes are a possible mechanism for the release of pathogen molecules from infected cells. The exact mechanisms for how these pathogen molecules escape their respective vacuoles and are trafficked to host exosomes is not fully understood, but it is likely to be unique for each pathogen as discussed in this review. The composition of pathogen-containing vacuoles is diverse and requires unique methods for the exchange of molecules between host and pathogen. *Mycobacteria* utilize secA, type VII secretion system (represented by blue channel), and possibly other secretion systems to secrete exosome-bound proteins from the *Mycobacterium* containing vacuole (MCV). *Plasmodium* containing vacuoles (PL-PVs) conversely contain pores (represented by dashed vacuole boarder) through which small molecules may pass freely between the PV lumen and host cytosol, presenting easy access of pathogen molecules to host cytosol and exosome processes. *Leishmania* parasitophorous vacuoles (LPVs) are dynamic compartments that interact with the host's endocytic and secretory pathways. Multimembranous structures within LPVs whose cellular origin is not known, may transport molecules from LPVs to host cell organelles including MVBs. Dashed arrows represent speculative pathways for trafficking of pathogen molecules into host ILVs. **(B, C)** Exosome biogenesis can occur by two general mechanisms- either ESCRT-dependent or ESCRT-independent. **(B)** ESCRT, or endosomal sorting complexes required for transport, is a specialized multi-subunit complex which allows for the recruitment of ubiquitinated proteins and the inward budding and scission of ILVs. ESCRT-0 recruits ubiquitinated proteins while ESCRT-I, ESCRT-II, and ESCRT-III facilitate ILV budding, and finally Vsp4 facilitates membrane scission. Accessory proteins such as ALIX are also involved which perform deubiquitylation for cargo loading. **(C)** Less is currently known about the mechanisms of ESCRT-independent exosome biogenesis, however it is proposed that ceramide and other lipids, such as sphingomyelin and cholesterol, as well as tetraspanins play a part in the trafficking of proteins and inward budding. Created with BioRender.com.

EUKARYOTIC PATHOGENS

Brief Review of *Plasmodium* biology

Plasmodium parasites are apicomplexan parasites that cause malaria. It is estimated that over 100 million people are infected worldwide, and just under 1 million people succumb to these infections each year (66). Infections in humans are initiated by sporozoites deposited into a host by female Anopheles mosquitoes when they take a blood meal. The sporozoites establish a productive infection when they infect liver cells. Although hepatocytes are the principal hosts of parasites in the liver, it has been shown that sporozoites take up transient residence in Kupfer cells that mediate their access to hepatocytes (67, 68). It was also shown that after infection of hepatocytes, a small subset of liver parasites is acquired by monocyte-derived CD11c+ cells (69). Infection of CD11c+ cells and hepatocytes were shown to be dependent on their expression of the tetraspanin CD81, which coincidentally is a vital component of exosomes (70). The parasitophorous vacuoles (PVs) in which the parasites reside in hepatocytes exhibit unique characteristics compared to PVs that harbor other Apicomplexan parasites. For example, *Plasmodium* containing PVs rest close to the cell nucleus and establish interactions with the Endoplasmic Reticulum (ER), which is in contrast to *Toxoplasma* whose PVs establish a tight association with the Golgi apparatus, Mitochondria, and Endoplasmic Reticulum (ER) (71) of the host cell, Furthermore, *Plasmodium*-containing PVs have been shown to have pores through which nutrients smaller than 3000 Da can be exchanged between the PV lumen and cell cytosol (71). Parasites in PVs within liver cells undergo rapid division into merozoites. The PVs enlarge into giant syncytium-like compartments (71). Upon their release from the liver, merozoites enter the blood circulation, where they infect red blood cells. Of the five species of *Plasmodium* parasites

that infect humans, *Plasmodium falciparum* and *Plasmodium knowlesi* infect all red blood cells. In contrast, *Plasmodium vivax* and *Plasmodium ovale* infect only reticulocytes. *Plasmodium malariae* infect older red blood cells. Many mechanistic studies on *Plasmodium* infections have been performed in experimental models with parasites of rodents, including *P. berghei, P. yoelii* and *P. chabaudi* that exhibit similarities and differences with *Plasmodium falciparum* and *Plasmodium vivax*, depending on the stage of infection.

Exosomes in *Plasmodium* Infections

As discussed above, during their life cycle, *Plasmodium* parasites infect distinct cell types that should be expected to employ mechanisms for exosome biogenesis. Several studies have explored the role of exosomes and microvesicles (previously called microparticles) in *Plasmodium* infections. Mature red blood cells are devoid of a nucleus and the endocytic cell machinery in their cytoplasm, including multivesicular bodies (MVBs) that play a critical role in exosome biogenesis in nucleated cells. *Plasmodium* within mature red blood cells have been shown to translocate over 300 parasite-derived proteins from their PVs into the red blood cell cytosol. These molecules that are distributed throughout the red blood cell, including on its cell surface, have been implicated in several functions, including the formation of Maurer's clefts that appear to play some role in exosome formation in *Plasmodium*-infected cells (72). It is striking that only a subset of the molecules that are translocated into the red cell has been identified in EVs that are recovered from the supernatant fluid of cultured infected erythrocytes (73, 74). While EVs included proteins from the PV membrane and some well-studied surface molecules such as PfEBA and knob-associated molecules, they however, lacked other well studied molecules, including PfEMP1(a knob associated protein) and AMA-1. This observation suggests that there is a machinery outside of the parasite in the red blood cell that plays a pivotal role in selecting molecules for inclusion in EVs. Abdi et al. (74) analyzed exosomes released from red blood cells infected with a relatively earlier parasite passage. They identified over 50 more *Plasmodium* molecules in those EVs as compared to exosomes produced from a parasite line that had long been adapted to the *in vitro* culture conditions (74). Not surprisingly, many of the molecules that were identified in the study with the low passage parasites were involved in virulence. That study underscored the need to evaluate recently obtained field isolates and suggested that molecules in exosomes may play a role in the parasites' virulence.

A couple of elegant studies have shown that exosomes can mediate intracellular communication between parasites within infected red blood cells [reviewed in (75)]. Studies using transgenic parasites expressing a drug resistance marker showed that DNA packaged in EVs could be exchanged by parasites in an infected cell, which results in the spread of a resistance marker (72). Another study showed that infected red blood cells selectively took up EVs produced by other infected cells, which then stimulated gametocyte production in the recipient infected cells (73). Exosomes have also been shown to stimulate the immune response by activating macrophages and neutrophils [reviewed in (75)]. They also play significant roles in cerebral malaria where among other activities, they promote vascular changes, including endothelial cell activation [reviewed in (76)]. Together, those studies demonstrated the critical role of EVs in *Plasmodium* infections and suggested that a greater understanding of their biogenesis and functions could be exploited to modify the course of malaria.

Studies on the ATP binding cassette transporter A1 have suggested a role for this molecule in EV biogenesis in *Plasmodium* infections. It had been shown that ATP binding cassette transporter A-1 (ABCA-1) plays a role in phosphatidylserine distribution at the plasma membrane (77). ABCA-1 knock-out mice were subsequently shown to be defective in EV release. Red blood cells from these mice produced reduced levels of EVs, which implicated this molecule in EV biogenesis in red blood cells [reviewed in (76)]. As mentioned briefly above, the molecules localized to Maurer's clefts were identified in EVs from *Plasmodium*-infected RBCs. Studies by Regev-Rudzki et al. (72) identified and tracked the PfEMP1 trafficking protein (PfPTP) that associates with Maurer's cleft (72). They proceeded to show that parasites that were genetically altered to lack expression of PTP-2 were defective in EV release when used to infect red blood cells. This provided compelling evidence of the role of Maurer's clefts in EV biogenesis in infected cells.

In contrast to mature red blood cells, reticulocytes are nucleated and possess the biosynthetic machinery of mammalian nucleated cells. The composition and functions of exosomes released from *Plasmodium*-infected reticulocytes and liver cells have been described. The studies of Martin-Jaular et al. (78) that characterized exosomes released by BALB/c mice infected with non-lethal *Plasmodium yoelii* 17X described the presence of parasite-derived molecules in exosomes from infected reticulocytes (78). In that experimental model, where *Plasmodium yoelii* 17X infects reticulocytes, infections were initiated by intraperitoneal injection of infected cell blood cells. Up to 31 parasite-derived proteins were found to be included among the molecules in the reticulocyte-derive exosomes. Some of the parasite proteins that were identified included the serine-rich antigen (SERA) that is expressed by a multigene family and has been implicated in virulence [reviewed in (79)], merozoite surface antigens (MSP1 and MSP9), and heat shock protein 70. The mechanisms that led to their inclusion in reticulocyte derived exosomes have not been described. A more recent study by Gualdrón-López et al. (80) described the characterization of exosomes that were secreted from the liver stages of *Plasmodium vivax* infections (80). The research team took advantage of the human liver-chimeric (FRG huHep) mouse (81) in which an immunocompromised mouse with several genetic mutations was engrafted with human hepatocytes. FRG huHep mice support the complete development of the human parasites, *P. falciparum* (81) and *P. vivax* (82) that would not otherwise infect mice. The analysis of exosomes isolated from the blood plasma of the *P. vivax* infected FRG huHep mice (ExEF) identified 290 and 234 proteins from mouse and human origin, which included liver proteins that had previously been described from liver exosomes (80). This

analysis also identified 17 parasite-derived molecules that were included in exosomes from liver-infected cells. When the authors compared human ExEF exosomes from infected animals versus uninfected control mice, they stated that several proteins were differentially associated with *P. vivax* infections (P-value < 0.05). This finding is consistent with studies from other infections that have shown that the infection influences host-derived molecules' composition in exosomes. The list of parasite proteins in ExEF included heat shock protein 70 (HSP70), which was also seen in the study on infected reticulocyte-derived exosomes described above. A different variant of merozoite surface antigen (MSP3) was found in the ExEF, which differed from the variants found in the infected reticulocyte derived exosomes discussed above. Whether it is 17 or 31 parasite-derived proteins identified in exosomes from infected liver cells or from infected reticulocytes, it is currently unknown which characteristics of these proteins direct them to the host cellular exosome biogenesis machinery. It is also not known whether ubiquitination plays a role in exosome loading within *Plasmodium*-infected cells.

Toxoplasma

Toxoplasma are Apicomplexan parasites that can infect all warm-blooded animals, including mammals and birds. In humans, *Toxoplasma* have been implicated in a range of clinical presentations whose severity is determined by the individual's immune status. *Toxoplasma* is acquired by ingestion of raw or inadequately cooked meat. It can also be acquired upon ingestion of oocyst dispersed in the environment in cat feces. This later mode of acquiring the infection by pregnant women is the subject of public health campaigns that dissuade women from changing cat litter, as infection during pregnancy can lead to congenital transmission resulting in stillbirths or hydrocephalus or retinal infections of the newborn. *Toxoplasma* can infect all nucleated cells in mammals. Parasite entry into cells involves the sequential deployment of molecules from Apicomplexan-specific organelles. The release of proteins from Rhoptries follows the discharge of micronemal proteins. Dense granule proteins are then released, which contribute to the formation of the parasitophorous vacuole and the intravacuolar network. Rastogi et al. (83), Håkansson (84), and Nadipuram (85) have described the export machinery of proteins from the *Toxoplasma* PVM and provided examples of molecules that are transported to the host cell (83–85). Whether displayed on the PVM or translocated to other host cell organelles or the cytosol, most of these molecules are potentially accessible to the exosome biogenesis machinery.

Studies of the potential role of exosomes in toxoplasmosis have evaluated exosomes that are released from axenic cultures of parasites (86) or exosomes that are released from dendritic cells that are pulse with Toxoplasma antigens (lysate) (87, 88) or mammalian cells that are infected with Toxoplasma (56, 89). Despite the obvious differences in the sources of *Toxoplasma* molecules, exosomes containing *Toxoplasma* molecules were shown to be able to stimulate naïve recipient cells to secrete cytokines. Injection into hosts in experimental studies led to the elaboration of a variety of *Toxoplasma* specific responses. Some studies of exosomes secreted from *Toxoplasma*, have shown that infection with *Toxoplasma* induces the release of a unique profile of protein and nucleic acids that is different from those released by uninfected cells. In infections of human foreskin fibroblast cells, Wowk analyzed exosomes from cells infected with *Toxoplasma gondii* and compared their protein content to exosomes from axenic cultured tachyzoites. They found 69 unique parasite derived proteins in infection derived EVs, however the number of parasite derived proteins was not stated (90). In another study in which dendritic cells were infected with *Toxoplasma gondii*, 12 differentially expressed miRNAs compared to exosomes from uninfected cells were identified (91). Further analysis predicted that in recipient cells, these miRNAs could be associated with a variety of biological processes, including signaling pathways involved in host ubiquitin system, innate immunity, biosynthesis, and transferase activity. Future studies will no doubt provide greater insight on the trafficking of these parasites derived molecules in the infected host cells.

Leishmania

Brief Review of *Leishmania* Infections

Leishmania are members of the family Trypanomastidae in the order Kinetoplastida. *Leishmania* parasites are grouped into two subgenera: *Leishmania* (*Leishmania*) and *Leishmania* (Viannia) that are further classified into species and subspecies. Infection of humans results in a disease presentation that is mostly dependent on the parasite species. Parasites of the *Leishmania* (*Leishmania*) subgenus including *L.(L) donovani*, *L.(L) infantum* and *L.(L) chagasi* (with a few exceptions including *L.(L) amazonensis and L.(L) major, L.(L) tropica* that cause cutaneous infections) are the primary causative agents of visceral disease. In contrast, parasites of the *Leishmania* (Viannia) subgenus, including *L.(V) braziliensis*, *L.(V) panamensis*, cause cutaneous infections that can manifest as self-limiting lesions or disseminated lesions or mucocutaneous infections [reviewed in (92, 93)]. However, there are reports of visceral disease caused by parasites that ordinarily lead to cutaneous lesions, while other reports of cutaneous lesions have implicated parasites species that typically lead to visceral disease [reviewed in (94)]. These 'unexpected' disease presentations underscore the complexity of these infections and may be due to host genetics contributions and poorly defined environmental factors (94, 95). *Leishmania* parasites are transmitted by sandflies. Once inside the mammalian host, *Leishmania* infects phagocytic cells wherein they reside in *Leishmania*-containing parasitophorous vacuoles (LPVs). The *Leishmania* species determine LPV morphology. At the extremes of morphological differences, parasites of the *L. mexicana* complex (*L. mexicana*, *L. amazonensis*) reside within large communal LPVs that continuously distend. At the other extreme, *L. donovani*, *L. chagasi/L. Infantum* reside in tight LPVs that harbor a single parasite. After parasite replication and fission, daughter parasites segregate into secondary LPVs that also house individual parasites. All other *Leishmania* species reside in LPVs that may house one to four parasites. It is presently not known how LPV morphology differences affect

Leishmania pathogenesis. LPVs are dynamic compartments composed of molecules from the host secretory pathway, including the endoplasmic reticulum (ER) and the endocytic pathway, including late endosomes and lysosomes (96). Although much has been learned about the molecular composition of LPVs, there are still unanswered questions about the biology of LPVs, including how *Leishmania* derived molecules are translocated across the LPV membrane and which signals mediate the trafficking of parasite-derived molecules to the intracellular sites where they express their functions. On this topic, a recent publication provided evidence of traffic of *Leishmania* proteins from LPVs to the ER in vesicles that otherwise transmit cargo between the Golgi and the ER (97). The authors proposed that this could be one route through which parasite molecules are retrieved from LPVs for distribution in the infected cell and beyond.

In natural infections, the parasite's promastigote form is deposited in the skin of the host by the sandfly. The parasites commence a skin phase of the infection. After a transient residence in neutrophils, parasites are transferred to macrophages wherein they undergo replication as amastigotes (98, 99). In cutaneous infections, inflammatory cells are recruited to the bite site, which results in a cutaneous lesion over time. In infections by parasites that cause visceral infections, there is also an initial cutaneous phase (can last for several weeks) after which infected cells migrate to visceral organs where they replicate and form inflammatory lesions; this was first demonstrated in infections of hamsters (100). Parasites such as *L. amazonensis* and *L. braziliensis* that disseminate to secondary sites, proliferate for much longer periods at the primary site (months to years) before dissemination. Recent studies that have explored the phenotype of cells at primary and secondary sites in experimental infections with *L. major*, highlighted the expression of chemokine receptors $CCR2^+$ and $CX3CR1^+$ on the monocyte-derived cells that are the primary host cells of these parasites (99, 101). Infections in knockout mice that lack these receptors were limited, which suggested a role for chemokines in *Leishmania*-infected cell dissemination [Also reviewed in (102)]. Nonetheless, neither the triggers for disseminating the infection nor the factors that determine the selection of secondary sites to which parasites spread are not known. Could some of the mechanisms that promote metastatic tumor dissemination, such as the roles played by exosomes in tissue homing or organotropism (reviewed in (103, 104), be also important in the dissemination of *Leishmania* infections?

After parasites take up residence at a tissue site, remodeling of the site ensues. Analyses of skin lesions in humans revealed the noticeable presence of blood vessels of varying morphologies at these sites (105, 106). Experimental infections of cutaneous and visceral leishmaniasis also undergo vascular changes at the lesion site. Horst et al. (107) reported that cutaneous infection by *L. major* parasites in the hindfoot of C57BL/6 wild-type mice resulted in extensively vascularized lesions because the lymphatic and blood vessels were readily evident as the infection established (107). The authors implicated the expression of carcinoembryonic antigen-related cell adhesion molecule 1 (CEACAM1) on mononuclear cells ($CD11b^{hi}$ cells) as essential mediators of angiogenesis in *L. major* infected lesions. Also performing studies with *L. major*, Weinkopff et al. (108), showed that there was increased expression of vascular endothelial growth factor-A (VEGF-A) and vascular endothelial growth factor receptor (VEGFR-2) at the site of infection that mirrored the increase in lesion size and parasite numbers (108). In infections with *L. donovani*, where lesions form in visceral tissue, Yurdakul et al. (109), described vascularization and neovascularization of the red pulp and white pulp regions of the spleen, respectively (109). They attributed splenic vascularization to Ly6C+ inflammatory monocytes. In a more recent study, Dalton et al. (110), showed that neurotrophic tyrosine kinase receptor type 2 (Ntrk2, also known as TrkB) was aberrantly expressed on splenic endothelial cells following *Leishmania* infections (110). The study then showed that macrophages expressed the ligand(s) for Ntrk2 in the infected spleen and that inhibition of signaling through Ntrk2 blocked white pulp neovascularization.

Exosomes in *Leishmania* Infections

Natural *Leishmania* infections are initiated with promastigotes, which are a transient stage within the mammalian host. Within 24 hours of internalization into macrophages, they transform into amastigotes. The characteristics of this transformation that is triggered by temperature and pH changes were described by Zilberstein and colleagues (111, 112). The present challenge is to determine which molecules are released from long-term infections. Many *Leishmania* virulence factors have been described; however, as Kaye et al. (113) noted in their recent review, no *Leishmania* parasite-derived factors that cause tissue damage are known (113). It is likely, though, that exosomes released from infected cells carry molecules that could play a role in lesion development and immune response activation. *Leishmania* parasites themselves produce a variety of extracellular vesicles, including exosomes, which enable them to interact with and respond to their environment. *Leishmania* promastigotes were found to release vesicles with an average diameter of 30-70nm, consistent with exosomes released by other cell types (114). The molecular composition of these parasite-derived exosomes has been evaluated and shown to contain homologs of some mammalian exosome markers, as well as molecules that may enhance infectivity (114, 115). Up to 329 molecules have been identified in exosomes released from axenic promastigotes, accounting for greater than 52% of the parasite secretome (115). Atayde et al. (116) showed that *L. major* parasites secrete exosomes within the sandfly midgut, which, when injected with parasites during the initial insect bite of a mammalian host, enhance infection and lesion development in mice (116). Additionally, the exosomes produced by axenic *Leishmania* promastigotes modulate the chemotactic activity and cytokine secretion of macrophages *in vitro* to suppress the immune response and enhance permissiveness to subsequent infection (115). The vesicles also have the capacity to activate the immune system of the host. Exosomes released from *L. major* parasites were shown to induce Th2 polarization and enhanced disease progression in mice, indicating that parasite-derived vesicles are immunosuppressive and proparasitic in nature.

The *Leishmania* major surface protease (MSP), also referred to as GP63, is an important virulence factor, which contributes to enhanced phagocytosis by macrophages and promoting the survival of the parasite during both promastigote and amastigote life stages. There are three pools of GP63: surface-localized, internal, or released, that are believed to traffic separately through the cell and then released into the extracellular environment (117). Upon infection of macrophages, released GP63 is captured in vesicles and may also access the macrophage cytoplasm, though the exact mechanism of GP63 delivery to the host cytoplasm remains unclear; *Leishmania* parasites lack secretion systems comparable to those found in pathogenic bacteria (118). Exosomes released by *L. mexicana*-infected J774 macrophages for 24 hours were found to contain GP63, suggesting that parasite molecules from this intracellular pathogen can access host exosomes and then be released widely (119).

Recent research also indicates that macrophages infected with *L. donovani* amastigotes release exosomes containing a mixture of unique host and parasite proteins contributing to pathogenic processes (120). In that study, infections of RAW264.7 macrophages were initiated with *L. donovani* promastigotes, and infections were allowed to continue for 72 hours (about 3 days) to evaluate mature infections. After 72 hours of infection, extracellular vesicles were purified from media supernatants using differential centrifugation and then subjected to liquid chromatography combined with tandem mass spectrometry. In-solution and in-gel protocols for tryptic digestion were used prior to the mass spectrometry-based analysis, and data combined to yield protein composition profiles for uninfected and infected macrophage-derived EVs. Consequently, this approach led to a confident identification of 59 parasite proteins in EVs released by infected macrophages. These proteins included a putative Vasohibin, nucleoside transporter 1, kinesin, DNA directed RNA polymerase II subunit 2, dynein heavy chain, and putative protein kinases. Interestingly, some of the same protein families were also identified in a study of circulating immune complexes in the peripheral blood of 115 human patients with active *L. donovani* infections (121). In that clinical study, circulating immune complexes (CICs) were purified from patient serum using PEG-assisted precipitation and centrifugation, CIC antigens and antibodies were then dissociated using an acidic buffer, and the antibody was removed using protein A agarose to yield purified antigens. The researchers then used 2D gel electrophoresis and mass spectrometry of these purified CIC antigens to identify parasite proteins, revealing 31 proteins present during active infection before drug treatment. While there appears to be an elevated level of congruence between the parasite-derived protein profiles of these CICs and EVs isolated from infected macrophages, it is difficult to resolve this relationship past the family level. Finding similarities when comparing data between projects can be complicated due to differences in mass spectrometry approach, poor protein annotations, and the overall redundancy of *Leishmania* protein databases currently in use. In addition, it can be challenging to match proteins exactly across different experiments by reported accession numbers. However, the parity between these profiles at the protein family level remains intriguing. Along with what is known about exosomes and their ability to circulate through the body and deliver their contents to tissues distant from their origin, these findings suggest that *L. donovani* infected macrophages release exosomes containing parasite factors that may aid in their circulation throughout the host.

It is also worth noting that exosomes released by infected macrophages contain only 59 parasite-derived proteins, a significantly smaller number than the 329 parasite proteins identified in *Leishmania* promastigote secreted exosomes (122). Comparing the parasite-derived profiles of exosomes from promastigotes versus exosomes from amastigote infected macrophages, we again see several overlapping protein families, including elongation factor 1-alpha, serine/threonine-protein kinase, kinesin, and calpain-like cysteine peptidase. Strikingly, many of the molecules present only in promastigote-derived exosomes are homologs of mammalian exosome structural components (5). The absence of these parasite proteins in exosomes released by infected macrophages may be the result of two biological phenomena. First, the expression of parasite proteins may be differentially regulated between the promastigote and amastigote life stages. For example, a sizable portion of promastigote proteins are downregulated during macrophage infection as the parasites adapt to life in the intracellular environment. Alternatively, it may be unnecessary for the structural proteins of EVs to be contributed by the parasites during infection, as the parasites may be able to hijack the existing host machinery for protein secretion and exosome biogenesis. To be sure, the mammalian counterparts of these structural proteins were identified in EVs from infected macrophages, suggesting that *Leishmania* amastigotes may translocate their molecules across the LPVM into the host cytosol to utilize normal host processes to their advantage for the secretion of specific parasite molecules. EVs released by *Leishmania*-infected macrophages were also found to enhance several measures of endothelial cell activation *in vitro*, including tube formation, cell migration, and enhanced production of VEGF and IL8, which suggests that infection-induced EVs may play a role in neovascularization and pathogenesis (120).

CONCLUSION

All eukaryotic cells release EVs, including exosomes. The biogenesis of EVs released by cells under various normal and abnormal conditions has been well-studied. There is ample evidence that intrinsic cell characteristics and environmental queues determine the composition of EVs. This results in unique exosome compositions that could be monitored for diagnostic value. Ongoing studies have shown that intracellular pathogens, including viruses, bacteria, and parasites, can take advantage of the host exosome machinery to release virulence factors. Pathogens may smuggle pathogen-encoded virulence factors and other molecules that collectively contribute to their

pathogenesis. The existence of these mechanisms suggests that pathogens have evolved adaptations to take advantage of host protein trafficking mechanisms for exosomal packaging. For its part, the host cells also modulate exosome composition as an anti-pathogen strategy since exosomes induce immune responses directed against specific pathogens. More research is needed to evaluate specific mechanisms by which pathogen-derived molecules are targeted to multivesicular bodies within infected cells and further packaged into host-derived exosomes. This information will elucidate a large gap in our understanding of intracellular host-pathogen interactions and identify novel drug targets for infection control.

AUTHOR CONTRIBUTIONS

AG wrote and edited the manuscript. ME wrote and edited the manuscript. PEK developed the manuscript focus, wrote and edited manuscript. All authors contributed to the article and approved the submitted version.

FUNDING

PEK was supported by an R56 AI143293 grant from the NIH. ME was supported by the R03 AI-135610 grant from NIH.

REFERENCES

1. Epelman S, Lavine KJ, Randolph GJ. Origin and functions of tissue macrophages. *Immunity* (2014) 41(1):21–35. doi: 10.1016/j.immuni.2014.06.013
2. Schorey JS, Cheng Y, Singh PP, Smith VL. Exosomes and other extracellular vesicles in host-pathogen interactions. *EMBO Rep* (2015) 16(1):24–43. doi: 10.15252/embr.201439363
3. Atayde VD, Hassani K, da Silva Lira Filho A, Borges AR, Adhikari A, Martel C, et al. Leishmania exosomes and other virulence factors: Impact on innate immune response and macrophage functions. *Cell Immunol* (2016) 309:7–18. doi: 10.1016/j.cellimm.2016.07.013
4. Alenquer M, Amorim MJ. Exosome Biogenesis, Regulation, and Function in Viral Infection. *Viruses* (2015) 7(9):5066–83. doi: 10.3390/v7092862
5. Raposo G, Stoorvogel W. Extracellular vesicles: exosomes, microvesicles, and friends. *J Cell Biol* (2013) 200(4):373–83. doi: 10.1083/jcb.201211138
6. Yáñez-Mó M, Siljander PR, Andreu Z, Zavec AB, Borràs FE, Buzas EI, et al. Biological properties of extracellular vesicles and their physiological functions. *J Extracell Vesicles* (2015) 4:27066. doi: 10.3402/jev.v4.27066
7. Gould SJ, Raposo G. As we wait: coping with an imperfect nomenclature for extracellular vesicles. *J Extracell Vesicles* (2013) 2. doi: 10.3402/jev.v2i0.20389
8. Kerr JF, Wyllie AH, Currie AR. Apoptosis: a basic biological phenomenon with wide-ranging implications in tissue kinetics. *Br J Cancer* (1972) 26 (4):239–57. doi: 10.1038/bjc.1972.33
9. Colombo M, Raposo G, Théry C. Biogenesis, secretion, and intercellular interactions of exosomes and other extracellular vesicles. *Annu Rev Cell Dev Biol* (2014) 30:255–89. doi: 10.1146/annurev-cellbio-101512-122326
10. Merchant ML, Rood IM, Deegens JKJ, Klein JB. Isolation and characterization of urinary extracellular vesicles: implications for biomarker discovery. *Nat Rev Nephrol* (2017) 13(12):731–49. doi: 10.1038/nrneph.2017.148
11. van Niel G, D'Angelo G, Raposo G. Shedding light on the cell biology of extracellular vesicles. *Nat Rev Mol Cell Biol* (2018) 19(4):213–28. doi: 10.1038/nrm.2017.125
12. Tricarico C, Clancy J, D'Souza-Schorey C. Biology and biogenesis of shed microvesicles. *Small GTPases* (2017) 8(4):220–32. doi: 10.1080/21541248.2016.1215283
13. Maas SLN, Breakefield XO, Weaver AM. Extracellular Vesicles: Unique Intercellular Delivery Vehicles. *Trends Cell Biol* (2017) 27(3):172–88. doi: 10.1016/j.tcb.2016.11.003
14. Lötvall J, Hill AF, Hochberg F, Buzás EI, Di Vizio D, Gardiner C, et al. Minimal experimental requirements for definition of extracellular vesicles and their functions: a position statement from the International Society for Extracellular Vesicles. *J Extracell Vesicles* (2014) 3:26913. doi: 10.3402/jev.v3.26913
15. Johnstone RM, Adam M, Hammond JR, Orr L, Turbide C. Vesicle formation during reticulocyte maturation. Association of plasma membrane activities with released vesicles (exosomes). *J Biol Chem* (1987) 262(19):9412–20. doi: 10.1016/S0021-9258(18)48095-7
16. Vidal M. Exosomes: Revisiting their role as "garbage bags". *Traffic* (2019) 20 (11):815–28. doi: 10.1111/tra.12687
17. O'Neill CP, Gilligan KE, Dwyer RM. Role of Extracellular Vesicles (EVs) in Cell Stress Response and Resistance to Cancer Therapy. *Cancers (Basel)* (2019) 11(2). doi: 10.3390/cancers11020136
18. Morshed A, Karawdeniya BI, Bandara YMND, Kim MJ, Dutta P. Mechanical characterization of vesicles and cells: A review. *Electrophoresis* (2020) 41(7-8):449–70. doi: 10.1002/elps.201900362
19. Pant S, Hilton H, Burczynski ME. The multifaceted exosome: biogenesis, role in normal and aberrant cellular function, and frontiers for pharmacological and biomarker opportunities. *Biochem Pharmacol* (2012) 83(11):1484–94. doi: 10.1016/j.bcp.2011.12.037
20. Doyle LM, Wang MZ. Overview of Extracellular Vesicles, Their Origin, Composition, Purpose, and Methods for Exosome Isolation and Analysis. *Cells* (2019) 8(7). doi: 10.3390/cells8070727
21. Christianson HC, Svensson KJ, van Kuppevelt TH, Li JP, Belting M. Cancer cell exosomes depend on cell-surface heparan sulfate proteoglycans for their internalization and functional activity. *Proc Natl Acad Sci U S A* (2013) 110 (43):17380–5. doi: 10.1073/pnas.1304266110
22. Villarroya-Beltri C, Baixauli F, Gutiérrez-Vázquez C, Sánchez-Madrid F, Mittelbrunn M. Sorting it out: regulation of exosome loading. *Semin Cancer Biol* (2014) 28:3–13. doi: 10.1016/j.semcancer.2014.04.009
23. Katzmann DJ, Babst M, Emr SD. Ubiquitin-dependent sorting into the multivesicular body pathway requires the function of a conserved endosomal protein sorting complex, ESCRT-I. *Cell* (2001) 106(2):145–55. doi: 10.1016/s0092-8674(01)00434-2
24. Catalano M, O'Driscoll L. Inhibiting extracellular vesicles formation and release: a review of EV inhibitors. *J Extracell Vesicles* (2020) 9(1):1703244. doi: 10.1080/20013078.2019.1703244
25. Juan T, Fürthauer M. Biogenesis and function of ESCRT-dependent extracellular vesicles. *Semin Cell Dev Biol* (2018) 74:66–77. doi: 10.1016/j.semcdb.2017.08.022
26. Hurley JH. ESCRTs are everywhere. *EMBO J* (2015) 34(19):2398–407. doi: 10.15252/embj.201592484
27. Hurley JH. ESCRT complexes and the biogenesis of multivesicular bodies. *Curr Opin Cell Biol* (2008) 20(1):4–11. doi: 10.1016/j.ceb.2007.12.002
28. Henne WM, Stenmark H, Emr SD. Molecular mechanisms of the membrane sculpting ESCRT pathway. *Cold Spring Harb Perspect Biol* (2013) 5(9). doi: 10.1101/cshperspect.a016766
29. Raiborg C, Bache KG, Mehlum A, Stang E, Stenmark H. Hrs recruits clathrin to early endosomes. *EMBO J* (2001) 20(17):5008–21. doi: 10.1093/emboj/20.17.5008
30. Henne WM, Buchkovich NJ, Emr SD. The ESCRT pathway. *Dev Cell* (2011) 21(1):77–91. doi: 10.1016/j.devcel.2011.05.015
31. Kostelansky MS, Schluter C, Tam YY, Lee S, Ghirlando R, Beach B, et al. Molecular architecture and functional model of the complete yeast ESCRT-I heterotetramer. *Cell* (2007) 129(3):485–98. doi: 10.1016/j.cell.2007.03.016
32. Langelier C, von Schwedler UK, Fisher RD, De Domenico I, White PL, Hill CP, et al. Human ESCRT-II complex and its role in human immunodeficiency virus type 1 release. *J Virol* (2006) 80(19):9465–80. doi: 10.1128/JVI.01049-06

33. Babst M, Katzmann DJ, Snyder WB, Wendland B, Emr SD. Endosome-associated complex, ESCRT-II, recruits transport machinery for protein sorting at the multivesicular body. *Dev Cell* (2002) 3(2):283–9. doi: 10.1016/s1534-5807(02)00219-8
34. Odorizzi G, Katzmann DJ, Babst M, Audhya A, Emr SD. Bro1 is an endosome-associated protein that functions in the MVB pathway in Saccharomyces cerevisiae. *J Cell Sci* (2003) 116(Pt 10):1893–903. doi: 10.1242/jcs.00395
35. Babst M, Wendland B, Estepa EJ, Emr SD. The Vps4p AAA ATPase regulates membrane association of a Vps protein complex required for normal endosome function. *EMBO J* (1998) 17(11):2982–93. doi: 10.1093/emboj/17.11.2982
36. Ghossoub R, Lembo F, Rubio A, Gaillard CB, Bouchet J, Vitale N, et al. Syntenin-ALIX exosome biogenesis and budding into multivesicular bodies are controlled by ARF6 and PLD2. *Nat Commun* (2014) 5:3477. doi: 10.1038/ncomms4477
37. Stuffers S, Sem Wegner C, Stenmark H, Brech A. Multivesicular endosome biogenesis in the absence of ESCRTs. *Traffic* (2009) 10(7):925–37. doi: 10.1111/j.1600-0854.2009.00920.x
38. Chen S, Datta-Chaudhuri A, Deme P, Dickens A, Dastgheyb R, Bhargava P, et al. Lipidomic characterization of extracellular vesicles in human serum. *J Circ Biomark* (2019) 8:1849454419879848. doi: 10.1177/1849454419879848
39. Trajkovic K, Hsu C, Chiantia S, Rajendran L, Wenzel D, Wieland F, et al. Ceramide triggers budding of exosome vesicles into multivesicular endosomes. *Science* (2008) 319(5867):1244–7. doi: 10.1126/science.1153124
40. Wubbolts R, Leckie RS, Veenhuizen PT, Schwarzmann G, Möbius W, Hoernschemeyer J, et al. Proteomic and biochemical analyses of human B cell-derived exosomes. Potential implications for their function and multivesicular body formation. *J Biol Chem* (2003) 278(13):10963–72. doi: 10.1074/jbc.M207550200
41. Matsuo H, Chevallier J, Mayran N, Le Blanc I, Ferguson C, Fauré J, et al. Role of LBPA and Alix in multivesicular liposome formation and endosome organization. *Science* (2004) 303(5657):531–4. doi: 10.1126/science.1092425
42. van Niel G, Charrin S, Simoes S, Romao M, Rochin L, Saftig P, et al. The tetraspanin CD63 regulates ESCRT-independent and -dependent endosomal sorting during melanogenesis. *Dev Cell* (2011) 21(4):708–21. doi: 10.1016/j.devcel.2011.08.019
43. Chairoungdua A, Smith DL, Pochard P, Hull M, Caplan MJ. Exosome release of β-catenin: a novel mechanism that antagonizes Wnt signaling. *J Cell Biol* (2010) 190(6):1079–91. doi: 10.1083/jcb.201002049
44. Perez-Hernandez D, Gutiérrez-Vázquez C, Jorge I, López-Martín S, Ursa A, Sánchez-Madrid F, et al. The intracellular interactome of tetraspanin-enriched microdomains reveals their function as sorting machineries toward exosomes. *J Biol Chem* (2013) 288(17):11649–61. doi: 10.1074/jbc.M112.445304
45. Moreno-Gonzalo O, Villarroya-Beltri C, Sánchez-Madrid F. Post-translational modifications of exosomal proteins. *Front Immunol* (2014) 5:383. doi: 10.3389/fimmu.2014.00383
46. Villarroya-Beltri C, Gutiérrez-Vázquez C, Sánchez-Cabo F, Pérez-Hernández D, Vázquez J, Martin-Cofreces N, et al. Sumoylated hnRNPA2B1 controls the sorting of miRNAs into exosomes through binding to specific motifs. *Nat Commun* (2013) 4:2980. doi: 10.1038/ncomms3980
47. Zuccato E, Blott EJ, Holt O, Sigismund S, Shaw M, Bossi G, et al. Sorting of Fas ligand to secretory lysosomes is regulated by mono-ubiquitylation and phosphorylation. *J Cell Sci* (2007) 120(Pt 1):191–9. doi: 10.1242/jcs.03315
48. Zhang X, Yuan X, Shi H, Wu L, Qian H, Xu W. Exosomes in cancer: small particle, big player. *J Hematol Oncol* (2015) 8:83. doi: 10.1186/s13045-015-0181-x
49. Hui WW, Hercik K, Belsare S, Alugubelly N, Clapp B, Rinaldi C, et al. Salmonella enterica Serovar Typhimurium Alters the Extracellular Proteome of Macrophages and Leads to the Production of Proinflammatory Exosomes. *Infect Immun* (2018) 86(2). doi: 10.1128/IAI.00386-17
50. Cheng Y, Schorey JS. Exosomes carrying mycobacterial antigens can protect mice against Mycobacterium tuberculosis infection. *Eur J Immunol* (2013) 43(12):3279–90. doi: 10.1002/eji.201343727
51. Cohen SB, Gern BH, Delahaye JL, Adams KN, Plumlee CR, Winkler JK, et al. Alveolar Macrophages Provide an Early Mycobacterium tuberculosis Niche and Initiate Dissemination. *Cell Host Microbe* (2018) 24(3):439–46.e4. doi: 10.1016/j.chom.2018.08.001
52. Armstrong JA, Hart PD. Phagosome-lysosome interactions in cultured macrophages infected with virulent tubercle bacilli. Reversal of the usual nonfusion pattern and observations on bacterial survival. *J Exp Med* (1975) 142(1):1–16. doi: 10.1084/jem.142.1.1
53. Via LE, Deretic D, Ulmer RJ, Hibler NS, Huber LA, Deretic V. Arrest of mycobacterial phagosome maturation is caused by a block in vesicle fusion between stages controlled by rab5 and rab7. *J Biol Chem* (1997) 272 (20):13326–31. doi: 10.1074/jbc.272.20.13326
54. Xu S, Cooper A, Sturgill-Koszycki S, van Heyningen T, Chatterjee D, Orme I, et al. Intracellular trafficking in Mycobacterium tuberculosis and Mycobacterium avium-infected macrophages. *J Immunol* (1994) 153 (6):2568–78.
55. Zulauf KE, Sullivan JT, Braunstein M. The SecA2 pathway of Mycobacterium tuberculosis exports effectors that work in concert to arrest phagosome and autophagosome maturation. *PloS Pathog* (2018) 14 (4):e1007011. doi: 10.1371/journal.ppat.1007011
56. Bhatnagar S, Schorey JS. Exosomes released from infected macrophages contain Mycobacterium avium glycopeptidolipids and are proinflammatory. *J Biol Chem* (2007) 282(35):25779–89. doi: 10.1074/jbc.M702277200
57. Bhatnagar S, Shinagawa K, Castellino FJ, Schorey JS. Exosomes released from macrophages infected with intracellular pathogens stimulate a proinflammatory response in vitro and in vivo. *Blood* (2007) 110(9):3234–44. doi: 10.1182/blood-2007-03-079152
58. Singh PP, Smith VL, Karakousis PC, Schorey JS. Exosomes isolated from mycobacteria-infected mice or cultured macrophages can recruit and activate immune cells in vitro and in vivo. *J Immunol* (2012) 189(2):777–85. doi: 10.4049/jimmunol.1103638
59. Smith VL, Cheng Y, Bryant BR, Schorey JS. Exosomes function in antigen presentation during an in vivo Mycobacterium tuberculosis infection. *Sci Rep* (2017) 7:43578. doi: 10.1038/srep43578
60. Ostrowski M, Carmo NB, Krumeich S, Fanget I, Raposo G, Savina A, et al. Rab27a and Rab27b control different steps of the exosome secretion pathway. *Nat Cell Biol* (2010) 12(1):19–30; sup pp 1-13. doi: 10.1038/ncb2000
61. Giri PK, Kruh NA, Dobos KM, Schorey JS. Proteomic analysis identifies highly antigenic proteins in exosomes from M. tuberculosis-infected and culture filtrate protein-treated macrophages. *Proteomics* (2010) 10 (17):3190–202. doi: 10.1002/pmic.200900840
62. Kruh-Garcia NA, Wolfe LM, Chaisson LH, Worodria WO, Nahid P, Schorey JS, et al. Detection of Mycobacterium tuberculosis peptides in the exosomes of patients with active and latent M. tuberculosis infection using MRM-MS. *PloS One* (2014) 9(7):e103811. doi: 10.1371/journal.pone.0103811
63. Smith VL, Jackson L, Schorey JS. Ubiquitination as a Mechanism To Transport Soluble Mycobacterial and Eukaryotic Proteins to Exosomes. *J Immunol* (2015) 195(6):2722–30. doi: 10.4049/jimmunol.1403186
64. Cheng Y, Schorey JS. Targeting soluble proteins to exosomes using a ubiquitin tag. *Biotechnol Bioeng* (2016) 113(6):1315–24. doi: 10.1002/bit.25884
65. Singh PP, Li L, Schorey JS. Exosomal RNA from Mycobacterium tuberculosis-Infected Cells Is Functional in Recipient Macrophages. *Traffic* (2015) 16(6):555–71. doi: 10.1111/tra.12278
66. World Health Organization. *Malaria* (2020). Available at: https://www.who.int/news-room/fact-sheets/detail/malaria.
67. Sibley LD. Intracellular parasite invasion strategies. *Science* (2004) 304 (5668):248–53. doi: 10.1126/science.1094717
68. Pradel G, Frevert U. Malaria sporozoites actively enter and pass through rat Kupffer cells prior to hepatocyte invasion. *Hepatology* (2001) 33(5):1154–65. doi: 10.1053/jhep.2001.24237
69. Kurup SP, Anthony SM, Hancox LS, Vijay R, Pewe LL, Moioffer SJ, et al. Monocyte-Derived CD11c. *Cell Host Microbe* (2019) 25(4):565–77.e6. doi: 10.1016/j.chom.2019.02.014
70. Silvie O, Rubinstein E, Franetich JF, Prenant M, Belnoue E, Rénia L, et al. Hepatocyte CD81 is required for Plasmodium falciparum and Plasmodium yoelii sporozoite infectivity. *Nat Med* (2003) 9(1):93–6. doi: 10.1038/nm808
71. Bano N, Romano JD, Jayabalasingham B, Coppens I. Cellular interactions of Plasmodium liver stage with its host mammalian cell. *Int J Parasitol* (2007) 37(12):1329–41. doi: 10.1016/j.ijpara.2007.04.005

72. Regev-Rudzki N, Wilson DW, Carvalho TG, Sisquella X, Coleman BM, Rug M, et al. Cell-cell communication between malaria-infected red blood cells via exosome-like vesicles. *Cell* (2013) 153(5):1120–33. doi: 10.1016/j.cell.2013.04.029
73. Mantel PY, Hoang AN, Goldowitz I, Potashnikova D, Hamza B, Vorobjev I, et al. Malaria-infected erythrocyte-derived microvesicles mediate cellular communication within the parasite population and with the host immune system. *Cell Host Microbe* (2013) 13(5):521–34. doi: 10.1016/j.chom.2013.04.009
74. Abdi A, Yu L, Goulding D, Rono MK, Bejon P, Choudhary J, et al. Proteomic analysis of extracellular vesicles from a. *Wellcome Open Res* (2017) 2:50. doi: 10.12688/wellcomeopenres.11910.2
75. Mantel PY, Marti M. The role of extracellular vesicles in Plasmodium and other protozoan parasites. *Cell Microbiol* (2014) 16(3):344–54. doi: 10.1111/cmi.12259
76. Debs S, Cohen A, Hosseini-Beheshti E, Chimini G, Hunt NH, Grau GER. Interplay of extracellular vesicles and other players in cerebral malaria pathogenesis. *Biochim Biophys Acta Gen Subj* (2019) 1863(2):325–31. doi: 10.1016/j.bbagen.2018.10.012
77. Combes V, Coltel N, Faille D, Wassmer SC, Grau GE. Cerebral malaria: role of microparticles and platelets in alterations of the blood-brain barrier. *Int J Parasitol* (2006) 36(5):541–6. doi: 10.1016/j.ijpara.2006.02.005
78. Martin-Jaular L, Nakayasu ES, Ferrer M, Almeida IC, Del Portillo HA. Exosomes from Plasmodium yoelii-infected reticulocytes protect mice from lethal infections. *PloS One* (2011) 6(10):e26588. doi: 10.1371/journal.pone.0026588
79. Arisue N, Palacpac NMQ, Tougan T, Horii T. Characteristic features of the SERA multigene family in the malaria parasite. *Parasit Vectors* (2020) 13(1):170. doi: 10.1186/s13071-020-04044-y
80. Gualdrón-López M, Flannery EL, Kangwanrangsan N, Chuenchob V, Fernandez-Orth D, Segui-Barber J, et al. Characterization of Plasmodium vivax Proteins in Plasma-Derived Exosomes from Malaria-Infected Liver-Chimeric Humanized Mice. *Characterization of Front Microbiol* (2018) 9:1271. doi: 10.3389/fmicb.2018.01271
81. Vaughan AM, Mikolajczak SA, Wilson EM, Grompe M, Kaushansky A, Camargo N, et al. Complete Plasmodium falciparum liver-stage development in liver-chimeric mice. *J Clin Invest* (2012) 122(10):3618–28. doi: 10.1172/JCI62684
82. Mikolajczak SA, Vaughan AM, Kangwanrangsan N, Roobsoong W, Fishbaugher M, Yimamnuaychok N, et al. Plasmodium vivax liver stage development and hypnozoite persistence in human liver-chimeric mice. *Cell Host Microbe* (2015) 17(4):526–35. doi: 10.1016/j.chom.2015.02.011
83. Rastogi S, Cygan AM, Boothroyd JC. Translocation of effector proteins into host cells by Toxoplasma gondii. *Curr Opin Microbiol* (2019) 52:130–8. doi: 10.1016/j.mib.2019.07.002
84. Håkansson S, Charron AJ, Sibley LD. Toxoplasma evacuoles: a two-step process of secretion and fusion forms the parasitophorous vacuole. *EMBO J* (2001) 20(12):3132–44. doi: 10.1093/emboj/20.12.3132
85. Nadipuram SM, Kim EW, Vashisht AA, Lin AH, Bell HN, Coppens I, et al. In Vivo Biotinylation of the Toxoplasma Parasitophorous Vacuole Reveals Novel Dense Granule Proteins Important for Parasite Growth and Pathogenesis. *mBio* (2016) 7(4). doi: 10.1128/mBio.00808-16
86. Li Y, Liu Y, Xiu F, Wang J, Cong H, He S, et al. Characterization of exosomes derived from. *Int J Nanomed* (2018) 13:467–77. doi: 10.2147/IJN.S151110
87. Aline F, Bout D, Amigorena S, Roingeard P, Dimier-Poisson I. Toxoplasma gondii antigen-pulsed-dendritic cell-derived exosomes induce a protective immune response against T. gondii infection. *Infect Immun* (2004) 72(7):4127–37. doi: 10.1128/IAI.72.7.4127-4137.2004
88. Beauvillain C, Ruiz S, Guiton R, Bout D, Dimier-Poisson I. A vaccine based on exosomes secreted by a dendritic cell line confers protection against T. gondii infection in syngeneic and allogeneic mice. *Microbes Infect* (2007) 9(14-15):1614–22. doi: 10.1016/j.micinf.2007.07.002
89. Pope SM, Lässer C. Toxoplasma gondii infection of fibroblasts causes the production of exosome-like vesicles containing a unique array of mRNA and miRNA transcripts compared to serum starvation. *J Extracell Vesicles* (2013) 2. doi: 10.3402/jev.v2i0.22484
90. Wowk PF, Zardo ML, Miot HT, Goldenberg S, Carvalho PC, Mörking PA. Proteomic profiling of extracellular vesicles secreted from Toxoplasma gondii. *Proteomics* (2017) 17(15-16). doi: 10.1002/pmic.201600477
91. Li DL, Zou WH, Deng SQ, Peng HJ. Analysis of the Differential Exosomal miRNAs of DC2.4 Dendritic Cells Induced by. *Int J Mol Sci* (2019) 20(21). doi: 10.3390/ijms20215506
92. Pearson RD, Sousa AQ. Clinical spectrum of Leishmaniasis. *Clin Infect Dis* (1996) 22(1):1–13. doi: 10.1093/clinids/22.1.1
93. McMahon-Pratt D, Alexander J. Does the Leishmania major paradigm of pathogenesis and protection hold for New World cutaneous leishmaniases or the visceral disease? *Immunol Rev* (2004) 201:206–24. doi: 10.1111/j.0105-2896.2004.00190.x
94. Wilson ME, Jeronimo SM, Pearson RD. Immunopathogenesis of infection with the visceralizing Leishmania species. *Microb Pathog* (2005) 38(4):147–60. doi: 10.1016/j.micpath.2004.11.002
95. Blackwell JM, Fakiola M, Ibrahim ME, Jamieson SE, Jeronimo SB, Miller EN, et al. Genetics and visceral leishmaniasis: of mice and man. *Parasite Immunol* (2009) 31(5):254–66. doi: 10.1111/j.1365-3024.2009.01102.x
96. Ndjamen B, Kang BH, Hatsuzawa K, Kima PE. Leishmania parasitophorous vacuoles interact continuously with the host cell's endoplasmic reticulum; parasitophorous vacuoles are hybrid compartments. *Cell Microbiol* (2010) 12(10):1480–94. doi: 10.1111/j.1462-5822.2010.01483.x
97. Arango Duque G, Jardim A, Gagnon É, Fukuda M, Descoteaux A. The host cell secretory pathway mediates the export of Leishmania virulence factors out of the parasitophorous vacuole. *PloS Pathog* (2019) 15(7):e1007982. doi: 10.1371/journal.ppat.1007982
98. Peters NC, Egen JG, Secundino N, Debrabant A, Kimblin N, Kamhawi S, et al. In vivo imaging reveals an essential role for neutrophils in leishmaniasis transmitted by sand flies. *Science* (2008) 321(5891):970–4. doi: 10.1126/science.1159194
99. Romano A, Carneiro MBH, Doria NA, Roma EH, Ribeiro-Gomes FL, Inbar E, et al. Divergent roles for Ly6C+CCR2+CX3CR1+ inflammatory monocytes during primary or secondary infection of the skin with the intra-phagosomal pathogen Leishmania major. *PloS Pathog* (2017) 13(6):e1006479. doi: 10.1371/journal.ppat.1006479
100. Wilson ME, Innes DJ, Sousa AD, Pearson RD. Early histopathology of experimental infection with Leishmania donovani in hamsters. *J Parasitol* (1987) 73(1):55–63. doi: 10.2307/3282344
101. Costa DL, Lima-Júnior DS, Nascimento MS, Sacramento LA, Almeida RP, Carregaro V, et al. CCR2 signaling contributes to the differentiation of protective inflammatory dendritic cells in Leishmania braziliensis infection. *J Leukoc Biol* (2016) 100(2):423–32. doi: 10.1189/jlb.4A0715-288R
102. Kaye PM, Beattie L. Lessons from other diseases: granulomatous inflammation in leishmaniasis. *Semin Immunopathol* (2016) 38(2):249–60. doi: 10.1007/s00281-015-0548-7
103. Steinbichler TB, Dudás J, Riechelmann H, Skvortsova II. The role of exosomes in cancer metastasis. *Semin Cancer Biol* (2017) 44:170–81. doi: 10.1016/j.semcancer.2017.02.006
104. Wortzel I, Dror S, Kenific CM, Lyden D. Exosome-Mediated Metastasis: Communication from a Distance. *Dev Cell* (2019) 49(3):347–60. doi: 10.1016/j.devcel.2019.04.011
105. Caltagirone F, Pistone G, Arico M, Vitale F, Sorbello D, Rizzo D, et al. Vascular patterns in cutaneous leishmaniasis: A videodermatoscopic study. *Indian J Dermatol Venereol Leprol* (2015) 81(4):394–8. doi: 10.4103/0378-6323.159939
106. Taheri AR, Pishgooei N, Maleki M, Goyonlo VM, Kiafar B, Banihashemi M, et al. Dermoscopic features of cutaneous leishmaniasis. *Int J Dermatol* (2013) 52(11):1361–6. doi: 10.1111/ijd.12114
107. Horst AK, Bickert T, Brewig N, Ludewig P, van Rooijen N, Schumacher U, et al. CEACAM1+ myeloid cells control angiogenesis in inflammation. *Blood* (2009) 113(26):6726–36. doi: 10.1182/blood-2008-10-184556
108. Weinkopff T, Konradt C, Christian DA, Discher DE, Hunter CA, Scott P. Leishmania major Infection-Induced VEGF-A/VEGFR-2 Signaling Promotes Lymphangiogenesis That Controls Disease. *J Immunol* (2016) 197(5):1823–31. doi: 10.4049/jimmunol.1600717
109. Yurdakul P, Dalton J, Beattie L, Brown N, Erguven S, Maroof A, et al. Compartment-specific remodeling of splenic micro-architecture during experimental visceral leishmaniasis. *Am J Pathol* (2011) 179(1):23–9. doi: 10.1016/j.ajpath.2011.03.009
110. Dalton JE, Glover AC, Hoodless L, Lim EK, Beattie L, Kirby A, et al. The neurotrophic receptor Ntrk2 directs lymphoid tissue neovascularization

during Leishmania donovani infection. *PloS Pathog* (2015) 11(2):e1004681. doi: 10.1371/journal.ppat.1004681
111. Barak E, Amin-Spector S, Gerliak E, Goyard S, Holland N, Zilberstein D. Differentiation of Leishmania donovani in host-free system: analysis of signal perception and response. *Mol Biochem Parasitol* (2005) 141(1):99–108. doi: 10.1016/j.molbiopara.2005.02.004
112. Tsigankov P, Gherardini PF, Helmer-Citterich M, Späth GF, Myler PJ, Zilberstein D. Regulation dynamics of Leishmania differentiation: deconvoluting signals and identifying phosphorylation trends. *Mol Cell Proteomics* (2014) 13(7):1787–99. doi: 10.1074/mcp.M114.037705
113. Kaye PM, Cruz I, Picado A, Van Bocxlaer K, Croft SL. Leishmaniasis immunopathology-impact on design and use of vaccines, diagnostics and drugs. *Semin Immunopathol* (2020) 42(3):247–64. doi: 10.1007/s00281-020-00788-y
114. Silverman JM, Clos J, de'Oliveira CC, Shirvani O, Fang Y, Wang C, et al. An exosome-based secretion pathway is responsible for protein export from Leishmania and communication with macrophages. *J Cell Sci* (2010) 123(Pt 6):842–52. doi: 10.1242/jcs.056465
115. Silverman JM, Clos J, Horakova E, Wang AY, Wiesgigl M, Kelly I, et al. Leishmania exosomes modulate innate and adaptive immune responses through effects on monocytes and dendritic cells. *J Immunol* (2010) 185 (9):5011–22. doi: 10.4049/jimmunol.1000541
116. Atayde VD, Aslan H, Townsend S, Hassani K, Kamhawi S, Olivier M. Exosome Secretion by the Parasitic Protozoan Leishmania within the Sand Fly Midgut. *Cell Rep* (2015) 13(5):957–67. doi: 10.1016/j.celrep.2015.09.058
117. Yao C, Donelson JE, Wilson ME. Internal and surface-localized major surface proteases of Leishmania spp. and their differential release from promastigotes. *Eukaryot Cell* (2007) 6(10):1905–12. doi: 10.1128/EC.00073-07
118. Isnard A, Christian JG, Kodiha M, Stochaj U, McMaster WR, Olivier M. Impact of Leishmania infection on host macrophage nuclear physiology and nucleopore complex integrity. *PloS Pathog* (2015) 11(3):e1004776. doi: 10.1371/journal.ppat.1004776
119. Hassani K, Olivier M. Immunomodulatory impact of leishmania-induced macrophage exosomes: a comparative proteomic and functional analysis. *PloS Negl Trop Dis* (2013) 7(5):e2185. doi: 10.1371/journal.pntd.0002185
120. Gioseffi A, Hamerly T, Van K, Zhang N, Dinglasan RR, Yates PA, et al. -infected macrophages release extracellular vesicles that can promote lesion development. *Life Sci Alliance* (2020) 3(12). doi: 10.26508/lsa.202000742
121. Jamal F, Shivam P, Kumari S, Singh MK, Sardar AH, Pushpanjali, et al. Identification of Leishmania donovani antigen in circulating immune complexes of visceral leishmaniasis subjects for diagnosis. *PloS One* (2017) 12(8):e0182474. doi: 10.1371/journal.pone.0182474
122. Silverman JM, Chan SK, Robinson DP, Dwyer DM, Nandan D, Foster LJ, et al. Proteomic analysis of the secretome of Leishmania donovani. *Genome Biol* (2008) 9(2):R35. doi: 10.1186/gb-2008-9-2-r35

Conflict of Interest: The authors declare that the research was conducted in the absence of any commercial or financial relationships that could be construed as a potential conflict of interest.

Copyright © 2021 Gioseffi, Edelmann and Kima. This is an open-access article distributed under the terms of the Creative Commons Attribution License (CC BY). The use, distribution or reproduction in other forums is permitted, provided the original author(s) and the copyright owner(s) are credited and that the original publication in this journal is cited, in accordance with accepted academic practice. No use, distribution or reproduction is permitted which does not comply with these terms.

frontiers in Immunology

REVIEW
published: 20 April 2021
doi: 10.3389/fimmu.2021.631714

Cellular Responses to the Efferocytosis of Apoptotic Cells

Charles Yin[1,2] *and Bryan Heit*[1,2,3]*

[1] Department of Microbiology and Immunology, Schulich School of Medicine and Dentistry, Western University, London, ON, Canada, [2] Center for Human Immunology, Western University, London, ON, Canada, [3] Robarts Research Institute, London, ON, Canada

The rapid and efficient phagocytic clearance of apoptotic cells, termed efferocytosis, is a critical mechanism in the maintenance of tissue homeostasis. Removal of apoptotic cells through efferocytosis prevents secondary necrosis and the resultant inflammation caused by the release of intracellular contents. The importance of efferocytosis in homeostasis is underscored by the large number of inflammatory and autoimmune disorders, including atherosclerosis and systemic lupus erythematosus, that are characterized by defective apoptotic cell clearance. Although mechanistically similar to the phagocytic clearance of pathogens, efferocytosis differs from phagocytosis in that it is immunologically silent and induces a tissue repair response. Efferocytes face unique challenges resulting from the internalization of apoptotic cells, including degradation of the apoptotic cell, dealing with the extra metabolic load imposed by the processing of apoptotic cell contents, and the coordination of an anti-inflammatory, pro-tissue repair response. This review will discuss recent advances in our understanding of the cellular response to apoptotic cell uptake, including trafficking of apoptotic cell cargo and antigen presentation, signaling and transcriptional events initiated by efferocytosis, the coordination of an anti-inflammatory response and tissue repair, unique cellular metabolic responses and the role of efferocytosis in host defense. A better understanding of how efferocytic cells respond to apoptotic cell uptake will be critical in unraveling the complex connections between apoptotic cell removal and inflammation resolution and maintenance of tissue homeostasis.

Keywords: efferocytosis, intracellular trafficking, transcriptional regulation, cellular metabolism, inflammation resolution, host defense

OPEN ACCESS

Edited by:
Gregory D. Fairn, St. Michael's Hospital, Canada

Reviewed by:
Luisa Martinez-Pomares, University of Nottingham, United Kingdom
Arif Yurdagul, Louisiana State University Health Shreveport, United States

***Correspondence:**
Bryan Heit
bheit@uwo.ca

Specialty section:
This article was submitted to Molecular Innate Immunity, a section of the journal Frontiers in Immunology

Received: *20 November 2020*
Accepted: *29 March 2021*
Published: *20 April 2021*

Citation:
Yin C and Heit B (2021) Cellular Responses to the Efferocytosis of Apoptotic Cells. Front. Immunol. 12:631714. doi: 10.3389/fimmu.2021.631714

INTRODUCTION

Efferocytosis is the process of rapid and efficient clearance of apoptotic cells by both professional and non-professional phagocytic cells (1, 2). From an evolutionary perspective, efferocytosis is an ancient mechanism that allowed early multicellular organisms to regulate their growth through the disposal of dying cells during development (3). In complex multicellular organisms, efferocytosis is

Abbreviations: LAP, LC3-associated phagocytosis; PI3KCIII, class III phosphatidylinositol-3-kinase; TLR, Toll-like receptor; DCs, dendritic cells; PtdSer, phosphatidylserine; LXR, liver X receptor; PPAR, peroxisome proliferator-activated receptor; SPM, pro-resolving mediator.

critical in growth and development, for the resolution of inflammation, and for maintaining tissue homeostasis (4–6). Mechanistically, efferocytosis closely resembles phagocytosis—the internalization and clearance of pathogens and other foreign particulates (7). Indeed, though efferocytosis utilizes a distinct and well-characterized set of cell surface receptors (e.g. TAM family receptors, Tim4, α_V integrins) and soluble opsonins (e.g. Gas6, MFGE8, CD93) that bind to ligands found on the plasma membrane of apoptotic cells (e.g. phosphatidylserine), much of the processes downstream of apoptotic cell internalization such as intracellular trafficking of apoptotic cell cargo and cellular responses to internalized of apoptotic cell contents are either thought to be wholly analogous to phagocytosis or to be poorly understood (1, 7–10). Strikingly, efferocytes such as macrophages can distinguish between normal apoptotic cells and those infected with an intracellular pathogen, despite the fact that much of the contents of an infected apoptotic cell (e.g. lipids, nucleic acids, proteins) are identical to that of a non-infected cell, allowing the efferocyte to mount an appropriate immunological response to pathogens within efferocytosed cells (3). This demonstrates that efferocytosis is a distinct process from phagocytosis, that and efferocytes are fine-tuned to be able to distinguish between apoptotic versus pathogenic cargo.

The major efferocytic cell—or efferocyte—within the body is the macrophage (11). These immune cells are responsible for clearance of apoptotic cells and debris across many tissues (12, 13). There is emerging evidence that efferocytic macrophages form a distinct subset of tissue-resident macrophages that differ in both function and pattern of gene expression compared to other tissue-resident macrophage populations (14, 15). Indeed, A-Gonzalez et al. (14) found that tissue-resident murine efferocytic macrophages from across a range of different tissues share a common transcriptional profile, which is characterized by downregulation of proinflammatory cytokines such as IL1β and expression of the mannose receptor CD206 (14). Interestingly, although this population upregulates several anti-inflammatory genes, it's gene expression profile does not co-cluster with alternatively activated (M2) macrophages (14). This suggests that efferocytic macrophages cannot simply to be thought of as "anti-inflammatory" macrophages, and instead occupy a distinct space in the macrophage transcriptional landscape.

The purpose of this review will be to discuss the distinct cellular responses elicited upon uptake of apoptotic cells by an efferocyte, with a focus on macrophages as the major efferocytic cell population within the body. In particular, we will review differences in trafficking of apoptotic cell cargo and presentation of antigens following internalization, alterations in cell signaling and transcriptional regulation, as well as explore how changes in cargo trafficking and gene expression contribute to the anti-inflammatory phenotype that characterize efferocytes. Further, we will explore recent advances in our understanding of how efferocytes deal with the metabolic stress of internalizing apoptotic cells, how efferocytes respond upon uptake of infected apoptotic cells, and the role of efferocytosis in host defense.

EFFEROSOME TRAFFICKING AND ANTIGEN PRESENTATION

Following recognition, apoptotic cells are engulfed by the efferocyte into a plasma membrane-derived vacuole termed an efferosome (8). Similar to phagosomes that contain internalized pathogens, efferosomes undergo a highly regulated series of sequential fusions with early endosomes, late endosomes, and finally lysosomes (**Figure 1**) (16–18). These fusion events are regulated by proteins including Rab GTPases and SNAREs, with the fusion events delivering the hydrolytic enzymes which degrade the apoptotic cell within the efferosome (19–23). This process is termed efferosome maturation and is analogous to the maturation processes observed following phagocytosis and endocytosis (8, 24).

The efferosome maturation process bears many similarities to phagosome maturation, including the recruitment of the Rab GTPases Rab5 and Rab7 (23, 25, 26). Rab5 is recruited to efferosomes as the apoptotic cell is internalized, and remains bound to the efferosome for several minutes following the release of the efferosome from the plasma membrane (19, 27). Here, Rab5 mediates the fusion of the efferosome with early endosomes, beginning the degradative process which will ultimately disassemble the apoptotic cell (19, 20). Rab5 is exchanged for Rab7 several minutes after efferosome formation, with Rab7 mediating the fusion of late endosomes and lysosomes to the efferosome – thus generating a highly hydrolytic environment capable of the complete degradation of the apoptotic cell (18, 27). Recent work by our group and others have demonstrate important differences between the regulation of efferosome maturation versus phagosome maturation (27, 28). Efferosome acidification is a central process that facilitates the degradation of apoptotic cargo through activation of lysosomal proteases (29, 30).

Efferosomes have also been shown to employ LC3-associated phagocytosis (LAP, **Figure 1**), a noncanonical form of autophagy that involves recruitment of autophagy mediators including the class III phosphatidylinositol-3-kinase (PI3KCIII) complex ATG5 and ATG7 to the surface of nascent efferosomes (31, 32). These elements then direct the rapid maturation of the efferosome and processing of the apoptotic cargo in a manner that suppresses antigen presentation and serves to polarize macrophages towards an anti-inflammatory phenotype (33). While the exact signals which allow for LAP to be employed for efferosome maturation remain unknown, work from the Medzhitov group has demonstrated that phagosome-derived Toll-like receptor (TLR) signaling is required to direct materials into the classical phagocytic (e.g. non-LAP) pathway where they then undergo antigen presentation (34, 35). This indicates that the detection of pathogen products *via* TLR's serves not only to induce the expression of genes involved in inflammation and antigen presentation, but also induces immediate differences in the trafficking of cargo bearing TLR ligands compared to those lacking these ligands (36). Rab39a may serve to inhibit LAP following phagocytosis, as this GTPase inhibits autophagy following TLR signaling, and is required for

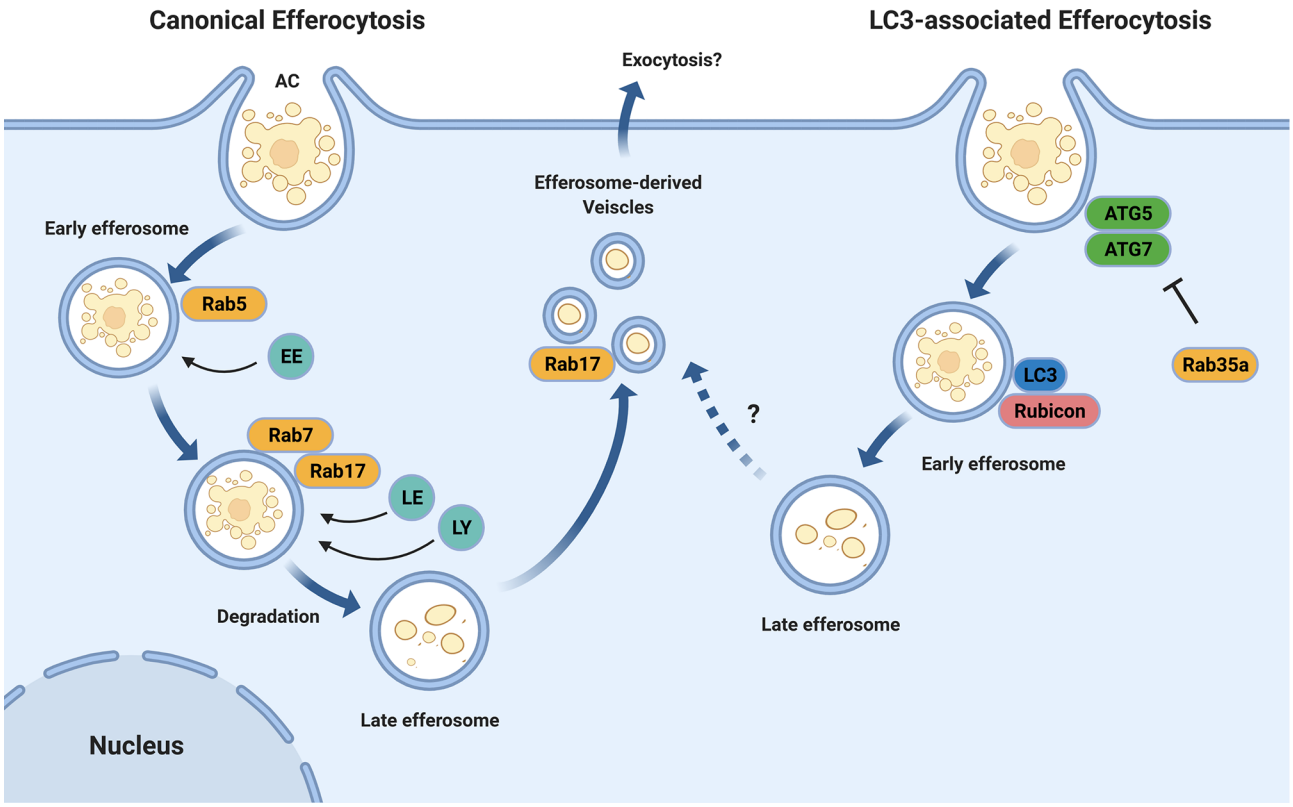

FIGURE 1 | Efferosome Maturation Pathways. Efferocytosis can occur through the canonical endo-lysosomal maturation pathway (left) in which the GTPases Rab5 and Rab7 mediate the sequential fusion of early endosomes (EE), late endosomes (LE), and lysosomes (LY) with the maturing efferosome. Unlike phagocytosis, this efferosome maturation pathway also involves Rab17 which directs the degraded contents from the efferosome to the recycling endosome from where they may be exocytosed, thereby avoiding the delivery of these materials to antigen loading compartments. In addition to the canonical pathway, some efferosomes may mature through an LC3-mediated, autophagy-like pathway (right). In this pathway, the efferosome recruits the protein LC3 which then mediates a rapid degradation of the efferosome in a fashion which suppresses antigen presentation. Similar to LC3-associated phagocytosis, the recruitment of the autophagy-related proteins ATG5 and ATG7, as well as Rubicon to the nascent efferosome appear to be important for efferocytosis through this pathway. The activity of ATG5 and ATG7 are inhibited by Rab35a, which is activated downstream of TLR signaling. Figure produced using BioRender.

the delivery of MHC I to phagosomes for antigen cross-presentation (37, 38). However, there are no published studies of the role of Rab39a in efferocytosis, and therefore its role in efferocytosis-associated LAP remains unclear. Interestingly, LAP and the formation of LC3-associated efferosomes is dependent on the Beclin1-interacting protein Rubicon (39). Rubicon is a negative regulator of canonical autophagy and downregulation of this protein results in an increase in the number of autophagosomes (39, 40). Indeed, deletion of Rubicon in a mouse model of autoimmune disease significantly increases susceptibility to the development of systemic lupus erythematosus-like features in these animals, potentially due to altered processing of apoptotic cells (41).

Differences in acidification and trafficking of efferosomes, as compared to phagosomes, also plays a role in ensuring the immunologically silent degradation of apoptotic cells (34, 42, 43). There is conflicting evidence in the literature on the kinetics of efferosome maturation as compared to phagosome maturation (35, 42). Erwig et al. reported that in murine macrophages, early maturation and acidification of efferosomes containing apoptotic neutrophils proceeded at a faster rate than phagosomes containing IgG-opsonized neutrophils (42). Inhibition of the small GTPase RhoA using a small molecule inhibitor was sufficient to negate these differences (42). In contrast, Blander and Medzhitov have shown that efferosome maturation proceeded at a slower rate than phagosomes (35). Of note, in the case of Blander and Medzhitov, the phagocytic target employed was inactivated *Escherichia coli* and the authors argue that it was activation of TLR2 and TLR4 signaling that drove accelerated phagosome maturation (35). In contrast, the IgG-coated neutrophils used by Erwig and colleagues would not have stimulated TLRs in the same fashion (42).

Our group has recently demonstrated that efferosome localization appears to play a role in distinguishing the fate of apoptotic cargo (28). Canonically, phagosomes undergo dynein-mediated trafficking towards the cell centre as they mature, where lysosomes are concentrated due to a similar dynein-mediated trafficking pathway (16, 44–46). Thus, by moving to the cell centre, phagosomes can efficiently undergo fusion with lysosomes to acquire the hydrolytic enzymes that degrade

phagosome cargos (29, 47). In contrast, we have shown that while efferosomes also undergo an initial migration towards the cell centre where they fuse with lysosomes, they subsequently fragment into smaller efferosome-derived vesicles (EDVs) which migrate away from the cell centre and towards the periphery (28). At the periphery, EDVs undergo fusion with the recycling endosome compartment, presumably to facilitate exocytosis of degraded apoptotic cargo or resorption of nutrients (28). This process is driven by the small GTPase Rab17 (**Figure 1**), which is required for both the fragmentation of efferosomes into EDVs and for the movement of the EDVs to the cell periphery (27, 28). Macrophages that overexpress a dominant-negative mutant of Rab17 accumulate efferosomes at the cell center (28). Furthermore, the presence of Rab17 on efferosomes also prevents the delivery of MHC class II, circumventing autoantigen presentation from degraded apoptotic cargo (27). Expression of a dominant-negative Rab17 impairs this pathway, leading to MHC II accumulation in mature efferosomes (27).

The presence of three processes that work simultaneously to limit antigen presentation of efferosome-derived antigens – LAP, accelerated maturation, and Rab17-mediated redirection of cargo out of the maturing efferosome – indicates that limiting autoantigen presentation is a fundamental response of phagocytes following efferocytosis. Moreover, efferocytes engage in non-trafficking-based mechanisms to limit autoimmune responses to efferocytosed materials. As described later in this review, efferocytosis is often accompanied by the upregulation of cytokines such as IL-10 which suppress the activity of mature T cells and promotes the formation of T_{reg} cells from naive T cells (48). Consequentially, T cell responses are inhibited following efferocytosis. For example, Rodriguez-Fernandez et al. demonstrated that in human DCs, efferocytosis of PtdSer-containing liposomes biased the stimulation of autologous T cells from a proliferative to a tolerogenic profile, likely through altered cytokine expression by the DCs (49). Consistent with these mechanisms acting to limit autoreactivity, emerging evidence indicate that defects in the suppression of antigen presentation following efferocytosis is a driver of autoimmune disease (50, 51). In mouse models of systemic lupus erythematosus, dysregulated expression of specific pro-efferocytic receptors such as Tim4, C1q or CLM-1 result in either deficient apoptotic cell clearance or inappropriate antigen presentation that then promotes the development of autoimmune disease in these mice (52). In humans, mutations in efferocytic receptors, especially in MERTK and its opsonins, are associated with a similar increase in the risk of autoimmune disorders including multiple sclerosis and rheumatoid arthritis, highlighting the importance of efficient efferocytosis in limiting autoimmunity (53–57).

Interestingly, some professional antigen presenting cells have mechanisms that allow efferosome-derived antigens to be cross-presented on MHC I. A recent study by Canton et al. demonstrated that type 1 conventional dendritic cells use the receptor DNGR-1 to recognize actin-myosin complexes exposed to the efferosome lumen during the early stage of efferosome maturation (58). Recognition of actin-myosin complexes leads to an alternative maturation pathway where the efferosome does not acquire its normal degradative capacity, and instead, Syk-induced NADPH oxidase activity damages the efferosomal membrane, releasing the efferosome's cargo into the cytosol. Once in the cytosol, the efferocytosed materials are processed and presented *via* the canonical MHC I presentation pathway [reviewed in (59)]. Interestingly, the restriction of this process to the early stages of efferosome maturation suggests that this process may only occur in response to engulfed cells that have pre-exposed actin-myosin complexes – e.g. cells which have lost membrane integrity as they progress through late stage apoptosis, or cells which have died a lytic form of cell death such as necroptosis or necrosis (9). Alternatively, this pathway may enable the routine "screening" of apoptotic cell-derived antigens *via* MHC I, which because it relies on T cells previously activated to the same antigen presented on MHC II by professional antigen presenting cells, lacks the autoimmune potential of MHC II presentation (60).

CELL SIGNALING AND TRANSCRIPTIONAL REGULATION

Differences between the cellular response of phagocytes to efferocytosis of apoptotic cells versus phagocytosis of pathogens require that there be efferocytosis-specific signal transduction events and transcriptional regulation (1, 2). We are just beginning to develop an understanding of the key transcriptional factors that control the cellular events that occur following efferocytosis. Two key families of transcriptional factors that drive this response are members of the liver X receptor (LXR) and peroxisome proliferator-activated receptor (PPAR) families of nuclear receptors (61–63). These transcription factor families bind to the same DNA motifs, and often act as heterodimers, meaning that their functions are often overlapping and redundant (64). Both receptor families bind to many of the same ligands, notably lipid-derived metabolites, with their activation leading to the preferential formation of heterodimers that then bind to direct 5' – RGKTCA – 3' repeats (65). Once bound, these LXRs and PPARs coordinate with other transcription factors to either activate or repress transcription (64, 66, 67).

LXRs are well-characterized regulators of cholesterol, glucose and fatty acid metabolism (68). The two members of the LXR family, LXRα and LXRβ, are both activated following efferocytic apoptotic cell uptake, and in turn increase the cell's efferocytic capacity *via* two distinct mechanisms (69). The first mechanism – described in-detail later in this review – is the upregulation of the metabolic pathways required to process the large quantities of lipids, sterols and proteins present in an efferocytosed apoptotic cell. The second mechanism is the upregulation of efferocytic receptors and signaling molecules. Stimulation of LXRs *in vivo* with apoptotic thymocytes has been shown to upregulate MERTK, a key efferocytic receptor involved in apoptotic cell recognition and uptake (69, 70). This enhances the efferocytic capacity of the efferocyte, and increases MERTK-mediated anti-inflammatory activity *via* increased activation of SOCS3, a suppressor of cytokine-induced JAK/STAT signaling (71). Conversely, peritoneal macrophages isolated from LXR double-knockout mice have been shown to have diminished capacity to engage in

efferocytosis, without any impairment in the phagocytosis of *E. coli* (69). Indeed, activation of LXRα/β appears to be required to shift macrophages away from a pro-inflammatory state following efferocytosis, with exposure of LXR double-knockout macrophages to apoptotic thymocytes resulting in increased expression of several pro-inflammatory mediators including IL1β, MCP-1 and the scavenger receptor MARCO (69).

Given the functional overlap between LXRs and PPARs, it is of no surprise that the observed role of the PPAR family in efferocytosis closely parallels the role of LXRs. As with LXRs, PPARs have previously been implicated in macrophage polarization and in enhancing lipids metabolism and synthesis of lipid-derived molecules such as eicosanoids and arachidonic acid (72). Similar to the LXR family of transcription factors, activation of certain members of the PPAR family, including PPARγ and PPARδ, appear to directly enhance efferocytic activity in macrophages (63, 66, 73). Majai et al. demonstrated that downregulation of PPARγ activity using a small-molecule inhibitor resulted in a diminished capacity of human monocyte-derived macrophages to efferocytosed apoptotic neutrophils (66). This resulted from the downregulation of several key efferocytic receptors including CD36, AXL, TG2 and PTX3 (66). Using PPARγ-specific agonists, Zizzo & Cohen demonstrated that PPARγ activation leads directly to upregulation of MERTK and its opsonin Gas6 in macrophages, as well as to polarization of macrophages to a pro-efferocytic M2c phenotype (74). Furthermore, efferocytosis of apoptotic cells by macrophages has been shown to directly suppress key inflammatory pathways, including activation of PKCα, a kinase involved in many cellular functions including inflammatory cytokine transcription and the generation of bactericidal free radicals (64). Indeed, activation of PPARγ in response to efferocytosis of apoptotic cells in murine macrophages has been shown to attenuate reactive oxygen species formation in response to proinflammatory mediators (64). Similarly, efferocytosis induces the expression of SOCS1 and SOCS3, which in turn inhibit Jak/STAT signaling through inflammatory cytokine receptors, thereby reducing the responsiveness of efferocytic macrophages to inflammatory stimuli (75). Finally, the uptake of apoptotic thymocytes by murine bone marrow-derived macrophages has been shown by Mukundan and colleagues to upregulate PPARδ and stimulate PPARδ-dependent expression of C1qb, a member of the complement cascade that has been identified as an opsonin involved in the efferocytic clearance of apoptotic macrophages (63).

Defects in efferocytosis have been implicated in the pathogenesis of several inflammatory and autoimmune disorders, including atherosclerosis (76, 77). Our group recently discovered that atherosclerotic macrophages upregulated the hematopoietic transcription factor GATA2 in response to modified lipoproteins (78). Upregulation of GATA2 led to the downregulation of multiple proteins required for efficient efferocytosis, including downregulation of the efferocytic receptor α_X integrin, multiple signaling molecules required for these receptors function including multiple Src-family kinases, impaired efferosome-lysosome fusion *via* decreased expression of Rab7, and impairment in multiple degradative pathways needed for the degradation of apoptotic cargos including lysosomal acidification (10, 78). Interestingly, mutations in the GATA2 gene has been linked to increased risk of cardiovascular disease in human cohort studies (79). It remains to be seen whether there are other transcription factors that act to impair efferocytosis during autoimmune or inflammatory diseases.

RESOLUTION OF INFLAMMATION

A key feature of efferocytosis is the limitation of inflammation and the resolution of inflammatory responses (5, 9). We have previously discussed how efferosome maturation acts to prevent antigen presentation on MHC II, and how efferocytosis activates transcriptional programs that restrain inflammation (27, 78). It is well established that efferocytosis induces the production of anti-inflammatory mediators (80, 81). Meagher et al. showed as early as 1992 that the uptake of apoptotic neutrophils by macrophages does not lead to release of the pro-inflammatory mediator thromboxane A2, in contrast with phagocytosis of bacterial pathogens (80). Only a few years later Fadok and colleagues demonstrated that efferocytosis in macrophages resulted in suppression of a host of proinflammatory molecules including IL1β, IL8, IL10, GM-CSF and TNFα (81). Furthermore, these investigators determined that efferocytosis upregulated anti-inflammatory mediators including TGFβ and prostaglandin E2 (81).

More recent studies have demonstrated that efferocytic macrophages carry anti-inflammatory functions and gene expression signatures. A landmark study in 2017 showed that pro-efferocytic macrophages across various tissues carried a distinct gene expression signature that differentiated them from other tissue-resident macrophages (14). In particular, this pro-efferocytic signature is characterized by downregulation of the inflammatory cytokine IL1β (14). Campana et al. further demonstrated that in a sterile liver inflammation model, efferocytosis of apoptotic hepatocytes induced a M2-like phenotype and activation of the STAT3-IL6-IL10 pathway (82). Finally, in an acute coronary ligature model, Howangyin and colleagues demonstrated that mouse macrophages lacking the efferocytic receptor MERTK and its opsonin MFGE8 had decreased production of the vascular tissue repair factor VEGF-A and increased tissue damage in a model of myocardial infarct (83).

Beyond simply downregulating the production of pro-inflammatory factors, there is growing evidence that efferocytosis also directly induces the resolution of inflammation (61, 84). Specialized pro-resolving mediators (SPMs) are a class of signaling molecules including resolvins and lipoxins that are derived from free fatty acids that play a key role in limiting inflammation in physiological settings (85). The work of Cai et al. demonstrated that mice lacking the efferocytic receptor MERTK have decreased levels of LXA_4 and RvD1 when challenged with zymosan in a model of inducible peritonitis (86). These authors further demonstrated that activation of MERTK using a cross-linking antibody resulted in decreased levels of the enzyme 5-lipooxygenase in the macrophage nucleus, which has previously been shown to result in increased SPM production (86). Interestingly, SPM signaling enhances the efferocytic capacity of

macrophages and reduces their sensitivity to efferocytosis-induced cell stress, suggesting that SPM production may be a self-reinforcing stimuli which acts in an autocrine or paracrine manner to enhance the efferocytic capacity within a tissue when apoptotic cells are present (87, 88).

EFFEROCYTE METABOLISM

The uptake and degradation of apoptotic cells places a unique metabolic demand on efferocytes (89). These cells must not only quickly degrade the apoptotic cell, but must also ensure that components of the degraded apoptotic cell - especially excess lipids and cholesterol - are redistributed and not allowed to accumulate within the efferocyte (90, 91). A failure to prevent the accumulation of metabolites such as cholesterol and lipids is a source of significant cellular stress that promotes inflammation and can lead to the death of the efferocyte (92, 93). Evidence indicates that efferocytes such as macrophages have unique means of dealing with this additional metabolic load (94, 95). Lipid catabolism is enhanced *via* a distinctive metabolome characterized by an increase in the generation of ATP from the β-oxidation, accompanied by a concordant enhancement of the mitochondrial electron transport chain, fatty acid oxidation, and oxidative phosphorylation (**Figure 2**) (94). These adaptations allow efferocytes to rapidly process excess lipids obtained from internalized apoptotic cells.

Efferocytes have multiple molecular mechanisms in place to deal with the metabolic stress induced by cholesterol accumulation, most of which converge on increasing the rate of cholesterol export from the cell (96, 97). Following uptake of an apoptotic cell, cholesterol is exported from the efferosome by NPC1 and NPC2 to cytosolic cholesterol carriers (98). These carriers transport cholesterol throughout the cell, but in the absence of cholesterol export, these carriers ultimately deliver cholesterol to the ER (98, 99). Here, cholesterol accumulates within the ER membrane, eventually forming lipid droplets (100). Unaddressed, these droplets can accumulate to the point where they induce the ER's unfolded protein response, leading to apoptosis of the efferocyte (92). Efferocytes such as macrophages

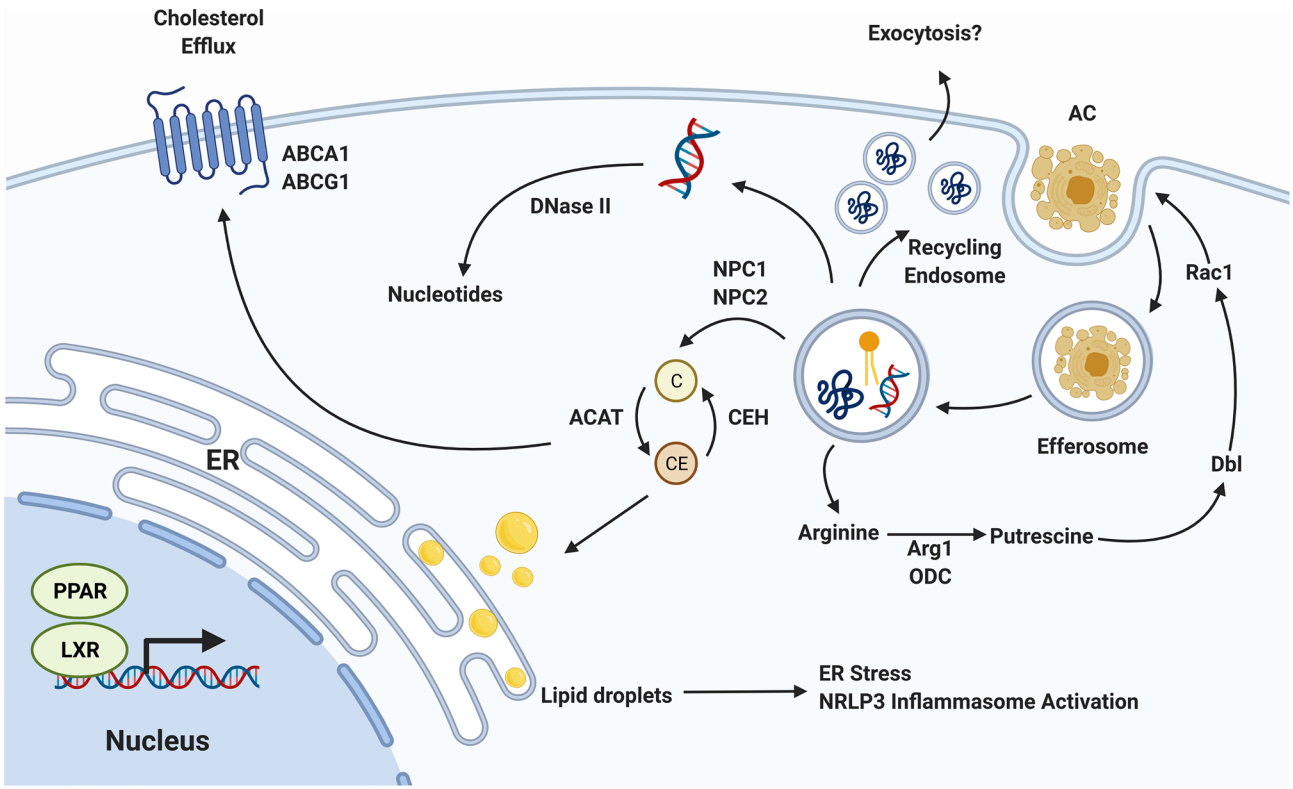

FIGURE 2 | Efferocyte Metabolism. The biomolecules released as efferocytosed apoptotic cells are degraded must be processed by the efferocyte, incurring a significant metabolic load. Cholesterol (C) is exported from the efferosome to cytosolic carriers which, in the presence of cholesterol transporters such as pABCA1 and ABCG1, can export this cholesterol to circulating high density lipoprotein. In the absence of sufficient export, cholesterol is esterified into cholesterol esters (CE) which can accumulate in the endoplasmic reticulum (ER). DNA is degraded in the efferosome by DNase II, and proteins by a range of cathepsin and other proteases, with the resulting nucleotides and amino acids transported into the cytosol where they are recycled. The amino acid arginine is converted in the cytosol to the putrescine, which activates Dbl to enhance Rac1 activity, thereby promoting the efferocytosis of additional apoptotic cells. Lastly, the activation or PPAR and LXR nuclear receptors by lipid-derived metabolites induces a pro-efferocytic metabolic profile *via* upregulation of cholesterol export machinery and upregulation of lipid β-oxidation. Figure prepared in BioRender.

increase the expression of genes involved in cholesterol export to avoid this fate, notably the cholesterol efflux pumps ABCA1 and ABCG1, which export cytosolic cholesterol to lipid-poor apolipoproteins and HDL (**Figure 2**) (101, 102). Macrophages have multiple pathways by which these cholesterol efflux pumps can be induced. This includes the induction of ABCA1 transcription by LXR following apoptotic cell uptake (103). In parallel, signaling through the efferocytic receptor BAI1 induces a signaling through the BAI1/ELMO/Rac1 pathway that leads to upregulation of ABCA1 in an LXR-independent manner (104). Both the LXR-dependent and -independent pathways enable macrophages to export excess cholesterol absorbed during efferocytosis, thus maintaining cholesterol homeostasis within the cell and avoiding death of the efferocyte (103, 104). The consequences of impaired cholesterol efflux can be dire. The increased ER stress caused by lipid droplet formation not only leads to death *via* the unfolded protein response but is also inflammatory due to activation of the NLRP3 inflammasome (105). In addition to causing cell death, the accumulation of cholesterol can directly impair efferocytosis. In one study, Viaud et al. inhibited lysosomal acid lipase, an enzyme required for hydrolysis of cholesterol esters within lysosomes into free cholesterol prior to their export *via* NPC1/2 to cytosolic carriers (106). This resulted in accumulation of cholesterol esters within the lysosome interfered with Rac1 activation, blocking the engulfment of additional apoptotic cells (106).

In addition to excess lipids and cholesterol, efferocytes must also deal with excess amino acids, short peptides, and apoptotic cell DNA (107). While amino acids and peptides are exported from efferosomes by lysosomal transporters, and via trafficking to the recycling endosome, apoptotic cell DNA is degraded by DNase II in professional efferocytes such as macrophages (108). This is a critical step in maintaining the immunologically silent nature of efferocytosis, with deletion of DNase II from macrophages resulting in the upregulation of pro-inflammatory mediators such as TNFα, likely *via* activation of TLR9 by partially digested DNA fragments containing unmethylated CpG motifs (108, 109).

Another important alteration to cellular metabolism following efferocytosis are those allowing for additional rounds of efferocytosis (110). Professional efferocytes such as macrophages must often clear multiple apoptotic cells in succession, and impaired clearance of multiple apoptotic cells is regarded as a marker of defective efferocytosis (110, 111). Several components of cellular metabolism are altered in order to facilitate continuous efferocytosis. Wang et al. showed that efferocytic uptake of apoptotic cells induced Drp1-mediated mitochondrial fission along with mitochondrial calcium ion release (110). When this fission process was inhibited macrophages lost their ability to successively engulf apoptotic cells. These macrophages exhibited defective sealing of the efferosome and decreased continuous efferocytic capacity (110). Interestingly, this process is accompanied by a loss of mitochondrial membrane potential driven by the uncoupling protein Ucp2, increased glucose uptake *via* SLC2A1, and a shift to glycolysis over oxidative phsophroylation (2, 111, 112). In parallel, these cells upregulate the lactate transporter SLC16A1, enabling the rapid export of the end-product of glycolysis (112). This shift in cellular energetics may be required to sustain rapid, successive apoptotic cell uptake and degradation, although how the decoupling of oxidative phosphorylation observed in these studies occurs in cells seemingly also requiring increased oxidative phosphorylation for the β-oxidation of fatty acids remains unresolved (94, 95, 112). Broadly speaking, mitochondrial fission and fusion are important processes that serve to regulate mitochondrial DNA segregation, mitochondrial reactive oxygen species levels and calcium homeostasis (113). These processes have also been shown to be coupled to particular metabolic states in macrophages (113, 114). For example, classically activated, pro-inflammatory macrophages require massive upregulation of glycolysis within the cell (114). Nair et al. demonstrated that blockade of mitochondrial fission with Mdivi-1, a mitochondrial division inhibitor, led to reversal of metabolic reprogramming towards glycolysis in macrophages treated with LPS (115). Therefore, alteration of mitochondrial fusion and fission following efferocytosis may represent alignment with the unique metabolic state adopted by efferocytes following apoptotic cell internalization. Finally, recent work has shown that apoptotic cell-derived arginine and ornithine are converted by macrophages into to putrescine through the activity of the enzymes arginase 1 and ornithine decarboxylase (116). Putrescine subsequently increases Rac1 activity through upregulation of the GTP exchange factor Dbl, enhancing the ability of the efferocyte to engulf additional apoptotic cells (**Figure 2**) (116). During efferocytosis, macrophages further process putrescine into other polyamines such as spermidine and spermine, but these don't appear to have the same efferocytosis-enhancing effect as putrescine (116). However, it should be noted that some polyamines, in particular spermidine, confer protection from atherosclerosis by promoting enhanced cholesterol efflux and appear to have cardioprotective effects in animal models of heart failure (117, 118).

HOST DEFENSE

An often-underappreciated role of efferocytosis is its role in host defense (3, 119). Efferocytosis plays an important role in control of intracellular pathogens, most notably, control of *Mycobacterium tuberculosis* (120). In its natural life cycle, *M. tuberculosis* is internalized by macrophages, where it persists within the phagosome by halting phagosome maturation prior to acidification (121). But while *M. tuberculosis* can proliferate within these phagosomes, the infected macrophages eventually undergo apoptosis and are cleared through efferocytosis by other, healthy macrophages (3, 121). Because the bacterium is trapped within the apoptotic cell, it is unable to inhibit efferosome maturation as efficiently as it inhibits phagosome maturation (122). Consequentially, the clearance of infected macrophages by efferocytosis is an important mechanism for controlling *M. tuberculosis* through killing within fully matured efferosomes (3, 120). Importantly, the efferocytic degradation of *M. tuberculosis*-infected apoptotic cells results in antigen presentation on MHC II – unlike what is observed with uninfected apoptotic cells. While the exact mechanism which

allows for the normally non-immunogenic efferocytic pathway to result in antigen presentation remains unclear, it is mediated at least in part by annexin 1, which is required for cross-presentation of *M. tuberculosis* antigens on MHC I to CD8+ T cells (123).

The ability of macrophages to recognize intracellular pathogens within infected apoptotic cells is a relatively new finding, and the mechanisms that underlie this process remain incompletely defined. It is thought that engagement of TLRs within the maturing efferosome is required, with TLR4 known to be required for the recognition of infected apoptotic cells in other models (124). The detection of pathogens within apoptotic cells is not restricted to bacteria. Efferocytosis of apoptotic cells infected by the herpes simplex virus appears to trigger recognition within the efferosome and subsequent preparation and cross-presentation of viral antigens to CD8+ T cells, where it plays an important role in the control of the virus in a mouse models of infection (125).

It is also unclear whether differences exist in how efferocytes handle the processing of excess cholesterol, lipids and nucleic acids derived from apoptotic cell uptake should that cell be infected with an intracellular pathogen. Indeed, the lipidomic response to pathogen phagocytosis appears to be the opposite of that following efferocytosis. Lipid synthesis is increased following pathogen phagocytosis, including synthesis of ceramides on the phagosome itself (126), and an accompanying upregulation of lipogenesis *via* TLR-mediated activation of the transcription factors sterol regulatory element binding transcription factor 1 and 2 (SREBP1/2) (127–130). To our knowledge however, no study to date has examined whether a similar phenomenon occurs in maturing efferosomes or whether there is any difference in how efferocytes handle excess lipids and other metabolites following uptake of an infected apoptotic cell.

DISCUSSION

Efferocytosis is an essential homeostatic mechanism which clears apoptotic cells and debris before the dying cell progresses to necrosis and induces an inflammatory response (1, 13). Although mechanistically similar to phagocytosis, efferocytosis is mediated by a distinct set of receptors, engages a unique maturation pathway, and ultimately results in the efficient degradation of internalized apoptotic cells while avoiding antigen presentation and inflammation (16). To engage in efferocytosis, macrophages take on a unique gene expression and metabolic profile to ensure they are equipped with the necessary metabolic capacity to process the contents of multiple dying cells (14, 94). In this review, we explored several cellular responses to apoptotic cell uptake observed in efferocytes, especially in professional efferocytic cells such as macrophages.

The process of efferosome maturation is similar to that of phagosome maturation, with processes ultimately resulting in cargo degradation (8). However, while phagosomes acquire antigen-presentation machinery – resulting in the presentation of phagosome-derived antigens on both MHC I and II – efferosomes avoid this process and instead dispose of apoptotic cargo in an immunologically silent fashion (1, 28). Similarly, while phagocytosis results in activation of several signaling cascades that lead to generation of a pro-inflammatory response, efferocytosis engages a different set of pathways which upregulate anti-inflammatory and tissue remodeling mediators. This is accomplished through the activation of distinct transcription factors in cells undergoing phagocytosis versus efferocytosis. Indeed, efferocytic macrophages carry a common gene expression signature associated with these functions that distinguish them from pro-inflammatory, tissue patrolling, and other tissue-resident macrophages (14). Efferocytosis of apoptotic cells also appears to induce a unique set of metabolic adaptations designed to permit the efferocyte to effectively deal with the increase burden of lipids, cholesterol and other apoptotic cell-derived macromolecules, while simultaneously priming the cell to engage in additional rounds of efferocytosis (94, 110). Finally, efferocytosis has a role in host defense against intracellular pathogens, including both bacteria and viruses (119, 120, 125).

Although there have been significant advances in our understanding of efferocytosis over the past few decades, there remain significant gaps in our understanding – especially regarding the role of efferocytosis in pathogen clearance, and in our understanding of the metabolic reprogramming of efferocytes. In particular, we current lack a detailed mechanistic understanding of how efferocytes are able to distinguish between infected versus non-infected apoptotic cells. It is further unclear how efferocytes respond metabolically to infected apoptotic cells. Furthermore, it remains unclear whether differences in immunological outcomes following pathogen versus apoptotic cell uptake are solely the result of differences in the receptors used to recognize each type of cargo, or if the processing of cargo within the phagosome or efferosome also plays a significant role. Finally, we are only beginning to unravel the complexities of immunometabolic responses to apoptotic cell uptake and further work is needed to fully define how efferocytes are able to cope efficiently with the massive intake of lipids, proteins and nucleic acids. With a growing body of evidence that defects in efferocytosis are involved in inflammatory and autoimmune disease, a clearer understanding of how professional efferocytes such as macrophages respond to apoptotic cell uptake will be crucial in furthering our understanding of the pathogenesis of these disorders and identifying potential therapeutic options.

AUTHOR CONTRIBUTIONS

CY and BH contributed equally to the authoring of this manuscript. All authors contributed to the article and approved the submitted version.

FUNDING

This study was funded by a Heart and Stroke Foundation of Canada Grant-In-Aid and an Ontario Ministry of Research and Innovation Early Research Award to BH. CY was funded by a Vanier PhD Scholarship and Canadian Institutes for Health Research (CIHR) MD/PhD studentship.

REFERENCES

1. Henson PM. Cell Removal: Efferocytosis. *Annu Rev Cell Dev Biol* (2017) 33:1–18. doi: 10.1146/annurev-cellbio-111315-125315
2. Morioka S, Maueröder C, Ravichandran KS. Living on the Edge: Efferocytosis at the Interface of Homeostasis and Pathology. *Immunity* (2019) 50(5):1149–62. doi: 10.1016/j.immuni.2019.04.018
3. Martin CJ, Peters KN, Behar SM. Macrophages Clean Up: Efferocytosis and Microbial Control. *Curr Opin Microbiol* (2014) 17:17–23. doi: 10.1016/j.mib.2013.10.007.Macrophages
4. Brill A, Torchinsky A, Carp H, Toder V. The role of apoptosis in normal and abnormal embryonic development. *J Assist Reprod Genet* (1999) 16:512–9. doi: 10.1023/A:1020541019347
5. Sachet M, Liang YY, Oehler R. The immune response to secondary necrotic cells. *Apoptosis* (2017) 22(10):1189–204. doi: 10.1007/s10495-017-1413-z
6. Tabas I. 2016 Russell Ross Memorial Lecture in Vascular Biology. *Arterioscler Thromb Vasc Biol* (2016) 37(2):183–9. doi: 10.1161/ATVBAHA.116.308036
7. Freeman SA, Grinstein S. Phagocytosis: Receptors, signal integration, and the cytoskeleton. *Immunol Rev* (2014) 262:193–215. doi: 10.1111/imr.12212
8. Kinchen JM, Ravichandran KS. Phagosome maturation: going through the acid test. *Nat Rev Mol Cell Biol* (2008) 9:781–95. doi: 10.1038/nrm2515
9. Nagata S. Apoptosis and Clearance of Apoptotic Cells. *Annu Rev Immunol* (2018) 361829:1–18. doi: 10.1146/annurev-immunol
10. Blackburn JWD, Lau DHC, Liu EY, Ellins J, Vrieze AM, Pawlak EN, et al. Soluble CD93 is an apoptotic cell opsonin recognized by $\alpha_x\beta_2$. *Eur J Immunol* (2019) 49(4):1–23. doi: 10.1002/eji.201847801
11. Thorp E, Subramanian M, Tabas I. The role of macrophages and dendritic cells in the clearance of apoptotic cells in advanced atherosclerosis. *Eur J Immunol* (2011) 41:2515–8. doi: 10.1002/eji.201141719
12. Gregory CD, Pound JD. Cell death in the neighbourhood: Direct microenvironmental effects of apoptosis in normal and neoplastic tissues. *J Pathol* (2011) 223:177–94. doi: 10.1002/path.2792
13. Gordon S, Plüddemann A. Macrophage Clearance of Apoptotic Cells: A Critical Assessment. *Front Immunol* (2018) 9:127. doi: 10.3389/fimmu.2018.00127
14. A-Gonzalez N, Quintana JA, García-Silva S, Mazariegos M, González de la Aleja A, Nicolás-Ávila JA, et al. Phagocytosis imprints heterogeneity in tissue-resident macrophages. *J Exp Med* (2017) 214:1281–96. doi: 10.1084/jem.20161375
15. Cochain C, Vafadarnejad E, Arampatzi P, Pelisek J, Winkels H, Ley K, et al. Single-Cell RNA-Seq Reveals the Transcriptional Landscape and Heterogeneity of Aortic Macrophages in Murine Atherosclerosis. *Circ Res* (2018) 122:1661–74. doi: 10.1161/CIRCRESAHA.117.312509
16. Kinchen JM, Doukoumetzidis K, Almendinger J, Stergiou L, Tosello-Trampont A, Sifri CD, et al. A pathway for phagosome maturation during engulfment of apoptotic cells. *Nat Cell Biol* (2008) 10:556–66. doi: 10.1038/ncb1718
17. Roberts RL, Barbieri MA, Ullrich J, Stahl PD. Dynamics of rab5 activation in endocytosis and phagocytosis. *J Leukoc Biol* (2000) 68:627–32.
18. Harrison RE, Bucci C, Vieira OV, Schroer TA, Grinstein S. Phagosomes fuse with late endosomes and/or lysosomes by extension of membrane protrusions along microtubules: role of Rab7 and RILP. *Mol Cell Biol* (2003) 23:6494–506. doi: 10.1128/MCB.23.18.6494
19. Mills IG, Jones AT, Clague MJ. Involvement of the endosomal autoantigen EEA1 in homotypic fusion of early endosomes. *Curr Biol* (1998) 8:881–4. doi: 10.1016/S0960-9822(07)00351-X
20. Gorvel JP, Chavrier P, Zerial M, Gruenberg J. Rab5 Controls Early Endosome Fusion in Vitro. *Cell* (1991) 64:915–25. doi: 10.1016/0092-8674(91)90316-Q
21. Simonsen A, Gaullier JM, D'Arrigo A, Stenmark H. The Rab5 effector EEA1 interacts directly with syntaxin-6. *J Biol Chem* (1999) 274:28857–60. doi: 10.1074/jbc.274.41.28857
22. Chen YA, Scheller RH. SNARE-mediated membrane fusion. *Nat Rev Mol Cell Biol* (2001) 2:98–106. doi: 10.1038/35052017
23. Taefehshokr N, Yin C, Heit B. Rab GTPases in the differential processing of phagocytosed pathogens versus efferocytosed apoptotic cells. *Histol Histopathol* (2020) 18252. doi: 10.14670/HH-18-252
24. Flannagan RS, Jaumouillé V, Grinstein S. The Cell Biology of Phagocytosis. *Annu Rev Pathol* (2011) 7:61–98. doi: 10.1146/annurev-pathol-011811-132445
25. Poteryaev D, Datta S, Ackema K, Zerial M, Spang A. Identification of the switch in early-to-late endosome transition. *Cell* (2010) 141:497–508. doi: 10.1016/j.cell.2010.03.011
26. Cui Y, Zhao Q, Gao C, Ding Y, Zeng Y, Ueda T, et al. Activation of the Rab7 GTPase by the MON1-CCZ1 Complex Is Essential for PVC-to-Vacuole Trafficking and Plant Growth in Arabidopsis. *Plant Cell* (2014) 26:2080–97. doi: 10.1105/tpc.114.123141
27. Yin C, Kim Y, Argintaru D, Heit B. Rab17 mediates differential antigen sorting following efferocytosis and phagocytosis. *Cell Death Dis* (2016) 7:e2529. doi: 10.1038/cddis.2016.431
28. Yin C, Argintaru D, Heit B. Rab17 mediates intermixing of phagocytosed apoptotic cells with recycling endosomes. *Small GTPases* (2017) 1–9. doi: 10.1080/21541248.2017.1308852
29. Yin J, Huang Y, Guo P, Hu S, Yoshina S, Xuan N, et al. GOP-1 promotes apoptotic cell degradation by activating the small GTPase Rab2 in C. elegans. *J Cell Biol* (2017) 216:1775–94. doi: 10.1083/jcb.201610001
30. Ward MG, Li G, Hao M. Apoptotic beta-cells induce macrophage reprogramming under diabetic conditions. *J Biol Chem* (2018) 293(42):16160–73. doi: 10.1074/jbc.RA118.004565
31. Li B, Castano AP, Hudson TE, Nowlin BT, Lin S-L, Bonventre JV, et al. The melanoma-associated transmembrane glycoprotein Gpnmb controls trafficking of cellular debris for degradation and is essential for tissue repair. *FASEB J* (2010) 24:4767–81. doi: 10.1096/fj.10.154757
32. Heckmann BL, Green DR. LC3-associated phagocytosis at a glance. *J Cell Sci* (2019) 132. doi: 10.1242/jcs.231472
33. Wan J, Weiss E, Ben Mkaddem S, Mabire M, Choinier P-M, Picq O, et al. LC3-associated phagocytosis protects against inflammation and liver fibrosis via immunoreceptor inhibitory signaling. *Sci Transl Med* (2020) 12:eaaw8523. doi: 10.1126/scitranslmed.aaw8523
34. Blander JM, Medzhitov R. Toll-dependent selection of microbial antigens for presentation by dendritic cells. *Nature* (2006) 440:808–12. doi: 10.1038/nature04596
35. Blander JM, Medzhitov R. Regulation of Phagosome Maturation by Signals from Toll-Like Receptors. *Science* (2011) 1014:1014–8. doi: 10.1126/science.1096158
36. Blander JM, Medzhitov R. On regulation of phagosome maturation and antigen presentation. *Nat Immunol* (2006) 7:1029–35. doi: 10.1038/ni1006-1029
37. Seto S, Sugaya K, Tsujimura K, Nagata T, Horii T, Koide Y. Rab39a interacts with phosphatidylinositol 3-kinase and negatively regulates autophagy induced by lipopolysaccharide stimulation in macrophages. *PloS One* (2013) 8:1–13. doi: 10.1371/journal.pone.0083324
38. Cruz FM, Colbert JD, Rock KL. The GTP ase Rab39a promotes phagosome maturation into MHC -I antigen-presenting compartments. *EMBO J* (2020) 39:1–21. doi: 10.15252/embj.2019102020
39. Martinez J, Malireddi RKS, Lu Q, Cunha LD, Pelletier S, Gingras S, et al. Molecular characterization of LC3-associated phagocytosis reveals distinct roles for Rubicon, NOX2 and autophagy proteins. *Nat Cell Biol* (2015) 17:893–906. doi: 10.1038/ncb3192
40. Bhargava HK, Tabata K, Byck JM, Hamasaki M, Farrell DP, Anishchenko I, et al. Structural basis for autophagy inhibition by the human Rubicon-Rab7 complex. *Proc Natl Acad Sci USA* (2020) 117:17003–10. doi: 10.1073/pnas.2008030117
41. Wong SW, Sil P, Martinez J. Rubicon: LC3-associated phagocytosis and beyond. *FEBS J* (2018) 285:1379–88. doi: 10.1111/febs.14354
42. Erwig L-P, McPhilips KA, Wynes MW, Ivetic A, Ridley AJ, Henson PM. Differential regulation of phagosome maturation in macrophages and dendritic cells mediated by Rho GTPases and ezrin–radixin–moesin (ERM) proteins. *Proc Natl Acad Sci USA* (2006) 103:12825–30. doi: 10.1155/2015/359153
43. Canton J, Khezri R, Glogauer M, Grinstein S. Contrasting phagosome pH regulation and maturation in human M1 and M2 macrophages. *Mol Biol Cell* (2014) 25:3330–41. doi: 10.1091/mbc.E14-05-0967
44. De Luca M, Cogli L, Progida C, Nisi V, Pascolutti R, Sigismund S, et al. RILP regulates vacuolar ATPase through interaction with the V1G1 subunit. *J Cell Sci* (2015) 128:2565–5. doi: 10.1242/jcs.175323

45. Trivedi PC, Bartlett JJ, Pulinilkunnil T. Lysosomal Biology and Function: Modern View of Cellular Debris Bin. *Cells* (2020) 9:1–35. doi: 10.3390/cells9051131
46. Rai A, Pathak D, Thakur S, Singh S, Dubey AK, Mallik R. Dynein Clusters into Lipid Microdomains on Phagosomes to Drive Rapid Transport toward Lysosomes. *Cell* (2016) 164:722–34. doi: 10.1016/j.cell.2015.12.054
47. Fairn GD, Grinstein S. How nascent phagosomes mature to become phagolysosomes. *Trends Immunol* (2012) 33(8):1–9. doi: 10.1016/j.it.2012.03.003
48. Heo YJ, Bin JY, Oh HJ, Park MK, Heo YM, Cho M, et al. IL-10 suppresses Th17 cells and promotes regulatory T cells in the CD4+ T cell population of rheumatoid arthritis patients. *Immunol Lett* (2010) 127:150–6. doi: 10.1016/j.imlet.2009.10.006
49. Rodriguez-Fernandez S, Pujol-Autonell I, Brianso F, Perna-Barrull D, Cano-Sarabia M, Garcia-Jimeno S, et al. Phosphatidylserine-liposomes promote tolerogenic features on dendritic cells in human type 1 diabetes by apoptotic mimicry. *Front Immunol* (2018) 9:253. doi: 10.3389/fimmu.2018.00253
50. Yurdagul A, Doran AC, Cai B, Fredman G, Tabas IA. Mechanisms and Consequences of Defective Efferocytosis in Atherosclerosis. *Front Cardiovasc Med* (2017) 4:1–10. doi: 10.3389/fcvm.2017.00086
51. Abdolmaleki F, Farahani N, Hayat SMG, Pirro M, Bianconi V, Barreto GE, et al. The role of efferocytosis in autoimmune diseases. *Front Immunol* (2018) 9:1645. doi: 10.3389/fimmu.2018.01645
52. Kimani SG, Geng K, Kasikara C, Kumar S, Sriram G, Wu Y, et al. Contribution of Defective PS Recognition and Efferocytosis to Chronic Inflammation and Autoimmunity. *Front Immunol* (2014) 5:566. doi: 10.3389/fimmu.2014.00566
53. Zizzo G, Guerrieri J, Dittman LM, Merrill JT, Cohen PL. Circulating levels of soluble MER in lupus reflect M2c activation of monocytes/macrophages, autoantibody specificities and disease activity. *Arthritis Res Ther* (2013) 15:R212–R227. doi: 10.1186/ar4407
54. Waterborg CEJ, Beermann S, Broeren MGA, Bennink MB, Alves-filho JC. Protective role of the Mer Tyrosine Kinase via efferocytosis in rheumatoid arthritis Models. *Front Immunol* (2018) 9:742. doi: 10.3389/fimmu.2018.00742
55. Ma GZM, Stankovich J, Kilpatrick TJ, Binder MD, Field J, Bahlo M, et al. Polymorphisms in the receptor tyrosine kinase MERTK gene are associated with Multiple Sclerosis susceptibility. *PloS One* (2011) 6:2–7. doi: 10.1371/journal.pone.0016964
56. Zaza R, Ibayyan L, El-Khateeb M, Bahou YG, Khreisat E, Al-Khateeb W, et al. Association of genetic polymorphisms of MERTK with multiple sclerosis among Jordanians. *BioMed Res* (2017) 28:399–404.
57. Binder MD, Fox AD, Merlo D, Johnson LJ, Giuffrida L, Calvert SE, et al. Common and Low Frequency Variants in MERTK Are Independently Associated with Multiple Sclerosis Susceptibility with Discordant Association Dependent upon HLA-DRB1*15:01 Status. *PloS Genet* (2016) 12:1–25. doi: 10.1371/journal.pgen.1005853
58. Canton J, Blees H, Henry CM, Buck MD, Schulz O, Rogers NC, et al. The receptor DNGR-1 signals for phagosomal rupture to promote cross-presentation of dead-cell-associated antigens. *Nat Immunol* (2021) 22:140–53. doi: 10.1038/s41590-020-00824-x
59. Rock KL, Reits E, Neefjes J. Present Yourself! By MHC Class I and MHC Class II Molecules. *Trends Immunol* (2016) 37:724–37. doi: 10.1016/j.it.2016.08.010
60. Zhang N, Bevan MJ. CD8(+) T cells: foot soldiers of the immune system. *Immunity* (2011) 35:161–8. doi: 10.1016/j.immuni.2011.07.010
61. Korns D, Frasch SC, Fernandez-Boyanapalli R, Henson PM, Bratton DL. Modulation of macrophage efferocytosis in inflammation. *Front Immunol* (2011) 2:57. doi: 10.3389/fimmu.2011.00057
62. Rébé C, Raveneau M, Chevriaux A, Lakomy D, Sberna A-L, Costa A, et al. Induction of transglutaminase 2 by a liver X receptor/retinoic acid receptor alpha pathway increases the clearance of apoptotic cells by human macrophages. *Circ Res* (2009) 105:393–401. doi: 10.1161/CIRCRESAHA.109.201855
63. Mukundan L, Odegaard JI, Morel CR, Heredia JE, Mwangi JW, Ricardo-gonzalez RR, et al. PPAR- δ senses and orchestrates clearance of apoptotic cells to promote tolerance. *Nat Med* (2009) 15:1266–73. doi: 10.1038/nm.2048
64. Johann AM, von Knethen A, Lindemann D, Brüne B. Recognition of apoptotic cells by macrophages activates the peroxisome proliferator-activated receptor-γ and attenuates the oxidative burst. *Cell Death Differ* (2006) 13:1533–40. doi: 10.1038/sj.cdd.4401832
65. Penvose A, Keenan JL, Bray D, Ramlall V, Siggers T. Comprehensive study of nuclear receptor DNA binding provides a revised framework for understanding receptor specificity. *Nat Commun* (2019) 10:1–15. doi: 10.1038/s41467-019-10264-3
66. Majai G, Sarang Z, Csomós K, Zahuczky G, Fésüs L. PPARγ-dependent regulation of human macrophages in phagocytosis of apoptotic cells. *Eur J Immunol* (2007) 37:1343–54. doi: 10.1002/eji.200636398
67. Wang LH, Yang XY, Zhang X, Huang J, Hou J, Li J, et al. Transcriptional Inactivation of STAT3 by PPARγ Suppresses IL-6-Responsive Multiple Myeloma Cells. *Immunity* (2004) 20:205–18. doi: 10.1016/S1074-7613(04)00030-5
68. Wang B, Tontonoz P. Liver X receptors in lipid signalling and membrane homeostasis. *Nat Rev Endocrinol* (2018) 14:452–63. doi: 10.1038/s41574-018-0037-x
69. A-Gonzalez N, Bensinger SJ, Hong C, Beceiro S, Bradley MN, Zelcer N, et al. Apoptotic cells promote their own clearance and immune tolerance through activation of the nuclear receptor LXR. *Immunity* (2009) 31:245–58. doi: 10.1016/j.immuni.2009.06.018
70. Pastore M, Grimaudo S, Pipitone RM, Lori G, Raggi C, Petta S, et al. Role of myeloid-epithelial-reproductive tyrosine kinase and macrophage polarization in the progression of atherosclerotic lesions associated with nonalcoholic fatty liver disease. *Front Pharmacol* (2019) 10:604. doi: 10.3389/fphar.2019.00604
71. Zhang B, Fang L, Wu HM, Ding PS, Xu K, Liu RY. Mer receptor tyrosine kinase negatively regulates lipoteichoic acid-induced inflammatory response via PI3K/Akt and SOCS3. *Mol Immunol* (2016) 76:98–107. doi: 10.1016/j.molimm.2016.06.016
72. Berger J, Moller DE. The mechanisms of action of PPARs. *Annu Rev Med* (2002) 53:409–35. doi: 10.1146/annurev.med.53.082901.104018
73. Croasdell A, Duffney PF, Kim N, Lacy SH, Sime PJ, Phipps RP. PPARy and the Innate Immune System Mediate the Resolution of Inflammation. *PPAR Res* (2015) 2015:1–20. doi: 10.1155/2015/549691
74. Zizzo G, Cohen PL. The PPAR-γ antagonist GW9662 elicits differentiation of M2c-like cells and upregulation of the MerTK/Gas6 axis: A key role for PPAR-γ in human macrophage polarization. *J Inflamm (United Kingdom)* (2015) 12:1–16. doi: 10.1186/s12950-015-0081-4
75. Gordon P, Okai B, Hoare JI, Erwig LP, Wilson HM. SOCS3 is a modulator of human macrophage phagocytosis. *J Leukoc Biol* (2016) 100:771–80. doi: 10.1189/jlb.3a1215-554rr
76. Thorp E, Tabas I. Mechanisms and consequences of efferocytosis in advanced atherosclerosis. *J Leukoc Biol* (2009) 86:1089–95. doi: 10.1189/jlb.0209115
77. Linton MF, Babaev VR, Huang J, Linton EF, Tao H, Yancey PG. Macrophage Apoptosis and Efferocytosis in the Pathogenesis of Atherosclerosis. *Circ J* (2016) 80:2259–68. doi: 10.1253/circj.CJ-16-0924
78. Yin C, Vrieze AM, Rosoga M, Akingbasote J, Pawlak EN, Jacob RA, et al. Efferocytic Defects in Early Atherosclerosis Are Driven by GATA2 Overexpression in Macrophages. *Front Immunol* (2020) 11:594136. doi: 10.3389/fimmu.2020.594136
79. Muiya NP, Wakil S, Al-Najai M, Tahir AI, Baz B, Andres E, et al. A study of the role of GATA2 gene polymorphism in coronary artery disease risk traits. *Gene* (2014) 544:152–8. doi: 10.1016/j.gene.2014.04.064
80. Meagher LC, Savill JS, Baker A, Fuller RW, Haslett C. Phagocytosis of apoptotic neutrophils does not induce macrophage release of thromboxane B2. *J Leukoc Biol* (1992) 52:269–73. doi: 10.1002/jlb.52.3.269
81. Fadok VA, Bratton DL, Konowal A, Freed PW, Westcott JY, Henson PM. Macrophages that have ingested apoptotic cells in vitro inhibit proinflammatory cytokine production through autocrine/paracrine mechanisms involving TGF-β, PGE2, and PAF. *J Clin Invest* (1998) 101:890–8. doi: 10.1172/JCI1112
82. Campana L, Starkey Lewis PJ, Pellicoro A, Aucott RL, Man J, O'Duibhir E, et al. The STAT3–IL-10–IL-6 Pathway Is a Novel Regulator of Macrophage Efferocytosis and Phenotypic Conversion in Sterile Liver Injury. *J Immunol* (2018) 200:1169–87. doi: 10.4049/jimmunol.1701247

83. Howangyin KY, Zlatanova I, Pinto C, Ngkelo A, Cochain C, Rouanet M, et al. Myeloid-Epithelial-Reproductive Receptor Tyrosine Kinase and Milk Fat Globule Epidermal Growth Factor 8 Coordinately Improve Remodeling after Myocardial Infarction via Local Delivery of Vascular Endothelial Growth Factor. *Circulation* (2016) 133:826–39. doi: 10.1161/CIRCULATIONAHA.115.020857
84. Tabas I. Macrophage death and defective inflammation resolution in atherosclerosis. *Nat Rev Immunol* (2009) 10:36–46. doi: 10.1038/nri2675
85. Lehmann C, Homann J, Ball AK, Blöcher R, Kleinschmidt TK, Basavarajappa D, et al. Lipoxin and resolvin biosynthesis is dependent on 5-lipoxygenase activating protein. *FASEB J* (2015) 29:5029–43. doi: 10.1096/fj.15-275487
86. Cai B, Thorp EB, Doran AC, Subramanian M, Sansbury BE, Lin C-S, et al. MerTK cleavage limits proresolving mediator biosynthesis and exacerbates tissue inflammation. *Proc Natl Acad Sci* (2016) 113:6526–31. doi: 10.1073/pnas.1524292113
87. Lee HN, Surh YJ. Resolvin D1-mediated NOX2 inactivation rescues macrophages undertaking efferocytosis from oxidative stress-induced apoptosis. *Biochem Pharmacol* (2013) 86:759–69. doi: 10.1016/j.bcp.2013.07.002
88. Rymut N, Heinz J, Sadhu S, Hosseini Z, Riley CO, Marinello M, et al. Resolvin D1 promotes efferocytosis in aging by limiting senescent cell-induced MerTK cleavage. *FASEB J* (2020) 34:597–609. doi: 10.1096/fj.201902126R
89. Han CZ, Ravichandran KS. Metabolic connections during apoptotic cell engulfment. *Cell* (2011) 147:1442–5. doi: 10.1016/j.cell.2011.12.006
90. Westover E. Cholesterol in Health and Disease. *J Clin Invest* (2002) 110:583–90. doi: 10.1172/JCI200216381.Imagine
91. Chistiakov DA, Melnichenko AA, Myasoedova VA, Grechko AV, Orekhov AN. Mechanisms of foam cell formation in atherosclerosis. *J Mol Med* (2017) 95:1153–65. doi: 10.1007/s00109-017-1575-8
92. Li Y, Schwabe RF, DeVries-Seimon T, Yao PM, Gerbod-Giannone MC, Tall AR, et al. Free cholesterol-loaded macrophages are an abundant source of tumor necrosis factor-α and interleukin-6: Model of NF-κB- and map kinase-dependent inflammation in advanced atherosclerosis. *J Biol Chem* (2005) 280:21763–72. doi: 10.1074/jbc.M501759200
93. Lara-Guzmán OJ, Gil-Izquierdo Á, Medina S, Osorio E, Álvarez-Quintero R, Zuluaga N, et al. Oxidized LDL triggers changes in oxidative stress and inflammatory biomarkers in human macrophages. *Redox Biol* (2018) 15:1–11. doi: 10.1016/j.redox.2017.11.017
94. Zhang S, Weinberg S, DeBerge M, Gainullina A, Schipma M, Kinchen JM, et al. Efferocytosis Fuels Requirements of Fatty Acid Oxidation and the Electron Transport Chain to Polarize Macrophages for Tissue Repair. *Cell Metab* (2019) 29:443–456.e5. doi: 10.1016/j.cmet.2018.12.004
95. Cummings RJ, Barbet G, Bongers G, Hartmann BM, Gettler K, Muniz L, et al. Different tissue phagocytes sample apoptotic cells to direct distinct homeostasis programs. *Nature* (2016) 539:565–9. doi: 10.1038/nature20138
96. Yvan-Charvet L, Pagler TA, Seimon TA, Thorp E, Welch CL, Witztum JL, et al. ABCA1 and ABCG1 protect against oxidative stress-induced macrophage apoptosis during efferocytosis. *Circ Res* (2010) 106:1861–9. doi: 10.1161/CIRCRESAHA.110.217281
97. Costet P, Lalanne F, Gerbod-Giannone MC, Molina JR, Fu X, Lund EG, et al. Retinoic Acid Receptor-Mediated Induction of ABCA1 in Macrophages. *Mol Cell Biol* (2003) 23:7756–66. doi: 10.1128/mcb.23.21.7756-7766.2003
98. Subramanian K, Balch WE. NPC1/NPC2 function as a tag team duo to mobilize cholesterol. *Proc Natl Acad Sci USA* (2008) 105:15223–4. doi: 10.1073/pnas.0808256105
99. Dron JS, Hegele RA. Genetics of Lipid and Lipoprotein Disorders and Traits. *Curr Genet Med Rep* (2017) 5:115–5. doi: 10.1007/s40142-017-0117-6
100. Tangirala RK, Jerome WG, Jones NL, Small DM, Johnson WJ, Glick JM, et al. Formation of cholesterol monohydrate crystals in macrophage-derived foam cells. *J Lipid Res* (1994) 35:93–104. doi: 10.1016/S0022-2275(20)40131-2
101. Wang X, Collins HL, Ranalletta M, Fuki IV, Billheimer JT, Rothblat GH, et al. Macrophage ABCA1 and ABCG1, but not SR-BI, promote macrophage reverse cholesterol transport in vivo. *J Clin Invest* (2007) 117:2216–24. doi: 10.1172/JCI32057
102. Yvan-Charvet L, Wang N, Tall AR. Role of HDL, ABCA1, and ABCG1 transporters in cholesterol efflux and immune responses. *Arterioscler Thromb Vasc Biol* (2010) 30:139–43. doi: 10.1161/ATVBAHA.108.179283
103. Tamehiro N, Park MH, Hawxhurst V, Nagpal K, Adams ME, Zannis VI, et al. LXR Agonism Upregulates the Macrophage ABCA1/Syntrophin Protein Complex That Can Bind ApoA-I and Stabilized ABCA1 Protein, but Complex Loss Does Not Inhibit Lipid Efflux. *Biochemistry* (2015) 54:6931–41. doi: 10.1021/acs.biochem.5b00894
104. Fond AM, Lee CS, Schulman IG, Kiss RS, Ravichandran KS. Apoptotic cells trigger a membrane-initiated pathway to increase ABCA1. *J Clin Invest* (2015) 125:2748–58. doi: 10.1172/JCI80300
105. Duewell P, Kono H, Rayner KJ, Sirois CM, Vladimer G, Bauernfeind FG, et al. NLRP3 inflammasomes are required for atherogenesis and activated by cholesterol crystals. *Nature* (2010) 464:1357–61. doi: 10.1038/nature08938
106. Viaud M, Ivanov S, Vujic N, Duta-mare M, Aira L, Barouillet T, et al. Lysosomal cholesterol hydrolysis couples efferocytosis to anti-inflammatory oxysterol production. *Circ Res* (2019) 122:1369–84. doi: 10.1161/CIRCRESAHA.117.312333.Lysosomal
107. Boada-romero E, Martinez J, Heckmann BL, Green DR, Group I, Park T. Mechanisms and physiology of the clearance of dead cells by efferocytosis. *Nat Rev Cell Biol* (2020) 21:398–414. doi: 10.1038/s41580-020-0232-1.Mechanisms
108. Kawane K, Ohtani M, Miwa K, Kizawa T, Kanbara Y, Yoshioka Y, et al. Chronic polyarthritis caused by mammalian DNA that escapes from degradation in macrophages. *Nature* (2006) 443:998–1002. doi: 10.1038/nature05245
109. Saito Y, Hikita H, Nozaki Y, Kai Y, Makino Y, Nakabori T, et al. DNase II activated by the mitochondrial apoptotic pathway regulates RIP1-dependent non-apoptotic hepatocyte death via the TLR9/IFN-β signaling pathway. *Cell Death Differ* (2019) 26:470–86. doi: 10.1038/s41418-018-0131-6
110. Wang Y, Subramanian M, Yurdagul A, Barbosa-Lorenzi VC, Cai B, de Juan-Sanz J, et al. Mitochondrial Fission Promotes the Continued Clearance of Apoptotic Cells by Macrophages. *Cell* (2017) 171:331–345.e22. doi: 10.1016/j.cell.2017.08.041
111. Park D, Han CZ, Elliott MR, Kinchen JM, Trampont PC, Das S, et al. Continued clearance of apoptotic cells critically depends on the phagocyte Ucp2 protein. *Nature* (2011) 477:220–4. doi: 10.1038/nature10340
112. Morioka S, Perry JSA, Raymond MH, Medina CB, Zhu Y, Zhao L, et al. Efferocytosis induces a novel SLC program to promote glucose uptake and lactate release. *Nature* (2018) 563(7733):714–8. doi: 10.1038/s41586-018-0735-5
113. Rambold AS, Pearce EL. Mitochondrial Dynamics at the Interface of Immune Cell Metabolism and Function. *Trends Immunol* (2018) 39:6–18. doi: 10.1016/j.it.2017.08.006
114. Benmoussa K, Garaude J, Acín-Pérez R. How Mitochondrial Metabolism Contributes to Macrophage Phenotype and Functions. *J Mol Biol* (2018) 430:3906–21. doi: 10.1016/j.jmb.2018.07.003
115. Nair S, Sobotka KS, Joshi P, Gressens P, Fleiss B, Thornton C, et al. Lipopolysaccharide-induced alteration of mitochondrial morphology induces a metabolic shift in microglia modulating the inflammatory response in vitro and in vivo. *Glia* (2019) 67:1047–61. doi: 10.1002/glia.23587
116. Yurdagul A, Subramanian M, Wang X, Crown SB, Ilkayeva OR, Darville L, et al. Macrophage Metabolism of Apoptotic Cell-Derived Arginine Promotes Continual Efferocytosis and Resolution of Injury. *Cell Metab* (2020) 31:518–533.e10. doi: 10.1016/j.cmet.2020.01.001
117. Eisenberg T, Abdellatif M, Schroeder S, Primessnig U, Stekovic S, Pendl T, et al. Cardioprotection and lifespan extension by the natural polyamine spermidine. *Nat Med* (2016) 22:1428–38. doi: 10.1038/nm.4222
118. Michiels CF, Kurdi A, Timmermans J-P, De Meyer GRY, Martinet W. Spermidine reduces lipid accumulation and necrotic core formation in atherosclerotic plaques via induction of autophagy. *Atherosclerosis* (2016) 251:319–27. doi: 10.1016/j.atherosclerosis.2016.07.899
119. Zheng DJ, Abou Taka M, Heit B. Role of Apoptotic Cell Clearance in Pneumonia and Inflammatory Lung Disease. *Pathogens (Basel Switzerland)* (2021) 10. doi: 10.3390/pathogens10020134
120. Martin CJ, Booty MG, Rosebrock TR, Nunes-Alves C, Desjardins DM, Keren I, et al. Efferocytosis is an innate antibacterial mechanism. *Cell Host Microbe* (2012) 12:289–300. doi: 10.1016/j.chom.2012.06.010
121. Vandal OH, Nathan CF, Ehrt S. Acid resistance in Mycobacterium tuberculosis. *J Bacteriol* (2009) 191:4714–21. doi: 10.1128/JB.00305-09

122. Behar SM, Martin CJ, Booty MG, Nishimura T, Zhao X, Gan HX, et al. Apoptosis is an innate defense function of macrophages against Mycobacterium tuberculosis. *Mucosal Immunol* (2011) 4:279–87. doi: 10.1038/mi.2011.3
123. Tzelepis F, Verway M, Daoud J, Gillard J, Hassani-Ardakani K, Dunn J, et al. Annexin1 regulates DC efferocytosis and cross-presentation during Mycobacterium tuberculosis infection. *J Clin Invest* (2015) 125:752–68. doi: 10.1172/JCI77014
124. Zhang Y, Bliska JB. Role of toll-like receptor signaling in the apoptotic response of macrophages to Yersinia infection. *Infect Immun* (2003) 71:1513–9. doi: 10.1128/IAI.71.3.1513-1519.2003
125. Subramanian M, Hayes CD, Thome JJ, Thorp E, Matsushima GK, Herz J, et al. An AXL/LRP-1/RANBP9 complex mediates DC efferocytosis and antigen cross-presentation in vivo. *J Clin Invest* (2014) 124:1296–308. doi: 10.1172/JCI72051
126. Pathak D, Mehendale N, Singh S, Mallik R, Kamat SS. Lipidomics Suggests a New Role for Ceramide Synthase in Phagocytosis. *ACS Chem Biol* (2018) 13:2280–7. doi: 10.1021/acschembio.8b00438
127. Shimano H, Sato R. SREBP-regulated lipid metabolism: Convergent physiology-divergent pathophysiology. *Nat Rev Endocrinol* (2017) 13:710–30. doi: 10.1038/nrendo.2017.91
128. Jeon T, Osborne TF. SREBPs: Metabolic integrators in physiology and metabolism. *Trends Endocrinol Metab* (2012) 23:65–72. doi: 10.1016/j.tem.2011.10.004
129. Im SS, Yousef L, Blaschitz C, Liu JZ, Edwards RA, Young SG, et al. Linking lipid metabolism to the innate immune response in macrophages through sterol regulatory element binding protein-1a. *Cell Metab* (2011) 13:540–9. doi: 10.1016/j.cmet.2011.04.001
130. Oishi Y, Spann NJ, Link VM, Muse ED, Strid T, Edillor C, et al. SREBP1 Contributes to Resolution of Pro-inflammatory TLR4 Signaling by Reprogramming Fatty Acid Metabolism. *Cell Metab* (2017) 25:412–27. doi: 10.1016/j.cmet.2016.11.009

Conflict of Interest: The authors declare that the research was conducted in the absence of any commercial or financial relationships that could be construed as a potential conflict of interest.

Copyright © 2021 Yin and Heit. This is an open-access article distributed under the terms of the Creative Commons Attribution License (CC BY). The use, distribution or reproduction in other forums is permitted, provided the original author(s) and the copyright owner(s) are credited and that the original publication in this journal is cited, in accordance with accepted academic practice. No use, distribution or reproduction is permitted which does not comply with these terms.

frontiers in Immunology

REVIEW
published: 29 April 2021
doi: 10.3389/fimmu.2021.662063

Microbial Phagocytic Receptors and Their Potential Involvement in Cytokine Induction in Macrophages

Yan Lin Fu[1,2] *and Rene E. Harrison*[1,2*]

[1] Department of Cell & Systems Biology, University of Toronto, Toronto, ON, Canada, [2] Department of Biological Sciences, University of Toronto Scarborough, Toronto, ON, Canada

Phagocytosis is an essential process for the uptake of large (>0.5 μm) particulate matter including microbes and dying cells. Specialized cells in the body perform phagocytosis which is enabled by cell surface receptors that recognize and bind target cells. Professional phagocytes play a prominent role in innate immunity and include macrophages, neutrophils and dendritic cells. These cells display a repertoire of phagocytic receptors that engage the target cells directly, or indirectly *via* opsonins, to mediate binding and internalization of the target into a phagosome. Phagosome maturation then proceeds to cause destruction and recycling of the phagosome contents. Key subsequent events include antigen presentation and cytokine production to alert and recruit cells involved in the adaptive immune response. Bridging the innate and adaptive immunity, macrophages secrete a broad selection of inflammatory mediators to orchestrate the type and magnitude of an inflammatory response. This review will focus on cytokines produced by NF-κB signaling which is activated by extracellular ligands and serves a master regulator of the inflammatory response to microbes. Macrophages secrete pro-inflammatory cytokines including TNFα, IL1β, IL6, IL8 and IL12 which together increases vascular permeability and promotes recruitment of other immune cells. The major anti-inflammatory cytokines produced by macrophages include IL10 and TGFβ which act to suppress inflammatory gene expression in macrophages and other immune cells. Typically, macrophage cytokines are synthesized, trafficked intracellularly and released in response to activation of pattern recognition receptors (PRRs) or inflammasomes. Direct evidence linking the event of phagocytosis to cytokine production in macrophages is lacking. This review will focus on cytokine output after engagement of macrophage phagocytic receptors by particulate microbial targets. Microbial receptors include the PRRs: Toll-like receptors (TLRs), scavenger receptors (SRs), C-type lectin and the opsonic receptors. Our current understanding of how macrophage receptor stimulation impacts cytokine production is largely based on work utilizing soluble ligands that are destined for endocytosis. We will instead focus this review on research examining receptor ligation during uptake of particulate microbes and how

OPEN ACCESS

Edited by:
Valentin Jaumouillé, Simon Fraser University, Canada

Reviewed by:
Michelle R. Lennartz, Albany Medical College, United States
Sanja Arandjelovic, University of Virginia, United States

***Correspondence:**
Rene E. Harrison
rene.harrison@utoronto.ca

Specialty section:
This article was submitted to Molecular Innate Immunity, a section of the journal Frontiers in Immunology

Received: *31 January 2021*
Accepted: *30 March 2021*
Published: *29 April 2021*

Citation:
Fu YL and Harrison RE (2021) Microbial Phagocytic Receptors and Their Potential Involvement in Cytokine Induction in Macrophages. Front. Immunol. 12:662063. doi: 10.3389/fimmu.2021.662063

this complex internalization process may influence inflammatory cytokine production in macrophages.

Keywords: macrophage, cytokine, receptor, inflammation, phagocyte

PHAGOCYTOSIS RECEPTORS AND CYTOKINE INDUCTION IN MACROPHAGES

Phagocytosis is a receptor-mediated process designed to engulf and destroy large target cells, including microbes, from the body. Professional phagocytes possess specialized receptors that can engage with the target directly or *via* intermediary products including opsonins. We will review known phagocytic targets for each receptor and the literature documenting cytokine induction during phagocytosis in macrophages (**Figure 1**). The mechanism by which an inflammatory outcome is signaled is unique to each receptor and we will consider some examples.

Toll-Like Receptors (TLRs) and CD14

Phagocytic targets: Within the TLR superfamily, TLR2, TLR4 and TLR5 are considered phagocytic receptors in macrophages (1) (**Figure 2**). While, TLR2 often forms heterodimers with TLR1 and TLR6, TLR2 ligation is most essential for uptake of *Leishmania donovani (L. donovani)* promastigotes and *Escherichia coli* (*E. coli*) in macrophages (2, 3). TLR2 heterodimers recognize lipopeptides, peptidoglycan and lipoteichoic acid (LTA), lipoarabinomannan, zymosan and the hemagglutinin protein on the surface of bacteria, viruses, mycobacteria and parasites (4, 5). Alternatively, TLR4 binds to lipopolysaccharide (LPS) on the outer membrane of gram-negative bacteria to promote their uptake into macrophages (6, 7). While this review will focus on particulate microbial antigens, TLR2 and TLR4 are also the major receptors that recognize danger-associated molecular patterns (DAMPs) that are expressed on apoptotic or necrotic cells. The role of other TLRs in phagocytosis is more ambiguous, however it was recently shown that TLR5 ligation to bacteria flagella is responsible for uptake of *Pseudomonas aeruginosa* (*P. aeruginosa*) by alveolar macrophages (8). CD14 is a TLR4 co-receptor expressed on the cell surface of monocytes, macrophages and dendritic cells and is responsible for the uptake and clearance of gram-negative bacteria including nontypeable *Haemophilus influenzae* (NTHi), *Acinetobacter baumannii (A. baumannii)* and *E. coli* (9–11).

Cytokine Induction: Cytokine induction by TLR2, TLR4 and CD14 signaling in macrophages is strongly pro-inflammatory. Pro-inflammatory cytokine induction by soluble ligands to TLR2 and TLR4 have been well-studied and is reviewed elsewhere (4, 5, 7, 12, 13). Insight into TLR signaling events during phagocytosis of intact microbes has been gained from the use of receptor

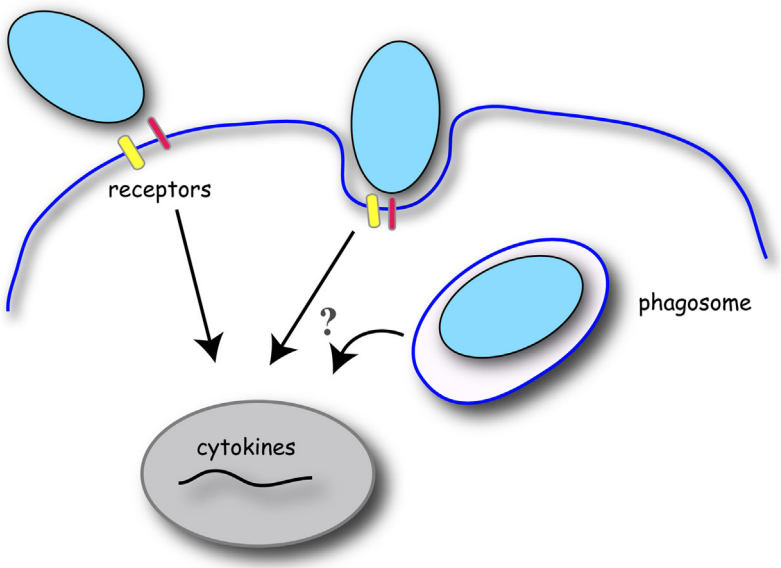

FIGURE 1 | Schematic of phagocytosis and cytokine gene induction in macrophages. Phagocytosis is initiated by the binding of target particles to the macrophage cell surface *via* specific receptors. Receptor signaling initiates localized changes in the plasma membrane and underlying cytoskeleton to engulf and internalize the target particle into a membrane-bound phagosome. Receptor ligation to the target particle induces signal transduction to promote gene expression of pro- or anti-inflammatory cytokines. Conflicting evidence exists for the relevance of particle internalization and phagosome maturation in cytokine production in macrophages.

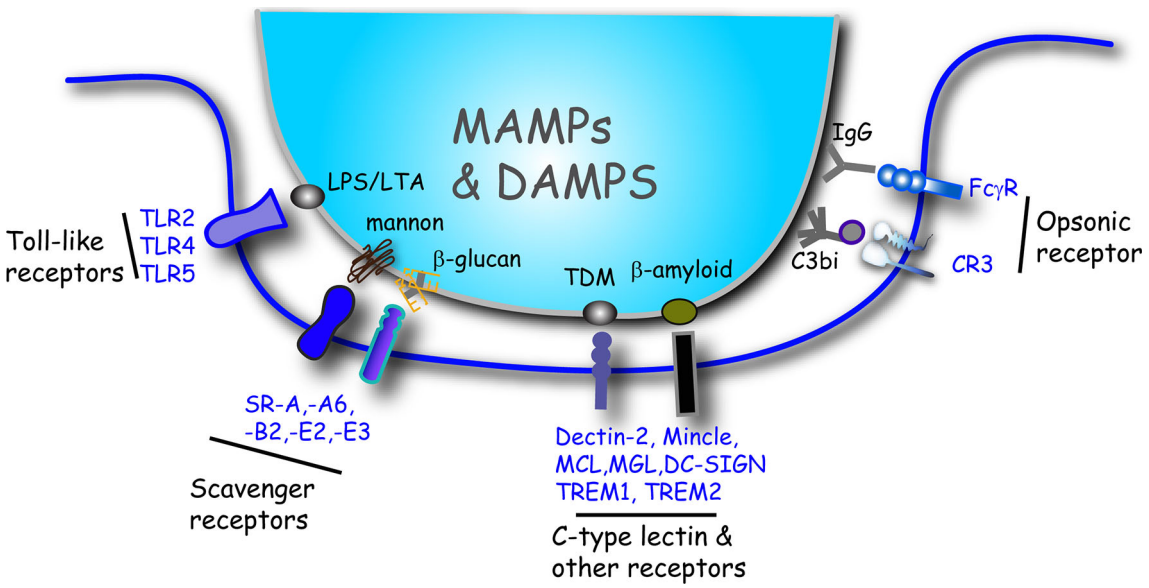

FIGURE 2 | Summary illustration of the major receptor/ligand interactions that initiate phagocytosis of microbes and induce cytokine release in macrophages. Macrophages bind to targets directly or indirectly *via* opsonins. Toll-like receptors, scavenger receptors and other phagocytic receptors interact with ligands inherent to the surface of microbes that includes MAMPs and DAMPs. Some representative ligand examples are shown. Target particles that are coated (opsonized) with either IgG or C3bi bind to the FcγR or CR3 receptors, respectively. DAMP, damage-associated molecular pattern; LPS, lipopolysaccharide; LTA, lipoteichoic acid; MAMP, microbe-associated molecular pattern; SR, scavenger receptor; TDM, trehalose 6,6-dimycolate.

knockout mice or antibody-blocking experiments (see **Table 1** for complete list). For example, ingestion of NTHi by alveolar macrophages, null for either TLR4 or CD14, caused a marked reduction in secreted TNFα protein levels, compared to control macrophages (10). *Staphylococcus aureus* (*S. aureus*) or *S. epidermidis* exposure to macrophages from TLR2 knockout mice resulted in attenuated TNFα and IL6 secretion, compared to control macrophages (14, 15). Additionally, bone marrow-derived macrophages (BMDMs) from TLR2 and TLR4 double knockout mice had blunted TNFα and IL6 release during uptake of the oral bacterium *Fusobacterium nucleatum* or *Aggregatibacter actinomycetemcomitans* (19). Finally, alveolar macrophages from TLR5 knockout mice had dampened IL1β production during ingestion of *P. aeruginosa* (8). Thus, similar to the extensive research on soluble ligands, stimulation of TLR2, TLR4, TLR5 and CD14 by particulate antigens induces a robust pro-inflammatory response in macrophages.

Ligation of TLR2 and TLR4 also modulates cytokine expression when other phagocytic receptors on macrophages are co-engaged by the same microbial target. This includes scavenger receptors like Dectin-1 as well as the opsonic receptors (**Table 1**) and we discuss receptor signaling cross-talk in subsequent sections.

Scavenger Receptors (SRs)

Phagocytic targets: Scavenger receptors are another prominent family of phagocytosis receptors utilized by macrophages to bind and destroy microbes. These receptors include: Scavenger receptor-A (SR-A), SR-A6 (macrophage receptor with collagenous structure; MARCO), SR-B2 (CD36), SR-E2 (Dectin-1) and SR-E3 (Mannose Receptor; MR) (**Figure 2**). Scavenger receptors are PRRs that bind to several microbe-associated molecular patterns (MAMPs) and DAMPs on microbes. SR-A protects the host against the invasion of various pathogens including gram-positive bacteria such as *S. aureus*, *Listeria monocytogenes* (*L. monocytogenes*), *Streptococcus pneumoniae* (*S. pneumoniae*) and gram-negative bacteria including *Neisseria meningitides* (*N. meningitides*) (58). This protective effect is due to SR-A-mediated bacterial clearance through phagocytosis by macrophages. The scavenger receptor MARCO is expressed on macrophages of the splenic marginal zone, medullary cords of the lymph nodes and alveolar macrophages of the lung (59–62) and is used to bind *E. coli* and *S. aureus* for clearance in the spleen (63).

CD36 belongs to the class B scavenger receptor family (64) and the phagocytic targets of CD36 include *S. aureus*, *E. coli*, as well as apoptotic cells and fibrillar β-amyloid (25, 65, 66). Dectin-1 directly mediates the phagocytosis of various kinds of fungi including fungal pathogens as well as fungal particles like zymosan (67–69). With assistance from TLR2, Dectin-1 also induces uptake of *Aspergillus fumigatus* conidia by murine macrophages (70). Mannose receptors recognize and phagocytose microbial targets expressing terminal mannose residues (71–76). While some studies indicate that the mannose receptor does not discriminate between pathogenic and non-pathogenic mycobacteria (77), other evidence indicates that the mannose receptor binds and internalizes virulent *M. tuberculosis* strains more efficiently compared to attenuated bacteria strains (78, 79).

Cytokine Induction: Phagocytosis induced by SRs in macrophages frequently induces pro-inflammatory cytokine production and often with TLR help (see **Table 1** for complete list). While phagocytosis of *N. meningitides* is reduced in

TABLE 1 | Research articles investigating phagocytic receptors and cytokine production when macrophages were exposed to particulate microbial antigens.

Phagocytic receptor	Phagocytic target/ligand	Macrophage cell type	Experimental model	Receptor-induced pro-inflammatory cytokines	Receptor-induced anti-inflammatory cytokines	Literature cited
TOLL-LIKE RECEPTORS (TLRs)						
TLR2	nontypeable *Haemophilus influenzae* (NTHi)	alveolar macrophages	TLR2-/- mice	↑TNFα		(10)
	Staphylococcus epidermidis (*S. epidermidis*)	peritoneal macrophages	TLR2-/- mice	↑TNFα ↑IL6		(14)
	Staphylococcus aureus (S. aureus)	peritoneal macrophages	TLR2-/- mice	↑TNFα ↑IL6		(15)
	zymosan	bone marrow-derived macrophages (BMDMs)	TLR2-/- mice	↑TNFα		(16)
	Candida albicans (*C. albicans*) cell wall	human monocytes	anti-TLR2 antibody	↑TNFα		(17)
TLR4	NTHi	alveolar macrophages	TLR4-/- mice	↑TNFα		(10)
	mutant *Neisseria meningitides* (*N. meningitides)*	murine BMDMs	*N. meningitides* strain lacking LPS	↑TNFα ↑IL6		(18)
+TLR2	*Fusobacterium nucleatum* and *Aggregatibacter actinomycetemcomitans*	BMDMs	TLR2 and TLR4 double -/- mice	↑TNFα ↑IL6		(19)
TLR5	*Pseudomonas aeruginosa*	alveolar macrophages	TLR5-/- mice	↑IL1β		(8)
CD14 co-receptor	*Streptococcus pneumococci* (*S. pneumococci*), or purified *S. pneumococci* cell wall	THP1 human macrophages	anti-CD14 antibody	↑TNFα ↑IL6 ↑IL1		(20)
	group B *streptococci* type III (GBS)	human monocytes	anti-CD14 antibody	↑TNFα		(21)
	NTHi	alveolar macrophages	CD14-/- mice	↑TNFα		(10)
SCAVENGER RECEPTORS (SRs)						
SR-A	*N. meningitides*	BMDMs	SR-A-/- mice	–TNFα –IL12	–IL10	(18)
+TLR4	*N. meningitides*	BMDMs	TLR4-/- mice	↑TNFα ↑IL12		
	Trehalose 6,6′-dimycolate (TDM)-coated beads	resident peritoneal macrophages	SR-A-/- mice	↑TNFα		(22)
+TLR2/4,CD14, MARCO	TDM-beads	HEK293 cells	Co-expression of MARCO, CD14 and TLR2 or SR-A, CD14, TLR2, MD2 and TLR4	↑NF-κB activation		
SR-A6	TDM-beads	RAW264.7 cells	MARCO overexpression	↑TNFα		(22)
Macrophage receptor (MARCO)		peritoneal macrophages	MARCO-/- mice	↑IL6 ↑TNFα ↑IL1β		
+TLR2/4,CD14, SR-A		HEK293 cells	Co-expression of MARCO, CD14 and TLR2 or SR-A, CD14, TLR2, MD2 and TLR4	↑NF-κB activation		
SR-B2 (CD36)	*Plasmodium falciparum* (*P. falciparum*) malaria-parasitized erythrocytes	human peripheral blood mononuclear cells and murine peritoneal macrophages	anti-CD36 antibody	–TNFα		(23)
+TLR2	*Cryptococcus neoformans*	RAW264.7 macrophages	CD36 knockdown	↑IL1β		(24)
	S. aureus or *E. coli*	BMDMs	CD36-/- rat	↑IL6 ↑TNFα		(25)

(Continued)

TABLE 1 | Continued

Phagocytic receptor	Phagocytic target/ligand	Macrophage cell type	Experimental model	Receptor-induced pro-inflammatory cytokines	Receptor-induced anti-inflammatory cytokines	Literature cited
	β-amyloid	peritoneal macrophages	CD36 downstream signaling kinase knockdown	↑MCP1		(26)
SR-E2 (Dectin-1)	zymosan, live *C. albicans* and *S. cerevisiae*	RAW264.7 cells	Dectin-1 overexpression	↑TNFα		(16)
	zymosan	RAW264.7 cells	Dectin-1 overexpression	↑TNFα		(27)
	Candida glabrata (*C. glabrata*)	thioglycollate-elicited macrophages	Dectin-1-/- mice	↑TNFα ↑IL6	↑IL10	(28)
+TLR4	*Exserohilum rostratum* (*E. rostratum*)	BMDMs	Dectin-1-/- mice	↑TNFα		(29)
	E. rostratum + LPS	BMDMs	Dectin-1-/- mice	↑IL1β compared to LPS		
	Aspergillus fumigatus germ tubes	murine peritoneal macrophages	anti-Dectin-1 antibody	↑TNFα		(30)
	zymosan and soluble and particulate β-glucan	resident peritoneal macrophages, alveolar macrophages		↑TNFα		(31)
		RAW264.7 cells	Dectin-1 overexpression	↑TNFα		
+TLR2	zymosan	HEK293 cells	Dectin-1 and TLR2 overexpression	↑NF-κB activation		(27)
		RAW264.7 cells with endogenous TLR2	Dectin-1 overexpression	↑TNFα		
SR-E3 (Mannose Receptor (MR))	*C. albicans*	thioglycollate-elicited peritoneal macrophages	MR knockdown	↑IL1β mRNA ↑IL6 mRNA		(32)
	C. albicans	thioglycollate-elicited peritoneal macrophages	MR-/-mice	↑TNFα ↑MCP1		(33)
	zymosan	thioglycollate-elicited peritoneal macrophages	MR-/-mice	–MCP1 –TNFα		
	Pneumocystis carinii (P. carinii)	human alveolar macrophages	MR-blocking ligand and MR knockdown	↑NF-κB nuclear translocation		(34)
	P. carinii	human alveolar macrophages	MR-blocking ligand and MR knockdown	↑NF-κB activation –IL1β –IL6 –TNFα		(35)
C-TYPE LECTIN RECEPTORS						
Dectin-2	*C. glabrata*	peritoneal macrophages	Dectin-2-/- mice	↓TNFα ↓IL6		(36)
	C. albicans yeast	peritoneal macrophages	Dectin-2-/- mice	↓IL1β		
	C. albicans hyphae	peritoneal macrophages	Dectin-2-/- mice	↓IL1β		
	C. glabrata	thioglycollate-elicited macrophage	Dectin-2-/- mice	↑TNFα ↑IL6	↓IL10	(28)
Mincle	*Tannerella forsythia*	THP1 cells	Mincle knockdown	↑TNFα	↑IL10	(37)
	Malassezia	BMDMs	Mincle-/- mice	↑TNFα ↑IL6	↑IL10	(38)
	C. albicans	BMDMs	Mincle-/- mice	↑TNFα		(39)
+TLR2	TDM-coated beads + Pam3CSK4	BMDMs	Mincle-/- mice	↑TNFα	↑ IL10	(40)
	Mycobacterium bovis Bacillus Calmette–Guérin (*M. bovis* BCG)	BMDMs	Mincle-/- mice		↑ IL10	
	M. tuberculosis H37Rv	BMDMs	Mincle-/- mice	↑TNFα mRNA		(41)

(Continued)

TABLE 1 | Continued

Phagocytic receptor	Phagocytic target/ligand	Macrophage cell type	Experimental model	Receptor-induced pro-inflammatory cytokines	Receptor-induced anti-inflammatory cytokines	Literature cited
Macrophage C-type lectin (MCL)	*M. tuberculosis*	BMDMs	MCL-/- mice	↑TNFα mRNA		(42)
OTHER RECEPTORS						
Macrophage galactose-type lectin (MGL)	*Trypanosoma cruzi*	peritoneal macrophages	MGL-/- mice	↑TNFα	↑IL10	(43)
Dendritic Cell-Specific Intercellular adhesion molecule-3-Grabbing Non-integrin (DC-SIGN)	*M. tuberculosis*	human MDMs	DC-SIGN knockdown	↓TNFα mRNA ↓IL6 mRNA ↓IL1β mRNA ↓TNFα ↓IL6		(44)
Triggering receptor expressed on myeloid cells 1 (TREM1)	*M. tuberculosis* cell lysates	BMDMs	TREM1-/- mice	↑TNFα ↑IL1β (mRNA and protein)	↑IL10 mRNA	(45)
	heat-killed *S. pneumoniae*	BMDMs and alveolar macrophages	TREM1/3-/- mice	↑TNFα		(46)
TREM2	*M. bovis* BCG	peritoneal macrophages	TREM2-/-mice	↓MCP1		(47)
	E. coli	peritoneal macrophages	TREM2-/- mice and TREM2 overexpression	↓IL6		(48)
OPSONIC RECEPTORS						
FcγR	IgG-coated tissue culture plates	human monocytes		↑H_2O_2 release		(49)
	IgG-coated beads	murine peritoneal macrophages		↑arachidonic acid		(50)
	IgG-opsonized sheep red blood cells (sRBCs)	BMDMs		–TNFα –IL1β –IL6		(51)
+TLR4	IgG-opsonized sRBCs	LPS-stimulated BMDMs		Low IgG: ↑IL12 High IgG: ↓IL12	Low IgG: ↓IL10 High IgG: ↑IL10	(52, 53)
+CD36	*P. falciparum*-infected erythrocytes opsonized with pooled patient immune serum	IFN-γ-primed human MDMs		↑TNFα ↑IL1β ↑IL6		(54)
+TLR2	heat aggregated gamma-globulins +P3C (soluble TLR2 ligand)	IFN-γ-primed human MDMs			↑IL10	(55)
Complement receptor3 (CR3)	IgM-C3bi-coated beads	murine peritoneal macrophages		–arachidonic acid		(50)
	C3b- or C3bi- coated tissue culture plates	human monocytes		–H_2O_2 release		(49)
	C3bi-opsonized sRBCs	BMDMs		↑TNFα ↑IL1β ↑IL6		(51)
+Dectin-1	heat-killed *Histoplasma capsulatum (H. capsulatum)*	peritoneal macrophages	CR3 and Dectin-1 single and double -/- mice	↑TNFα ↑IL6		(56)
+Dectin-1	heat-killed *H. capsulatum*	peritoneal macrophages	anti-CR3 and anti-Dectin-1 antibodies	↑TNFα ↑IL6		(57)

Phagocytic receptor and target particles are listed as well as the type of primary macrophage or macrophage cell line utilized. Experimental strategies to test receptor involvement are also briefly described. Finally, the effect of receptor stimulation on either pro- or anti-inflammatory cytokine production is summarized.

macrophages from SR-A-/- mice, the pro-inflammatory response is not impacted and is dependent on TLR4 expression and ligation to LPS (18) (**Table 1**). This is likely attributed to the inherent structure of SR-A, which does not have an intracellular signaling domain. However, peritoneal macrophages from SR-A-/- mice showed decreased TNFα production during uptake of latex beads coated with trehalose 6,6′-dimycolate (TDM), the cell wall glycolipid of *M. tuberculosis* (22), indicating a more direct role for SR-A in cytokine signaling, or the involvement of another as of yet identified signaling co-receptor. Likewise, MARCO is implicated in tethering and phagocytosis of *M. tuberculosis* but does not have an intracellular signaling moiety and requires TLR2 stimulation and signaling for cytokine induction in macrophages (22) (**Table 1**).

In macrophages, CD36 can either independently, or in cooperation with TLR2 receptors, mediate pro-inflammatory cytokine release during phagocytosis. CD36 presents bacterial LTA as well as diacylated lipoproteins to TLR2/6 heterodimers (80). Phagocytosis studies in macrophages have confirmed that CD36 signaling mediates internalization of microbes but requires TLR2 signaling for pro-inflammatory cytokine secretion (23, 24) (**Table 1**). Dectin-1 also synergizes with TLR2 for the production of pro-inflammatory cytokines in macrophages (16, 27) (**Table 1**). Phagocytosis of zymosan by macrophages occurred through either Dectin-1 or the mannose receptor, but only Dectin-1-mediated phagocytosis of zymosan led to the production of superoxide (77). As discussed later, Dectin-1-mediated cytokine induction during phagocytosis also depends on ligand density and the activation status of macrophages.

Stimulation of the mannose receptor during phagocytosis has varying effects on cytokine production in murine macrophages (**Table 1**). *C. albicans* binding to mannose receptors on thioglycollate-elicited peritoneal macrophages induced transcription of IL6 and IL1β (32), indicating a pro-inflammatory response. The mannose receptor is the main receptor for phagocytosis of unopsonized *Pneumocystis*, a pathogen that causes pneumonia (72, 81). While mannose receptor ligation to *Pneumocystis carinii (P. carinii)* induced NF-κB nuclear translocation in human alveolar macrophages, the expression and secretion of IL1β, IL6 and TNFα did not occur (34, 35). The observed effects on NF-κB translocation may be related to the different bacteria MOIs used in these studies (34, 35). NF-κB activation requires a particular threshold of signal density from PRRs, including input from MAPKs, for transcription of cytokine genes to occur (82). Other receptor involvement may also be required for pro-inflammatory cytokine production during *P. carinii* uptake, for instance through bacteria opsonization. In support of this, immune serum opsonization of *Pneumocystis* bacteria promoted significant TNFα production, compared to unopsonized bacteria, in macrophages (83).

C-Type Lectin Receptors and Other PRR Phagocytic Receptors

Phagocytic targets: Dectin-2 belongs to the C-type lectin phagocytic receptors which also include macrophage inducible C-type lectin (Mincle) and macrophage C-type lectin (MCL) (**Figure 2**). Dectin-2 mediates the phagocytosis and killing of *Candida glabrata* (*C. glabrata*) by macrophages (36). Both Mincle and MCL are TDM receptors, where Mincle recognizes the carbohydrate part of TDM and MCL recognizes the lipid portion of TDM (84). Mincle ligation drives the phagocytosis of *Klebsiella pneumonia* (85), but not *C. albicans*, although interestingly Mincle is localized to both the phagocytic cup and *C. albicans*-containing phagosomes (39, 86). Mincle can form heterodimers with MCL and serves as a bridge between MCL and FcRγ. The Mincle-MCL-FcRγ complex has a much higher phagocytosis capacity for anti-Mincle- or anti-MCL-coated beads in macrophages (87).

Other phagocytic PRR receptors include macrophage galactose-type lectin (MGL) which recognizes Gal/GalNAc residues present in N- and O-glycans on glycoproteins and/or glycosphingolipids and thus MGL binds tumor antigens, apoptotic cells and foreign glycoproteins on helminth parasites (88). Dendritic cell-specific ICAM-3 grabbing non-integrin (DC-SIGN) is another C-type lectin receptor which has a carbohydrate recognition domain that recognizes glycoproteins with mannose-containing structures (89). Triggering receptor expressed on myeloid cells 1 (TREM1) and TREM2 are expressed in macrophages and other cells of the myeloid lineage (90). TREM1 mediates the phagocytosis of β-amyloid peptides by human monocytes and promotes the uptake of heat-killed *S. pneumoniae* by BMDMs and alveolar macrophages (46). TREM2, is required for the phagocytosis of *K. pneumoniae* (91), and is also responsible for the uptake of *E. coli*, *S. aureus*, zymosan and β-amyloid (Aβ 1-42) (48, 92, 93).

Cytokine Induction: There are conflicting studies on the role of Dectin-2 in cytokine release during phagocytosis in macrophages. In one study, Dectin-2-deficient peritoneal macrophages released more pro-inflammatory cytokines after *C. glabrata* and *C. albicans* stimulation, compared to control macrophages (36). However, another study examining thioglycollate-elicited peritoneal macrophages from Dectin-2-/- mice, showed reduced TNFα and IL6 levels and enhanced IL10 levels after *C. glabrata* infection, compared to control macrophages (28). The activation status of the macrophages may be impacting the signaling capacity for Dectin-2, which lacks signaling domains and must associate with the adaptor FcRγ chain that contains an immunoreceptor tyrosine-based activation motif (ITAM) (94).

Mincle activation can promote the release of both pro- and anti-inflammatory cytokines when macrophages engage with gram-negative bacterium, mycobacteria, fungi and inorganic particles. For instance, while Mincle was not required for the phagocytosis of the gram-negative *Tannerella forsythia* (*T. forsythia*) bacteria, Mincle ligation to *T. forsythia* promoted pro-inflammatory cytokine TNFα and anti-inflammatory cytokine IL10 release in macrophages (37) (**Table 1**). Mincle also mediated the release of TNFα, IL6 and IL10 in BMDMs ingesting the fungi *Malassezia* (38). Mincle activity can synergize with TLR2 in macrophages to promote pro- and anti-inflammatory cytokine release. As an example, BMDMs stimulated with the TLR2 agonist Pam3CSK4 produced more pro-inflammatory TNFα and anti-inflammatory cytokine IL10

when co-stimulated with TDM-coated beads, that was depended on Mincle signaling (40). While MCL has not received as much attention as other C-type lectin receptors, BMDMs from MCL-/- mice had reduced levels of TNF mRNA after *M. tuberculosis* H37Rv stimulation, compared to control macrophages (42) (**Table 1**), indicating that this receptor may signal for cytokine gene expression in a similar manner to Mincle. Similarly, little has been reported about cytokine induction during phagocytosis induced by MGL ligation, however one study of peritoneal macrophages from MGL-/- mice showed reduced TNFα and IL10 secretion during phagocytosis of *Trypanosoma cruzi* parasites, compared to control macrophages (43) (**Table 1**).

In contrast to other C-type lectin receptors, DC-SIGN signaling during phagocytosis dampens pro-inflammatory signaling in macrophages. For instance, when DC-SIGN receptor levels were experimentally downregulated in human monocyte-derived macrophages (MDMs) exposed to *M. tuberculosis*, the mRNA and secreted protein levels of TNFα, IL6, and IL1β were increased, compared to control macrophages (44) (**Table 1**). DC-SIGN is more abundant in dendritic cells, where inhibitory PRRs are more common (95), and act to the advantage of the pathogen to actively suppress host immune defenses. It is quite probable that most macrophage PRRs are strongly pro-inflammatory to reflect the front-line response of macrophages in infections.

Finally, TREM1 ligation induces a pro-inflammatory response during bacterial uptake and accordingly, TREM1 inhibition is protective in septic shock animal models (90). Macrophages from TREM1 knockout mice have attenuated TNFα and IL1β mRNA and protein levels after *M. tuberculosis* exposure (45) (**Table 1**). TNFα secretion is also reduced from TREM1/3-/- BMDMs and alveolar macrophages during uptake of heat-killed *S. pneumoniae* (46). Compared to TREM1, TREM2 is more anti-inflammatory.

Knocking out the TREM2 gene in macrophages engaging *M. bovis* BCG increased the BCG-induced release of the pro-inflammatory cytokine, MCP1 (47). Similarly, TREM2-/- peritoneal macrophages had higher IL6 secretion after engagement with *E. coli* while RAW264.7 cells overexpressing TREM2 had attenuated IL6 release after *E. coli* stimulation, compared to control cells (48). Why might there be such a variation in cytokine induction by TREM1 and TREM2? One possibility is that TREM2 does not induce complete phosphorylation of the required adaptor, DAP12. The ITAM of DAP12 becomes only partially phosphorylated if the associated receptor has a low affinity or avidity to ligand (96). Incomplete phosphorylation of the ITAM recruits the SH2 domain-containing protein tyrosine phosphatase SHP-1, leading to dephosphorylation of downstream targets of Syk (97).

Opsonic Receptors

Phagocytic targets: Fcγ receptors (FcγR) bind to the fragment crystalline (Fc) region of IgG exposed on opsonized targets that have been recognized with the fragment antigen binding (Fab) portion of IgG (98) (**Figure 2**). Once ligated, clustered FcγRs use the ITAM either in the cytosolic domain of the receptor or in associated subunits (FcRγ or FcεRIβ chain) to activate downstream signaling cascades. The complement system is activated either through the classic pathway, the alternative pathway or the lectin pathway, which leads to the generation of C3b that can bind to exposed hydroxyl and amino groups on the surface of pathogens (99). Bound C3b can also be cleaved into an inactivated form that is called C3bi (99). Phagocytes express CR3 receptors, which upon inside-out activation can bind to deposited C3b or C3bi on target cells (99, 100) (**Figure 2**).

Cytokine Induction: While the study of phagocytosis has centered on uptake by the opsonic receptors, there is relatively little work on their connectedness with cytokine induction in macrophages (**Table 1**). An early study of human monocytes plated on IgG-coated substrates showed a significantly higher production of H_2O_2 in these cells, compared to macrophages on a control surface (49). In contrast, H_2O_2 levels remained unchanged in monocytes plated on C3b- or C3bi-coated substrates (49). A follow-up study of murine peritoneal macrophages revealed that internalization of opsonized latex beads through Fcγ receptors, but not CRs, caused elevated arachidonic acid production, which is a potent inflammatory mediator of vascular permeability (50). This led to the belief that phagocytosis through Fcγ, but not CR3, was pro-inflammatory. However, our lab recently showed that the phagocytosis of C3bi-opsonized sRBCs increased the release of a host of pro-inflammatory cytokines including TNFα, IL1β and IL6, compared to control macrophages and those ingesting IgG-sRBCs (51) (**Table 1**). CR3 is an integrin, and we identified a role for the downstream signaling protein, calpain, in mediating this response (51).

Recent evidence suggests that FcγRs do not induce cytokine production directly, but can modulate cytokine release mediated by other receptors. For example, IFN-γ-primed human MDMs produced much higher pro-inflammatory cytokines (TNFα, IL1β, IL6) when ingesting *P. falciparum*-infected erythrocytes opsonized with pooled patient immune serum, compared to unopsonized targets (54) (**Table 1**). Complement receptors are also well-known to coordinate with TLRs for inflammatory responses when macrophages engage with targets coated with both respective ligands (101, 102). CR3 also synergizes with Dectin-1 in pro-inflammatory cytokine release when macrophages interact with microbes. For example, macrophages exposed to heat-killed *Histoplasma capsulatum* have significantly reduced TNFα and IL6 secretion when both CR3 and Dectin-1 signaling is blunted, compared to single receptor inhibition (56, 57). **Table 1** captures the available literature investigating microbial phagocytic receptor involvement in cytokine production in macrophages. We will next discuss putative cytokine-invoking signaling elements that are activated during phagocytosis and the contributions of particulate ligands and the internalization process in the inflammatory response.

SHARED SIGNALING ELEMENTS IN PHAGOCYTOSIS AND CYTOKINE PRODUCTION IN MACROPHAGES

The intracellular signaling events that lead to NF-κB activation and pro-inflammatory cytokine gene expression in macrophages

is best understood for TLRs and is described in several comprehensive reviews (4, 5, 103) (**Figure 3**). We have mentioned several phagocytosis receptors that cooperate with TLR-mediated signaling for cytokine induction (**Table 1**) (**Figure 3**). However, some phagocytosis receptors signal independently and induce cytokine expression in the absence of TLR ligation. These signal transduction pathways are not as well-understood due to inherent challenges when blocking receptors and the consequent impact on particle binding/internalization. Thus, it is difficult to uncouple these events and address whether the pronounced F-actin remodeling events in phagocytosis signal to the nucleus for a pro-inflammatory response. However, we are beginning to understand some of the signaling commonalities between phagocytosis and cytokine induction in macrophages. For phagocytosis, a wealth of literature exists describing the signaling events during FcγR-mediated phagocytosis (reviewed in (104, 105)). Dissecting this comprehensive signal transduction pathway allows us opportunities to identify major areas of signaling overlap (**Figure 3**) that have been substantiated with experimental evidence.

Phagocytosis is initiated by receptor engagement with the microbe and subsequent receptor clustering along the plasma membrane. The ITAMs within the receptor or adaptor proteins become phosphorylated by Src-family kinases to allow docking and activation of Syk (106, 107). Syk is also activated in the NF-κB signaling pathway induced by soluble ligands to TLR4 (108, 109) and thus represents a potential signaling hub between phagocytosis and cytokine induction in macrophages. Binding of Dectin-1 to its target leads to Syk phosphorylation which activates the caspase recruitment domain family member 9 (CARD9)/B-cell lymphoma 10 (BCL-10)/mucosa-associated lymphoid tissue lymphoma translocation protein 1 (MALT1) protein complex leading to the activation of NF-κB (107). While phagocytic receptors like FcγRIIA contain an ITAM, or hemITAM (Dectin-1), for signal transduction, others like Dectin-2 and the TREM family proteins utilize adaptor proteins containing ITAMs, which vary in their ability to induce pro- or anti-inflammatory gene expression. CD36 does not possess an ITAM and associates with the ITAM-bearing adaptor FcRγ for signaling to Syk (110). Similarly, the FcRγ ITAM becomes phosphorylated after Mincle stimulation with ligand, which in turn recruits Syk. Syk then activates the MALT1 signalosomes leading to NF-κB activation (84).

Syk activation during FcγR-mediated phagocytosis recruits PI3K and phospholipase Cγ (PLCγ) for key lipid modifications at the phagocytic cup (104, 111, 112). The production of diacylglycerol by PLCγ activity triggers calcium release that stimulates protein kinase C (PKC) and Erk1/2 and p38 MAPKs (104). PKC-ε is required for membrane delivery to the phagocytic cup (113) and also for LPS-induced 1L12 secretion (114), and thus may serve as an intersection point between phagocytosis and cytokine production in macrophages (**Figure 3**). Similarly, the MAPK family plays pivotal functions in both particle internalization and NF-κB activation. Following LPS stimulation of TLRs in macrophages, Erk1/2, p38 and JNK are

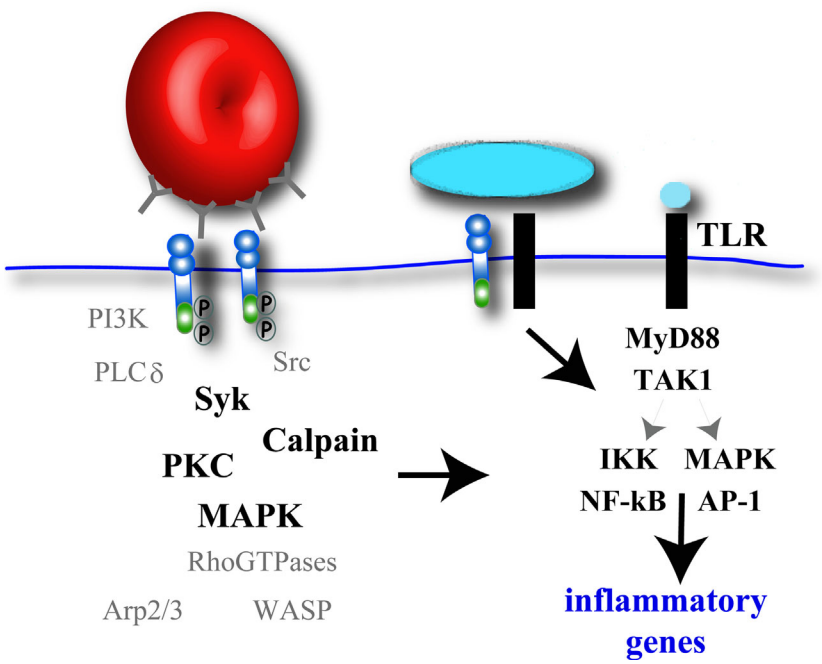

FIGURE 3 | Potential signaling molecules involved in pro-inflammatory cytokine gene expression during phagocytosis. Macrophage phagocytic receptor clustering will activate F-actin-remodeling signaling elements, some kinases of which (black bold), have also been implicated in canonical TLR signaling induced by soluble ligands. While some phagocytosis receptors can independently activate an inflammatory response, other phagocytosis receptors require co-ligation of TLR receptors and subsequent TLR signaling to promote NF-κB and AP-1 activation and pro-inflammatory cytokine gene expression.

activated by TGFβ-activated kinase 1 (TAK1 kinase) (115). MAPKs activate the transcription factor activator protein 1 (AP-1) leading to additional cytokine gene transcription (4, 7) (**Figure 3**). Relevant to phagocytosis, Erk1/2 is activated and required for FcγR-mediated phagocytosis in macrophages (116, 117). MARCO null macrophages exposed to TDM beads had reduced MAPK activation and TNFα, IL6, and IL1β production, compared to control macrophages (22) (**Table 1**). CD36-mediated uptake of fibrillar β-amyloid by CD36 induced Lyn signaling to Fyn and MAPK, which were necessary for pro-inflammatory reactive oxygen species (ROS) and MCP1 production in peritoneal macrophages (26). Both the amino and carboxy termini of CD36 are cytosolic and palmitoylated which targets CD36 to lipid rafts containing Src kinase family members that can activate p38 and Erk1/2 (26). Similarly, Dectin-1-mediated phagocytosis of *C. glabrata* and subsequent secretion of IL6, TNFα and IL10 in thioglycollate-elicited peritoneal macrophages was induced by the activation of MAPK and NF-κB pathways (28).

We recently identified calpain as a potential mediator of cytokine production during CR3-mediated phagocytosis in macrophages (51) (**Figure 3**). Calpain is a cysteine protease that has been shown to degrade IkBα (118), the inhibitory subunit for NF-κB (119, 120). In canonical TLR signaling, TAK1 activates the IKK complex whereby the IKKβ subunit phosphorylates IκBα. Phosphorylated IκBα is degraded by the proteasome and NF-κB is freed for translocation into the nucleus to turn on pro-inflammatory genes (**Figure 3**).

It remains to be seen whether the robust F-actin machinery involved in particle internalization (Rac1, RhoA, WAVE, Arp2/3, etc.) plays a direct signaling role in cytokine production in macrophages (**Figure 3**). F-actin depolymerizing agents have an impact on cytokine production in macrophages (described below) but these experiments do not address the role of individual F-actin signaling elements in cytokine induction and is worthy of further investigation.

CYTOKINE INDUCTION BY MICROBES VERSUS SOLUBLE LIGANDS IN MACROPHAGES

Utilizing soluble ligands to study phagocytic receptor signaling allows a simplified analysis of its potential role in cytokine induction. However, soluble ligands engage fewer receptors than intact microbes and do not induce receptor clustering and cross-linking, which strongly impacts the type and amplitude of downstream signaling events. In an elegant Dectin-1 study, macrophages were exposed to either soluble β-glucans or particulate/immobilized β-glucan and assayed for pro-inflammatory responses (121). While uptake of soluble β-glucans did not induce TNFα release and reactive oxygen species (ROS) production in macrophages, both particulate β-glucan and zymosan induced a significant pro-inflammatory response. Additionally, when soluble β-glucans were adhered to 0.8 μm latex beads to promote phagocytosis, ROS production was enhanced in macrophages (121). Immunofluorescence analysis of the macrophages plated on surface-immobilized β-glucan showed that Dectin-1 adherence to large targets removed/excluded the inhibitory CD45 and CD148 proteins from the "phagocytic synapse". Clearance of these proteins is believed to allow the Src-Syk-MAPK signaling cascade induced by Dectin-1 to induce pro-inflammatory gene expression (121). Related to this, a recent study engineered a nanoarray of TLR1/2 ligands to recreate the phagocytic synapse. The researchers were able to manipulate the spatial organization of ligands and observed that closer spacing of ligands (and presumably receptors) enhanced TNFα release in RAW264.7 cells, up to an intrinsic limit (122). While a wealth of receptor signaling information can be gleaned from studying soluble ligands, there is value in investigating large targets where the magnitude of receptor ligation and clustering may impact intracellular signaling events.

VARIATIONS IN CYTOKINE SIGNAL STRENGTH AND CROSS-TALK BY PHAGOCYTOSIS RECEPTORS

Many signaling proteins overlap during phagocytosis and NF-κB activation pathways, yet the type of pro-inflammatory cytokines and magnitude of the secreted cytokine levels varies widely. Studies in our lab have directly compared cytokine secretion after stimulation of macrophages with different ligands. TLR signaling induced an order of magnitude higher cytokine production in macrophages, compared to CR3 or FcγR stimulation using opsonized sRBCs (51, 52). As mentioned earlier, opsonization of microbes is known to influence the cytokine production profile induced by other receptors. Antibody-opsonized targets are indicative of a measured adaptive immune response and may not signal the urgency of a new infection represented by microbes solely displaying MAMPs.

The degree of opsonization also strongly influences cytokine production in macrophages. In LPS-stimulated macrophages, increasing IgG on RBCs to saturation inhibited IL12 production and surprisingly, induced secretion of the anti-inflammatory cytokine, IL10 (53). Equivalent amounts of soluble antibody added to media had no effect suggesting that the ligand must be present at high enough densities to cluster FcγRs. This FcγR-mediated influence on TLR signaling included pronounced Erk1/2 activation, known to induce histone modifications associated with the IL10 gene promotor (123). The coinciding increase in sRBC phagocytosis at higher opsonin concentrations also begs the question of whether the enhanced internalized particles also contributed to altered cytokine gene expression. Potential receptor signaling contributions during particle uptake and from phagosome membranes are discussed in the next sections.

Dectin-1-mediated cytokine expression during phagocytosis is also dependent on the density and type of fungal ligands. Fungi with higher levels of β-glucans on the cell wall induces more Dectin-1 engagement and pro-inflammatory cytokine release, compared to fungi with lower β-glucans levels. For example, macrophage uptake of *A. fumigatus* resting conidia did not

induce pro-inflammatory signals while maturing *A. fumigatus* germ tubes caused pronounced NF-κB activation and the production of TNFα and ROS in macrophages (30).

In addition to ligand density, microbes contain multiple ligands and activate PRRs and opsonic receptors of the same or different type(s). These findings underscore the importance of using intact microbes to decipher the relationship between phagocytosis and cytokine induction. As detailed in **Table 1**, complexities in cytokine induction in macrophages arise when more than one phagocytic receptor is engaged. For instance, a synergistic production of pro-inflammatory cytokine production was observed when both CR3 and Dectin-1 were engaged in macrophages ingesting *H. capsulatum*. The signal amplification by these receptors occurred *via* pronounced Syk activation, which then enhanced downstream Syk-JNK-AP-1 signaling (56). Dectin-1 co-ligation also magnifies TLR2 or TLR4 signaling during phagocytosis. For instance, the uptake of *Exserohilum rostratum* (*E. rostratum*) in the presence of LPS, provoked a much higher IL1β release in macrophages, compared to LPS or *E. rostratum* stimulation alone (29). Dectin-1 signaling also synergizes with TLR2 for NF-κB activation after zymosan stimulation (27). As we have discussed, MAPK may represent a common node for signaling by phagocytic receptors and parallel activation of MAPK *via* different pathways could lead to synergistic cytokine expression outcomes. The opsonization of bacteria activates both FcγR and TLR signaling pathways often leading to amplified cytokine responses in macrophages (52, 53) (**Table 1**). There likely exists a hierarchy of responses by PRRs to the threat at hand which is mediated by co-ligation of different receptor combinations.

ROLE OF PARTICLE INTERNALIZATION IN CYTOKINE INDUCTION IN MACROPHAGES

Phagocytosis is typified by dramatic F-actin remodeling and plasma membrane protrusions but is this unique morphological event required for inflammatory signaling? Some clues to help answer this question can be provided by experiments that block microbial uptake or utilize targets that cannot be internalized. Inhibition of particle internalization can be achieved with F-actin depolymerizing agents. Treatment of thioglycollate-elicited BMDMs with cytochalasin D (cyto D) to block uptake of heat-killed *S. aureus* did not impact TNF or IL10 release, suggesting that internalization was not required for TLR2/4-mediated pro-inflammatory signaling (124). In contrast, cyto D treatment to inhibit internalization of *K. pneumoniae* through TLR2 and Dectin-1 receptors, blocked secretion of the pro-inflammatory cytokine, IL8 (125). Impeding phagocytosis of gram-positive bacteria using cyto D also reduced the expectant IL12 response (126). While the latter observations were made in respiratory epithelium and monocytes, respectively, the results warrant investigation in macrophages. Cyto D is a blunt tool to block microbial internalization and we have utilized Src and Syk inhibitors in our own work to prevent particle uptake in macrophages (51). While we observed a marked reduction in pro-inflammatory cytokine secretion in drug-treated BMDMs, phagocytosis still proceeded at a lower level in Src- and Syk-inhibited cells, confounding the results (51).

Another strategy to delineate receptor signaling events is to employ "frustrated phagocytosis" assays where ligand is bound to a coverslip and thus cannot be internalized. Exploiting such an assay, robust TNFα and ROS production was seen in BMDMs engaged with plate-immobilized β-glucan, validating the cell surface as a predominant cytokine signaling locale for the Dectin-1 phagocytic receptor (121). Similarly, there was a Dectin-1-dependent secretion of TNFα when macrophages were bound to *E. rostratum*, a bacteria that cannot be internalized (29). In contrast, compelling evidence for an internalization requirement for cytokine secretion in macrophages came from a study on the rough and smooth varieties of *Mycobacteria abscessus* (*M. abscessus*), where the topology of the rough strain impedes effective engulfment by macrophages (127). Interestingly, human PMBCs engaged with rough *M. abscessus* strains produced significantly less TNF and IL10 cytokines than after engulfment of the smooth bacteria strain (127). There are a few potential reasons for this. As we discussed, shared signaling elements between phagocytosis and NF-κB activation pathways may amplify the response when microbes are internalized. Furthermore, phagocytic receptor signaling may acutely persist on the phagosome (**Figure 1**), which is the next topic of discussion.

PHAGOCYTIC RECEPTOR SIGNALING IN PHAGOSOMES

Do phagocytosis receptors signal within phagosomes for cytokine induction? As previously mentioned, it is inherently difficult to uncouple signaling events during particle uptake with cytokine gene expression, as down-regulating the receptor usually blocks internalization. However, it is well-known that after uptake of soluble ligands, internalized TLR4 can recruit TRAM and TRIF that lead to the activation of NF-κB-mediated pro-inflammatory cytokine gene expression and type I IFN gene expression (4). While TLR4 can signal at both the cell surface and within endosomes, other TLR family members signal only at the plasma membrane or from endosomal compartments (128). CARD9, an important downstream signaling element for Dectin-1, is recruited to early phagosomes where it may exert some of its pro-inflammatory effects (31). It remains to be determined if other *bona fide* phagocytic receptors mediate inflammatory signaling at the plasma membrane and/or along phagosomes (**Figure 1**). Once internalized, the newly formed phagosome organelle is quickly remodeled as it fuses sequentially with vesicles of endocytic lineage in a process known as phagosome maturation, reviewed in (105). Membrane fission events from the phagosome also occurs to collect microbe fragments for antigen presentation and to recycle receptors (129). It is unlikely that FcγR signals extensively from the phagosomal membrane as the rapid loss of F-actin from the nascent phagosomes (111) implies a termination of the signal. Interestingly, we observed recruitment and successive F-actin flashes on CR3-phagosomes that were rarely observed in FcγR-phagosomes (130).

F-actin flashes also occur on some bacteria-containing phagosomes (131) and apart from mechanically fragmenting cargo (130), these F-actin accumulations may represent phagocytic receptor signaling hubs important in cytokine production.

Maturing phagosomes ultimately fuse with lysosomes for terminal cargo destruction and killing of internalized microorganisms (105). The progressive loss of receptors from the phagosome resulting from fission events likely attenuates any long-term intracellular signaling. Interestingly, mannose receptors were recruited to *C. albicans*-containing phagosomes 20 minutes after uptake and were implicated in stimulating TNFα and MCP1 production post-internalization (33). While it is not clear if phagocytic receptor signaling commonly promotes cytokine induction from the phagosome, the routing of microbial contents to lysosomes triggers additional inflammatory receptors, including intracellular PRRs (reviewed in (132)). A larger pool of ligands is obscured in intact microbes and becomes accessible only after phagolysosome formation and digestion of the microorganism. Phagosome degradation of bacteria exposes additional TLR2 ligands as well as releasing DNA to activate intracellular TLR9 and downstream inflammatory responses (133). Ultimately, phagosome membrane remodeling and saturation of intracellular receptors will cease signaling to signify removal of the microbe and defeat of the threat (134).

MACROPHAGE POLARIZATION AND CYTOKINE INDUCTION DURING PHAGOCYTOSIS

Macrophages exist in "resting" states and various forms of activation/polarization *in vitro* and *in vivo*. M1 macrophages are primed with microbial products like LPS and the cytokine IFN-γ and subsequently secrete many pro-inflammatory cytokines including TNFα, IL6, IL12, IL18 and IL1β (135). In contrast, IL4-induced M2 macrophages secrete anti-inflammatory cytokines such as IL8, IL10, TGFβ and MCP1 and are ascribed a wound healing role (135). While phagocytosis of pathogens in particular will polarize macrophages, it is still unclear whether pre-programmed, polarized macrophage subsets have a different inflammatory response upon encounter with a target, compared to naïve macrophages. The results surveyed in this review largely describe resting or resident macrophages, but some studies utilized PMA-treated or thioglycollate-elicited macrophages (**Table 1**), which may influence the inflammatory outcome. For instance, while resting macrophages undergoing Dectin-1-mediated uptake of zymosan did not induce NF-κB activation and TNFα production, priming of the macrophages with either GM-CSF or IFN-γ led to Dectin-1-CARD9-mediated TNFα production (31). Macrophage priming also enhanced the surface expression of Dectin-1 (31), which may account for enhanced pro-inflammatory signaling. Interestingly, we have shown that classical activation (IFN-γ + LPS) of macrophages promotes TLR4 delivery to the cell surface (136). Circulating IFN-γ is indicative of an ongoing infection, and consequent changes in phagocytic receptor display may create macrophage populations prepared for this circumstance. Our lab has also shown that classically activated macrophages have a dramatically enhanced stable microtubule population (137, 138). In M1 macrophages, these stabilized microtubule subsets have a prominent role in transporting vesicles containing matrix metalloproteinase-9, important for invasion (139). It will be of interest to determine whether phagocytosis receptor- and cytokine-containing vesicles also mobilize these stabilized tracks and whether this augments a pro-inflammatory response during phagocytosis.

CONCLUSIONS

In this review, we summarize the numerous macrophage receptors that serve as PRRs to recognize and engulf microbes and trigger pro- or anti-inflammatory outcomes. Many of the pro-inflammatory responses during phagocytosis are activated through TLR signaling pathways alone or with other receptors collaborating with TLRs. TLRs, in concert with other phagocytic receptors, can together enhance the macrophages' ability to target a variety of pathogens while utilizing the robust TLR signaling pathways to induce and regulate cytokine gene expression. The purpose of this review was to highlight the importance of understanding the macrophage response to whole microbes, versus soluble MAMPs, since these are the major players in infections. Future studies investigating additional receptor cross-talk during phagocytosis will likely reveal more physiological insights into cytokine outcomes for particles with multiple target moieties for macrophage engagement. Importantly, understanding how the phagocytosis machinery responsible for the uptake of large apoptotic and necrotic cells contributes to the well-described anti-inflammatory response in macrophages will add valuable insight to the field.

AUTHOR CONTRIBUTIONS

YF wrote the first draft and **Table 1**. RH edited the manuscript and did the figures. All authors contributed to the article and approved the submitted version.

FUNDING

This project was funded by a Natural Sciences and Engineering Research Council grant (RGPIN 2017-06087) and a grant from Canadian Institutes of Health Research grant (PJT-166084) to RH.

ACKNOWLEDGMENTS

We would like to thank Dr. Christina Guzzo (University of Toronto) for thoughtful discussions and critical reading of this manuscript.

REFERENCES

1. McDonald PP, Fadok VA, Bratton D, Henson PM. Transcriptional and translational regulation of inflammatory mediator production by endogenous TGF-β in macrophages that have ingested apoptotic cells. *J Immunol* (1999) 163(11):6164–72.
2. Flandin JF, Chano F, Descoteaux A. RNA interference reveals a role for TLR2 and TLR3 in the recognition of Leishmania donovani promastigotes by interferon-γ-primed macrophages. *Eur J Immunol* (2006) 36:411–20. doi: 10.1002/eji.200535079
3. Blander JM, Medzhitov R. Regulation of Phagosome Maturation by Signals from Toll-Like Receptors. *Science* (2004) 304:1014–18. doi: 10.1126/science.1096158
4. Kawasaki T, Kawai T. Toll-like receptor signaling pathways. *Front Immunol* (2014) 5:1–8. doi: 10.3389/fimmu.2014.00461
5. Kawai T, Akira S. The role of pattern-recognition receptors in innate immunity: Update on toll-like receptors. *Nat Immunol* (2010) 11:373–84. doi: 10.1038/ni.1863
6. Park BS, Song DH, Kim HM, Choi BS, Lee H, Lee JO. The structural basis of lipopolysaccharide recognition by the TLR4-MD-2 complex. *Nature* (2009) 458:1191–5. doi: 10.1038/nature07830
7. Takeuchi O, Akira S. Pattern Recognition Receptors and Inflammation. *Cell* (2010) 140:805–20. doi: 10.1016/j.cell.2010.01.022
8. Descamps D, Le Gars M, Balloy V, Barbier D, Maschalidi S, Tohme M, et al. Toll-like receptor 5 (TLR5), IL-1β secretion, and asparagine endopeptidase are critical factors for alveolar macrophage phagocytosis and bacterial killing. *Proc Natl Acad Sci USA* (2012) 109:1619–24. doi: 10.1073/pnas.1108464109
9. Knapp S, Wieland CW, Florquin S, Pantophlet R, Dijkshoorn L, Tshimbalanga N, et al. Differential roles of CD14 and Toll-like receptors 4 and 2 in murine Acinetobacter pneumonia. *Am J Respir Crit Care Med* (2006) 173:122–9. doi: 10.1164/rccm.200505-730OC
10. Wieland CW, Florquin S, Maris NA, Hoebe K, Beutler B, Takeda K, et al. The MyD88-Dependent, but Not the MyD88-Independent, Pathway of TLR4 Signaling Is Important in Clearing Nontypeable Haemophilus influenzae from the Mouse Lung. *J Immunol* (2005) 175:6042–9. doi: 10.4049/jimmunol.175.9.6042
11. Frevert CW, Matute-Bello G, Skerrett SJ, Goodman RB, Kajikawa O, Sittipunt C, et al. Effect of CD14 Blockade in Rabbits with Escherichia coli Pneumonia and Sepsis. *J Immunol* (2000) 64:5439–45. doi: 10.4049/jimmunol.164.10.5439
12. Janeway CA, Medzhitov R. Innate immune recognition. *Annu Rev Immunol* (2002) 20:197–216. doi: 10.1146/annurev.immunol.20.083001.084359
13. Akira S, Takeda K. Toll-like receptor signalling. *Nat Rev Immunol* (2004) 4:499–511. doi: 10.1038/nri1391
14. Strunk T, Coombs MRP, Currie AJ, Richmond P, Golenbock DT, Stoler-Barak L, et al. TLR2 mediates recognition of live Staphylococcus epidermidis and clearance of bacteremia. *PloS One* (2010) 5:1–8. doi: 10.1371/journal.pone.0010111
15. Yimin, Kohanawa M, Zhao S, Ozaki M, Haga S, Nan G, et al. Contribution of Toll-Like Receptor 2 to the Innate Response against Staphylococcus aureus Infection in Mice. *PloS One* (2013) 8:1–11. doi: 10.1371/journal.pone.0074287
16. Brown GD, Herre J, Williams DL, Willment JA, Marshall ASJ, Gordon S. Dectin-1 mediates the biological effects of β-glucans. *J Exp Med* (2003) 197:1119–24. doi: 10.1084/jem.20021890
17. Tada H, Nemoto E, Shimauchi H, Watanabe T, Mikami T, Matsumoto T, et al. Saccharomyces cerevisiae- and Candida albicans-derived mannan induced production of tumor necrosis factor alpha by human monocytes in a CD14- and Toll-like receptor 4-dependent manner. *Microbiol Immunol* (2002) 46:503–12. doi: 10.1111/j.1348-0421.2002.tb02727.x
18. Peiser L, De Winther MPJ, Makepeace K, Hollinshead M, Coull P, Plested J, et al. The class A macrophage scavenger receptor is a major pattern recognition receptor for Neisseria meningitidis which is independent of lipopolysaccharide and not required for secretory responses. *Infect Immun* (2002) 70:5346–54. doi: 10.1128/IAI.70.10.5346-5354.2002
19. Park SR, Kim DJ, Han SH, Kang MJ, Lee JY, Jeong YJ, et al. Diverse toll-like receptors mediate cytokine production by fusobacterium nucleatum and aggregatibacter actinomycetemcomitans in macrophages. *Infect Immun* (2014) 82:1914–20. doi: 10.1128/IAI.01226-13
20. Cauwels A, Wan E, Leismann M, Tuomanen E. Coexistence of CD14-dependent and independent pathways for stimulation of human monocytes by gram-positive bacteria. *Infect Immun* (1997) 65:3255–60. doi: 10.1128/iai.65.8.3255-3260.1997
21. Cuzzola M, Mancuso G, Beninati C, Biondo C, Von Hunolstein C, Orefici Z, et al. Human monocyte receptors involved in tumor necrosis factor responses to group B streptococcal products. *Infect Immun* (2000) 68:994–8. doi: 10.1128/IAI.68.2.994-998.2000
22. Bowdish DME, Sakamoto K, Kim MJ, Kroos M, Mukhopadhyay S, Leifer CA, et al. TLR2, and CD14 are required for macrophage cytokine responses to mycobacterial trehalose dimycolate and Mycobacterium tuberculosis. *PloS Pathog* (2009) 5:1–14. doi: 10.1371/journal.ppat.1000474
23. Erdman LK, Cosio G, Helmers AJ, Gowda DC, Grinstein S, Kain KC. CD36 and TLR Interactions in Inflammation and Phagocytosis: Implications for Malaria. *J Immunol* (2009) 183:6452–9. doi: 10.4049/jimmunol.0901374
24. Means TK, Mylonakis E, Tampakakis E, Colvin RA, Seung E, Puckett L, et al. Evolutionarily conserved recognition and innate immunity to fungal pathogens by the scavenger receptors SCARF1 and CD36. *J Exp Med* (2009) 206:637–53. doi: 10.1084/jem.20082109
25. Baranova IN, Kurlander R, Bocharov AV, Vishnyakova TG, Chen Z, Remaley AT, et al. Role of Human CD36 in Bacterial Recognition, Phagocytosis, and Pathogen-Induced JNK-Mediated Signaling. *J Immunol* (2008) 181:7147–56. doi: 10.4049/jimmunol.181.10.7147
26. Moore KJ, El Khoury J, Medeiros LA, Terada K, Geula C, Luster AD, et al. A CD36-initiated signaling cascade mediates inflammatory effects of β-amyloid. *J Biol Chem* (2002) 277:47373–9. doi: 10.1074/jbc.M208788200
27. Gantner BN, Simmons RM, Canavera SJ, Akira S, Underhill DM. Collaborative induction of inflammatory responses by dectin-1 and toll-like receptor 2. *J Exp Med* (2003) 197(9):1107–17. doi: 10.1084/jem.20021787
28. Chen SM, Shen H, Zhang T, Huang X, Liu XQ, Guo SY, et al. Dectin-1 plays an important role in host defense against systemic Candida glabrata infection. *Virulence* (2017) 8:1643–56. doi: 10.1080/21505594.2017.1346756
29. Reedy JL, Negoro PE, Feliu M, Lord AK, Khan NS, Lukason DP, et al. The carbohydrate lectin receptor dectin-1 mediates the immune response to Exserohilum rostratum. *Infect Immun* (2017) 85:1–18. doi: 10.1128/IAI.00903-16
30. Gersuk GM, Underhill DM, Zhu L, Marr KA. Dectin-1 and TLRs Permit Macrophages to Distinguish between Different Aspergillus fumigatus Cellular States. *J Immunol* (2006) 176:3717–24. doi: 10.4049/jimmunol.176.6.3717
31. Goodridge HS, Shimada T, Wolf AJ, Hsu Y-MS, Becker CA, Lin X, et al. Differential utilization of CARD9 by Dectin-1 in macrophages and dendritic cells. *J Immunol* (2013) 182:1146–54. doi: 10.1002/ana.22528s
32. Yamamoto Y, Klein TW, Friedman H. Involvement of mannose receptor in cytokine interleukin- 1β (IL-1β), IL-6, and granulocyte-macrophage colony-stimulating factor responses, but not in chemokine macrophage inflammatory protein 1β (MIP-1β), MIP-2, and KC responses, caused by attachment of C. *Infect Immun* (1997) 65:1077–82. doi: 10.1128/iai.65.3.1077-1082.1997
33. Heinsbroek SEM, Taylor PR, Martinez FO, Martinez-Pomares L, Brown GD, Gordon S. Stage-specific sampling by pattern recognition receptors during Candida albicans phagocytosis. *PloS Pathog* (2008) 4:1–11. doi: 10.1371/journal.ppat.1000218
34. Zhang J, Zhu J, Imrich A, Cushion M, Kinane TB, Koziel H. Pneumocystis activates human alveolar macrophage NF-κB signaling through mannose receptors. *Infect Immun* (2004) 2:3147–60. doi: 10.1128/IAI.72.6.3147-3160.2004
35. Zhang J, Tachado SD, Patel N, Zhu J, Imrich A, Manfruelli P, et al. Negative regulatory role of mannose receptors on human alveolar macrophage proinflammatory cytokine release in vitro. *J Leukoc Biol* (2005) 78:665–74. doi: 10.1189/jlb.1204699
36. Ifrim DC, Bain JM, Reid DM, Oosting M, Verschueren I, Gow NAR, et al. Role of dectin-2 for host defense against systemic infection with Candida glabrata. *Infect Immun* (2014) 82:1064–73. doi: 10.1128/IAI.01189-13

37. Chinthamani S, Settem RP, Honma K, Kay JG, Sharma A. Macrophage inducible C-type lectin (Mincle) recognizes glycosylated surface (S)-layer of the periodontal pathogen Tannerella forsythia. *PloS One* (2017) 12:1–3. doi: 10.1371/journal.pone.0173394
38. Yamasaki S, Matsumoto M, Takeuchi O, Matsuzawa T, Ishikawa E, Sakuma M, et al. C-type lectin Mincle is an activating receptor for pathogenic fungus, Malassezia. *Proc Natl Acad Sci USA* (2009 106:1897–902. doi: 10.1073/pnas.0805177106
39. Wells CA, Salvage-Jones JA, Li X, Hitchens K, Butcher S, Murray RZ, et al. The Macrophage-Inducible C-Type Lectin, Mincle, Is an Essential Component of the Innate Immune Response to Candida albicans. *J Immunol* (2008) 180:7404–13. doi: 10.4049/jimmunol.180.11.7404
40. Patin EC, Willcocks S, Orr S, Ward TH, Lang R, Schaible UE. Mincle-mediated anti-inflammatory IL-10 response counter-regulates IL-12 in vitro. *Innate Immun* (2016) 22:181–5. doi: 10.1177/1753425916636671
41. Ishikawa E, Ishikawa T, Morita YS, Toyonaga K, Yamada H, Takeuchi O, et al. Direct recognition of the mycobacterial glycolipid, trehalose dimycolate, by C-type lectin Mincle. *J Exp Med* (2009) 206:2879–88. doi: 10.1084/jem.20091750
42. Miyake Y, Toyonaga K, Mori D, Kakuta S, Hoshino Y, Oyamada A, et al. C-type Lectin MCL Is an FcRγ-Coupled Receptor that Mediates the Adjuvanticity of Mycobacterial Cord Factor. *Immunity* (2013) 38:1050–62. doi: 10.1016/j.immuni.2013.03.010
43. Vázquez A, Ruiz-Rosado J de D, Terrazas LI, Juárez I, Gomez-Garcia L, Calleja E, et al. Mouse macrophage galactose-type lectin (mMGL) is critical for host resistance against Trypanosoma cruzi infection. *Int J Biol Sci* (2014) 10:909–20. doi: 10.7150/ijbs.9214
44. Lugo-Villarino G, Troegeler A, Balboa L, Lastrucci C, Duval C, Mercier I, et al. The C-type lectin receptor DC-SIGN has an anti-inflammatory role in Human M(IL-4) macrophages in response to Mycobacterium tuberculosis. *Front Immunol* (2018) 9:1–15. doi: 10.3389/fimmu.2018.01123
45. Feng JY, Su WJ, Chuang FY, Pan SW, Yeh YC, Lin YY, et al. TREM-1 enhances Mycobacterium tuberculosis-induced inflammatory responses in macrophages. *Microbes Infect* (2020) 23:1–9. doi: 10.1016/j.micinf.2020.10.001
46. Hommes TJ, Hoogendijk AJ, Dessing MC, Van'T Veer C, Florquin S, Colonna M, et al. Triggering receptor expressed on myeloid cells-1 (TREM-1) improves host defence in pneumococcal pneumonia. *J Pathol* (2014) 233:357–67. doi: 10.1002/path.4361
47. Iizasa E, Chuma Y, Uematsu T, Kubota M, Kawaguchi H, Umemura M, et al. Contrasting roles of the innate receptors TREM2 versus Mincle in the recognition and response of macrophages to mycolic acid-containing lipids in mycobacterial cell walls. (2020). doi: 10.21203/rs.3.rs-37581/v1
48. Gawish R, Martins R, Böhm B, Wimberger T, Sharif O, Lakovits K, et al. Triggering receptor expressed on myeloid cells-2 fine-tunes inflammatory responses in murine Gram-negative sepsis. *FASEB J* (2015) 29:1247–57. doi: 10.1096/fj.14-260067
49. Wright SD, Silverstein SC. Receptors for C3b and C3bi promote phagocytosis but not the release of toxic oxygen from human phagocytes. *J Exp Med* (1983) 158:2016–23. doi: 10.1084/jem.158.6.2016
50. Aderem AA, Wright SD, Silverstein SC, Cohn ZA. Ligated complement receptors do not activate the arachidonic acid cascade in resident peritoneal macrophages. *J Exp Med* (1985) 161:617–22. doi: 10.1084/jem.161.3.617
51. Acharya D, Li XR, Heineman RES, Harrison RE. Complement Receptor-Mediated Phagocytosis Induces Proinflammatory Cytokine Production in Murine Macrophages. *Front Immunol* (2020) 10(3049):1–15. doi: 10.3389/fimmu.2019.03049
52. Sutterwala FS, Noel GJ, Salgame P, Mosser DM. Reversal of proinflammatory responses by ligating the macrophage Fcγ receptor type I. *J Exp Med* (1998) 188:217–22. doi: 10.1084/jem.188.1.217
53. Gallo P, Gonçalves R, Mosser DM. The influence of IgG density and macrophage Fc (gamma) receptor cross-linking on phagocytosis and IL-10 production. *Immunol Lett* (2010) 133:70–7. doi: 10.1016/j.imlet.2010.07.004
54. Zhou J, Ludlow LE, Hasang W, Rogerson SJ, Jaworowski A. Opsonization of malaria-infected erythrocytes activates the inflammasome and enhances inflammatory cytokine secretion by human macrophages. *Malar J* (2012) 11(343):1–13. doi: 10.1186/1475-2875-11-343
55. Ambarus CA, Santegoets KCM, van Bon L, Wenink MH, Tak PP, Radstake TRDJ, et al. Soluble immune complexes shift the TLR-induced cytokine production of distinct polarized human macrophage subsets towards IL-10. *PloS One* (2012) 7:1–10. doi: 10.1371/journal.pone.0035994
56. Huang JH, Lin CY, Wu SY, Chen WY, Chu CL, Brown GD, et al. CR3 and Dectin-1 Collaborate in Macrophage Cytokine Response through Association on Lipid Rafts and Activation of Syk-JNK-AP-1 Pathway. *PloS Pathog* (2015) 11:1–26. doi: 10.1371/journal.ppat.1004985
57. Lin J-S, Huang J-H, Hung L-Y, Wu S-Y, Wu-Hsieh BA. Distinct roles of complement receptor 3, Dectin-1, and sialic acids in murine macrophage interaction with Histoplasma yeast. *J Leukoc Biol* (2010) 88:95–106. doi: 10.1189/jlb.1109717
58. Kelley JL, Ozment TR, Li C, Schweitzer JB, Williams DL. Scavenger receptor-A (CD204): A two-edged sword in health and disease. *Crit Rev Immunol* (2014) 34:241–61. doi: 10.1615/CritRevImmunol.2014010267
59. Kraal G, Van Der Laan LJW, Elomaa O, Tryggvason K. The macrophage receptor MARCO. *Microbes Infect* (2000) 2:313–6. doi: 10.1016/S1286-4579(00)00296-3
60. Palecanda A, Paulauskis J, Al-Mutairi E, Imrich A, Qin G, Suzuki H, et al. Role of the scavenger receptor MARCO in alveolar macrophage binding of unopsonized environmental particles. *J Exp Med* (1999) 189:1497–506. doi: 10.1084/jem.189.9.1497
61. Elomaa O, Kangas M, Sahlberg C, Tuukkanen J, Sormunen R, Liakka A, et al. Cloning of a novel bacteria-binding receptor structurally related to scavenger receptors and expressed in a subset of macrophages. *Cell* (1995) 80:603–9. doi: 10.1016/0092-8674(95)90514-6
62. Benard EL, Roobol SJ, Spaink HP, Meijer AH. Phagocytosis of mycobacteria by zebrafish macrophages is dependent on the scavenger receptor Marco, a key control factor of pro-inflammatory signalling. *Dev Comp Immunol* (2014) 47:223–33. doi: 10.1016/j.dci.2014.07.022
63. van der Laan LJ, Döpp EA, Haworth R, Pikkarainen T, Kangas M, Elomaa O, et al. Regulation and functional involvement of macrophage scavenger receptor MARCO in clearance of bacteria in vivo. *J Immunol* (1999) 162:939–47.
64. PrabhuDas MR, Baldwin CL, Bollyky PL, Bowdish DME, Drickamer K, Febbraio M, et al. A Consensus Definitive Classification of Scavenger Receptors and Their Roles in Health and Disease. *J Immunol* (2017) 198:3775–89. doi: 10.4049/jimmunol.1700373
65. Febbraio M, Hajjar DP, Silverstein RL. CD36: A class B scavenger receptor involved in angiogenesis, atherosclerosis, inflammation, and lipid metabolism. *J Clin Invest* (2001) 108:785–91. doi: 10.1172/JCI14006
66. Medeiros LA, Khan T, El Khoury JB, Pham CLL, Hatters DM, Howlett GJ, et al. Fibrillar Amyloid Protein Present in Atheroma Activates CD36 Signal Transduction. *J Biol Chem* (2004) 279:10643–8. doi: 10.1074/jbc.M311735200
67. Gantner BN, Simmons RM, Underhill DM. Dectin-1 mediates macrophage recognition of Candida albicans yeast but not filaments. *EMBO J* (2005) 24:1277–86. doi: 10.1038/sj.emboj.7600594
68. Herre J, Marshall ASJ, Caron E, Edwards AD, Williams DL, Schweighoffer E, et al. Dectin-1 uses novel mechanisms for yeast phagocytosis in macrophages. *Blood* (2004) 104:4038–45. doi: 10.1182/blood-2004-03-1140
69. Steele C, Marrero L, Swain S, Harmsen AG, Zheng M, Brown GD, et al. Alveolar Macrophage-mediated Killing of Pneumocystis carinii f. sp. muris Involves Molecular Recognition by the Dectin-1 β-Glucan Receptor. *J Exp Med* (2003) 198:1677–88. doi: 10.1084/jem.20030932
70. Luther K, Torosantucci A, Brakhage AA, Heesemann J, Ebel F. Phagocytosis of Aspergillus fumigatus conidia by murine macrophages involves recognition by the dectin-1 beta-glucan receptor and Toll-like receptor 2. *Cell Microbiol* (2007) 9:368–81. doi: 10.1111/j.1462-5822.2006.00796.x
71. Speert DP, Wright SD, Silverstein SC, Mah B. Functional characterization of macrophage receptors for in vitro phagocytosis of unopsonized Pseudomonas aeruginosa. *J Clin Invest* (1988) 82:872–9. doi: 10.1172/JCI113692
72. Ezekowitz RAB, Williams DJ, Koziel H, Armstrong MYK, Warner A, Richards FF, et al. Uptake of Pneumocystis carinii mediated by the macrophage mannose receptor. *Nature* (1991) 351:155–8. doi: 10.1038/351155a0

73. Wilson ME, Pearson RD. Evidence that Leishmania donovani utilizes a mannose receptor on human mononuclear phagocytes to establish intracellular parasitism. *J Immunol* (1986) 136:4681–8.
74. Bermudez LE, Young LS, Enkel H. Interaction of Mycobacterium avium complex with human macrophages: Roles of membrane receptors and serum proteins. *Infect Immun* (1991) 59:1697–702. doi: 10.1128/iai.59.5.1697-1702.1991
75. Roecklein JA, Swartz RP, Yeager H. Nonopsonic uptake of Mycobacterium avium complex by human monocytes and alveolar macrophages. *J Lab Clin Med* (1992) 119:772–81. doi: 10.5555/uri:pii:0022214392903044
76. Alan R, Ezekowitz B, Sastry K, Bailly P, Warner A. Molecular characterization of the human macrophage mannose receptor: Demonstration of multiple carbohydrate recognition-like domains and phagocytosis of yeasts in cos-1 cells. *J Exp Med* (1990) 172:1785–94. doi: 10.1084/jem.172.6.1785
77. Astarie-Dequeker C, N'Diaye EN, Le Cabec V, Rittig MG, Prandi J, Maridonneau-Parini I. The mannose receptor mediates uptake of pathogenic and nonpathogenic mycobacteria and bypasses bactericidal responses in human macrophages. *Infect Immun* (1999) 67:469–77. doi: 10.1128/iai.67.2.469-477.1999
78. Schlesinger LS. Macrophage phagocytosis of virulent but not attenuated strains of Mycobacterium tuberculosis is mediated by mannose receptors in addition to complement receptors. *J Immunol* (1993) 150:2920–30.
79. Schlesinger LS, Kaufman TM, Iyer S, Hull SR, Marchiando LK. Differences in mannose receptor-mediated uptake of lipoarabinomannan from virulent and attenuated strains of Mycobacterium tuberculosis by human macrophages. *J Immunol* (1996) 157:4568–75.
80. Triantafilou M, Gamper FGJ, Haston RM, Mouratis MA, Morath S, Hartung T, et al. Membrane sorting of toll-like receptor (TLR)-2/6 and TLR2/1 heterodimers at the cell surface determines heterotypic associations with CD36 and intracellular targeting. *J Biol Chem* (2006) 281:31002–11. doi: 10.1074/jbc.M602794200
81. Koziel H, Eichbaum Q, Kruskal BA, Pinkston P, Rogers RA, Armstrong MYK, et al. Reduced binding and phagocytosis of Pneumocystis carinii by alveolar macrophages from persons infected with HIV-1 correlates with mannose receptor downregulation. *J Clin Invest* (1998) 102:1332–44. doi: 10.1172/JCI560
82. Gottschalk RA, Martins AJ, Angermann BR, Dutta B, Ng CE, Uderhardt S, et al. Distinct NF-κB and MAPK Activation Thresholds Uncouple Steady-State Microbe Sensing from Anti-pathogen Inflammatory Responses. *Cell Syst* (2016) 2:378–90. doi: 10.1016/j.cels.2016.04.016
83. Neese LW, Standing JE, Olson EJ, Castro M, Limper AH. Vitronectin, fibronectin, and gp120 antibody enhance macrophage release of TNF-α in response to Pneumocystis carinii. *J Immunol* (1994) 152:4549–56.
84. Richardson MB, Williams SJ. MCL and Mincle: C-type lectin receptors that sense damaged self and pathogen-associated molecular patterns. *Front Immunol* (2014) 5:288. doi: 10.3389/fimmu.2014.00288
85. Sharma A, Steichen AL, Jondle CN, Mishra BB, Sharma J. Protective role of mincle in bacterial pneumonia by regulation of neutrophil mediated phagocytosis and extracellular trap formation. *J Infect Dis* (2014) 209:1837–46. doi: 10.1093/infdis/jit820
86. Rabes A, Zimmermann S, Reppe K, Lang R, Seeberger PH, Suttorp N, et al. The C-type lectin receptor mincle binds to streptococcus pneumoniae but plays a limited role in the anti-pneumococcal innate immune response. *PloS One* (2015) 10:1–12. doi: 10.1371/journal.pone.0117022
87. Lobato-Pascual A, Saether PC, Fossum S, Dissen E, Daws MR. Mincle, the receptor for mycobacterial cord factor, forms a functional receptor complex with MCL and FcεRI-γ. *Eur J Immunol* (2013) 43:3167–74. doi: 10.1002/eji.201343752
88. Yuita H, Tsuiji M, Tajika Y, Matsumoto Y, Hirano K, Suzuki N, et al. Retardation of removal of radiation-induced apoptotic cells in developing neural tubes in macrophage galactose-type C-type lectin-1-deficient mouse embryos. *Glycobiology* (2005) 15:1368–75. doi: 10.1093/glycob/cwj028
89. Van Kooyk Y, Geijtenbeek TBH. DC-SIGN: Escape mechanism for pathogens. *Nat Rev Immunol* (2003) 3:697–709. doi: 10.1038/nri1182
90. Roe K, Gibot S, Verma S. Triggering receptor expressed on myeloid cells-1 (TREM-1): A new player in antiviral immunity? *Front Microbiol* (2014) 5 (627):1–11. doi: 10.3389/fmicb.2014.00627
91. Hommes TJ, Dessing MC, Van't Veer C, Florquin S, Colonna M, De Vos AF, et al. Role of triggering receptor expressed on myeloid cells-1/3 in klebsiella-derived pneumosepsis. *Am J Respir Cell Mol Biol* (2015) 53:647–55. doi: 10.1165/rcmb.2014-0485OC
92. Kleinberger G, Yamanishi Y, Suárez-Calvet M, Czirr E, Lohmann E, Cuyvers E, et al. TREM2 mutations implicated in neurodegeneration impair cell surface transport and phagocytosis. *Sci Transl Med* (2014) 6:1–12. doi: 10.1126/scitranslmed.3009093
93. N'Diaye EN, Branda CS, Branda SS, Nevarez L, Colonna M, Lowell C, et al. TREM-2 (triggering receptor expressed on myeloid cells 2) is a phagocytic receptor for bacteria. *J Cell Biol* (2009) 184:215–23. doi: 10.1083/jcb.200808080
94. Graham LM, Brown GD. The Dectin-2 family of C-type lectins in immunity and homeostasis. *Cytokine* (2009) 48:148–55. doi: 10.1016/j.cyto.2009.07.010
95. Fraser IP, Stuart L, Ezekowitz RAB. TLR-independent pattern recognition receptors and anti-inflammatory mechanisms. *J Endotoxin Res* (2004) 10:120–4. doi: 10.1179/096805104225004013
96. Turnbull IR, Gilfillan S, Cella M, Aoshi T, Miller M, Piccio L, et al. Cutting Edge: TREM-2 Attenuates Macrophage Activation. *J Immunol* (2006) 177:3520–4. doi: 10.4049/jimmunol.177.6.3520
97. Peng Q, Malhotra S, Torchia JA, Kerr WG, Coggeshall KM, Humphrey MB. TREM2- and DAP12-dependent activation of PI3K requires DAP10 and is inhibited by SHIP1. *Sci Signal* (2010) 3:1–30. doi: 10.1126/scisignal.2000500
98. Indik ZK, Park J-G, Hunter S, Schreiber AD. The molecular dissection of Fc gamma receptor mediated phagocytosis. *Am Soc Hematol* (1995) 86:4389–99. doi: 10.1182/blood.V86.12.4389.bloodjournal86124389
99. Mosser DM, Zhang X. Measuring opsonic phagocytosis via Fcγ receptors and complement receptors on macrophages. *Curr Protoc Immunol* (2011) 14:1–12. doi: 10.1002/0471142735.im1427s95
100. Helmy KY, Katschke KJ, Gorgani NN, Kljavin NM, Elliott JM, Diehl L, et al. CRIg: A macrophage complement receptor required for phagocytosis of circulating pathogens. *Cell* (2006) 124:915–27. doi: 10.1016/j.cell.2005.12.039
101. Hajishengallis G, Lambris JD. More than complementing Tolls: complement–Toll-like receptor synergy and crosstalk in innate immunity and inflammation. *Immunol Rev* (2016) 274:233–44. doi: 10.1111/imr.12467
102. Han C, Jin J, Xu S, Liu H, Li N, Cao X. Integrin CD11b negatively regulates TLR-triggered inflammatory responses by activating Syk and promoting degradation of MyD88 and TRIF via Cbl-b. *Nat Immunol* (2010) 11:734–42. doi: 10.1038/ni.1908
103. Takeda K, Kaisho T, Akira S. Toll-like receptors. *Annu Rev Immunol* (2003) 21:335–76. doi: 10.1146/annurev.immunol.21.120601.141126
104. Uribe-querol E, Rosales C. Phagocytosis : Our Current Understanding of a Universal Biological Process. *Front Immunol* (2020) 11:1–13. doi: 10.3389/fimmu.2020.01066
105. Niedergang F, Grinstein S. How to build a phagosome: new concepts for an old process. *Curr Opin Cell Biol* (2018) 50:57–63. doi: 10.1016/j.ceb.2018.01.009
106. Berton G, Mócsai A, Lowell CA. Src and Syk kinases: Key regulators of phagocytic cell activation. *Trends Immunol* (2005) 26:208–14. doi: 10.1016/j.it.2005.02.002
107. Brown GD. Dectin-1 : A signalling non-TLR pattern-recognition receptor. *Nat Rev Immunol* (2006) 6:33–43. doi: 10.1038/nri1745
108. Kim JY, Lee YG, Kim MY, Byeon SE, Rhee MH, Park J, et al. Src-mediated regulation of inflammatory responses by actin polymerization. *Biochem Pharmacol* (2010) 79:431–43. doi: 10.1016/j.bcp.2009.09.016
109. Yi YS, Son YJ, Ryou C, Sung GH, Kim JH, Cho JY. Functional roles of Syk in macrophage-mediated inflammatory responses. *Mediators Inflammation* (2014) 2014:1–12. doi: 10.1155/2014/270302
110. Heit B, Kim H, Cosío G, Castaño D, Collins R, Lowell CA, et al. Multimolecular signaling complexes enable Syk-mediated signaling of CD36 internalization. *Dev Cell* (2013) 24:372–83. doi: 10.1016/j.devcel.2013.01.007
111. Scott CC, Dobson W, Botelho RJ, Coady-Osberg N, Chavrier P, Knecht DA, et al. Phosphatidylinositol-4, 5-bisphosphate hydrolysis directs actin remodeling during phagocytosis. *J Cell Biol* (2005) 169:139–49. doi: 10.1083/jcb.200412162
112. Cox D, Tseng CC, Bjekic G, Greenberg S. A requirement for phosphatidylinositol 3-kinase in pseudopod extension. *J Biol Chem* (1999) 274:1240–7. doi: 10.1074/jbc.274.3.1240

113. Lennartz M. Protein Kinase C-epsilon in Membrane Delivery during Phagocytosis. *J Immunol Sci* (2018) 2:26–32. doi: 10.29245/2578-3009/2018/2.1134
114. Fronhofer V, Lennartz MR, Loegering DJ. Role of PKC isoforms in the FcγR-mediated inhibition of LPS-stimulated IL-12 secretion by macrophages. *J Leukoc Biol* (2006) 79:408–15. doi: 10.1189/jlb.0805438
115. Ajibade AA, Wang HY, Wang RF. Cell type-specific function of TAK1 in innate immune signaling. *Trends Immunol* (2013) 34:307–16. doi: 10.1016/j.it.2013.03.007
116. Botelho RJ, Harrison RE, Stone JC, Hancock JF, Philips MR, Jongstra-Bilen J, et al. Localized diacylglycerol-dependent stimulation of Ras and Rap1 during phagocytosis. *J Biol Chem* (2009) 284:28522–32. doi: 10.1074/jbc.M109.009514
117. García-García E, Rosales R, Rosales C. Phosphatidylinositol 3-kinase and extracellular signal-regulated kinase are recruited for Fc receptor-mediated phagocytosis during monocyte-to-macrophage differentiation. *J Leukoc Biol* (2002) 72:107–14. doi: 10.1189/jlb.72.1.107
118. Shumway SD, Maki M, Miyamoto S. The PEST domain of IκBα is necessary and sufficient for in vitro degradation by μ-calpain. *J Biol Chem* (1999) 274:30874–81. doi: 10.1074/jbc.274.43.30874
119. Schaecher K, Goust JM, Banik NL. The effects of calpain inhibition on IkBα degradation after activation of PBMCs: Identification of the calpain cleavage sites. *Neurochem Res* (2004) 29:1443–51. doi: 10.1023/B:NERE.0000026410.56000.dd
120. Li X, Luo R, Chen R, Song L, Zhang S, Hua W, et al. Cleavage of IκBα by calpain induces myocardial NF-κB activation, TNF-α expression, and cardiac dysfunction in septic mice. *Am J Physiol Hear Circ Physiol* (2014) 306:H833–43. doi: 10.1152/ajpheart.00893.2012
121. Goodridge HS, Reyes CN, Becker CA, Katsumoto TR, Ma J, Wolf AJ, et al. Activation of the innate immune receptor Dectin-1 upon formation of a Phagocytic synapse. *Nature* (2011) 472:471–5. doi: 10.1038/nature10071
122. Li M, Wang H, Li W, Xu XG, Yu Y. Macrophage activation on "phagocytic synapse" arrays: Spacing of nanoclustered ligands directs TLR1/2 signaling with an intrinsic limit. *Sci Adv* (2020) 6:1–11. doi: 10.1126/sciadv.abc8482
123. Lucas M, Zhang X, Prasanna V, Mosser DM. ERK Activation Following Macrophage FcγR Ligation Leads to Chromatin Modifications at the IL-10 Locus. *J Immunol* (2005) 175:469–77. doi: 10.4049/jimmunol.175.1.469
124. Kapetanovic R, Nahori MA, Balloy V, Fitting C, Philpott DJ, Cavaillon JM, et al. Contribution of phagocytosis and intracellular sensing for cytokine production by Staphylococcus aureus-activated macrophages. *Infect Immun* (2007) 75:830–7. doi: 10.1128/IAI.01199-06
125. Nica Regueiro V, Campos MA, Pons J, Albertí SN, Bengoechea JA, Es J. The uptake of a Klebsiella pneumoniae capsule polysaccharide mutant triggers an inflammatory response by human airway epithelial cells. *Microbiology* (2006) 152:555–66. doi: 10.1099/mic.0.28285-0
126. Barkman C, Martner A, Hessle C, Wold AE. Soluble bacterial constituents down-regulate secretion of IL-12 in response to intact Gram-positive bacteria. *Microbes Infect* (2008) 10:1484–93. doi: 10.1016/j.micinf.2008.08.011
127. Jönsson B, Ridell M, Wold AE. Phagocytosis and cytokine response to rough and smooth colony variants of Mycobacterium abscessus by human peripheral blood mononuclear cells. *APMIS* (2013) 121:45–55. doi: 10.1111/j.1600-0463.2012.02932.x
128. Brubaker SW, Bonham KS, Zanoni I, Kagan JC. Innate immune pattern recognition: A cell biological perspective. *Annu Rev Immunol* (2015) 33:257–90. doi: 10.1146/annurev-immunol-032414-112240
129. Silver KE, Harrison RE. Kinesin 5B Is Necessary for Delivery of Membrane and Receptors during FcγR-Mediated Phagocytosis. *J Immunol* (2011) 186:816–25. doi: 10.4049/jimmunol.1002161
130. Poirier MB, Fiorino C, Rajasekar TK, Harrison RE. F-actin flashes on phagosomes mechanically deform contents for efficient digestion in macrophages. *J Cell Sci* (2020) 133:1–13. doi: 10.1242/jcs.239384
131. Yam PT, Theriot JA. Repeated cycles of rapid actin assembly and disassembly on epithelial cell phagosomes. *Mol Biol Cell* (2004) 15:5647–58. doi: 10.1091/mbc.E04-06-0509
132. Zhou H, Coveney AP, Wu M, Huang J, Blankson S, Zhao H, et al. Activation of both TLR and NOD signaling confers host innate immunity-mediated protection against microbial infection. *Front Immunol* (2019) 9:1–15. doi: 10.3389/fimmu.2018.03082
133. Wolf AJ, Arruda A, Reyes CN, Kaplan AT, Shimada T, Shimada K, et al. Phagosomal Degradation Increases TLR Access to Bacterial Ligands and Enhances Macrophage Sensitivity to Bacteria. *J Immunol* (2011) 187:6002–10. doi: 10.4049/jimmunol.1100232
134. Underhill DM, Goodridge HS. Information processing during phagocytosis. *Nat Rev Immunol* (2012) 12:492–502. doi: 10.1038/nri3244
135. Atri C, Guerfali FZ, Laouini D. Role of human macrophage polarization in inflammation during infectious diseases. *Int J Mol Sci* (2018) 19(1801):1–15. doi: 10.3390/ijms19061801
136. Xu K, Harrison RE. Down-regulation of stathmin is required for the phenotypic changes and classical activation of macrophages. *J Biol Chem* (2015) 290:19245–60. doi: 10.1074/jbc.M115.639625
137. Patel PC, Fisher KH, Yang ECC, Deane CM, Harrison RE. Proteomic analysis of microtubule-associated proteins during macrophage activation. *Mol Cell Proteomics* (2009) 8:2500–14. doi: 10.1074/mcp.M900190-MCP200
138. Khandani A, Eng E, Jongstra-Bilen J, Schreiber AD, Douda D, Samavarchi-Tehrani P, et al. Microtubules regulate PI-3K activity and recruitment to the phagocytic cup during Fcγ receptor-mediated phagocytosis in nonelicited macrophages. *J Leukoc Biol* (2007) 82:417–28. doi: 10.1189/jlb.0706469
139. Hanania R, Sun HS, Xu K, Pustylnik S, Jeganathan S, Harrison RE. Classically activated macrophages use stable microtubules for matrix metalloproteinase-9 (MMP-9) secretion. *J Biol Chem* (2012) 287:8468–83. doi: 10.1074/jbc.M111.290676

Conflict of Interest: The authors declare that the research was conducted in the absence of any commercial or financial relationships that could be construed as a potential conflict of interest.

Copyright © 2021 Fu and Harrison. This is an open-access article distributed under the terms of the Creative Commons Attribution License (CC BY). The use, distribution or reproduction in other forums is permitted, provided the original author(s) and the copyright owner(s) are credited and that the original publication in this journal is cited, in accordance with accepted academic practice. No use, distribution or reproduction is permitted which does not comply with these terms.

frontiers in Immunology

ORIGINAL RESEARCH
published: 31 May 2021
doi: 10.3389/fimmu.2021.649600

Rab10-Positive Tubular Structures Represent a Novel Endocytic Pathway That Diverges From Canonical Macropinocytosis in RAW264 Macrophages

*Katsuhisa Kawai, Arata Nishigaki, Seiji Moriya, Youhei Egami and Nobukazu Araki**

Department of Histology and Cell Biology, School of Medicine, Kagawa University, Miki, Japan

OPEN ACCESS

Edited by:
Gregory D. Fairn, Dalhousie University, Canada

Reviewed by:
Jason Kay, University at Buffalo, United States
Rachael Zoe Murray, Queensland University of Technology, Australia

***Correspondence:**
Nobukazu Araki
naraki@med.kagawa-u.ac.jp

Specialty section:
This article was submitted to Molecular Innate Immunity, a section of the journal Frontiers in Immunology

Received: *05 January 2021*
Accepted: *11 May 2021*
Published: *31 May 2021*

Citation:
Kawai K, Nishigaki A, Moriya S, Egami Y and Araki N (2021) Rab10-Positive Tubular Structures Represent a Novel Endocytic Pathway That Diverges From Canonical Macropinocytosis in RAW264 Macrophages. Front. Immunol. 12:649600. doi: 10.3389/fimmu.2021.649600

Using the optogenetic photo-manipulation of photoactivatable (PA)-Rac1, remarkable cell surface ruffling and the formation of a macropinocytic cup (premacropinosome) could be induced in the region of RAW264 macrophages irradiated with blue light due to the activation of PA-Rac1. However, the completion of macropinosome formation did not occur until Rac1 was deactivated by the removal of the light stimulus. Following PA-Rac1 deactivation, some premacropinosomes closed into intracellular macropinosomes, whereas many others transformed into long Rab10-positive tubules without forming typical macropinosomes. These Rab10-positive tubules moved centripetally towards the perinuclear Golgi region along microtubules. Surprisingly, these Rab10-positive tubules did not contain any endosome/lysosome compartment markers, such as Rab5, Rab7, or LAMP1, suggesting that the Rab10-positive tubules were not part of the degradation pathway for lysosomes. These Rab10-positive tubules were distinct from recycling endosomal compartments, which are labeled with Rab4, Rab11, or SNX1. These findings suggested that these Rab10-positive tubules may be a part of non-degradative endocytic pathway that has never been known. The formation of Rab10-positive tubules from premacropinosomes was also observed in control and phorbol myristate acetate (PMA)-stimulated macrophages, although their frequencies were low. Interestingly, the formation of Rab10-positive premacropinosomes and tubules was not inhibited by phosphoinositide 3-kinase (PI3K) inhibitors, while the classical macropinosome formation requires PI3K activity. Thus, this study provides evidence to support the existence of Rab10-positive tubules as a novel endocytic pathway that diverges from canonical macropinocytosis.

Keywords: macropinocytosis, Rab10, tubules, endocytosis, macrophages, live-cell imaging

INTRODUCTION

Macropinocytosis is a form of clathrin-independent, actin-dependent endocytosis that mediates the non-selective uptake of extracellular fluids and solutes into 0.2 – several μm diameter endocytic vesicles called macropinosomes. Newly-formed macropinosomes undergo a maturation process, during which they fuse with other endocytic compartments and eventually merged with lysosomes (1, 2). In macrophages and dendritic cells, this endocytic pathway is involved in immune surveillance and antigen presentation (3). In tumor cells, macropinocytosis serves as an amino acid supply route to support active cell proliferation (4). In neuronal cells, macropinocytosis has been proposed to be involved in the uptake and propagation of pathogenic protein aggregates associated with neurodegenerative diseases such as Alzheimer's disease and Parkinson's disease (5). In addition, many pathogenic bacteria and viruses exploit macropinocytosis pathways to gain entry into host cells during infection (6). Therefore, a better understanding of the molecular mechanisms underlying macropinocytosis and its related pathways has implications for cell biology and the establishment of therapeutic strategies to combat various diseases, including cancer and viral infections.

Phosphoinositide metabolism and small GTPases of the Ras superfamily, including the Rho and Rab families, coordinately regulate macropinosome formation and maturation (7, 8). Macropinocytosis is initiated by the plasma membrane ruffle formation driven by the actin polymerization and reorganization which is upregulated by Rac1, a member of the Rho family GTPases. Using an optogenetic technology in which RAW macrophages express photoactivatable Rac1 (PA-Rac1), we have found that Rac1 activation is sufficient to induce plasma membrane ruffling and circular ruffle/macropinocytic cup formation; however, persistent Rac1 activation stalls at the macropinocytic cup stage without progressing to the complete formation of macropinosomes. Rac1 deactivation following temporal activation enables some macropinocytic cups to form macropinosomes (9). By repeating the activation and deactivation of PA-Rac1 at a certain interval, macropinocytosis can be efficiently induced. However, many macropinocytic cups collapse prior to the completion of macropinosome formation. It is also known that a considerable number of circular ruffles or macropinocytic cups in macrophages under normal conditions disappear without resulting in intracellular macropinosome formation (1). Nonetheless, no attention has been paid to the phenomenon of cup collapse so far. Therefore, in this study, we focused our attention on the differences between collapsing macropinocytic cups and typical cups that form macropinosomes.

The Rab family GTPases comprise more than 60 members in mammals and are key regulators of membrane trafficking (10, 11). One protein, Rab10, has been implicated in a variety of membrane trafficking pathways (12–17). More recently, Rab10 was identified as a novel protein regulator of tubular recycling endosome formation through interaction with the kinesin motor protein KIF13 (18). Furthermore, it was reported that Rab10 phosphorylation by leucine-rich repeat kinase 2 (LRRK2) has been associated with the regulation of macropinosome early maturation (19).

In this study, while studying RAW264 macrophages expressing a fluorescent protein-tagged Rab10 and PA-Rac1, we unexpectedly discovered that macropinocytic cup or pocket-like structures (premacropinosomes) that were intensively associated with Rab10 collapsed and disappeared by transforming into Rab10-positive tubules, whereas those premacropinosomes that were only faintly or briefly associated with Rab10 became intracellular macropinosomes. The Rab10-positive tubules that originated from premacropinosomes were distinct from known endocytic compartments having Rab4, Rab5, Rab7, Rab11, SNX1, or lysosomal associated membrane protein 1 (LAMP1). Here, we provide evidence to support the existence of a new endocytic pathway that diverges from canonical macropinocytosis.

MATERIALS AND METHODS

Chemicals and Plasmids

pEGFP-C1, pECFP-C1, and pmCherry-C1 were obtained from Clontech. pEGFP-Rab8a, pEGFP-Rab10, pmCherry-Rab10, pEGFP-Rab35-4E, EGFP-tubulin, pEGFP-EHBP1, pEGFP-EHD1, pEGFP-MICAL-L1, and pEGFP-SNX1 were generated by amplifying the full-length open reading frames of each gene by polymerase chain reaction (PCR), followed by the cloning of the resultant PCR products into pEGFP-C1, or pmCherry-C1. The pmCitrine-Rab4, pmCitrine-Rab5, pmCitrine-Rab7, pmCitrine-LAMP1, and pmCitrine-Akt-PH domain were provided by Dr. Joel A. Swanson (University of Michigan). pEGFP-Rab11 was provided by Dr. Marino Zerial (Max Planck Institute). pTriEx/mCherry-PA-Rac1 was obtained from Dr. Klaus Hahn through Addgene (Plasmid #22027, Cambridge, MA). pECFP-PA-Rac1 was created by the insertion of the PA-Rac1 fragment into pECFP-C1.

Other reagents were purchased from Sigma-Aldrich (St. Louis, MO) or Nakalai Tesque (Kyoto, Japan) unless otherwise indicated.

Cell Culture and Transfection

RAW264 cells were obtained from Riken Cell Bank (Tsukuba, Japan) and maintained in Dulbecco's modified Eagle medium supplemented with 10% heat-inactivated fetal bovine serum and antibiotics (100 U/mL of penicillin and 0.1 mg/mL streptomycin) at 37°C in a humidified atmosphere containing 5% CO_2. Cells were transfected with vectors using the Neon Transfection System (Life Technologies), according to the manufacturer's protocol. Briefly, 100 μL of a RAW264 cell suspension (1.0×10^7 cells/mL) in Buffer R was mixed with 1.0–3.0 μg of the indicated plasmids and electroporated once at 1,680 V for 20 ms. The cells were then seeded onto 25-mm circular coverslips in culture dishes containing the culture medium. At 10–24 h after transfection, the cells were subjected to live-cell imaging.

Live-Cell Imaging and Optogenetic Photo-Manipulation

RAW264 cells transfected with plasmids were cultured on 25-mm circular coverslips. The coverslip was assembled in an Attofluor cell chamber (A7816, Molecular Probes, Eugene, OR)

filled with Ringer's buffer (RB), consisting of 155 mM NaCl, 5 mM KCl, 1 mM $MgCl_2$, 2 mM Na_2HPO_4, 10 mM glucose, 10 mM HEPES and 0.5 mg/mL bovine serum albumin (BSA) at pH 7.2. The chamber was settled onto a thermo-controlled stage (Tokai Hit, Shizuoka, Japan) attached to a confocal laser microscope (Zeiss LSM700) or an epifluorescence microscope (Leica DMI6000B).

The optogenetic photo-manipulation of PA-Rac1 activity was performed as previously described (9, 20). Briefly, cells were transfected with pTriEx/mCherry- or pECFP-PA-Rac1 (21) and observed under the LSM700 confocal microscope controlled by ZEN (Zeiss) By illuminating a blue-light laser (445 or 488 nm wavelength) to the cells expressing PA-Rac1 under the indicated conditions, PA-Rac1 was activated through the conformational change of the light oxygen voltage 2 domain (LOV2) of PA-Rac1 in either a local area or the whole-cell region. PA-Rac1 can be reversibly deactivated by turning off the blue-light illumination (21). To observe the dynamics of a red fluorescent protein-tagged protein during PA-Rac1 photo-manipulation, pECFP-PA-Rac1 was employed. In some optogenetic photo-manipulation experiments were performed using the Leica DMI6000B automated epifluorescence microscopy system, controlled by MetaMorph software (Molecular Devices) (20). The acquired fluorescence images were processed using the Safir denoising software (INRIA) and the nearest neighbor deconvolution algorism of the MetaMorph software. Microscopic images are representative of ≥7 cells from at least three separate experiments.

Data Presentation and Statistical Analysis

Quantitation of macropinosome and premacropinosome formation was performed by counting phase-bright macropinosomes and Rab10-positive premacropinosomes larger than 2 μm in diameter using time-lapse microscopic movies. The number of macropinosomes/premacropinosomes formed during 10 min/cell was calculated. Quantitative data are expresses as the means ± standard deviations (SD, n≥7 cells from at least three independent experiments). Significant differences in mean values were determined by a two-tailed unpaired *t-test*. *P*-values less than 0.05 were considered statistically significant.

RESULTS

Reversible Optogenetic Control of PA-Rac1 Activity Induces Rab10-Positive Tubule Formation

Through the optogenetic control of PA- Rac1 activity in RAW264 cells, we were able to manipulate the process of macropinocytosis (9). The activation of PA-Rac1 by local irradiation with blue light-induced cell surface ruffling. Continuous blue-light irradiation applied to the same area results in the formation of numerous bubble-like structures underneath the ruffles. Our previous study revealed that these bubble-like structures are unclosed macropinocytic cups or pockets, which we refer to as premacropinosomes. After turning off the blue-light irradiation, some premacropinosomes were closed into intracellular macropinosomes, but many other premacropinosomes (~70%) disappear without forming macropinosomes (**Figure 1A**, **Supplementary Movie 1**), as we have previously reported (9).

To clarify the involvement of Rab10 in this process, enhanced green fluorescent protein (EGFP) - or mCherry-tagged Rab10 was co-expressed together with enhanced cyan fluorescent protein (ECFP)-tagged PA-Rac1 and observed in live RAW264 cells during the optogenetic control of PA-Rac1 activity. We found that most PA-Rac1induced premacropinosomes were intensively positive for Rab10. Following the deactivation of PA-Rac1, these Rab10-positive premacropinosomes transformed into tubular structures. Under phase-contrast microscopy, premacropinosomes appeared to collapse and return to the cell surface without forming phase-bright macropinosomes; however, they actually transformed into tubular structures. Curiously, only Rab10-negative premacropinosomes, ~30% of all premacropinosomes, became phase-bright macropinosomes (**Figures 1A, B**, **Supplementary Figures S1**).

When we observed EGFP-Rab10 dynamics in RAW264 cells co-expressing with mCherry-PA-Rac1, which was temporally activated by 488 nm excitation for EGFP-Rab10 observation with 15-sec intervals, we found that the Rab10-positive tubules frequently form from the Rab10-positive premacropinosomes (**Figures 1C, D**). By live-cell imaging of RAW264 cells co-expressing EGFP-Rab10 with PA-Rac1, it was apparently shown that a few Rab10-tubules extended from one peripheral premacropinosome toward the cell center perinuclear region. The body of the premacropinosome gradually shrunk and disappeared without moving into the cell center (**Figure 1D**, **Supplementary Movie 2**). We were able to constantly induce the formation of Rab10-positive tubules from multiple premacropinosomes over a 30-min observation period through repeating PA-Rac1 activation (ON) and deactivation (OFF) cycles with the 488 nm-excitation light for EGFP observation.

The Rab10-Positive Tubular Endocytic Pathway Exists in Cells Under Near-Physiological Conditions

Rab10-positive tubule may reflect an artificial structure that is an artifact of PA-Rac1 photo-manipulation. To rule out this possibility, we examined whether Rab10-positive tubules could be observed in RAW264 cells under near-physiological conditions. In RAW264 cells stimulated with 100 nM phorbol myristate acetate (PMA), membrane ruffling and macropinosome formation were enhanced. During the normal process of macropinosome formation, Rab10 transiently localized to nascent macropinosomes. The Rab10 localization to macropinosomal membranes was much sparser than that on premacropinosomes formed by the photo-manipulation of PA-Rac1 ON-OFF cycling. During a long and careful observation, we observed that Rab10-positive premacropinosomes and tubules were occasionally formed in PMA-stimulated cells (**Figure 2**, **Supplementary Movie 3**). Counting the number of Rab10-positive premacropinosomes and Rab10-negative macropinosomes formed showed that the percentage of Rab10-positive premacropinosomes across all

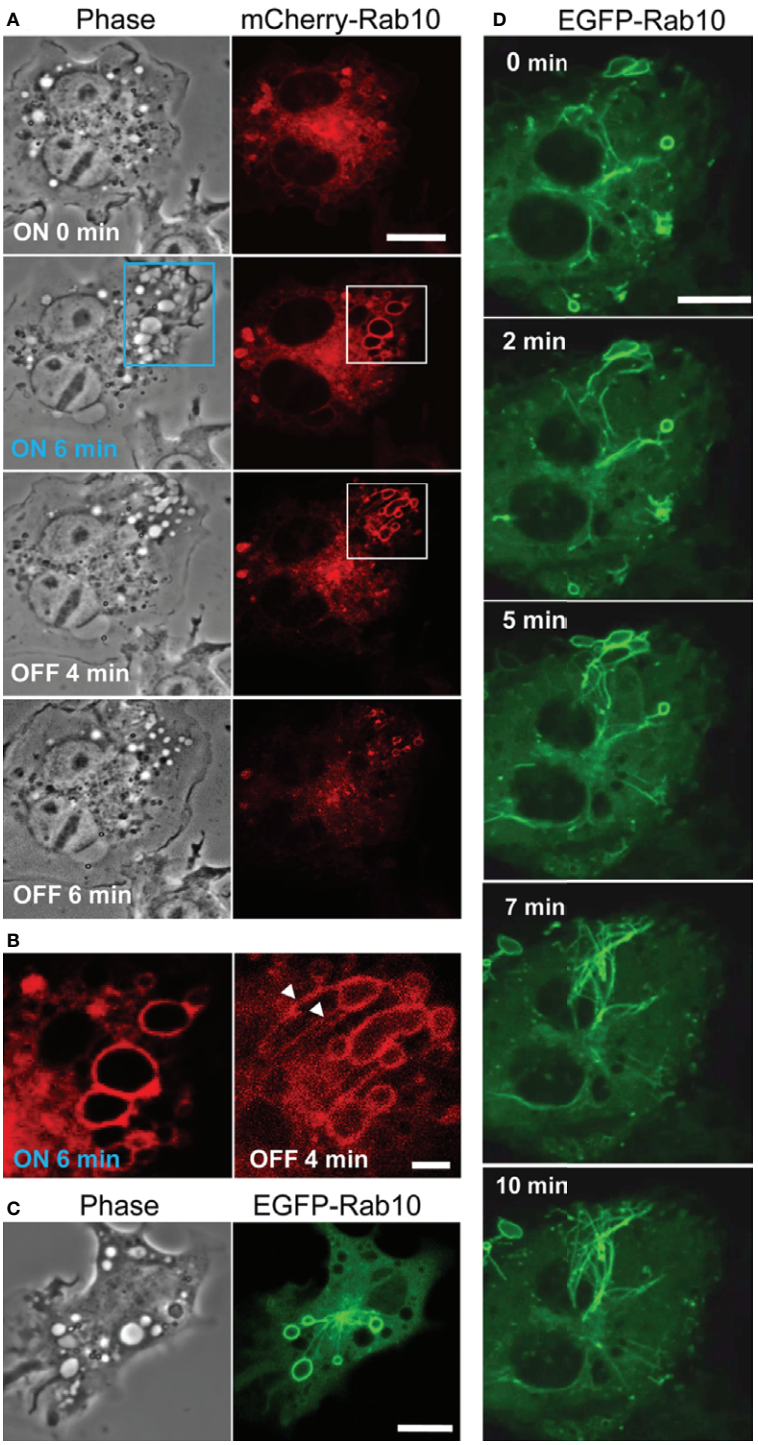

FIGURE 1 | Rab10 dynamics in live RAW264 cells under the optogenetic control of PA-Rac1 activity. **(A)** The blue boxed area of a cell expressing ECFP-PA-Rac1 was irradiated with a blue laser to photoactivate PA-Rac1. Phase-contrast (left) and mCherry-Rab10 (right) images were acquired at the indicated times after PA-Rac1 activation (ON) and deactivation (OFF). Scale bar =10 μm. **(B)** Enlarged images of the white boxed area in **(A)** Following local PA-Rac1 activation, Rab10-positive premacropinosomes were formed in the area. After PA-Rac1 OFF, a few Rab10-positive tubules extended from a premacropinosome (arrowheads). Scale bar = 2 μm. **(C)** Representative phase-contrast and EGFP-Rab10 fluorescence images of RAW264 cells during PA-Rac1 ON-OFF cycles. **(D)** Confocal time-lapse microscopy of EGFP-Rab10 in RAW264 cells during PA-Rac1 ON-OFF cycles. Selected frames from the time-lapse movie are presented. Elapsed times are shown in the frame. Scale bar = 10 μm. The corresponding movie is available in the **Supplementary Material Movie 2**.

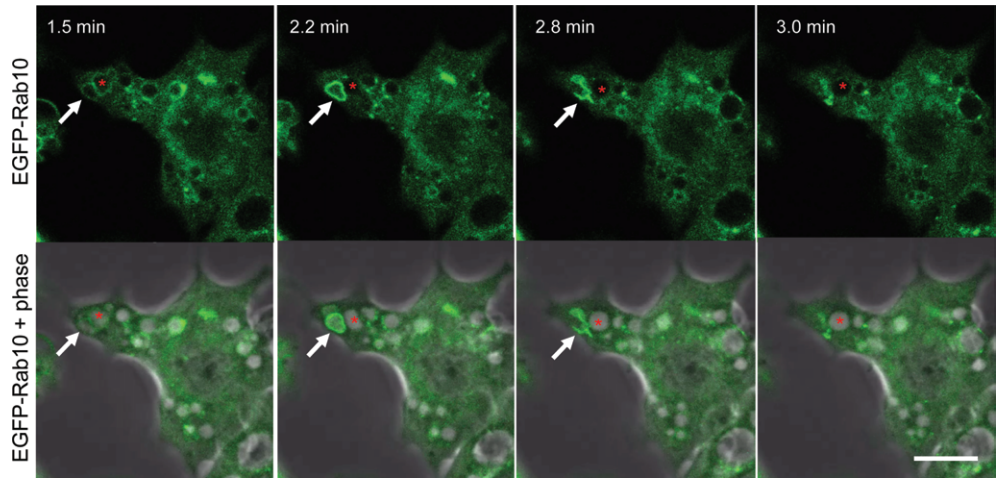

FIGURE 2 | Short-lived Rab10-positive premacropinosomal structures exist in RAW264 cells under near-physiological conditions. Confocal live-cell imaging of RAW 264 cells expressing EGFP-Rab10 stimulated with 10 nM phorbol myristate acetate (PMA). Elapsed times after the addition of PMA are shown in the frame. Arrows indicate a Rab10-positive premacropinosome which disappears within a few minutes. Asterisks indicate a Rab10-negative macropinosomal structure that remains as a phase-bright macropinosome. Scale bar = 10 μm. The corresponding movie is available in the **Supplementary Material Movie 3**.

macropinosomal structures was ~23%, which is a much lower proportion than was observed in RAW cells during the photo-manipulation of PA-Rac1 ON-OFF cycling (~68%) (**Supplementary Figure S1C**). Similarly, the formation of Rab10-positive premacropinosomes was also observed in control RAW264 cells, although the frequency of this event is lower than in PMA-stimulated cells (**Supplementary Figure S1C**). Thus, Rab10-positive premacropinosomes and tubules exist in cells under near-physiological conditions, although they were likely easily overlooked due to their shorter lifetimes and lower frequency of appearance. They disappeared within a few minutes by transforming to tubular profiles.

Compared with near-physiological conditions, the frequency of Rab10-positive premacropinosome formation significantly increases under photo-manipulation conditions, therefore, we attempted to characterize these Rab10-positive premacropinosomes and tubules mainly under the condition of repeating PA-Rac1 ON-OFF cycles.

Rab10-Positive Tubules Originate From Unclosed Macropinocytic Cups

Our previous study indicated that the premacropinosomes induced by the PA-Rac1 photoactivation are unclosed, and continuous with the cell surface plasma membrane by the lipophilic dye FM4-64 staining (9). However, it is unknown if the Rab10-positive tubules originate from the membrane of unclosed premacropinosomes or closed macropinosomes. To solve this question, the FM4-64 was added to the cells immediately after confirming the formation of EGFP-Rab10-positive tubules by the photo-manipulation of PA-Rac1 ON-OFF cycling (**Figure 3A**). Examining EGFP-Rab10 localization and FM4-64 labeling, we found that the preexisting Rab10-positive premacropinosomes and tubules were labeled with FM4-64 within 20 seconds after the addition of FM4-64 (**Figure 3B**). This result suggested that these Rab10-positive tubules elongated directly from the membrane of unclosed premacropinosomes, although the possibility that new Rab10-tubules will extend from the closed macropinosomes cannot be ruled out.

Rab10-Positive Tubules That Extend From Premacropinosomes Centripetally Move Along Microtubules

Next, we examined whether Rab10-positive tubule movement was dependent on microtubules using RAW264 cells co-expressing EGFP-tubulin, mCherry-Rab10, and PA-Rac1. When Rab10-tubule formation was induced by PA-Rac1 ON-OFF cycling, long Rab10-positive tubules were observed to move along microtubules centripetally (**Figures 4A, B**, **Supplementary Movies 4**, **5**). The long-distance vectorial movement of Rab10-positive tubules toward the perinuclear region was disturbed when microtubules were disrupted by the addition of 3.3 μM nocodazole, a microtubule depolymerizer (**Figure 4C**, **Supplementary Movie 6**). However, the budding of short Rab10-positive tubules from premacropinosomes that displayed short-distance, non-vectorial movements was occasionally observed, even in the presence of nocodazole. These findings indicated that the vectorial movement of Rab10-positive tubules was highly dependent on microtubules, although the budding of Rab10-positive tubules from premacropinosomes may not require microtubules.

The Rab10 Effectors EHBP1 and MICAL-L1 May Link Rab10 to EHD1 for Membrane Tubulation

Eps15 homology domain-binding protein 1 (EHBP1) is known as a Rab10 effector in the endocytic recycling pathway in *Caenorhabditis elegans*. It is reported that EHBP1 links EH domain-containing

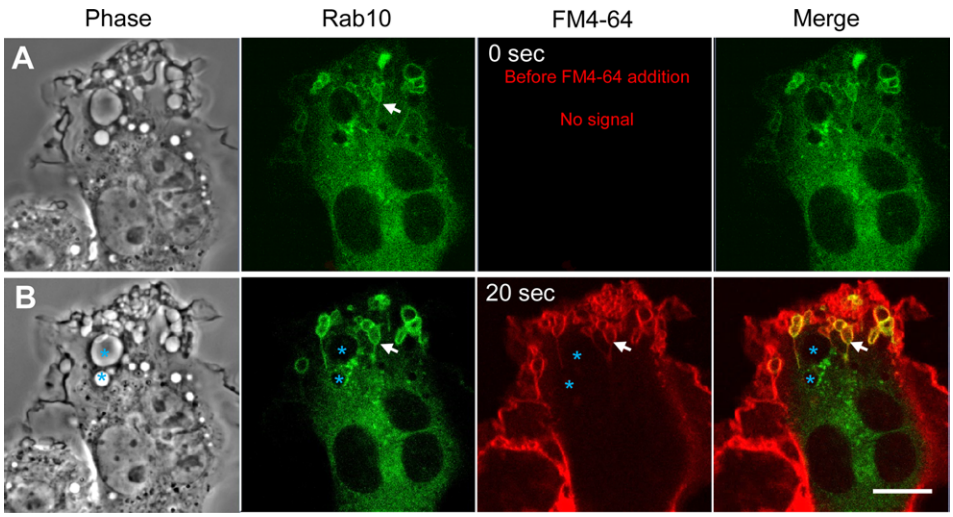

FIGURE 3 | Rab10-positive tubules originate from unclosed macropinocytic cups (premacropinosomes). Rab10-positive macropinosome-like structures were induced by PA-Rac1 ON-OFF cycling. After confirming the formation of Rab10-positive tubules elongated from macropinosome-like structures, the FM4-64 membrane-impermeable dye was added to the medium to label the cell surface plasma membrane during image recording. **(A)** Images acquired just before the addition of FM4-64 (time 0 sec). Rab10-positive tubules elongated from Rab10-positive macropinosome-like structures were confirmed (arrows). **(B)** The EGFP-Rab10 and FM4-64 images were acquired at 20 sec after the FM4-64 addition. Although phase-bright Rab10-negative macropinosomes (blue asterisks) were unlabeled with the FM4-64, Rab10-positive macropinocytic structures with extending tubules (arrows) were labeled with the FM4-64. Scale bar = 10 μm.

protein 1 (EHD1) to Rab10 to promote endosome tubulation (22, 23). Therefore, we investigated the involvement of EHBP1 in Rab10-positive tubules from premacropinosomes in RAW264 cells co-expressing EGFP-EHBP1 and mCherry-Rab10. As expected, we observed the colocalization of Rab10 and EHBP1 in the premacropinosome and tubular structures induced by the PA-Rac1 ON-OFF photo-manipulation (**Figure 5A**, **Supplementary Movie 7**). EHD1 has membrane tubulation activity in an ATP-dependent manner and plays a role in the regulation of tubular recycling endosome trafficking to the plasma membrane (24). Consistently, EGFP-EHD1 was found to localize to the tubules budding from Rab10-positive premacropinosomes (**Figure 5B**, **Supplementary Movie 8**). Similarly, MICAL-L1, a Rab10 effector that links Rab10 to EHD1 (25, 26), was also observed in Rab10-positive tubules (data not shown). These results implied that EHBP1 and/or MICAL-L1 may link Rab10 to EHD1 which may cause the tubulation of membranes.

Rab10-Positive Tubular Structures Represent a Novel Endocytic Pathway of Membrane Trafficking

Classical macropinosomes undergo a maturation process through the acquisition of Rab 5 and Rab7 before merging with lysosomes, where their contents are degraded. Therefore, we examined whether Rab10-positive tubules matured or fused with other endocytic compartments by performing a time-lapse image analysis in RAW264 cells co-expressing mCherry-Rab10 and various fluorescent protein-tagged endocytic marker proteins. Rab10-negative or faintly-positive compartments transiently acquire Rab5, an early endocytic protein. In contrast, Rab10-positive profiles do not become Rab5-positive (**Figures 6A, B**, **Supplementary Movie 9**). Also, Rab10-positive profiles were never observed to fuse with Rab7-positive late endocytic compartments or with LAMP1-positive lysosomal compartments (**Figures 7A, B**, **Supplementary Movies 10**, **11**). These findings indicated that these Rab10-positive profiles represented distinct entities from conventional endocytic pathways for lysosomal degradation.

Next, we examined the relationship between Rab10-positive tubules and recycling compartments using Rab4, which mediates fast recycling, or Rab11 which mediates slow recycling (27, 28). Although EGFP-Rab11was slightly observed on the membranes of Rab10-positive premacropinosomes, Rab11 was not localized on Rab10-positive tubules. EGFP-Rab4 was also not observed on Rab10-positive premacropinosomes or tubules. These findings indicated that the Rab10-positive tubules that extended from premacropinosomes were not recycling compartments (**Figures 7C, D**, **Supplementary Movie 12**). Sorting nexin 1 (SNX1), which contains BAR (Bin/Amphiphysin/Rvs) domains, localizes to early macropinosomes and tubules that extended from the early macropinosomes (29–31). However, we did not observe SNX1 localization on Rab10-positive compartments (**Figure 7E**, **Supplementary Movie 13**). To determine the destination of Rab10-positive tubules, we observed the relationship between the Rab10-positive tubules and the Golgi complex using EGFP-Rab35-4E, a Golgi marker that was created by a C-terminal mutation of Rab35 (32). The front end of Rab10-positive tubules appeared to reach out to the center of the Golgi region (**Supplementary Movie 13**). However, we could not see the fate of tubules because there is no specific tracer. Thus, Rab10-positive profiles likely exist as non-degradative

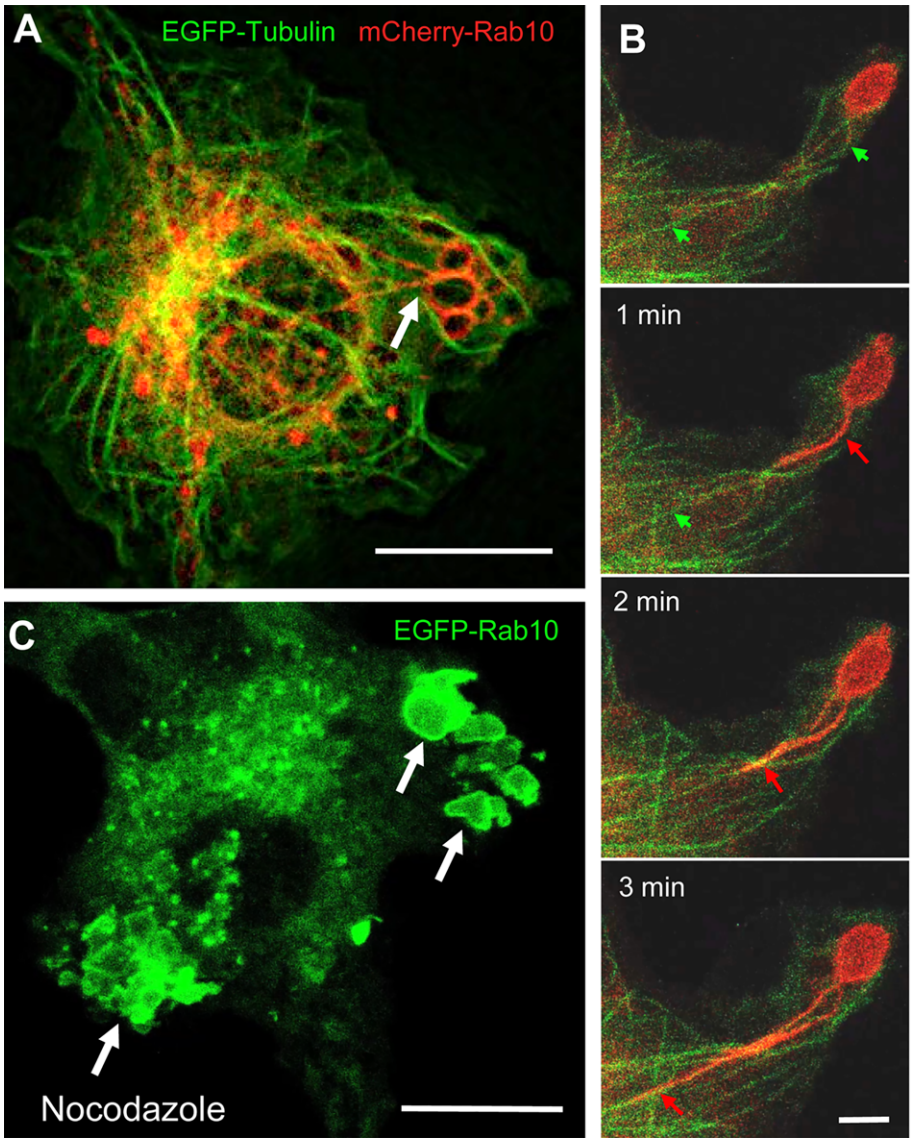

FIGURE 4 | The retrograde movement of Rab10-positive tubules is dependent on microtubules. **(A)** Epifluorescence microscopy of mCherry-Rab10 and EGFP-tubulin in live RAW 264 cells during PA-Rac1 ON-OFF cycling. Arrow indicates a Rab10-positive tubule extended from a peripheral premacropinosome. Scale bar=10 μm. **(B)** Higher-magnification view of extending Rab10-positive tubules (red arrows) along microtubules (green arrows). Scale bar = 2 μm. **(C)** The extension of EGFP-Rab10 tubules was inhibited in nocodazole-treated RAW264 cells, while many Rab10-positive premacropinosomes (arrows) were formed. Scale bar = 10 μm. The corresponding movies are available in the (**Supplementary Material Movies 4–6**).

compartments that are distinct from canonical endosomes or recycling compartments. Among various Rab proteins that we examined, Rab8a, a Rab protein very closely related to Rab10, is found to be colocalized with Rab10 in the premacropinosomes and tubules (**Figure 7F**, **Supplementary Movie 14**).

Rab10-Positive Premacropinosome and Tubule Formation Is Not Dependent on PI3K

It is well-known that PI(3,4,5)P_3 production by class I PI3K is critical for macropinosome closure during the process of classical macropinocytosis (33, 34). However, the dependency of Rab10-positive premacropinosome and tubule formation on PI3K has not yet been determined. Therefore, we examined the PI3K-dependency of the Rab10-positive endocytic pathway using pharmacological inhibitors and mCitrine-fused Akt pleckstrin homology (PH) domain (Akt-PH), which binds to PI(3,4,5)P_3/PI(3,4)P_2. In RAW 264 cells during PA-Rac1 ON-OFF cycling, the localization of Rab10 to macropinocytic cups or nascent macropinosomes was frequently observed. However, in most cases, the recruitment of Rab10 to these structures was transient and small in amount (**Figure 8A**, **Supplementary Movie 15**).

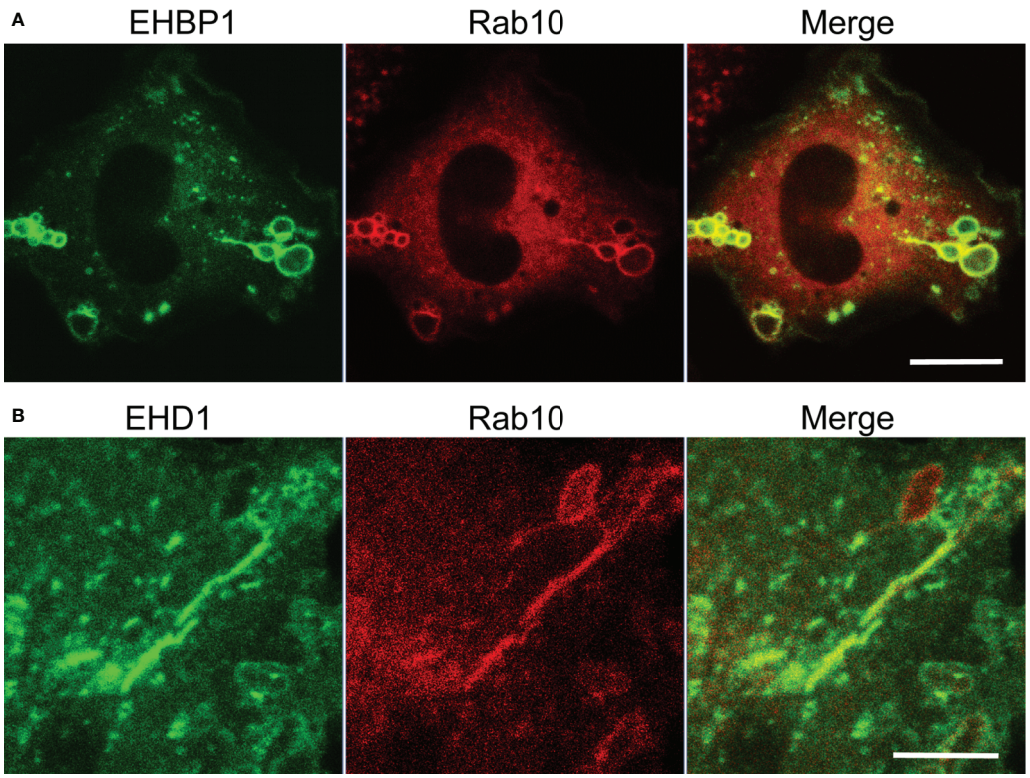

FIGURE 5 | Localizations of EHBP1 and EHD1 on Rab10-positive premacropinosomes and tubules. **(A)** EHBP1 colocalized with Rab10 in premacropinosomes and tubules. Scale bar = 10 μm. **(B)** EHD1 predominantly localized on Rab10-positive tubules extended from premacropinosomes. Scale bar = 5 μm. Corresponding movies are available in the (**Supplementary Material Movies 7**, **8**).

Incontrast, when the cells were treated with a PI3K inhibitor (10 μM LY294002 or 100 nM wortmannin), the remarkable accumulation of Rab10 in macropinocytic cups was frequently observed, although Rab10-negative macropinosomes were hardly seen (**Figure 8B**, **Supplementary Movie 15**). As a consequence, large macropinosomes rarely formed, whereas Rab10-positive tubule formation from premacropinosomes was not perturbed. Although Rab10 accumulation on the Akt-PH-positive macropinosomal membrane was not seen in RAW cells during PA-Rac1 ON-OFF cycling, Rab10-positive premacropinosomes without Akt-PH signals were frequently observed after treatment with PI3K inhibitors (**Figures 8A, B**, **Supplementary Movie 15**). These results suggested that Rab10-recruitment and Rab10-positive premacropinosome formation were PI3K-independent.

DISCUSSION

In this study, we first identified a novel endocytic pathway that diverges from canonical macropinocytosis using the optogenetic photo-manipulation of Rac1 activity. As we have reported previously (9), local PA-Rac1 activation induced the formation of premacropinosomes, which opened to the cell surface. Following the deactivation of PA-Rac1, some of the premacropinosomes closed into intracellular macropinosomes, whereas the majority of these structures (~70%) disappeared within several minutes. Through the co-expression of PA-Rac1 and EGFP-Rab10, we found that Rab10-negative premacropinosomes became intracellular macropinosomes, whereas Rab10-enriched premacropinosomes shrank and disappeared without forming intracellular macropinosomes. Instead, Rab10-positive premacropinosomes transformed into Rab10-positive tubules that extended toward the perinuclear region. Because the premacropinosomes were unclosed, the fluid contents of the premacropinosomes were likely to be returned to the extracellular fluid, and premacropinosome membranes can be efficiently transported because the Rab10-tubule features a much smaller diameter with a larger surface area/volume ratio than premacropinosomes. Thus, the abundant and sustained localization of Rab10 on premacropinosomes may change the mode of endocytosis from fluid-phase to membrane flow.

Previous studies have shown that Rab10 is involved in membrane recycling to the plasma membrane, associated with tubular recycling endosomes in other cell types (15, 16, 18, 23). Although the morphologies of these Rab10-positive tubular recycling endosomes are very similar to those observed in this study, the direction of movement for these tubular structures was

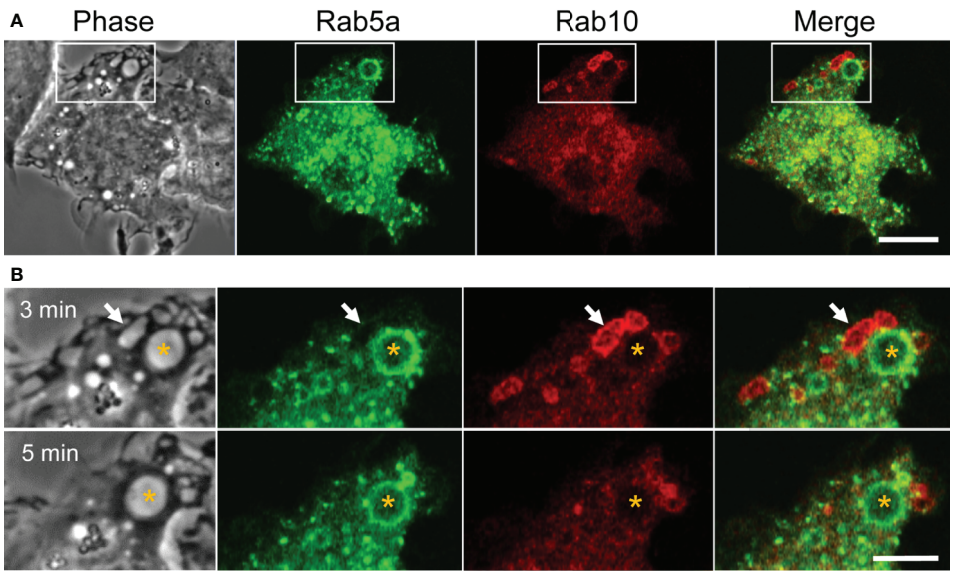

FIGURE 6 | Rab5, an early endocytic marker, is not recruited to Rab10-positive premacropinosomes and tubules. **(A)** Live-cell microscopy of RAW264 cells expressing EGFP-Rab5a and mCherry-Rab10. Scale bar = 10 μm. **(B)** Enlarged micrographs of the boxed area in **(A)**. Selective frames at two-time points as indicated. Rab5a-positive macropinosomes are Rab10-negative (asterisk). Rab10-positive compartments disappear within a few minutes without becoming Rab5a-positive, suggesting that Rab10-positive compartments are distinct from those of the classical macropinocytic pathway. Scale bar = 5 μm. The corresponding movie is available in the (**Supplementary Material Movie 9**).

the opposite of those observed here. Etoh and Fukuda revealed that Rab10-positive tubules extended from early endosomes in a microtubule-dependent manner and were anterogradely transported using the kinesin motors KIF13A and KIF13B (18). In contrast, the Rab10-positive tubules that extended from premacropinosomes were retrogradely transported along microtubules. Furthermore, the Rab10-positive tubules observed in this study were negative for Rab4 or Rab11, which are involved in fast recycling and slow recycling pathways, respectively (35), whereas the Rab10/Rab8a-positive tubules previously reported in other studies were associated with Rab4 or Rab11 proteins (13, 18, 36, 37). Thus, the identified Rab10-positive tubules in this study are likely distinct from recycling tubules that traffic toward the plasma membrane. Curiously, no other early or late endocytic marker proteins, such as Rab5, Rab7, or LAMP1, were recruited to the Rab10-positive tubules observed in this study, which suggested that the Rab10-positive tubules that originate from premacropinosomes represent a non-degradative pathway that diverges from macropinocytosis.

Although SNX1, a tubulation protein having a BAR domain, is known to be localized on tubular recycling endosomes that derive from early macropinosomes (29–31), we could not detect SNX1 on the Rab10-positive tubules. Therefore, Rab10-positive tubules from premacropinosomes appear to be distinct from SNX1-positive recycling tubules that derive from early macropinosomes. Taken together, these findings suggested that the Rab10-positive tubules that extend from premacropinosomes toward the perinuclear Golgi region represent a previously undefined endocytic pathway.

Among the various Rab proteins that we examined, Rab8a showed a very similar localization pattern to Rab10 in the premacropinosomes and tubules. Because Rab8a/b are highly homologous to Rab10, they share common effectors, such as MICAL-L1 and EHBP1, in addition to upstream regulators, GEF, and GAP proteins. Therefore, Rab10 and Rab8 may be functionally redundant. Wall et al. (38, 39) reported that Rab8a is localized to macropinosomes and tubular compartments that elongate from macropinosomes in lipopolysaccharide (LPS)-stimulated RAW264.7 macrophages (38, 39). Although they have regarded these Rab8-positive tubules as components of the conventional macropinocytosis pathway, the Rab8a-positive tubules observed in their studies may be identical to the Rab10-positive tubules observed in this study. In HeLaM cells, the knockout of Rab10 completely abolished Rab8- and MICAL-L1-positive tubular structures, whereas the Rab8a/b double-knockout did not perturb Rab10- and MICAL-L1-positive tubules (18). This study suggested that Rab10 plays a primary role in the formation of the tubular recycling endosome structure. Whether Rab10 and Rab8 play differential roles in macrophages should be clarified in future studies.

When exploring the underlying molecular mechanism responsible for Rab10-tubule formation, we found that EHBP1 and MICAL-L1, which are Rab10 effectors, both localized to Rab10-positive premacropinosomes and tubules. EHD1, a membrane tubulation protein, was also predominantly observed on Rab10-positive tubules. EHBP1 is known to link the EH domain-containing protein 1 (EHD1) to Rab10 to promote endosome tubulation (22, 23). MICAL-L1 also links EHD1 to

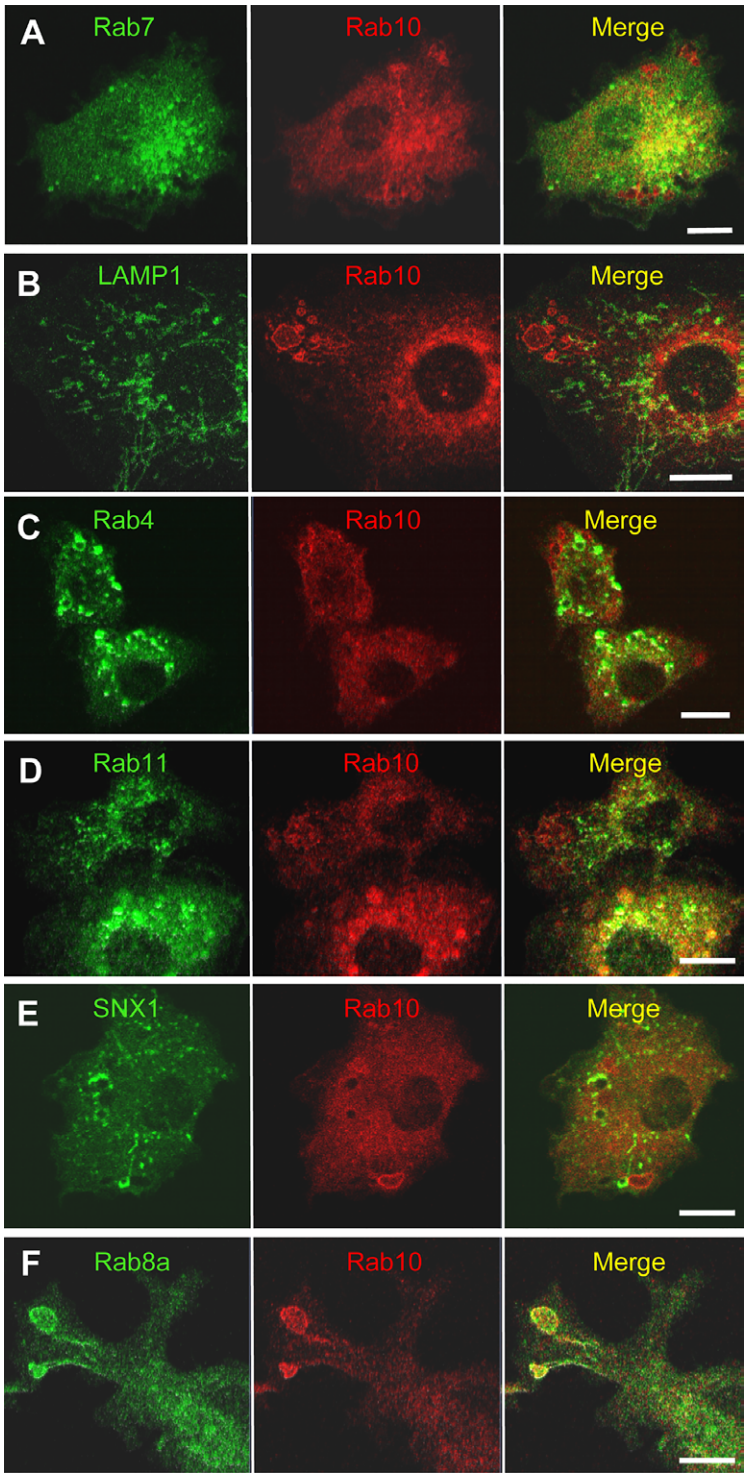

FIGURE 7 | Rab10-positive premacropinosomes and tubules are distinct from conventional degradative endocytic or recycling pathways. Rab10-positive premacropinosomes and tubules are not labeled with the late endosome/lysosome markers, Rab7- **(A)** or LAMP1 **(B)**. The recycling endosomal markers, Rab4 **(C)**, Rab11 **(D)**, and sorting nexin 1 (SNX1) **(E)** are faintly observed in Rab10-positive premacropinosomes and tubules, although they are only transiently recruited to the Rab10-negative conventional macropinosomes. Only Rab8a colocalized with Rab10 in the premacropinosomes and extending tubules **(F)**. All scale bars = 10 μm. The corresponding movies are available in the (**Supplementary Material Movies 10**–**14**).

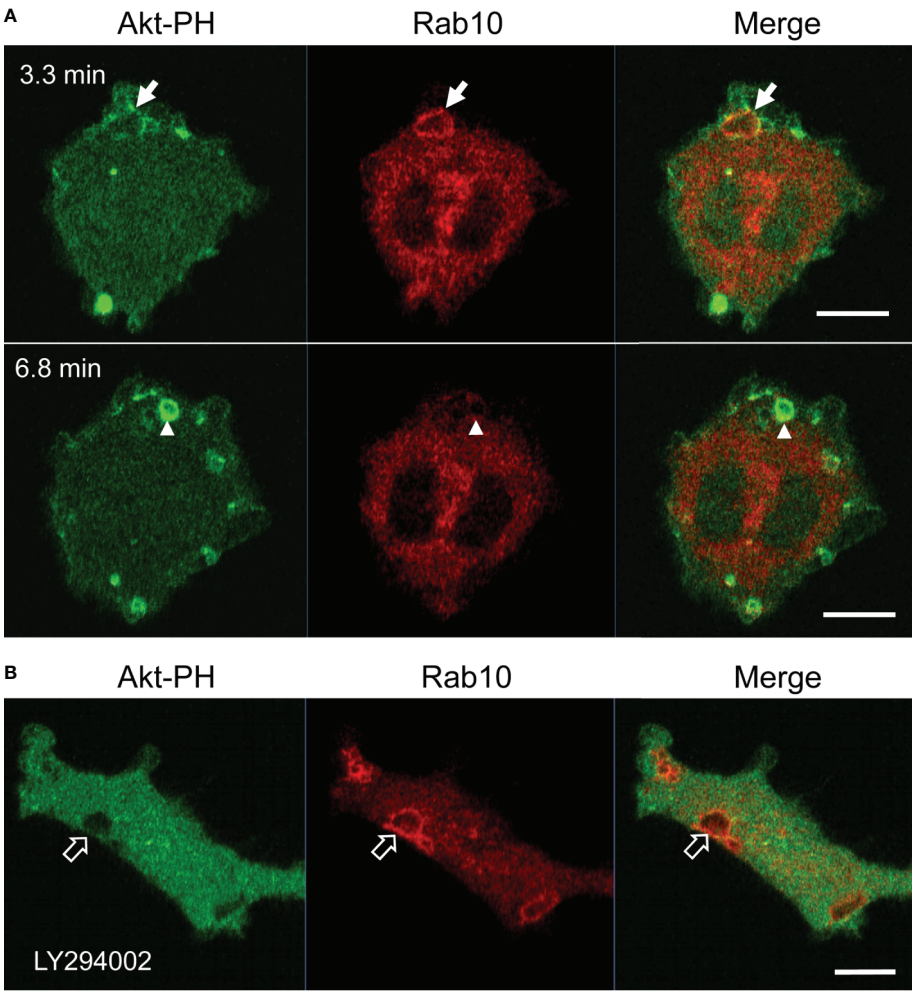

FIGURE 8 | Premacropinosome formation and the recruitment of Rab10 are not PI3K-dependent. The PI(3,4,5)P_3/PI(3,4)P_2 production by class I PI3K was monitored through the expression of mCitrine-Akt-PH domain (Akt-PH, green) in RAW264 cells during PA-Rac1 ON-OFF cycling **(A)** Although only small amounts of Akt-PH were observed on Rab10-positive premacropinosomes (arrows), Rab10-negative premacropinosomes were strongly positive for Akt-PH (arrowheads) at the timing of macropinosome closure. Elapsed time is shown in the frame. **(B)** In the presence of 10 μM LY294002, a PI3K inhibitor, the formation of Rab10-positive premacropinosomes was frequently seen (open arrows), whereas Akt-PH recruitment to the membrane was completely abolished. All scale bars = 10 μm. The corresponding movies are available in the (**Supplementary Material Movie 15**).

tubular recycling endosomes (25, 26). Therefore, it can be conceived that Rab10 may recruit EHD1 to premacropinosomes through EHBP1 and/or MICAL-L1, causing membrane tubule budding from premacropinosomes.

Macropinosome formation is well-known to depend on PI(3,4,5)P_3 production by class I PI3K (7, 8, 34, 40). Live-cell imaging of the fluorescent protein-tagged Akt-PH domain demonstrated that PI(3,4,5)P_3 levels in macropinocytic cup membranes rapidly increased at the timing of macropinosome closure (7, 38). However, PI(3,4,5)P_3 production was not observed upon the formation of Rab10-positive premacropinosomes. Furthermore, PI3K inhibition using pharmacological inhibitors did not reduce the formation of Rab10-positive premacropinosomes, whereas Rab10-negative macropinosome formation was drastically abolished. All Rab10-positive premacropinosomes were transformed into Rab10-positive tubules. These results suggested that the PI3K inhibition facilitates Rab10 localization to macropinocytic cups, leading to the transformation of premacropinosomes into tubules instead of macropinosome formation.

Recently, Liu et al. (19) reported the transitional association of Rab10 with early macropinosomes in RAW macrophages. In their study, the LRRK2-mediated phosphorylation of Rab10 was shown to play a regulatory role in macropinosome maturation (19). However, they did not mention the formation of Rab10-positive tubules derived from the premacropinosomes that are persistently Rab10-positive. This inconsistency may be due to differences in the experimental conditions. Under the condition

of PA-Rac1 photo-manipulation, the majority of the induced premacropinosomes transitioned into the Rab10-positive tubular endosome pathway, whereas LPS-induced macropinosomes underwent maturation in the classical macropinocytosis pathway. This difference is likely the reason why this Rab10-positive endocytic pathway has been overlooked or neglected. The identification of this novel pathway was a fortunate accident due to the use of innovative optogenetic technology. Importantly, we revealed that the Rab10-positive tubular endocytic pathway appears in macrophages even under near-physiological conditions, although the frequency is reduced under near-physiological conditions compared with PA-Rac1 photo-manipulation conditions. This finding suggested that the Rab10-positive endocytic pathway may play a significant role under physiological and pathological conditions.

Although the function of Rab10 in macrophages remains obscure, Rab10 has recently been reported to be involved in the transport of Toll-like receptor 4 (TLR4) to the plasma membrane in macrophages (16). The Rab10-positive endocytic route identified in this study may be responsible for the membrane trafficking of TLR4 and other membrane proteins. Further studies will be needed to clarify the cargos and destination of the Rab10-positive endocytic pathway. The present study has demonstrated that Rab10 mediates a tubular membrane trafficking pathway that diverges from the canonical fluid-phase uptake by macropinocytosis. The discovery of this non-degradative, endocytic pathway is likely to provide novel insights into the concepts of intracellular membrane trafficking. The intracellular pathway that avoids the lysosomal degradation system might be related to the pathophysiology of some metabolic diseases, and be utilized as a virus infection route.

DATA AVAILABILITY STATEMENT

The original contributions presented in the study are included in the article/**Supplementary Material**, further inquiries can be directed to the corresponding author.

AUTHOR CONTRIBUTIONS

Conceived and designed the experiments: KK and NA. Performed the experiments and collected image data: KK, AN, and SM. Analyzed the data: KK and NA. Contributed reagents/materials/analysis tools: KK, AN, SM, and YE. Wrote and edited the manuscript; NA and KK. All authors contributed to the article and approved the submitted version.

FUNDING

This study was supported by the Japan Society for the Promotion of Science (grant numbers: 18K06831 to NA, 19K07248 to KK, 20K07245 to YE).

ACKNOWLEDGMENTS

We are grateful to Drs. Joel A. Swanson (University of Michigan), Marino Zerial (Max Planck Institute), and Klaus Hahn (University of North Carolina) for providing plasmids; and to Mr. Toshitaka Nakagawa, Mr. Kazuhiro Yokoi, and Ms. Yukiko Iwabu for their skillful assistance. We also wish to thank Yuri Manabe, Akira Ikawa, Yusei Nonomiya, Daisuke Katayama, and Masana Hayashi, for their contribution to this research project in the undergraduate medical science research program at the Araki laboratory.

SUPPLEMENTARY MATERIAL

The Supplementary Material for this article can be found online at: https://www.frontiersin.org/articles/10.3389/fimmu.2021.649600/full#supplementary-material

Movie 1 | Optogenetic control of PA-Rac1 activity in RAW264 cells. The boxed area was locally irradiated with a blue laser to activate Rac1 (PA-Rac1 ON); then, the blue laser was turned off to deactivate Rac1 (PA-Rac1 OFF). ×80 speed. Scale bar = 10 μm.

Movie 2 | Time-lapse movie showing the formation of Rab10-positive premacropinosomes and tubules in RAW264 macrophages expressing EGFP-Rab10 by PA-Rac1 ON-OFF cycling. ×80 speed. Scale bar = 10 μm.

Movie 3 | EGFP-Rab10 and phase-contrast overlay images showing the formation of short-lifetime, EGFP-Rab10-positive premacropinosomes, and Rab10-negative classical macropinosomes in a PMA-stimulated RAW264 cell. ×80 speed. Scale bar = 10 μm.

Movie 4 | Time-lapse movie showing dynamics of mCherry-Rab10 and EGFP-tubulin in live RAW264 cells during PA-Rac1 ON-OFF cycling. ×30 speed. Scale bar = 10 μm.

Movie 5 | High-magnification movie showing extending Rab10-positive tubules (red) along microtubules (green). × 80 speed, Scale bar = 2 μm.

Movie 6 | Time-lapse movie showing dynamics of EGFP-Rab10 in a nocodazole-treated RAW264 cell during PA-Rac1 ON-OFF cycling. ×80 speed. Scale bar = 10 μm. 6:e1006093

Movie 7 | Dual-color time-lapse movie showing that EGFP-EHPB1 (green) is found to colocalize with mCherry-Rab10 (red) in premacropinosomes and tubules. ×80 speed. Scale bar = 10 μm.

Movie 8 | Dual-color time-lapse movie showing that EGFP-EHD1 (green) is predominantly localized on mCherry-Rab10 (red)-positive tubules extending from premacropinosomes. ×80 speed. Scale bar = 5 μm.

Movie 9 | Dual-color time-lapse movie showing that EGFP-Rab5a (green) and mCherry-Rab10 (red) localize to distinct compartments. Although the Rab10-negative, Rab5a-temporarily positive compartment remains a phase-bright macropinosome (arrow), mCherry-Rab10-positive compartments disappear within a few minutes without becoming Rab5a-positive. The merged image was overlaid with the corresponding phase-contrast image (right). ×80 speed. Scale bar = 10 μm.

Movie 10 | Dual-color time-lapse movie showing that mCherry-Rab10 (red)-positive tubules extending from Rab10-positive premacropinosomes do not obtain mCitrine-Rab7 (green). ×80 speed. Scale bar = 10 μm.

Movie 11 | Dual-color time-lapse movie showing that mCherry-Rab10 (red)-positive premacropinosomes and extending tubules do not merge with mCitrine-LAMP1 (green). ×80 speed. Scale bar=10 μm.

Movie 12 | Dual-color time-lapse movie showing that mCherry-Rab10 (red)-positive premacropinosomes and extending tubules are distinct compartments from EGFP-Rab4 (green)-positive fast recycling endosomal compartments **(A)** or EGFP-Rab11 (green)-positive recycling endosomal compartments **(B)**. ×80 speed. Scale bar = 10 μm.

Movie 13 | (A) Dual-color time-lapse movie showing that mCherry-Rab10 (red)-positive premacropinosomes and extending tubules are distinct compartments from EGFP-SNX1 (green)-positive recycling tubules that extend from conventional macropinosomes. ×80 speed. Scale bar = 10 μm. **(B)** Dual-color time-lapse movie showing the relationship between mCherry-Rab10 (red)-positive tubules and the Golgi apparatus labeled with an EGFP-Golgi marker (EGFP-Rab35-4E, green). ×80 speed. Scale bar = 10 μm.

Movie 14 | Dual-color time-lapse movie showing that EGFP-Rab8a (green) and mCherry-Rab10 colocalize on premacropinosomes and extending tubules. ×80 speed. Scale bar = 10 μm.

Movie 15 | Dual-color time-lapse movie showing $PI(3,4,5)P_3$/$PI(3,4)P_2$ production, monitored by the mCitrine-Akt PH domain (green) in a RAW264 cell during PA-Rac1 ON-OFF cycling. **(A)** Although only small amounts of Akt-PH are observed on Rab10-positive premacropinosomes (green arrow), Rab10-negative premacropinosomes are strongly positive for Akt-PH (red arrow). **(B)** LY294002 does not inhibit Rab10-positive premacropinosome formation, while the recruitment of mCitrine-Akt-PH (green) to Rab10-positive premacropinosomal membranes was completely abolished. Arrows indicate the formation of Rab10-positive premacropinosomes by PA-Rac1 ON-OFF cycling. ×80 speed. Scale bar = 10 μm.

REFERENCES

1. Swanson JA, Watts C. Macropinocytosis. *Trends Cell Biol* (1995) 5:424–8. doi: 10.1016/S0962-8924(00)89101-1
2. Kerr MC, Teasdale RD. Defining Macropinocytosis. *Traffic* (2009) 10:364–71. doi: 10.1111/j.1600-0854.2009.00878.x
3. Sallusto F, Cella M, Danieli C, Lanzavecchia A. Dendritic Cells Use Macropinocytosis and the Mannose Receptor to Concentrate Macromolecules in the Major Histocompatibility Complex Class II Compartment: Downregulation by Cytokines and Bacterial Products. *J Exp Med* (1995) 182:389–400. doi: 10.1084/jem.182.2.389
4. Commisso C, Davidson SM, Soydaner-Azeloglu RG, Parker SJ, Kamphorst JJ, Hackett S, et al. Macropinocytosis of Protein is an Amino Acid Supply Route in Ras-Transformed Cells. *Nature* (2013) 497:633–7. doi: 10.1038/nature12138
5. Zeineddine R, Yerbury JJ. The Role of Macropinocytosis in the Propagation of Protein Aggregation Associated With Neurodegenerative Diseases. *Front Physiol* (2015) 6:277. doi: 10.3389/fphys.2015.00277
6. Mercer J, Helenius A. Virus Entry by Macropinocytosis. *Nat Cell Biol* (2009) 11:510–20. doi: 10.1038/ncb0509-510
7. Araki N, Egami Y, Watanabe Y, Hatae T. Phosphoinositide Metabolism During Membrane Ruffling and Macropinosome Formation in EGF-Stimulated A431 Cells. *Exp Cell Res* (2007) 313:1496–507. doi: 10.1016/j.yexcr.2007.02.012
8. Egami Y, Taguchi T, Maekawa M, Arai H, Araki N. Small GTPases and Phosphoinositides in the Regulatory Mechanisms of Macropinosome Formation and Maturation. *Front Physiol* (2014) 5:374. doi: 10.3389/fphys.2014.00374
9. Fujii M, Kawai K, Egami Y, Araki N. Dissecting the Roles of Rac1 Activation and Deactivation in Macropinocytosis Using Microscopic Photo-Manipulation. *Sci Rep* (2013) 3:2385. doi: 10.1038/srep02385
10. Stenmark H. Rab GTPases as Coordinators of Vesicle Traffic. *Nat Rev Mol Cell Biol* (2009) 10:513–25. doi: 10.1038/nrm2728
11. Pfeffer S, Aivazian D. Targeting Rab GTPases to Distinct Membrane Compartments. *Nat Rev Mol Cell Biol* (2004) 5:886–98. doi: 10.1038/nrm1500
12. Babbey CM, Ahktar N, Wang E, Chen CCH, Grant BD, Dunn KW. Rab10 Regulates Membrane Transport Through Early Endosomes of Polarized Madin-Darby Canine Kidney Cells. *Mol Biol Cell* (2006) 17:3156–75. doi: 10.1091/mbc.E05-08-0799
13. Chua CEL, Tang BL. Rab 10—A Traffic Controller in Multiple Cellular Pathways and Locations. *J Cell Physiol* (2018) 233:6483–94. doi: 10.1002/jcp.26503
14. Sano H, Eguez L, Teruel MN, Fukuda M, Chuang TD, Chavez JA, et al. Rab10, a Target of the AS160 Rab GAP, is Required for Insulin-Stimulated Translocation of GLUT4 to the Adipocyte Plasma Membrane. *Cell Metab* (2007) 5:293–303. doi: 10.1016/j.cmet.2007.03.001
15. Shi A, Liu O, Koenig S, Banerjee R, Chen CC-H, Eimer S, et al. Rab-10-GTPase-mediated Regulation of Endosomal Phosphatidylinositol-4,5-Bisphosphate. *Proc Natl Acad Sci USA* (2012) 109:E2306–15. doi: 10.1073/pnas.1205278109
16. Wang D, Lou J, Ouyang C, Chen W, Liu Y, Liu X, et al. Ras-Related Protein Rab10 Facilitates TLR4 Signaling by Promoting Replenishment of TLR4 Onto the Plasma Membrane. *Proc Natl Acad Sci USA* (2010) 107:13806–11. doi: 10.1073/pnas.1009428107
17. Cardoso CMP, Jordao L, Vieira OV. Rab10 Regulates Phagosome Maturation and its Overexpression Rescues *Mycobacterium*-Containing Phagosomes Maturation. *Traffic* (2010) 11:221–35. doi: 10.1111/j.1600-0854.2009.01013.x
18. Etoh K, Fukuda M. Rab10 Regulates Tubular Endosome Formation Through KIF13A and KIF13B Motors. *J Cell Sci* (2019) 132:jcs236977. doi: 10.1242/jcs.226977
19. Liu Z, Xu E, Zhao HT, Cole T, West AB. LRRK2 and Rab10 Coordinate Macropinocytosis to Mediate Immunological Responses in Phagocytes. *EMBO J* (2020) 39:e104862. doi: 10.15252/embj.2020104862
20. Araki N, Ikeda Y, Kato T, Kawai K, Egami Y, Miyake K, et al. Development of an Automated Fluorescence Microscopy System for Photomanipulation of Genetically Encoded Photoactivatable Proteins (Optogenetics) in Live Cells. *Microscopy* (2014) 63:255–60. doi: 10.1093/jmicro/dfu003
21. Wu YI, Frey D, Lungu OI, Jaehrig A, Schlichting I, Kuhlman B, et al. A Genetically Encoded Photoactivatable Rac Controls the Motility of Living Cells. *Nature* (2009) 461:104–8. doi: 10.1038/nature08241
22. Shi A, Chen CCH, Banerjee R, Glodowski D, Audhya A, Rongo C, et al. EHBP-1 Functions With RAB-10 During Endocytic Recycling in Caenorhabditis Elegans. *Mol Biol Cell* (2010) 21:2930–43. doi: 10.1091/mbc.E10-02-0149
23. Wang P, Liu H, Wang Y, Liu O, Zhang J, Gleason A, et al. Rab-10 Promotes EHBP-1 Bridging of Filamentous Actin and Tubular Recycling Endosomes. *PloS Genet* (2016). doi: 10.1371/journal.pgen.1006093
24. Lee S, Uchida Y, Wang J, Matsudaira T, Nakagawa T, Kishimoto T, et al. Transport Through Recycling Endosomes Requires EHD1 Recruitment by a Phosphatidylserine Translocase. *EMBO J* (2015) 34:669–88. doi: 10.15252/embj.201489703
25. Sharma M, Giridharan SSP, Rahajeng J, Caplan S, Naslavsky N. Mical-L1. *Commun Integr Biol* (2010) 3:181–3. doi: 10.4161/cib.3.2.10845
26. Sharma M, Giridharan SSP, Rahajeng J, Naslavsky N, Caplan S. Mical-L1 Links EHD1 to Tubular Recycling Endosomes and Regulates Receptor Recycling. *Mol Biol Cell* (2009) 20:5181–94. doi: 10.1091/mbc.E09-06-0535
27. Pfeffer S. Membrane Domains in the Secretory and Endocytic Pathways. *Cell* (2003) 112:507–17. doi: 10.1016/S0092-8674(03)00118-1
28. Zerial M, McBride H. Rab Proteins as Membrane Organizers. *Nat Rev Mol Cell Biol* (2001) 2:107–17. doi: 10.1038/35052055
29. Buckley CM, King JS. Drinking Problems: Mechanisms of Macropinosome Formation and Maturation. *FEBS J* (2017) 284:3778–90. doi: 10.1111/febs.14115
30. Kerr MC, Lindsay MR, Luetterforst R, Hamilton N, Simpson F, Parton RG, et al. Visualisation of Macropinosome Maturation by the Recruitment of Sorting Nexins. *J Cell Sci* (2006) 119:3967–80. doi: 10.1242/jcs.03167
31. Lim JP, Gleeson PA, Teasdale RD. SNX5 is Essential for Efficient Macropinocytosis and Antigen Processing in Primary Macrophages. *Biol Open* (2012) 1:904–14. doi: 10.1242/bio.20122204
32. Kawai K, Egami Y, Nishigaki A, Araki N. Rab35 Targeting to the Plasma Membrane is Dependent on the C-Terminal Polybasic Cluster. *Acta Histochem Cytochem* (2020) 53:93–7. doi: 10.1267/ahc.20-00006
33. Cox D, Tseng CC, Bjekic G, Greenberg S. A Requirement for Phosphatidylinositol 3-Kinase in Pseudopod Extension. *J Biol Chem* (1999) 274:1240–7. doi: 10.1074/jbc.274.3.1240
34. Araki N, Johnson MT, Swanson JA. A Role for Phosphoinositide 3-Kinase in the Completion of Macropinocytosis and Phagocytosis by Macrophages. *J Cell Biol* (1996) 135:1249–60. doi: 10.1083/jcb.135.5.1249
35. Grant BD, Donaldson JG. Pathways and Mechanisms of Endocytic Recycling. *Nat Rev Mol Cell Biol* (2009) 10:597–608. doi: 10.1038/nrm2755

36. Lucken-Ardjomande Häsler S, Vallis Y, Pasche M, McMahon HT. GRAF2, WDR44, and MICAL1 Mediate Rab8/10/11–dependent Export of E-cadherin, MMP14, and CFTR Δf508. *J Cell Biol* (2020) 219:e201811014. doi: 10.1083/jcb.201811014
37. Chen Y, Wang Y, Zhang J, Deng Y, Jiang L, Song E, et al. Rab10 and Myosin-Va Mediate Insulin-Stimulated GLUT4 Storage Vesicle Translocation in Adipocytes. *J Cell Biol* (2012) 198:545–60. doi: 10.1083/jcb.201111091
38. Wall AA, Luo L, Hung Y, Tong SJ, Condon ND, Blumenthal A, et al. Small GTPase Rab8a-Recruited Phosphatidylinositol 3-Kinase γ Regulates Signaling and Cytokine Outputs From Endosomal Toll-Like Receptors. *J Biol Chem* (2017) 292:4411–22. doi: 10.1074/jbc.M116.766337
39. Wall AA, Condon ND, Luo L, Stow JL. Rab8a Localisation and Activation by Toll-Like Receptors on Macrophage Macropinosomes. *Philos Trans R Soc B Biol Sci* (2019) 374:20180151. doi: 10.1098/rstb.2018.0151
40. Yoshida S, Hoppe AD, Araki N, Swanson JA. Sequential Signaling in Plasma-Membrane Domains During Macropinosome Formation in Macrophages. *J Cell Sci* (2009) 122:3250–61. doi: 10.1242/jcs.053207

Conflict of Interest: The authors declare that the research was conducted in the absence of any commercial or financial relationships that could be construed as a potential conflict of interest.

Copyright © 2021 Kawai, Nishigaki, Moriya, Egami and Araki. This is an open-access article distributed under the terms of the Creative Commons Attribution License (CC BY). The use, distribution or reproduction in other forums is permitted, provided the original author(s) and the copyright owner(s) are credited and that the original publication in this journal is cited, in accordance with accepted academic practice. No use, distribution or reproduction is permitted which does not comply with these terms.

frontiers in Immunology

REVIEW
published: 10 June 2021
doi: 10.3389/fimmu.2021.660865

Pro-Resolving Ligands Orchestrate Phagocytosis

Christa Decker, Sudeshna Sadhu and Gabrielle Fredman *

The Department of Molecular and Cellular Physiology, Albany Medical College, Albany, NY, United States

The resolution of inflammation is a tissue protective program that is governed by several factors including specialized pro-resolving mediators (SPMs), proteins, gasses and nucleotides. Pro-resolving mediators activate counterregulatory programs to quell inflammation and promote tissue repair in a manner that does not compromise host defense. Phagocytes like neutrophils and macrophages play key roles in the resolution of inflammation because of their ability to remove debris, microbes and dead cells through processes including phagocytosis and efferocytosis. Emerging evidence suggests that failed resolution of inflammation and defective phagocytosis or efferocytosis underpins several prevalent human diseases. Therefore, understanding factors and mechanisms associated with enhancing these processes is a critical need. SPMs enhance phagocytosis and efferocytosis and this review will highlight mechanisms associated with their actions.

Keywords: macrophage, phagocytosis, efferocytosis, resolvin, inflammation

OPEN ACCESS

Edited by:
Valentin Jaumouillé, Simon Fraser University, Canada

Reviewed by:
Nan Chiang, Brigham and Women's Hospital and Harvard Medical School, United States
Amiram Ariel, University of Haifa, Israel
Jesmond Dalli, Queen Mary University of London, United Kingdom

***Correspondence:**
Gabrielle Fredman
fredmag@amc.edu

Specialty section:
This article was submitted to Molecular Innate Immunity, a section of the journal Frontiers in Immunology

Received: *29 January 2021*
Accepted: *06 April 2021*
Published: *10 June 2021*

Citation:
Decker C, Sadhu S and Fredman G (2021) Pro-Resolving Ligands Orchestrate Phagocytosis. Front. Immunol. 12:660865. doi: 10.3389/fimmu.2021.660865

INTRODUCTION

Elie Metchnikoff uncovered the significance of phagocytosis nearly 100 years ago (1). Since then, phagocytosis has been recognized as a critical cellular program for innate and adaptive immune responses to foreign material. Moreover, we now appreciate that engulfment and neutralization of invading organisms is key to maintain health. Phagocytes like PMN and macrophages promote microbial removal and wound debridement. Mechanisms associated with phagocytosis continue to be uncovered which has aided in our understanding of inflammation and disease. There are now numerous endogenous factors like lipid mediators (LMs), proteins, metabolites and gasses, that can promote phagocytosis. For example, LMs like specialized pro-resolving mediators (SPMs) are biosynthesized from arachidonate (AA), eicosapentaenoic acid (EPA), docosahexaenoic acid (DHA), or n-3 docosapentaenoic acid (DPA) (2, 3). SPMs are named lipoxins, resolvins, protectins, their aspirin-triggered isomers, maresins, cysteinyl-conjugated SPMs (CTRs) and 13-series resolvins (RvTs) (2, 4–9). Each of the SPMs has a distinct chemical structure (2) and several of the SPMs bind and signal through distinct G-protein coupled receptors (GPCRs) (10–14). SPMs in general exert a tissue protective action in as much as they can temper pro-inflammatory factors and promote the clearance of harmful stimuli and dead cells (i.e. phagocytosis). Pro-phagocytic ligands are not limited to SPMs and indeed the repertoire of these factors are growing and is summarized in **Table 1**.

Non-resolving inflammation is an underpinning of several prevalent diseases, including cardiovascular and neurodegenerative diseases, cancer, arthritis, asthma etc. Phagocytes play a major

TABLE 1 | Pro-resolving factors that promote phagocytosis.

			Phagocyte	Phagocytic action elicited	References
Lipid Mediators	EPA Derived	RvE1	Macrophages (human and murine) Neutrophils (human and murine)	-Increases phagocytosis of Zymosan, E. *coli*, C. *albicans* -Promotes efferocytosis of apoptotic PMN	(15–19)
		RvE2	Macrophages (human)	-Increases phagocytosis of Zymosan	(20)
		RvE4	Macrophages (human)	-Increases efferocytosis of apoptotic PMN, effete RBCs	(21, 22)
	DHA Derived	RvD1, AT-RvD1	Macrophages (human, murine, rat) Neutrophils (human and murine) Fibroblasts (human)	- Increases phagocytosis of Zymosan, E. *coli*, P. *aeruginosa*, NTHi, IgA-OVA-coated beads, Amyloidβ, clot particles, cancer cell debris - Promotes efferocytosis of apoptotic PMN, osteoblasts, Jurkats, macrophages, thymocytes, and sickle cell RBCs -Enhances clearance of necroptotic cells	(23–41)
		RvD2	Macrophages (human and murine) Neutrophils (human and murine)	-Enhances phagocytosis of live *E. coli* -Promotes efferocytosis of apoptotic PMN apoptotic osteoblasts	(29, 42–44)
		RvD3, AT-RvD3	Macrophages (human and murine)	-Enhances phagocytosis -Promotes efferocytosis of apoptotic PMN -Increases uptake of cancer cell debris	(40, 45)
		RvD4	Macrophages (human) Fibroblasts (Human) Whole blood phagocytes	-Enhances phagocytosis of *S. aureus, Zymosan* -Increases efferocytosis of apoptotic PMN	(25, 46)
		RvD5	Macrophages (human)	-Enhances phagocytosis of *E. coli*	(23)
		MaR1, MaR2	Macrophages (human and murine)	-Enhances phagocytosis of E. *coli*, Zymosan –Increases efferocytosis of apoptotic PMN	(47–50)
		PD1/NPD1, AT-PD1	Macrophages (human and murine)	-Increases efferocytosis of apoptotic PMN, thymocytes	(15, 23, 41, 51–54)
		Cys SPMs: MCTR1, MCTR2, MCTR3, PCTR1, PCTR2, PCTR3, RCTR1, RCTR2, RCTR3	Macrophages (human and murine)	-Enhances phagocytosis of *E. coli*, Zymosan -Increases efferocytosis of apoptotic PMN	(8, 55–59)
	n-3 DPA derived SPMs	$RvD5_{n-3}DPA$ $PD1_{n-3}DPA$ $Mar_{n-3}DPA$ $RvD_{n-3}DPA$ RvT	Macrophages (human and murine)	-Increases phagocytosis of S. aureus, Zymosan -Enhances efferocytosis of apoptotic HL-60 cells	(9, 14, 60)
	AA Derived	LXA_4, AT-LXA_4	Macrophages (human, murine, rat, THP-1 cells)	-Enhances efferocytosis of apoptotic PMN	(61–63)
		LXB_4, AT-LXB_4	Macrophages (human, murine, rat)	-Increases phagocytosis of E. *coli* -Enhances efferocytosis of apoptotic PMN	(63, 64)
Proteins		Annexin A1, Ac2-26	Macrophages (human)	-Enhances efferocytosis of apoptotic PMN	(65)
		DEL-1	Macrophages (murine)	-Increases efferocytosis of apoptotic PMN	(66)
		IL-10	Macrophages (human)	-Increases phagocytosis of E. *coli* -Enhances efferocytosis of apoptotic PMN	(67)
		IFN-β	Macrophages (murine)	-Enhances efferocytosis of apoptotic PMN	(68)

(Continued)

TABLE 1 | Continued

		Phagocyte	Phagocytic action elicited	References
	Galectin-1	Microglial cells Macrophages	-Enhances phagocytosis of myelin –Increases efferocytosis of apoptotic PMN	(69, 70)
	Galectin-3	Neutrophils (human) Macrophages (murine)	-Enhances phagocytosis IgG-RBCs –Increases efferocytosis of apoptotic PMN	(71, 72)
	Melanocortin	Macrophages (murine)	-Enhances phagocytosis of zymosan –Increases efferocytosis of apoptotic PMN	(73)
	Alpha-2-macroglobin	Macrophages (murine)	-Enhances phagocytosis of zymosan –Increases efferocytosis of apoptotic PMN	(74)
Gases	H_2S	Macrophages	-Enhances phagocytosis of bacteria	(75)
	CO	Macrophages (human)	-Increases phagocytosis of zymosan –Increases efferocytosis of apoptotic PMN	(76)
Nucleotides	Adenosine	PMN	-Stimulates Fc-mediated phagocytosis	(77)
Lipids	Estrogen	Microglial cells	-Stimulated efferocytosis of apoptotic PC12 cells	(78)

role in the resolution of inflammation because of their ability to neutralize and contain harmful stimuli and clear dead cells and debris, which is a feed-forward process that helps repair tissue injury. Not surprisingly, phagocyte functions in several diseases mentioned above have been shown to be dysregulated and are nicely reviewed in the following reference (79). Instead, we appreciate that aging is a major risk factor for several diseases and is a scourge of modern medicine. Therefore, this mini review will highlight some of the pro-phagocytic bioactions of SPMs, with a focus on aging. Lastly, we will offer some suggestions for future studies in this arena.

PRO-RESOLVING LIGANDS ENHANCE THE CLEARANCE OF MICROBES AND DEBRIS

We now appreciate that phagocytosis and thus the engulfment and neutralization of invading organisms is key to maintain health. There are several manners in which phagocytes like neutrophils or macrophages ingest pathogens, which is nicely reviewed by Flannagan RS et al. (80). Briefly, the removal of pathogens is a highly orchestrated event that involves cell surface receptors and specific signaling pathways to initiate recognition, engulfment and degradation. SPMs have been shown to increase phagocytosis (**Table 1**) of pathogens and some of the initial findings are described below. One of the earliest observations involved the SPM called Resolvin E1 (RvE1). RvE1 was shown to enhance the clearance of *Candida albicans* by human neutrophils and in a mouse model of candidiasis (17). In this same paper, RvE1 was also shown to be biosynthesized by C. *albicans.* Other pathogens like *Pseudomonas aeruginosa* (81), T. *gondii* (82) and T. *cruzi* (83) were also shown to biosynthesize SPMs. Collectively, these studies demonstrate an intimate link between host-derived SPMs and pathogens. Some questions remain, like why would microbes make SPMs? From the viewpoint of pathogens like Candida, RvE1 could potentially limit the number of recruited polymorphonuclear lymphocytes (PMN), allowing for its persistence. From the perspective of the host, Candida also increases IL-8 (which is a neutrophil chemoattractant) and the presence of RvE1 can enhance local phagocytes to clear Candida (17). From an evolutionary perspective, it is possible that mammalian hosts hijacked SPMs as important armament to protect against foreign invaders. Therefore it is possible that evolutionary pressures on the host are what drove SPMs to possess the ability to enhance phagocytosis. Along these lines, several SPMs such as RvD5, PD1, RvD1 and RvD2 each enhanced the clearance and neutralization of E. *coli* by neutrophils and macrophages (23, 42). An important finding was that these SPMs do not directly kill E. *coli*, but rather act on phagocytes to enhance killing in a contained manner. **Table 1** summarizes key papers associated with SPM's ability to enhance phagocytosis in numerous contexts. SPMs also promote phagocytosis of pathogens found in the lungs (34, 84, 85), which may be important for a return to homeostasis post airway infections. Along these lines, RvD1 and Mar1 contain and limit *Mycobacterium tuberculosis* intracellular growth in macrophages (86). RvD1 increased antimicrobial peptides including bactericidal/permeability-increasing protein (BPI) and LL-37 and Mar1 only increased BPI. The control and containment of Tuberculosis relies heavily on the balance between pro-inflammatory and pro-resolving factors (87). Moreover, RvD1 and Mar1 each stimulated NF-κB nuclear translocation but only Mar1 promoted Nrf2 localization. These results suggest that while RvD1 and Mar1 have overlapping functions, they also exert distinct actions and thus highlight the utter importance of having several distinct SPM species available to promote optimal function. A deeper understanding of the common and distinct actions of SPMs on phagocytosis are of interest.

Along these lines, uncovering mechanisms associated with SPM clearance of microbes and debris is an emerging area of research. As an example, aspirin-triggered lipoxin A_4 (or AT-LXA_4) was shown to enhance phagocytosis in a mannose scavenger receptor dependent manner (61) because inhibition of the mannose receptor by treatment with mannin completely abrogated AT-LXA_4's ability to enhance the clearance of E. *coli* (61). In this same

study, the authors also found that AT-LXA_4 required PI3K and p110γ to enhance phagocytosis (61). AT-LXA_4 binds and signals through a GPCR called ALX/FPR2 and so these results suggest that SPMs engage signaling pathways *via* their cell surface GPCRs. Accordingly, RvD2 binds and signals through a GPCR called GPR18 and knockdown of GPR18 abrogated RvD2's ability to enhance phagocytosis (43). Moreover, RvD2 enhanced the expression of key phagocytic recognition receptors like CD206 and CD163 (43). In a subsequent study, RvD2 was also found to increase phagocytosis through mechanisms involving cAMP, PKA and STAT3 (44). Other SPMs, like 13S,14S-epoxy-DHA (or eMaR) and RvD1 also increased surface levels of CD163 and CD206 on human macrophages (88). Also, n-3 docosapentaenoic acid–derived resolvin D5 ($RvD5_{n\text{-}3\ DPA}$) enhanced phagocytosis through mechanisms involving a GPCR called GPR101 (14). Collectively, these are only a few examples of how SPMs enhance phagocytosis and further understanding of the intricate signaling pathways associated with SPM-initiated phagocytosis are of immense interest. SPMs have also been reported to enhance the clearance of debris, including fibrin clots (35), which is an important process to maintain vascular homeostasis. Overall, SPMs enhance the clearance of microbes and debris. There are several remaining questions: Do particular subsets of macrophages or neutrophils respond optimally to SPMs, and if so which species of SPM? How are SPM GPCRs regulated during phagocytosis? How do SPMs impact macrophage or PMN metabolism when ingesting and neutralizing pathogens? Addressing these questions will likely yield important information as to how cells integrate SPM signals and may help inform the development of targeted therapies for particular infections. Another critical aspect to the maintenance of homeostasis is the clearance of dead cells. The next sections will focus on how SPMs enhance dead cell removal by phagocytes.

PRO-RESOLVING LIGANDS ENHANCE THE CLEARANCE OF DEAD CELLS

Billions of cells die daily in adult lives and so the efficient clearance of dead cells is utterly critical for homeostasis (89). Moreover, a large number of cells also die during the resolution of a pathological outcome, such as infection or tissue damage (89). The engulfment of dead cells by professional phagocytes like macrophages is called efferocytosis, which is a highly intricate process that ultimately allows for the recycling of cellular products and tissue repair (79, 90). Failure to clear dead cells can lead to accumulation of necrotic debris, which is associated with several prevalent human diseases, including atherosclerosis (91). Therefore, a major topic of interest in recent years has been the exploration of factors that increase efferocytosis to quell persistent inflammation, limit tissue necrosis and promote repair.

SPMs are of immense interest because of their ability to enhance efferocytosis. Lipoxin A_4 (LXA_4) was among the first SPMs that was published to enhance the clearance of apoptotic cells *in vitro* (62, 92). Mechanistically, the increase in efferocytosis is in part through LXA_4's ability to dephosphorylate MYH9, a protein involved with cytoskeletal rearrangement (92). This dephosphorylation results in the activation of components of a signaling cascade leading to cell polarization and increased phagocytosis. In addition to MYH9, LXA_4 also activates CDC42, which promotes engulfment (92).

Numerous SPMs, including the E-series, D-series, DPA-derived resolvins, protectins and maresins enhance the clearance of dead cells (93). This redundancy again suggests that SPMs and efferocytosis are utterly critical for tissue repair mechanisms and our survival. The mechanisms by which SPMs enhance efferocytosis are under investigation. Because SPMs have distinct structures, the first step in our understanding toward mechanisms is to investigate the receptors to which they bind. Indeed, several SPM receptors have been discovered and are highlighted in further detail by Chiang et al. (2). Removal of key receptors for SPMs demonstrate that SPMs initiate pro-efferocytotic programs through their cell surface receptors (14, 36, 43, 47).

Intracellular signaling associated with SPM mechanisms are also of immense interest. Resolvin D1 for example binds and signals through a GPCR called ALX/FPR2 (36). RvD1 initiates a cAMP-PKA signaling event and also limits the phosphorylation of p47, a crucial molecule involved in NADPH oxidase (NOX) activation (37). Limiting the activation of NOX aids in quelling inflammation by reducing the amount of ROS which trigger oxidative stress induced cellular damage (37). To this end, it is appreciated that certain pro-inflammatory cytokines, like TNF-α can limit efferocytosis through increased ROS in macrophages (94). RvD1 also limits LPS-induced TNF-α expression to rescue defective efferocytosis by controlling the classical $NF\text{-}_kB1$ pathway and activating an atypical pathway that suppresses the secretion of TNF-α and IL-1β (28). Moreover, through C-terminal cleavage of $NF\text{-}_kB1$, RvD1 initiates formation of a p50/p50 homodimer which competes for DNA binding with the classical heterodimer (28). Therefore, RvD1's actions in limiting the release of pro-inflammatory factors (28, 37, 95–97) may also aid in its ability to enhance efferocytosis. Another interesting angle is that oral administration of RvD1 was recently shown to control key transcriptional profiles in ingesting macrophages *in vivo* (98). For example, RvD1 reduced transcript levels of coactivator-associated arginine methyltransferase 1 (CARM1), histone aminotransferase 1 (HAT1), histone deacetylase 5 and 7 (HDAC5 and HDAC7), protein arginine *N*-methyltransferase 2 (PMRT2), and ribosomal protein S6 kinase, polypeptide 5 (RPS6KA5) in macrophages from inflammatory loci *ex vivo* (98). With regard to the regulation of CARM1, adoptive transfer of siCARM1-transfected human macrophages to zymosan-challenged mice resulted in a significant increase in PMN clearance, which suggests an important counter regulatory role for CARM1 and efferocytosis (98). RvD1 also decreased HDAC5 and HDAC7, which suggests that RvD1 may regulate epigenetic mechanisms (98). How RvD1-initated epigenetic control of macrophages impacts its efferocytic function is of interest. Along these lines, RvD1 also regulated a panel of miRNAs that might contribute to phagocytosis, efferocytosis and resolution of inflammation (99) and a deeper exploration of roles and mechanisms of pro-resolving and pro-phagocytic miRNAs are also of interest.

Another emerging area of interest is the macrophage's ability to carry out continual efferocytosis, which is the ability of individual macrophages to engulf multiple apoptotic cells consecutively. Early work in this arena demonstrated that CD11b levels were associated with a macrophage's ability to eat "a little" or "a lot" of apoptotic cells (100). We now appreciate that macrophages within tissues are very diverse with regard to function and phenotype and newer research suggests that macrophage metabolism is an important player in the ability of a macrophage to eat apoptotic cells (101–105). Apoptotic cell engulfment and the eventual breakdown of the corpse provides the fuel for metabolic programs like fatty acid oxidation (FAO) and oxidative phosphorylation (OXPHOS) (101). Macrophages also engage aerobic glycolysis to ingest apoptotic cells (105). Recent work by Yurdagul A et al. demonstrates a critical role for amino acid metabolism and continual efferocytosis (102, 103). Briefly, they found that arginine can be metabolized to ornithine by Arginase-1 in pro-resolving macrophages. Moreover they also found that pro-resolving macrophages converted ornithine into putrescine *via* ornithine decarboxylase (ODC) for continual efferocytosis. To further this mechanism they then found that ODC-dependent putrescine synthesis drives IL-10 production and inflammation-resolution *in vivo*. Moreover, putrescine promoted MerTK levels through sH3K9 di/trimethylation mechanisms. Together, these results uncover key players in our understanding of the link between macrophage metabolism, efferocytosis and inflammation resolution programs.

EFFEROCYTOSIS PROMOTES SPM BIOSYNTHESIS

Another fascinating finding is that the process of efferocytosis itself leads to the biosynthesis of more SPMs (15, 106, 107). This feed-forward circuit was first demonstrated in murine systems (15). Human macrophages that had ingested apoptotic PMN also had increased biosynthesis of SPMs, including RvD1, RvD2 and LXB_4 (106). A potential mechanism for the increase in SPMs during efferocytosis is transcellular biosynthesis (106). From a mechanistic perspective and to determine whether released SPMs enhance efferocytosis in a feed forward manner, Chiang N et al. knocked down a key SPM biosynthetic enzyme called 15-lipoxygenase (15-LOX) in human macrophages. They found the 15-LOX silenced macrophages had significantly impaired efferocytosis, which suggests a critical role for SPM synthesis and efficient clearance (76). Another mechanism that promotes SPMs during efferocytosis is through MerTK signaling (107). Cai B. et al. demonstrated that MerTK signaling led to increased SPMs and that silencing of MerTK resulted in less SPMs (107). Mechanisms through which MerTK increases SPMs may be through non-nuclear subcellular localization of a key SPM biosynthetic enzyme called 5-lipoxyeganse (5-LOX) (95, 107). Collectively, these papers point to a critical feed-forward mechanism in which efferocytosis stimulates SPMs and SPMs act locally to further enhance efferocytosis.

RELEASED SPMS AS IMPORTANT "GOOD-BYE" TISSUE MESSENGERS

SPMs and other lipid mediators were also shown to be released by apoptotic neutrophils (106). Interestingly some SPMs enhance the migration of monocytes and macrophages and so released SPMs by apoptotic cells may act as a signal for phagocytes to find these cells for swift clearance. Moreover, these findings suggest that apoptotic cells themselves are active participants in their own clearance. Newer work suggests that metabolites such as putrescine released by apoptotic cells also participate in their own clearance (108) and so released products from apoptotic cells may play critical roles in their swift clearance. More work regarding apoptotic cell secretomes and how released factors impact their clearance are of interest. In fact, Medina et al. profiled the metabolite secretome of apoptotic lymphocytes and macrophages and showed specific metabolites released by apoptotic cells act as "good-bye" messengers to modulate tissue functions. These metabolites reprogram the genes of neighboring healthy cells to facilitate an anti-inflammatory phenotype and promote tissue homeostasis (108).

Moreover, we know there are many modes of cell death beyond apoptosis. Lytic cell death like necroptosis, impacts phagocyte function given the pro-inflammatory nature of their death (109). In addition to the release of DAMPs, cytokines and chemokines, recent work from our lab suggests that necroptotic cells release prostanoids (26). Advanced atherosclerotic plaques from hypercholesterolemic *Mlkl*$^{-/-}$ mice had significantly more prostanoids like PGE_2, PGD_2, $PGF_{2\alpha}$, and thromboxane (TX) compared with wild type (Wt) controls (26). In vitro studies revealed that necroptotic macrophages and endothelial cells also released prostanoids, including TX and PGE_2 (26). Receptor antagonists for DP (i.e. PGD_2 receptor), EP2 (i.e. PGE_2 receptor) and TP (i.e. TX receptor) rescued defective efferocytosis caused by necroptotic cell releasate, suggesting that a prostanoid storm negatively impacts phagocyte behavior (26). Moreover, macrophages stimulated with a TP agonist called U46619 impaired the clearance of both apoptotic and necroptotic cells and so TX may be a novel "avoid me" signal (26). As mentioned above, certain pro-inflammatory cytokines also limit efferocytosis and so released factors from necroptotic cells (or cells that undergo a pro-inflammatory mode of death) may play a large role in negatively impacting phagocyte behavior in tissues.

SPMS PROMOTE THE CLEARANCE OF NECROPTOTIC CELLS

Necroptosis is a pro-inflammatory form of cell death (110, 111) and so the accumulation of necroptotic cells can be damaging to tissues (112). Therefore, uncovering mechanisms associated with necroptotic cell clearance is of immense interest. Earlier work demonstrated that necroptotic cells were cleared by macrophages in a distinct and less efficient manner than apoptotic cells (113, 114). However, detailed molecular mechanisms, quantification methods, and factors that augment the clearance of necroptotic cells were not

known. We recently found that necroptotic macrophages express high levels of a "don't eat me" signal called CD47 (27). Other work suggests that the exuberant expression of CD47 results from pro-inflammatory cytokines, like TNF-α (115), and so the pro-inflammatory nature of this cell death likely drives the increase of CD47. Moreover, because necroptotic cells have regions of disrupted membrane (109), we also found that elevated levels of CD47 were present in clusters on the surface of the necroptotic cell (27). The elevated levels and clustering of CD47 led to an inefficient "nibbling" of necroptotic cells *via* a RhoA-pMLC signaling event (27). RvD1 when given *in vitro* and *in vivo* was able to enhance the clearance of necroptotic cells by promoting whole cell engulfment (26, 27). RvD1-stimulated whole cell engulfment of necroptotic cells by macrophages was non-phlogistic and RvD1 acted by limiting RhoA-pMLC signaling and promoting CDC42 (27). Additionally, RvD1-stimulated macrophages swiftly recognized necroptotic cells for their engulfment and how RvD1 overcame the "don't eat me" recognition was of interest. ER-mediated phagocytosis is a process in which macrophages release calreticulin onto their target. In other contexts, ER-mediated phagocytosis has been described and is thought to be important for eating large cargo (116, 117). Our work suggests that RvD1 promotes the release of calreticulin from macrophages (117) and may be a mechanism through which RvD1 can swiftly recognize these cells for whole-cell clearance. This work highlights the intricate set of signals/signaling that a macrophage needs to decode for efficient engulfment and clearance of dead cells.

From a metabolic perspective RvD1 stimulates p-AMPK, fatty acid oxidation (FAO) and oxidative phosphorylation (OXHPOS) mechanisms in macrophages to allow for enhanced clearance of necroptotic cells (26). We found OXPHOS is not as readily activated in vehicle-treated macrophages that were ingesting necroptotic cells (26), which suggests that the cargo load within the macrophage may be important for initiating these programs. As mentioned above, apoptotic cell uptake and its eventual breakdown provides the fuel for FAO and OXPHOS in macrophages (101) and so these data suggest that RvD1 maintains this protective metabolic phenotype.

PRO-RESOLVING LIGANDS RESCUE AGE-RELATED DEFECTS IN EFFEROCYTOSIS

The population is rapidly aging, health care costs are already insurmountable and therapeutics to manage several age-related diseases are limited. Therefore aging and age-related diseases are the scourges of modern medicine. Aging is a complex process that involves genetic, environmental and biological factors. Therefore understanding a common mechanism that may link all of these diseases will inform the development of therapeutics that can promote health span. Persistent, non-resolving inflammation, or inflammaging, largely contributes to a panoply of age-related diseases including periodontal disease, neurodegenerative diseases, macular degeneration, and atherosclerotic cardiovascular disease (118). Defective efferocytosis in aging is well appreciated (119–123). Linehan et al. observed that peritoneal macrophages from old mice had diminished efferocytosis compared with peritoneal macrophages from young mice (121). Interestingly, they transferred peritoneal macrophages from young mice into the peritoneum of old mice, and found that the young macrophages exhibited defective

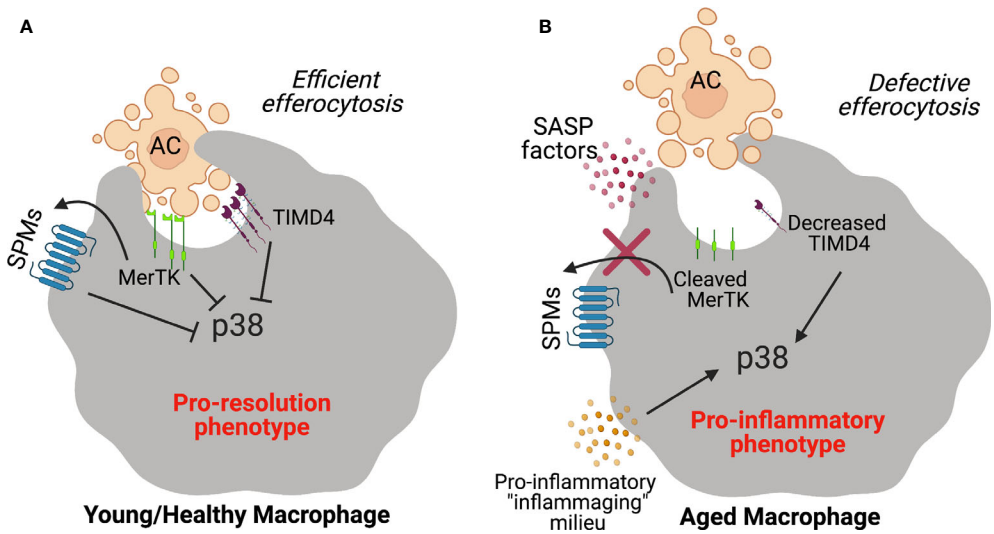

FIGURE 1 | Schematic diagram depicting failed efferocytosis mechanisms during aging. **(A)** Efferocytic receptors like MerTK or TIMD4 on young healthy macrophages interact with phosphatidyl serine on apoptotic cells to promote efficient clearance. SPMs promote efferocytosis and MerTK signaling in a feed forward manner which stimulates the synthesis of SPMs. In response to apoptotic cell ingestion, the pro-inflammatory p38 MAPK pathway is inhibited and macrophages prevent the production of pro-inflammatory programs. **(B)** In the context of aging, MerTK is cleaved by released factors from senescent cells (i.e. factors from the senescence-associated secretory phenotype or SASP) which limits apoptotic cell uptake and the feed-forward pro-resolution circuit. TIMD4 expression is also significantly decreased on macrophages from aging humans which drives the activation of p38 to propagate inflammation.

efferocytosis similar to that of macrophages from old mice (121), which suggests that the aging milieu drives defective efferocytosis (120, 121). Lung macrophages from old mice also exhibited defective efferocytosis, which may account for the accumulation of leukocytes and failed tissue repair in lungs from influenza-infected aged mice (124, 125).

Accumulation of senescent cells is also associated with inflammaging (126). Senescent cells acquire a senescence-associated secretory phenotype (SASP) which exacerbates inflammation (126) and contributes to inefficient clearance of dead cells (38). Briefly, we found that released factors from senescent cells promote the cleavage of a critical efferocytosis receptor on macrophages called MerTK to limit efferocytosis (38). RvD1 rescued senescent cell-induced defective efferocytosis *in vitro*. RvD1 treatment to old mice also increased *in situ* efferocytosis in lungs post hind-limb ischemia-reperfusion injury (38). MerTK is an interesting efferocytosis receptor because of its ability to stimulate a pro-resolution feed-forward circuit. In this regard, MerTK cleavage is associated with delayed temporal resolution, impaired SPM synthesis over pro-inflammatory lipid mediators and has been shown to promote atherosclerosis (107, 127). Also, with regard to other TAM receptors and aging, Frisch et al. found that Gas6, which is a ligand for MerTK (and other TAM receptors), was down regulated in the bone marrow from aged mice (123) which may account for defective efferocytosis in the aging bone marrow milieu. Moreover, they demonstrated loss-of-function of another efferocytic TAM receptor, Axl in bone marrow macrophages from aged mice which further leads to a significant increase in pro-inflammatory IL-1β signaling. Together, these results suggest that efferocytosis receptors and thus a feed-forward pro-resolution circuit may be dysfunctional in aging.

Along these lines, imbalances in the SPM to pro-inflammatory lipid mediator ratios have been observed in mice and humans in the context of inflammaging (122, 128). In elderly humans, urinary lipoxins (LXs) were decreased resulting in a profound imbalance between pro-resolving LXs and leukotrienes (LTs) (128). Other relevant age-related diseases like atherosclerosis, peripheral vascular disease, periodontal disease and Alzheimer's disease are also associated with imbalances in this critical ratio and restoration of defective SPMs to these pre-clinical models of disease result in protection (129–132). Nevertheless, how these imbalances arise in aging is of interest but work suggests that one mechanism (of many) may be through MerTK signaling (38). MerTK signaling in human macrophages decreased activity of the mitogen-activated protein kinase (MAPK) p38 and the kinase MK2, resulting in the increased non-phosphorylated, cytoplasmic form of 5-LOX and enhanced SPM biosynthesis (133). Therefore, downstream signaling events from efferocytic responses may drive SPM synthesis of pro-inflammatory mediators. Of note, RvD1 was shown to limit p38 activation which promotes a pro-resolution circuit in macrophages (95). Therefore, continued activation of p38 may not only drive defective efferocytosis but also impair resolution in aging (**Figure 1**).

Recent work demonstrated that the efferocytosis receptor, TIM-4 was decreased on macrophages from elderly humans in self-limited inflammatory loci (134). Reduced levels of TIM4 in elderly humans was attributed to increased p38 activation (134) and blockade of elevated p38 restored efferocytosis in the elderly. This work provides strong rationale for therapeutic strategies that target p38 to promote efferocytosis in aging (135). Together, phagocyte function in aging is impaired, which may be one of several factors that contributes to limited tissue repair in aging. A deeper exploration of efferocytosis mechanisms in aging may help inform the development of new tissue-reparative therapies.

CLOSING REMARKS: THERAPEUTIC OPPORTUNITY

SPMs and other pro-resolving ligands offer tremendous opportunities for therapeutic use. Currently, treating inflammation is difficult because we evolved inflammatory reactions to fight infection and repair wounds. Therefore anti-inflammatories possess a risk in which critical host defense mechanisms are weakened. Anti-inflammatories may halt the progression of ongoing inflammation, but do very little to repair the already damaged tissue. Ultimately what is lacking is a therapeutic strategy that can repair tissue damage once it has occurred. SPMs are protective in numerous pre-clinical models of disease and most recently have been shown to reduce PMN infiltration during acute sterile inflammation in humans (136). SPMs stimulate phagocytes to clear, and neutralize pathogens or accelerate the removal of unwanted dead cells or debris, all while dampening inflammatory mediators and stimulating necessary pro-repair factors (58). Thus, SPMs offer an entirely new way to control inflammation which includes enhancing the removal of harmful stimuli and promoting tissue repair.

AUTHOR CONTRIBUTIONS

CD, SS and GF wrote the manuscript. All authors contributed to the article and approved the submitted version.

FUNDING

This work was supported by NIH grants HL141127 (GF), HL153019 (GF).

REFERENCES

1. Gordon S. Phagocytosis: The Legacy of Metchnikoff. *Cell* (2016) 166 (5):1065–8. doi: 10.1016/j.cell.2016.08.017
2. Chiang N, Serhan CN. Specialized Pro-Resolving Mediator Network: An Update on Production and Actions. *Essays Biochem* (2020) 64(3):443–62. doi: 10.1042/EBC20200018
3. Serhan CN. Pro-Resolving Lipid Mediators Are Leads for Resolution Physiology. *Nature* (2014) 510(7503):92–101. doi: 10.1038/nature13479
4. Serhan CN, Hamberg M, Samuelsson B. Lipoxins: Novel Series of Biologically Active Compounds Formed From Arachidonic Acid in Human Leukocytes. *Proc Natl Acad Sci USA* (1984) 81(17):5335–9. doi: 10.1073/pnas.81.17.5335

5. Serhan CN, Clish CB, Brannon J, Colgan SP, Chiang N, Gronert K. Novel Functional Sets of Lipid-Derived Mediators With Antiinflammatory Actions Generated From Omega-3 Fatty Acids Via Cyclooxygenase 2-Nonsteroidal Antiinflammatory Drugs and Transcellular Processing. *J Exp Med* (2000) 192(8):1197–204. doi: 10.1084/jem.192.8.1197
6. Serhan CN, Hong S, Gronert K, Colgan SP, Devchand PR, Mirick G, et al. Resolvins: A Family of Bioactive Products of Omega-3 Fatty Acid Transformation Circuits Initiated by Aspirin Treatment That Counter Proinflammation Signals. *J Exp Med* (2002) 196(8):1025–37. doi: 10.1084/jem.20020760
7. Hong S, Gronert K, Devchand PR, Moussignac RL, Serhan CN. Novel Docosatrienes and 17S-Resolvins Generated From Docosahexaenoic Acid in Murine Brain, Human Blood, and Glial Cells. Autacoids in Anti-Inflammation. *J Biol Chem* (2003) 278(17):14677–87. doi: 10.1074/jbc.M300218200
8. Dalli J, Chiang N, Serhan CN. Identification of 14-Series Sulfido-Conjugated Mediators That Promote Resolution of Infection and Organ Protection. *Proc Natl Acad Sci USA* (2014) 111(44):E4753–61. doi: 10.1073/pnas.1415006111
9. Dalli J, Chiang N, Serhan CN. Elucidation of Novel 13-Series Resolvins That Increase With Atorvastatin and Clear Infections. *Nat Med* (2015) 21 (9):1071–5. doi: 10.1038/nm.3911
10. Fiore S, Maddox JF, Perez HD, Serhan CN. Identification of a Human cDNA Encoding a Functional High Affinity Lipoxin A4 Receptor. *J Exp Med* (1994) 180(1):253–60. doi: 10.1084/jem.180.1.253
11. Arita M, Bianchini F, Aliberti J, Sher A, Chiang N, Hong S, et al. Stereochemical Assignment, Antiinflammatory Properties, and Receptor for the Omega-3 Lipid Mediator Resolvin E1. *J Exp Med* (2005) 201 (5):713–22. doi: 10.1084/jem.20042031
12. Krishnamoorthy S, Recchiuti A, Chiang N, Fredman G, Serhan CN. Resolvin D1 Receptor Stereoselectivity and Regulation of Inflammation and Proresolving Micrornas. *Am J Pathol* (2012) 180(5):2018–27. doi: 10.1016/j.ajpath.2012.01.028
13. Chiang N, Serhan CN. Structural Elucidation and Physiologic Functions of Specialized Pro-Resolving Mediators and Their Receptors. *Mol Aspects Med* (2017) 58:114–29. doi: 10.1016/j.mam.2017.03.005
14. Flak MB, Koenis DS, Sobrino A, Smith J, Pistorius K, Palmas F, et al. GPR101 Mediates the Pro-Resolving Actions of RvD5n-3 DPA in Arthritis and Infections. *J Clin Invest* (2020) 130(1):359–73. doi: 10.1172/JCI131609
15. Schwab JM, Chiang N, Arita M, Serhan CN. Resolvin E1 and Protectin D1 Activate Inflammation-Resolution Programmes. *Nature* (2007) 447 (7146):869–74. doi: 10.1038/nature05877
16. Ohira T, Arita M, Omori K, Recchiuti A, Van Dyke TE, Serhan CN. Resolvin E1 Receptor Activation Signals Phosphorylation and Phagocytosis. *J Biol Chem* (2010) 285(5):3451–61. doi: 10.1074/jbc.M109.044131
17. Haas-Stapleton EJ, Lu Y, Hong S, Arita M, Favoreto S, Nigam S, et al. Candida Albicans Modulates Host Defense by Biosynthesizing the Pro-Resolving Mediator Resolvin E1. *PloS One* (2007) 2(12):e1316. doi: 10.1371/journal.pone.0001316
18. Oh SF, Pillai PS, Recchiuti A, Yang R, Serhan CN. Pro-Resolving Actions and Stereoselective Biosynthesis of 18S E-series Resolvins in Human Leukocytes and Murine Inflammation. *J Clin Invest* (2011) 121(2):569–81. doi: 10.1172/JCI42545
19. Fredman G, Oh SF, Ayilavarapu S, Hasturk H, Serhan CN, Van Dyke TE. Impaired Phagocytosis in Localized Aggressive Periodontitis: Rescue by Resolvin E1. *PloS One* (2011) 6(9):e24422. doi: 10.1371/journal.pone.0024422
20. Oh SF, Dona M, Fredman G, Krishnamoorthy S, Irimia D, Serhan CN. Resolvin E2 Formation and Impact in Inflammation Resolution. *J Immunol* (2012) 188(9):4527–34. doi: 10.4049/jimmunol.1103652
21. Libreros S, Shay AE, Nshimiyimana R, Fichtner D, Martin MJ, Wourms N, et al. A New E-Series Resolvin: Rve4 Stereochemistry and Function in Efferocytosis of Inflammation-Resolution. *Front Immunol* (2020) 11:631319. doi: 10.3389/fimmu.2020.631319
22. Norris PC, Libreros S, Serhan CN. Resolution Metabolomes Activated by Hypoxic Environment. *Sci Adv* (2019) 5(10):eaax4895. doi: 10.1126/sciadv.aax4895
23. Chiang N, Fredman G, Backhed F, Oh SF, Vickery T, Schmidt BA, et al. Infection Regulates Pro-Resolving Mediators That Lower Antibiotic Requirements. *Nature* (2012) 484(7395):524–8. doi: 10.1038/nature11042
24. Rogerio AP, Haworth O, Croze R, Oh SF, Uddin M, Carlo T, et al. Resolvin D1 and Aspirin-Triggered Resolvin D1 Promote Resolution of Allergic Airways Responses. *J Immunol* (2012) 189(4):1983–91. doi: 10.4049/jimmunol.1101665
25. Winkler JW, Orr SK, Dalli J, Cheng CY, Sanger JM, Chiang N, et al. Resolvin D4 Stereoassignment and its Novel Actions in Host Protection and Bacterial Clearance. *Sci Rep* (2016) 6:18972. doi: 10.1038/srep18972
26. Hosseini Z, Marinello M, Decker C, Sansbury BE, Sadhu S, Gerlach BD, et al. Resolvin D1 Enhances Necroptotic Cell Clearance Through Promoting Macrophage Fatty Acid Oxidation and Oxidative Phosphorylation. *Arterioscler Thromb Vasc Biol* (2021) 2021:ATVBAHA120315758. doi: 10.1161/ATVBAHA.120.315758
27. Gerlach BD, Marinello M, Heinz J, Rymut N, Sansbury BE, Riley CO, et al. Resolvin D1 Promotes the Targeting and Clearance of Necroptotic Cells. *Cell Death Differ* (2019) 27:525–39. doi: 10.1038/s41418-019-0370-1
28. Lee HN, Kundu JK, Cha YN, Surh YJ. Resolvin D1 Stimulates Efferocytosis Through p50/p50-Mediated Suppression of Tumor Necrosis Factor-Alpha Expression. *J Cell Sci* (2013) 126(Pt 17):4037–47. doi: 10.1242/jcs.131003
29. McCauley LK, Dalli J, Koh AJ, Chiang N, Serhan CN. Cutting Edge: Parathyroid Hormone Facilitates Macrophage Efferocytosis in Bone Marrow Via Proresolving Mediators Resolvin D1 and Resolvin D2. *J Immunol* (2014) 193(1):26–9. doi: 10.4049/jimmunol.1301945
30. Mizwicki MT, Liu G, Fiala M, Magpantay L, Sayre J, Siani A, et al. 1alpha,25-Dihydroxyvitamin D3 and Resolvin D1 Retune the Balance Between Amyloid-Beta Phagocytosis and Inflammation in Alzheimer's Disease Patients. *J Alzheimers Dis* (2013) 34(1):155–70. doi: 10.3233/JAD-121735
31. Croasdell A, Lacy SH, Thatcher TH, Sime PJ, Phipps RP. Resolvin D1 Dampens Pulmonary Inflammation and Promotes Clearance of Nontypeable Haemophilus Influenzae. *J Immunol* (2016) 196(6):2742–52. doi: 10.4049/jimmunol.1502331
32. Abdulnour RE, Sham HP, Douda DN, Colas RA, Dalli J, Bai Y, et al. Aspirin-Triggered Resolvin D1 Is Produced During Self-Resolving Gram-Negative Bacterial Pneumonia and Regulates Host Immune Responses for the Resolution of Lung Inflammation. *Mucosal Immunol* (2016) 9(5):1278–87. doi: 10.1038/mi.2015.129
33. Matte A, Recchiuti A, Federti E, Koehl B, Mintz T, El Nemer W, et al. Resolution of Sickle Cell Disease-Associated Inflammation and Tissue Damage With 17R-Resolvin D1. *Blood* (2019) 133(3):252–65. doi: 10.1182/blood-2018-07-865378
34. Codagnone M, Cianci E, Lamolinara A, Mari VC, Nespoli A, Isopi E, et al. Resolvin D1 Enhances the Resolution of Lung Inflammation Caused by Long-Term Pseudomonas Aeruginosa Infection. *Mucosal Immunol* (2018) 11(1):35–49. doi: 10.1038/mi.2017.36
35. Elajami TK, Colas RA, Dalli J, Chiang N, Serhan CN, Welty FK. Specialized Proresolving Lipid Mediators in Patients With Coronary Artery Disease and Their Potential for Clot Remodeling. *FASEB J* (2016) 30(8):2792–801. doi: 10.1096/fj.201500155R
36. Krishnamoorthy S, Recchiuti A, Chiang N, Yacoubian S, Lee CH, Yang R, et al. Resolvin D1 Binds Human Phagocytes With Evidence for Proresolving Receptors. *Proc Natl Acad Sci USA* (2010) 107(4):1660–5. doi: 10.1073/pnas.0907342107
37. Lee HN, Surh YJ. Resolvin D1-Mediated NOX2 Inactivation Rescues Macrophages Undertaking Efferocytosis From Oxidative Stress-Induced Apoptosis. *Biochem Pharmacol* (2013) 86(6):759–69. doi: 10.1016/j.bcp.2013.07.002
38. Rymut N, Heinz J, Sadhu S, Hosseini Z, Riley CO, Marinello M, et al. Resolvin D1 Promotes Efferocytosis in Aging by Limiting Senescent Cell-Induced MerTK Cleavage. *FASEB J* (2020) 34(1):597–609. doi: 10.1096/fj.201902126R
39. Luo B, Han F, Xu K, Wang J, Liu Z, Shen Z, et al. Resolvin D1 Programs Inflammation Resolution by Increasing TGF-Beta Expression Induced by Dying Cell Clearance in Experimental Autoimmune Neuritis. *J Neurosci* (2016) 36(37):9590–603. doi: 10.1523/JNEUROSCI.0020-16.2016
40. Gilligan MM, Gartung A, Sulciner ML, Norris PC, Sukhatme VP, Bielenberg DR, et al. Aspirin-Triggered Proresolving Mediators Stimulate Resolution in Cancer. *Proc Natl Acad Sci USA* (2019) 116(13):6292–7. doi: 10.1073/pnas.1804000116
41. Merched AJ, Ko K, Gotlinger KH, Serhan CN, Chan L. Atherosclerosis: Evidence for Impairment of Resolution of Vascular Inflammation Governed by Specific Lipid Mediators. *FASEB J* (2008) 22(10):3595–606. doi: 10.1096/fj.08-112201
42. Spite M, Norling LV, Summers L, Yang R, Cooper D, Petasis NA, et al. Resolvin D2 Is a Potent Regulator of Leukocytes and Controls Microbial Sepsis. *Nature* (2009) 461(7268):1287–91. doi: 10.1038/nature08541

43. Chiang N, Dalli J, Colas RA, Serhan CN. Identification of Resolvin D2 Receptor Mediating Resolution of Infections and Organ Protection. *J Exp Med* (2015) 212(8):1203–17. doi: 10.1084/jem.20150225
44. Chiang N, de la Rosa X, Libreros S, Serhan CN. Novel Resolvin D2 Receptor Axis in Infectious Inflammation. *J Immunol* (2017) 198(2):842–51. doi: 10.4049/jimmunol.1601650
45. Dalli J, Winkler JW, Colas RA, Arnardottir H, Cheng CY, Chiang N, et al. Resolvin D3 and Aspirin-Triggered Resolvin D3 Are Potent Immunoresolvents. *Chem Biol* (2013) 20(2):188–201. doi: 10.1016/j.chembiol.2012.11.010
46. Winkler JW, Libreros S, De La Rosa X, Sansbury BE, Norris PC, Chiang N, et al. Structural Insights Into Resolvin D4 Actions and Further Metabolites Via a New Total Organic Synthesis and Validation. *J Leukoc Biol* (2018) 103:995–1010. doi: 10.1002/JLB.3MI0617-254R
47. Chiang N, Libreros S, Norris PC, de la Rosa X, Serhan CN. Maresin 1 Activates LGR6 Receptor Promoting Phagocyte Immunoresolvent Functions. *J Clin Invest* (2019) 129(12):5294–311. doi: 10.1172/JCI129448
48. Serhan CN, Dalli J, Karamnov S, Choi A, Park CK, Xu ZZ, et al. Macrophage Proresolving Mediator Maresin 1 Stimulates Tissue Regeneration and Controls Pain. *FASEB J* (2012) 26(4):1755–65. doi: 10.1096/fj.11-201442
49. Deng B, Wang CW, Arnardottir HH, Li Y, Cheng CY, Dalli J, et al. Maresin Biosynthesis and Identification of Maresin 2, A New Anti-Inflammatory and Pro-Resolving Mediator From Human Macrophages. *PloS One* (2014) 9(7):e102362. doi: 10.1371/journal.pone.0102362
50. Serhan CN, Yang R, Martinod K, Kasuga K, Pillai PS, Porter TF, et al. Maresins: Novel Macrophage Mediators With Potent Antiinflammatory and Proresolving Actions. *J Exp Med* (2009) 206(1):15–23. doi: 10.1084/jem.20081880
51. Bang S, Xie YK, Zhang ZJ, Wang Z, Xu ZZ, Ji RR. GPR37 Regulates Macrophage Phagocytosis and Resolution of Inflammatory Pain. *J Clin Invest* (2018) 128(8):3568–82. doi: 10.1172/JCI99888
52. Mukherjee PK, Marcheselli VL, de Rivero Vaccari JC, Gordon WC, Jackson FE, Bazan NG. Photoreceptor Outer Segment Phagocytosis Attenuates Oxidative Stress-Induced Apoptosis With Concomitant Neuroprotectin D1 Synthesis. *Proc Natl Acad Sci USA* (2007) 104(32):13158–63. doi: 10.1073/pnas.0705963104
53. Serhan CN, Gotlinger K, Hong S, Lu Y, Siegelman J, Baer T, et al. Anti-Inflammatory Actions of Neuroprotectin D1/protectin D1 and its Natural Stereoisomers: Assignments of Dihydroxy-Containing Docosatrienes. *J Immunol* (2006) 176(3):1848–59. doi: 10.4049/jimmunol.176.3.1848
54. Serhan CN, Fredman G, Yang R, Karamnov S, Belayev LS, Bazan NG, et al. Novel Proresolving Aspirin-Triggered DHA Pathway. *Chem Biol* (2011) 18 (8):976–87. doi: 10.1016/j.chembiol.2011.06.008
55. Ramon S, Dalli J, Sanger JM, Winkler JW, Aursnes M, Tungen JE, et al. The Protectin Pctr1 Is Produced by Human M2 Macrophages and Enhances Resolution of Infectious Inflammation. *Am J Pathol* (2016) 186(4):962–73. doi: 10.1016/j.ajpath.2015.12.012
56. Dalli J, Sanger JM, Rodriguez AR, Chiang N, Spur BW, Serhan CN. Identification and Actions of a Novel Third Maresin Conjugate in Tissue Regeneration: Mctr3. *PloS One* (2016) 11(2):e0149319. doi: 10.1371/journal.pone.0149319
57. Chiang N, Riley IR, Dalli J, Rodriguez AR, Spur BW, Serhan CN. New Maresin Conjugates in Tissue Regeneration Pathway Counters Leukotriene D4-stimulated Vascular Responses. *FASEB J* (2018) 32(7):4043–52. doi: 10.1096/fj.201701493R
58. Dalli J, Ramon S, Norris PC, Colas RA, Serhan CN. Novel Proresolving and Tissue-Regenerative Resolvin and Protectin Sulfido-Conjugated Pathways. *FASEB J* (2015) 29(5):2120–36. doi: 10.1096/fj.14-268441
59. de la Rosa X, Norris PC, Chiang N, Rodriguez AR, Spur BW, Serhan CN. Identification and Complete Stereochemical Assignments of the New Resolvin Conjugates in Tissue Regeneration in Human Tissues That Stimulate Proresolving Phagocyte Functions and Tissue Regeneration. *Am J Pathol* (2018) 188(4):950–66. doi: 10.1016/j.ajpath.2018.01.004
60. Dalli J, Colas RA, Serhan CN. Novel N-3 Immunoresolvents: Structures and Actions. *Sci Rep* (2013) 3:1940. doi: 10.1038/srep01940
61. Prescott D, McKay DM. Aspirin-Triggered Lipoxin Enhances Macrophage Phagocytosis of Bacteria While Inhibiting Inflammatory Cytokine Production. *Am J Physiol Gastrointest Liver Physiol* (2011) 301(3):G487–97. doi: 10.1152/ajpgi.00042.2011
62. Godson C, Mitchell S, Harvey K, Petasis NA, Hogg N, Brady HR. Cutting Edge: Lipoxins Rapidly Stimulate Nonphlogistic Phagocytosis of Apoptotic Neutrophils by Monocyte-Derived Macrophages. *J Immunol* (2000) 164 (4):1663–7. doi: 10.4049/jimmunol.164.4.1663
63. Mitchell S, Thomas G, Harvey K, Cottell D, Reville K, Berlasconi G, et al. Lipoxins, Aspirin-Triggered Epi-Lipoxins, Lipoxin Stable Analogues, and the Resolution of Inflammation: Stimulation of Macrophage Phagocytosis of Apoptotic Neutrophils In Vivo. *J Am Soc Nephrol* (2002) 13(10):2497–507. doi: 10.1097/01.ASN.0000032417.73640.72
64. Norris PC, Libreros S, Chiang N. And Serhan Cn. A Cluster of Immunoresolvents Links Coagulation to Innate Host Defense in Human Blood. *Sci Signal* (2017) 10(490):eaan1471. doi: 10.1126/scisignal.aan1471
65. Maderna P, Yona S, Perretti M, Godson C. Modulation of Phagocytosis of Apoptotic Neutrophils by Supernatant From Dexamethasone-Treated Macrophages and Annexin-Derived Peptide Ac(2-26). *J Immunol* (2005) 174(6):3727–33. doi: 10.4049/jimmunol.174.6.3727
66. Kourtzelis I, Li X, Mitroulis I, Grosser D, Kajikawa T, Wang B, et al. DEL-1 Promotes Macrophage Efferocytosis and Clearance of Inflammation. *Nat Immunol* (2019) 20(1):40–9. doi: 10.1038/s41590-018-0249-1
67. Chiang N, de la Rosa X, Libreros S, Pan H, Dreyfuss JM, Serhan CN. Cysteinyl-Specialized Proresolving Mediators Link Resolution of Infectious Inflammation and Tissue Regeneration Via TRAF3 Activation. *Proc Natl Acad Sci USA* (2021) 118(10):e2013374118. doi: 10.1073/pnas.2013374118
68. Kumaran Satyanarayanan S, El Kebir D, Soboh S, Butenko S, Sekheri M, Saadi J, et al. IFN-Beta is a Macrophage-Derived Effector Cytokine Facilitating the Resolution of Bacterial Inflammation. *Nat Commun* (2019) 10(1):3471. doi: 10.1038/s41467-019-10903-9
69. Rinaldi M, Thomas L, Mathieu P, Carabias P, Troncoso MF, Pasquini JM, et al. Galectin-1 Circumvents Lysolecithin-Induced Demyelination Through the Modulation of Microglial Polarization/Phagocytosis and Oligodendroglial Differentiation. *Neurobiol Dis* (2016) 96:127–43. doi: 10.1016/j.nbd.2016.09.003
70. Yaseen H, Butenko S, Polishuk-Zotkin I, Schif-Zuck S, Perez-Saez JM, Rabinovich GA, et al. Galectin-1 Facilitates Macrophage Reprogramming and Resolution of Inflammation Through IFN-Beta. *Front Pharmacol* (2020) 11:901. doi: 10.3389/fphar.2020.00901
71. Wright RD, Souza PR, Flak MB, Thedchanamoorthy P, Norling LV, Cooper D. Galectin-3-null Mice Display Defective Neutrophil Clearance During Acute Inflammation. *J Leukoc Biol* (2017) 101(3):717–26. doi: 10.1189/jlb.3A0116-026RR
72. Fernandez GC, Ilarregui JM, Rubel CJ, Toscano MA, Gomez SA, Beigier Bompadre M, et al. Galectin-3 and Soluble Fibrinogen Act in Concert to Modulate Neutrophil Activation and Survival: Involvement of Alternative MAPK Pathways. *Glycobiology* (2005) 15(5):519–27. doi: 10.1093/glycob/cwi026
73. Montero-Melendez T, Patel HB, Seed M, Nielsen S, Jonassen TE, Perretti M. The Melanocortin Agonist AP214 Exerts Anti-Inflammatory and Proresolving Properties. *Am J Pathol* (2011) 179(1):259–69. doi: 10.1016/j.ajpath.2011.03.042
74. Dalli J, Norling LV, Montero-Melendez T, Federici Canova D, Lashin H, Pavlov AM, et al. Microparticle alpha-2-macroglobulin Enhances Pro-Resolving Responses and Promotes Survival in Sepsis. *EMBO Mol Med* (2014) 6(1):27–42. doi: 10.1002/emmm.201303503
75. Dufton N, Natividad J, Verdu EF, Wallace JL. Hydrogen Sulfide and Resolution of Acute Inflammation: A Comparative Study Utilizing a Novel Fluorescent Probe. *Sci Rep* (2012) 2:499. doi: 10.1038/srep00499
76. Chiang N, Shinohara M, Dalli J, Mirakaj V, Kibi M, Choi AM, et al. Inhaled Carbon Monoxide Accelerates Resolution of Inflammation Via Unique Proresolving Mediator-Heme Oxygenase-1 Circuits. *J Immunol* (2013) 190 (12):6378–88. doi: 10.4049/jimmunol.1202969
77. Salmon JE, Cronstein BN. Fc Gamma Receptor-Mediated Functions in Neutrophils are Modulated by Adenosine Receptor Occupancy. A1 Receptors are Stimulatory and A2 Receptors Are Inhibitory. *J Immunol* (1990) 145(7):2235–40.
78. Loiola RA, Wickstead ES, Solito E, McArthur S. Estrogen Promotes Pro-Resolving Microglial Behavior and Phagocytic Cell Clearance Through the Actions of Annexin A1. *Front Endocrinol (Lausanne)* (2019) 10:420. doi: 10.3389/fendo.2019.00420
79. Doran AC, Yurdagul AJr., Tabas I. Efferocytosis in Health and Disease. *Nat Rev Immunol* (2020) 20(4):254–67. doi: 10.1038/s41577-019-0240-6

80. Flannagan RS, Jaumouille V, Grinstein S. The Cell Biology of Phagocytosis. *Annu Rev Pathol* (2012) 7:61–98. doi: 10.1146/annurev-pathol-011811-132445
81. Vance RE, Hong S, Gronert K, Serhan CN, Mekalanos JJ. The Opportunistic Pathogen Pseudomonas Aeruginosa Carries a Secretable Arachidonate 15-Lipoxygenase. *Proc Natl Acad Sci USA* (2004) 101(7):2135–9. doi: 10.1073/pnas.0307308101
82. Bannenberg GL, Aliberti J, Hong S, Sher A, Serhan C. Exogenous Pathogen and Plant 15-Lipoxygenase Initiate Endogenous Lipoxin A4 Biosynthesis. *J Exp Med* (2004) 199(4):515–23. doi: 10.1084/jem.20031325
83. Colas RA, Ashton AW, Mukherjee S, Dalli J, Akide-Ndunge OB, Huang H, et al. Trypanosoma Cruzi Produces the Specialized Proresolving Mediators Resolvin D1, Resolvin D5, and Resolvin E2. *Infect Immun* (2018) 86(4):e00688–17. doi: 10.1128/IAI.00688-17
84. Sham HP, Walker KH, Abdulnour RE, Krishnamoorthy N, Douda DN, Norris PC, et al. 15-Epi-Lipoxin A4, Resolvin D2, and Resolvin D3 Induce NF-Kappab Regulators in Bacterial Pneumonia. *J Immunol* (2018) 200(8):2757–66. doi: 10.4049/jimmunol.1602090
85. Wang H, Anthony D, Yatmaz S, Wijburg O, Satzke C, Levy B, et al. Aspirin-Triggered Resolvin D1 Reduces Pneumococcal Lung Infection and Inflammation in a Viral and Bacterial Coinfection Pneumonia Model. *Clin Sci (Lond)* (2017) 131(18):2347–62. doi: 10.1042/CS20171006
86. Ruiz A, Sarabia C, Torres M, Juarez E. Resolvin D1 (RvD1) and Maresin 1 (Mar1) Contribute to Human Macrophage Control of M. Tuberculosis Infection While Resolving Inflammation. *Int Immunopharmacol* (2019) 74:105694. doi: 10.1016/j.intimp.2019.105694
87. Tobin DM, Ramakrishnan L. TB: The Yin and Yang of Lipid Mediators. *Curr Opin Pharmacol* (2013) 13(4):641–5. doi: 10.1016/j.coph.2013.06.007
88. Dalli J, Zhu M, Vlasenko NA, Deng B, Haeggstrom JZ, Petasis NA, et al. The Novel 13S,14S-Epoxy-Maresin is Converted by Human Macrophages to Maresin 1 (MaR1), Inhibits Leukotriene A4 Hydrolase (LTA4H), and Shifts Macrophage Phenotype. *FASEB J* (2013) 27(7):2573–83. doi: 10.1096/fj.13-227728
89. Boada-Romero E, Martinez J, Heckmann BL, Green DR. The Clearance of Dead Cells by Efferocytosis. *Nat Rev Mol Cell Biol* (2020) 21(7):398–414. doi: 10.1038/s41580-020-0232-1
90. Arandjelovic S, Ravichandran KS. Phagocytosis of Apoptotic Cells in Homeostasis. *Nat Immunol* (2015) 16(9):907–17. doi: 10.1038/ni.3253
91. Tabas I. Macrophage Death and Defective Inflammation Resolution in Atherosclerosis. *Nat Rev Immunol* (2010) 10(1):36–46. doi: 10.1038/nri2675
92. Reville K, Crean JK, Vivers S, Dransfield I, Godson C. Lipoxin A4 Redistributes Myosin IIA and Cdc42 in Macrophages: Implications for Phagocytosis of Apoptotic Leukocytes. *J Immunol* (2006) 176(3):1878–88. doi: 10.4049/jimmunol.176.3.1878
93. Dalli J, Serhan CN. Identification and Structure Elucidation of the Pro-Resolving Mediators Provides Novel Leads for Resolution Pharmacology. *Br J Pharmacol* (2019) 176(8):1024–37. doi: 10.1111/bph.14336
94. McPhillips K, Janssen WJ, Ghosh M, Byrne A, Gardai S, Remigio L, et al. TNF-Alpha Inhibits Macrophage Clearance of Apoptotic Cells Via Cytosolic Phospholipase A2 and Oxidant-Dependent Mechanisms. *J Immunol* (2007) 178(12):8117–26. doi: 10.4049/jimmunol.178.12.8117
95. Fredman G, Ozcan L, Spolitu S, Hellmann J, Spite M, Backs J, et al. Resolvin D1 Limits 5-Lipoxygenase Nuclear Localization and Leukotriene B4 Synthesis by Inhibiting a Calcium-Activated Kinase Pathway. *Proc Natl Acad Sci USA* (2014) 111(40):14530–5. doi: 10.1073/pnas.1410851111
96. Schmid M, Gemperle C, Rimann N, Hersberger M. Resolvin D1 Polarizes Primary Human Macrophages Toward a Proresolution Phenotype Through GPR32. *J Immunol* (2016) 196(8):3429–37. doi: 10.4049/jimmunol.1501701
97. Gu Z, Lamont GJ, Lamont RJ, Uriarte SM, Wang H, Scott DA. Resolvin D1, Resolvin D2 and Maresin 1 Activate the GSK3beta Anti-Inflammatory Axis in TLR4-Engaged Human Monocytes. *Innate Immun* (2016) 22(3):186–95. doi: 10.1177/1753425916628618
98. Recchiuti A, Codagnone M, Pierdomenico AM, Rossi C, Mari VC, Cianci E, et al. Immunoresolving Actions of Oral Resolvin D1 Include Selective Regulation of the Transcription Machinery in Resolution-Phase Mouse Macrophages. *FASEB J* (2014) 28(7):3090–102. doi: 10.1096/fj.13-248393
99. Recchiuti A, Krishnamoorthy S, Fredman G, Chiang N, Serhan CN. MicroRNAs in Resolution of Acute Inflammation: Identification of Novel Resolvin D1-miRNA Circuits. *FASEB J* (2010) 25(2):544–60. doi: 10.1096/fj.10-169599
100. Schif-Zuck S, Gross N, Assi S, Rostoker R, Serhan CN, Ariel A. Saturated-Efferocytosis Generates Pro-Resolving CD11b Low Macrophages: Modulation by Resolvins and Glucocorticoids. *Eur J Immunol* (2011) 41(2):366–79. doi: 10.1002/eji.201040801
101. Zhang S, Weinberg S, DeBerge M, Gainullina A, Schipma M, Kinchen JM, et al. Efferocytosis Fuels Requirements of Fatty Acid Oxidation and the Electron Transport Chain to Polarize Macrophages for Tissue Repair. *Cell Metab* (2019) 29(2):443–56 e5. doi: 10.1016/j.cmet.2018.12.004
102. Yurdagul AJr., Subramanian M, Wang X, Crown SB, Ilkayeva OR, Darville L, et al. Macrophage Metabolism of Apoptotic Cell-Derived Arginine Promotes Continual Efferocytosis and Resolution of Injury. *Cell Metab* (2020) 31(3):518–33 e10. doi: 10.1016/j.cmet.2020.01.001
103. Yurdagul AJr., Kong N, Gerlach BD, Wang X, Ampomah P, Kuriakose G, et al. Odc (Ornithine Decarboxylase)-Dependent Putrescine Synthesis Maintains MerTK (Mer Tyrosine-Protein Kinase) Expression to Drive Resolution. *Arterioscler Thromb Vasc Biol* (2021) 2021:ATVBAHA120315622. doi: 10.1161/ATVBAHA.120.315622
104. Butenko S, Satyanarayanan SK, Assi S, Schif-Zuck S, Sher N, Ariel A. Transcriptomic Analysis of Monocyte-Derived Non-Phagocytic Macrophages Favors a Role in Limiting Tissue Repair and Fibrosis. *Front Immunol* (2020) 11:405. doi: 10.3389/fimmu.2020.01003
105. Morioka S, Perry JSA, Raymond MH, Medina CB, Zhu Y, Zhao L, et al. Efferocytosis Induces a Novel SLC Program to Promote Glucose Uptake and Lactate Release. *Nature* (2018) 563(7733):714–8. doi: 10.1038/s41586-018-0735-5
106. Dalli J, Serhan CN. Specific Lipid Mediator Signatures of Human Phagocytes: Microparticles Stimulate Macrophage Efferocytosis and Pro-Resolving Mediators. *Blood* (2012) 120(15):e60–72. doi: 10.1182/blood-2012-04-423525
107. Cai B, Thorp EB, Doran AC, Subramanian M, Sansbury BE, Lin CS, et al. MerTK Cleavage Limits Proresolving Mediator Biosynthesis and Exacerbates Tissue Inflammation. *Proc Natl Acad Sci USA* (2016) 113(23):6526–31. doi: 10.1073/pnas.1524292113
108. Medina CB, Mehrotra P, Arandjelovic S, Perry JSA, Guo Y, Morioka S, et al. Metabolites Released From Apoptotic Cells Act as Tissue Messengers. *Nature* (2020) 580(7801):130–5. doi: 10.1038/s41586-020-2121-3
109. Gong YN, Guy C, Olauson H, Becker JU, Yang M, Fitzgerald P, et al. Escrt-Iii Acts Downstream of MLKL to Regulate Necroptotic Cell Death and Its Consequences. *Cell* (2017) 169(2):286–300.e16. doi: 10.1016/j.cell.2017.03.020
110. Wallach D, Kang TB, Dillon CP, Green DR. Programmed Necrosis in Inflammation: Toward Identification of the Effector Molecules. *Science* (2016) 352(6281):aaf2154. doi: 10.1126/science.aaf2154
111. Enyedi B, Jelcic M, Niethammer P. The Cell Nucleus Serves as a Mechanotransducer of Tissue Damage-Induced Inflammation. *Cell* (2016) 165(5):1160–70. doi: 10.1016/j.cell.2016.04.016
112. Rayner KJ. Cell Death in the Vessel Wall: The Good, the Bad, the Ugly. *Arterioscler Thromb Vasc Biol* (2017) 37(7):e75–81. doi: 10.1161/ATVBAHA.117.309229
113. Krysko DV, Denecker G, Festjens N, Gabriels S, Parthoens E, D'Herde K, et al. Macrophages Use Different Internalization Mechanisms to Clear Apoptotic and Necrotic Cells. *Cell Death Differ* (2006) 13(12):2011–22. doi: 10.1038/sj.cdd.4401900
114. Karunakaran D, Geoffrion M, Wei L, Gan W, Richards L, Shangari P, et al. Targeting Macrophage Necroptosis for Therapeutic and Diagnostic Interventions in Atherosclerosis. *Sci Adv* (2016) 2(7):e1600224. doi: 10.1126/sciadv.1600224
115. Kojima Y, Volkmer JP, McKenna K, Civelek M, Lusis AJ, Miller CL, et al. CD47-Blocking Antibodies Restore Phagocytosis and Prevent Atherosclerosis. *Nature* (2016) 536(7614):86–90. doi: 10.1038/nature18935
116. Gagnon E, Duclos S, Rondeau C, Chevet E, Cameron PH, Steele-Mortimer O, et al. Endoplasmic Reticulum-Mediated Phagocytosis Is a Mechanism of Entry Into Macrophages. *Cell* (2002) 110(1):119–31. doi: 10.1016/S0092-8674(02)00797-3

117. Becker T, Volchuk A, Rothman JE. Differential Use of Endoplasmic Reticulum Membrane for Phagocytosis in J774 Macrophages. *Proc Natl Acad Sci USA* (2005) 102(11):4022–6. doi: 10.1073/pnas.0409219102
118. Franceschi C, Campisi J. Chronic Inflammation (Inflammaging) and Its Potential Contribution to Age-Associated Diseases. *J Gerontol A Biol Sci Med Sci* (2014) 69(Suppl 1):S4–9. doi: 10.1093/gerona/glu057
119. Aprahamian T, Rifkin I, Bonegio R, Hugel B, Freyssinet JM, Sato K, et al. Impaired Clearance of Apoptotic Cells Promotes Synergy Between Atherogenesis and Autoimmune Disease. *J Exp Med* (2004) 199(8):1121–31. doi: 10.1084/jem.20031557
120. Aprahamian T, Takemura Y, Goukassian D, Walsh K. Ageing is Associated With Diminished Apoptotic Cell Clearance In Vivo. *Clin Exp Immunol* (2008) 152(3):448–55. doi: 10.1111/j.1365-2249.2008.03658.x
121. Linehan E, Dombrowski Y, Snoddy R, Fallon PG, Kissenpfennig A, Fitzgerald DC. Aging Impairs Peritoneal But Not Bone Marrow-Derived Macrophage Phagocytosis. *Aging Cell* (2014) 13(4):699–708. doi: 10.1111/acel.12223
122. Arnardottir HH, Dalli J, Colas RA, Shinohara M, Serhan CN. Aging Delays Resolution of Acute Inflammation in Mice: Reprogramming the Host Response With Novel Nano-Proresolving Medicines. *J Immunol* (2014) 193(8):4235–44. doi: 10.4049/jimmunol.1401313
123. Frisch BJ, Hoffman CM, Latchney SE, LaMere MW, Myers J, Ashton J, et al. Aged Marrow Macrophages Expand Platelet-Biased Hematopoietic Stem Cells Via Interleukin1B. *JCI Insight* (2019) 4(10):e124213. doi: 10.1172/jci.insight.124213
124. Kulkarni U, Zemans RL, Smith CA, Wood SC, Deng JC, Goldstein DR. Excessive Neutrophil Levels in the Lung Underlie the Age-Associated Increase in Influenza Mortality. *Mucosal Immunol* (2019) 12(2):545–54. doi: 10.1038/s41385-018-0115-3
125. Wong CK, Smith CA, Sakamoto K, Kaminski N, Koff JL, Goldstein DR. Aging Impairs Alveolar Macrophage Phagocytosis and Increases Influenza-Induced Mortality in Mice. *J Immunol* (2017) 199(3):1060–8. doi: 10.4049/jimmunol.1700397
126. Campisi J. Aging, Cellular Senescence, and Cancer. *Annu Rev Physiol* (2013) 75:685–705. doi: 10.1146/annurev-physiol-030212-183653
127. Cai B, Thorp EB, Doran AC, Sansbury BE, Daemen MJ, Dorweiler B, et al. MerTK Receptor Cleavage Promotes Plaque Necrosis and Defective Resolution in Atherosclerosis. *J Clin Invest* (2017) 127(2):564–8. doi: 10.1172/JCI90520
128. Gangemi S, Pescara L, D'Urbano E, Basile G, Nicita-Mauro V, Davi G, et al. Aging is Characterized by a Profound Reduction in Anti-Inflammatory Lipoxin A4 Levels. *Exp Gerontol* (2005) 40(7):612–4. doi: 10.1016/j.exger.2005.04.004
129. Fredman G, Hellmann J, Proto JD, Kuriakose G, Colas RA, Dorweiler B, et al. An Imbalance Between Specialized Pro-Resolving Lipid Mediators and Pro-Inflammatory Leukotrienes Promotes Instability of Atherosclerotic Plaques. *Nat Commun* (2016) 7:12859. doi: 10.1038/ncomms12859
130. Fredman G, Van Dyke TE, Serhan CN. Resolvin E1 Regulates Adenosine Diphosphate Activation of Human Platelets. *Arterioscler Thromb Vasc Biol* (2010) 30(10):2005–13. doi: 10.1161/ATVBAHA.110.209908
131. Whittington RA, Planel E, Terrando N. Impaired Resolution of Inflammation in Alzheimer's Disease: A Review. *Front Immunol* (2017) 8:1464. doi: 10.3389/fimmu.2017.01464
132. Ho KJ, Spite M, Owens CD, Lancero H, Kroemer AH, Pande R, et al. Aspirin-Triggered Lipoxin and Resolvin E1 Modulate Vascular Smooth Muscle Phenotype and Correlate With Peripheral Atherosclerosis. *Am J Pathol* (2010) 177(4):2116–23. doi: 10.2353/ajpath.2010.091082
133. Cai B, Kasikara C, Doran AC, Ramakrishnan R, Birge RB, Tabas I. MerTK Signaling in Macrophages Promotes the Synthesis of Inflammation Resolution Mediators by Suppressing CaMKII Activity. *Sci Signal* (2018) 11(549):eaar3721. doi: 10.1126/scisignal.aar3721
134. De Maeyer RPH, van de Merwe RC, Louie R, Bracken OV, Devine OP, Goldstein DR, et al. Blocking Elevated P38 MAPK Restores Efferocytosis and Inflammatory Resolution in the Elderly. *Nat Immunol* (2020) 21(6):615–25. doi: 10.1038/s41590-020-0646-0
135. Gilroy DW, De Maeyer RPH, Tepper M, O'Brien A, Uddin M, Chen J, et al. Treating Exuberant, Non-Resolving Inflammation in the Lung; Implications for Acute Respiratory Distress Syndrome and COVID-19. *Pharmacol Ther* (2020) 221:107745. doi: 10.1016/j.pharmthera.2020.107745
136. Motwani MP, Colas RA, George MJ, Flint JD, Dalli J, Richard-Loendt A, et al. Pro-Resolving Mediators Promote Resolution in a Human Skin Model of UV-Killed Escherichia Coli-Driven Acute Inflammation. *JCI Insight* (2018) 3(6):e94463. doi: 10.1172/jci.insight.94463

Conflict of Interest: The authors declare that the research was conducted in the absence of any commercial or financial relationships that could be construed as a potential conflict of interest.

Copyright © 2021 Decker, Sadhu and Fredman. This is an open-access article distributed under the terms of the Creative Commons Attribution License (CC BY). The use, distribution or reproduction in other forums is permitted, provided the original author(s) and the copyright owner(s) are credited and that the original publication in this journal is cited, in accordance with accepted academic practice. No use, distribution or reproduction is permitted which does not comply with these terms.

Advantages of publishing in Frontiers

OPEN ACCESS
Articles are free to read for greatest visibility and readership

FAST PUBLICATION
Around 90 days from submission to decision

HIGH QUALITY PEER-REVIEW
Rigorous, collaborative, and constructive peer-review

TRANSPARENT PEER-REVIEW
Editors and reviewers acknowledged by name on published articles

Frontiers
Avenue du Tribunal-Fédéral 34
1005 Lausanne | Switzerland

Visit us: www.frontiersin.org
Contact us: frontiersin.org/about/contact

REPRODUCIBILITY OF RESEARCH
Support open data and methods to enhance research reproducibility

DIGITAL PUBLISHING
Articles designed for optimal readership across devices

FOLLOW US
@frontiersin

IMPACT METRICS
Advanced article metrics track visibility across digital media

EXTENSIVE PROMOTION
Marketing and promotion of impactful research

LOOP RESEARCH NETWORK
Our network increases your article's readership